

Gold compact disc appended Tröger's base scaffolds as MALDI-TOF
biodetection probes

Glyn D. Hiatt-Gipson

Supervisor

Dr. S. P. Bew

School of Chemistry, University of East Anglia, Norwich Research Park, Norwich,

NR4 7TJ, UK

[g.hiatt-gipson @ uea.ac.uk](mailto:g.hiatt-gipson@uea.ac.uk)

Submitted as fulfilment to Doctor of Philosophy

January 2013

This copy of the thesis has been supplied on condition that anyone who consults it is understood to recognise that its copyright rests with the author and that use of any information derived there-from must be in accordance with current UK Copyright Law. In addition, any quotation or extract must include full attribution.

Abstract

Tröger's base was discovered in 1887 by J. Tröger and has a V-shaped structure with C_2 symmetry containing a chiral, hydrophobic cleft creating an angle of 90° . For many years its chiral cleft has been utilised for the stationary phase of chiral HPLC columns, a chiral resolving agent and as a chiral catalyst.

Over the past 30 years it has been reported that this interesting molecule can intercalate DNA, inhibit enzyme activity and behave as a synthetic receptor. The biological activity of the analogues of Tröger's base has only been narrowly investigated. This investigation has generated a plethora of biologically interesting Tröger's base derivatives *via* utilisation of 'click' chemistry on a novel *bis*-azido Tröger's base scaffold.

The detection of proteins quickly, efficiently and cheaply is a huge challenge and this project aims to use cheap, readily available gold compact discs as a novel platform for the portable detection and sensing of biological interactions on the gold CD surface. The use of a gold compact disc and its ability to bind self assembled monolayers will be investigated and the detection of these biological interactions *via* MALDI-TOF spectrometry will be probed. The (+)-biotin / streptavidin interaction will be used as a model study for these purposes with the ambition to develop this further with humanitarian and military applications.

The V-shape and 90° angle of Tröger's base will be exploited to investigate its use as a scaffold for binding to gold compact discs for the development of surface based biological assays and proteomics.

The incorporation of stable isotopes into organic molecules will also be investigated and we report a new protocol for the mild and efficient deuteration of terminal alkynes and their subsequent use in organic chemistry.

Acknowledgements

I would like to thank Dr. Sean Bew (UEA) for his help and guidance throughout the years and the opportunity to work in his laboratory. A huge thanks must be given to my colleagues throughout the years and also to the other members of the lab past and present.

Thanks to Dr. Stephen Ashworth, UEA, for his help and encouragement with the CD-player challenge, Dr Bertrand Leze and Dr Andrew Round, UEA, for SEM and AFM images and Dr David Evason, SAI Ltd, must be thanked for the MALDI-TOF analysis. I thank Dr. D. Hughes and Dr. M. Schorman (UEA) for crystal structure determinations reported in this thesis. Thank you to the EPSRC National mass spectrometry service for running the HRMS reported in this thesis

Thanks to Chemistry Innovation, Librarian Ltd and DSTL for funding that made this all possible.

Finally thanks to all my friends and family for their support over the last four years, especially to my fiancée Patricia Vives-Garcia, not only for her help with the biological side of this project, but for her support, patience and understanding during these studies.

Declaration

CERTIFICATE OF ORIGINALITY

I certify that the work contained in the thesis submitted by me for the degree of Doctor of Philosophy is my original work, except where due reference is made to other authors, and has not previously been submitted by me for a degree at this or any other University

Signed (candidate) Glyn D Hiatt-Gipson.....Date: 10 / 11 / 2013

Abbreviations List

AFM	Atomic force microscopy
Bz	Benzyl
Cbz	Carboxybenzyl
CD	Circular dichromism
CI	Chemical ionisation
CO ₂	Carbon dioxide
d	Doublet
DCM	Dichloromethane
dd	Doublet of doublets
DMAP	Dimethyl amino pyridine
DMF	Dimethylformamide
DNA	Deoxyribonucleotide acid
E ⁺	Electrophile
ELD	Electric Linear Dichromism
ES	Electrospray
ET ₂ NH	Diethylamine
Gly	Glycine
H ⁺	Acid
H ₂ O	Water
Halo	Halogen
HCl	Hydrochloric Acid
HObt	N-hydroxybenzotriazole

HPLC	High performance liquid chromatography
ⁱ Pr ₂ NH	Di-isopropylamine
KOH	Potassium hydroxide
LC-MS	Liquid Chromatography Mass Spectrometry
LiOH	Lithium hydroxide
m	Multiplet
MALDI-TOF	Matrix Assisted Laser Desorption/Ionisation Time of Flight mass spectrometry
Me	Methyl
MeCN	Acetonitrile
MeOH	Methanol
NMR	Nuclear Magnetic Resonance
Phe	Phenylalanine
poc	Propargyloxycarbonyl
Pro	Proline
q	Quartet
rt	Room temperature
SAMs	Self assembled monolayer
SEM	Scanning electron microscopy
s	Singlet
t	Triplet
TB	Trögers Base

TBTU	O-benzotriazole-1-yl -N,N,N',N'- tetramethyluronium tetrafluoroborate
TEA	Triethylamine
TFA	Trifluoroacetic Acid
THF	Tetrahydrofuran
TLC	Thin layer chromatography
Tyr	Tyrosine

Table of Contents

Abstract.....	2
Acknowledgements.....	3
Declaration.....	3
Abbreviations List.....	4
1 Introduction.....	10
1.1 Tröger's base.....	10
1.2 Analogues of Tröger's base	12
1.2.1 Chiral clefts.....	12
1.2.2 Tröger's base modifications at the 2 and 8 positions.....	12
1.2.3 Tröger's base modification at bridgehead methylene C13	13
1.2.4 Aryl extended and aryl modified Tröger's base analogues	14
1.3 Biological properties and interactions of Tröger's base analogues	16
1.3.1 Tröger's base analogues as thromboxane A ₂ (TxA ₂) synthase inhibitor	16
1.3.2 Tröger's base analogues and their interactions with ds-DNA	17
1.3.3 Tröger's base analogues as synthetic receptors	21
1.3.4 Stable isotope incorporated Tröger's base.....	24
1.4 Incorporation and reactions of stable isotopes into organic compounds	25
1.4.1 Deuterium in organic synthesis.....	25
1.4.2 Dueterium isotope effect.....	26
1.4.3 Deuterium in the pharmaceutical industry.....	26
1.4.4 Current methods for the synthesis of deuterated terminal alkynes	28
1.4.5 ² H-incorporated alkynes as building blocks for organic synthesis	29
1.5 Small molecule – protein interactions.....	30
1.5.1 Proteins	30
1.5.2 (+)-Biotin and (strept)avidin system.....	31
1.5.3 Chemical derivatisation of (+)-biotin	32
1.5.4 Biotin/(strept)avidin interactions on a surface.....	34
1.6.1 Self assembled monolayers (SAMs).....	37

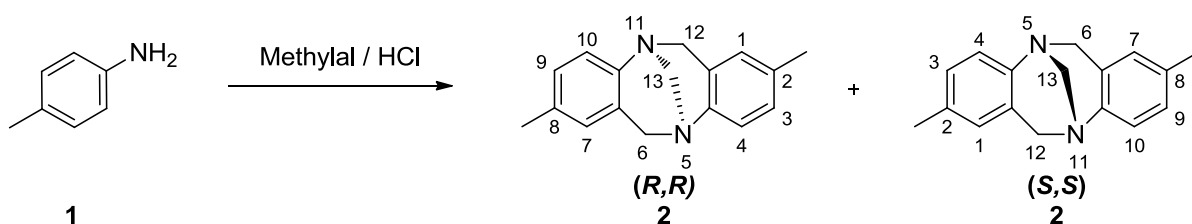
1.6.2 SAM formation on gold surfaces	38
1.6.3 SAM characterisation.....	39
1.6.4 SAMs for the detection of biological interactions	39
1.6.5 SAMs and matrix-assisted LASER-desorption/ionisation time of flight mass spectrometry (MALDI-TOF MS)	40
1.6.6 Binding events of biological interactions on SAMs analysed by MALDI-TOF MS	42
1.6.6 SAMs on compact discs.....	43
1.7 Compact discs and CD drives for biological assays	44
2 Aims of research	45
3 Methodology	46
3.1 Tröger's base synthesis and 'click' reaction.....	46
3.2 Stable isotope incorporation of alkynes and Tröger's base	49
3.3 Proof of concept for MALDI-TOF analysis of SAM (+)-biotin / streptavidin binding.....	50
3.4 Tröger's base modification for (+)-biotin and di-sulfide incorporation	51
4 Results and Discussion	53
4.1 Tröger's base synthesis and functionalisation	53
4.2 Propargyl esterification of (+)-biotin (+)-64.....	56
4.3 Propargyl ester synthesis of <i>N</i> -protected α / β - amino acids.....	58
4.4 Synthesis of 2,8- <i>bis</i> (4-substituted-5H-1,2,3-triazol-1-yl)-6,12-dihydro-5,11-methano dibenzo[b,f][1,5]diazocines	63
4.5 Synthesis of 2,8- <i>bis</i> (4- <i>N</i> -protected- α - or β -amino acids-5H-1,2,3-triazol-1-yl)-6,12-dihydro-5,11-methanodibenzo[b,f][1,5]diazocines	67
4.6 Synthesis of symmetrical 2,8- <i>bis</i> (4- <i>O</i> -protected-carbohydrates-5H-1,2,3-triazol-1-yl)-6,12-dihydro-5,11-methanodibenzo [b,f][1,5]diazocines.	70
4.7 Unsymmetrical 2-(4-substituted-5H-1,2,3-triazol-1-yl)-8-(4-substituted-5H-1,2,3-triazol-1-yl)-6,12-dihydro-5,11-methanodibenzo[b,f][1,5]diazocine.....	74
4.8 Biological testing of 2, 8-appended 1,2,3-triazole Tröger's bases	78
4.8.1 DNA intercalation.....	78
4.9 Mild conditions for the deuteration of terminal alkynes.....	81
4.10 ² H-incorporated terminal alkynes as building blocks for organic synthesis.....	89

4.11	Stable isotope incorporation within 2,8-appended Tröger's base (4-deutero) 1,2,3 triazoles ..	91
4.12	Incorporation of stable isotopes within the Tröger's base scaffold	94
4.13	Synthesis of (+)-biotin analogues for SAM formation.	97
4.14	Preparation of 24 karat gold compact discs for SAMs	104
4.15	Self Assembled Monolayer formation	107
4.16	Biotin / Streptavidin binding on a gold disc.	109
4.17	MALDI-TOF mass spectrometry analysis of binding events	109
4.18	Tröger's Base Scaffolds for SAMs	116
4.19	Methylene bridge removal from Tröger's base	116
4.20	Tröger's base C13 modification.....	119
4.21	Synthesis of (+)-biotin incorporated Tröger's bases.....	122
4.22	Synthesis of symmetrical 2,8-1,2,3-triazole Tröger's base C13 disulfide dimers	133
5.0	Discussion	134
6.0	Experimental.....	139
6.1	General Directions	139
6.2	Characterisation	139
	References.....	233
	Appendix.....	245

1 Introduction

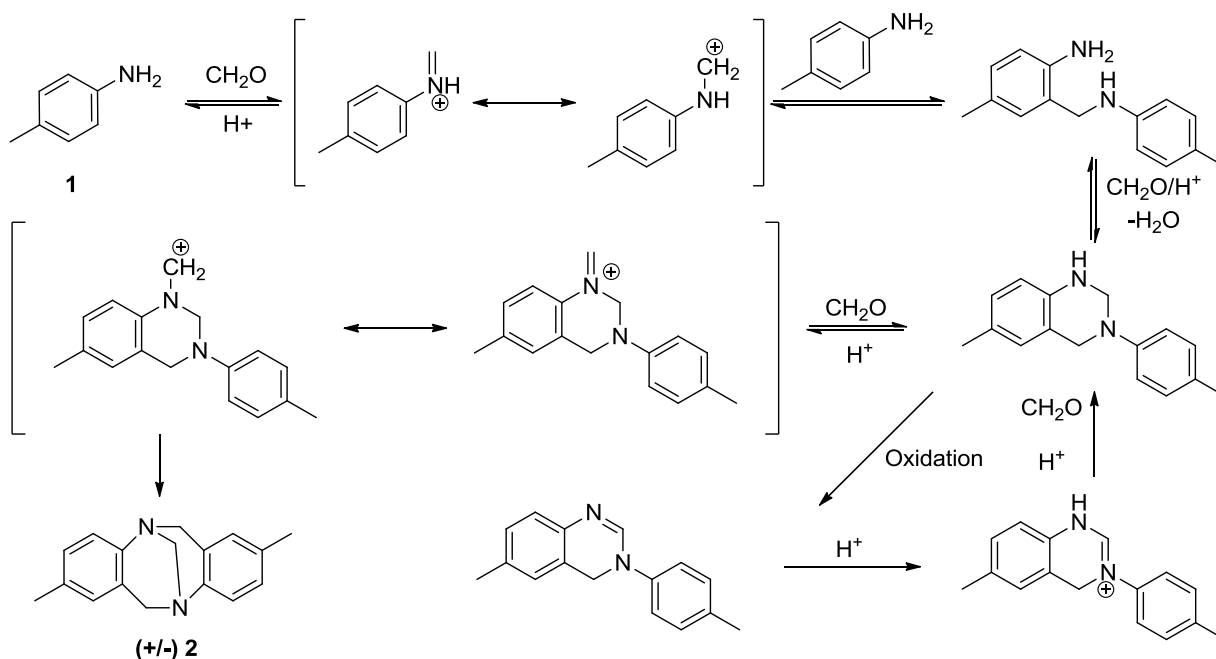
1.1 Tröger's base

In 1887 Carl Julius Ludwig Tröger published a paper on his results of the condensation of *para*-toluidine **1** with methylal $[\text{CH}_2-(\text{OCH}_3)_2]$ in an aqueous solution of hydrochloric acid. From this reaction he isolated an unexpected compound, which he described as 'base $\text{C}_{17}\text{H}_{18}\text{N}$ '.¹ It wasn't until 1935 that the correct chemical structure of this unusual base was finally determined by Spielman, who confirmed the structure of Tröger's base was in fact racemic 2,8-dimethyl-6,12-dihydro-5,11-methanodibenzo[b,f][1,5]diazocine **2**.²



Scheme 1 J. Tröger's synthesis of Tröger's base (2,8-dimethyl-6,12-dihydro-5,11-methanodibenzo[b,f][1,5]diazocine) **2**

In the same year, 1935, Wagner proposed the mechanism for the synthesis of racemic Tröger's base **2** (scheme 2 (*vide infra*)) via acid catalysed condensation of **1** with formaldehyde affording an iminium ion, which, reacts with a second equivalent of **1** affording the first intermediate. Subsequently this reacts with two methylenes, followed by ring closing to afford (+/-) **2**.³ This mechanism was further confirmed by Abella *et al.* in 2007 by mass spectrometry analysis of the intermediates formed during the condensation of **1** with paraformaldehyde.⁴



Scheme 2 Proposed mechanism for the synthesis of racemic Tröger's base **2** as described by Wagner

Prior to 1980 Tröger's base was mainly used for investigating separation techniques⁵ but since then Tröger's base and its various analogues have provoked much interest, due to its rigid shape and hydrophobic cavity, as supramolecular building blocks, molecular recognition tools, potential ligands for catalysis and as molecular tweezers.^{6,7,8} This C₂ symmetric heterocycle has its two aryl groups very nearly perpendicular to each other at angles between 90-100° and gives the structure a rigid backbone with a concave conformation and leads to a cavity or chiral cleft with hydrophobic behaviour⁹.

Tröger's base, a chiral diamine contains two stereogenic bridge-head nitrogens and has C₂ – symmetry.⁷ Therefore two enantiomers exist for this moiety, the resolution of **2** using (-)-1,1'-binaphthalene-2,2'-diyl hydrogen phosphate, (1:1) in ethanol affords (+)-enantiomer.¹⁰ This is commercially available from Aldrich, as a chiral resolving agent.

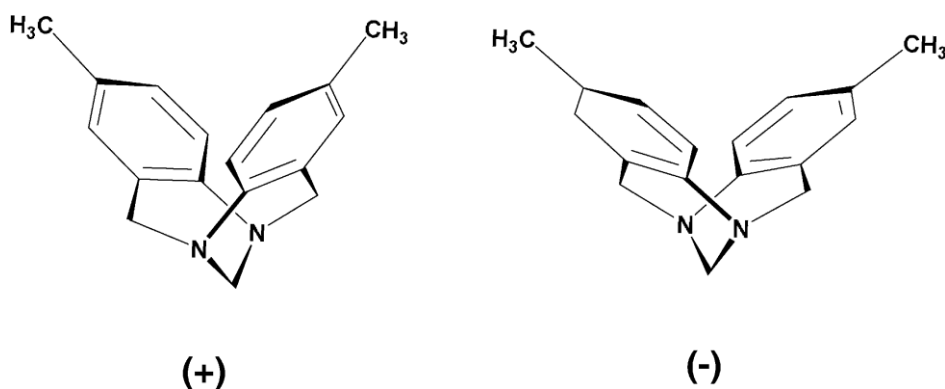


Figure 1 Enantiomers of Tröger's base **2** showing hydrophobic chiral cleft and C₂-symmetry.

The asymmetric synthesis of a Tröger's base analogue has been reported using 7-deoxycholic acid as a chiral steroid template prior to the bridged nitrogen formation.¹¹ Although separation of the enantiomers of this molecule does seem to be possible, there are problems with maintaining chiral purity during reaction procedures due to the high tendency of Tröger's base to racemise in acid conditions¹⁰.

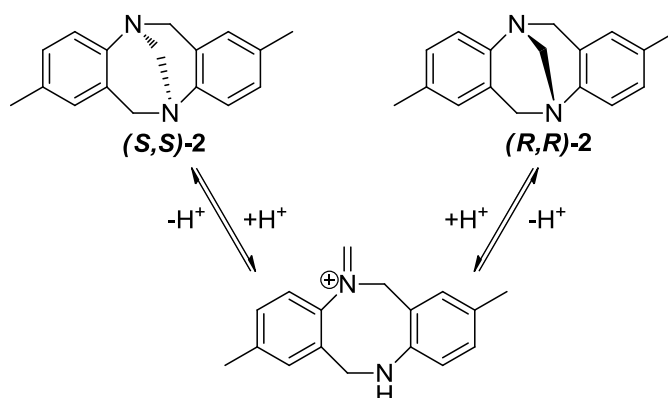


Figure 2 Proposed mechanism for Tröger's base racemisation under acidic conditions. Protonation on either of the tertiary amines causes ring opening to occur. This can then ring close from either face causing racemisation to occur.

1.2 Analogues of Tröger's base

1.2.1 Chiral clefts

Many analogues of Tröger's base, also known as [1,5] diazocines, have been synthesised that contain a chiral cleft, indeed many of these have been utilised in a plethora of chemical and biological disciplines. Thus an ether bridged carbocycle derivative **3** (*Kagan's ether*),¹² an unbridged dithiocene **4** and an α, β unsaturated ketone carbocycle **5**¹³ all contain clefts. Although **4** does not possess a chiral cleft it is an interesting example of a cleft molecule that doesn't contain a bridgehead atom to hold it in this conformation.

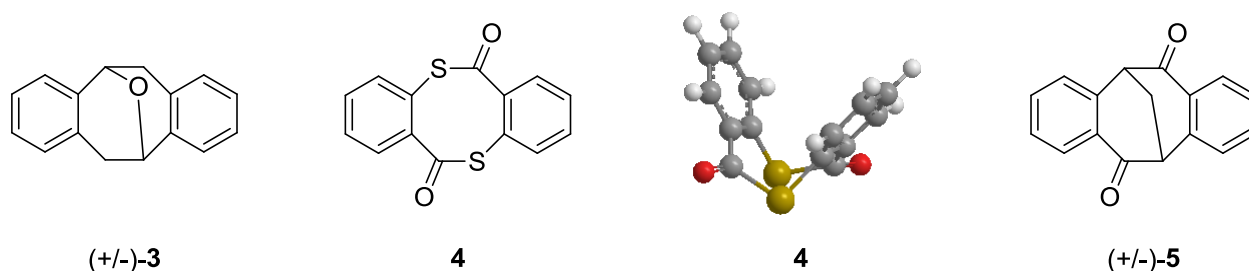
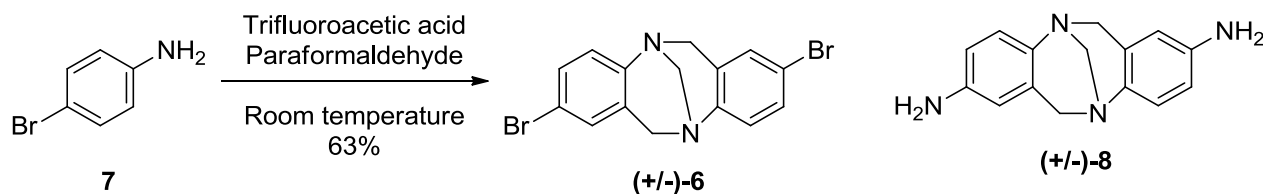


Figure 3 Examples of cleft containing compounds and Chem 3D representation of the unbridged di-thiocene **4**

1.2.2 Tröger's base modifications at the 2 and 8 positions

With a large variety of Tröger's base analogues reported in the literature, synthetic chemists require further functionalisation of the moiety in order to exploit the unique properties that Tröger's Base possess. The synthesis of racemic 2,8-*bis*-bromo-Tröger's base (+/-)-**6** by Jensen and Warnmark lead the way for functionalised analogues of the Tröger's base to be constructed. They reported the condensation of *para*-bromo aniline **7** with paraformaldehyde in neat trifluoroacetic acid¹⁴ afforded (+/-)-**6** in a 63% yield. Didier and Sergeev later reported a 2,8-di-amino analogue **8**, generated *via* transition metal catalysed aromatic amination of racemic-2, 8-*bis*-iodo Tröger's base.⁷

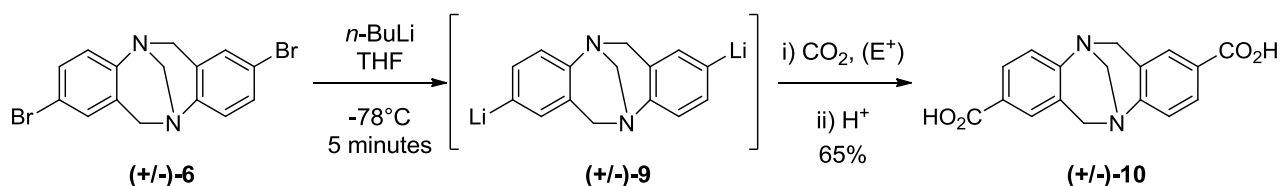


Scheme 3 racemic 2,8-*bis*-bromo Tröger's base (+/-)-**6** as reported by Warnmark *et al*

Figure 4 Didier and Sergeev reported (+/-)-**8** 2,8-*bis*-amino Tröger's base.

Following these developments Jensen *et al.* continued to functionalise the 2 and 8 positions of Tröger's base by utilising bromine-lithium exchange. Jensen *et al.* reacted (+/-)-**6** with *n*-butyl lithium which afforded *bis*-lithiated Tröger's base analogue (+/-)-**9** and then quenched the intermediate with a wide array of different electrophiles generating 2,8-*bis* substituted Tröger's base

analogues *i.e.* quenching (+/-)-**9** with CO₂ to generate (+/-)-**10**.¹⁵ This paved the way for synthetic chemists to utilise the 2 and 8 positions of Tröger's base for further functionalisation of these interesting molecules.



Scheme 4 Jenson *et al.* reported bromine-lithium exchange on (+/-)-**6** generating 2,8-*bis*-substituted Tröger's base analogues. Other electrophiles reported H₂O - 88%, TMSCl - 89%, PhCHO - 58%, Bu₃SnCl - 71%.

Bew *et al.* used this development to use Tröger's base as a scaffold for generating peptide derivatives (+/-)-**11**. The unique shape allows Tröger's base to be considered as a β-turn mimic or a hairpin which are widely found in natural peptides. The poly peptide TNYLFSPNGPIARAW binds to EphB4 (IC₅₀ 15 nM) and contains a 90° turn induced by proline-glycine di-peptide which was found to be essential for high affinity binding. It was reported that Tröger's base analogues could be used to probe these regions.⁹

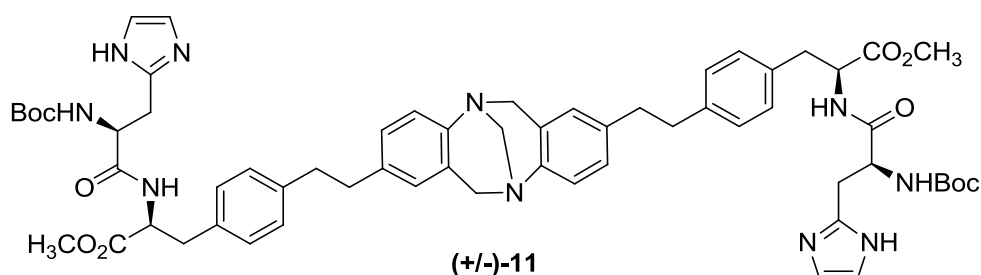
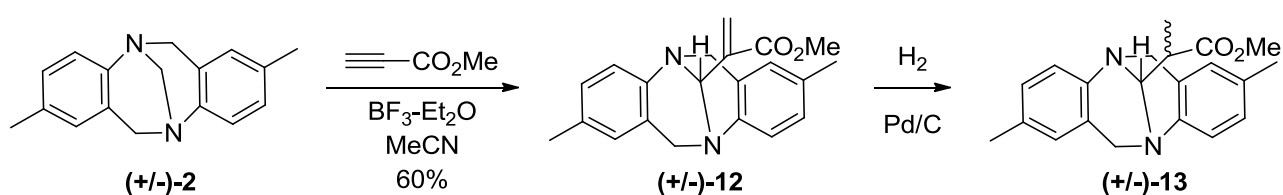


Figure 5 2,8-*bis*-peptidyl Tröger's base analogue generated as a β-turn director as reported by Bew *et al.*

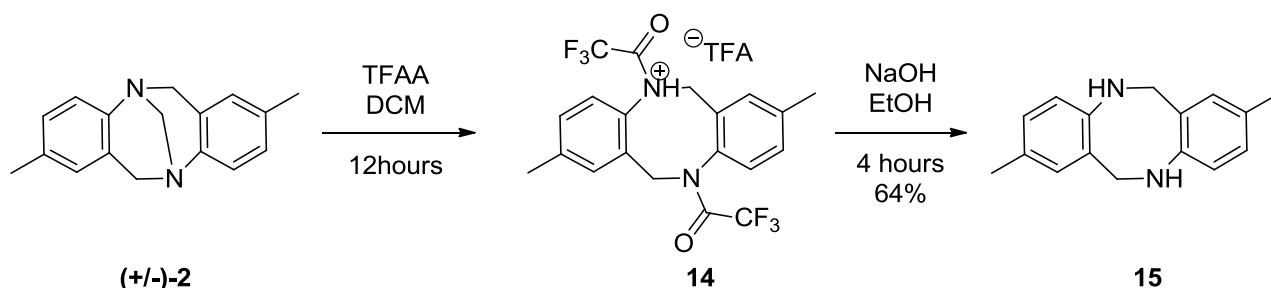
1.2.3 Tröger's base modification at bridgehead methylene C13

Lenev *et al.* reported a small library of analogues with substituent's at the bridged carbon, (C 13, Scheme 1) (+/-)-**12**, (+/-)-**13**. Reactions at the bicyclic core, were obtained by ring opening with boron trifluoride diethyl etherate and insertion of the activated acetylene *via* nucleophilic attack of the amine on the terminal acetylene carbon. This adduct then ring closes followed by allylic rearrangement which afforded (+/-)-**1**.¹⁶



Scheme 5 Lenev *et al.* reported modification of Tröger's base at the C13 position

Mahon *et al.* reported the complete removal of the Tröger's base methylene bridge C13, by reacting (+/-)-**2** with trifluoroacetic anhydride, which, afforded a trifluoroacetate salt of a bis-trifluoroacetylated dissecondary amine **14** this was then hydrolysed by ethanolysis affording the methylene removed Tröger's base derivative **15**.¹⁷



Scheme 6 Mahon *et al.* reported complete removal of the Tröger's base methylene bridge

In the same publication Mahon *et al.* reported the replacement of the methylene bridge by insertion of a bridging methylene component, benzaldehyde, into the diazocine framework. This was achieved *via* refluxing **15** with benzaldehyde in toluene affording (+/-)-**16**.¹⁸ Hamada *et al.* reported an ethano-bridged Tröger's base analogue (+/-)-**17** by treatment of (+/-)-**2** with 1,2-dibromoethane. It was suggested that this reacts *via* ammonium ion and dibromide intermediates before formation of (+/-)-**17** and bromomethane.¹⁹ The introduction of a spiro[4,5]lactone strap on Tröger's base was reported by Try *et al.* *via* treatment of (+/-)-**2** or **15** with phthaloyl dichloride and triethylamine affording analogue (+/-)-**18**.²⁰

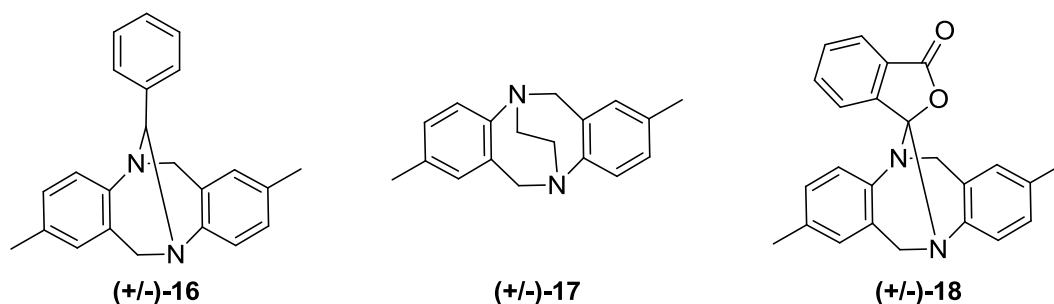


Figure 6 Tröger's base bridgehead methylene replaced derivatives

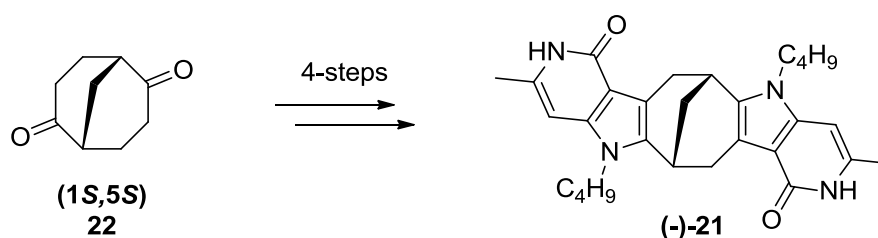
1.2.4 Aryl extended and aryl modified Tröger's base analogues

Various different aromatic systems, including thiophenes (+/-)-**19**²¹ as reported by Kobayashi and *N*-methyl pyrrole (+/-)-**20**,²² reported by Valik *et al.* In both cases they have replaced the standard benzene rings affording different aromatic, heterocyclic analogues. These were generated by replacing the aniline start material with 3-aminothiophene and 4-amino-1-methylpyrrole, respectively. They were then condensed with paraformaldehyde in hydrochloric acid.^{21, 22}



Figure 7 Thiophene (+/-)-**19** and *N*-methyl pyrrole (+/-)-**20** derivatives of Tröger's base.

Aza indole analogues (**R**)-**21** containing a molecular chiral cleft have been reported by Warnmark *et al.* with the purpose of self aggregation to form helical tubes with non-covalent, end to end, aggregation. These compounds can be synthesised as either enantiomer as the start material, (1*S*,5*S*)-bicyclo[3.3.1]nonane-2,6-dione (+/-)-**22** is available enantiomerically pure from Aldrich.²³



Scheme 7 Warnmark *et al.* synthesis of a chiral cleft containing aza indole Tröger's base analogue

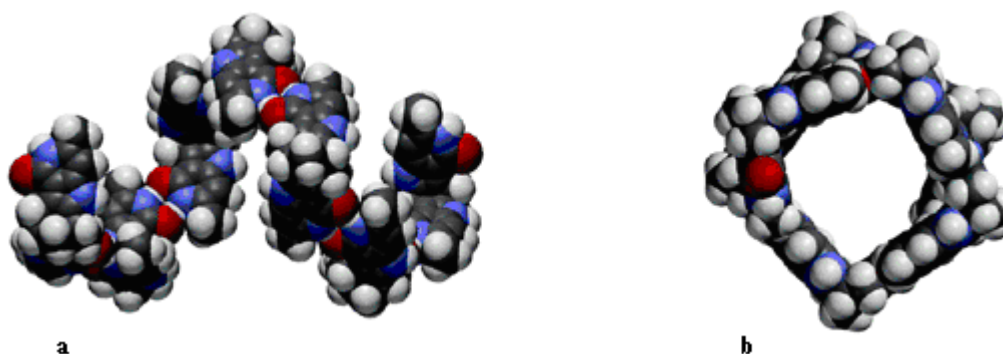


Figure 8 PM3-optimised geometry of a proposed homochiral helical assembly of (**R**)-**2**. Side view (a) and top view (b)

Valik *et al.* have reported the synthesis of a calix type Tröger's base molecule, this *tris* - Tröger's base was formed via annulation of three benzene rings to one, to give a cup or "calix" shaped molecule (+/-)-**23**. During the synthesis of (+/-)-**23** an isomer was also isolated to yield a "throne" shaped molecule (+/-)-**24**. These molecules are of significant interest to scientists at the nano-technology interface as possible "nano-reactors" or capping them to make "nano-capsules". The pharmaceutical industry is interested in (+/-)-**23** as potential drug delivery systems due to their ability to isomerise in acidic conditions.²⁴

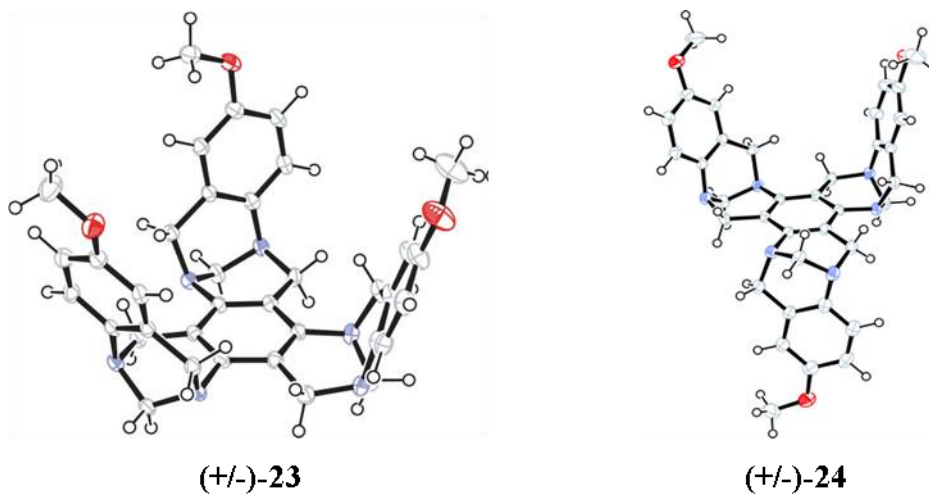
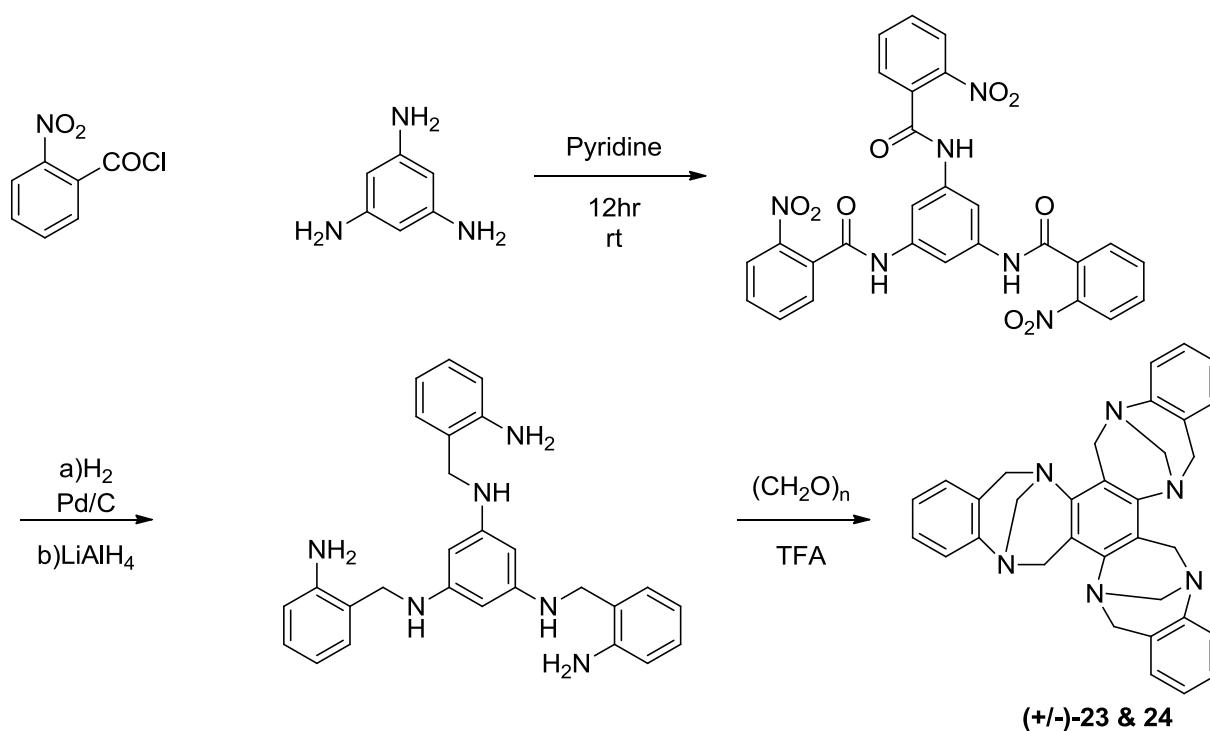


Figure 9 ORTEP style plots of 'calix' (+/-)-23 and 'throne' (+/-)-23 type Tröger's base analogues



Scheme 8 Reaction scheme for the preparation of *tris*-Tröger's base analogues as reported by Valik *et al*, 3% overall yield

1.3 Biological properties and interactions of Tröger's base analogues

1.3.1 Tröger's base analogues as thromboxane A₂ (TxA₂) synthase inhibitor

Johnson *et al.* report 2,8-*bis*-3-pyridylmethyl Tröger's base (+/-)-25 to be an efficient inhibitor of thromboxane A₂ (TxA₂) synthase. With *in vitro* assays affording an ED₅₀ of 30ng/ml. This level of activity is comparable with current (TxA₂) inhibitors, such as, sodium furegrelate **26**, dazoxiben **27** and OKY-1581 **28**, although it falls outside of the standard structure-activity correlations for

these inhibitors.²⁵ It was also reported that any modification to the C13 methylene bridge severely reduced the bioactivity as a TxA₂ inhibitor.

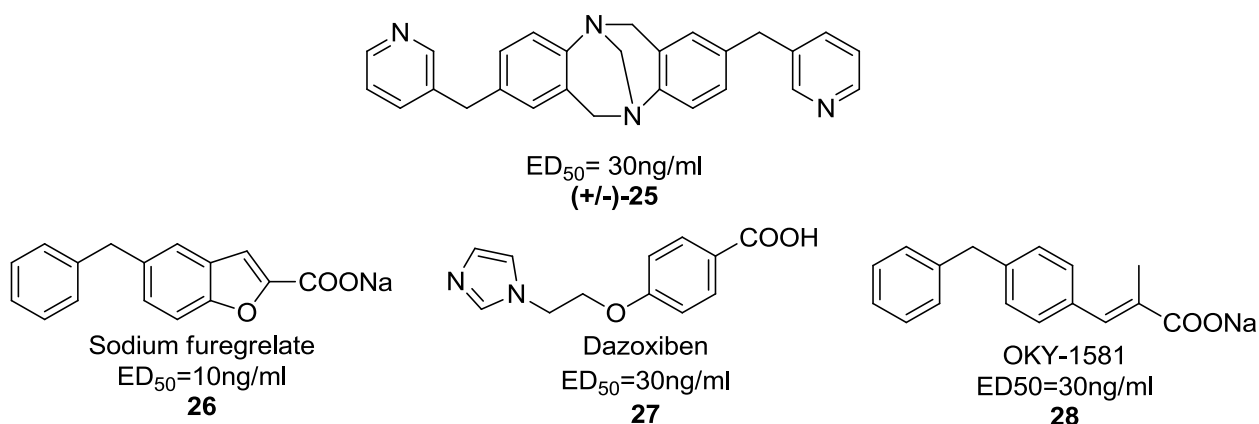


Figure 10 Tröger's base analogue (+/-)-25 affords an ED₅₀ that is comparable with currently marketed TxA₂ inhibitors.

1.3.2 Tröger's base analogues and their interactions with ds-DNA

Incorporating different aromatic systems into the Tröger's base scaffold and other carbocycles have been reported and many of these show a degree of biological activity towards ds-DNA. The ability of these molecules to direct appended substrates through different angles has been of major interest as the V shaped molecules can fit into the minor groove of ds-DNA.²⁶

Tatibouët *et al.* (1999) and Bailly *et al.* (2000) independently reported DNA affinity of a proflavine Tröger's base moiety (+/-)-29. Proflavine is a known DNA intercalator in the major and minor grooves.²⁷ Their studies show that the Tröger's base containing compound was not as efficient at binding, as the circular dichromism (CD) signals were weaker than values obtained for proflavine, but still had some interesting properties. It is thought that the Tröger's base moiety is not actually intercalating DNA as there is no evidence of the DNA unwinding and it is suggested that binding occurs in the minor groove. Interestingly, they have shown that the binding of the Tröger's base analogue to calf-thymus DNA (ct-DNA) is enantioselective and that the (-)-isomer has a much higher binding affinity than the (+) isomer. This was regarded as enantio-specific ligand towards DNA.²⁸

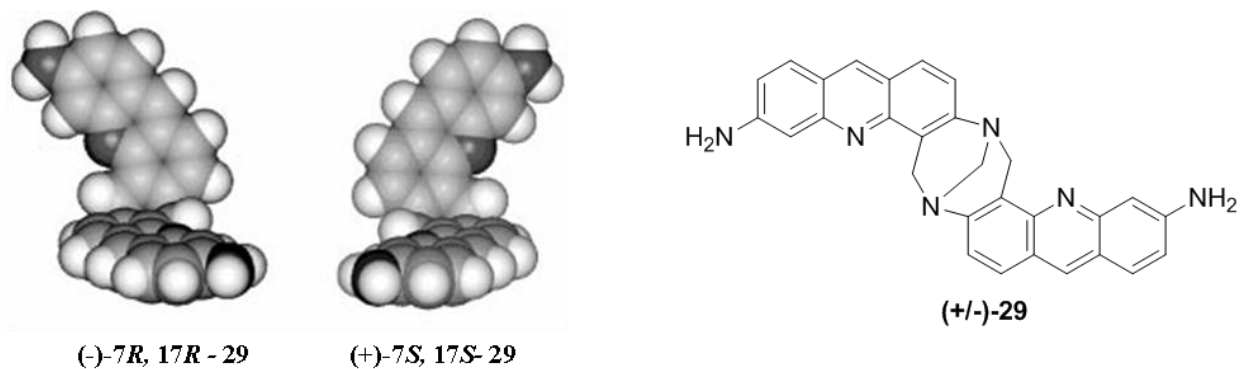


Figure 11 Molecular modelling representation of the two enantiomers of proflavine Tröger's base analogue (+/-)-29 and its structure.

DNase I footprinting was used to discover the sequence-selectivity of the (-) isomer and showed DNase I inhibition specifically at the A · T and G · C pairs. This crucially differs from other DNA intercalating agents which typically favour G · C pairs and minor groove binders favour the A · T pairs. There is potential for Tröger's base molecules and other analogues to be used as biological probes for nucleic acid structure determination.^{28,29}

Baldeyrou developed this model further by introducing a phenanthroline chromophore thus affording an unsymmetrical Tröger's base analogue (+/-)-30. Both chromophores are well known to bind DNA³⁰ and as shown previously the (-) *bis*-proflavine Tröger's base (-)-29 has a strong affinity to bind in the minor groove.²⁸ The mechanism for the binding of Tröger's base analogues is so far unknown due to the complications that arise from the symmetric nature of the analogues.³¹ Therefore, an investigation into unsymmetrical analogue may throw some light on the mechanisms of binding. Melting point analysis, where the change in melting point shows whether there is interaction between DNA and substrates, showed a strong binding of the (+/-)-30 to DNA as the temperature of decomposition was increased. Studies on the effect of the (+/-)-30 on poly (dAT)₂ showed stabilisation against thermal decomposition. CD and electric linear dichromism (ELD) measurements were recorded and showed the acridine ring is located parallel to base pairs, as is consistent with intercalative binding. As a consequence of the right angled orientation of Tröger's base it would suggest that the phenanthroline heterocycle is able to bind to the minor groove of DNA resulting in a bimodal process. The proflavine moiety is intercalated between the base pairs and the phenanthroline simultaneously bound to the minor groove. This bimodal action causes the molecule to have a different preferred site of interaction than its parent compounds. Footprinting with bovine pancreatic DNase I showed the Tröger's base moiety had moderate sequence selectivity and protected the sequence 5'-GTCACGACG from cleavage by the enzyme. Interestingly, the underlined segments were adjacent and anti-parallel triplets and was believed to be the preferred target sequence for the Tröger's base moiety.³¹ The footprinting also afforded an

increase in cleavage susceptibility at the sequences 5'-GGGTTT and 5'-AAAACGAC, *i.e.* at the “flanks” of the Tröger’s base preferred binding site. It was suggested that this was due to intercalation-induced structural re-arrangement thus promoting cutting by the enzyme.³¹

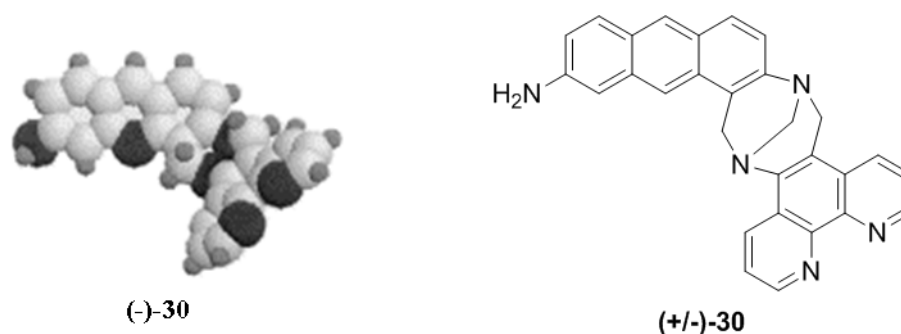


Figure 12 Energy minimised representation of proflavine-phenthroline Tröger’s base (-)-30 and structure of (+/-)-30

It has been shown that taking known DNA binding molecules and introducing these to a Tröger’s base scaffold has been successful in generating biologically active Tröger’s base molecules with different properties to the original parent compounds. Distamycin has the ability to bind to the minor groove of DNA with A·T selectivity and interestingly it can bind as a monomer and as anti-parallel dimers. Dystamycin is also known to inhibit protein interactions with G-quadruplex DNA and thus is a probe of protein interactions with double stranded DNA.³² A variety of linkers for dystamycin analogues were synthesised and it was found to be conformationally restrained linkers that were more effective at binding calf thymus DNA than flexible units. Stereochemical effects of the linkers have been reported to be critical to the binding affinity, making Tröger’s base a good scaffold. It was also reported that increasing the number of pyrrole units in analogues afforded a rise in A·T selectivity.²⁶ Dystamycin therefore seems to be a likely candidate to benefit from appendage to the Tröger’s base scaffold. This was carried out by Palivec *et al.* with *bis*-dystamycin Tröger’s base analogues (+/-)-31, using the *N*-methyl pyrrole Tröger’s base scaffold. A small number of analogues were synthesised with an increasing numbers of pyrrole units in a symmetrical fashion.

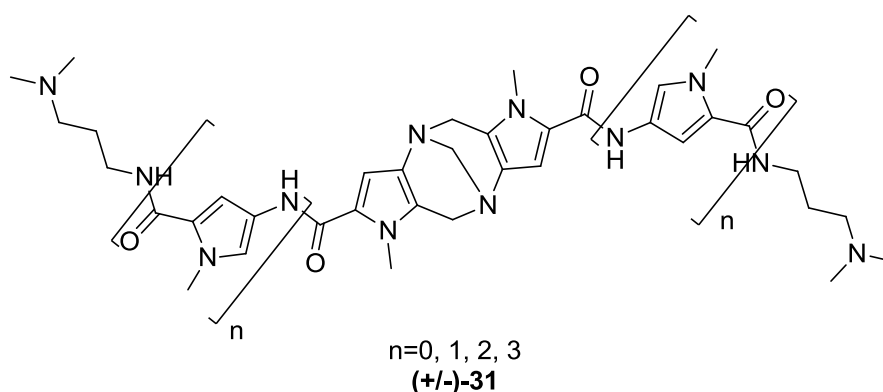


Figure 13 Dystamycin Tröger’s base analogues with DNA binding affinity where n=2 and n=3

Changes in UV-vis spectra were observed upon addition of (+/-)-**31**, where $n = 1-3$, to ct-DNA and gave evidence of complex formation. Only a weak interaction was observed where $n=0$. Electronic circular dichromism (ECD) showed signals in the 300-400nm range, where $n=2,3$, whereas neither the ct-DNA or (+/-)-**31** derivative controls have signals in this range. Where $n=3$ the signal was 3 times stronger than when $n=2$ thus proving it has a strong binding affinity to the minor groove. No signal was observed for $n=1$ and was assumed to be suppressed. There was an increase in DNA binding activity as the chain length was increased due to better arrangement of the complex with DNA. Sequence selectivity was determined using oligonucleotides (dA-dT)₁₀ and (dG-dC)₁₀ for $n=3$. ECD signals were observed for (dA-dT)₁₀ but not for (dG-dC)₁₀ therefore afforded an affinity for A·T rich sequences. The binding affinity was influenced greatly by temperature, as ECD signals strengthened as the temperature increased, due to the increased accessibility of the minor groove in β -form of the ct-DNA. The stereochemistry of the (+/-)-**31** analogue $n=3$ is not important for the binding affinities, but ECD experiments afforded different signs and symmetric patterns for the enantiomers, thus afforded differing chiroptical properties.²⁶

Chiral metal complexes have been used for enantioselective DNA configuration recognition.²⁹ Now a combination of chiral Tröger's base analogues (ligand) and a metal centre were synthesised. A *bis*-phenanthroline Tröger's base was generated and employed as a ligand and introduced to *cis*-[Ru(phen)₂(py)₂]²⁺ (phen = 1,10-phenanthroline) which afforded the complex [Ru(phen)₂ *bis*-phenanthroline Tröger's Base]²⁺ (+/-)-**32** as a racemic mixture. Subsequent purification by slow fractional crystallisation gave 80% enantiomerically pure *S*-isomer (*S*)-**32**.³³

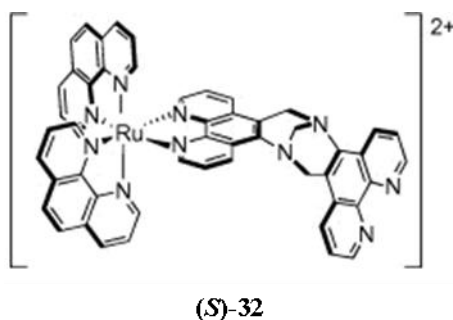


Figure 14 [Ru(phen)₂ *bis*-phenanthrolineTröger's base]²⁺ complex (*S*)-**32**

DNA binding isotherms were determined using luminescence intensities as ct-DNA was added in order to determine the interactions of the Tröger's base derivative (*S*)-**32** with calf thymus DNA. These experiments afforded a binding to ct-DNA that was stronger than the racemic mixture of the parent compound [Ru(phen)₃]²⁺ this was attributed to an increase in binding geometry given by the Tröger's base structure. The extra steric bulkiness given to the compound by the Tröger's base unit, over the parent compound hinders semi-intercalation which was the known binding method of

$[\text{Ru}(\text{phen})_3]^{2+}$.³⁴ Unfortunately no information was given on the sequence selectivity of the Tröger's base analogue and is assumed to be work in progress.

There have been clear interactions found between Tröger's base analogues and DNA but the research has so far been aimed at taking known DNA binding molecules and appending them to Tröger's base. As was shown there are many analogues of Tröger's base with differing cleft angles and appendages where no study into biological activity has been reported. This is an exciting time for Tröger's base as more and more analogues are being reported and are "calling out" to have their biological properties tested. Tröger's bases' unique structure has been shown to change the binding sites of known intercalaters and interfere with both the minor and major grooves of DNA with some surprising results and good sequence selectivity. Strangely there have been no reports of any experimental data on Tröger's base analogues with RNA which could yield some interesting results to explore the gap between DNA and protein formation. Perhaps this is due to the relative instability of RNA or maybe just an oversight.

1.3.3 Tröger's base analogues as synthetic receptors

Wilcox *et al.* have described the synthesis of Tröger's base analogues containing di-carboxylic acid groups (+/-)-**33** and these have been shown to act as hosts for adenine **34** and (+)-biotin (+)-**35** moieties.³⁵ The interaction was due to the formation of four hydrogen bonds between the carboxylic acid groups on the host and nitrogens on the guest substrate.

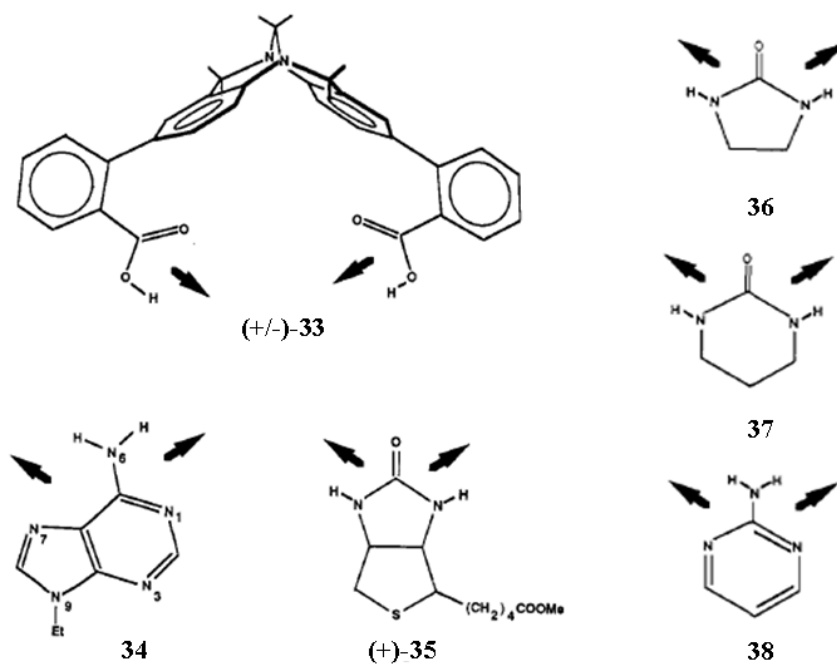


Figure 15 Tröger's base host (+/-)-**33** and guest binding coefficients in CDCl_3 : 9-ethyladenine **34** $K_a = (4.5 \pm 1.7) \times 10^4 \text{ M}^{-1}$, (+)-biotin methyl ester **35** $K_a = (1.7 \pm 0.3) \times 10^4 \text{ M}^{-1}$, 2-imidazoleidone **36** $K_a = (2.1 \pm 0.4) \times 10^4 \text{ M}^{-1}$,

trimethyleneurea **37** $K_a = (3.3 \pm 1.6) \times 10^4 \text{ M}^{-1}$, 2-aminopyrimidine **38** $K_a = (2.6 \pm 0.5) \times 10^3 \text{ M}^{-1}$. Figure taken from Wilcox *et al.*³⁵

Interactions between guest and host were measured using NMR and UV/fluorescence techniques and binding affinities were compared to benzoic acid ($K_a = 30\text{M}^{-1}$). The host was shown to hydrogen bond remarkably well to guests **34-38** all of which have two hydrogen bonding surfaces available. The ability to hydrogen bond with the guests was dependent on properly arranged carboxylic acid groups at an angle of 120° . The ability of the guest to interact is due to simultaneous Watson-Crick and Hoogsteen interactions. These interactions were observed with adenine *in vivo* for triple ribonucleic acid helix formation and protein–nucleic acid interactions.³⁵

Goswami *et al.* designed a series of amino pyridine Tröger's base analogues for the recognition of di-carboxylic acids. Here the amino pyridine heterocycles have a strong affinity to form hydrogen bonds with di-carboxylic acids and these scaffolds provide a well arranged system for the selective binding of the guest. The system can only bind with certain guests that fit into the concave area formed by the appended Tröger's base analogue.³⁶

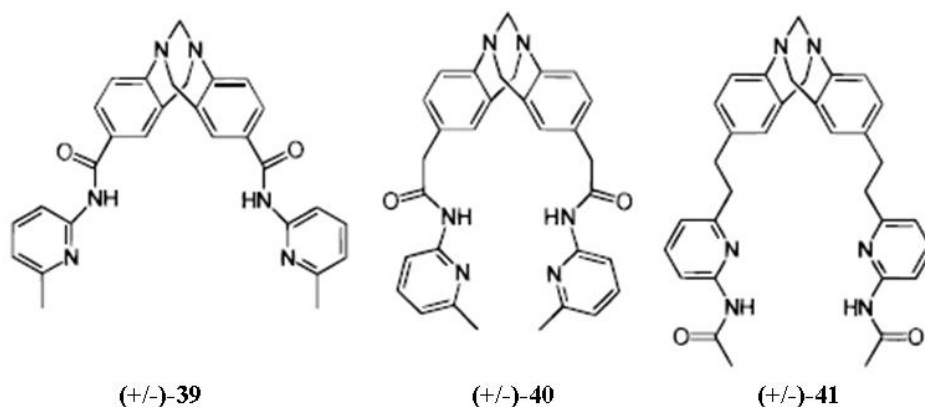
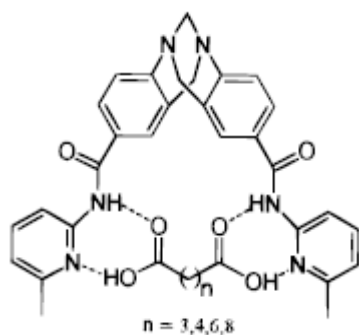


Figure 16 Synthetic Tröger's base binding receptors as described by Goswami.³⁶

^1H NMR titration studies were performed on a variety of guests with the above hosts **39-40** and changes in chemical shifts were processed as a function of concentration and subsequent Foster-Fyfe analysis yielded the binding constants.³⁶



Di-acids	$K_a(25^\circ\text{C}) \text{ M}^{-1}$	$\Delta G (25^\circ\text{C}), \text{ kcal/mol}$
Glutaric	1.0×10^3	-4.09
Adipic	1.69×10^3	-4.40
Suberic	1.5×10^4	-5.69
Sebaic	3.10×10^3	-4.76
Benzene-1,4-diacetic	2.88×10^2	-3.35

Table 1 Binding constants of host (+/-)-**39** with di-acids

Figure 17 Mode of complexation of di-acids with (+/-)-**39**

	Glutaric	Adipic	Suberic	Sebaic
(+/-)- 40	2.4×10^2	3.5×10^2	4.8×10^2	5.8×10^2
(+/-)- 41	1.1×10^2	5.3×10^2	1.01×10^3	6.54×10^3

Table 2 Binding constant values of receptors **40** and **41** K_a (M^{-1})

Fluorescence data provided by the Goswami *et al.* afforded strong complexation characteristics between host (+/-)-**39** and suberic acid to back up their findings from the titration experiments. Effects of chirality on the host were also studied using (+)-camphoric acid as guest and 1H NMR titration experiments afforded the amide proton peak has split into two. Subsequent analysis afforded differences in binding constant energy as shown in table 1 and 2. Attempts to prove the stereospecific interactions couldn't be completed due to the difficulties in resolving host (+/-)-**39**.³⁶

Macrocyclic Tröger's base derivatives have also been reported and shown to be useful synthetic receptors. Wilcox *et al.* reported the synthesis of optically pure, water soluble, cyclophane receptor **42** which binds to neutral alicyclic guests in a stereospecific manner.³⁷ Many cyclophanes have been developed to accept aromatic guests and a simple rectangular shape is sufficient to allow planer molecules into the pocket. Alicyclic guests required a much larger pocket to allow the bulkier substrates to bind. The minimum size required for a cyclohexane ring to be confined by two benzene rings is 8.5Å, therefore larger cyclophanes are required³⁷

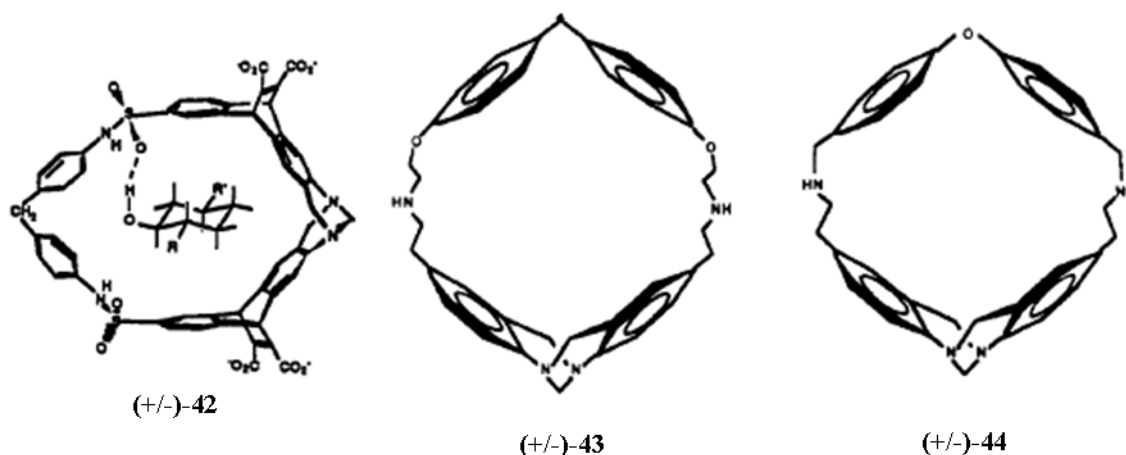
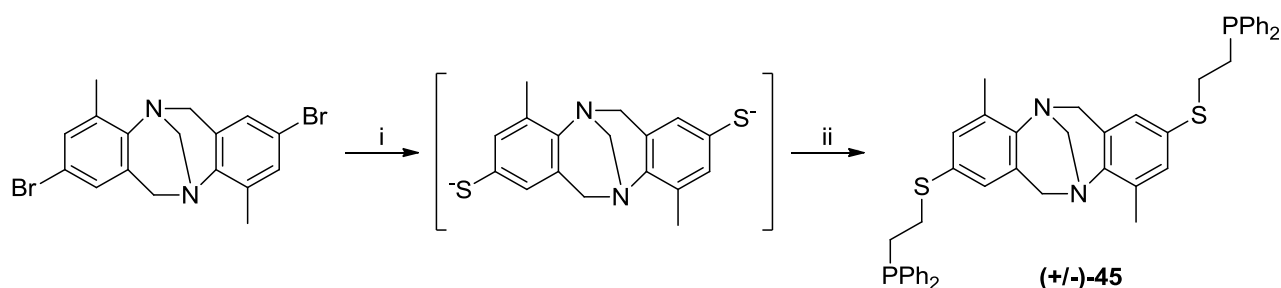


Figure 18 Tröger's base cyclophane (+/-)-**42** interacting with guest. Di-phenyl methane analogue (+/-)-**43** and di-phenyl ether analogue (+/-)-**44** as reported by Wilcox *et al.*³⁸

Other Tröger's base cyclophanes have also been generated within the Wilcox group, thus a Tröger's base unit bridged by a second diaryl unit (fig 18). They include a diphenyl ether (+/-)-**44** and a diphenyl methane (+/-)-**43** unit. These water soluble cyclophanes were shown, by 1H NMR titrations, to accommodate a range of guests. 1H NMR data showed strong up field shifts of guest

protons and titration curves gave rise to saturation phenomena, compared to control experiments. Both hosts (+/-)-**43** and (+/-)-**44** had binding energies in the range 2.1 – 3.3 kcal / mol with benzoidal substrates including 4-toluene sulfonic acid and 1,3-dihydroxynaphthalene.³⁸

Khoshbin *et al.* have reported the synthesis of metallomacrocycles containing hemilabile Tröger's base ligands. The ligands are comprised of phosphinoalkyl thioethers appended to Tröger's base (+/-)-**45**. These were subsequently reacted with copper(I) and rhodium(I) complexes generating the corresponding metallomacrocycles. These metallomacrocycles have some interesting geometries. Reaction with the Cu^I metal centre provided a bi-metallic closed metallomacrocycle (**46**) as is common for the tetrahedral favoured geometry of copper. Whereas, the square planer geometry of Rh^I meant that bi-metallic macrocycle systems weren't generated but tri-(**47**) and tetra-(**48**) macrometallic closed macrocycle systems were formed instead.³⁹



Scheme 9 Synthesis of (+/-)-**45** i) 4.4 eq *t*-BuLi, 3eq S₈, THF -78°C, ii) 2 eq Cl(CH₂)₂PPh₂, 0.2eq CsCO₃, MeCN, reflux.

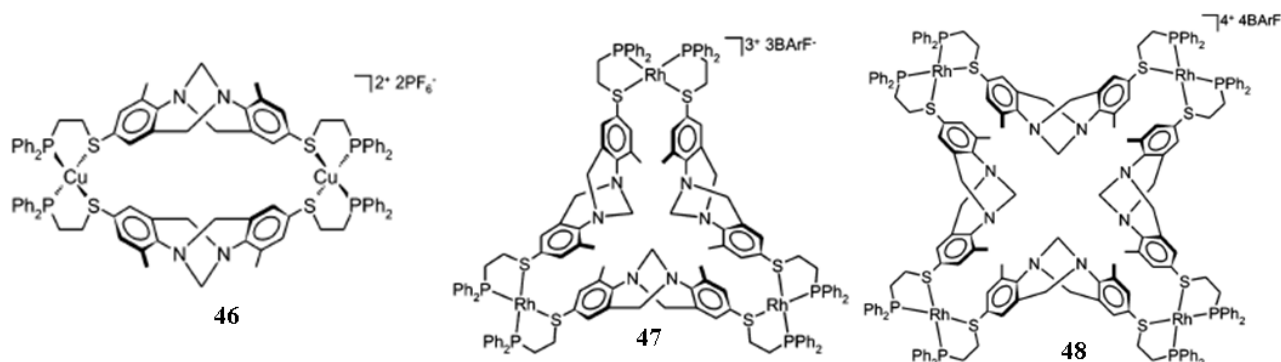


Figure 19 Open *bis*-metallic Cu Tröger's base metallocycle (**46**); closed *tri*-metallic Rh Tröger's base metallocycle (**47**) and closed *tetra*-metallic Rh Tröger's base metallocycle (**48**)

1.3.4 Stable isotope incorporated Tröger's base

Lenev *et al.* reported the synthesis two of d⁶-Tröger's base analogues (+/-)-**49** & **50** generated by replacing paraformaldehyde with d²-paraformaldehyde and condensing with anilines in neat TFA, however no yields were reported.⁴⁰ The resolution of (+/-)-**49** & **50** to (*R*)-**49** & (*S*)-**50** was

achieved by crystallisation of spherical homochiral druses from toluene, followed by manual separation and recrystallisation.⁴¹

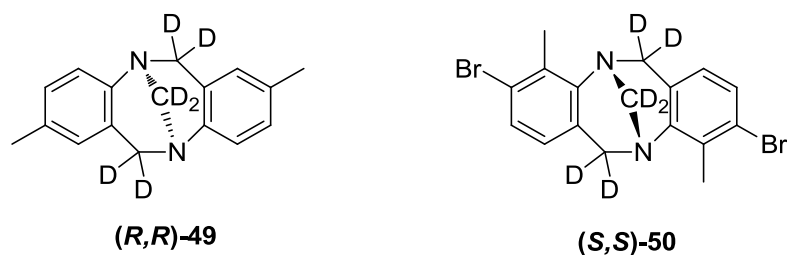


Figure 20 Deuterium incorporated Tröger's base analogues

Lenev *et al.* was investigating the rate of racemisation of **(R,R)-49** & **(S,S)-50** compared to its proteo counterparts. He observed the isotopic effects of deuterium on the rate of racemisation with **(R,R)-49** racemising more slowly than its proteo counterpart, however, for **(S,S)-50** the opposite was observed. He suggests this is due to an increased steric volume of H compared to D, affording retardation of racemisation in the sterically hindered proteo **(S,S)-50**.⁴⁰

In honour of Julius Tröger's discovery of Tröger's base 125 years ago, Runarsson *et al* published a review on the diverse uses and research undertaken, over the past 125 years, upto 2012 of this interesting and structurally unique compound.⁴²

1.4 Incorporation and reactions of stable isotopes into organic compounds

1.4.1 Deuterium in organic synthesis

The development of protocols that afford high value, deuterated molecules in high yields and, importantly, with excellent levels of deuterium incorporation is very important to academia and biotechnology, medicinal, analytical, pharmaceutical, and agrochemical industries.⁴³ A deuteron has 0.02% natural abundance and is made up of a proton and a neutron, the additional neutron (compared to its proteo ¹H counterpart) affords it with an atomic mass of 2.014u that is double the protium. This extra mass confers a difference of chemical properties to the ²H-isotope over the ¹H-isotope which is not seen in other isotopes of heavier elements, for example deuterium oxide is more viscous than water, has a melting point of 3.82°C, boiling point of 101.72°C and a density of 1.1056 g/mL (20°C).⁴⁴ The kinetic isotope effect (KIE) for deuterium is considerably more noticeable than for other isotopes of heavier elements because of the two fold increase in mass, equating to a theoretical maximum difference of 9 at 37°C. The higher mass affords a deuterium-carbon bond with a lower vibrational frequency and thus a lower zero point energy than the corresponding proton-carbon bond. This lower zero point energy translates into a higher activation

energy for carbon-deuterium bond cleavage and a slower reaction rate. This effect on reaction rate is known as the primary KIE for deuterium.⁴⁵

The KIE is the ratio of the rate of reaction between two different isotopically labelled molecules during a chemical reaction. For example the KIE for a proteo and deutero reaction is:

$$\text{KIE} = k_H/k_D$$

where, k_H and k_D are rate constants.⁴⁵ The specific KIE expressed above for deuterium and protium, is also known as the deuterium isotope effect (DIE).

1.4.2 Deuterium isotope effect

The primary DIE is the difference between the rates of reaction observed between a proton and deuterium atom substitution. DIE is an important tool in the elucidation of mechanisms in chemical synthesis due to the rate constant K_H observed for proteo species often exceeding the rate constant K_D for deutero species. The strength of the deuterium carbon bond is much stronger than its proteo counterpart, thus making it more resistant chemical or enzymatic cleavage.⁴⁶

1.4.3 Deuterium in the pharmaceutical industry

The incorporation of deuterium into a drug molecule has negligible steric and minimal effect on its physiochemical properties; however the resulting increase in bond stability, carbon-deuterium bond for example, may cause a dramatic change in biological properties. The increased bond stability has the potential to retard certain pathways of the drug molecules metabolism *in vivo*.⁴⁶ The substitution of deuterium atom for a proton at a specific site of metabolic cleavage could offer potential benefits including improved exposure profiles and a reduction of toxic metabolites. This could lead to greater efficacy, safety and tolerability. Incorporation of deuterium at positions not involved in metabolism, affords it to be metabolically silent, and has led to its use as a tracer.⁴⁵ One of the first reported instances of the DIE *in vivo* was the replacement of the α -hydrogens of tyramine **51** and tryptamine **52**, which when administered produced a marked intensification of blood pressure effects and nictitating membrane contractions.⁴⁷

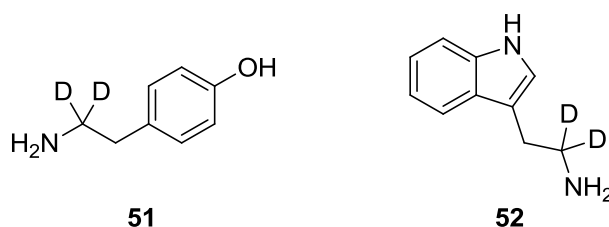


Figure 21 α -di-deutero tyramine **51** and α -di-deutero tryptamine **52** – two of the first reported deuterated drugs to exhibit deuterium kinetic isotope effects *in vivo*.

More recently (2008) Auspex Pharmaceuticals has developed a selectively deuterated analogue of venlafaxine (+/-)-**53**, an anti-depressant and subsequently issued a press release stating that after the phase I healthy volunteer study “exhibited a pharmacokinetic profile that appears to be superior to that of to that of venlafaxine”.⁴⁸

Concert Pharmaceuticals have developed a ²H-incorporated HIV protease inhibitor based on the scaffold of atazanavir **54** and has initiated multiple ascending dose studies. Its antiviral potency and pharmacokinetic profile has positive implications that it could be used without the need of the pharmacokinetic booster ritonavir, which causes problematic side effects.⁴⁸

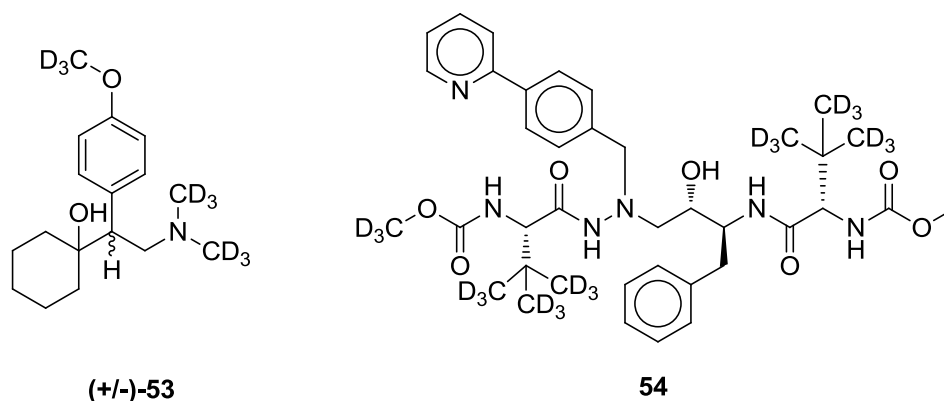
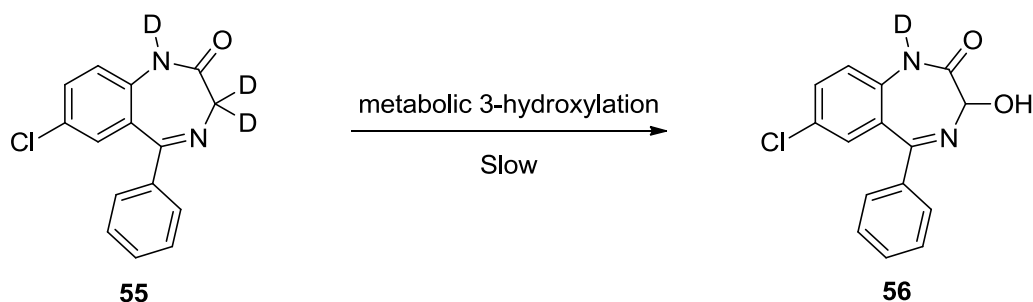


Figure 22 Auspex Pharmaceuticals deuterated venlafaxine (+/-)-**53** and Concert Pharmaceuticals deuterated atazanavir **54**. Both have been reported to have increased biological activities compared to their parent proteo analogues.

The inclusion of deuterium into biologically active molecules does not always offer benefits. The incorporation of deuterium to the DNA alkylating species 1,2-di-bromo ethane affords a slower metabolism thus results in more damage to the DNA than its proteo analogue. Similarly diazepam **55** requires metabolic oxidation to the active form oxepam **56** and deuteration inhibits the anticonvulsive properties of diazepam.⁴⁹



Scheme 10 Deuteration of diazepam **55** slows down the 3-hydroxylation to the active species oxepam **56** resulting in a loss of anticonvulsive properties.

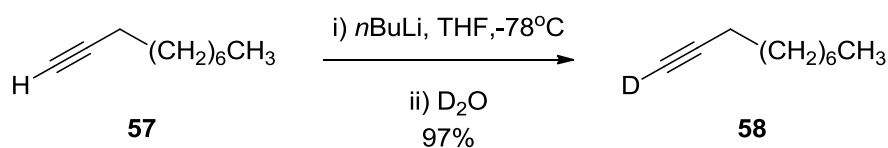
The success of a few deuterium incorporated drugs affording improved pharmacokinetics, longer half lives and the ability to patent them has lead to a need for more deuterated building blocks for the

synthesis of these important molecules. With the current trend in the utilization of the Azide-Alkyne Huisgen 1,3-dipolar cycloaddition ('click') reaction, the synthesis of deuterated terminal alkynes could lead to the synthesis of deuterated triazoles. The synthesis of a plethora of deuterated alkynes would allow for functionalization of these triazoles for incorporation into drug candidates.

1.4.4 Current methods for the synthesis of deuterated terminal alkynes

The requirement for deuterated building blocks with excellent levels of ^2H -incorporation for organic synthesis is very important for the research community. The incorporation of deuterium at specific points in a drug molecule, generally in regions where metabolism occurs 'soft spots', is currently a 'hot topic'. The ability to generate ^2H -alkynes will be beneficial to organic synthesis as precursors to ^2H -alkyne hydrogenation generates cis- or trans- ^2H -alkenes⁵⁰ or ^2H -alkanes.⁵¹ Alternatively aqueous gold salts afford ^2H -ketones,⁵² and ^2H -alkyne cyclotrimerization with a ruthenium catalyst affords ^2H -aromatics.⁵³

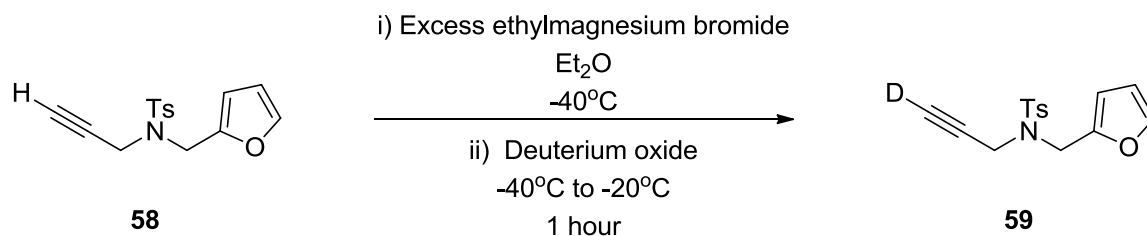
Hislop *et al.* reports the synthesis of deuterio-decyne **58** *via* deprotonation, with *n*-BuLi at -78°C followed by quenching of the lithiated intermediate with deuterium oxide in a 97% yield, however the ^2H -incorporation was only described as 'high'.⁵⁴



Scheme 11 Hislop *et al.* describe the synthesis of ^2H -decyne with *n*-BuLi and D_2O

Sabot *et al.* reported the synthesis of three deuterated alkynes using CDCl_3 as a deuterium donor and reported yields and ^2H -incorporations between 31% and 93% using catalytic triazabicyclodecene (TBD 10 mol%) for 12 hours.⁵⁵ Lewandos *et al.* reported the synthesis of ^2H -1-hexyne ^2H -incorporation 79%, ^2H -3-methyl-1-pentyne ^2H -incorporation 75% and ^2H -dimethyl-1-butyne ^2H -incorporation 80% *via* stirring with sodium hydroxide in deuterium oxide for 7 hours.⁵⁶

Other protocols for the synthesis of ^2H -incorporated alkynes including, Hashimi *et al.* This employed excess ethyl magnesium bromide at -40°C quenching with deuterium oxide followed by stirring for a further hour at -20°C . Unfortunately details of the level of ^2H -incorporation were not reported.⁵⁷



Scheme 12 Hashimi *et al.* reported the synthesis of deuterated alkynes *via* ethyl magnesium bromide.

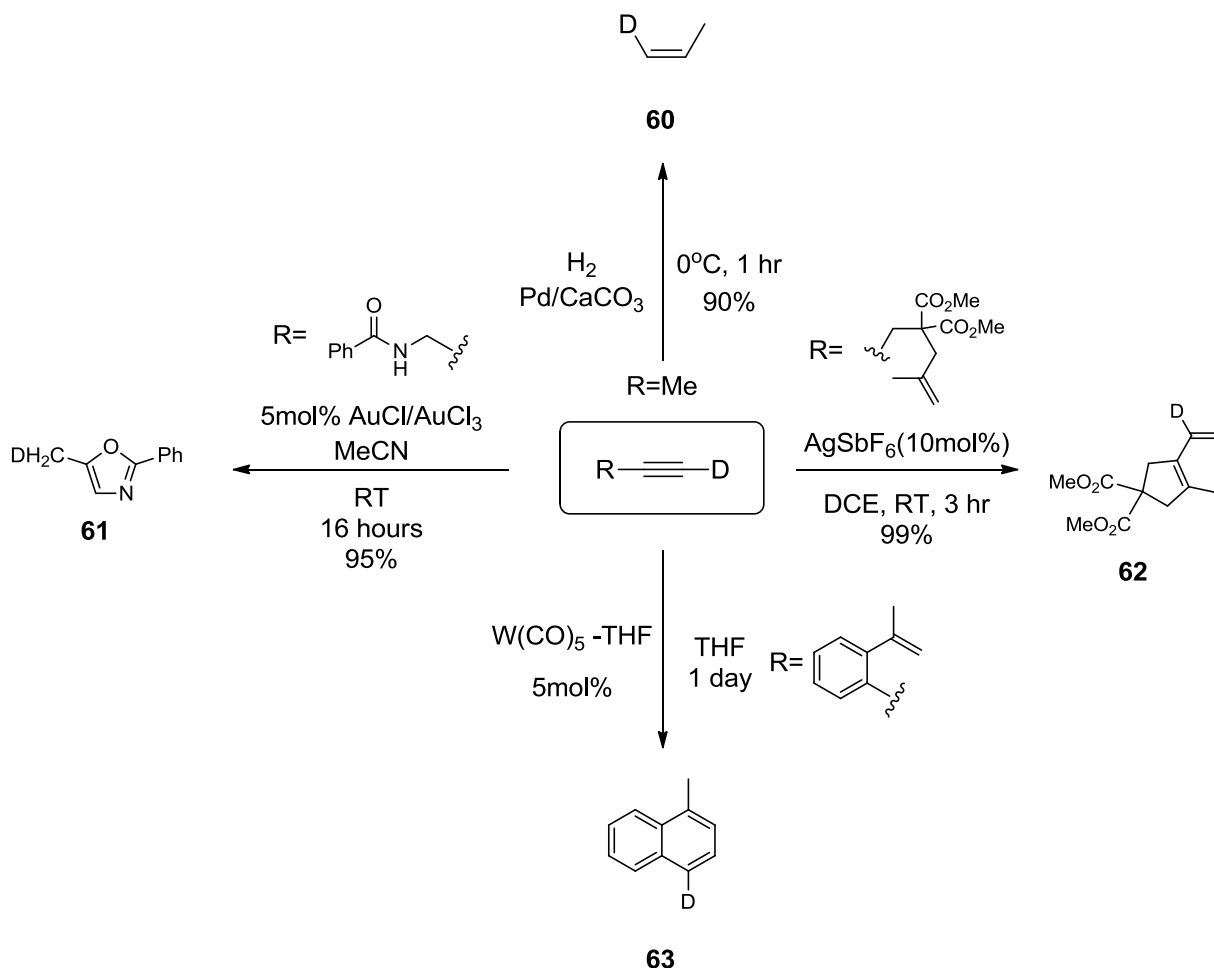
Although numerous syntheses of terminally deuterated alkynes are available in the literature many of these methods require extended reaction times, strong bases, low temperatures and strictly anhydrous reaction conditions to afford the ²H-alkyne analogues in high yield with high levels of ²H-incorporation. There is clearly a necessity to generate these compounds quickly, safely and with high yields.

1.4.5 ²H-incorporated alkynes as building blocks for organic synthesis

The ability to generate ²H-alkynes would be unfeasible if they couldn't be used for further synthesis. A Scifinder search for ²H-alkynes as a reactant affords over 500 references where they are used as start materials for more complex reactions.

Tanaka *et al.* reported the reduction of a deuterated alkyne to the corresponding deuterio-*Z*-alkene **60** *via* hydrogenation with a palladium catalyst (Scheme 13) with a 90% yield and deuterium incorporation.⁵⁸ Porcel *et al.* reported an elegant silver salt catalysed procedure for the cyclisation of α, ω -enynes **62** to a carbocycle, *via* a procedure that retained 99% ²H-incorporation.⁵⁹

Egorova *et al.* reported the gold(I) and gold(III) catalysed cyclisation which afforded heterocycle **61** *via* proto-deauration of a di-vinylgold species affording a mono-deuterated methyl group (Scheme 13).⁵⁹ For the final example of ²H-alkynes as building blocks for synthesis; Maeyama *et al.* reports the synthesis of bicyclic aromatics from aromatic enyne *via* an electrocyclisation with a catalytic amount (5 mol%) tungsten pentacarbonyl•THF complex. This afforded **63** in a 99% ²H-incorporation and good yield.⁶⁰ Interestingly the deuterium atom finishes at the 4-position suggesting a 1,2 migration has occurred.



Scheme 13 Reported syntheses utilising 2H -incorporated terminal alkynes affording selectively deuterated products **60-63**.

1.5 Small molecule – protein interactions

1.5.1 Proteins

Proteins are long polymer chains of amino acids, ranging from 50-200 monomer amino acid units. They are ubiquitous in nature with many different shapes and sizes. They are synthesised using genetic information encoded in cells and are essential for life. Problems with the biosynthesis of proteins within organisms are responsible for many diseases, such as sickle cell anaemia which is caused by an error in the gene which codes for the amino acid sequence that forms haemoglobin. This causes one amino acid in the whole protein sequence to be wrong with dramatic consequences.

Not all proteins have positive ‘outcomes’ for organisms for example the protein produced by *Bacillus anthracis*, the Anthrax toxin is comprised of three proteins known as the protective antigen, edema factor and lethal factor. These three proteins all work together to attack the immune system in mammals and if left untreated will, ultimately, kill the host.⁶¹ Another protein toxin is cholera

toxin which is secreted by the bacterium *Vibrio cholerae*. This causes the symptoms of cholera and again if left untreated will kill the host.

Protein research is of great importance to the pharmaceutical industry, medicine, military and academics alike. A model substrate for developing novel detection techniques of small molecules and proteins comes from the strong interaction of (+)-biotin and streptavidin/avidin proteins.⁶²

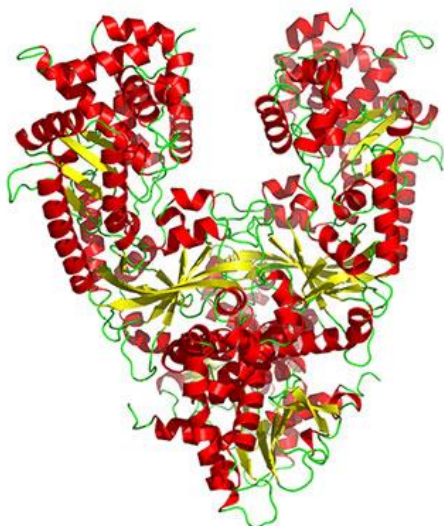


Figure 23 Crystal structure of the anthrax toxin

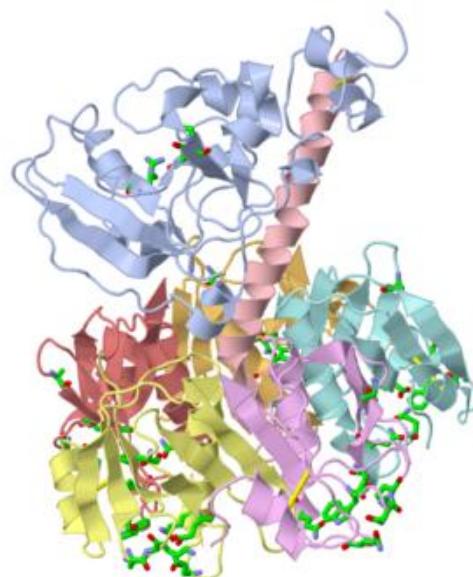


Figure 24 Crystal structure of cholera lethal factor

1.5.2 (+)-Biotin and (strept)avidin system

Avidin is a 67kDa glycoprotein, found in egg white, consisting of 4 identical subunits of 128 amino acids each. Streptavidin is a similar protein that is extracted from the culture broth of *S.avidinii* and is again comprised of four identical subunits. Streptavidin doesn't contain any carbohydrates and has a slightly lower mass of 60 kDa in its native form. Much of the commercially available streptavidin reports a mass of 50-60 kDa depending on supplier and the mass is dependent on the purification technique employed as proteolytic digestion at both *N* and *C* terminus can occur, thus a lower mass material can be generated.⁶² Both streptavidin and avidin bind to (+)-biotin (+)-**64** non-covalently with a formation (affinity) constant of 10^{15}L/mol^{-1} , this puts it among the highest formation constants reported. To put this into context this interaction is 10^3 - 10^6 times stronger than those found between ligands and their specific antibodies. Both avidin and streptavidin proteins possess four binding sites for (+)biotin per molecule which make it possible to form multibiotinylated moieties.⁶²

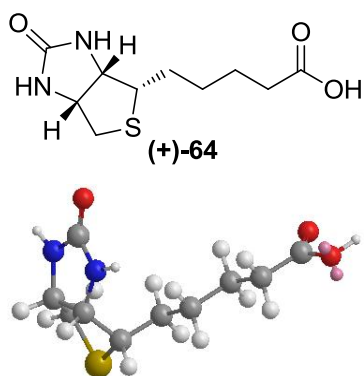


Figure 25 Structure and Chem 3D representation of (+)-biotin (+)-64

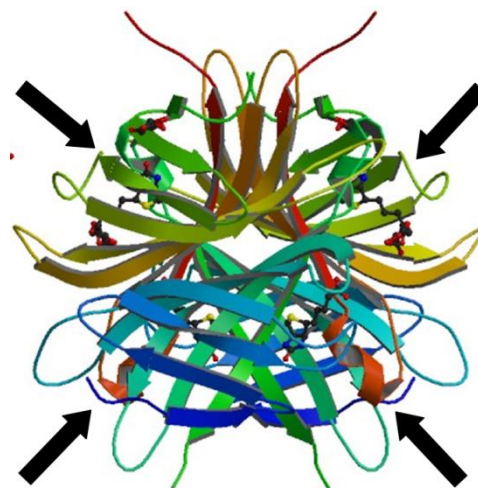


Figure 26 tetrameric streptavidin structure showing binding sites of (+)-biotin(+)-64

(+)-Biotin (+)-64 (vitamin H or coenzyme R) is a small molecule with a molecular weight of 244 Da which when introduced to a biologically active macromolecule, such as DNA the biological activity is generally not affected. This has resulted in its use within a diverse range of applications including; biotinylated anti-lectins for localisation of lectin receptors, biotinylated enzymes for immunological assays, biotinylated agarose or cellulose for affinity chromatography, biotinylated DNA and nucleotides for nucleic acid hybridisation, molecular mass markers and DNA sequencing.⁶² These applications often require the chemical modification of (+)-biotin (+)-64 usually *via* the appendage of organic compounds and this has to be achieved without destroying the binding ability of the (+)-biotin (+)-64 to (strept)avidin. However it has been reported that chemical derivatisation of (+)-biotin can also decrease the affinity constant for binding with avidin but not for streptavidin.⁶³

1.5.3 Chemical derivatisation of (+)-biotin

A diverse array of (+)-biotin derivatives are currently commercially available from suppliers such as Sigma. The commercial availability of (+)-65 and (+)-66 have found uses for coupling directly to the C or N-terminus of proteins allowing them to be biotinylated relatively simply and allows for the recovery of the biotinylated protein by affinity chromatography. This has also led to the straight forward synthesis of many alternative derivatives of (+)-biotin *via* coupling to amines and forming an amide bond with the (+)-biotin carboxylic acid. Particularly note worthy is the synthesis of cleavable (+)-biotin linkers which allow for ‘catch and release’ methodology to be applied. Szychowski *et al.* reported the inclusion of an *L*-homopropargyl glycine as a methionine surrogate during a protein synthesis and then utilised an azido (+)-biotin derivative to ‘click’ to the synthesised protein. Eluting through a streptavidin column elutes non-biotinylated proteins and the

biotinylated proteins remain bound. The cleavable linker is then activated to release the new protein and allow it to be eluted.⁶⁴

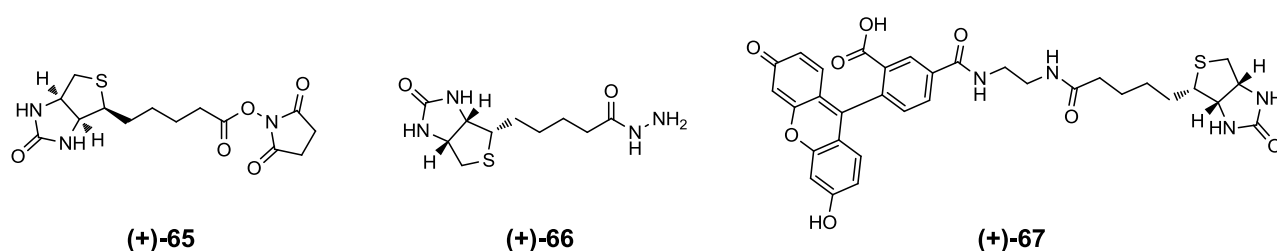


Figure 27 Commercially available (+)-biotin derivatives. (+)-65 *N*-hydroxy succinamide ester (NHS), activated ester for coupling to amines. (+)-66 biotin hydrazide for coupling to carboxyl groups and (+)-67 biotin-4-fluorescein, incorporated fluorophore for labelling DNA.

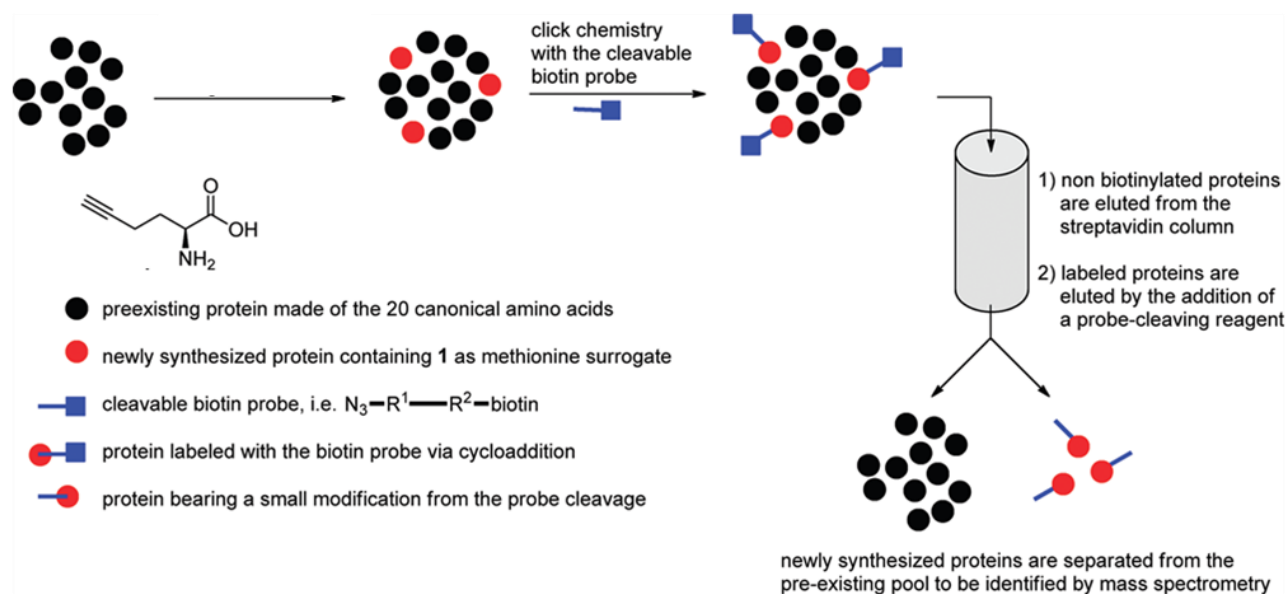
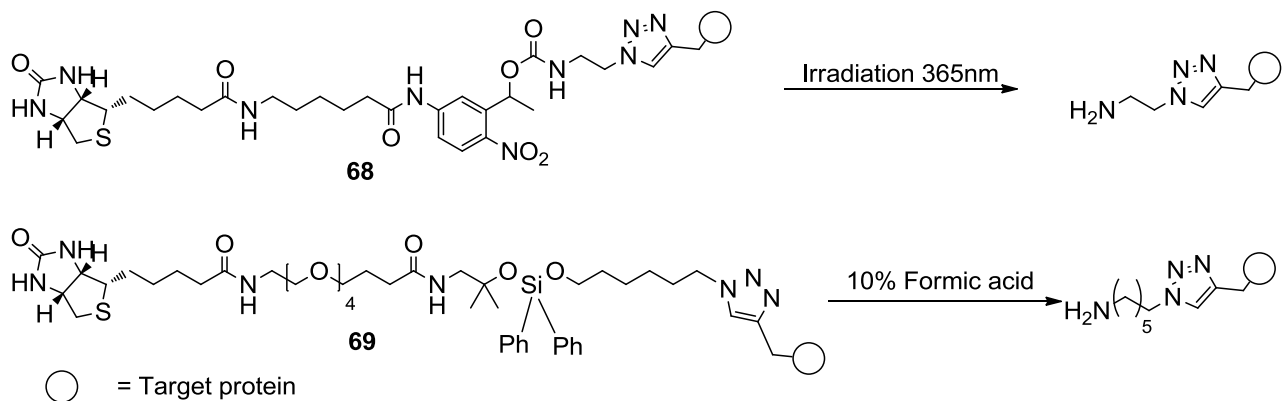


Figure 28 Catch and release methodology as described by Szychowski *et al.* for biotinylating proteins and eluting through a streptavidin column, followed by cleavage and elution off the column.⁶⁴

Different (+)-biotin analogues were developed that would cleave under different conditions these included two which resulted in 98% efficiency a photocleavable analogue and an acid cleavable silicon based analogue.⁶⁴



Scheme 14 Szychowski *et al.* reported a photocleavable linker for release of target protein from streptavidin linker(top) and formic acid cleaved-silicon based linker (bottom) both gave 98% cleavage efficiency.

The ‘click’ reaction is an extremely popular protocol due to its high yields (99%), quick reaction times (1 hour) and its relative simplicity. This has resulted in a number of (+)-biotin analogues containing azido (see Scheme 14) and alkynyl functionalities.⁶⁵⁻⁶⁷

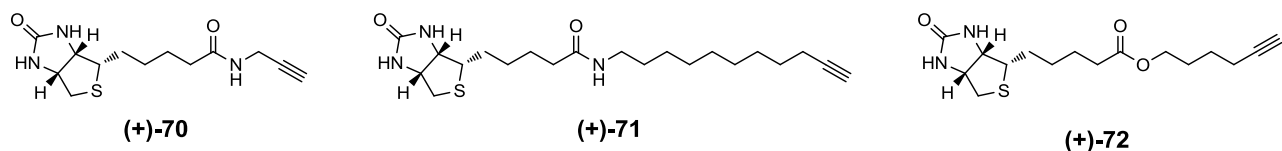


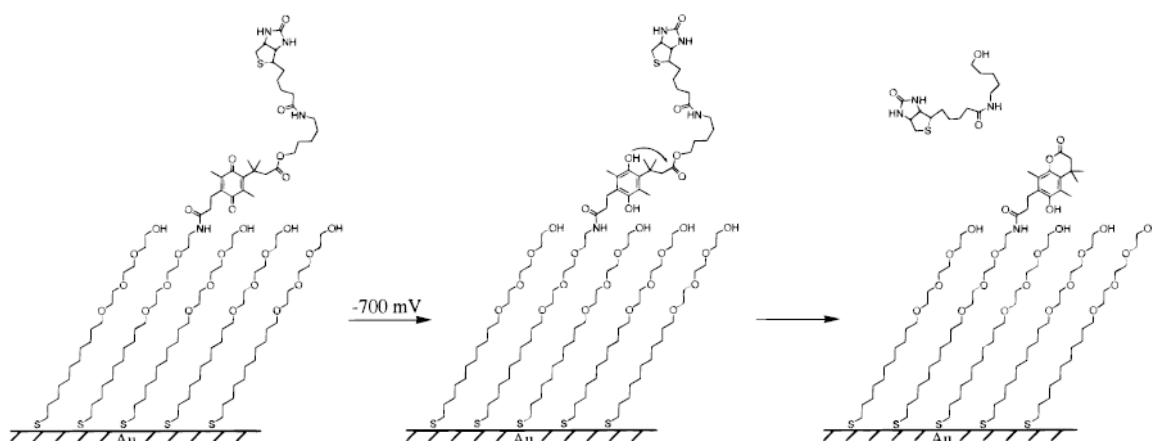
Figure 29 Xu *et al.* reported the synthesis of (+)-70 *via* stirring NHS-biotin with propargyl amine and triethylamine, Crisp *et al.* reported (+)-71 *via* stirring NHS-biotin with 1-amino-11-undecyne in DMF and Renhack *et al.* reported (+)-72 *via* stirring biotin with 1-hydroxy-6 hexyne, TBTU, DIPEA and DMF at room temperature for 5 h.

1.5.4 Biotin/(strept)avidin interactions on a surface

The biotin/streptavidin interaction has been utilised at the surface interface for a handful of applications. Wong *et al.* reported the functionalisation of an atomic force microscopy (AFM) probe with avidin *via* binding (+)-biotin to the AFM tip followed by addition of avidin using two of the four available binding sites. An agarose bead was subsequently functionalised with (+)-biotin and bound to a mica surface which was then analysed by AFM using the streptavidin modified AFM tip. As the tip passed over the biotinylated bead the remaining two avidin binding sites interacted with the (+)-biotin affording an interaction between the bead and the tip. As the AFM tip moved further away from the bead the bond is effectively ‘pulled apart’ and this can be translated, mathematically, into a binding constant for the avidin/biotin interaction.⁶⁸

Hodneland *et al.* bound (+)-biotin to a gold surface *via* a mixed SAM formation of hydroxyl terminated alkane thiolates and (+)-biotin terminated alkane thiolates. The (+)-biotin moiety incorporated a quinone propionic ester linker which can undergo electrochemical reduction and

subsequent lactonisation liberating the (+)-biotin from the surface,⁶⁹ scheme 15 outlines this process.



Scheme 15 Hodneland *et al.* report SAM formation with an electrochemical reducible linker to a gold surface. Upon treatment of a voltage of 700mV across the gold layer the linker undergoes reduction to hydroquinone and immediate lactonisation releasing the (+)-biotin.⁶⁹

Hodneland *et al.* employed surface plasmon resonance (SPR) to demonstrate the (+)-biotin had been released. The biotinylated surface was submitted to SPR and streptavidin passed across the surface and the binding event recorded. The surface was then treated with 700mV across the gold layer to release the (+)-biotin and streptavidin complex. This same sample was re-submitted to SPR analysis after streptavidin exposure and no binding event was observed.⁶⁹

Pérez-Luna *et al.* synthesised (+)-biotin alkane thiols **73-75** [Figure 30] and bound them to a gold sputtered mica surface for investigating the association and dissociation constants of wild-type streptavidin and streptavidin mutants. Two types of SAM were investigated, mixed SAMs (biotinylated and non-biotinylated) and pure biotinylated SAMs. Interestingly they reported that the mixed SAMs were more easily disassociated from the streptavidin protein by introduction of 'free' non-bound streptavidin in solution and that streptavidin bound to a surface has a much larger dissociation constant. Very nearly all the streptavidin bound to the surface *via* the mixed SAM could be dissociated with 'free' (+)-biotin. They suggested that the difference between the dissociation of mixed and pure SAMs with streptavidin was due to the closer packing of the pure SAM, this affords more crossovers between the streptavidin *i.e.* the closer packing of the SAMs leaves less space around the streptavidin for dissociation to occur.⁷⁰

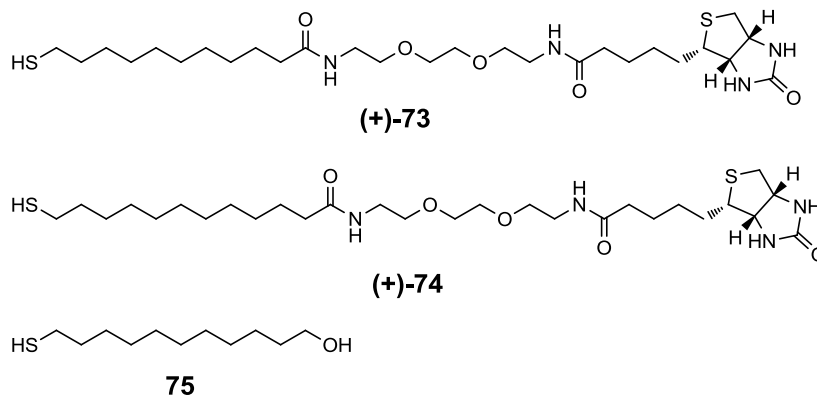


Figure 30 (+)-Biotin thiolates (+)-73 and (+)-74 were bound to gold as ‘pure’ SAMs and mixed SAMs with 75. The mixed SAMs afforded lower dissociation energies with streptavidin whilst the C₁₂-alkane thiolate (+)-74 afforded a more ordered structure of SAM than C₁₁ (+)-73.

Dupont-Fillard *et al.* has reported a reversible DNA sensor using the (+)-biotin/avidin interaction. Electropolymerisation of a (+)-biotin pyrrole unit (+)-76 to a polymer surface followed by binding of avidin to the immobilised (+)-biotin (see Figure 31). Single stranded biotinylated DNA (ODN-bio) (see Figure 31) was bound to the remaining sites of avidin and then this was incubated with complimentary and/or non complimentary biotinylated oligionucleotides (ODNc-bio) (see Figure 31). In the presence of the ss-DNA the two sequences hybridise to form a ds-DNA. This was then treated with a fluorophore (*R*-phycoerythrin) incorporated streptavidin (SAPE) which binds to the newly incorporated strand of ds-DNA provided hybridisation has occurred and the fluorophore can then be detected confirming hybridisation event.⁷¹

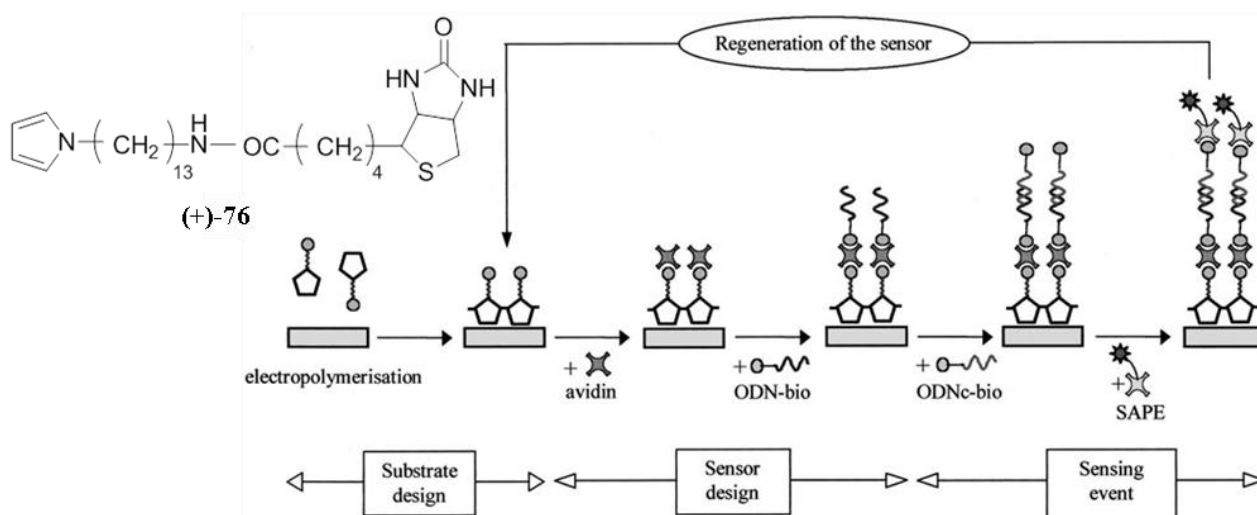


Figure 31 Pyrrole biotin analogue (+)-76 for electrochemical binding to polymer surface and scheme showing (+)-biotin-streptavidin based DNA hybridisation detection.⁷¹

Fang *et al.* and Pan *et al.* have also reported very similar methodologies to Dupont-Fillard to investigate the same hybridisations *via* (+)-biotin (strept)avidin interactions. Fang *et al.* reported

using a fluorescence marker and a quencher on the ss-DNA sequence, which was not fluorescent, and after hybridisation occurs a change in the structure of the ds-DNA activates the fluorescence properties of the fluorophore.⁷² Pan *et al.* employed the methodology outlined in figure 31 however the biotinylated substrate has been bound to a gold electrode using alkane-thiolates to form mixed SAMs.⁷³

1.6.1 Self assembled monolayers (SAMs)

Self Assembled Monolayers (SAMs) are a branch of nanoscience which involves the study of objects and systems with dimensions of between 1 and 100nm.⁷⁴ An organic SAM is comprised of a surface substrate (usually a noble metal or silicon wafer), ligand or head group (this varies depending on the surface *i.e.* thiols on gold or alcohols on silica), a spacer unit, usually an alkane chain and finally a terminal functional group.⁷⁴

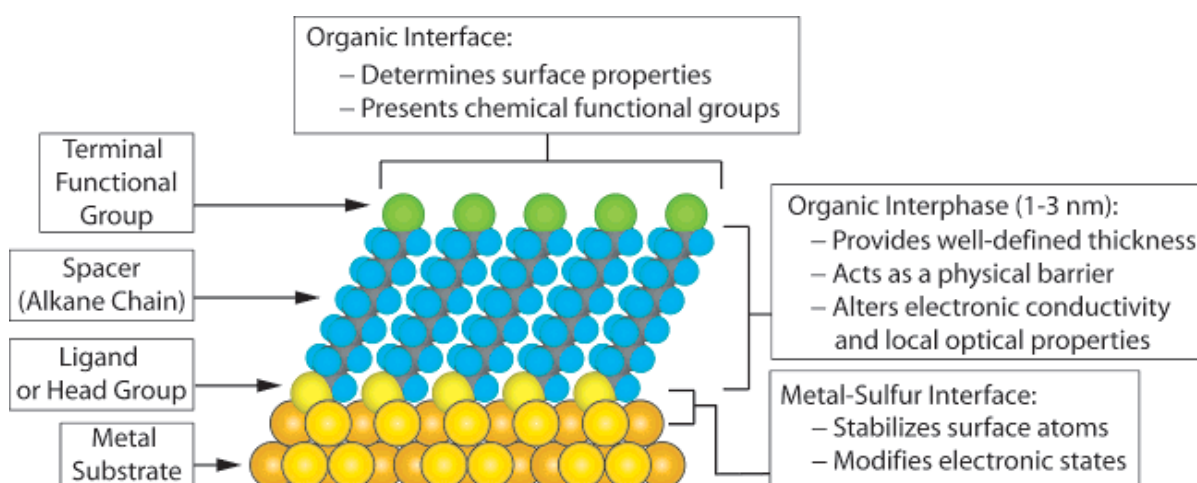


Figure 32 The “ideal” SAM between a gold surface and alkanethiolates, showing characteristics of the monolayer.⁷⁴

These nanostructures exhibit a plethora of physical behaviours derived from quantum phenomena including electron confinement, quantum entanglement, electron tunnelling and ballistic transport.⁷⁴ Since the introduction of alkanethiolates on a gold substrate by Nazzo *et al.* in 1983⁷⁵ a broad range of applications have been generated for application in many areas of science these include nano fabrication, biomolecular recognition and electron-transfer processes.⁷⁶ The ability of the organic chemist to perform chemical reactions at the terminal functional group and to vary the chain length and shape has proved to be central to the applications mentioned above.⁷⁶ By way of an example chemical reactions that have been performed at the terminal functional group include Sonogashira and Suzuki couplings, imine formations, ‘click’ chemistry and amide bond formation.⁷⁶

1.6.2 SAM formation on gold surfaces

Self assembly is the spontaneous formation of an ordered molecular ensemble, the self assembly of monolayers is achieved *via* immersion of a suitable substrate in an adsorbate solution.⁷⁷ This project will concentrate the SAM formation of thiols on a clean gold surface exclusively. The binding of sulfur groups, which can take the form of thiols,⁷⁸ disulfides⁷⁹ and/or thiosulfates,⁸⁰ occurs as a two step process. The first step is adsorption, a fast process that typically lasts a few minutes and covers the around 80-90% of the surface. This followed by the second step, adsorption and reorganisation which are much slower and the reorganisation process can take several days.⁸¹ The interaction of the head group sulfur and the gold substrate dominates generating a strong semi-covalent bond (~50 kcal/mol) and the alkane chains pack together leaving the functionalised tail group at the interface.⁷⁴ There is evidence that a low density lying down phase is formed first, with the alkyl chains lying parallel to the gold surface, before reorganisation forces the 3D structure associated with high density SAMs to be generated.⁷⁴

Strong *et al.* has used electron diffraction of docosanethiol ($\text{CH}_3(\text{CH}_2)_{21}\text{SH}$) on gold film single crystals and concluded that the packing is an incommensurate hexagonal array on Au(111) with interchain distances of 4.97 \AA .⁸² Two years later the results were re analysed by Chidsey *et al.* and they concluded the diffraction patterns were consistent with commensurate $(\sqrt{3} \times \sqrt{3})R30^\circ$ overlayer.⁸³

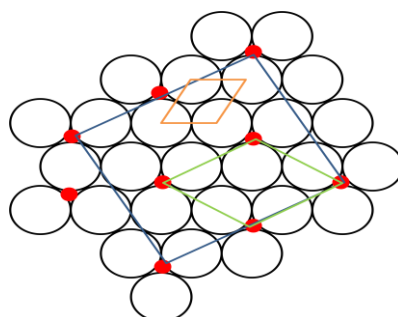


Figure 33 Schematic diagram, white circles represent Au(111) lattice with gold unit cell (orange), red circles represent arrangement of alkane thiol bound to Au(111), green box represents $(\sqrt{3} \times \sqrt{3})R30^\circ$ unit cell and blue box is the simplest representation of $c(4 \times 2)$ super lattice.

Poirier *et al.* has however found evidence for a $c(4 \times 2)$ super lattice again *via* electron diffraction for simple alkane thiol moieties⁸⁴ and Alves *et al.* have reported $c(7 \times 7)$ unit cells for SAMs with fluorinated alkane thiol SAMs as these have larger van der Waals diameter than the 5 \AA maximum for $(\sqrt{3} \times \sqrt{3})R30^\circ$ unit cell.⁸⁵ X-ray studies have also shown pairings of neighbouring sulfur head groups⁸⁶ which is incompatible with the $(\sqrt{3} \times \sqrt{3})R30^\circ$ unit cell and a dispute still remains as to the Au(111) surface-sites which the sulfur atoms bind to. Most studies indicate the thiolate is bound to

the hollow site between three neighbouring Au (111) atoms.⁷⁴ There is still much to learn about the exact locations of binding to gold and how the SAMs are generated.

1.6.3 SAM characterisation

Characterisation of SAMs bound to a surface has proved difficult. Unlike ‘free’ compounds in solution a simple NMR experiment can not be performed so alternative analytical methods were developed to allow their characterisation. Scanning probe microscopy, such as atomic force microscopy (AFM), have been developed to provide structural information on SAMs. Alternative spectroscopic methods have also been utilised that allow information to be obtained including reflection absorption infra red spectroscopy (RAIRS).⁷⁴ The increased resolution available from scanning electron microscopes⁸⁷ and tunnelling electron microscopes has shown images of SAMs with astonishing clarity as shown by Sharma *et al.* with this image of 1-octane-thiol on Au111 (figure 34)⁸⁸.

Optical techniques for the characterisation of SAMs are well established, ellipsometry has been used for investigating surfaces and thin films. Ellipsometry is a simple, non-destructive technique which allows the thickness of the monolayer to be measured at the angstrom scale.⁸⁹ A beam of polarised light is directed onto the monolayer surface and the change in the polarisation of the reflected light is detected and the thickness can be calculated.⁷⁷

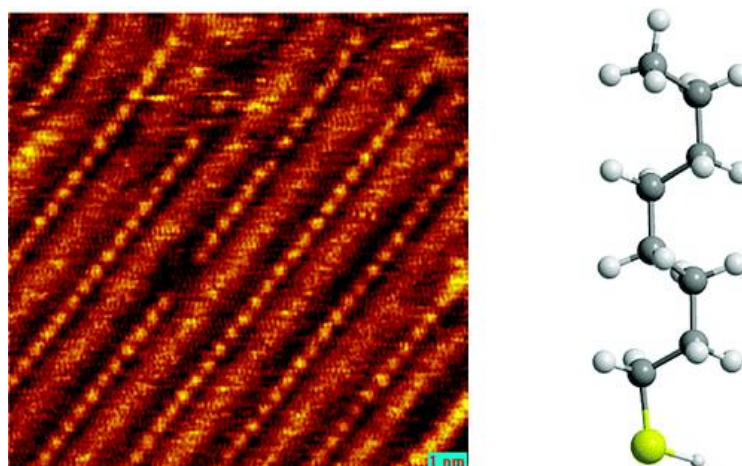


Figure 34 Image of 1-octane thiol (right) on gold substrate as seen by tunnelling electron microscopy (left) ⁸⁸

1.6.4 SAMs for the detection of biological interactions

Surface plasmon resonance (SPR) has been developed by Biacore, a company who manufacture equipment for investigating biomolecular interactions on a surface. These instruments integrate an optical detector, a gold coated sensor chip and a micro-fluidic arrangement of flow cells. Self assembly is used on the gold chip for binding molecular probes and upon exposure to the flow cell

containing analytes, in solution, binding to the probe occurs. The binding event is measured by a change in angle of resonance allowing the detection of the binding event to be recorded. Which is reported in the form of a ‘sensorgram’ that allows determination of mass and the kinetics of association and dissociation in real time. Applications of this are used for protein-protein interactions, drug discovery and antibody characterisation.⁹⁰

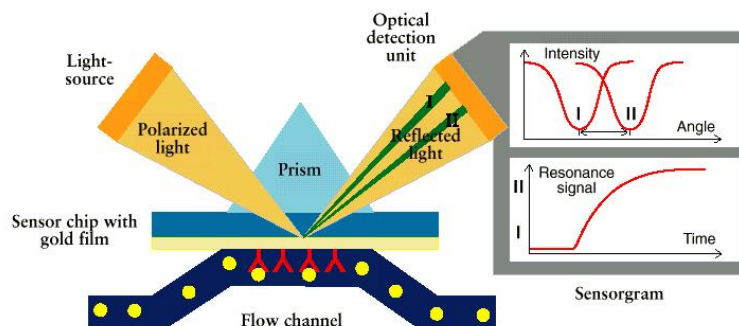


Figure 35 Biacore SPR schematic, illustrating the principles of the SPR detection technique.⁹¹

The ability to add functionality to the SAM has allowed a wide variety of biologically active compounds to be immobilised onto the gold surface allowing rapid testing for binding events using Matrix Assisted Laser Desorption Ionisation Time of Flight Mass Spectrometry (MALDI-TOF MS). The ability of SAMs to form organised layers with good control over density and orientation on an inert substrate makes this an attractive method for bio-assays in a high throughput (HT) manner⁹².

1.6.5 SAMs and matrix-assisted LASER-desorption/ionisation time of flight mass spectrometry (MALDI-TOF MS)

Matrix-assisted LASER-desorption/ionisation time of flight mass spectrometry (MALDI-TOF MS) is a soft ionisation technique for recording the mass spectrum of high mass biomolecules for example (proteins, DNA) and large organic compounds (polymers). The advantages of this technique over other mass analysis techniques other than being able to analyse large compounds (2000+ Da) is that it produces far less mass ions compared to some of the harsher analysis (chemical ionisation for example). MALDI analysis occurs by; first the desorption of the substrate *via* LASER irradiation, in combination with a chemical matrix (medium to aid in the absorption of LASER energy) leads to the ablation of the top layer of matrix and analyte. The plume of molecules following ablation contains many species of ionised, neutral, protonated and non-protonated matrix molecules. These then ionise the analyte molecules in the hot plume and become charged. These charged species are then detected by time of flight mass detector to afford the spectrum of the required analyte⁹³.

With SAMs on metal surfaces being notoriously difficult to characterise by normal analytical methods, MALDI-TOF spectrometry appeared to offer a significant advantage due to the necessity of the analytes needing to be on the surface of the MALDI plate. Detection of the analyte in the modern day with favourable conditions can be as low as the atto mole (10^{-18} mol) scale, making the detection of very small amounts of compound detectable⁹³. This appears to be a perfect system for analysing SAMs.

Su *et al.* report the MALDI-TOF analysis of SAMs on a gold surface and their subsequent chemical reactions. A SAM of a PEG chain terminating at the tail group with maleimide functional group was bound to a gold surface and treated with 2,5-dihydroxyl benzoic acid (10mg/mL, 1 μ L) as the matrix. The sample was then analysed by MALDI-TOF ms and generated the mass spectrum which afforded three large ion peaks for the disulfide moieties as sodium adducts (Figure36). Another sample was then tested following reaction of the maleimide *via* Diels-Alder reaction with pentamethyl cyclopentadiene and this generated a new mass ion confirming the reaction on the surface had been a success. This was repeated on two other SAMs and identical results were obtained⁹⁴.

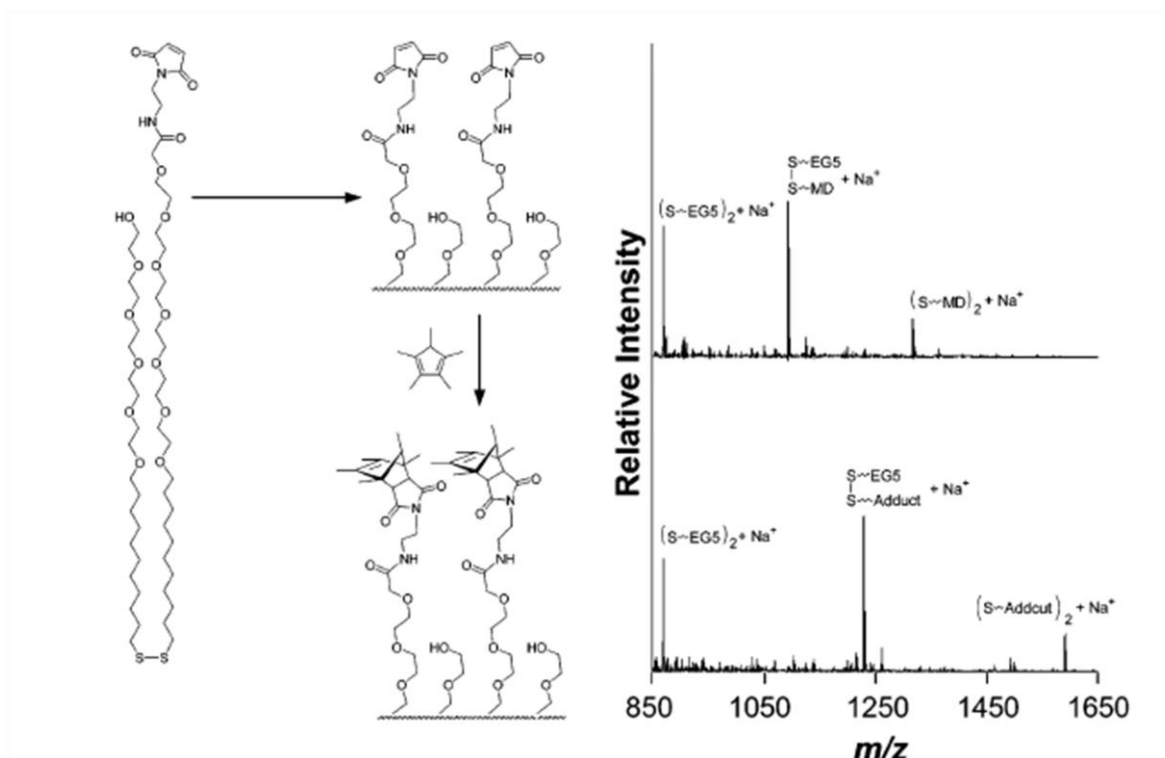


Figure 36 Su *et al.* reported the MALDI-TOF analysis of maleimide SAM (top spectrum) and MALDI-TOF analysis following Diels-Alder reaction of maleimide with pentamethyl cyclopentadiene (bottom spectrum).⁹⁴

Su suggested disulfide bonds were being generated in the plume of the ablation by dimerisation of the ionised species; however, Ha *et al.* has subsequently reported evidence that the dimers are being produced by dissolution of the SAMs into the matrix crystals by using alcoholic solvents for matrix

application. Ha tried applying the matrix in an aqueous solution which resulted in no observation of the di-sulfide species, he subsequently took another sample and applied the matrix in ethanol and let it dry. The matrix crystals at the surface were then removed and directly placed onto a MALDI target and analysed affording the dimer signals once more. This led him to conclude that the matrix and solvent were critical for the analysis of SAMs by MALDI-TOF spectrometry.⁹⁵

Ha has also reported the matrix free MALDI-TOF analysis of SAMs using sodium and potassium iodide as a matrix replacement. He has described this procedure as CALDI ms (cation assisted laser desorption ionisation mass spectrometry) and Ha obtained very clear mass ion peaks of simple SAMs as the disulfide sodium or potassium adducts. He also noted that the power of the LASER for ablation was critical as high LASER powers produced gold salts and produced saturation of the mass spectrum. The CALDI protocol was also successful in the analysis of SAM modified gold nano-particles.⁹⁶

1.6.6 Binding events of biological interactions on SAMs analysed by MALDI-TOF MS

With the ability to detect SAMs on a surface by MALDI-TOF MS the next step was to generate evidence of binding events taking place on the SAM surface. The interactions of proteins are ideally suited to analysis by MALDI-TOF MS as the high mass of proteins easily fit within the detection parameters of MALDI-TOF MS. Su *et al.* reported the synthesis of α -mannose incorporated tail group on a gold platform. This was subsequently treated with a buffered solution of the lectin Concanavalin A, the excess was washed off and submitted for MALDI analysis. They were able to detect the ions for the singly charged and doubly charged monomer units and doubly ionised trimer and tetramer units of the protein.⁹⁷

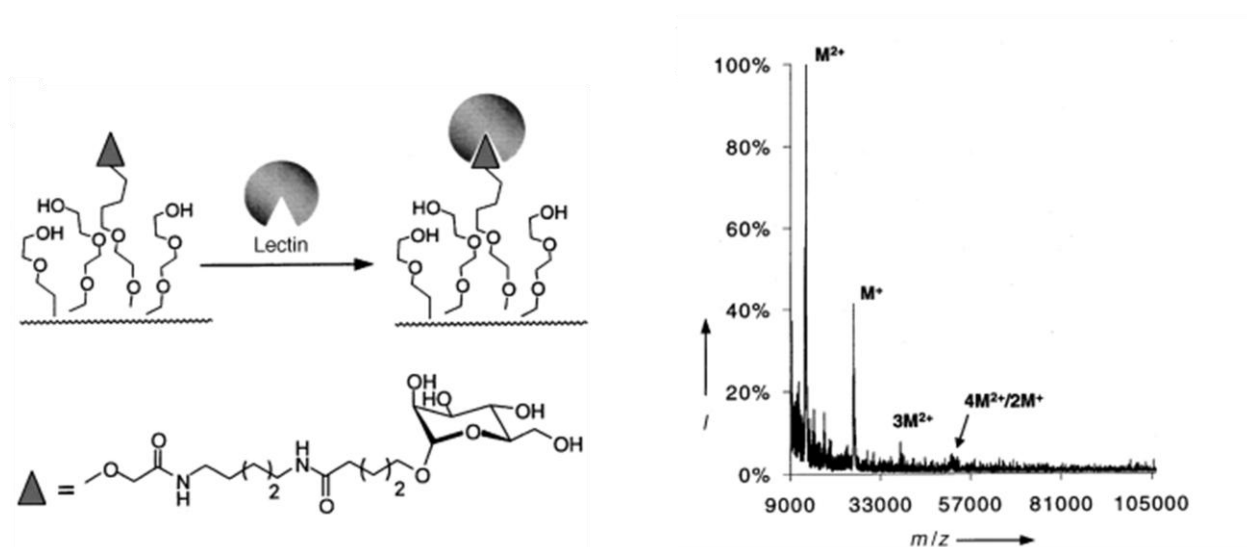


Figure 37 Su *et al.* report the detection of binding events between mannose and lectin on a gold surface. Monomer, trimer and tetramer units of the lectin protein can be observed.⁹⁷

Dal-Hee *et al.* reported analysis of anthrax inhibitors by immobilising small compound libraries onto a gold surface and incubating with the lethal factor protease (LF-protease). The excess LF-protease was washed off and then analysed using MALDI-TOF MS. The LF-protease targets a specific peptide sequence and cleaves the peptide at that point. By analysing the before and after *m/z* spectra it was possible to observe the difference in mass between the starting peptide and the cleaved peptide. After analysing many synthetic peptides, synthesised *via* solid phase peptide synthesis, he found only one that was cleaved by the LF-protease. He confirmed the results *via* solution phase cell based assays of the peptide.⁹⁸

It appears that the use of SAMs for detection of binding events at a surface *via* MALDI-TOF MS is clearly possible and using these methods for the high-throughput screening of new drug candidates should be possible.

1.6.6 SAMs on compact discs

With much of our lives now revolving around computers in some shape or form there has been a massive demand for storage and security of computer files. This has meant that there has been a huge amount of research done on data storage. With this being the case gold has been used to make high end CD-Rs for archiving the huge amounts of sensitive data which needs to be stored securely for long periods of time. The inert nature of gold to many of the compounds and elements found in the atmosphere has allowed it to replace aluminium as the reflective layer in some CD-R brands. Thus a gold CD is a cheap and readily available media that with little modification can be used as a platform for SAM formation. The gold layer is only 50 nm thick and has a slightly flatter surface than found on commercially available gold slides.⁹⁹ This makes it a perfect surface for SAM formation. Yu has reported a method to modify gold compact disks and remove the protective coating *via* treatment with 70% nitric acid to expose the bare gold surface which is immediately ready for SAM formation. Subsequent treatment of the exposed gold layer with alkanethiols has produced SAMs on the CD surface. Contact angles and other measurements performed on these SAMs have shown next to no differences to those recorded on standard commercially available gold plated glass slides.⁹⁹

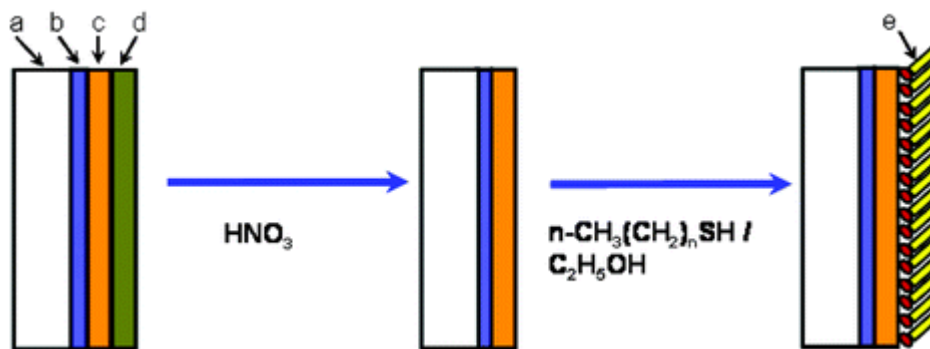


Figure 38 Yu *et al.* has shown the composition of the compact disc a) poly carbonate base, the major part of the CD, b) photosensitive dye layer (CD-R), c) gold layer ~50nm thick, d) polymer film as protective coating, e) SAM formed on gold surface.⁹⁹

Yu published his paper on SAMs on gold CDs in 2001 and there are currently no more published examples of SAM formation on CDs. There are reports of using the gold CDs as electrodes for electrochemical reactions and they are as good as commercially available gold electrodes and are much cheaper.¹⁰⁰

1.7 Compact discs and CD drives for biological assays

The idea of bioassays on a CD surface is not new and there are a handful of papers in the literature reporting binding events that have been detected using standard CD players and unmodified CDs (without removal of the protective lacquer). Li bound molecules to the polycarbonate by activating the surface with ozone to form carboxylic acid groups followed by forming amide bonds with a DNA tether. The DNA was then hybridized with biotin and coated with streptavidin/gold nano particle conjugates. This was subsequently placed in a standard CD drive on a PC and an error diagnostic program was run, therefore, errors were shown at the coordinates of the modified surface.¹⁰¹ Similar experiments have also been shown to work by La Clair using very similar methodology but different substrates and using a different error diagnostic tool.¹⁰²

Potyrailo *et al.* has taken this idea to a different level by converting the CD drive in order to extract the analogue signal directly from the LASER diode.¹⁰³ This gives many benefits to the quality of the data compared to the previous examples. The CD player has a built in microprocessor which converts the analogue signal to digital signal before it is sent to the computer as it only understands binary format therefore giving, for example, 1 for signal or 0 for error. The analogue signal is then processed by an oscilloscope which allows a variety of different voltages to be recorded. This gives more information to the user as all values can be read rather than just 1 or 0, therefore, this could be used as a fingerprint of the bound molecules. This was tested using calcium sensitive films which were treated with different concentrations of Ca^{2+} to give a gradient, which was then

analysed using his modified CD drive. As expected, the oscilloscope data showed different values depending on concentration.¹⁰³



Figure 39 Potyrailos CD with different concentrations of Ca^{2+} .

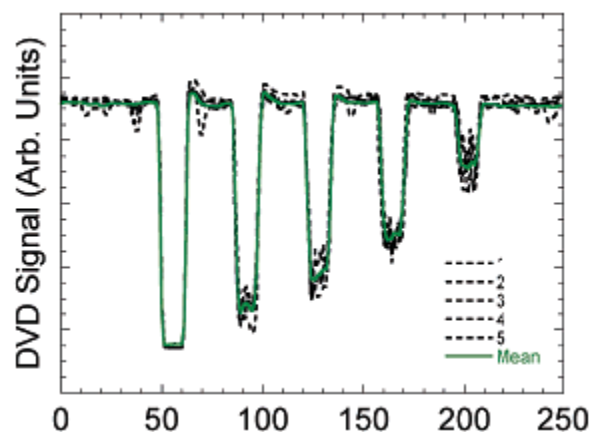


Figure 40 Potyrailos results from least concentrated to most concentrated (left to right) showing more signal returning to diode at lower concentrations.¹⁰³

So far there have been no reports in the literature of overlap between SAM formation on CD and using a conventional, but modified, CD drive to recognise binding events or even simply as a characterisation method to confirm the SAM formation. This would be an extremely interesting concept and could allow bio-screening to be performed on a large scale and very quickly using already available, cheap, apparatus.

2 Aims of research

In this project we aimed to investigate the potential of utilising gold compact discs as a cheap and readily available media for detection of proteins *via* MALDI-TOF spectroscopy. This model study will endeavour to utilise the strong (+)-biotin / streptavidin interaction to develop a proof of concept protocol which could then be extrapolated to substrates of a more useful nature. Since the events of September 11th the threat of terrorist attacks across the world is a real and present danger including the use of Anthrax and Ricin, both of which are protein based toxins. It is hoped that this work could make the detection of these and other toxic proteins much quicker and more reliable to determine whether the threat posed by unknown substances is real. The humanitarian applications of this project could also be revealed by the detection of the Cholera toxin, another deadly protein, in drinking water.

The detection of binding events with proteins and small molecules would be of huge interest to the pharmaceutical industry as many diseases are caused by proteins Alzheimer's, CJD and some cancers. The analysis of small molecule drug candidates with proteins could be a valuable asset to this industry. Quick and cheap methods for the discovery of new drugs would not only benefit them but also the general population as the cost of finding new drugs becomes cheaper.

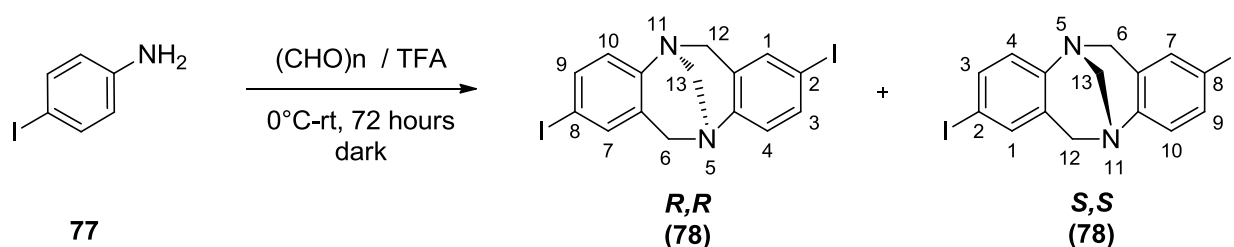
Once the proof of concept has been developed we will endeavour to use Tröger base as a scaffold for binding to the gold CD, through modification of the methylene bridge to incorporate a sulfur group for SAM formation. The 2 and 8 positions of the Tröger's base scaffold will be modified to incorporate a novel *bis*-azido functionality append the (+)-biotin warheads *via* 'click' chemistry, with varying lengths of linkers between the warhead and scaffold. It is hoped that the chiral cleft and the 90° angle found in Tröger's base will push the two warheads in opposite directions to ensure there is enough space to bind strongly to the streptavidin protein.

These will then be bound to the CD surface and the protein applied before being submitted for MALDI-TOF spectrometry analysis.

3 Methodology

3.1 Tröger's base synthesis and 'click' reaction

The synthesis of racemic *bis*-iodo Tröger's base (+/-)-**78** has been reported by Warnmark *et al.* by the condensation of *para*-iodo aniline **77** with paraformaldehyde in neat trifluoroacetic acid.¹⁵

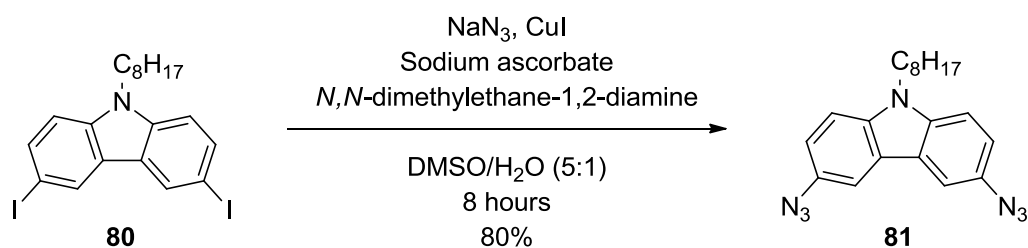


Scheme 16 Proposed synthesis of racemic *bis*-iodo Tröger's base

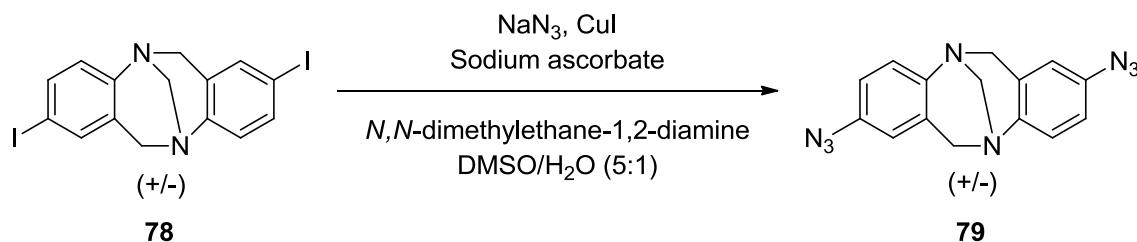
It is suggested that the reaction be kept in the dark to prevent cleavage of the carbon iodine bond, which is susceptible to cleavage by light. The reaction mixture will be cooled to 0°C as the addition of TFA to the mixture of aniline and paraformaldehyde is reported to be highly exothermic.¹⁵

The modification of Tröger's base (+/-)-**78** at the 2- and 8- positions to an azide moiety will be performed by a procedure adapted from Li *et al.* as racemic 2,8-*bis*-azido Tröger's base (+/-)-**79** has

not been reported in the literature. Li generated a *bis*-azido functionality of 3,6-diiodo-9-octyl-9H-carbazole **80** *via* a copper(I) catalysed transformation (Scheme 17).¹⁰⁴



Scheme 17 Li *et al.* reported the synthesis of a *bis*-azido adduct containing a tertiary amine at the *para* position.

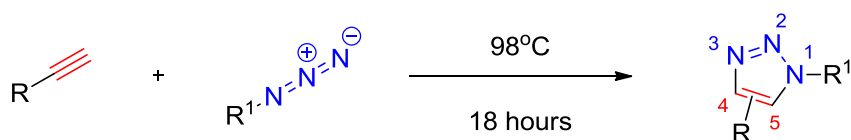


Scheme 18 Proposed synthesis of racemic *bis*-azido Tröger's base (+/-)-**79**

If successful it will be a good candidate for synthesis in a microwave reactor, due to the polar solvents used in this reaction, in an attempt to decrease the reaction time.

Before attempting to generate a (+)-biotin derivative capable of 'click' chemistry we need to ensure that (+/-)-**79** is capable forming a 1,2,3-1,4-triazole ring and the bicyclic core is stable to the conditions necessary for 1,2,3-triazole formation. Following a procedure reported by Bew *et al*¹⁰⁵ a series of propargyl substrates will be synthesised and 'clicked' to the scaffold. A simple and mild protocol, utilising *N*-protected α - and β - amino acids to generate their propargyl esters with propargyl bromide and potassium carbonate will be attempted.

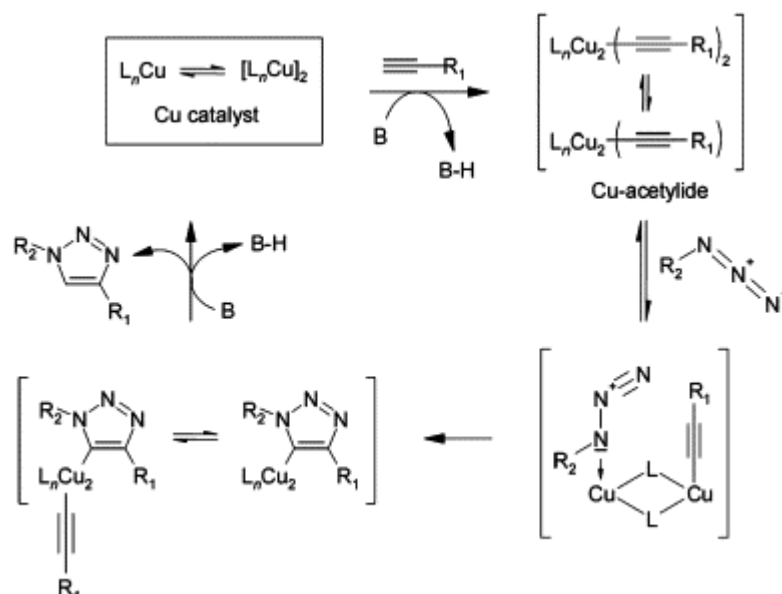
The propargyl esters will be coupled to the scaffold *via* the azide-alkyne Huisgen cycloaddition reaction. This 1,3 cycloaddition was coined 'click' reaction by Sharpless although the scope of the reaction was originally determined by Rolf Huisgen.



Scheme 19 Azide-alkyne Huisgen cycloaddition

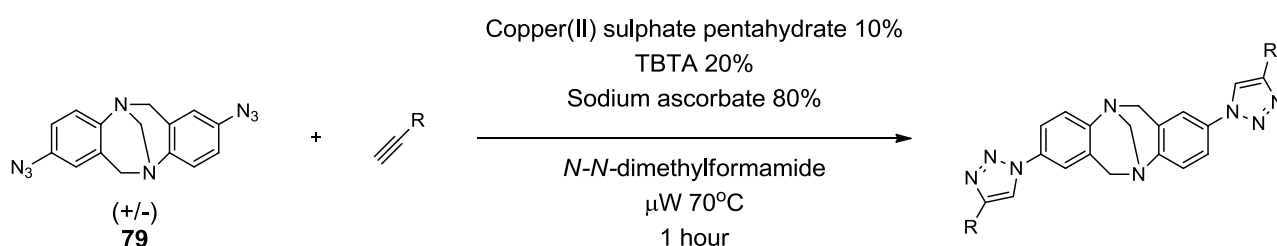
In the cycloaddition shown in Scheme 20, a long reaction time is required and a high temperature is necessary for reaction to progress. This also yields a mixture of 1,4 and 1,5 adducts as products. By introducing a copper or ruthenium catalyst to this reaction, the time required for reaction and

temperature requirements are greatly reduced. The copper(I) catalysed variant will afford predominantly the 1,4 substituted 1,2,3 triazole (usually greater than 95%) and the ruthenium catalyst will afford predominantly the 1,5 substituted 1,2,3 triazole.



Scheme 20 Proposed mechanism for copper(I) catalysed alkyne-azide cycloaddition

To ensure the chiral cleft and 90° angle of Tröger's base are used to push the 2 and 8 appended substituent's away from each other we require the 1,2,3 triazole to be in the 1,4 orientation. To achieve this, a copper catalysed procedure will need to be employed as described by Bew *et al.* The procedure employs copper(II) sulphate pentahydrate, TBTA (*tris*[(1-benzyl-1H-1,2,3-triazol-4-yl)methyl]amine) as a proton accepting ligand which negates the need for a base in the reaction and sodium-*L*-ascorbate, as a reducing agent to reduce the copper salt from copper(II) to copper (I).¹⁰⁶

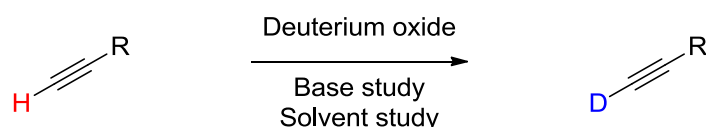


Scheme 21 Proposed synthesis of copper(I) catalysed azide-alkyne cycloaddition to afford the 1,4 substituted 1,2,3 triazole.

Should this be successful then it will be the first synthesis of a 2,8-*bis*-azido Tröger's base (+/-)-**79** and also the first 1,2,3 triazole containing Tröger's base analogue.

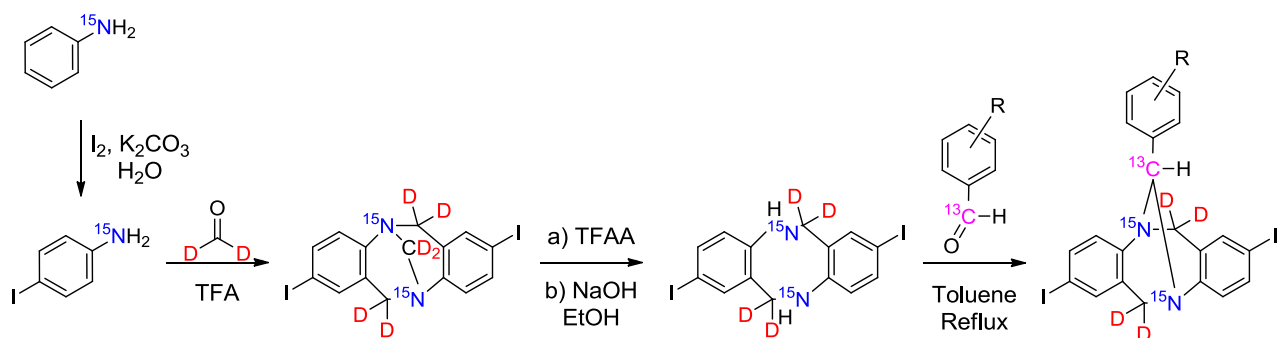
3.2 Stable isotope incorporation of alkynes and Tröger's base

The incorporation of stable isotopes into organic molecules is of great interest to many science disciplines, including chemists for mechanism elucidation¹⁰⁷ and biologists following the pathways of compounds through biological systems. During a project to generate deuterated propargyl diazoacetate it became apparent that the terminal alkyne of the propargyl functionality had been deuterated under particularly mild conditions. This observation was worth perusing further as current protocols require strong bases *ie* ethyl lithium,¹⁰⁸ low temperatures *ie* -50°C¹⁰⁹ or extended reaction times *ie* several weeks¹¹⁰ with poor ²H incorporations >70% or no mention of ²H incorporation. With aspirations to generate propargyl esters an experiment was designed to optimise this exchange for ²H-incorporation <95%.⁴³



Scheme 22 Optimisation strategy for the deuteration of terminal alkynes

Lenev *et al.* reported the synthesis of d₆-bis-methyl Tröger's base analogue by employing the condensation of d₂-paraformaldehyde with toluidine.⁴⁰ With ¹⁵N-aniline commercially available a simple electrophilic aromatic substitution to afford ¹⁵N-*para*-iodo-aniline, followed by condensing this with d₂-paraformaldehyde should afford ¹⁵N-d₆-Tröger's base (Scheme 23).



Scheme 23 Proposed synthesis of ¹⁵N, d₄, ¹³C – multi isotopically labelled Tröger's base analogue.

This could be followed by removal of the methylene bridge as described by Mahon *et al.* with TFAA and NaOH/EtOH and replacement with an α ¹³C-benzaldehyde¹⁸ should afford a novel multi isotopically labelled Tröger's base. Subsequent reaction of this labelled Tröger's base *via* copper(I) catalysed azide insertion and 'click' reaction (scheme 20) with a deuterated alkyne has the potential to afford a deuterated 1,2,3-triazole analogue.

3.3 Proof of concept for MALDI-TOF analysis of SAM (+)-biotin / streptavidin binding

Before synthesising Tröger's base incorporated SAMs it will be prudent to see if the binding of (+)-biotin and streptavidin on a compact disc is detectable by MALDI-TOF spectrometry. To do this a series of simple (+)-biotin with linkers will be required. Different lengths of linkers will be examined to ascertain optimum binding of biotin to streptavidin. The carboxylic acid functionality on the (+)-biotin moiety is the most feasible position for modification. To utilise the 'click' reaction for coupling to a disulfide linker, as will be used on the Tröger's base scaffold, an alkynyl group will need to be incorporated at this position. Reports in the literature utilise this functionality for amide bond formation *via* activation of the carboxylic acid with *N,N'*-dicyclohexylcarbodiimide¹¹¹ (DCC), however this was generated in a low 60% yield and the removal of the urea generated as a by product is notoriously difficult. Esterification is another possibility, however, the literature doesn't afford any hits on the Fisher esterification using propargyl alcohol or any alkyne moiety. The esterification by displacement of an alkynyl bromide, is another possibility for this coupling.

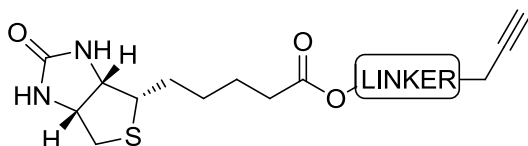
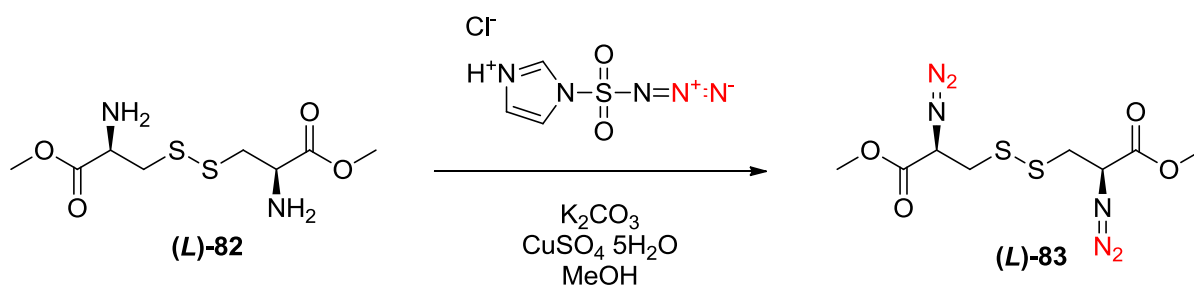


Figure 41 Required (+)-biotin linker incorporating a alkyne for subsequent 'click' reaction

A di-sulfide, a self protected thiol, and azide containing linker will be necessary for coupling to the biotin moiety and to bind to the gold CD. A readily available substrate that already contains a disulfide bond and an amine for conversion to an azide is the amino acid (*L*)-cystine. The carboxylic acid will need to be protected and this will be accomplished by an HCl catalysed Fisher esterification with methanol according to the procedure of Guerrero.¹¹² This will subsequently be converted to the *bis*-azide-(*L*)-cystine using imidazole sulfonyl azide hydrochloride as described by Goddard *et al.*¹¹³ This procedure is preferred to diazotisation followed by displacement with nucleophilic azide as Goddard reports the stereocentre of the (*L*)-cystine is unaffected as imidazole sulfonyl azide is a diazo transfer reagent.



Scheme 24 Proposed synthesis of *L*-cystine-*bis*-azide-methyl ester (*L*)-83

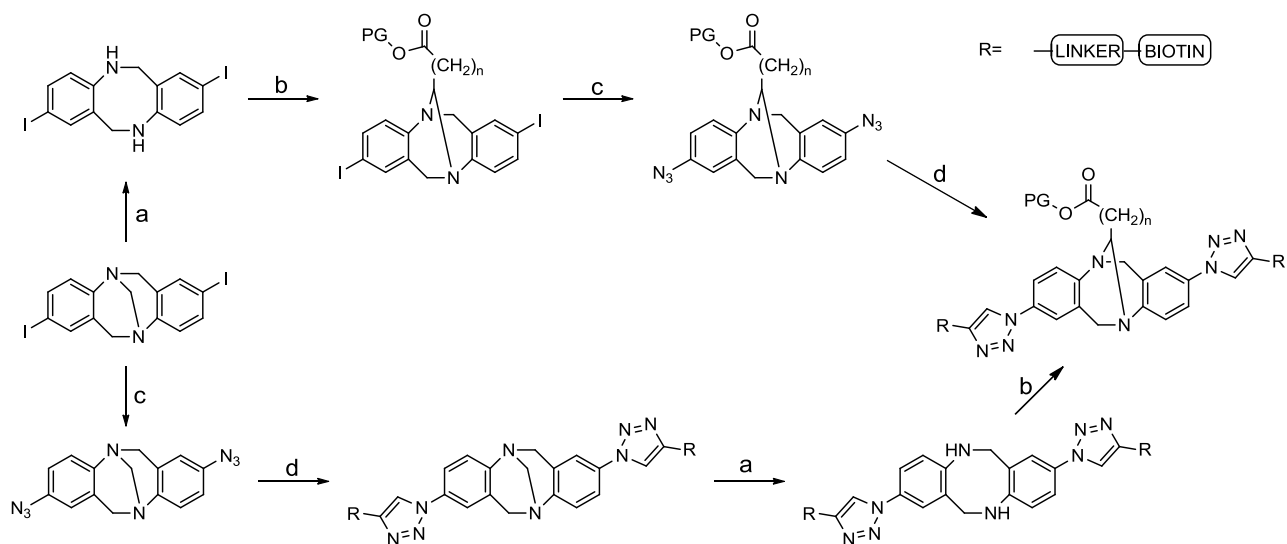
This will subsequently be 'clicked' to the biotin linkers affording di-sulfide, connected to a 'biotin warhead' with different length linker units between them. These will need to be bound to the gold CD surface prior to analysis by MALDI-TOF spectroscopy.

The CD surface will need to be cleaned and the protective lacquer removed prior to binding of the substrates. Yu has reported a procedure for removal of the lacquer by immersion of the compact disk in 70% nitric acid.¹¹⁴ Energy-dispersive X-ray spectroscopy (EDS), scanning electron microscopy (SEM) and atomic force microscopy (AFM) analysis of the gold surface will then be performed to ensure the surface is flat and the gold layer has been exposed. A suitable method for cutting the CD into small sections will be necessary for analysis to be performed.

A protocol will need to be developed to aid formation of the SAMs as simply spotting a solution of the disulfide and biotin linker onto the surface will result in evaporation of the solvent. We intended to design a rig for the application of the solution to the gold, therefore ensuring the compounds remain in solution during the SAM formation over a 24 hour period. The same procedure will be necessary for applying the streptavidin solution to the SAM, again for a 24 hour period. The resulting SAM/streptavidin binding event will need to be analysed by MALDI-TOF spectroscopy. Collaboration will be sought, from an outside source, as we have been expressly told not to disassemble the in house MALDI-TOF spectrometer.

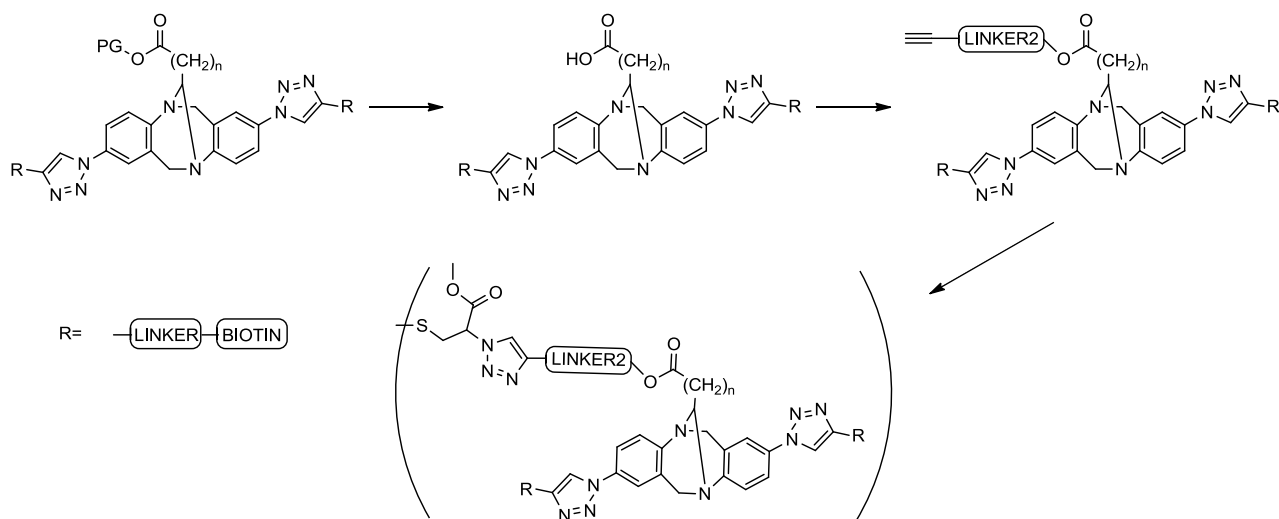
3.4 Tröger's base modification for (+)-biotin and di-sulfide incorporation

The Tröger's base will need to be modified at the 2, 8 and 13 position to allow for a disulfide linker to be attached at position 13, and (+)-biotin linkers to be appended at the 2 and 8 positions. It is hoped that by incorporating two (+)-biotin linkers onto the scaffold an increase in binding effectiveness will be observed. To modify the C13 of Tröger's base the methylene bridge will have to be removed and replaced with a suitable linker capable of modification to afford extended linkers and finally the disulfide unit. This will be achieved by synthesis of a linear alkyl chain with an aldehyde at one end, for incorporation at the C13 position and a protected carboxylic acid, for future deprotection, coupling to linkers and finally to the di-sulfide moiety.



Scheme 25 Synthetic strategies for synthesis of protected *bis*-4-biotin-linker 1,2,3 Tröger's base. a) i) Trifluoroacetic anhydride, DCM. ii) NaOH/EtOH. b) aldehyde, reflux, toluene. c) Copper(I) iodide, sodium ascorbate, N^1,N^2 -dimethylethane-1,2-diamine, sodium azide, DMSO/H₂O. d) Copper(II) sulphate pentahydrate, sodium ascorbate, TBTA, alkyne, DMF.

Following deprotection other linkers will be incorporated off the carboxylic acid functionality to investigate the effect of varying the length of the linker on SAM formation. This will also include an alkynyl group for final dimerisation to the disulfide moiety [scheme 26].



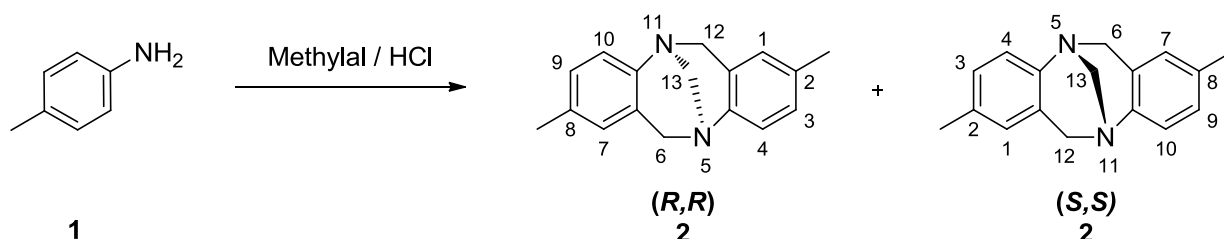
Scheme 26 Proposed strategy for synthesis of dimerised Tröger's base analogue through di-sulfide linker

This series of dimerised compounds will be bound to the surface of the compact disc using a rig to ensure they remain in solution during the SAM formation process. They will then be treated with a streptavidin solution to allow the interaction to take place. The gold CD segments will then be analysed by MALDI-TOF spectrometry to confirm whether or not a binding event can be observed.

4 Results and Discussion

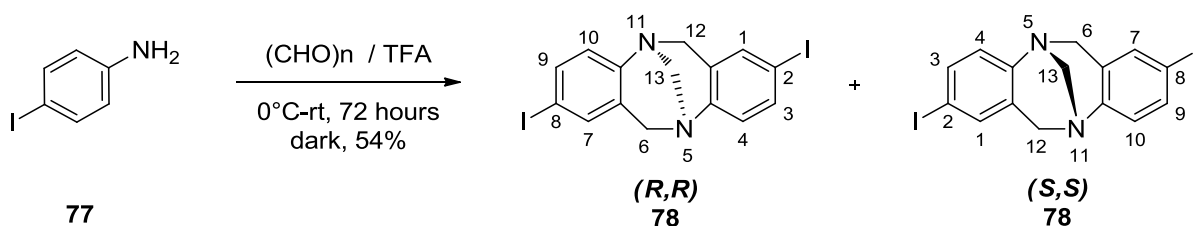
4.1 Tröger's base synthesis and functionalisation

The original synthesis of 2,8 di-methyl Tröger's base (+/-)-**2** by Julius Tröger in 1887 was performed by the condensation of *para*-toluidine **1** with methylal [CH₂-(CH₃O)₂] in an aqueous hydrochloric acid solution [Scheme 27].¹



Scheme 27 J. Tröger's synthesis of Tröger's base (2,8-dimethyl-6,12-dihydro-5,11-methanodibenzo[b,f][1,5]diazocine) **2**

A modified variation of J. Tröger's synthesis is still used today for preparing functionalised Tröger's bases' at the 2- and 8-positions. Warnmark *et al.* reported the synthesis of (+/-)-2,8-bis-iodo-6,12-dihydro-5,11-methanodibenzo[b,f][1,5]diazocine (+/-)-**78** via the condensation of *para*-iodoaniline **77** with paraformaldehyde in neat trifluoroacetic acid affording (+/-)-**78** in a 41% yield.¹¹⁵ Warnmark's procedure for (+/-)-**78** needed to be optimised to improve the yield for generating multigram quantities of (+/-)-**78**. After much experimentation this was achieved by premixing one equivalent of *para*-iodoaniline **77** with 1.5 equivalents of paraformaldehyde and adding, in portions, to vigorously stirred neat anhydrous trifluoroacetic acid at 0°C. [Scheme 28] The reaction mixture was protected from the light by covering the round-bottom flask in aluminium foil and left to stir for 72 hours under an argon atmosphere.



Scheme 28 Synthesis of racemic 2,8-bis-iodo Tröger's base (+/-)-**78**

This slightly altered protocol was found to be more effective for the multigram synthesis of (+/-)-**78**, than the literature protocol (41%), giving an increase in yield of 13%, to 54%. The synthesis of (+/-)-**78** generates a racemic mixture and all attempts to resolve the enantiomers, using 0.5 equivalents of (+)-camphor-10-sulfonic acid or *d*-mandelic acid failed. The ¹H-NMR (400MHz) spectrum of (+/-)-**78** was very interesting. Rather than observing a singlet for the equivalent

protons at positions C6 and C12 [Figure42], a splitting was observed resulting in two doublets, the first at δ 4.61, corresponding to the *exo* protons of C6 and C12. The second doublet was further upfield at δ 4.07 and corresponds to the *endo* protons. A coupling constant of 16.8Hz was observed between the *endo* and *exo* protons of C6 and C12 and was in agreement with $^1\text{H-NMR}$ study of (+/-)-**2** reported by Pardo *et al.*¹¹⁶ All data for (+/-)-**78** was in agreement with the literature provided by Warnmark *et al.*¹¹⁵

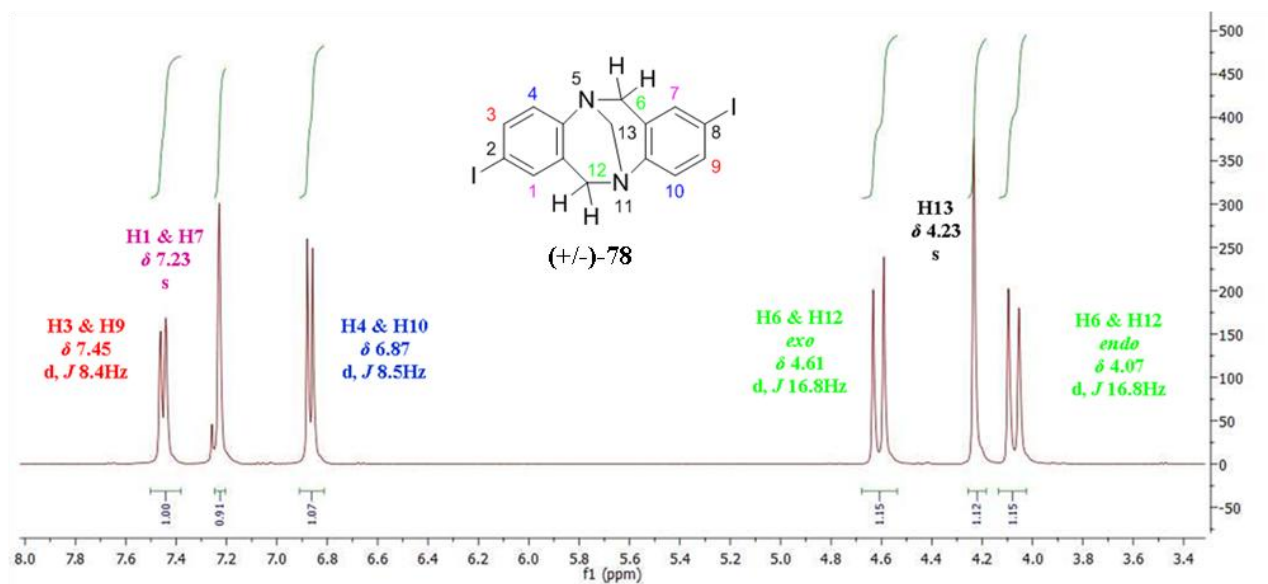
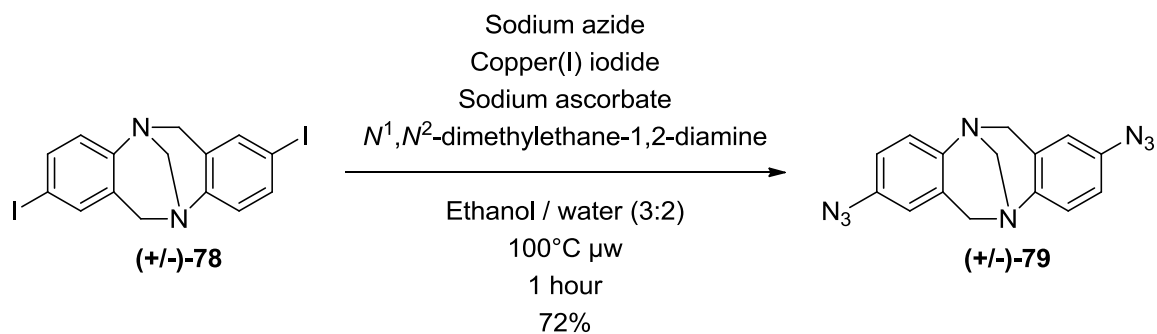


Figure 42 $^1\text{H-NMR}$ (400 MHz) of racemic 2,8-bis-iodo Tröger's base (+/-)-**78**

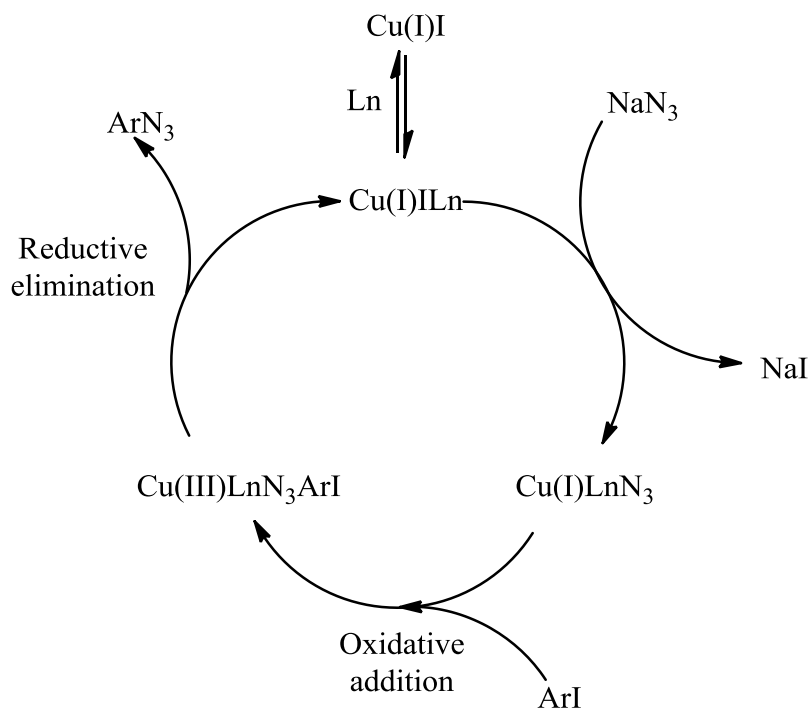
With Tröger's base (+/-)-**78** in hand, it was now possible to initiate studies functionalising the 2,8-positions of (+/-)-**78**. A wide variety of functionalised analogues such as, 2,8-bis-formyl, carboxylic acid, cyano, hydroxy¹⁵ and amino¹¹⁷ have been reported. In the first instance we decided to emulate Li *et al*, who demonstrated the conversion of an aryl iodide to an aryl azide using a copper(I) catalysed procedure [Scheme 29].¹⁰⁴ We opted to modify this procedure slightly, by utilizing a microwave reactor¹ which took the total reaction time down to only one hour at 100°C, a significant improvement on the reported 8 hour reflux.¹⁰⁴

¹ Microwave reactors can decrease reaction times by increasing bond vibration of polar solvents and this results in extra collisions, therefore, reaction times improve.



Scheme 29 Synthesis of racemic 2, 8-*bis*-azido Tröger's base (+/-)-**79**

Scheme 30 (*infra vide*) outlines the proposed catalytic cycle for the conversion of aryl iodides to aryl azides *via* a copper(I) catalysed procedure. The copper(I) iodide associates with the ligand, followed by introduction of the azide anion with loss of sodium iodide. This then undergoes oxidative addition with the aryl iodide, forming a copper(III) adduct. Reductive elimination affords the aryl azide product and regeneration of the original copper ligand catalyst.



Scheme 30 Proposed catalytic cycle for the synthesis of aryl azides from aryl halides.

Following purification of (+/-)-**79** by flash chromatography the desired novel Tröger's base analogue, (+/-)-2,8-*bis*-azido-6,12-dihydro-5,11-methanodibenzo[b,f][1,5]diazocine (+/-)-**79** was afforded in an unoptimised 72% yield. That we had generated (+/-)-**79** was confirmed by full physicochemical analysis for example the ¹H-NMR (400MHz) [Figure 43] observed a shift in peaks in the aromatic region, from δ 7.45(d, *J*8.4 Hz), δ 7.23 (s) and δ 6.87 (d, *J*8.5 Hz) in (+/-)-**78** to δ 7.08 (d, *J*8.5 Hz), 6.81 (d, *J*8.4 Hz), 6.55 (s), in the *bis*-azide (+/-)-**79**. In the ¹³C-NMR (75 MHz) [Figure 44] a clear shift of the C2 and C8 from δ 87.7 found in the carbon iodine bond to δ 118.68,

117.23 in the carbon azide bond. The presence of the azide group on the product was indicated by FT-IR with a strong peak at 2112 cm^{-1} .

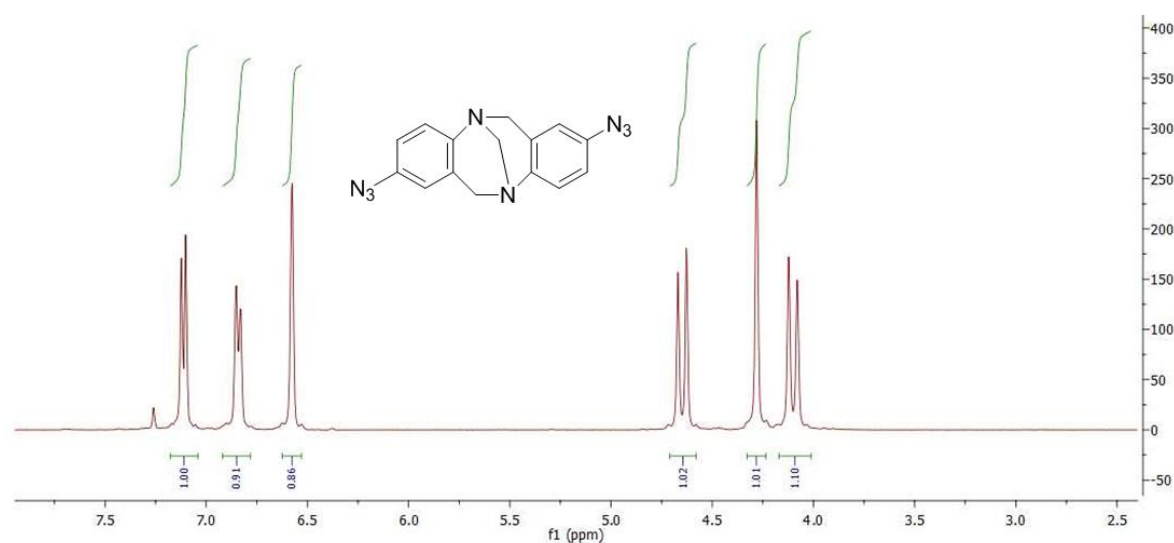


Figure 43 $^1\text{H-NMR}$ (400MHz) of racemic 2, 8-bis-azido Tröger's base (+/-)-79.

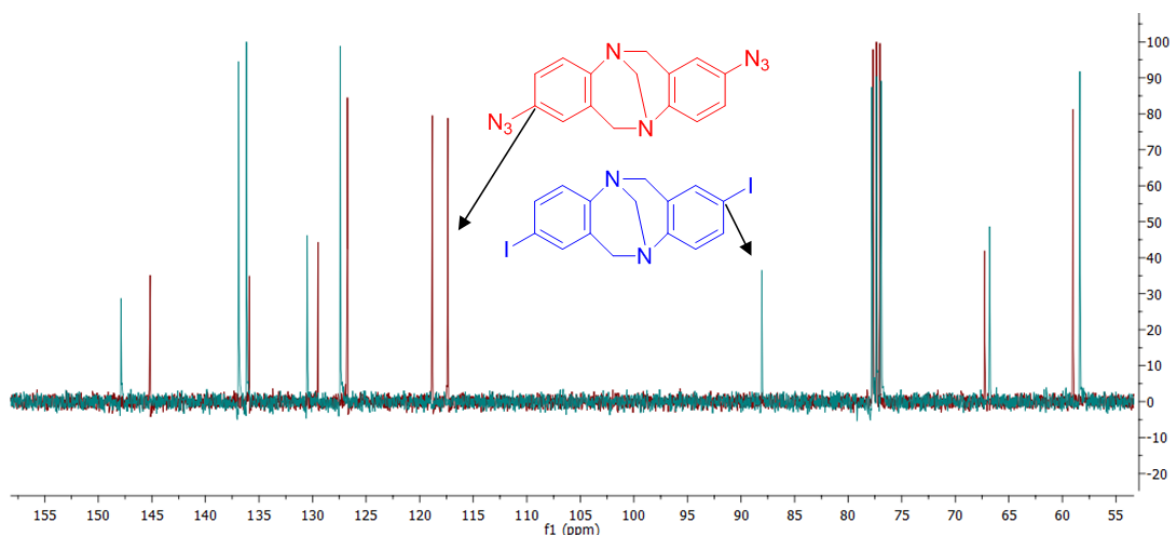


Figure 44 $^{13}\text{C-NMR}$ spectrum comparing racemic 2, 8-bis-iodo Tröger's base (+/-)-78 (blue) and racemic 2, 8-bis-azido Tröger's base (+/-)-79 (red).

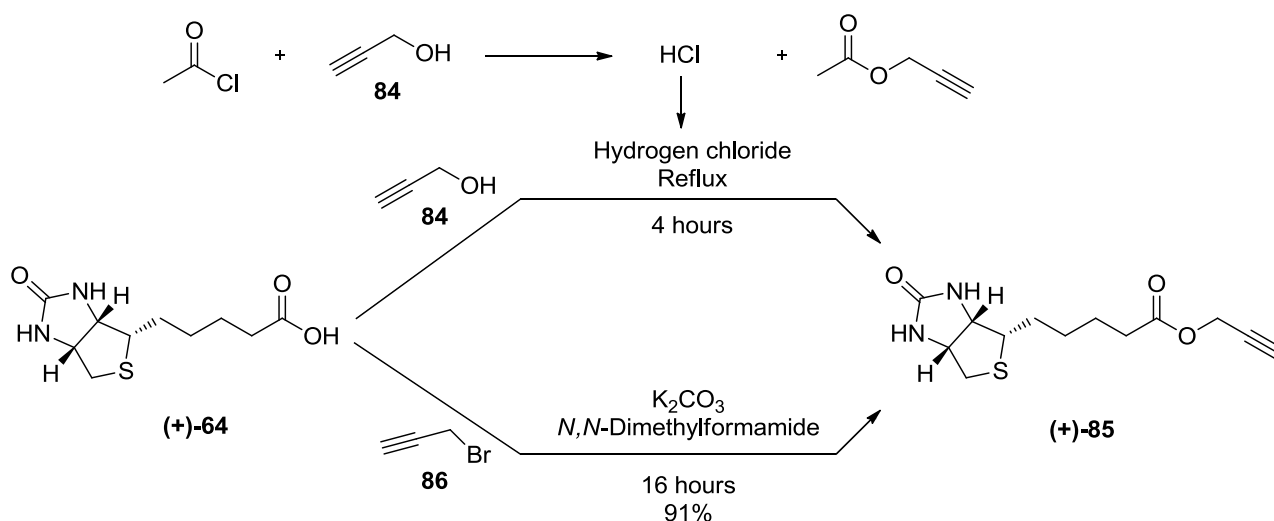
4.2 Propargyl esterification of (+)-biotin (+)-64

With the synthesis of (+/-)-79 completed it was necessary to synthesise a suite of compounds with suitable functionality to react with the azide of (+/-)-79. The azide functionality can be used to generate amines *via* reduction in the Staudinger reaction or hydrogenation, tetrazoles *via* reaction with cyanides, tetrazolinones *via* reaction with isocyanates and mercaptotetrazoles *via* reaction with isothiocyanates.¹¹⁸ We opted to generate 1, 4-bis substituted-1,2,3-triazoles from terminal alkynes *via* 'click' utilising a copper(I) catalysed Huisgen 1,3-dipolar cycloaddition reaction. For the

purpose of utilising Tröger's base as a scaffold for the detection of proteins on a compact disc it was necessary to incorporate a suitable ligand capable of forming strong bonds with a protein. It is known that the (+)-biotin – streptavidin interaction is one of the strongest non covalent bonds in Nature, with a dissociation constant (K_d) of approximately 10^{-14} mol/L.¹¹⁹ This interaction has been employed as a model study for the development of protein detection systems and has been used, as such, on the surfaces of nanoparticles¹¹⁹ and other surfaces *i.e.* silica.¹²⁰ We envisage this interaction would make an ideal model for the detection of proteins on the surface of a compact disk.

The synthesis of an alkynyl derived (+)-biotin (+)-**64** would be necessary to utilise the (+)-biotin / streptavidin interaction with our azide containing scaffold (+/-)-**79**. We envisage the esterification of the carboxylic acid functionality with propargyl alcohol **84** *via* a Fisher esterification, which utilises the acid-catalysed, typically hydrogen chloride, condensation of an alcohol and carboxylic acid, should afford (+)-**85** [Scheme 31]. A Scifinder search, at the time, for (+)-**85**, afforded no hits but (+)-**85** was subsequently reported by Zhang *et al*² in 2012.¹²¹

The attempted Fisher esterification of (+)-**64** by refluxing (+)-biotin (+)-**64** in propargyl alcohol **84** with 10 mol% of hydrogen chloride, formed *in situ* by the reaction of acetyl chloride with propargyl alcohol **84** was disappointing and afforded a brown tar after 4 hours. Analysis of this tar by ¹H-NMR (400MHz) couldn't confirm conclusively that (+)-**85** had been formed.



Scheme 31 Synthesis of (+)-biotin propargyl ester (+)-**85** top reaction pathway affords the unsuccessful synthesis *via* Fisher esterification and bottom pathway affords the successful synthesis.

² Disappointingly Zhang didn't cite the Letter, published by Bew and Hiatt-Gipson, that brought the facile synthesis of propargyl esters to the literature in 2010.

Using this protocol the Fisher esterification was disappointing. As no product was isolated and because the cost of (+)-biotin (+)-**64**, approaching £50 a gram, (Sigma Aldrich 2012) it was crucial to find a more efficient synthesis of (+)-**85**. A literature search on the synthesis of propargyl esters was, surprisingly, rather limited. The reported procedures employed relatively expensive reagents *i.e.* *N*-(3-dimethylaminopropyl)-*N*-ethylcarbodiimide hydrochloride (£15/gram Sigma Aldrich 2012)¹²² and extended reaction times *i.e.* 48 hours.¹²³ Sudhir *et al.* reported the synthesis of the propargyl ether of (*S*)-tyrosine and the *bis*-propargyl ester of (*S*)-aspartic acid using propargyl bromide **86** and potassium carbonate.¹²⁴ We opted to employ this method for the esterification of (+)-biotin (+)-**64** and gratifyingly the required ester (+)-**85** was afforded in an unoptimised 91% yield. The ¹H-NMR (400MHz) spectrum of (+)-**85** displayed a triplet at δ 2.45 (t, *J*2.5 Hz) and a singlet at δ 4.61 (d, *J*2.5 Hz) corresponding to the alkynyl proton and the propargyl methylene protons respectively, see [Figure 45].

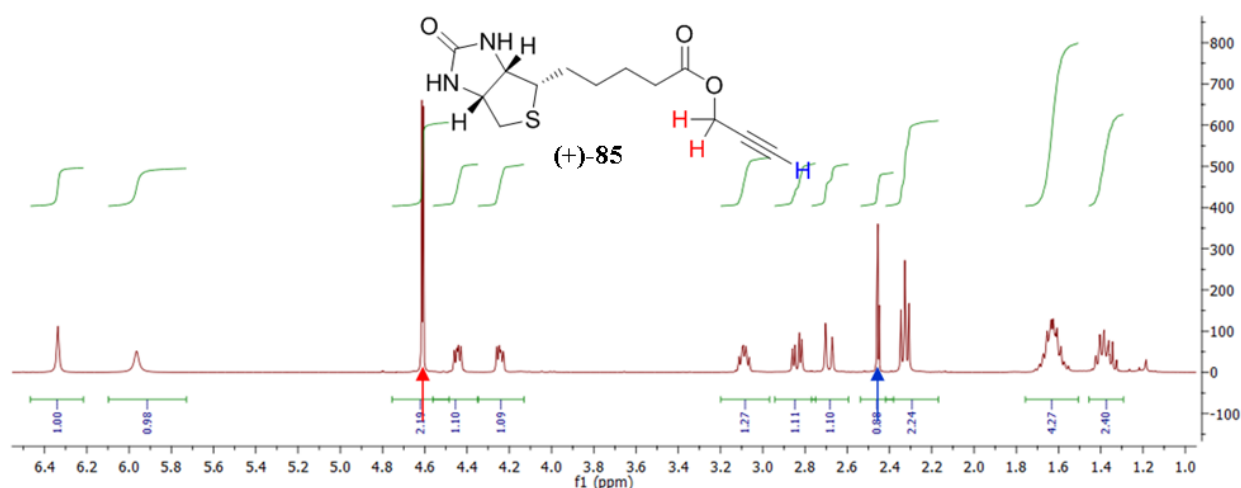
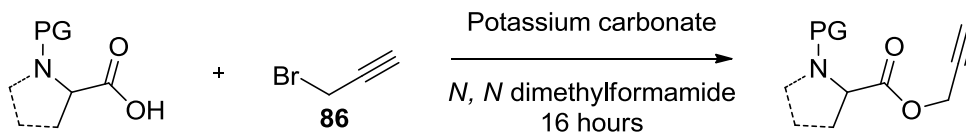


Figure 45 ¹H-NMR (400MHz) spectrum of (+)-biotin propargyl ester (+)-**85**.

The *O*-propargylation of carboxylic acids has not been widely reported, and a Scifinder search afforded only ~10 hits (2010), with the increasing popularity of ‘click’ (Huisgen 1,3-dipolar cycloaddition) chemistry amongst the research community it was thought that development of the facile *O*-propargylation reaction should be more extensively investigated.

4.3 Propargyl ester synthesis of *N*-protected α / β - amino acids

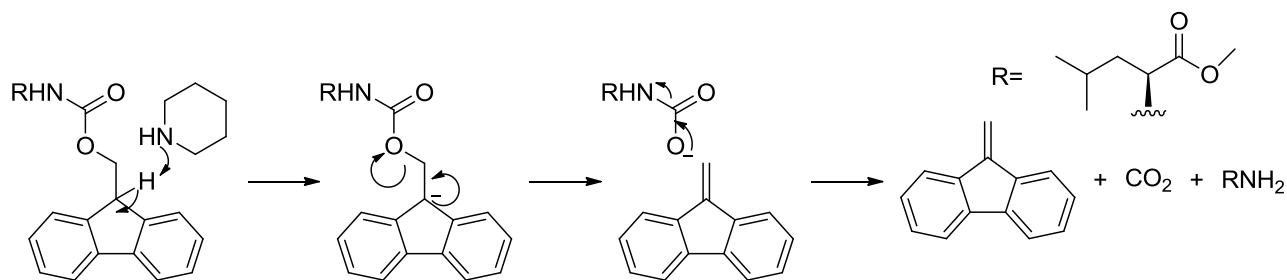
A selection of structurally and functionally diverse *N*-protected α - or β - amino acids were chosen, including known *O*-propargyl esters which afforded poor yields or were synthesised by other methods. Investigating the possibility that our reaction would be an improvement, these were subjected to our reaction conditions [Scheme 32].



Scheme 32 General reaction scheme for the mild synthesis of propargyl esters **87-104**

The S_N2 *O*-propargylation [Scheme 32], afforded the corresponding esters **87-104** [Table 1] for a plethora of *N*-protected α - and β -amino acids. The carboxylic acid functionality of natural, unnatural, α - and β -amino acid substrates were successfully *O*-propargylated in good to excellent yields *i.e.* 41-95%. [Table 1] However, *N*-fmoc and *N*-acetyl protecting groups were not compatible with our conditions, it is known that these groups are removed by relatively weak basic reaction conditions [Scheme 33].¹²⁵ It was also essential that the optical activity of the stereogenic centre within the α -amino acids was retained during the reaction as basic conditions have been reported to racemise enantiomerically pure α -amino acids.¹²⁵

After an aqueous work up **87-104** was filtered through NH_2 loaded silica³, eluting with dichloromethane, this removed unreacted α - or β -amino acid and propargyl bromide **86**. Subsequent ¹H-NMR (400MHz) analysis confirmed the desired compounds were generated in purities <95% and did not require flash chromatography.



Scheme 33 Reaction mechanism for *N*-Fmoc deprotection with piperidine

Product	Yield %	Product	Yield %	Product	Yield %
 (+/-) 87	83	 (S)-88	95	 (S)-89	65 (14)

³ Isolute preppacked flash chromatography cartridge, containing amino functionalised silica.

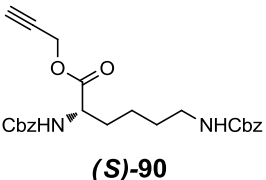
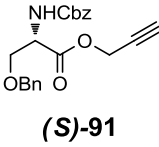
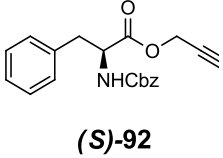
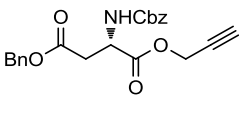
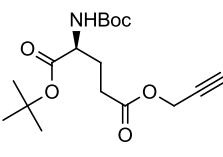
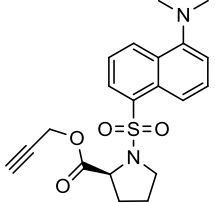
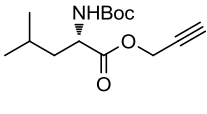
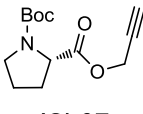
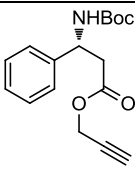
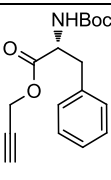
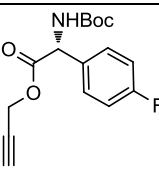
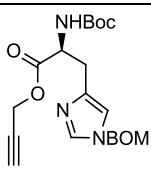
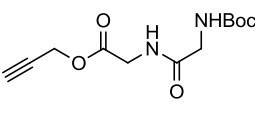
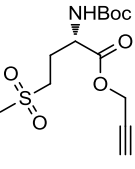
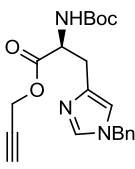
	85		81		86 (62)
(S)-90		(S)-91		(S)-92	
	82		89		85
(S)-93		(S)-94		(S)-95	
	92		95		85
(S)-96		(S)-97		(R)-98	
	91		86		43
(R)-99		(R)-100		(S)-101	
	67		71		41
102		(S)-103		(S)-104	

Table 1 Synthesis of α -, β - amino acid derived propargyl esters

The *O*-propargyl ester of (+)-biotin (+)-**85** was excluded from the communication for several reasons; firstly it was not a *N*-protected amino acid and secondly it required purification, unlike the α -, β -amino acids, *via* flash column chromatography.¹⁰⁵ We were delighted to see that the structurally and functionally diverse propargyl esters **87-104** were synthesised in good to excellent yields *i.e.* (43-95%). It was particularly noteworthy that the new procedure afforded improved yields for the synthesis of *N*-boc-(*S*)-serine-*O*-propargyl ester (**S**)-**89**, reported by Sanda *et al.* in a disappointing 14% yield *via* 1-[3-(dimethylaminopropyl)-3-ethylcarbodiimide hydrochloride (EDC•HCl) coupling of *N*-boc-(*S*)-serine with propargyl alcohol **84**.¹²² *N*-Cbz-(*S*)-phenylalanine propargyl ester **92** was also reported in 1977 by Loeffler *et al.* with a 62% yield, using a triethylamine base, however, this required elevated temperatures (75°C) and purification by flash

column chromatography.¹²⁶ The propargyl esters **87-104** are the first examples of such compounds, reported by Bew and Hiatt-Gipson.¹⁰⁵

Synthesis of *N*-dansyl-*L*-proline propargyl ester (**S**)-**95** employing our procedure was particularly gratifying. It was felt that this substrate could have significant potential as a readily employed 'clickable' end capping fluorophore for protein and peptide applications and could easily be utilized by biologists as a fluorescence probe, both in *vitro* and *vivo*.¹²⁷

The ¹H-NMR (400MHz) spectra of (**S**)-**95** displayed a clear triplet for the alkynyl proton δ2.44 (t, *J*2.5 Hz) and the propargyl methylene δ4.50 (d, *J*2.5 Hz). The ¹H-NMR(400MHz) spectrum [Figure 46] following purification by Isolute NH₂ loaded silica, is shown below and indicates the excellent levels of purity routinely generated in this protocol, >95% by ¹H-NMR.

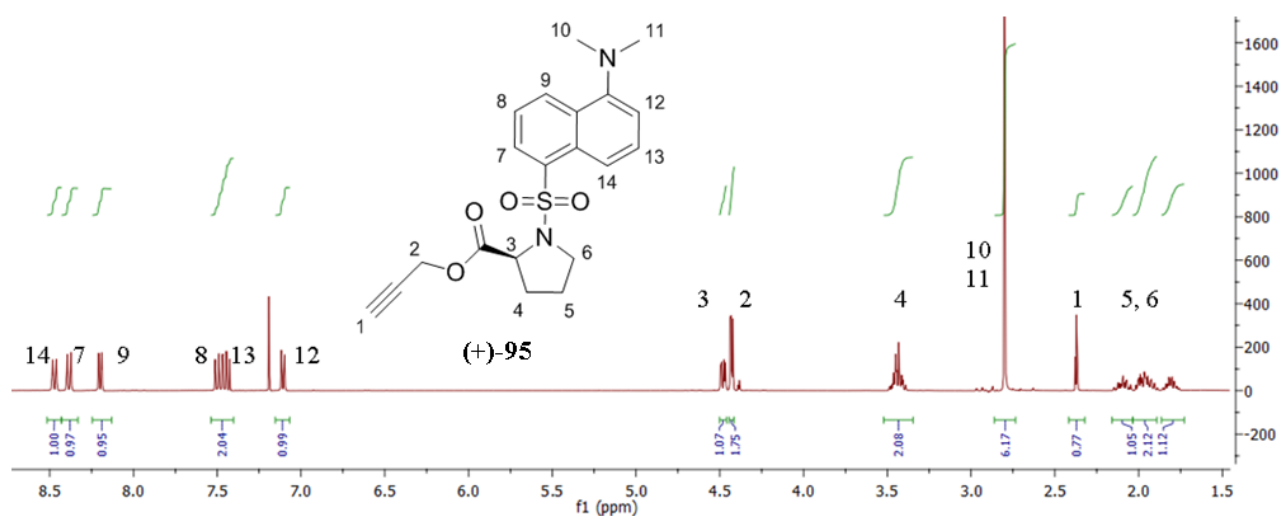
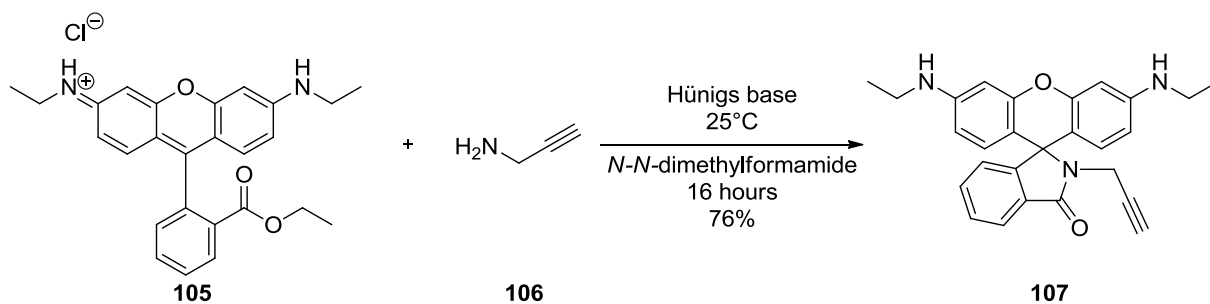


Figure 46 ¹H-NMR of *N*-dansyl-(*L*)-proline-*O*-propargyl ester a novel 'clickable' fluorophore

The synthesis of 'clickable' fluorophores is of interest to the research community; they are frequently used in molecular biology, for 'tracing' interactions in *vivo* and *vitro*,¹²⁷ and in physical chemistry, for excitation by LASER radiation.¹²⁸ Rhodamine 6G **105** is routinely employed as a LASER dye that is excited by Nd:YAG and nitrogen LASERS at 1064 nm and 331.1 nm respectively. A procedure to modify rhodamine 6G **105** into a 'clickable' substrate was, at the time we required it, unreported. With this in mind we opted to adapt a procedure reported to incorporate a propargyl group. With this in mind rhodamine 6G **105** was left to stir for 16 hours, under an atmosphere of argon at room temperature, with propargylamine **106** and Hünigs base in *N,N*-dimethylformamide. Following an aqueous workup and recrystallisation from ethanol afforded a crystalline pink solid. The small pink platelets were submitted for X-ray crystallographic diffraction analysis. Thus confirming a propargyl rhodamine analogue **107**, had indeed been generated and in good yield 76%.



Scheme 34 Synthesis of propargyl rhodamine 6G **107**

Interestingly the X-ray structure of **107** showed that there was no π – stacking observed, which, was peculiar for this type of aromatic compound. Presumably this was due to the perpendicular group, in a fixed configuration, that was hindering the stacking.

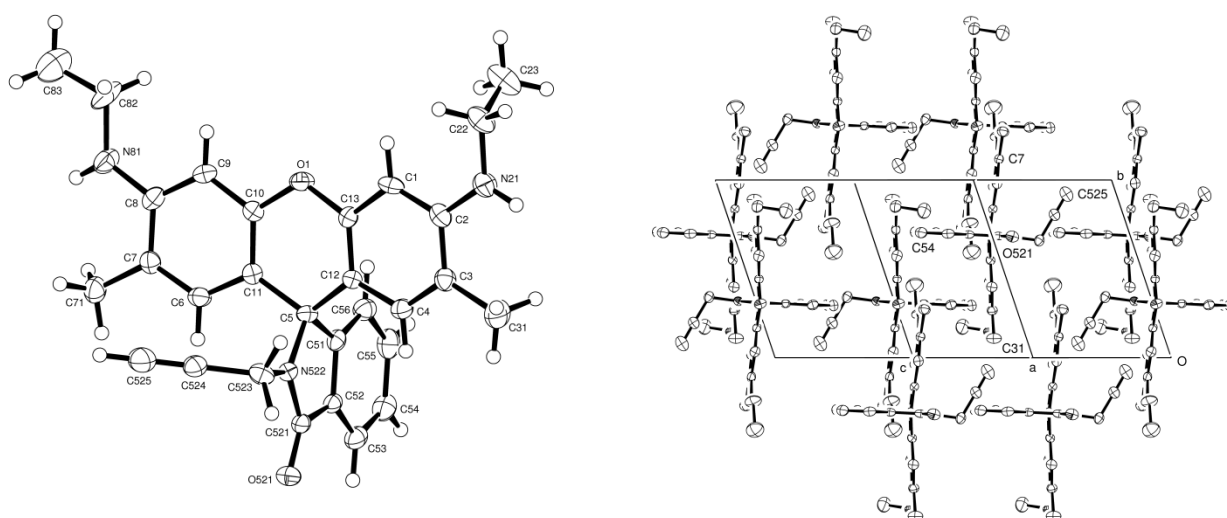
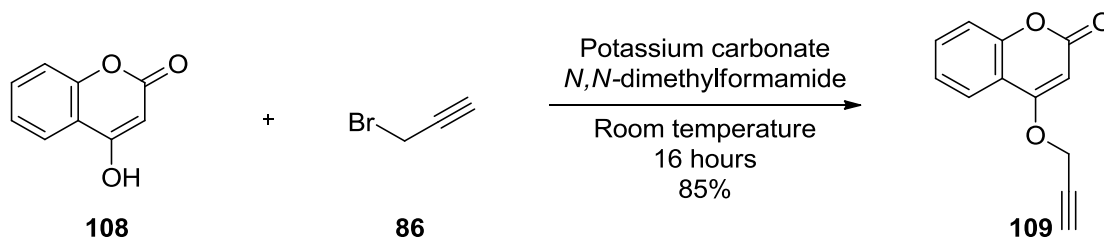


Figure 47 Crystal structure of propargyl rhodamine 6G **107**. Data collected and structure solved by Dr. D. Hughes, UEA.

Finally, 4-hydroxycoumarin **108**, a member of the vitamin K antagonists anticoagulant drug molecules, was subjected to our procedure (outlined in Scheme 35) thus affording phenolic propargyl ether 4-hydroxy coumarin **109**. This utilised the stability of the phenoxide type anion, to increase the nucleophilicity of the alcohol.



Scheme 35 Synthesis of 4-propargyl ether coumarin **109**

4.4 Synthesis of 2,8-bis(4-substituted-5H-1,2,3-triazol-1-yl)-6,12-dihydro-5,11-methano dibenzo[b,f][1,5]diazocines

With a selection of alkynes **87–104** and 2,8-bis-azido Tröger's base motif (+/-)-**79** in hand, we were ready to attempt the synthesis of 2,8-bis-(4-substituted-5H-1,2,3-triazol-1-yl)-6,12-dihydro-5,11-methanodibenzo[b,f][1,5]diazocines **112–120**. Although Tröger's base is not a traditional *beta*-turn director, as it turns through only 90°, it bears a resemblance to proline, a known constituent of *beta*-turn directors. Proline has an angle of 90° [Figure 48 A], however when it's found in a peptide chain it will direct through 180°. Figure 48 B and C display the 90° turn of the Tröger's base scaffold, the 1,2,3 triazole should be in the 1,4-configuration and not in the 1, 5-configuration [Figure 48 B and C] this we anticipate would aid Tröger's base afford a 90° turn between the 2, 8- appended motifs.

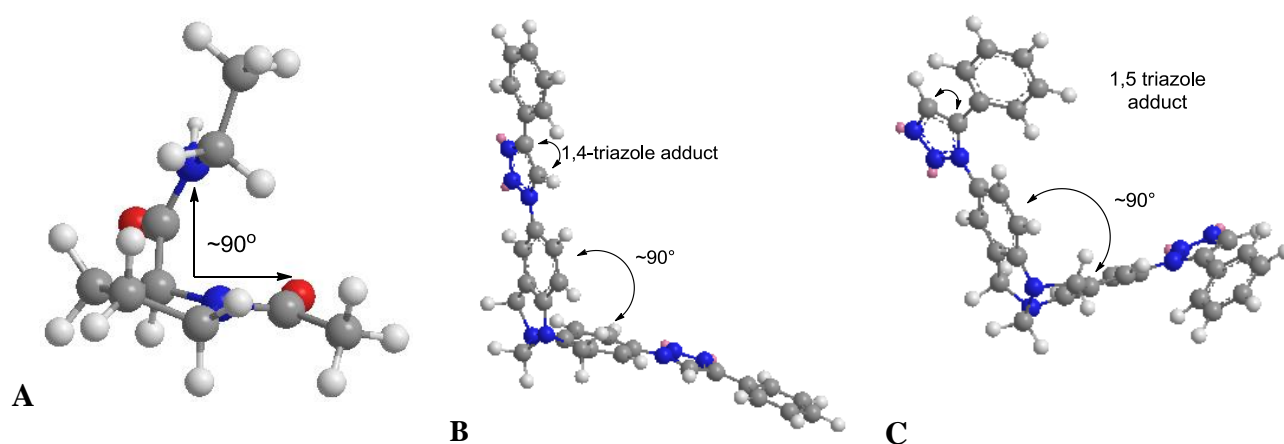
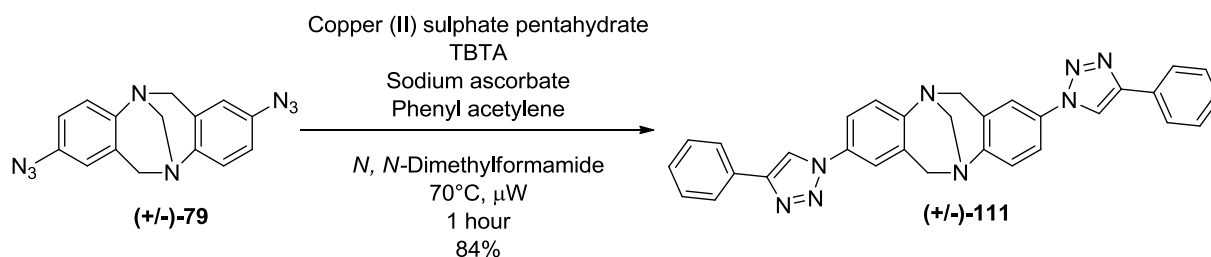


Figure 48 A) Chem 3D structure of β -turn director (L)-proline affording a 90° turn *via* the amino and carboxylic acid functionality. B) Tröger's base analogue affording a 90° angle and extension properties of the 4-substituted 1,2,3-triazole. C) Tröger's base analogue affording 90° angle and non-extending properties of 5-substituted 1,2,3-triazole.

A model reaction with phenyl acetylene **110** and (+/-)-**79** was attempted using a copper(I) catalysed Huisgen 1,3-dipolar cycloaddition. Copper(II) sulfate pentahydrate, TBTA (*tris*[(1-benzyl-1H-1,2,3-triazol-4-yl)methyl]amine), sodium-(L)-ascorbate in *N,N*-dimethylformamide the synthesis of (+/-) **111** was attempted. 2,8-Bis-azido Tröger's base (+/-)-**79**, phenyl acetylene **110** and the above reagents were sealed in a microwave vial and heated to 70°C, (*via*-microwave irradiation) for 1 hour, before an aqueous work up and extraction with ethyl acetate was employed to remove the *N,N*-dimethylformamide.



Scheme 36 Model 'click' reaction of 2,8-*bis*-azido Tröger's base (+/-)-**79** with phenylacetylene **110**

Purification of (+/-)-**111** by flash column chromatography on silica gel, eluting with diethyl-ether, afforded a white solid that was recrystallised from dichloromethane (+/-)-**111** was afforded as orthorhombic, colourless crystals. Subsequent X-ray diffraction analysis confirmed the product had not only been synthesised in a good yield (84%) but it was also in the desired 1,4-configuration [Figure 49 A]. The crystal structure affords both enantiomers (*RR*)-**111** and (*SS*)-**111** were formed in equal amounts [Figure 49 B] and an interlocking packing system [Figure 49 C], which indicates the π -stacking of the aromatic systems of the triazoles, Tröger's base and phenyl ring systems. The angle between the aromatic planes of (+/-)-**111** was calculated using:

Least-squares planes (x,y,z in crystal coordinates) and deviations from them
 (* indicates atom used to define plane)

$$13.0261 (0.0131) x + 1.6108 (0.0062) y - 8.4602 (0.0045) z = 8.8029 (0.0101)$$

- * 0.1179 (0.0007) N1_\$1
- * -0.0980 (0.0007) N1
- * -0.1333 (0.0010) C1_\$1
- * 0.0710 (0.0009) C11
- * 0.0424 (0.0010) C16

Rms deviation of fitted atoms = 0.0981

$$13.0261 (0.0131) x + 1.6108 (0.0062) y + 8.4602 (0.0045) z = 11.5416 (0.0101)$$

Angle to previous plane (with approximate su) = 71.97 (0.04)

- * 0.0980 (0.0007) N1_\$1
- * -0.1179 (0.0007) N1
- * 0.1333 (0.0010) C1
- * -0.0710 (0.0009) C11_\$1
- * -0.0424 (0.0010) C16_\$1

Rms deviation of fitted atoms = 0.0981

Thus the angle between the planes equals $180 - 71.97 = 108.03^\circ$ (+/- 0.04)

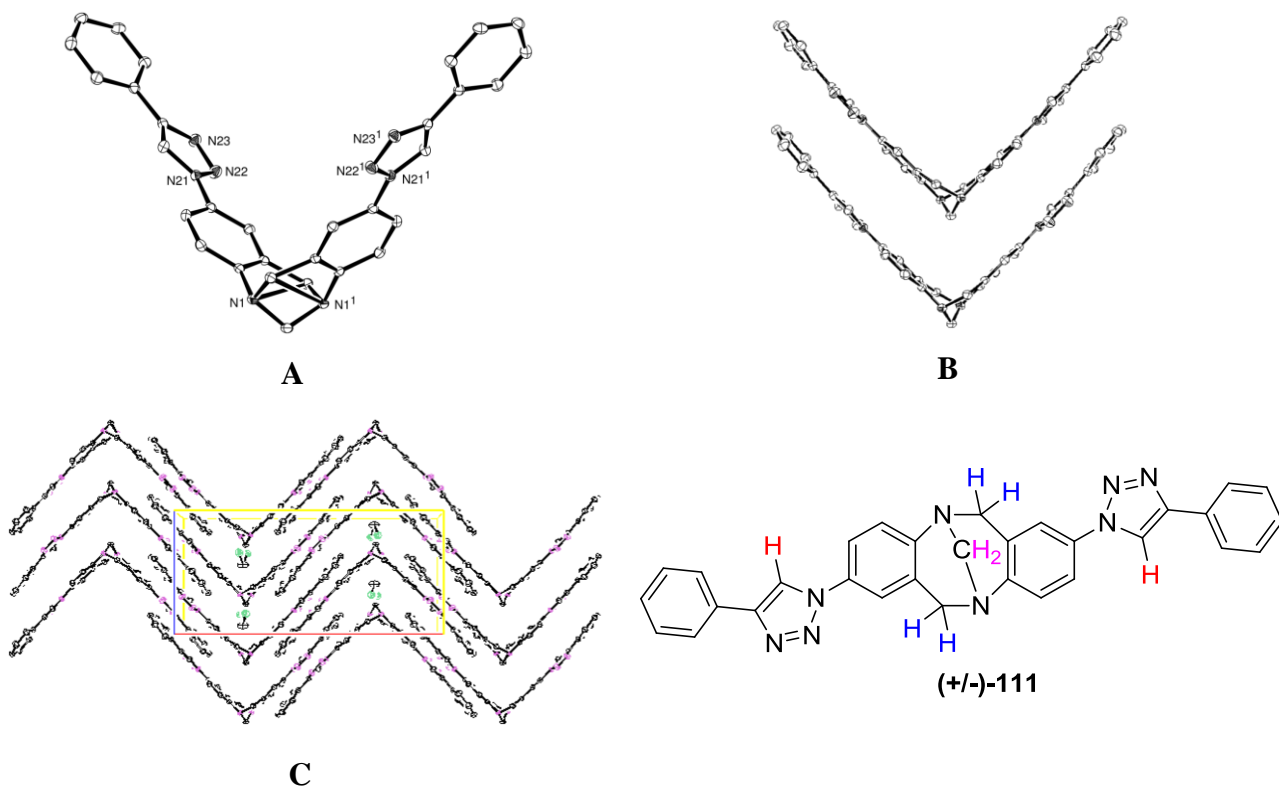


Figure 49 Crystal structure of 2, 8 bis-(4-phenyl-1H-1,2,3-triazole)-6H, 12H-5, 11-methandibenzo[b,f][1,5]diazocine (+/-)-**111** and structure of (+/-)-**111**. Data collected and structure solved by Dr. M. Schorman, UEA

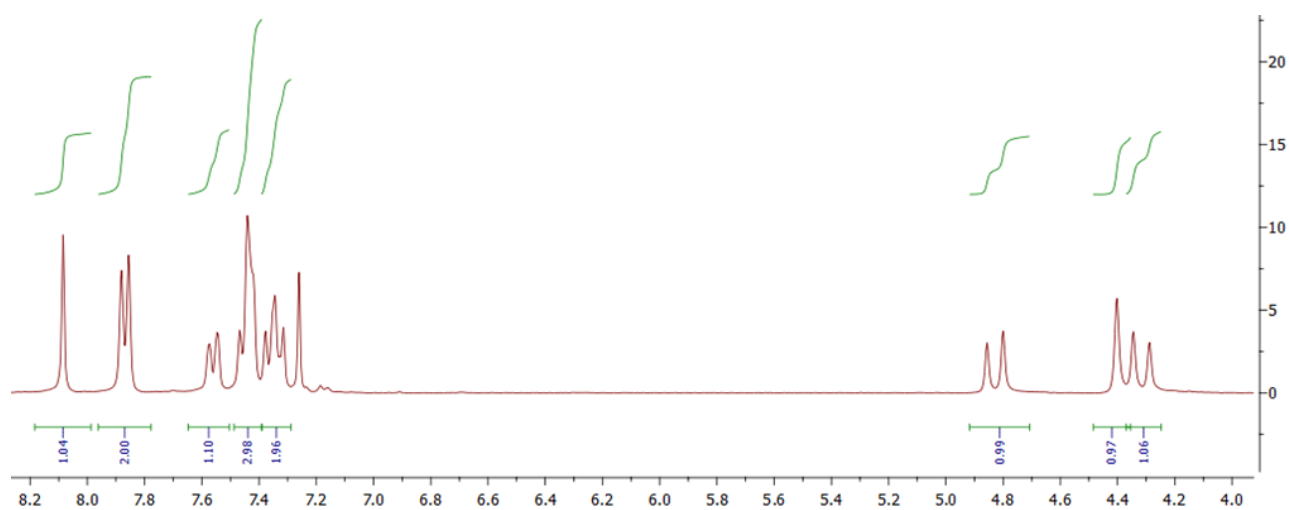


Figure 50 $^1\text{H-NMR}$ (300MHz) of (+/-)-**111**

The $^1\text{H-NMR}$ (300 MHz) of (+/-)-**111** shows the C₅ triazole proton, as a singlet at δ 8.08, this agrees with literature values for a proton on the C₅ of a 1,2,3-triazole. The Tröger's base *exo* and *endo* methylenes of (+/-)-**111** were doublets at δ 4.83 (J 16.8 Hz) and δ 4.32 (J 16.8 Hz) respectively, the singlet at δ 4.40 was associated with the bridge head methylene protons, indicating the scaffold was not ring opened by the reaction conditions employed. With the success of this, the first example of a 1,2,3-triazole containing Tröger's base analogue (+/-)-**111**, we opted to construct a small library of *bis*-appended analogues [**112-120**].

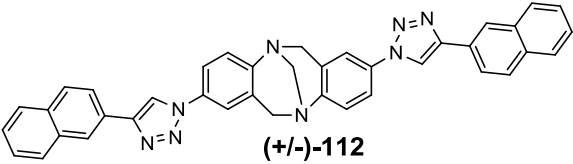
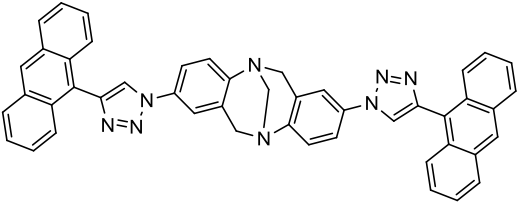
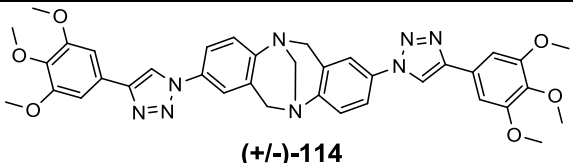
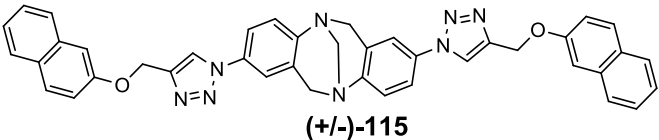
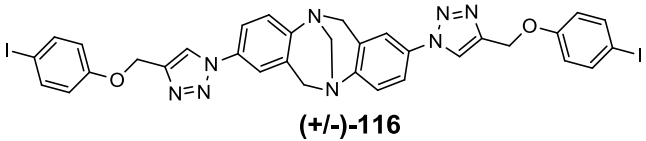
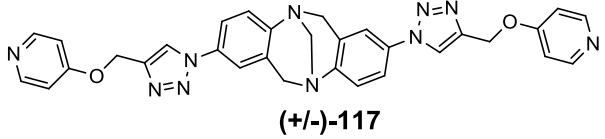
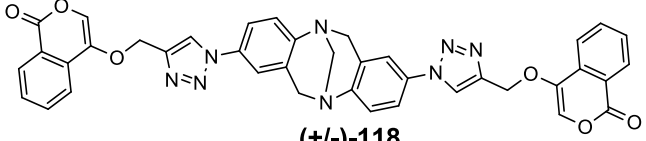
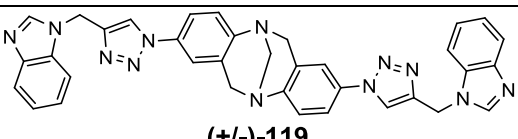
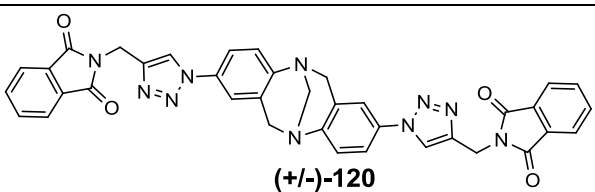
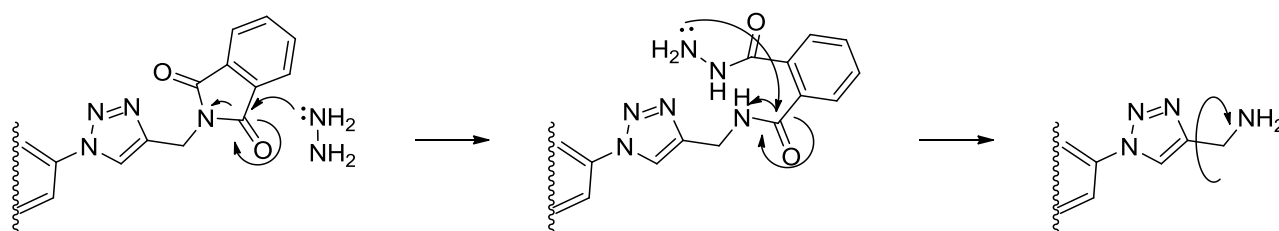
2,8-bis(4-substituted-5H-1,2,3-triazol-1-yl)-6,12-dihydro-5,11-methanodibenzo[b,f][1,5]diazocines 112-120	1,2,3 Triazole C ₅ Proton ppm	Yield %
 <p style="text-align: center;">(+/-)-112</p>	88.32 (CDCl ₃)	95
 <p style="text-align: center;">(+/-)-113</p>	88.53 (CDCl ₃)	74
 <p style="text-align: center;">(+/-)-114</p>	88.06 (CDCl ₃)	93
 <p style="text-align: center;">(+/-)-115</p>	87.95 (CDCl ₃)	70
 <p style="text-align: center;">(+/-)-116</p>	δ 7.88 (CDCl ₃)	78
 <p style="text-align: center;">(+/-)-117</p>	δ 8.66 (DMSO)	55
 <p style="text-align: center;">(+/-)-118</p>	δ 7.98 (CDCl ₃)	70
 <p style="text-align: center;">(+/-)-119</p>	δ 8.02 (CDCl ₃)	72
 <p style="text-align: center;">(+/-)-120</p>	δ 7.90 (CDCl ₃)	74

Table 2 Synthesis of racemic 2,8-bis(4-substituted-5H-1,2,3-triazol-1-yl)-6,12-dihydro-5,11-methanodibenzo[b,f][1,5]-diazocines **112-120**.

111 - 120 were all synthesised in good *i.e.* 55% to excellent *i.e.* 95% yields, of particular interest within this library is (+/-)-**116** and (+/-)-**120**. (+/-)-**116** provides access to an aryl extended Tröger's base with the possibility of functionalising the carbon-iodine bond using transition-metal based chemistry for example Sonogashira or Suzuki couplings. (+/-)-**120** is the phthalimide protected amine which can be liberated to form the amine by hydrazinolysis.[Scheme 37] This would be useful for subsequent amine coupling reactions for example amide bond formation and the methylene between the triazole and amine would allow for greater rotation.



Scheme 37 Proposed Gabriel deprotection of phthalimide Tröger's base derivative (+/-)-**120** affording a primary amine with rotation around the methylene.

4.5 Synthesis of 2,8-bis(4-*N*-protected- α - or β -amino acids-5H-1,2,3-triazol-1-yl)-6,12-dihydro-5,11-methanodibenzo[b,f][1,5]diazocines

With **111-120** in hand, we turned our attention to the application of the *O*-propargyl-*N*-protected amino acids **121-130**, submitting them to the same procedure as the above examples **111 – 120**.

2,8-bis(4- <i>N</i> -protected-amino acid-5H-1,2,3-triazol-1-yl)-6,12-dihydro-5,11-methanodibenzo[b,f][1,5]diazocines 121-130	1,2,3 Triazole C ₅ Proton ppm	Yield %
<p style="text-align: center;">121</p>	7.97 (CDCl ₃)	74
<p style="text-align: center;">122</p>	7.82 (CDCl ₃)	76
<p style="text-align: center;">123</p>	7.82 (CDCl ₃)	74

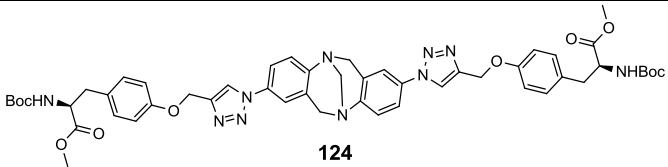
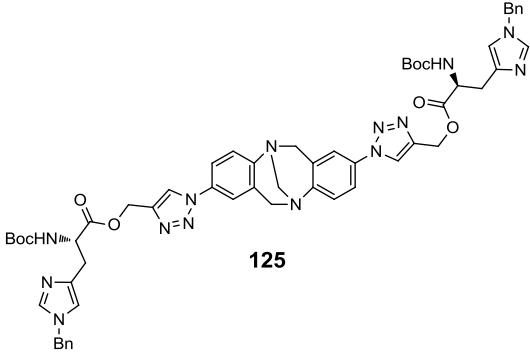
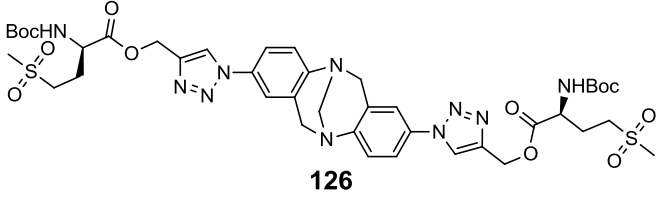
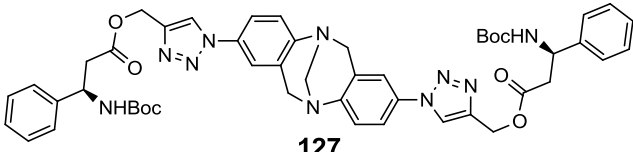
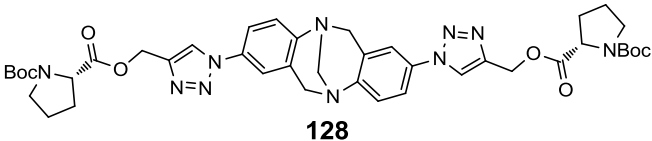
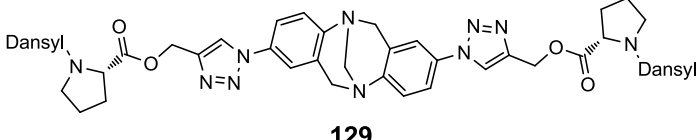
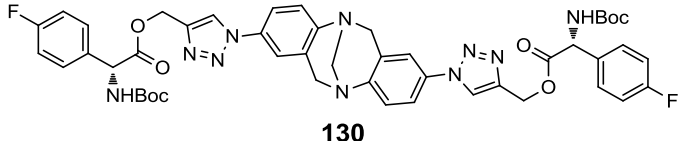
 <p style="text-align: center;">124</p>	7.91 (CDCl ₃)	63
 <p style="text-align: center;">125</p>	7.99 (CDCl ₃)	71
 <p style="text-align: center;">126</p>	7.96 (CDCl ₃)	64
 <p style="text-align: center;">127</p>	7.72 (CDCl ₃)	61
 <p style="text-align: center;">128</p>	8.08 (CDCl ₃)	60
 <p style="text-align: center;">129</p>	8.46 (CDCl ₃)	68
 <p style="text-align: center;">130</p>	7.73 (CDCl ₃)	57

Table 3 Synthesis of 2,8-bis(4-*N*-protected-amino acid-5H-1,2,3-triazol-1-yl)-6,12-dihydro-5,11-methanodibenzo[b,f][1,5]diazocines **121-130**.

The copper(I) catalysed Huisgen 1,3-dipolar cycloaddition worked very well affording the desired *N*-protected- α - β -amino acid derived substrates **121-130** in good yields *i.e.* 57-74%. Of particular interest was the incorporation of unnatural *para*-fluoro-*N*-boc-(*R*)-phenylglycine **130**, it was envisaged that this could serve as an unusual biological probe using ¹⁹F-NMR analysis. As fluorine is rarely found in natural biological systems it can be incorporated into peptides and the changes in

conformation due to interactions with the lipid membranes of cells can be traced by ^{19}F -NMR analysis see Figure 51.¹²⁹

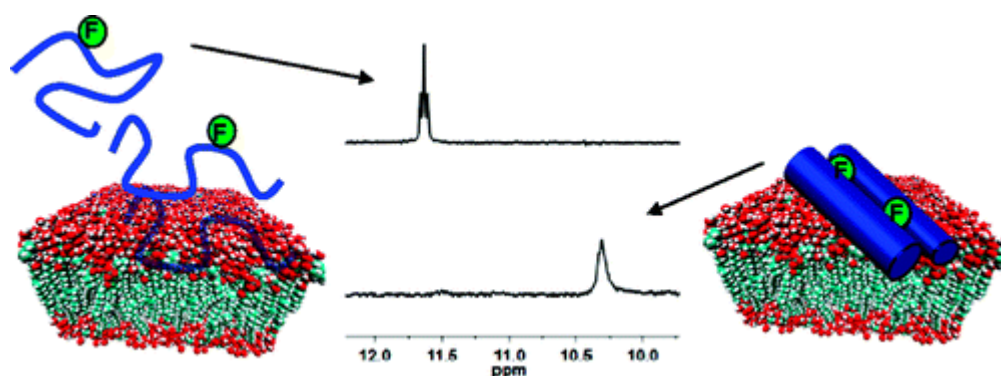


Figure 51 Incorporation of fluorine into peptides, followed by introduction to cells affords changes in conformation that can be detected by ^{19}F -NMR analysis.¹²⁹

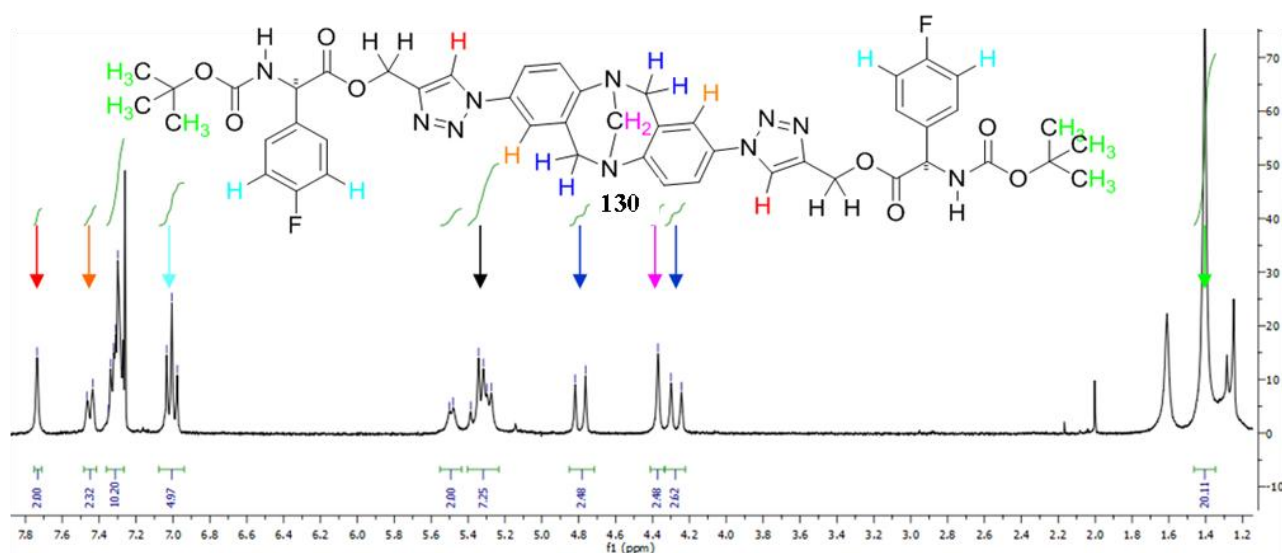
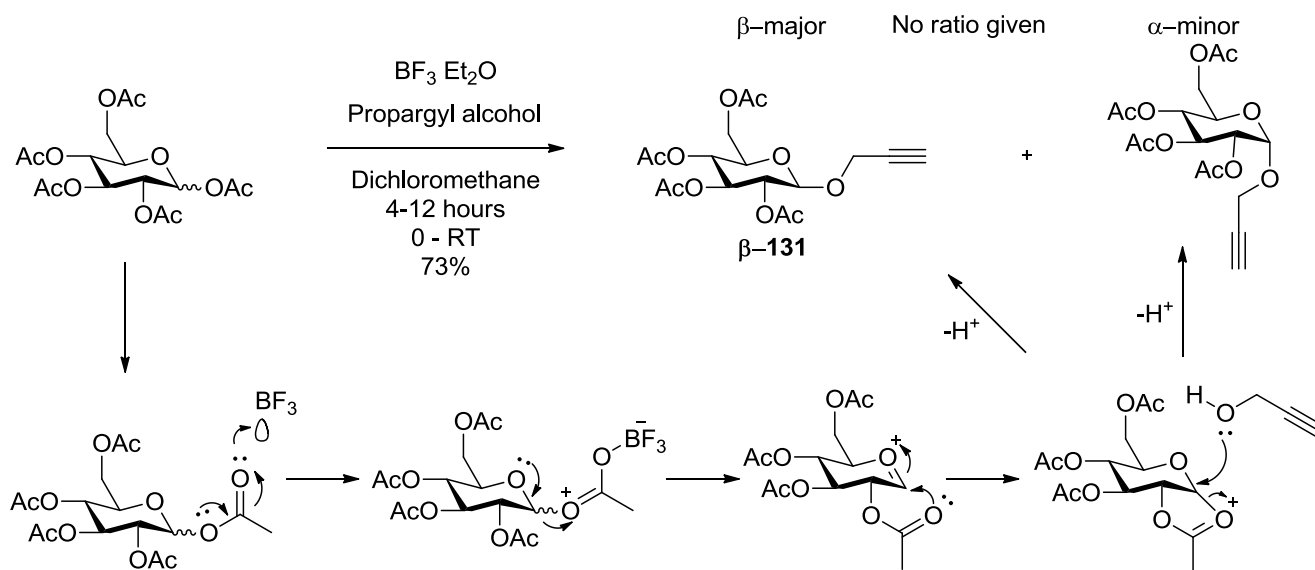


Figure 52 ^1H -NMR (300 MHz) of **130**

In the ^1H -NMR (300MHz) spectrum of **130** the C_5 -1,2,3-triazole proton was observed as a singlet at $\delta 7.73$, the characteristic Tröger's base *exo* and *endo* methylenes were observed as doublets at $\delta 4.79$ ($J_{16.7}$ Hz) and $\delta 4.27$ ($J_{17.0}$ Hz) respectively, and the singlet at $\delta 4.37$ corresponds to the bridge head methylene protons. The expected doublet associated with the *meta*-protons (light blue on aromatic ring) was split by the neighbouring fluorine affording a triplet at $\delta 7.01$ ($J_{8.6}$ Hz). An optical rotation of **130**, $[\alpha]_{\text{D}}^{26} -8.6$ (c 1.0, CHCl_3), indicated that the stereogenic centre of **130** has been preserved, however, no further investigations were undertaken *i.e.* chiral HPLC analysis, to confirm this.

4.6 Synthesis of symmetrical 2,8-bis(4-*O*-protected-carbohydrates-5H-1,2,3-triazol-1-yl)-6,12-dihydro-5,11-methanodibenzo [b,f][1,5]diazocines.

Following the successful synthesis of α - β -*N*-protected amino acid derived analogues **121-130** we turned our attention to the synthesis of carbohydrate derived Tröger's base analogues **121-130**. Protected *O*-acetate monosaccharide's, (*i.e.* glucose, galactose, mannose) and disaccharides (*i.e.* lactose, maltose) were *O*-propargylated at the anomeric-carbon using a protocol of Mereyala *et al*, who took *O*-acetate-protected carbohydrates, stirring them with the Lewis acid boron trifluoride diethyl etherate and an excess of propargyl alcohol **84**.¹³⁰



Scheme 38 Reaction mechanism for synthesis of *O*-acetate protected propargyl- β -glucose utilising the neighbouring effect of the C₂ acetate group.

By employing the *O*-acetate protecting group we have strategically employed the neighbouring group effect which affects the ratio of α - and β - glycoside formation. In summary the acetate at C₂ forms the acetoxonium ion which hinders attack of propargyl alcohol **84** from the bottom face, therefore affording the β -glycoside in preference to the α -glycoside. The major product of the glycosylation was the β -glycoside (**β** -131). The β -propargyl glycosides of glucose **131**, galactose, maltose and lactose *O*-acetates, were all synthesised following Mereyala *et al.* procedure. These were all separated from the α -anomer by column chromatography and data collected matched the literature values for the β -anomers.¹³⁰ The ¹H-NMR (300MHz) spectra of (**β** -131 [Figure 53] afforded signals matching the β -anomer as reported by Mereyala *et al.*¹³⁰ The coupling constant between C₁ δ 5.20 (t, *J*9.5 Hz) and C₂ 4.97 (dd, *J*9.6 Hz) afforded an axial-axial interaction, affording an angle of 180° between the protons thus a greater coupling constant than would be observed for the α -anomer.

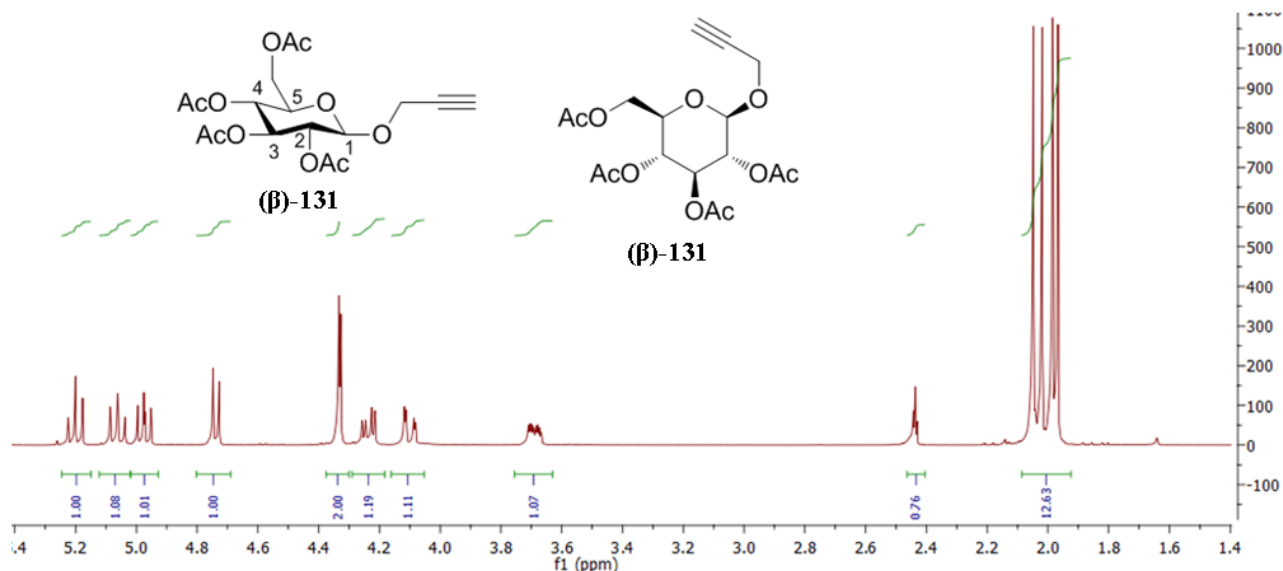
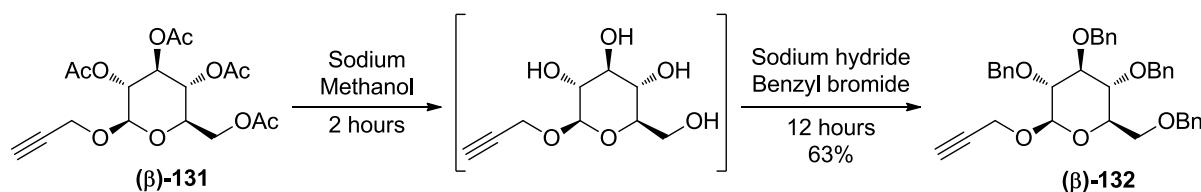


Figure 53 $^1\text{H-NMR}$ (300MHz) spectrum of *O*-acetate- β -glucose-propargyl ether (**β -131**)

For the *O*-benzyl protected- β -glucose (**β -132**) the *tetra-O*-acetate (**β -131**) was reacted with sodium in methanol, generating sodium methoxide *in situ*, this hydrolysed the acetates allowing the deprotonation of the hydroxyls with sodium hydride and addition of benzyl bromide afforded the corresponding *O*-benzyl protected β glucose (**β -132**). The physicochemical analysis of this substrate matched that reported by Wardrop *et al.*¹³¹



Scheme 39 Synthetic route to *O*-benzyl- β -glucose-propargyl ether **β -132**

The propargyl β -carbohydrates were then coupled to the Tröger's base scaffold (+/-)-**79** via a copper(I) catalysed Huisgen 1,3-dipolar cycloaddition using the same conditions as previously described, affording **133-136**.

Symmetrical 2,8- <i>bis</i> (4- <i>O</i> -protected- β -carbohydrates-5H-1,2,3-triazol-1-yl)-6,12-dihydro-5,11-methanodibenzo [b,f][1,5]diazocines	1,2,3 Triazole C ₅ Proton ppm	Yield %
<p style="text-align: center;">133</p>	7.76 (CDCl ₃)	82

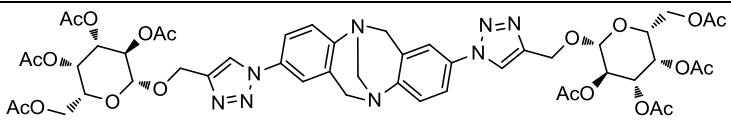
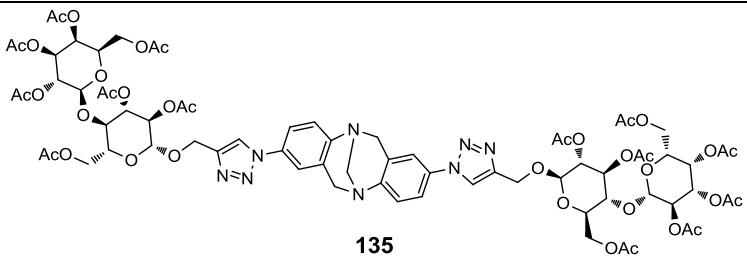
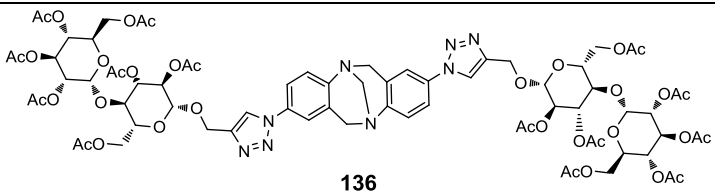
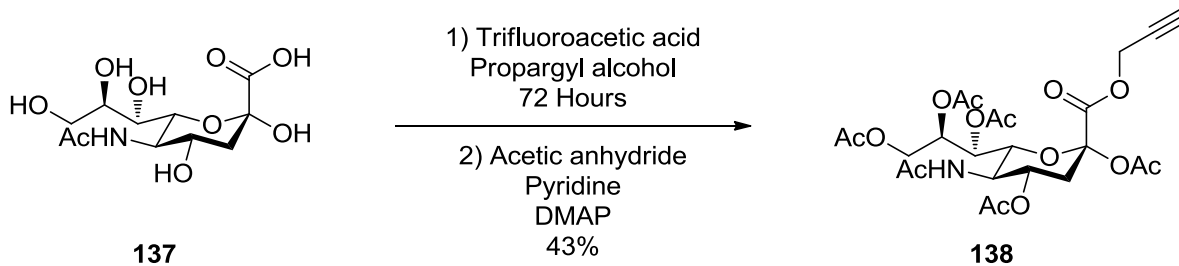
 <p style="text-align: center;">134</p>	7.88 (CDCl ₃)	82
 <p style="text-align: center;">135</p>	7.78 (CDCl ₃)	80
 <p style="text-align: center;">136</p>	7.85 (CDCl ₃)	68

Table 4 Synthesis of Symmetrical 2,8-*bis*(4-*O*-protected- β -carbohydrates-5H-1,2,3-triazol-1-yl)-6,12-dihydro-5,11-methanodibenzo [b,f][1,5]diazocines **133-136**.

For the final carbohydrate derivative in this series, a Sialic acid, *N*-acetylneuraminic acid (Neu5Ac) **137** was chosen due to its importance in nature as it is found on the surface of all mammalian cells. Sialic acids are found in many cells, including both prokaryotic and eukaryotic, they have an important role in biological processes such as cell-cell recognition and small molecule-cell recognition. The generic term Sialic acid is used to describe the family of nine carbon containing carbohydrate acids and they are found at the surface of many eukaryotic cells. They confer important properties to the cell surface. Bacteria have found a use for Sialic acids in order to resist the hosts' immune responses and to interact with host cell surfaces. The most abundant of these Sialic acids is Neu5Ac.¹³²

137 was modified to afford the first example propargylated Neu5Ac **138**. **138** was prepared following a modified procedure by Baumberger *et al.* who reported an example of a methyl ester derivative of Neu5Ac. The sialic acid **137** was suspended in propargyl alcohol **84** and one equivalent of trifluoroacetic acid added. The suspension was warmed to 40°C and left to stir for 72 hours under an atmosphere of argon.¹³³ The unreacted Neu5Ac **137** was filtered off through a short plug of silica and the solvent removed. The residue was redissolved in pyridine, followed by addition of acetic anhydride and a catalytic amount (10 mol%) of DMAP. Following flash chromatography on silica, eluting with ethyl acetate, a white solid was isolated. Subsequent physicochemical analysis indicated this was the required derivative **138** generated in a 43% yield.



Scheme 40 Synthesis of *per*-acetylated Neu5Ac propargyl ester **138**

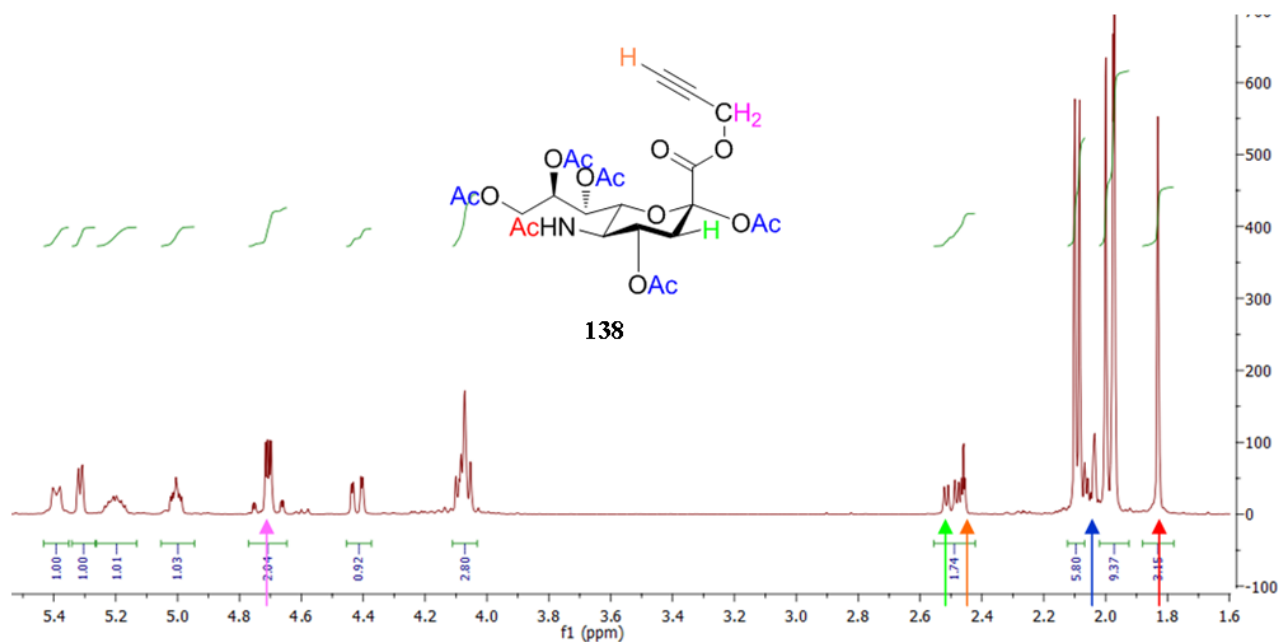


Figure 54 $^1\text{H-NMR}$ (400 MHz) of *per*-acetylated Neu5Ac propargyl ester **138**

The $^1\text{H-NMR}$ (400MHz) spectrum [Figure 54] of **138** displayed the propargyl methylene multiplet at $\delta 4.74$, the signal shown in green, (partially obscured by the alkynyl proton (orange) at $\delta 2.52$) is the equatorial proton, as reported by Johannes *et al.*, with the axial proton found upfield,¹³⁴ which in our case, is totally obscured by the *O*-acetate signals. The signal observed at $\delta 1.86$ ppm, shown in red, corresponds to the *N*-acetyl protecting group. FT-IR spectroscopy affords a strong peak 3277 & 2129cm^{-1} corresponding to the terminal alkyne proton stretch and C-C alkyne respectively.

138 was subsequently '*clicked*' under milder reaction conditions (as opposed to μW irradiation at 70° , 1 hour), to prevent its thermal decomposition a problem reported by Baumberger *et al.* at temperatures greater than 40°C .¹³³ Our procedure employed the same reagents used for previous '*click*' reactions, however, the reaction was left to stir at room temperature for 24 hours. The desired *bis*-substituted sialic acid Tröger's base adduct **139** was afforded in a 58% yield. Gratifyingly, both *N*-acetyl and *O*-acetate protecting groups were retained, [Figure 55] and an optical rotation of **139** $[\alpha]_D^{23} -27$ (c 1.0, CHCl_3) suggests that stereogenic centres were present, however, no further analysis to prove this was undertaken.

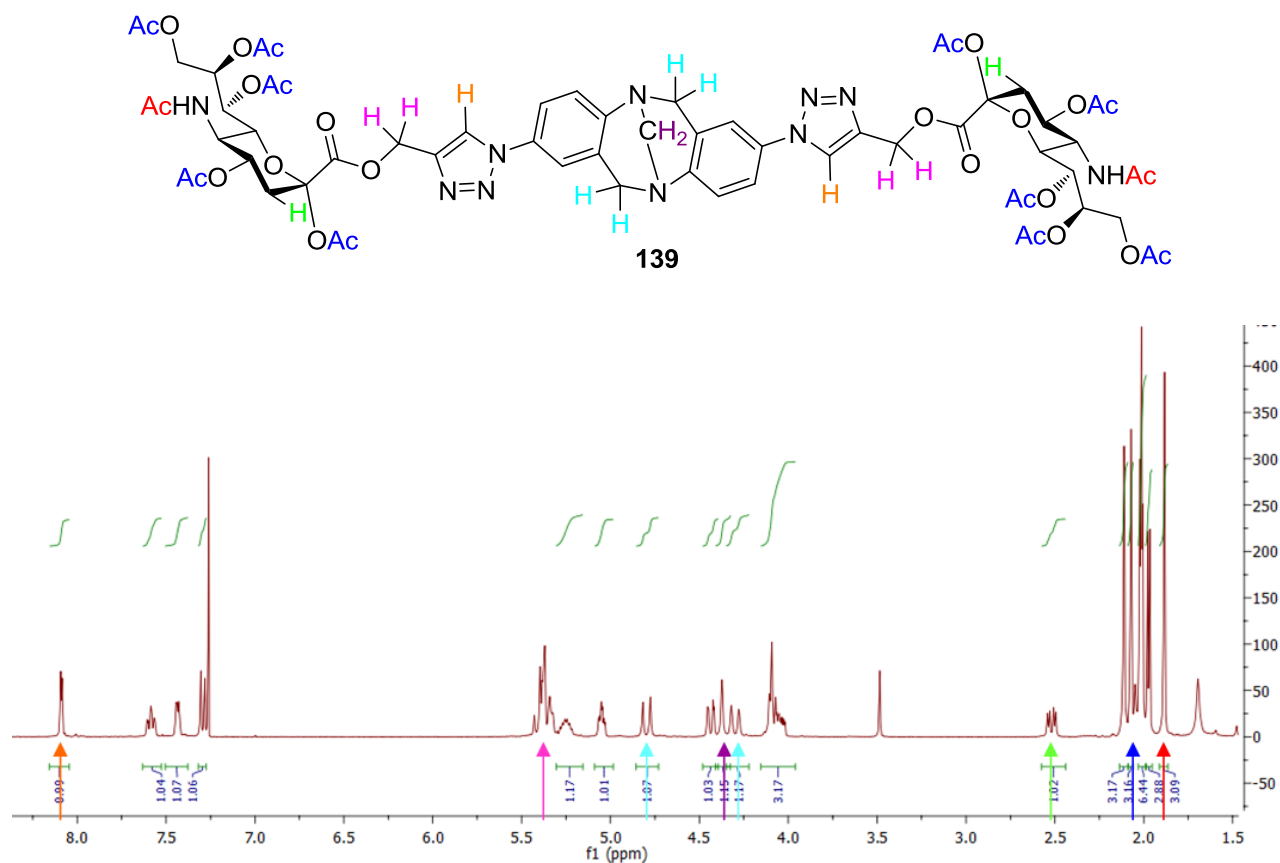
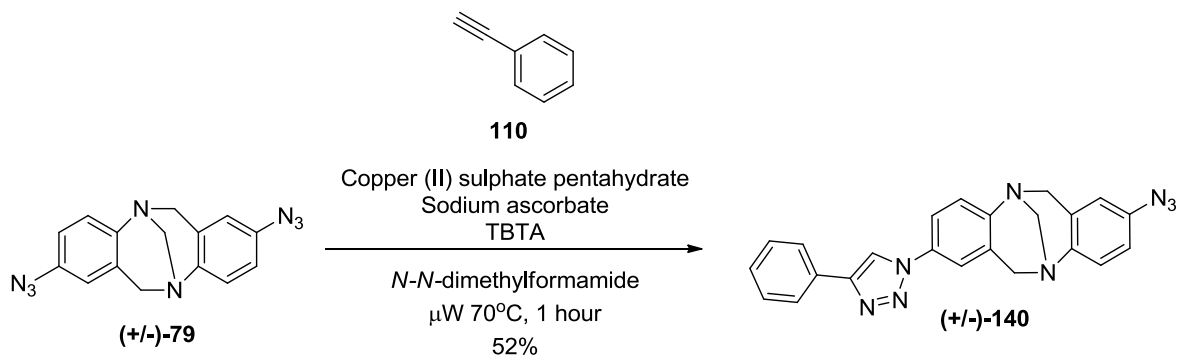


Figure 55 Structure and $^1\text{H-NMR}$ (400MHz) of 2, 8 *bis*-(((1*S*,2*R*)-1-((2*R*,3*R*,4*S*,6*R*)-3-acetamido-4,6-diacetoxy-6-(((1*H*-1,2,3-triazol-4-yl)methoxy)carbonyl) tetrahydro-2*H*-pyran-2-yl)propane-1,2,3-triyl triacetate))-6*H*, 12*H*-5, 11-methanodibenzo[*b*,*f*] [1,5]diazocine **139**

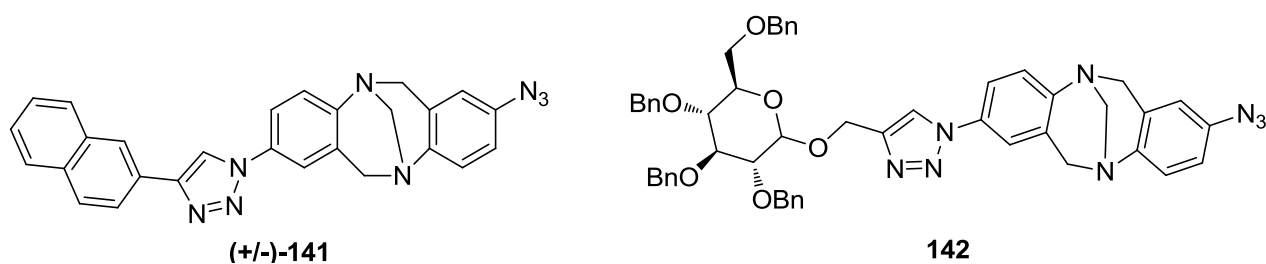
From the $^1\text{H-NMR}$ (400MHz) spectra of **139** [Figure 55], the diagnostic signal of the Neu5Ac C₃ equatorial proton at δ 2.46 (dd, J 13.4, 5.0 Hz) was clearly visible. The aromatics δ 7.52 (t, J 7.9 Hz), 7.37 (d, J 5.4 Hz), 7.23 (d, J 8.7 Hz) and methylenes 4.73 (d, J 16.9 Hz), 4.31 (s, 2H), 4.24 (d, J 17.1 Hz) (light blue and purple) associated with the Tröger's base scaffold were observed. The signal of the axial C₃ proton of Neu5Ac is still obscured by the *O*-acetates and the 1,2,3 triazole C₅ protons (orange) were observed at δ 8.09 (d, J 3.1 Hz)

4.7 Unsymmetrical 2-(4-substituted-5*H*-1,2,3-triazol-1-yl)-8-(4-substituted-5*H*-1,2,3-triazol-1-yl)-6,12-dihydro-5,11-methanodibenzo[*b*,*f*][1,5]diazocine

With the synthesis of a plethora of symmetrical 2,8-*bis*-1,2,3 triazole containing Tröger's base analogues accomplished, we attempted to de-symmetrise Tröger's base *via* chemoselective ligation at the 2- and 8- positions. One equivalent of phenyl acetylene **110** was reacted with (+/-)-**79**, using the same coupling reagents as previously employed, however the reaction was diluted to approximately 0.05M to promote a mono 'click' coupling. Gratifyingly a *mono*-substituted-1,2,3 triazole containing Tröger's base scaffold (+/-)-**140** was afforded in a 52% yield.



Scheme 41 Synthesis of 2-azido-8-(4-phenyl-1H-1,2,3-triazol-1-yl)-6,12-dihydro-5,11-methanodibenzo[b,f][1,5]diazocine (+/-)-**140**



Yield	51%		Azide FT-IR	2112 cm^{-1}		Yield	47%		Azide FT-IR	2115 cm^{-1}
-------	-----	--	----------------	-----------------------	--	-------	-----	--	----------------	-----------------------

The reaction afforded the desired product (+/-)-**140** in an unoptimised but gratifying 52% yield, following an aqueous work up and flash chromatography on silica gel eluting with diethyl ether. Recovery of the unreacted azide 27% (+/-)-**79** and the *bis*-substituted product 13% (+/-)-**111**, afforded an overall 92% recovered yield. The presence of an intact azide in (+/-)-**140** was confirmed by FT-IR spectroscopy, a strong signal was observed at 2113 cm^{-1} . This procedure was elaborated to incorporate a *mono*-substituted 2-naphthalene (+/-)-**141** and *O*-benzyl glucose **142** derivatives. All three examples afforded the required products **140-142** in reasonable yields 47-52%. The *O*-benzyl glucose derivative was inseparable from the *bis*-substituted product by flash chromatography, FT-IR of the mixture afforded an azide peak at 2115 cm^{-1} and $^1\text{H-NMR}$ analysis afforded a purity of 85% so was used for subsequent reaction without further purification.

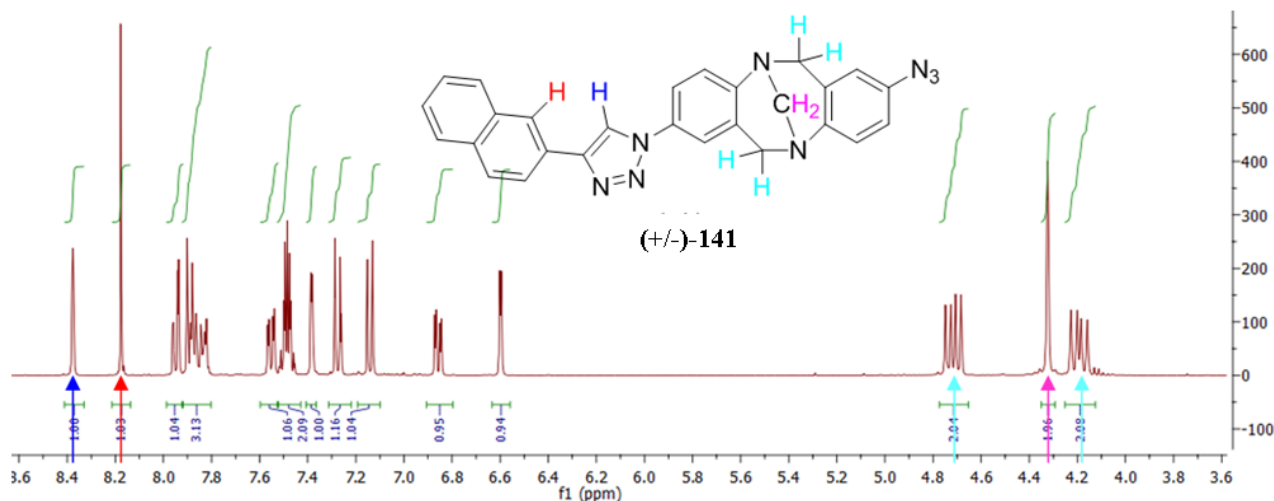


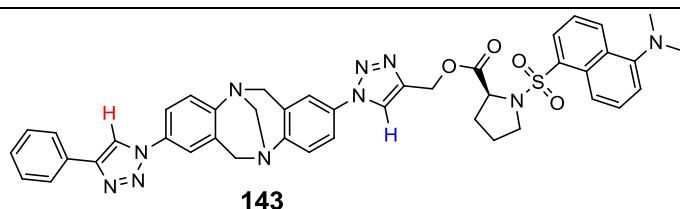
Figure 56 $^1\text{H-NMR}$ (400MHz) spectrum of 2-azido-8-(4-(naphthalen-2-yl)-1H-1,2,3-triazol-1-yl)-6,12-dihydro-5,11-methanodibenzo[b,f][1,5]diazocine (+/-)-**141**

The $^1\text{H-NMR}$ (400MHz) spectrum [Figure 56] of (+/-)-**141** afforded a more complex spectrum than the *bis*-substituted (+/-)-**112** due to the unsymmetric ‘click’ coupling. The singlet of the 1,2,3-triazole C_5 proton (dark blue) at $\delta 8.38$ was observed and the singlet at $\delta 8.18$ corresponds to the 1-naphthyl proton (red). The Tröger’s base C_{13} proton (pink) was observed as a singlet at $\delta 4.32$, the *endo* and *exo* protons (light blue) were split into a doublet of doublets at $\delta 4.72$ (dd, $J_{16.8}, 9.3$ Hz) and $\delta 4.19$ (dd, $J_{16.9}, 10.4$ Hz).

With *mono*-substituted analogues **140-142** in hand, their unsymmetrical elaboration was completed *via* a second ‘click’ reaction on the remaining azide. This time employing a different alkyne *via* the same methodology as previously employed for the symmetrical coupling (μW irradiation 70°C , 1 hour). The Neu5Ac derivative **149** was not heated and was left at room temperature for 24 hours to prevent thermal degradation.

Unsymmetrical 2-(4-substituted-5H-1,2,3-triazol-1-yl)-8-(4-substituted-5H-1,2,3-triazol-1-yl)-6,12-dihydro-5,11-methanodibenzo[b,f][1,5]diazocines
143-149

1,2,3-Triazole C_5 proton ppm Yield %



8.07
8.01
(CDCl_3) 72

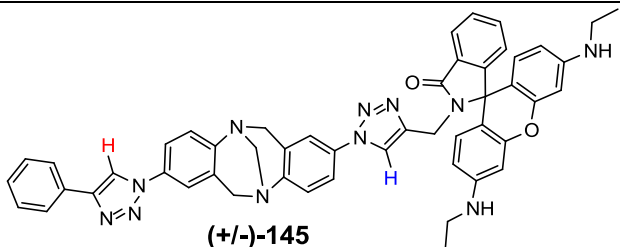
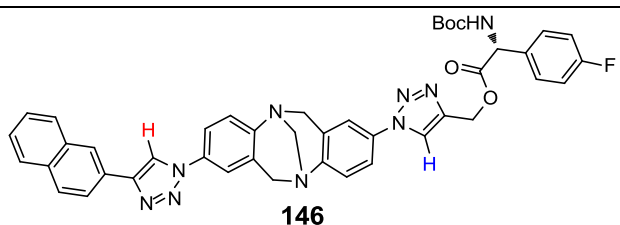
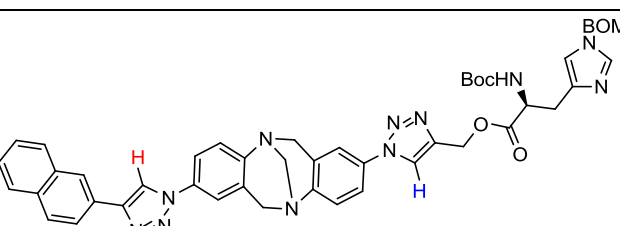
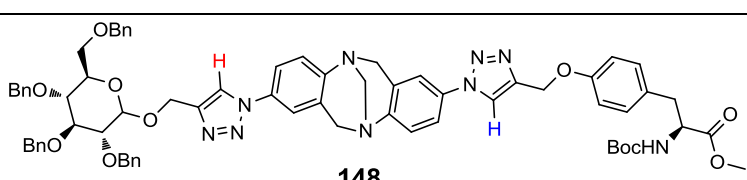
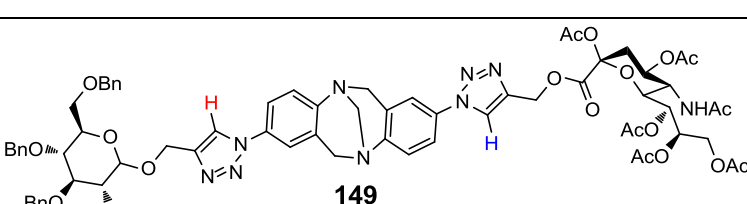
 <p style="text-align: center;">(+/-)-145</p>	<p>8.08 7.95 (CDCl₃)</p>	71
 <p style="text-align: center;">146</p>	<p>8.39 8.20 (CDCl₃)</p>	72
 <p style="text-align: center;">147</p>	<p>8.39 8.20 (CDCl₃)</p>	73
 <p style="text-align: center;">148</p>	<p>7.93 7.87 (CDCl₃)</p>	58
 <p style="text-align: center;">149</p>	<p>8.08 7.84 (CDCl₃)</p>	64

Table 5 Synthesis of Unsymmetrical 2-(4-substituted-5H-1,2,3-triazol-1-yl)-8-(4-substituted-5H-1,2,3-triazol-1-yl)-6,12-dihydro-5,11-methanodibenzo[b,f][1,5]diazocines **143-149**.

The ¹H-NMR (400 MHz) spectrum of **143** [Figure 57] afforded two singlet signals at δ8.07 and δ8.01 they corresponded to the 1,2,3-triazole C₅ protons of the phenyl-triazole and the *N*-dansyl-*L*-proline-*O*-triazole respectively. This was determined by matching the singlet for the 1,2,3-triazole found on the mono-substituted scaffold and comparing this with the new 1,2,3-triazole singlet. The quartet at δ5.25 (*J*13.0 Hz) corresponded to the methylene adjacent to the 1,2,3-triazole of the *N*-dansyl-*L*-proline functionality. The Tröger's base methylenes (green) at C₆ and C₁₂, and their *endo* and *exo* protons, were observed as a doublet of doublets at δ4.78 (*J*17.6, 8.4 Hz) and δ4.27 (*J*17.4, 7.6 Hz) the matching *J* values were a strong indication that these were the correct assignments. The C₁₃ bridgehead methylene (orange) of the Tröger's base afforded a singlet at δ4.37. The methyl protons of the dansyl fluorophore were observed as a singlet at δ2.84. The disappearance of the

azide peak in the FT-IR spectra confirmed the azide moiety had been consumed during the second ‘click’ reaction.

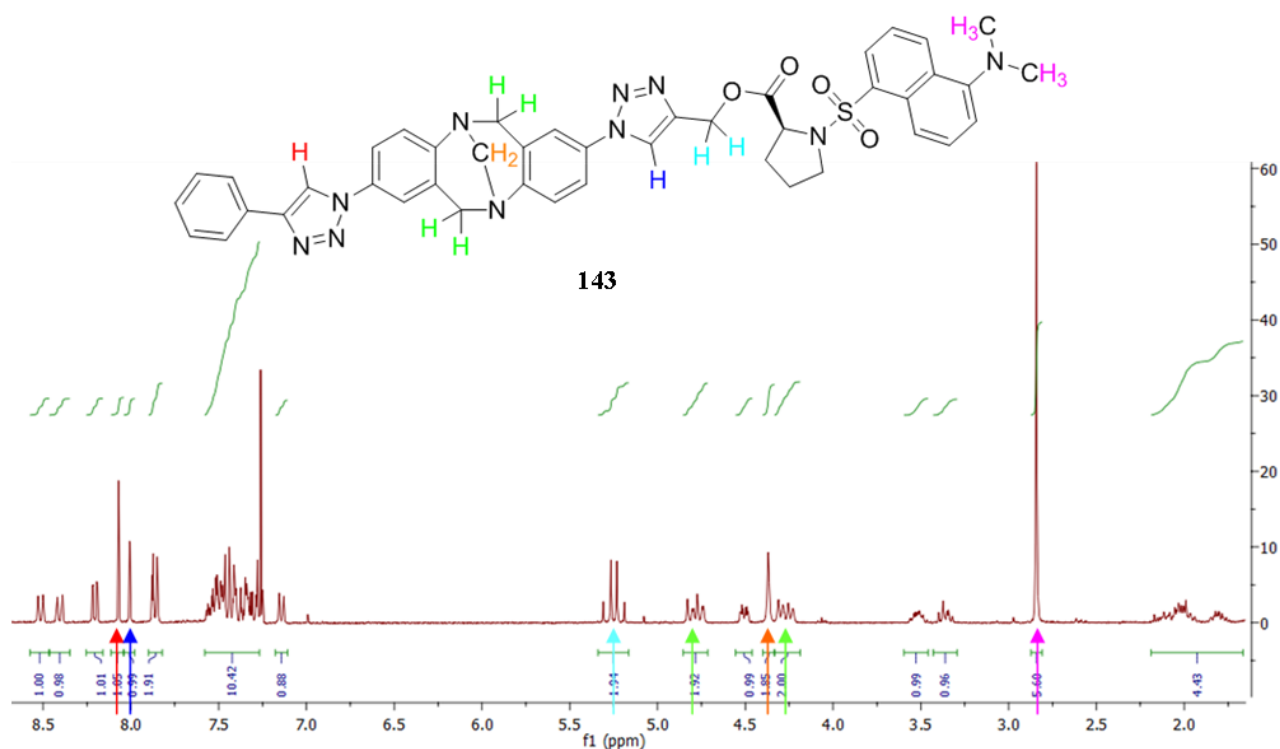


Figure 57 $^1\text{H-NMR}$ (400MHz) of 2,-(4-phenyl-1H-1,2,3-triazole),8,-((S)-(1H-1,2,3-triazol-4-yl)methyl 1-(5-(dimethylamino)naphthalen-1-ylsulfonyl)pyrrolidine-2-carboxylate)-6H, 12H-5, 11-methanodibenzo [b,f][1,5]diazocine **143**.

4.8 Biological testing of 2, 8-appended 1,2,3-triazole Tröger’s bases

4.8.1 DNA intercalation

Veale *et al*, Tatibouët *et al*, Baldeyrou *et al*. and Bailly *et al*. have all independently reported on the DNA intercalation properties of Tröger’s base analogues.^{28, 31, 135, 136} Tatibouët *et al*. reported the binding of the acridine analogue of Tröger’s base (-)-**150** to calf thymus B-DNA to be an enantiospecific process and the (-)-**150** enantiomer affording a preference for binding. This was determined *via* the resolution of (+/-)-**150**, achieved by crystallisation of racemic (+/-)-**150** with the (+)-dibenzoyl tartrate salts which afforded (-)-**150** in an 80% *ee*. The resolved (-)-**150** was subsequently submitted to liquid-liquid partition experiments between an aqueous solution of ct-DNA and (-)-**150** in *n*-butanol. This biphasic mixture was vigorously stirred and the *n*-butanol layer separated and analysed by circular dichromism (CD).¹³⁵ This afforded a broad band in the CD spectra which increased as the DNA concentration was increased. Bailly *et al*. confirmed the

Tatibouët results *via* melting point temperature experiments and DNase I footprinting experiments,⁴ Bailly demonstrated that the (-)-**150** was not only preferred for binding but was specific to certain DNA sequences that contained A • T and G • C base pairs.²⁸ Baldeyrou *et al.* reported that an unsymmetrical (-)-acridine – phenanthroline Tröger's base (-)-**151** also afforded sequence specific DNA binding properties to calf thymus B-DNA. They also determined this *via* DNase footprinting experiments and that (-)-**151** had a strong preference for sites containing adjacent 5'-GTC•5-GAC triplets.³¹

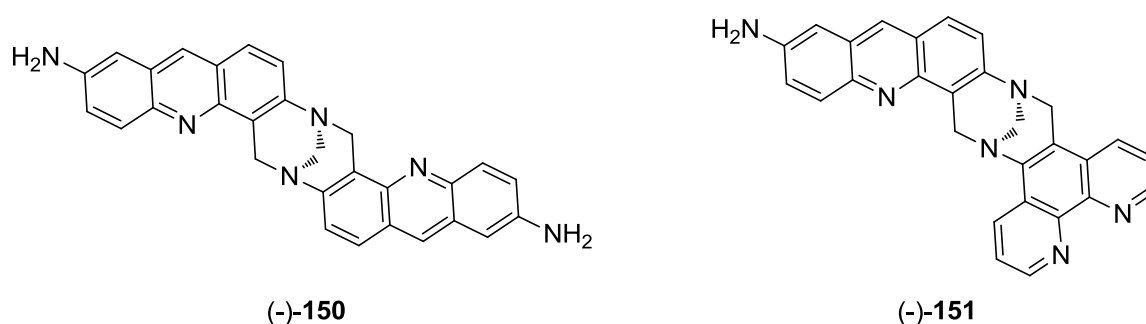


Figure 58 Tröger's base analogues capable of the enantiospecific binding to ds-DNA.

Veale *et al.* reported the binding of three *bis*-1,8-naphthalamide-containing Tröger's bases **152-154** to calf thymus double stranded DNA. Photophysical investigations, UV-vis and fluorescence spectroscopy of **152-154** afforded evidence for strong binding affinities, with K_b s of 10^{-6} M, to DNA. They reported the binding to be irreversible and this stabilised the DNA double helix. However there was no mention of their enantiospecific binding.¹³⁶

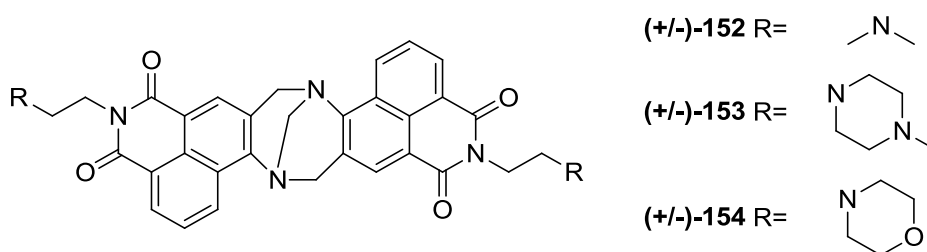


Figure 59 Tröger's base analogues **152-154** capable of binding to and stabilising ds-DNA.

With a plethora of novel Tröger's base analogues to hand, a select few, with potential DNA intercalative properties, *i.e.* planer compounds anthracene (+/-)-**113**, naphthyl (+/-)-**112**, (+/-)-**141**, **147**, (+/-)-**115**, phenyl **143** and 4-pyridyl **117**, were tested for their ability to interact with double stranded DNA by gel shift assay. A modified procedure of Furlan *et al.* was used to examine the target compounds. A mixture of *Bam*HI linearized plasmids, pUC 19 (2,6 kb) 50ng/ μ L, 2 μ L and the target compounds [Table 6] 100 ng/ μ L, 1 μ L in deionised water 7 μ L, this was left at 37°C for

⁴ DNase footprinting is a technique for determining DNA binding events and where they occur. DNase enzymes cleave DNA producing a footprint of the segments. If a binding event was occurring between DNA and an introduced compound, this can change the structure of DNA and hinder cleavage sites for the enzyme, therefore the footprint will change.

one hour, before being transferred to a well in a 1% agarose gel. The gel was run at 85V for two hours before being stained by ethidium bromide solution (10ppm).¹³⁷ Echinomycin, a known intercalating antibiotic, was prepared in an identical way and was used as the positive control.

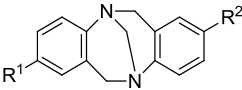
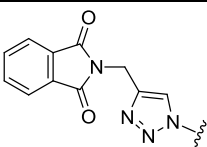
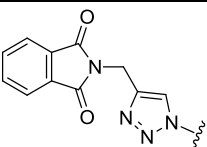
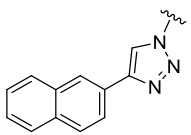
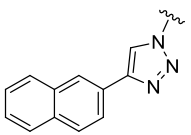
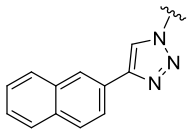
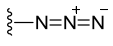
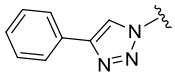
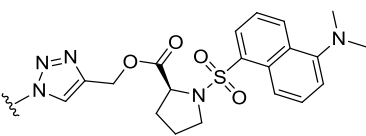
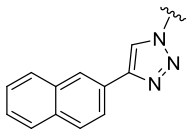
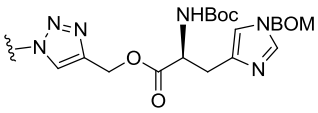
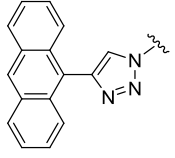
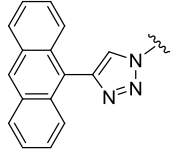
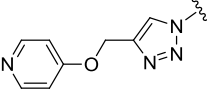
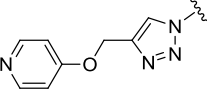
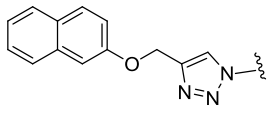
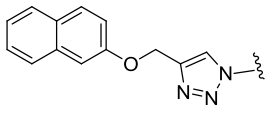
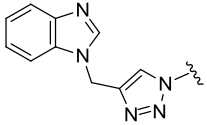
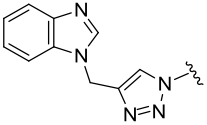
		
Tröger's base analogue	R ¹	R ²
(+/-)-120		
(+/-)-112		
(+/-)-141		
143		
147		
(+/-)-113		
(+/-)-117		
(+/-)-115		
(+/-)-119		

Table 6 Tröger's base analogues submitted for DNA intercalation experiments.

Gel position	Compound
1	Ladder 1Kb
2	Control
3	Echinamycin
4	(+/-)-120
5	(+/-)-112
6	(+/-)-141
7	143
8	147
9	(+/-)-113
10	(+/-)-117
11	(+/-)-115
12	(+/-)-119

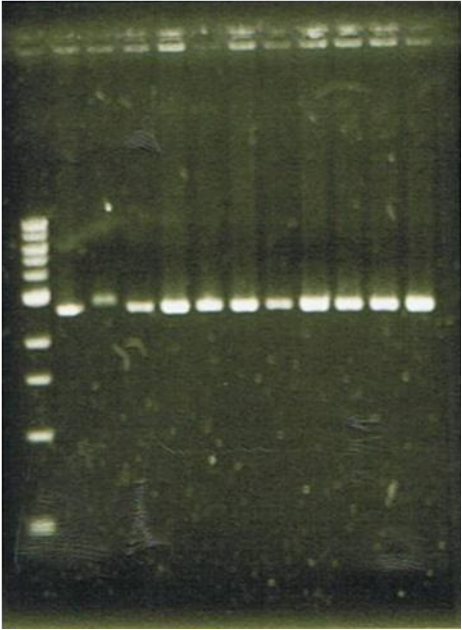


Table 7 Results from gel-shift assay

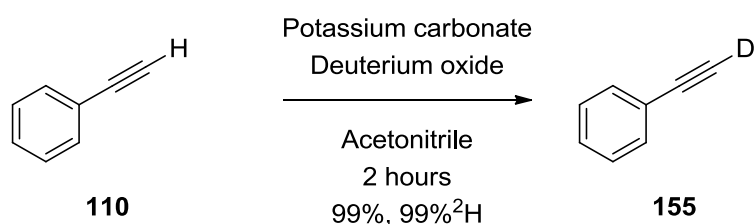
From the gel shift assay [Table 7] we can observe that only the known DNA intercalater, Echinomycin (lane 3) generated a small shift in the DNA band. This suggests that our protocol worked for detecting DNA intercalation properties, however, no DNA binding was detected for our analogues *via* this technique. Subsequent analysis, such as, thermal melting point analysis, would be required to definitively prove whether a binding event is occurring between the ct-DNA and Tröger's base analogues.

4.9 Mild conditions for the deuteration of terminal alkynes

The development of stable isotope enriched building blocks for organic synthesis is of great importance to the pharmaceutical industry, biotechnology and academics alike. ^2H -labelled compounds often need to be synthesised in high yields, for cost viability, and perhaps more importantly with high levels of ^2H -incorporation. ^2H -alkynes are valuable, synthetically useful entities⁴³ capable of being used for the synthesis of additional deuterated molecules; *e.g.*, ^2H -alkyne hydrogenation generates *cis*- or *trans*- ^2H -alkenes or ^2H -alkanes.⁵⁰ Alternatively aqueous gold salts afford ^2H -ketones,⁵² and ^2H -alkyne cyclotrimerization affords ^2H -aromatics.⁵³

During an unrelated project involving the deuteration of propargyl diazoacetate, it became apparent that the proton of the terminal alkyne had exchanged for ^2H under very mild reaction conditions, stir in acetonitrile with potassium carbonate and deuterium oxide. This unexpected result was investigated further with the library of propargyl compounds **87-104**. The method employed was

simple:- stirring a terminal proteo alkyne with potassium carbonate in acetonitrile followed by addition of deuterium oxide.



Scheme 42 Reaction conditions for the mild deuteration of terminal alkynes

During the reaction it was clear that a gas was afforded during the exchange, as seen by a build up of pressure in the reaction vial used to conduct the experiment in. Bubbling the evolved gas through lime water caused it to turn cloudy suggesting that carbon dioxide was present. This observation lead to the conclusion that the potassium carbonate was important for the exchange as carbon dioxide must have been released by the potassium carbonate. The literature provides examples of the deuteration of terminal alkynes using *n*-butyl-lithium or lithium di-isopropylamine and low temperatures -78°C ⁵⁴ or Grignard reagents at -40°C .⁵⁷ However the literature failed to provide any deuteration protocols that afford the exchange at ambient temperature in less than two hours. To investigate the effect of the base further, a range of bases, inorganic, organic and polymer supported, were chosen and the exchanges attempted on phenyl acetylene as a model substrate **110** [Table 8].

Base	Yield %	Deuterium incorporation %*
Sodium hydrogen carbonate	99	99%
Caesium carbonate	97	96%
Sodium carbonate	98	96%
Triethylamine	92	94%
Polymer supported trisamine	90	93%
None	0 (99% proteo alkyne recovered)	0

Table 8 Base study for mild deuteration of terminal alkynes

* (determined by $^1\text{H-NMR}$ (300MHz))

Table 8 allows us to conclude that the inclusion of a base was essential to the $\text{H}/^2\text{H}$ exchange process, however, which base had little impact on either the yield or ^2H -incorporation. The inorganic bases facilitated the exchange more efficiently, presumably due to the loss of carbon dioxide, a factor that may help drive the reaction forward.

Efforts to simplify the exchange further by utilising a non miscible organic solvent which would allow the two phases to separate after the exchange was completed. Upon collection the organic layer it was hoped this would afford the required ^2H -alkyne without work up. However, this was not the case and a plethora of non water miscible organic solvents were employed and the deuterium incorporation suffered.

Non-miscible solvent	Yield	Deuterium Incorporation %*
Dichloromethane	99% (recovered)	28
Diethyl ether	98% (recovered)	25
Toluene	99% (recovered)	32
Hexane	97% (recovered)	12
Ethyl Acetate	99% (recovered)	26
1,2 Dichloroethane	99% (recovered)	16
Miscible solvent		
1,4-dioxane	98	99
Tetrahydrofuran	97	99

Table 9 Solvent study for mild deuteration of terminal alkynes.

* (determined by ^1H -NMR (300MHz))

With non-miscible solvents deteriorating the exchange, other water miscible solvents were employed and were just as efficient as acetonitrile and didn't offer any significant advantage.

A ^1H -NMR (300MHz) experiment was initiated in an attempt to follow the ^2H -exchange '*in situ*'. An NMR tube was charged with phenylacetylene **110** and potassium carbonate in deuterated acetonitrile (500 μL) was added. The sample was locked and shimmed and a t=0 spectra was accumulated, this was followed by addition of deuterium oxide (50 μL). The sample was immediately re-submitted for ^1H -NMR analysis. However, to our surprise the H/ ^2H exchange reaction was already complete. The triplet alkyne peak had completely disappeared and a HOD peak could be seen at δ 2.10

With the procedure unchanged from the original, alkyne (1 equivalent), potassium carbonate (1.5 equivalents) and deuterium oxide (25 equivalents) in acetonitrile, a series of alkynes **156-167** were subjected to the deuteration conditions.

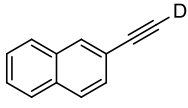
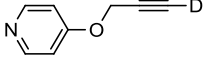
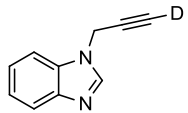
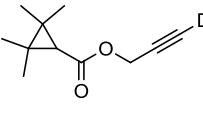
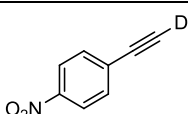
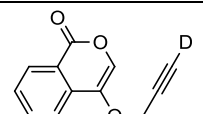
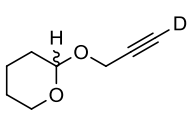
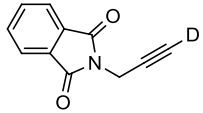
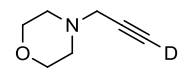
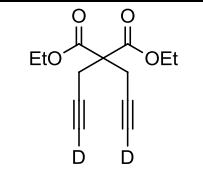
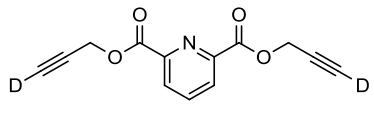
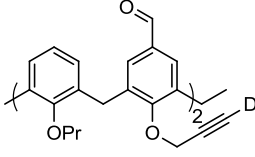
Deuterated terminal alkynes	Yield %	Deuterium Incorporation %*	Deuterated terminal alkynes	Yield %	Deuterium Incorporation %*
	99	98		98	99
	99	99		99	99
	99	99		99	99
	99	95		99	99
	93	95		99	99
	Yield 99%	Deuterium incorporation 96%		Yield 99%	Deuterium incorporation 97%

Table 10 Synthesis of deuterated terminal alkynes **156-157**

*(determined by $^1\text{H-NMR}$ (300MHz))

This very simple procedure worked well with ^2H -incorporations often >95% and practically quantitative yield in all cases. Gratifyingly, the $\text{H}/^2\text{H}$ exchange was just as efficient in affording deuterated compounds containing more than one terminal alkyne **165-167**, including a calix[4]arene **167** substrate, afforded a yield of 99% and a ^2H -incorporation of 97%. All compounds were fully characterised and deuterium incorporation was confirmed by mass spectrometry and $^{13}\text{C-NMR}$.

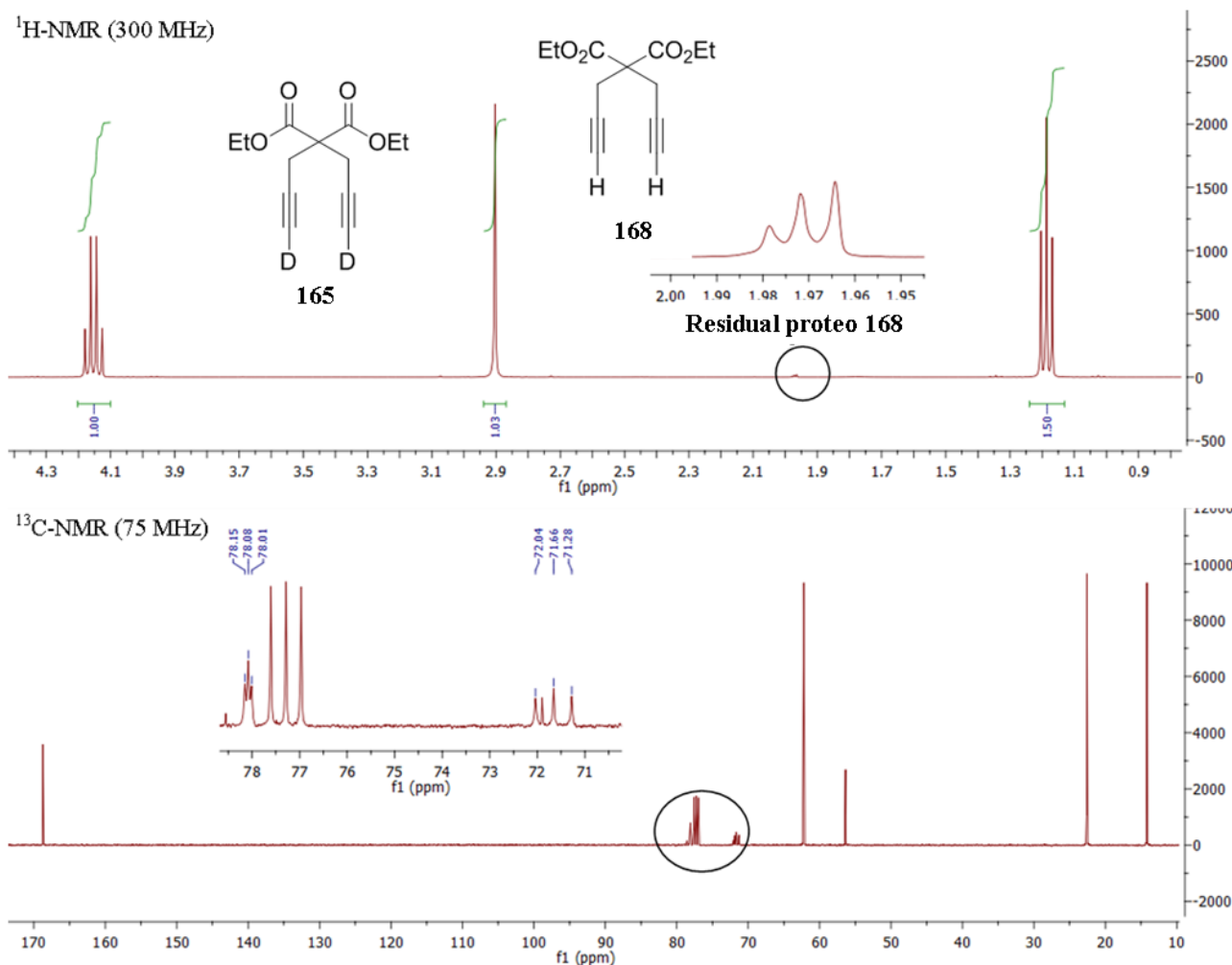
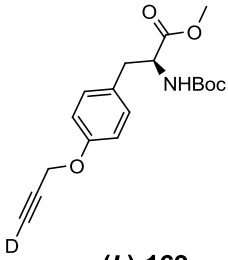
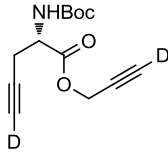
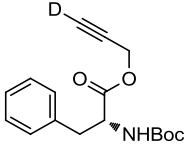
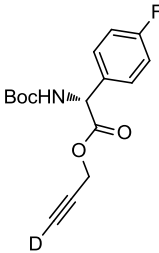
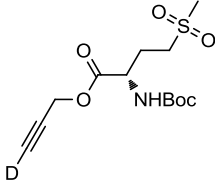
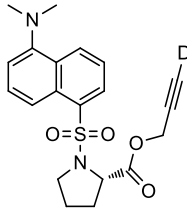
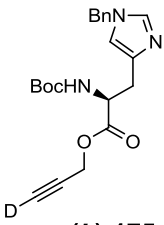
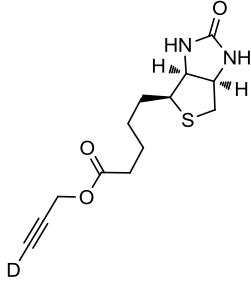
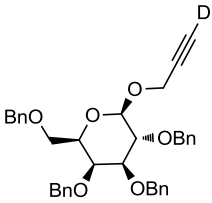
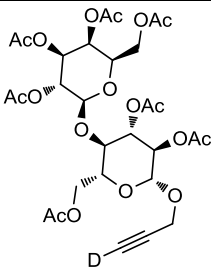
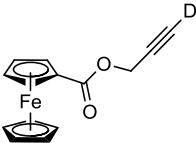


Figure 60 ¹H-NMR(300 MHz) and ¹³C-NMR(75 MHz) of diethyl 2,2-di(deutero-prop-2-ynyl)malonate **165**

In the ¹H-NMR (300 MHz) spectra of **165** the residual proteo-terminal alkyne δ 1.97 needed to be greatly expanded before it could be observed; effectively the peak had disappeared [see Fig 60]. In the ¹³C-NMR (75 MHz) the signals of the terminal and the internal alkynyl carbon have been split into triplets by ²H-¹³C coupling. The triplets were observed at δ 78.08 and δ 71.66 and correspond to the internal carbon and terminal carbon of the alkyne respectively, the ²H-bound to the terminal carbon has a spin of -1, 0, +1 and as the NMR spectrometer was not ²H decoupled, this afforded a three way splitting of the terminal alkyne carbon. The observed triplet of the alkynes 'internal' ¹³C was due to 'two bond' coupling of the ²H with the ¹³C. The poor intensities of the alkynyl ¹³C signals, due to the ¹³C-²H coupling and the relative abundance of ¹³C (1.1%), require a very concentrated sample and a very long acquisition time to detect these signals. With the success of the ²H-exchange on **156-167**, the procedure was employed for *O*-propargyl-*N*-protected amino acid derivatives **169-176** and carbohydrates **177-178**.

Deuterated terminal alkynes	Yield %	Deuterium Incorporation %	Deuterated terminal alkynes	Yield %	Deuterium Incorporation %
 (L)-169	95	99	 (L)-170	99	99
 (D)-171	99	99	 (R)-172	94	96
 (L)-173	99	95	 (L)-174	98	98
 (L)-175	98	98	 (+)-176	89	98
 (β)-177	99	99	 (β)-178	99	99
 179	98	99	<p>*(determined by ¹H-NMR(300MHz))</p> <p>Table 11 Synthesis of deuterated terminal alkynes 169-179</p>		

Gratifyingly our mild reaction conditions for H/²H exchange afforded the terminal alkynyl ²H-incorporated *N*-protected- α -amino acid-*O*-propargyl esters **169-175**, *O*-benzyl propargyl glucose (β)-**177**, *O*-hepta-acetate propargyl lactose (β)-**178** and 1-ferrocene propargyl ester **179** afforded the desired compounds in excellent yields 89-99% with excellent levels of ²H-incorporation >95%. Interestingly the (+)-biotin derivative (+)-**176** underwent a small amount of decomposition to an unisolatable by-product, however, purification *via* flash chromatography on silica gel eluting with 3% methanol in dichloromethane, afforded the required ²H-incorporated product (+)-**176** in a 89% yield. The ability to purify the ²H-alkynes on silica indicated their stability to reverse ²H/H-exchange *i.e.* no loss of ²H-incorporation was observed. The ferrocene propargyl ester derivative **179**, was also successful with no scrambling of the protons on the cyclopentadiene ring observed.

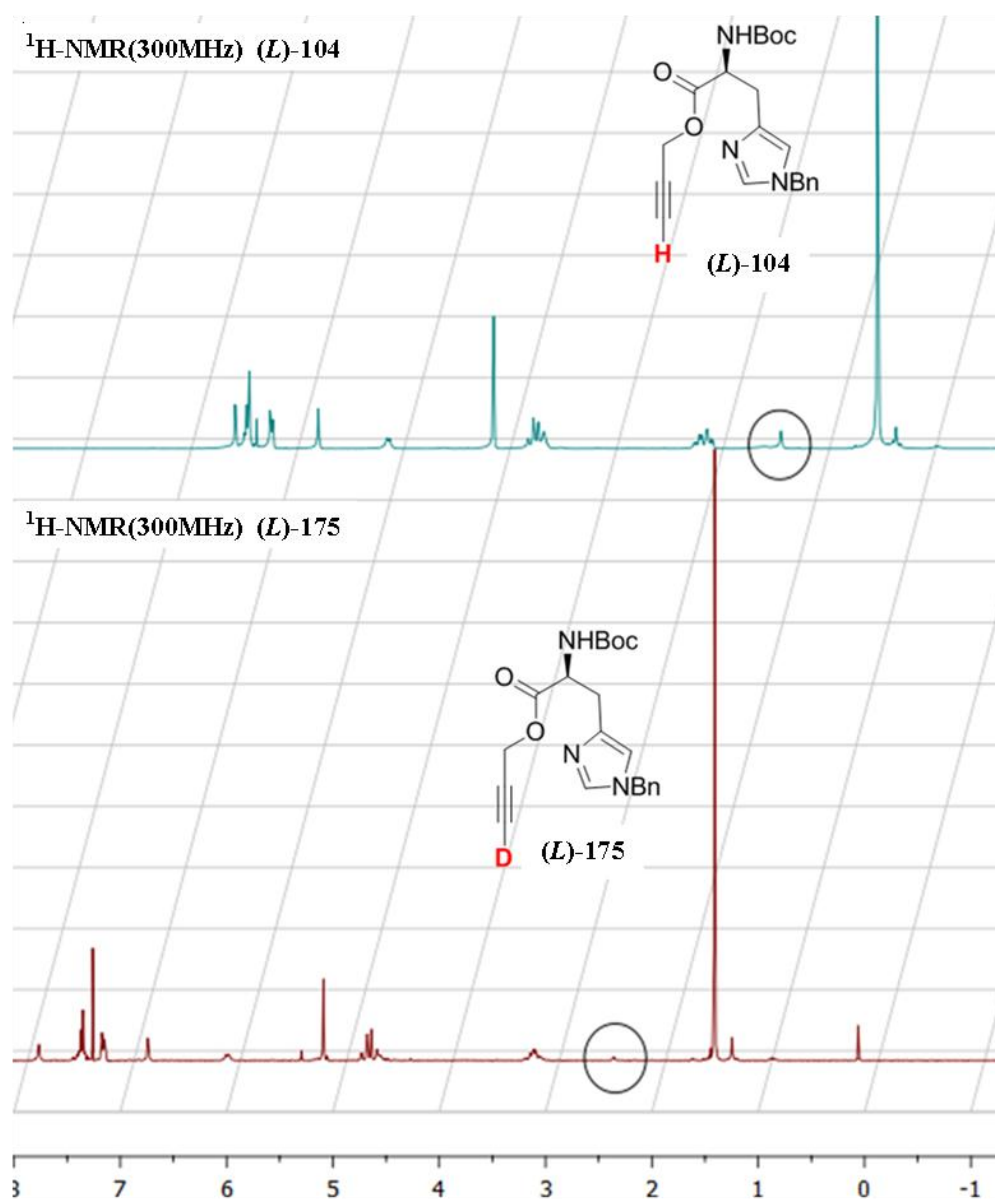


Figure 61 ¹H-NMR (300MHz) spectra of (L)-104 and (L)-175 as a comparison of proteo versus deuterio terminal alkynes.

In the $^1\text{H-NMR}$ (300MHz) spectrum of (*L*)-**175** [Figure 61 bottom] we observed almost complete disappearance of the alkynyl proton of (*L*)-**104** originally located at δ 2.32 (t, J 2.4 Hz)[Figure 61 top] and in the $^{13}\text{C-NMR}$ (75 MHz) spectra of (*L*)-**104** [Figure 62 top] and (*L*)-**175** [Figure 62 bottom] we observed a peak that has been split into a triplet by the deuterium coupling with the ^{13}C , the second triplet has been obscured by the chloroform peak.

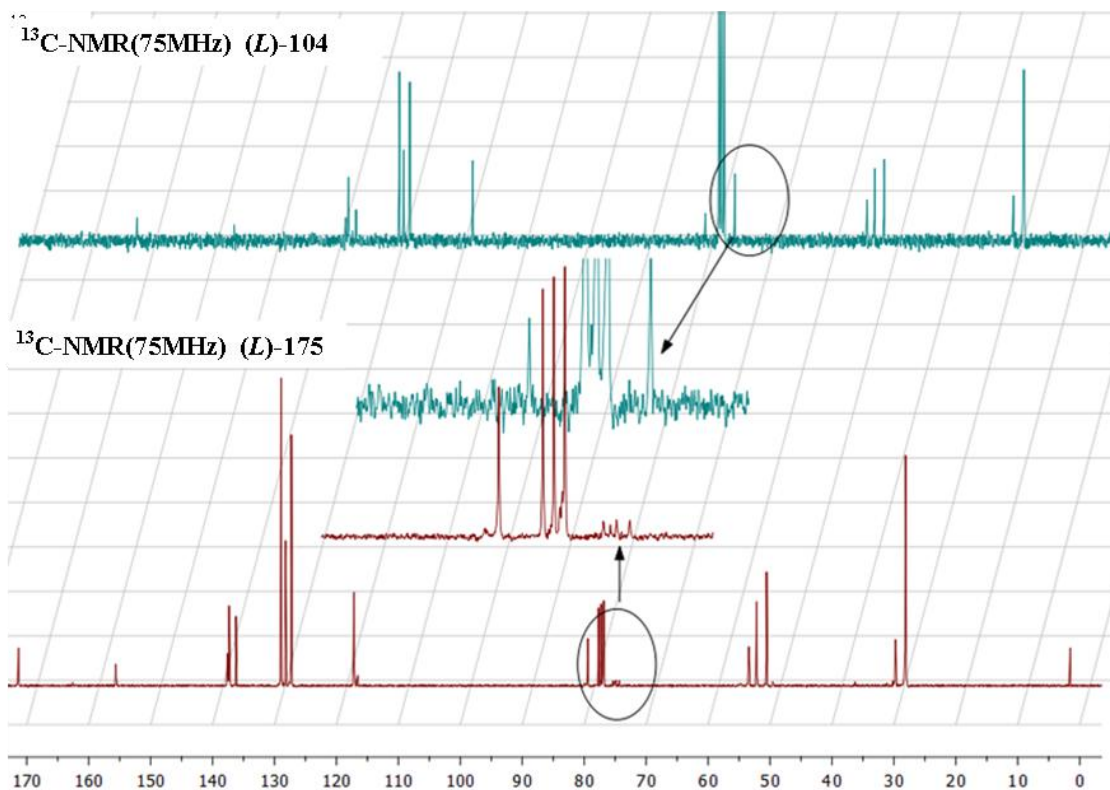
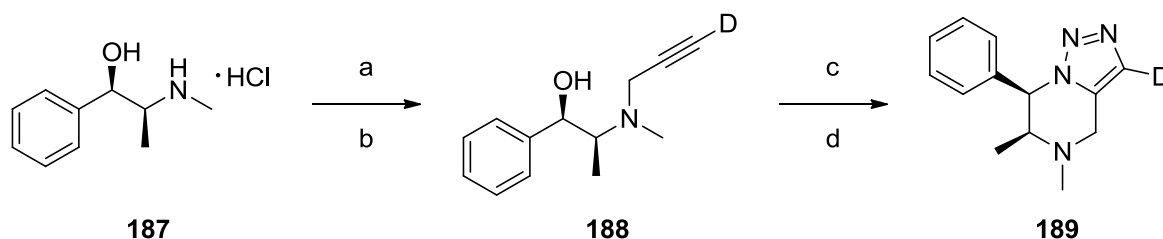


Figure 62 $^{13}\text{C-NMR}$ (75 MHz) spectra of (*L*)-**104** and (*L*)-**175** as a comparison of proteo versus deuterio terminal alkynes.

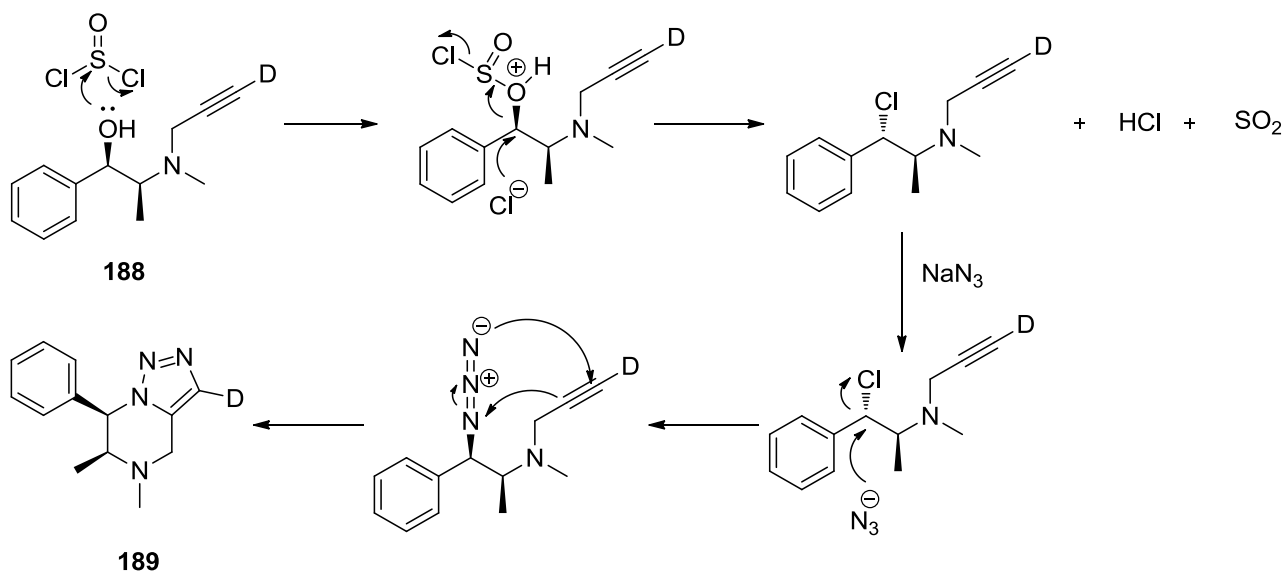
Our standard procedure was not always compatible with all compounds tested, for example, attempts to use the potassium carbonate mediated H^2 Hexchange on the antibiotic derived *O*-propargyl tazobactam **180** and *O*-propargyl cefazolin **181** substrates failed. A range of bases [Table 8], as already discussed in the previous study (see page 73), were investigated but to no avail. The reactivity of the β -lactam ring to ring-opening when subjected to basic conditions seemed to be at the root of the problem, as the ring strain of the 4-membered β -lactam ring makes it highly susceptible to hydrolysis. Undeterred by this minor setback, the problem afforded us with the perfect situation to ensure that the deuterated compounds were in fact useful for further chemistry.

result further enhances the protocol and its application in synthesis and could be used or incorporated as a building block in organic synthesis. To prove this point further we sought to exploit our protocol in the synthesis of deuterated 1,2,3-triazole-piperidine **189**, *via* intramolecular cycloaddition of a, β -amino azide, as described by Couty *et al.*¹³⁸



Scheme 43 Synthesis of deuterated 1,2,3-triazole-piperidine **189**. a) Propargyl bromide, potassium carbonate in *N,N*-dimethylformamide 12 hours. b) Deuterium oxide, ambient temperature 2 hours. c) thionyl chloride 1 hour. d) Sodium azide, d^6 -DMSO, 110°C, μ W, 1 hour.

189 was synthesised using (+)-ephedrine hydrochloride **187** as the start material in a two step, one pot propargylation of the amine and subsequent deuteration of the terminal alkyne **188**, was afforded in a 94% yield and with 99% deuterium incorporation. This was followed by the *in situ* chlorination of **188** *via* displacement of the hydroxyl group, with a chloride anion. This was immediately transferred to a microwave vial and sodium azide and deuterated dimethyl sulfoxide were added. The vial was sealed and heated to 110°C under microwave irradiation for 1 hour.



Scheme 44 Reaction mechanism for the synthesis of **189**

Following flash column chromatography on silica gel, eluting with 20% ethanol in diethyl ether, the required product **189** was afforded as a yellow oil in a 64% yield and with 95% deuterium incorporation. Subsequent physicochemical analysis confirmed this to be the required compound with our data and the data matching that reported by Couty,¹³⁸ with the exception of a missing

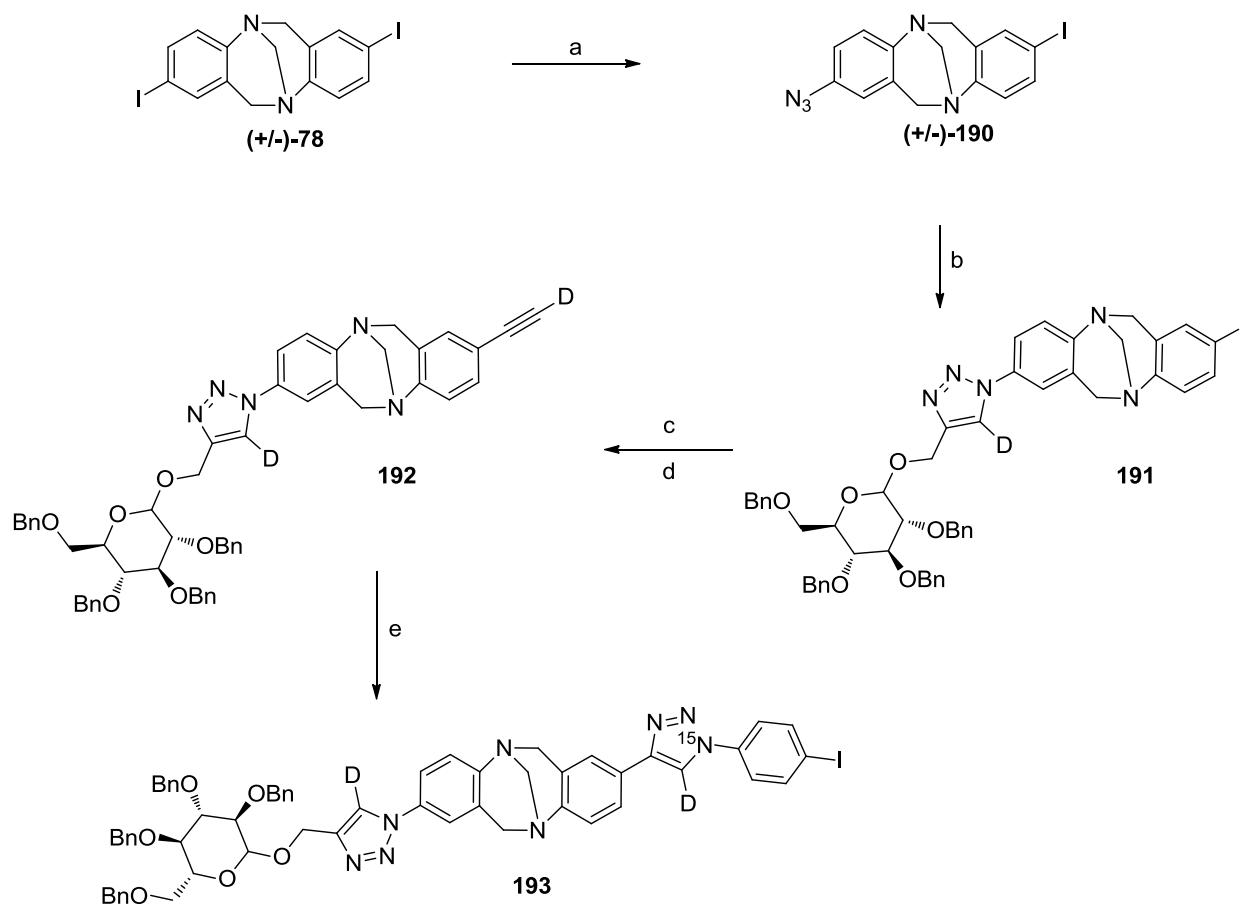
triazole peak in the $^1\text{H-NMR}$ (400MHz) spectrum, due to the incorporation of a ^2H at the C_4 position of the 1,2,3-triazole ring, and LCMS [ES] $^+$ M+H 230.1.

4.11 Stable isotope incorporation within 2,8-appended Tröger's base (4-deutero) 1,2,3 triazoles

With the success of the Tröger's base 'click' reactions and the discovery of a novel procedure for the deuteration of alkynes, the two were combined to attempt the synthesis of a 1,2,3- C_5 deuterated triazoles appended to a Tröger's base scaffold. 2,8-Bis-iodo-Tröger's base (+/-)-**78** was desymmetrised to 2-azido-8-iodo Tröger's base (+/-)-**190** in a 43% yield, followed by 'clicking' with *O*-benzyl protected deuterio-propargyl β -glucose (**β**)-**177**. To achieve this required we undertake a solvent study as employing our standard 'click' procedure afforded deuterium incorporations of the 1,2,3- C_5 deuterated triazole **191** below 95%. After much experimentation we were delighted that a biphasic mixture 1:1 of deuterated chloroform and deuterium oxide with an extended reaction time of 72 hours generated the required deuterated 1,2,3-triazoles **191-193** with a ^2H -incorporation of >95%.

Solvent	^2H -Incorporation	Solvent	^2H -Incorporation
DMF	75%	d^6 - DMSO	78%
THF	71%	$\text{CDCl}_3/\text{D}_2\text{O}$	97%

Table 12 Solvent study for synthesis of C_5 -deutero-1,2,3-triazoles



Scheme 45 a) Sodium azide, copper(I) iodide, sodium ascorbate, *N,N*-dimethylethane-1,2-diamine, ethanol : water 3:2, 100°C μ W, 1 hour, 43%; b) *O*-benzyl β -glucose deuteropropargyl ether, copper(II) sulfate pentadeuterate, Sodium ascorbate, deuterium oxide : d-chloroform 1 : 1, 72 hours, ambient temperature, 60%. c) Trimethylsilylacetylene, *tetrakis*(triphenylphosphine) palladium(0), copper(I) iodide, triethylamine, tetrahydrofuran. d) Methanol, potassium carbonate, 2 hours then acetonitrile, potassium carbonate, deuterium oxide, 1 hour, 81%. e) ¹⁵N-4-iodoaniline, copper(II) sulfate pentadeuterate, Sodium ascorbate, deuterium oxide : d³-chloroform 1 : 1, 72 hours, ambient temperature.

With **191** in hand the opportunity was taken to investigate utilising the carbon-iodine bond for palladium(0) catalysed Sonogashira couplings with trimethylsilylacetylene, utilising a procedure previously reported by Bew *et al*, affording a trimethylsilyl protected alkyne Tröger's base¹³⁹ this was desilylated and deuterated in one step. Stirring with potassium carbonate in acetonitrile, followed by addition of deuterium oxide, afforded **192** with 95% ²H-incorporation at the newly installed alkyne **192**. **192** was subsequently 'clicked' with a ¹⁵N-labelled *para*-azido-iodobenzene **194**, synthesised by iodination of ¹⁵N-aniline and subsequent diazotisation with *tert*-butyl nitrite and formation of the azide with trimethylsilyl azide. This afforded an aryl extended Tröger's base, **193** functionalisable at a later stage *via* the carbon-iodine bond [Scheme 45].

193 now contained two ²H-C₅-deuterated 1,2,3-triazoles and also, a ¹⁵N isotopically enriched ¹⁵N₁-1,2,3-triazole was incorporated. This is the first example of a multisotopermeric *i.e.* 2 x ²H and ¹⁵N

synthesis of a compound *via* ‘click’ chemistry. The confirmation of the isotopic incorporation of **193** was generated by ^2H and ^{15}N -NMR spectra figure 68.

In the ^{15}N -NMR (51 MHz) spectra of **193** [Figure 68] the shift of the ^{15}N peak from δ -288.01 for the azide **194** [FIGURE67] to δ -127.18 for the 1,2,3-triazole of **193** (referenced to nitromethane) was observed. The ^2H -NMR (77MHz) spectra affords two peaks at δ 8.13 and 7.89 this is the region where the C₅-1,2,3- triazole proton signals would be observed in ^1H -NMR spectrum.

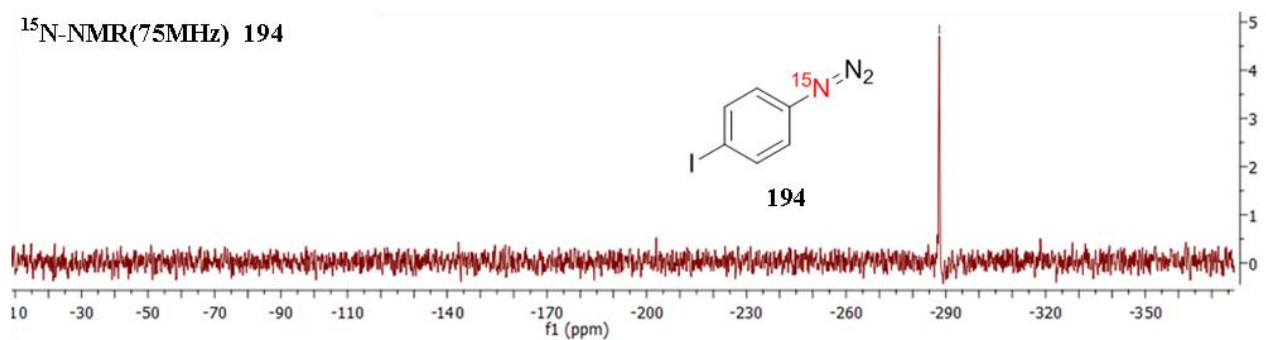


Figure 67 ^{15}N -NMR(51 MHz) of 194

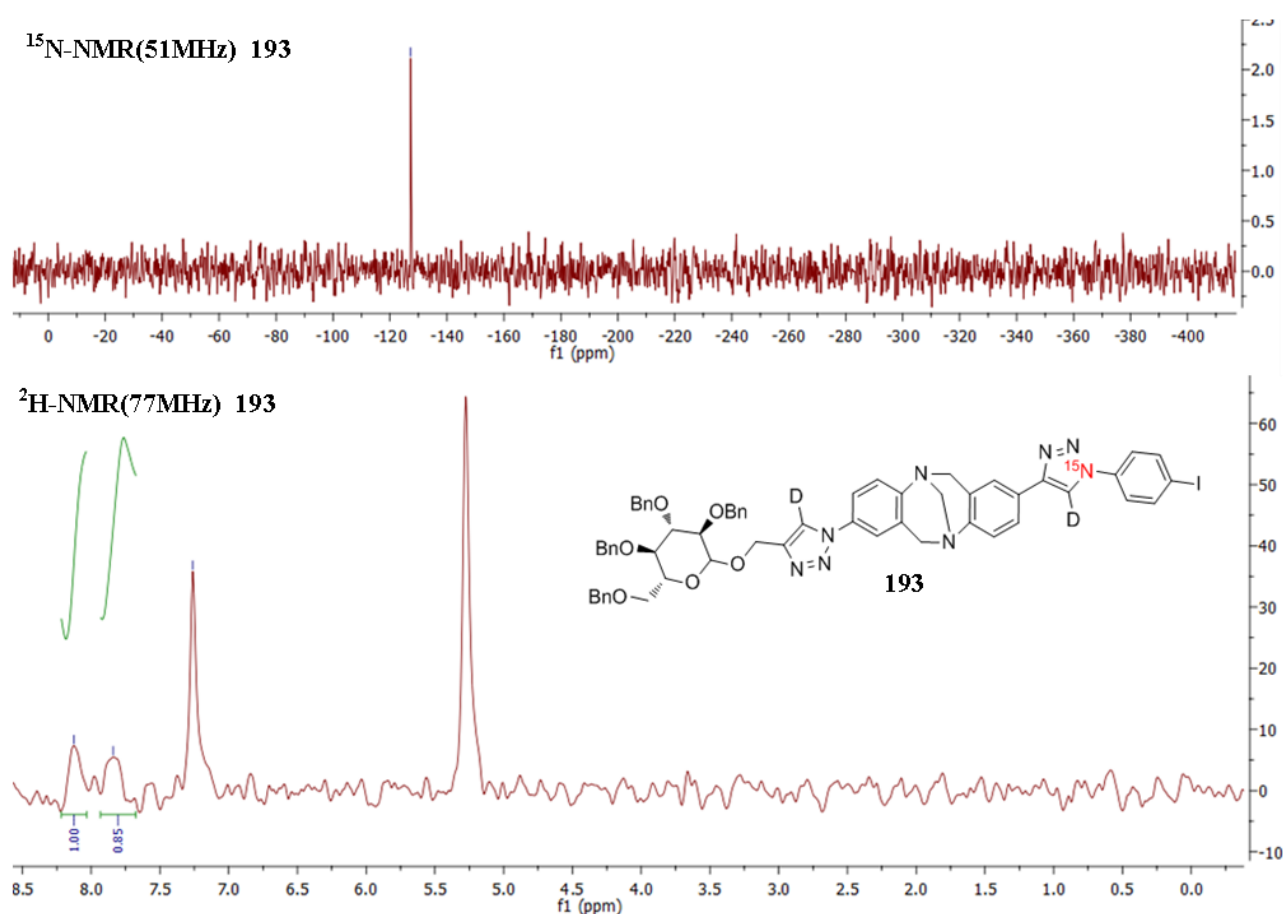
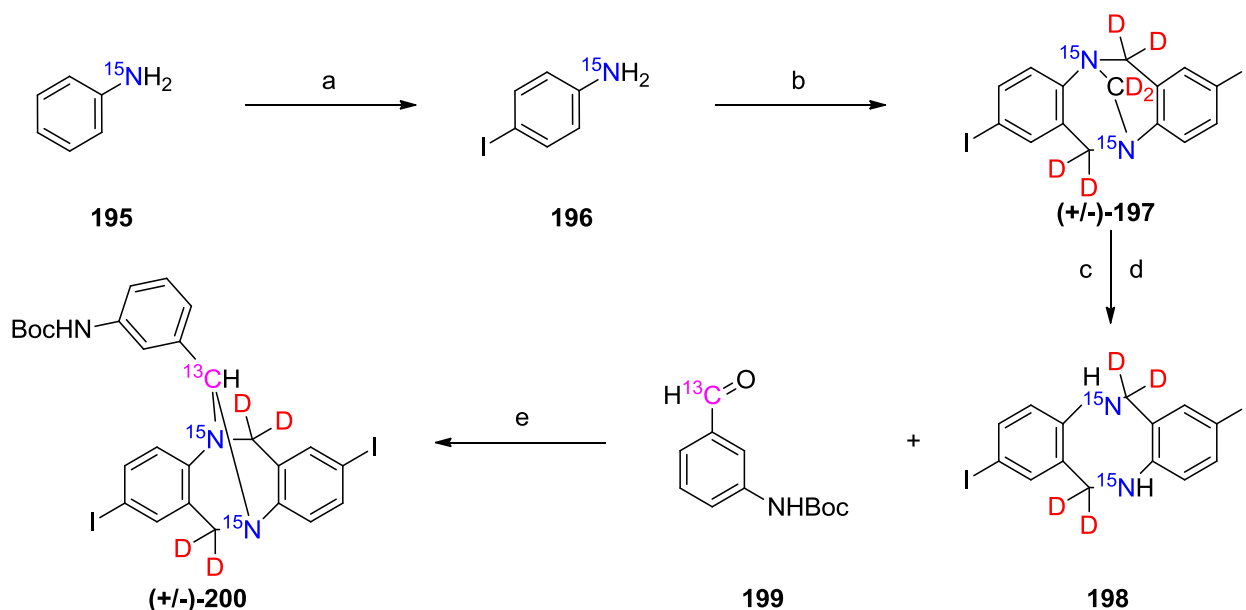


Figure 68 ^{15}N -NMR (51 MHz) and ^2H -NMR (77 MHz) of **193**

4.12 Incorporation of stable isotopes within the Tröger's base scaffold

With the success of the stable isotope enriched 2,8 appended Tröger's base **193**, the synthesis of a ^{15}N - and ^2H -labelled Tröger's base scaffold was attempted.



Scheme 46 a) Sodium bicarbonate, iodine, water, $0-5^\circ\text{C}$, 1 hour, 88%. b) d_2 -paraformaldehyde, d_3 -trifluoroacetic acid, dark, 72 hours, 54%. c) Trifluoroacetic anhydride, dichloromethane, 16 hours, d) sodium hydroxide and ethanol, 4 hours, 90%. e) toluene, reflux, 4\AA molecular sieves 24 hours, 53%.

^{15}N -labelled aniline **195** was iodinated at the *para*-position with sodium bicarbonate and iodine in water, ^{15}N -4-iodo-aniline **196** was afforded in an 89% yield. Condensing **196** with deuterated-*para*-formaldehyde in neat deuterated trifluoroacetic acid afforded ^{15}N - and ^2H -labelled 2,8-iodo-Tröger's base in a 54% yield (**(+/-)-197**) [Scheme 46]. The NMR analysis of (**(+/-)-197**) was very interesting; the ^1H -NMR (500MHz) spectrum [Figure 69 top] afforded no aliphatic peaks and the ^2H -NMR (77MHz) spectrum afforded signals in the expected region ^2H - $\delta 4.52$ *exo*, ^2H - $\delta 4.15$ C_{13} and ^2H - $\delta 4.00$ *endo*. The splitting in the ^{13}C -NMR (100MHz) spectrum of (**(+/-)-197**) had a complex splitting pattern. The aliphatic ^{13}C -signals C_6 , C_{12} at $\delta 57.35$ and C_{13} $\delta 65.78$ are split by both the ^2H - and ^{15}N -nuclei afforded a visible quintet and triplet. The triplet was only part of the splitting pattern as the intensity of the signal was reduced as there were half as many ^{13}C atoms compared to the quintet. To improve the resolution of these peaks it would be necessary to use more sample or run the acquisition for an extended time. The splitting pattern observed is due to the NMR spectrometer not being deuterium and ^{15}N decoupled. The nuclear spin of deuterium is 1 and causes the attached ^{13}C signal to be split into 3 signals (in a similar manner to CDCl_3 peak in ^{13}C -NMR spectra). As the ^{15}N is also coupled to the ^{13}C , and has a spin of $1/2$, this causes the already split ^{13}C signal to be further split into 2 signals, thus affording the complicated signal as seen in figure 69. The next step was to remove the methylene bridge C_{13} of (**(+/-)-197**). This was attempted by employing a method reported by Mahon *et al.* who used trifluoroacetic anhydride to form an *N*-

trifluoroacetamide intermediate.¹⁷ Ethanolysis of the intermediate afforded the required diamine **198** in a 90% yield. **198** was then refluxed with α -¹³C-labelled 3-*N*-Boc benzaldehyde **199** in toluene, as described by Mahon *et al.* This inserted the ¹³C-label at the bridgehead position affording (+/-)-**200** in a 53% yield. Subsequent physicochemical analysis of (+/-)-**200** including ¹⁵N-NMR (51MHz) afforded two signals, at δ -335.12, -338.22 with respect to internal standard CH₃NO₂, for what appears to be chemically identical nitrogens.

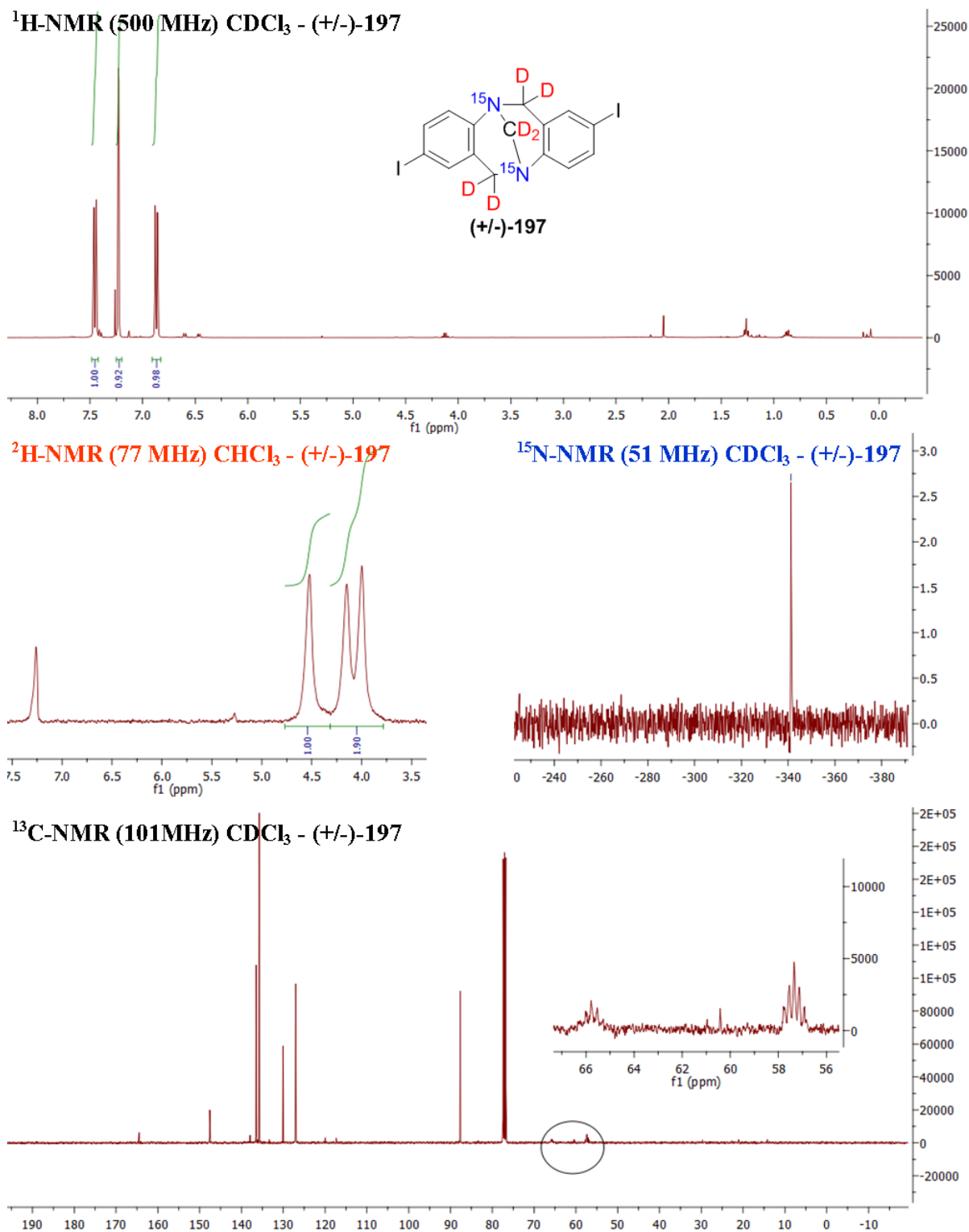
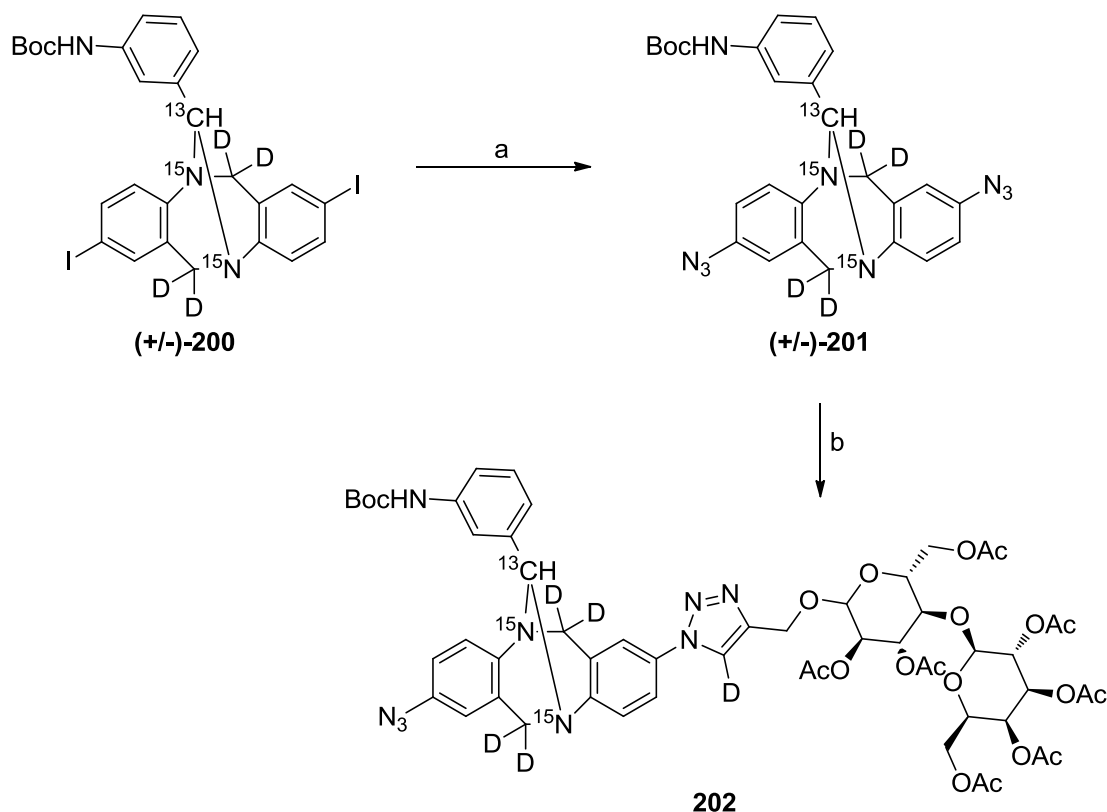


Figure 69 ¹H-, ²H-, ¹⁵N- and ¹³C- NMR analysis of (+/-)-**197**

(+/-)-**200** was transformed to (+/-)-**201** via the copper(I) catalysed procedure employed earlier, followed by a de-symmetrising ‘click’ procedure with *O*-acetate deuterio-propargyl lactose (**β**)-**178** which afforded **202** in 40% yield and with >95% deuterium incorporation.



Scheme 47 a) Sodium azide, copper(I) iodide, sodium ascorbate, *N,N*-dimethylethane-1,2-diamine, dimethylsulfoxide : water 5:1, 100°C μW , 1 hour, 80%. b) *O*-acetate β -lactose deuterio-propargyl ether, copper(II) sulfate pentadeuterate, sodium ascorbate, deuterium oxide : d-chloroform 1 : 1, 72 hours, ambient temperature, 40%.

202 was subsequently ‘clicked’ with *N*-Boc-*O*-methyl ester deuterio-propargyl ether (*L*)-tyrosine (***L***)-**169** and deuterio-*O*-propargyl-ester of *N*-Boc-*para*-fluoro-(*R*)-phenyl glycine (***R***)-**172**. This afforded the first example of multi-isotopically labelled, natural and unnatural α -amino acids and carbohydrate based 2,8-appended Tröger’s base derivatives **203** and **204**.

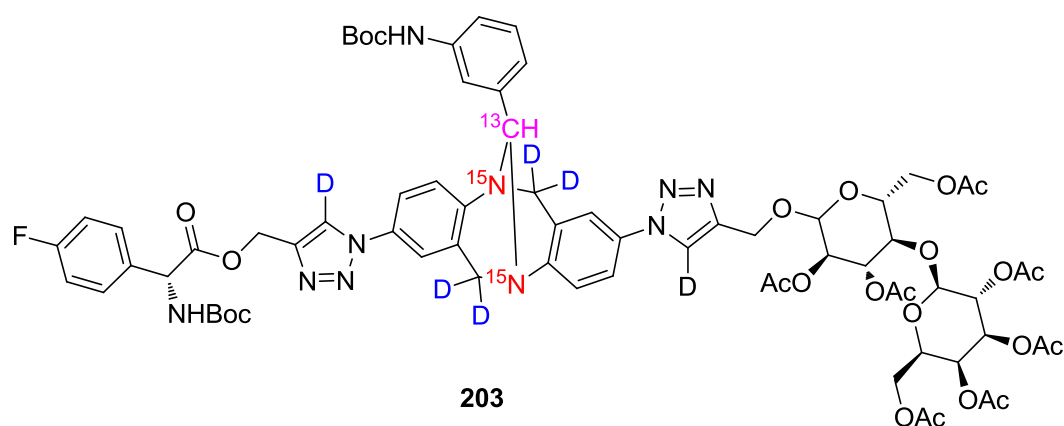


Figure 70 Structure of multi-isotopically labelled Tröger’s base derivative **203**

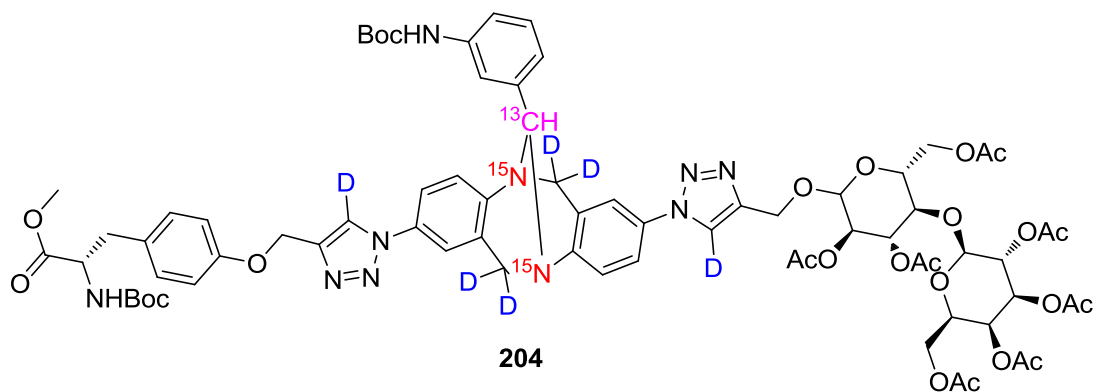
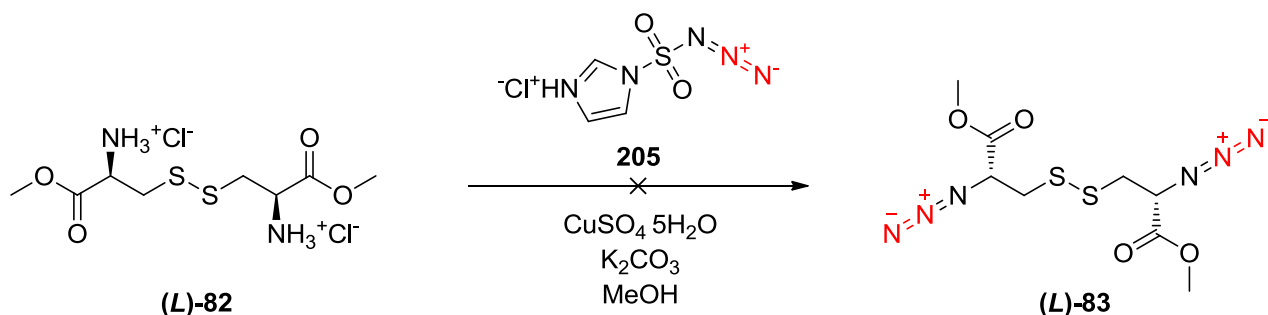


Figure 71 Structure of multi-isotopically labelled Tröger's base derivative **204**

4.13 Synthesis of (+)-biotin analogues for SAM formation.

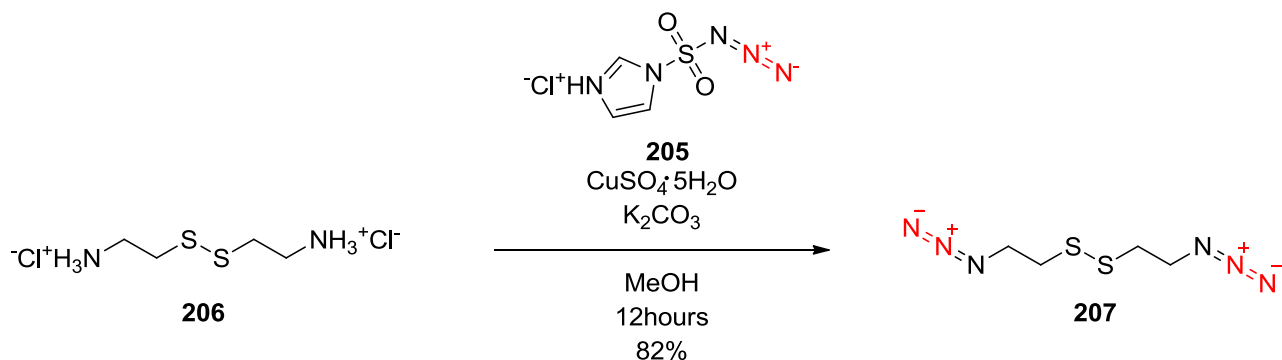
With intentions of binding compounds to the surface of the CD the synthesis of a range of substrates was required to bind to the gold layer. These substrates would need to be bifunctional, namely capable of binding to the gold and interacting with a protein. To show proof of principle the model study of the interaction between (+)-biotin and the protein streptavidin was chosen to be investigated. The interaction between this protein and ligand is one of the strongest non-covalent interactions, found in nature. The first biotin derivative was synthesised from the propargyl biotin (+)-**85**, in order for this to bind to gold a sulfur group needs to be incorporated. This can take the form of a thiol, a disulfide or a thiosulfate. To allow for coupling to the propargyl group of the (+)-biotin derivative an azide group needs to be introduced to the sulfur containing linker. A cheap, readily available source containing a disulfide and amine, which, can be converted to an azide is the amino acid *L*-cystine. It was hoped that the methyl ester of *L*-cystine (**L**)-**82** could be converted to the *N*-bis-azide-*L*-cystine-*O*-methyl ester (**L**)-**83** derivative using the diazo donor, imidazole sulfonyl azide hydrochloride **205**, as described by Goddard-Borger.¹¹³



Scheme 48 Failed synthesis of (**L**)-**83**

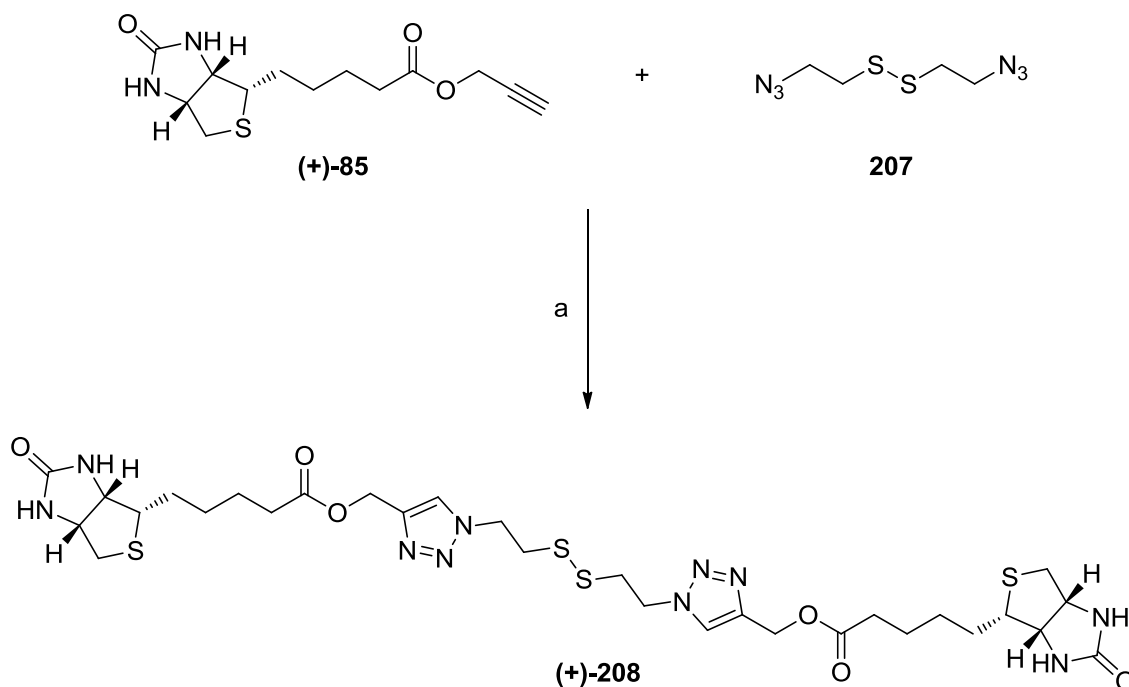
This reaction was unsuccessful and resulted in the formation of a black sticky tar within minutes of adding the reagents. Why this reaction failed is still to be determined. The reported procedure has many examples of successful α -amino acid azide derivatives, however (*L*)-cystine was not

included.¹¹³ Another method was needed to form the disulfide and azide containing intermediate. This was finally over come using de-carboxylated cystine hydrochloride or 2,2'-disulfanediyldiethaniminium chloride **206**.



Scheme 49 Synthesis of **207** using imidazole sulfonyl azide hydrochloride

Gratifyingly, the desired compound **207** was synthesised in an 82% yield and common with other sulfur containing compounds had a strong onion odour. **207** was filtered through a short silica plug, eluting with ether before being used for further reaction. Decomposition was rapid if left on the bench for as little as an hour. The FT-IR spectra afforded a strong peak at 2101 cm^{-1} confirming the presence of the azide. **207** was coupled to the propargyl (+)-biotin (+)-**85** affording a 1,2,3-triazole linked disulfide **208**, for SAM formation and the (+)-biotin ‘warhead’ for protein interaction. The reaction outlined [Scheme 50] was carried out using the standard ‘click’ procedure ($\text{CuSO}_4 \cdot 5\text{H}_2\text{O}$, TBTA, sodium ascorbate, DMF, 70°C μW , 1 hour) as previously employed.



Scheme 50 Synthesis of (+)-**208** a) $\text{CuSO}_4 \cdot 5\text{H}_2\text{O}$, TBTA, sodium ascorbate, DMF, 70°C μW , 1 hour, 88%

Gratifyingly this was successful affording the required product (+)-**208** in an 88% yield. The product was highly polar and 10% methanol in dichloromethane eluent was required to elute (+)-**208** from a silica column.

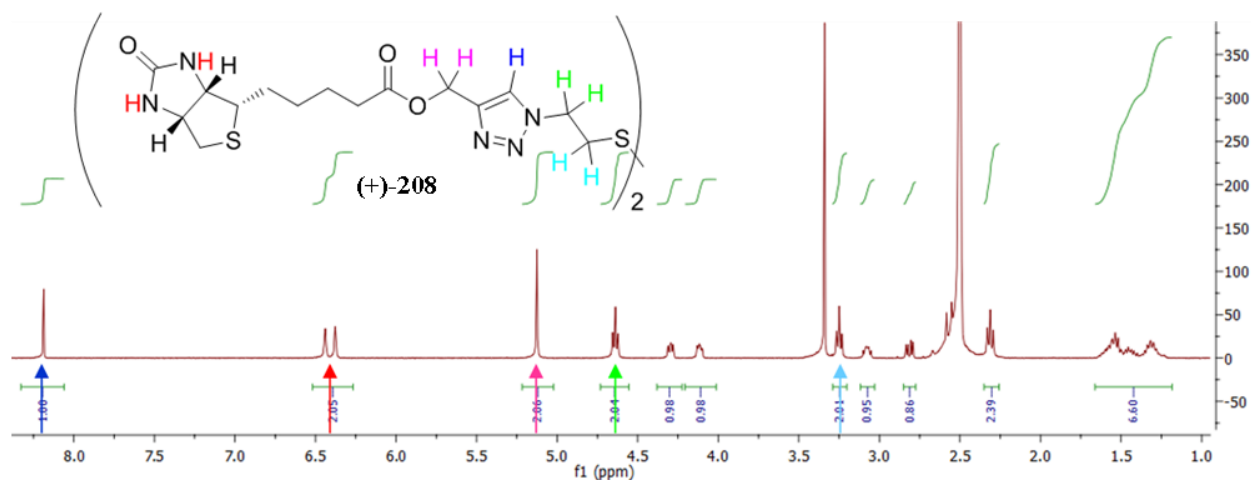
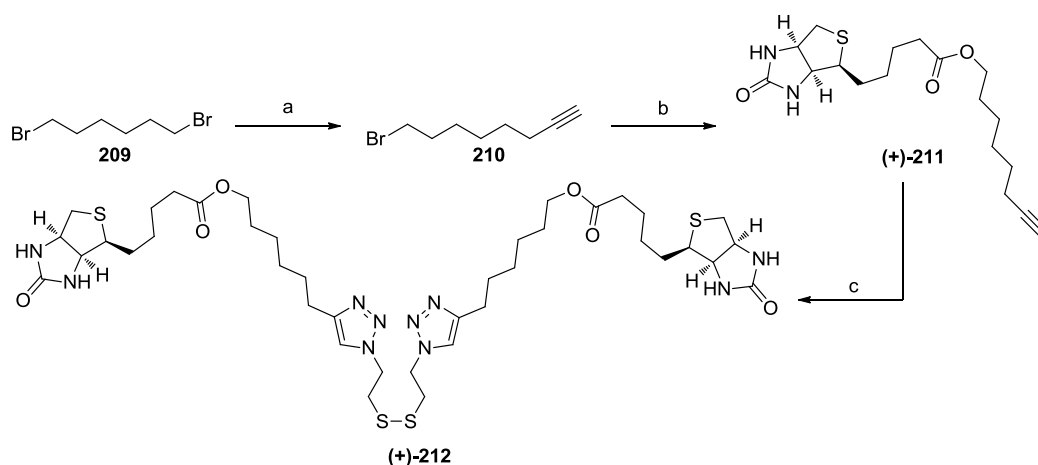


Figure 72 $^1\text{H-NMR}$ (400 MHz) of **208**

In the $^1\text{H-NMR}$ (400MHz, d_6 -DMSO) the 1,2,3- C_5 -triazole peak can clearly be seen at $\delta 8.19$ as a singlet and the diagnostic (+)-biotin amide signals, as two singlets, at $\delta 6.44$ and $\delta 6.38$ can be observed. The methylene between the 1,2,3-triazole and carbonyl group was observed at $\delta 5.13$ as a singlet and the methylenes from the disulfide linker were observed as triplets $\delta 4.64$ (t, $J 6.6$ Hz) and $\delta 3.25$ (t, $J 6.5$ Hz).

Gratifyingly, both (+)-**85** and the disulfide from **207** had survived the conditions for ‘click’ and formed (+)-**208**, we were concerned that the sulfur may chelate to the copper. The literature suggests that the length of the SAM linker effects the ability of the protein (streptavidin) binding of a ligand (+)-biotin) when bound to a surface.⁷⁰ With this in mind a selection of extended linkers were synthesised.



Scheme 51 a) Sodium acetylide, DMF, 12 hours, 50%. b) (+)-biotin (+)-**64**, K_2CO_3 , N,N -dimethylformamide, 16 hours, 94%. c) **207**, $\text{CuSO}_4 \cdot 5\text{H}_2\text{O}$, TBTA, sodium ascorbate, DMF, 70°C μW , 1 hour, 78%.

210 was generated by the desymmetrisation of 1,6-dibromohexane **209** with sodium acetylide affording 8-bromo-octyne **210**. This was followed by the displacement of the remaining bromide by the carboxylate of (+)-biotin (+)-**64** affording the 8 membered linker (+)-**211** complete with alkyne for coupling to the azido linker **207**. The ¹H-NMR(500 MHz) of (+)-**211** [Figure 73] affords the alkynyl triplet, at δ1.89 originating from the 8-bromo-octyne **210** and the broad amide protons seen at δ6.06 and 5.73 originate from the (+)-biotin (+)-**64**.

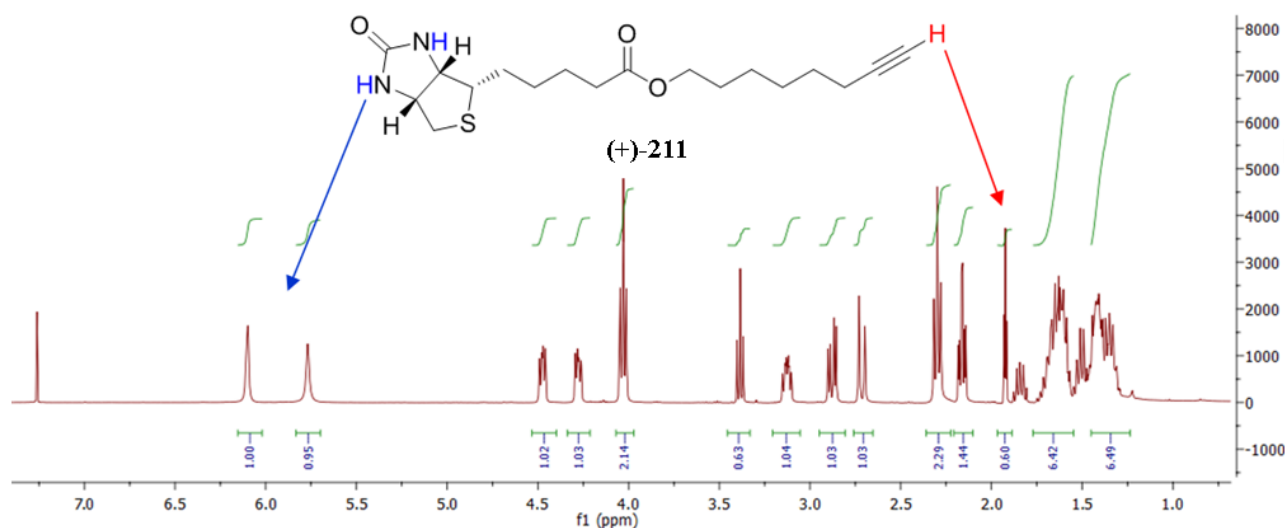


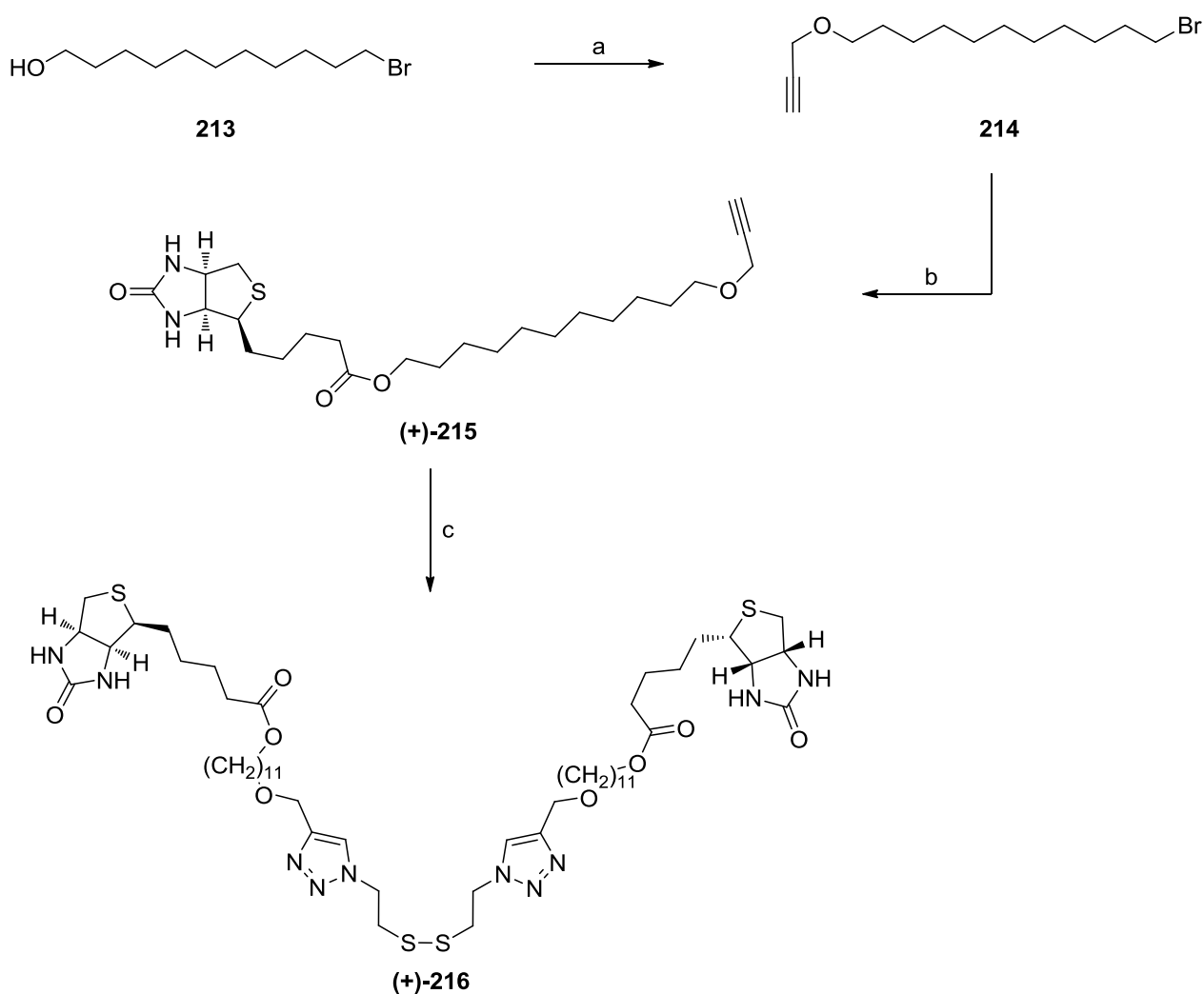
Figure 73 ¹H-NMR (500MHz) of (+)-**211**

Subsequently the standard ‘click’ conditions (CuSO₄•5H₂O, TBTA, sodium ascorbate, DMF, 70°C μW, 1 hour) were employed to couple (+)-**211** and **207** affording (+)-**212**.

Compound (+)-**212** was very polar and required a highly polar eluent 10% methanol in dichloromethane to elute it from the silica column. The solubility of the product in chloroform and methanol was poor, however, a mixture of chloroform and methanol afforded good solubility. This afforded a very broad ¹H-NMR (500MHz) spectrum but the 1,2,3-C₅-triazole peak could clearly be observed at δ7.52. Mass spectrometry afforded a strong ion at, *m/z* [ESI]⁺ M+Na 931.2 suggesting, along with full physiochemical analysis, FT-IR KBr(neat) 1750 C=O, 1683 C=O cm⁻¹, the product (+)-**212** had been generated.

The linker was then increased using 11-bromoundecanol **213**. After attempts to use sodium acetylide to displace the bromide failed, due to the strong basic nature of the sodium acetylide, the deprotonation of the alcohol to form an alkoxide was favoured. To negate this **213** was deprotonated at the alcohol using sodium hydride followed by the addition of an excess of 5 equivalents of propargyl bromide **86** affording the corresponding propargyl ether **214**. The subsequent displacement of the bromide by the (+)-biotin (+)-**64** carboxylate afforded the required (+)-biotin derivative **215**. **215** was subsequently ‘clicked’ to the disulfide linker **207**, using the

standard conditions ($\text{CuSO}_4 \cdot 5\text{H}_2\text{O}$, TBTA, sodium ascorbate, DMF, 70°C μW , 1 hour), affording **216** in good yield 80%.



Scheme 52 a) Sodium hydride(60% dispersion in mineral oil), propargyl bromide, THF, 72%. b) (+)-biotin (**64**), potassium carbonate, DMF, 80% c) **207**, $\text{CuSO}_4 \cdot 5\text{H}_2\text{O}$, TBTA, sodium ascorbate, DMF, 70°C μW , 1 hour, 86%.

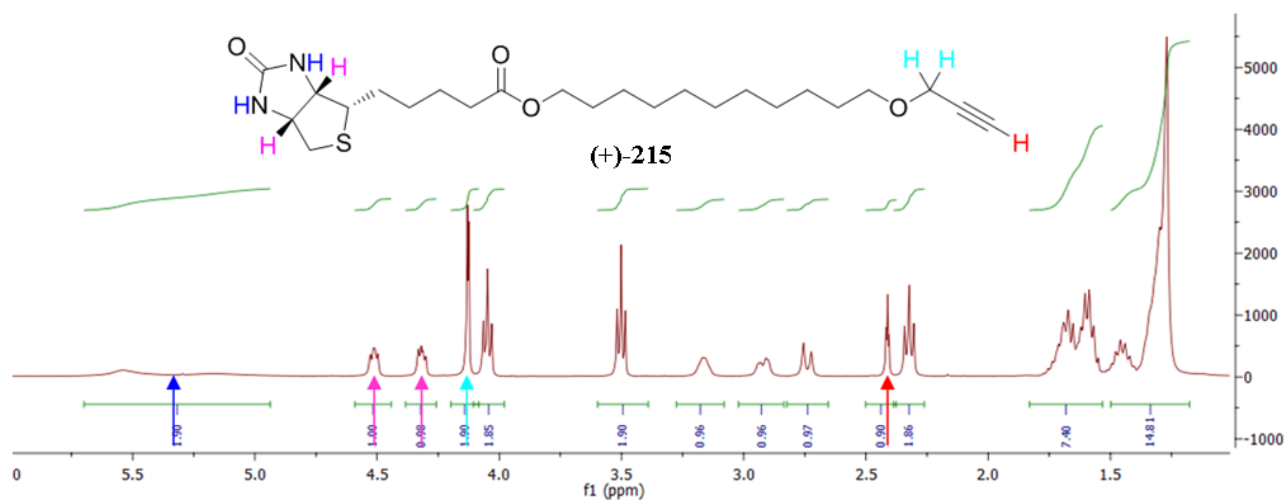


Figure 74 $^1\text{H-NMR}$ (400MHz) spectra of **(+)-215**

In the $^1\text{H-NMR}$ (400MHz) spectra of (+)-**215** (Figure 74) the alkynyl proton at $\delta 2.44$ (t, $J_{2.3}$ Hz) and is coupled to the propargyl methylene at $\delta 4.15$ (d, $J_{2.3}$ Hz) and the broad singlet at $\delta 1.27$ showing the aliphatic chain from the linker and the broad multiplets between $\delta 1.31$ and 1.75 correspond to the aliphatic chain of the (+)-biotin. The (+)-biotin signals can also be observed, the two central (+)-biotin protons (pink) at $\delta 4.62$ and 4.34 and the amide protons are very broad and are located at around $\delta 5.34$. Mass spectrometry afforded an ion at m/z $[\text{ES}]^+ \text{M}+\text{Na}$ 475.2 affording a strong indication that (+)-**216** had been generated.

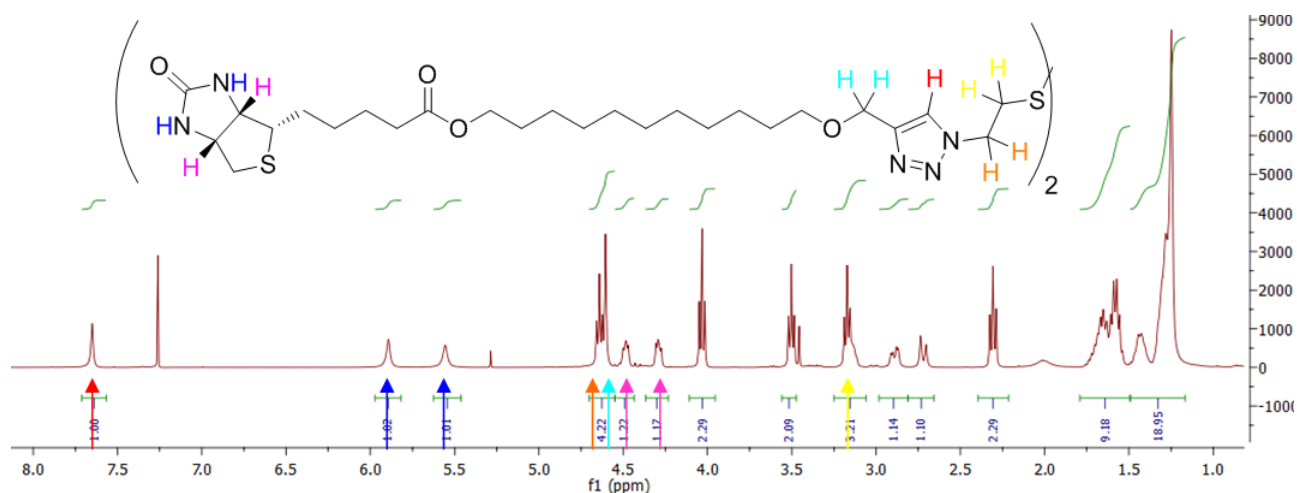
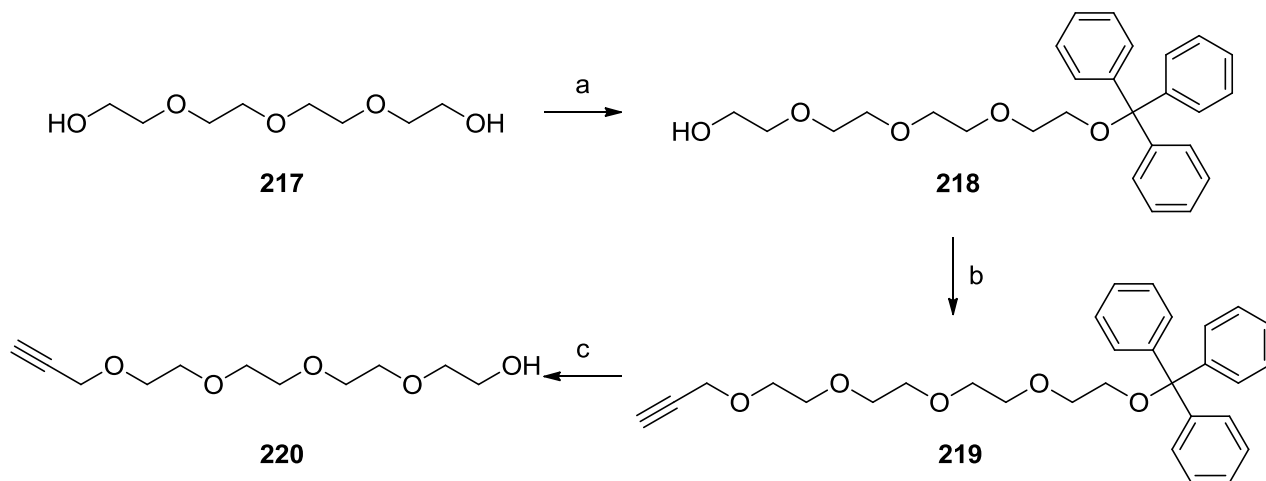


Figure 75 $^1\text{H-NMR}$ (500MHz) spectra of (+)-**216**

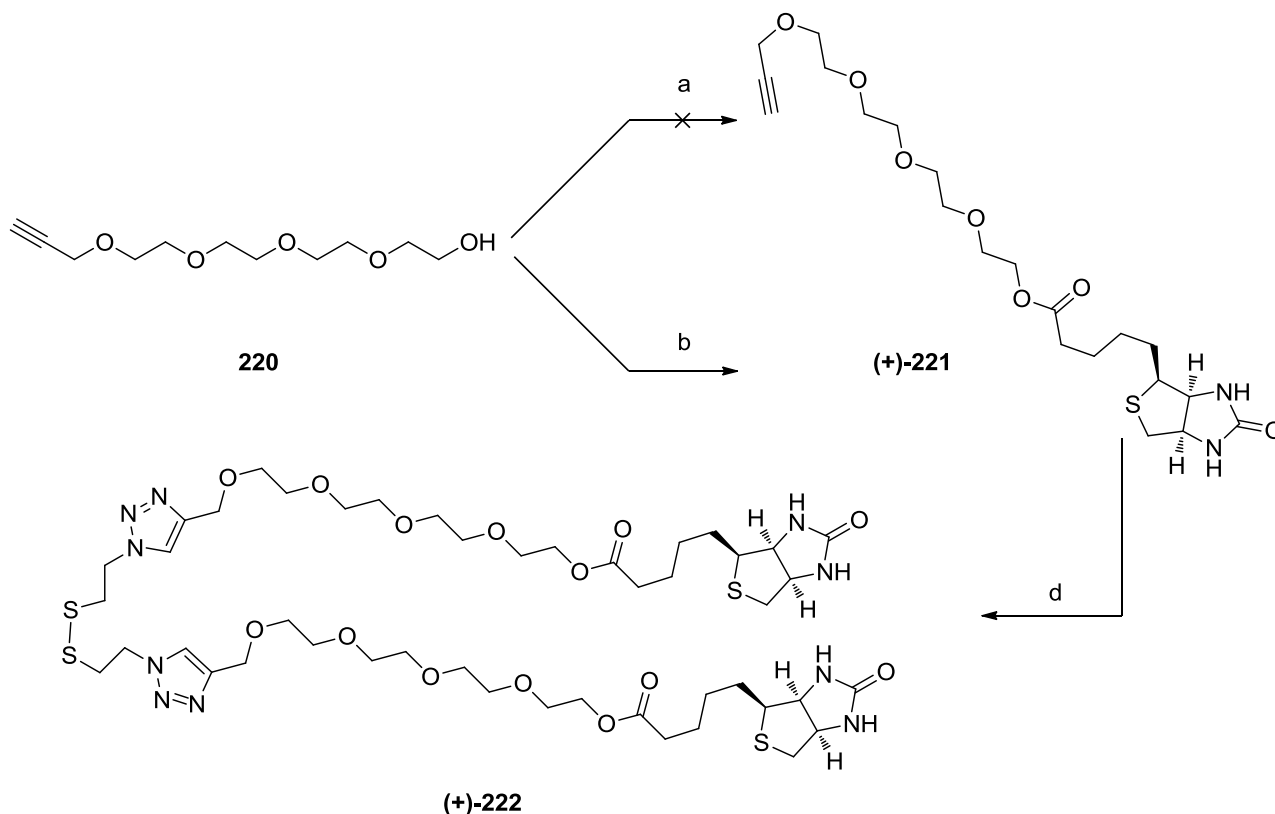
In the $^1\text{H-NMR}$ (500MHz) spectra of (+)-**216** [Figure 75] the 1,2,3- C_5 triazole peak at $\delta 7.60$ was observed and the disappearance of the alkynyl proton (Figure 74 $\delta 2.44$). The methylene between the 1,2,3-triazole and oxygen (light blue, Figure 75) was shifted from $\delta 4.15$ downfield to $\delta 4.59$ affording a strong indication that the chemical environment of the protons has changed to the expected more deshielded environment. The amide NHs, from (+)-biotin were observed at $\delta 5.84$ and $\delta 5.50$, and the two central (+)-biotin protons (pink) were observed at $\delta 4.44$ and $\delta 4.29$. The methylenes from the disulfide linker can be observed as triplets at $\delta 4.59$ (t, $J_{6.6}$ Hz) and $\delta 3.12$ (t, $J_{6.7}$ Hz).

The final extended linker was synthesised using *tetraethylene glycol* (PEG₄) **217**. One of the free hydroxyl groups was protected with a trityl group affording the triphenyl methyl ether **218**. Subsequent deprotonation of the remaining hydroxyl with sodium hydride and attack of the resulting alkoxide anion on propargyl bromide afforded a trityl protected PEG₄ propargyl ether **219**. **219** was *O*-trityl-protected with *para*-toluene sulfonic acid hydrate generating the free hydroxyl containing **220** [Scheme 53].



Scheme 53 a) Trityl chloride, pyridine, 12 hours, 45%. b) Sodium hydride (60% dispersion in mineral oil, propargyl bromide, THF, 2 hours, 74%. c) *para*-toluene sulfonic acid hydrate, methanol, 4 hours, 92%.

Attempts to couple **220** to (+)-biotin (+)-**64** using *in situ* formation of an ‘activated’ ester, using TBTU, [Scheme 54 path a] of (+)-biotin failed affording only start material **220**. This was overcome by refluxing (+)-biotin (+)-**64** with **220** and catalytic *para*-toluene sulfonic acid hydrate in toluene, the water generated during this condensation reaction was removed *via* a Dean-Stark trap. This reaction afforded a low yield 35%, presumably due to polymerisation of the linker, generating a dark brown sticky residue during the reaction. Careful flash column chromatography on silica gel eluting with 10% methanol in dichloromethane afforded the required product (+)-**221** in a 35% yield.



Scheme 54 a) TBTU, diisopropylethylamine, (+)-biotin (+)-**64**, -20°C – ambient temperature, no reaction. b) (+)-biotin

(+)-**64**, *para*-toluene sulfonic acid hydrate, toluene, reflux, 4 hours, 35%. d) 207, CuSO₄•5H₂O, TBTA, sodium ascorbate, DMF, 70°C μ W, 1 hour, 82%.

Compound (+)-**221** was subsequently coupled to the disulfide linker **207** following the normal ‘click’ protocol (CuSO₄•5H₂O, TBTA, sodium ascorbate, DMF, 70°C μ W, 1 hour) in good yield 74%. In the ¹H-NMR(500MHz) spectrum of (+)-**222** [Figure 76] the 1,2,3-C₅-triazole peak is observed at δ 7.68. A large signal at δ 3.59 corresponds to the ethylene groups from PEG. The diagnostic (+)-biotin peaks were observed at δ 6.08 and δ 5.39 for the amides, the central (+)-biotin (blue) signals were observed at δ 4.43 and δ 4.22. The methylene between the triazole and oxygen was observed as a singlet at δ 4.59 and finally the two methylenes from the disulfide linker were observed as triplets at δ 4.59 (t, *J*6.9 Hz) ppm and 3.13 (t, *J*6.6 Hz). FT-IR afforded disappearance of the azide peak at 2101cm⁻¹, and mass spectrometry afforded an ion at *m/z* [ES]⁺ M+Na 1143.3.

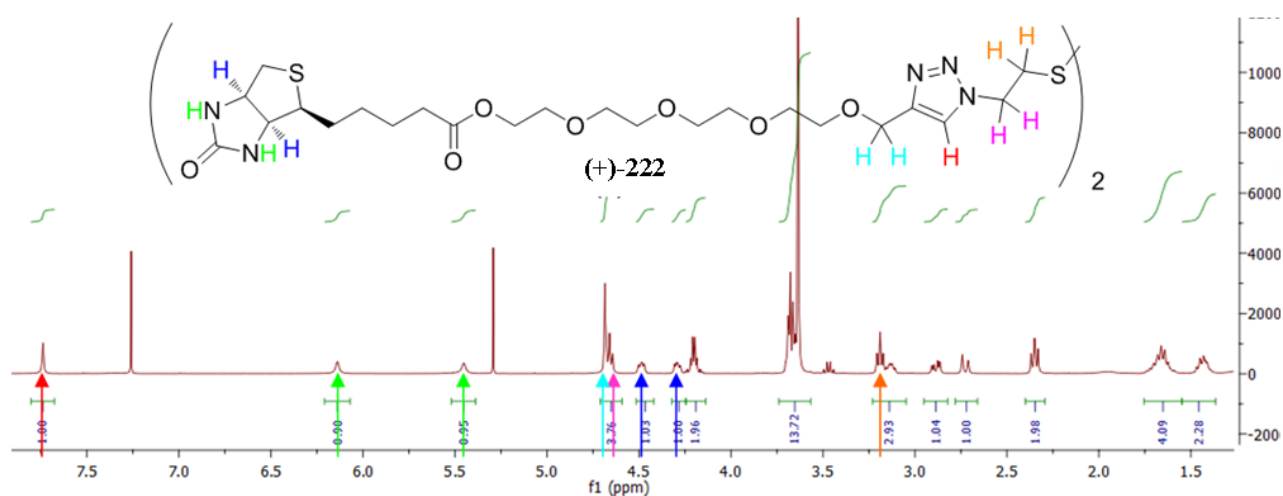


Figure 76 ¹H-NMR(500MHz) spectrum (+)-**222**

4.14 Preparation of 24 karat gold compact discs for SAMs

The preparation of the compact disc, to expose the 24 karat gold layer, has been described by Yu. The lacquer layer, which protects the gold surface, was removed by treating the top surface, identifiable *via* the writing on the top face, with a solution of 70% nitric acid for 3-5 minutes, followed by washing with deionised water and absolute ethanol.¹¹⁴ The compact disc was submerged in 70% nitric acid in a 7 inch shallow beaker. This was left until the surface took on a ‘crackled’ appearance and then removed from the acid and washed with deionised water and absolute ethanol. An air line was used to blow the remaining lacquer from the surface and the exposed gold layer was washed again with absolute ethanol and dried with an air line. The disc was then placed in a desiccator and stored under argon.

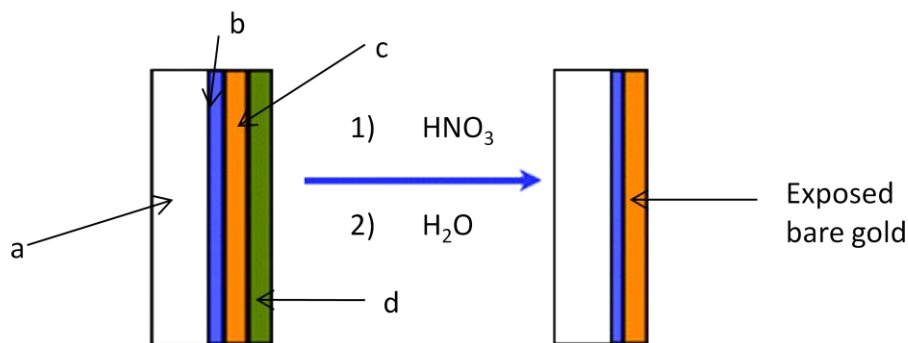


Figure 77 Components of a gold compact disc. a) polycarbonate backing, makes up most of the CD. b) photosensitive dye layer CD-R. c) gold layer ~50 nm. d) protective lacquer. The protective lacquer is removed by immersion of the CD in 70% nitric acid.

This process was essentially simple, however, the compact disc needed to be cut up to allow for analysis by scanning electron microscopy (SEM) and Energy-dispersive X-ray spectroscopy (EDS). This proved to be rather challenging, as cutting the compact disc after the lacquer had been removed resulted in the displacement of the gold from the polycarbonate backing. A variety of techniques were attempted including a hot knife, metal press, scissors and guillotine but all resulted in displacement of the gold. The problem was finally solved by cutting the compact disc, into pieces approximately the size of microscope slides and then removing the lacquer. A small amount of damage was caused to the edge of the slides but the centre area remained bound to the surface of the polycarbonate layer. To remove the lacquer from the compact disc centre required more care than from a complete disc. Submerging the slides into nitric acid resulted in total removal of the gold layer from the base. To negate this problem 200 μL of nitric acid was pipetted onto the surface and care was taken not to spill it on the edges of the slide. This was left for approximately five minutes before being removed by pipette. This left a crackled area in the centre of the slide, where the lacquer had come away from the gold, and this was removed by washing with a jet of water. The slide was then treated with an air line to blow the lacquer off of the surface leaving the bare gold layer exposed. This was then washed with ethanol and dried before being stored in a dessiccator under argon.

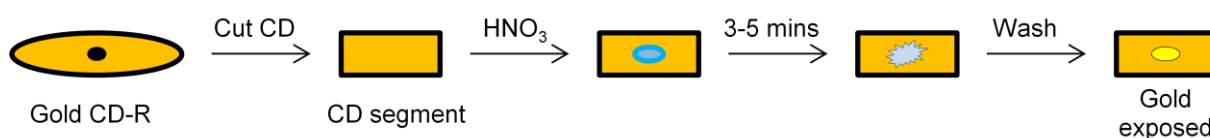


Figure 78 Successful route to generating segments of CD for analysis and subsequent removal of protective lacquer.

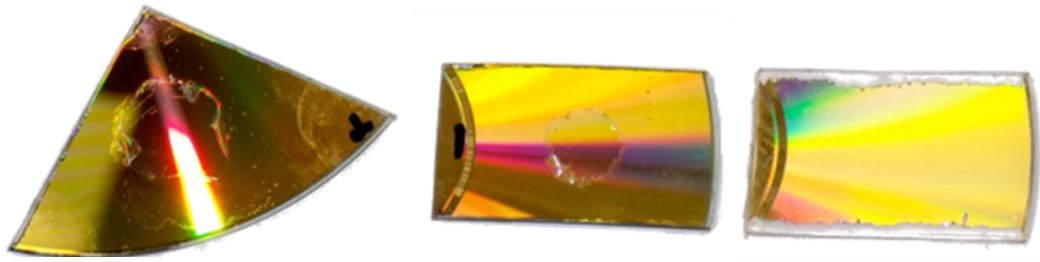


Figure 79 Segments of CD with protective lacquer removed *via* route shown in Figure 78

These segments were then analysed by SEM, atomic force microscopy (AFM) and EDS to confirm the gold layer had been exposed and that the surface was flat enough to afford for the formation of self assembled monolayer (SAM).

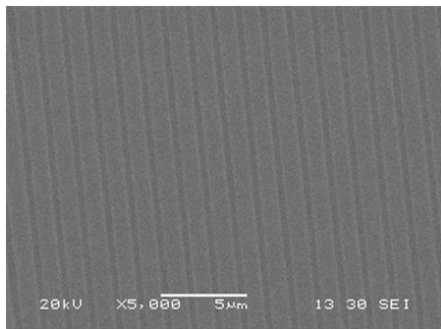


Figure 80 SEM image of gold surface of the CD the grooves are used for alignment of the LASER during reading / writing

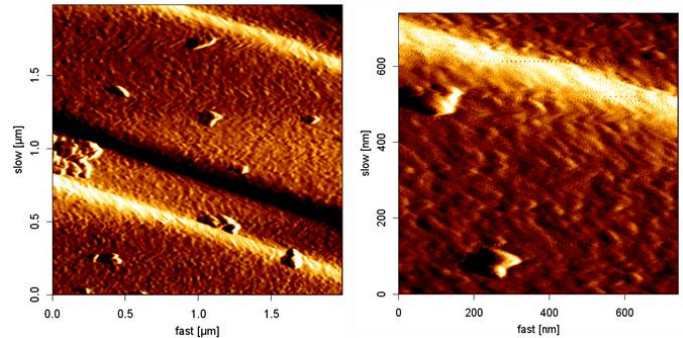


Figure 81 AFM image of gold CD surface affording closer images of the pregroove and feathered appearance of the gold layer.

The SEM image [Figure 80] shows a $25 \mu\text{m}^2$ area of the bare gold on the compact disc, the lines seen are trenches which are built into the polycarbonate disc before the gold surface is applied. These are called the pregroove and are used to guide the LASER to the read/write areas on the disc. The AFM images [Figure 81] show the width of this groove is just under $0.5 \mu\text{m}$ wide. The AFM images show the surface in more detail and the slight imperfections on the surface can be observed. Discussions with the microscopist suggest that the surface of the disc is slightly flatter than a sputter coated slides but not quite as flat as mica. The image to the right shows the feathering pattern of the gold at the hundreds of nanometre scale. Below is an AFM depth map which shows clearly a difference in height of the pregrooves, with dark being the deeper areas.

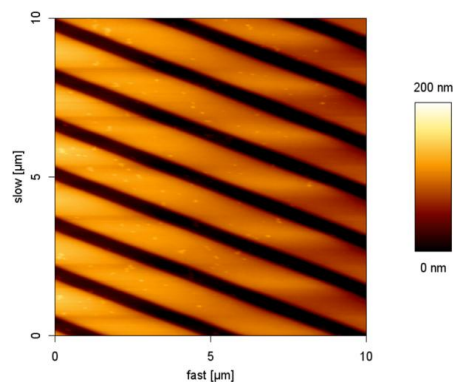


Figure 82 AFM depth map of the CD surface, the pregroove can be seen as the darker areas, therefore, deeper region compared to the lighter coloured area.

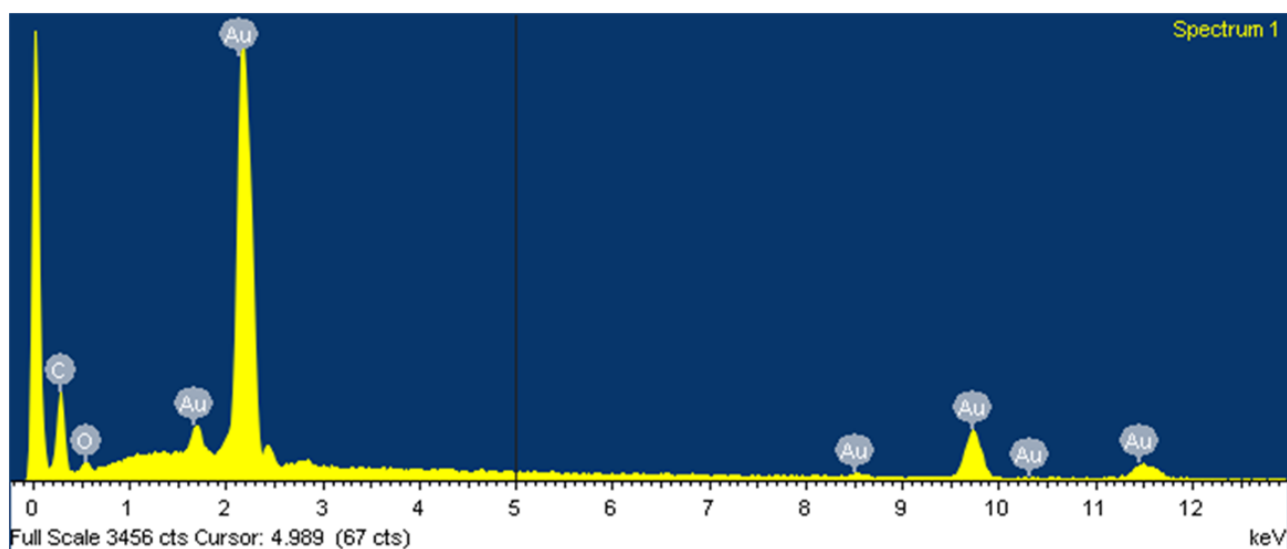


Figure 83 Energy Dispersive X-ray Spectroscopy spectrum showing the signature fingerprint of gold from the surface of the compact disc

The EDS data [Figure 83] shows the gold layer has been successfully exposed affording a very strong signal in the gold region.

4.15 Self Assembled Monolayer formation

With the (+)-biotin analogues (+)-**208**, (+)-**212**, (+)-**216** and (+)-**222** in hand, we were ready to attempt their use as SAM precursors on a gold disc. A 5 mg sample of (+)-**208**, (+)-**212**, (+)-**216** and (+)-**222** were dissolved in 500 μL of dimethylsulfoxide and 50 μL was loaded into a 1 mL syringe. The syringe had the air pushed out and the dimethylsulfoxide solution was held by its meniscus protruding from the end of the syringe. This was clamped and the segment of gold disc raised *via* a lab jack until the hanging drop of solution was resting on the gold surface. This ensured that the sample would not dry out whilst the SAMs were forming.

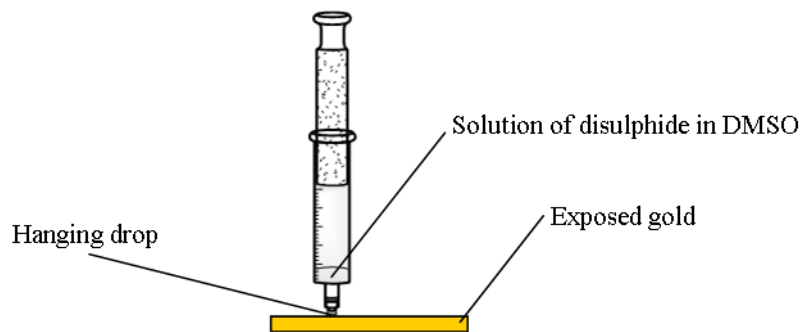


Figure 84 Hanging drop method of applying di-sulfides (+)-**208**, (+)-**212**, (+)-**216** and (+)-**222** to the surface of the compact disc to ensure (+)-**208**, (+)-**212**, (+)-**216** and (+)-**222** remained in solution during the SAM formation process.

The solution was left for 24 hours before being carefully removed and the gold surface washed with deionised water and absolute ethanol, thoroughly dried and returned to a desiccator for storage under argon. Attempts to establish if the SAM had indeed been formed turned out to be problematic. Attempts to obtain an FT-IR spectrum of the monolayer using Reflection Absorption Infra Red Spectroscopy (RAIRS) failed due to the weak signal afforded from the tiny quantity of sample. Attempts to visualise the SAM using AFM and SEM also drew a blank. However, discussions with a mass spectrometry company, ‘SAI Limited’ were fruitful and they kindly agreed to do some testing for us. The sample of (+)-**208** was sent and some interesting results came back.

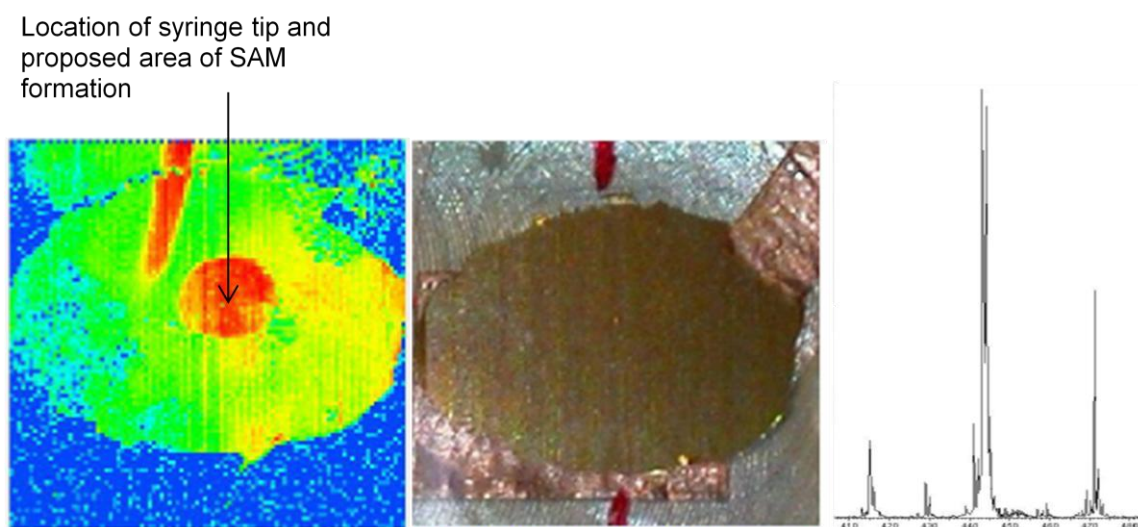


Figure 85 The MALDI-TOF MS image of the SAM applied region of the compact disc segment, red indicates strong ion count (left). Image of the gold segment in the MALDI-TOF mass spectrometer (centre) and the mass spectrum of the SAM region indicating mass of around 440 Da (right).

The image in the centre, [Figure 85] affords the gold surface inside the MALDI-TOF and to the left is an image map of the mass analysis of the sample. The blue area corresponds to no signal, the yellow and green correspond to low signal and red corresponds to a strong signal. Clearly the area where the syringe was applied affords an incredibly strong signal and has a well defined shape. This red region shows a mass on the right of around 440 mass units, which is approximately half of

the mass of the disulfide. This was the clearest indication that the SAM had been formed. The mass is not exact, however SAI say that calibration was off due to the extra height of the sample in the MALDI-TOF spectrometer. A snippet of their assessment can be seen below.

We again performed an imaging experiment over the solution sample using the same laser power and conditions as above collecting 10 shots per pixel. In Figure 4 its clear to see a high intensity region in the centre of the gold plate for mass around 440. We assume this is the area with the biotin attached.

Again the re areas are the most intense going through yellow, green then blue the least intense.

Note the calibration maybe a small amount off as we calibrated on a different plate that was a slightly different thickness

With some evidence of SAM formation taking place at the surface the other examples (+)-**208**, (+)-**212**, (+)-**216** and (+)-**222** were then bound to gold discs in an identical fashion. The raster used to complete the MALDI-TOF image of the gold surface was very intensive on the equipment and it was noted by SAI that 1% of the total LASER life of the spectrometer had been consumed during this one experiment.

4.16 Biotin / Streptavidin binding on a gold disc.

With evidence that the (+)-biotin compound (+)-**208** had bound to the gold CD surface, the application of streptavidin was investigated. Once again a rig was made from a syringe and 100µL of a solution of 11.32 µM streptavidin in deionised water was applied using the hanging drop method. This was left in a warm place ~30°C for 16 hours to encourage binding and reorganisation to occur. The syringe was carefully removed and the applied area was washed with water and ethanol. These were then stored under argon in a dessicator, before being transferred to SAI for analysis.

4.17 MALDI-TOF mass spectrometry analysis of binding events

The samples were subjected to MALDI-TOF mass spectrometry at SAI Ltd using a LaserToF TT mass spectromer. This is a top of the range time of flight mass spectrometer, designed for peptide and protein analysis. The SAI research model was used as it could be easily modified to accommodate the disc segments.



Figure 86 SAI LaserToF TT mass spectrometer
Figure 87 Durability test to ensure the CD could withstand the LASER energy from the MALDI-TOF spectrometer

The durability of the disc was tested to ensure the gold layer and CD would stand up to the LASERs intense ionisation. A power of 75% was selected on advice from SAI, stating that in their opinion this power was suitable for successful proteomic analysis, and a blank CD segment was bombarded with 1 – 10,000 shots of the LASER in small 200 µm raster. This showed that the damage started to occur over 100 shots but was not clearly visible until over 1000 shots. Out of curiosity the LASER was then set to 100% power and fired at the blank sample, unsurprisingly, this obliterated the gold layer and caused visible damage to the polycarbonate layer very quickly.

Generating a reference streptavidin MALDI-TOF mass spectrum with the parameters outlined above, a 10 µL sample of 11.32 µM streptavidin in water was placed on the surface of a CD segment and left to evaporate, following this 1 µL of a 20 mg/mL aqueous solution of α -cyano-4-hydroxycinnamic acid (CHCA) was added to the streptavidin as a matrix to aid in ionisation of the sample. This was subjected to MALDI analysis to give a reference of the streptavidin protein.

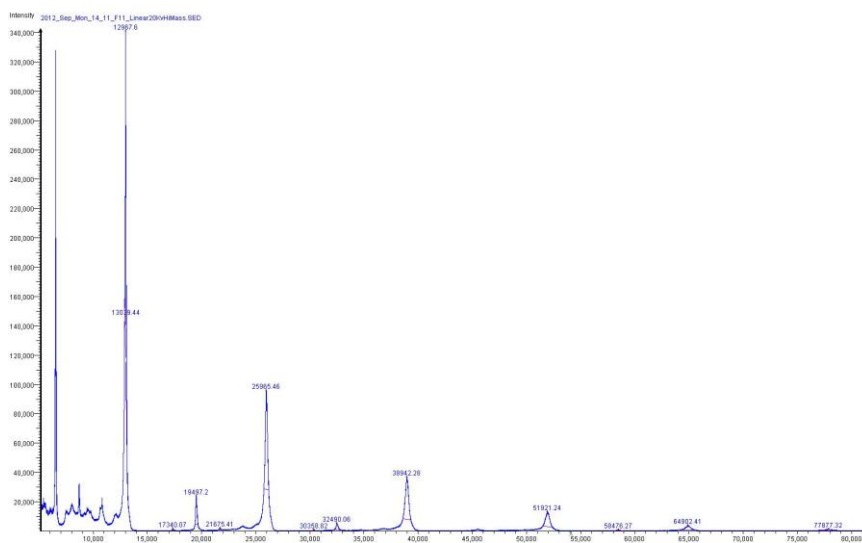


Figure 88 MALDI-TOF MS spectrum of streptavidin with CHCA matrix

The units of the streptavidin protein can clearly be seen, at 12,967 Da for the monomer, 25,985 Da for the dimer, 38,942 Da for the trimer and 51,921 Da for the tetramer. A decrease in intensity is observed as the oligomer gets larger and is presumably due to the high energy of the LASER disrupting the bonding between the units, resulting in a higher proportion of streptavidin monomers being detected. This is in agreement with the literature value of the monomer unit reported by Beavis who calculated the mass of the amino acid residues 14 - 136 of the streptavidin sequence 12,971 Da. Beavis offers an experimental value of $12,969 \pm 2$ Da from experimental results.¹⁴⁰

Streptavidin is a tetrameric protein, made up of four identical monomer units each capable of binding a (+)-biotin unit. Due to the shape of streptavidin we expect two of the four streptavidin binding sites to be occupied by (+)-biotin analogues. The high energy of the LASER radiation used to ionise the sample will cause the streptavidin to break into its constituent monomers. [Figure 89]

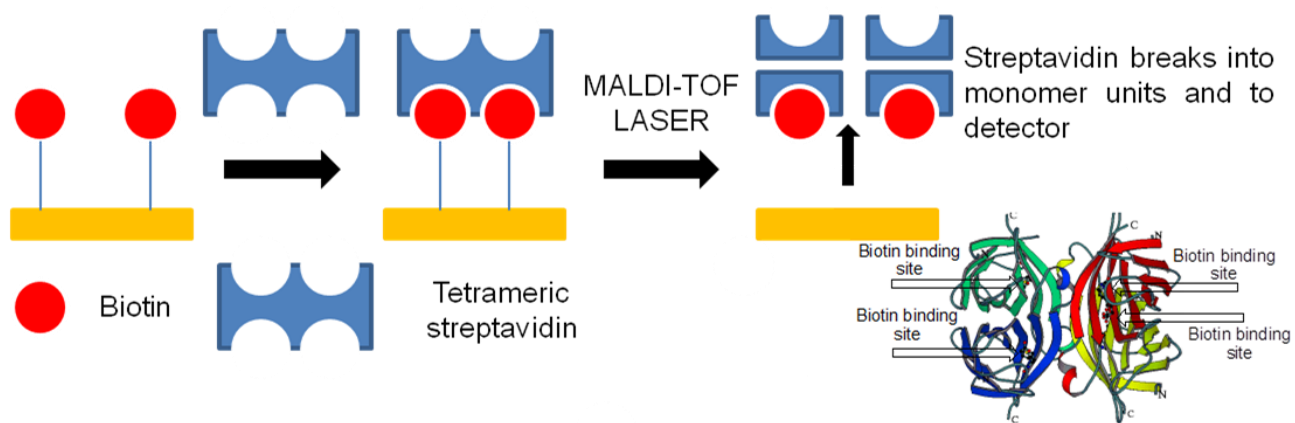


Figure 89 Schematic of (+)-biotin and its interaction with streptavidin on a gold surface. It is thought that two of the 4 available streptavidin binding sites will interact with the (+)-biotin. MALDI-TOF ablation of the streptavidin and (+)-biotin linker will release it from its tether and allow it to be detected.

This was followed by a control sample, where, streptavidin was applied to the gold disc, using the syringe hanging drop method as previously described, but this had not previously been treated with a (+)-biotin substrate. The control was treated in an identical fashion to the biotinylated samples and was washed with deionised water and absolute ethanol, dried and stored in a desiccater.

The raster choice was essential, as firing on the spot once would obliterate the sample, the second shot would then be firing on bare gold and lead to an unnecessary number shots being used and a diminished result. The raster was set to 'fire' and move to ensure the same region was not ablated twice.

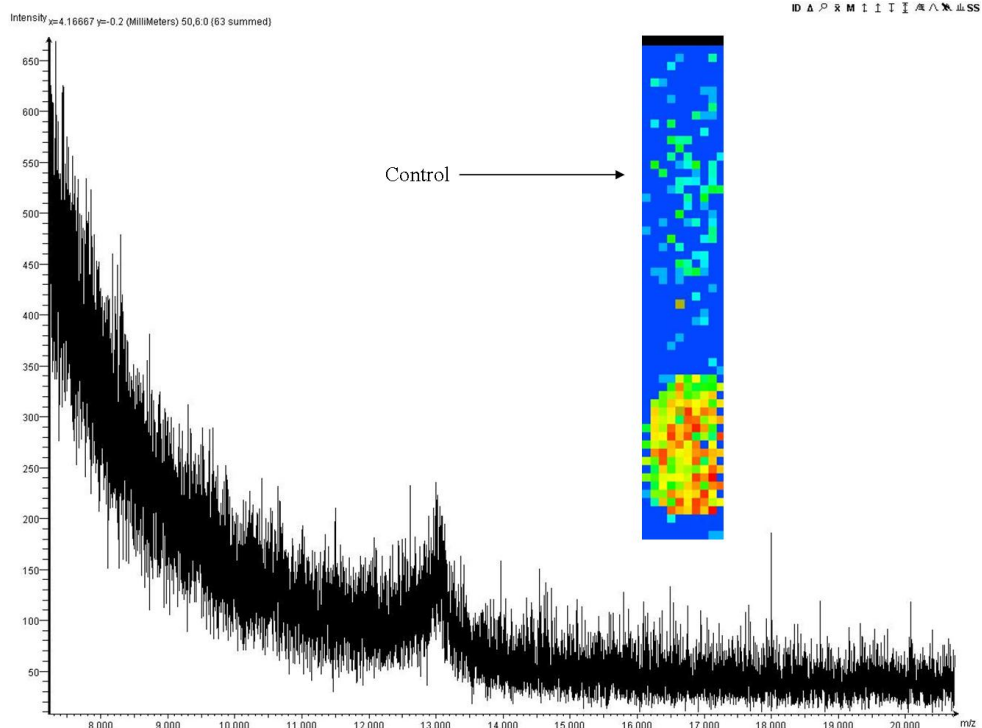


Figure 90 MALDI-TOF image and spectrum used as a control for non-specific binding.

The spot below the control sample was of neat streptavidin, freshly applied before analysis as a spectrometer control. A very low intensity peak at ~13 kDa can be seen which is from a very small amount of residual streptavidin but is hardly detectable.

The mass spectrometrist could only run these samples with a maximum detection limit of 30 kDa in order to use the imaging functionalities. To modify the spectrometer for analysis up to 60 kDa would have required ‘major electronic changes’ so this limit was deemed suitable as the two strongest intensities of the streptavidin (monomer and dimer) would still be able to be seen. Smaller rasters and imaging areas were necessary to prolong the life of the LASER.

The first sample to be analysed was (+)-**208** the (+)-biotin unit where the linker was shortest, $n = 6$. (6 atoms between (+)-biotin and the sulfur head group) The spot seen below the sample was of neat streptavidin as a control, this allows us to be confident that MALDI-TOF spectrometer was functioning correctly. The mass spectrum shown was the sums of only the target spot, the control was not included.

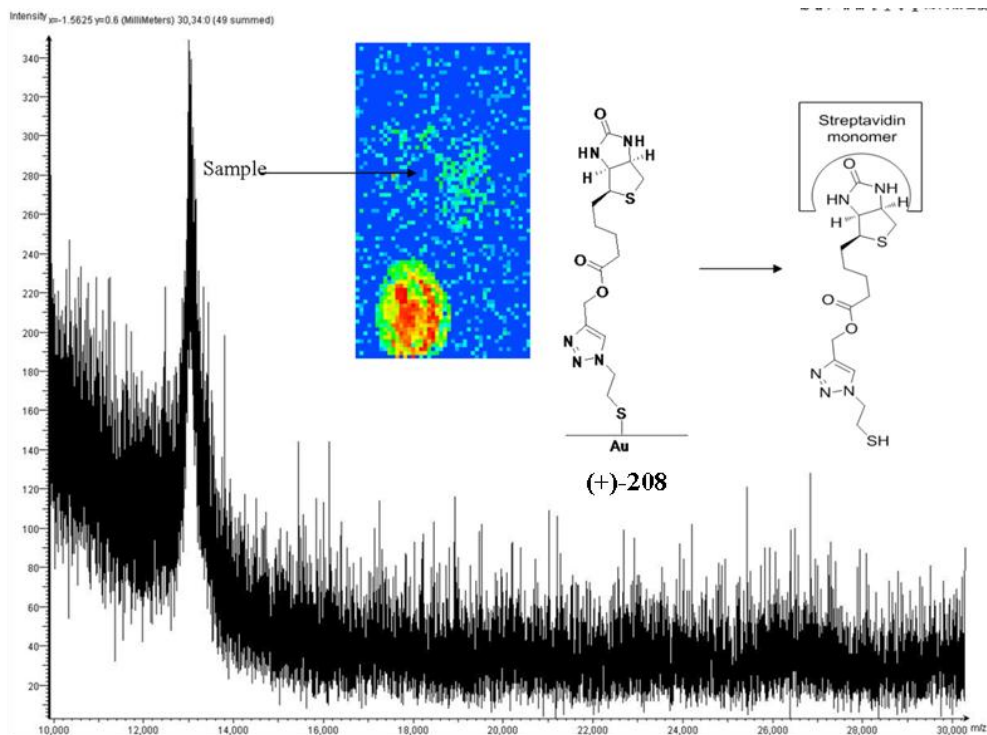


Figure 91 MALDI-TOF image and spectrum of sample (+)-208

The mass spectrum above [Figure 91] has a very weak signal corresponding to the streptavidin monomer with a very low intensity of mass ions ~ 340 with an incredibly poor signal to noise ratio $\sim 4:1$. The peak at ~ 13 kDa is of the monomer and a slight hump at ~ 26 kDa can just be made out, however, this is far from conclusive but was looking promising as it was more intense than the control sample. This was followed by (+)-212, where, $n = 11$ and again the spot below the sample is a spectrometer control.

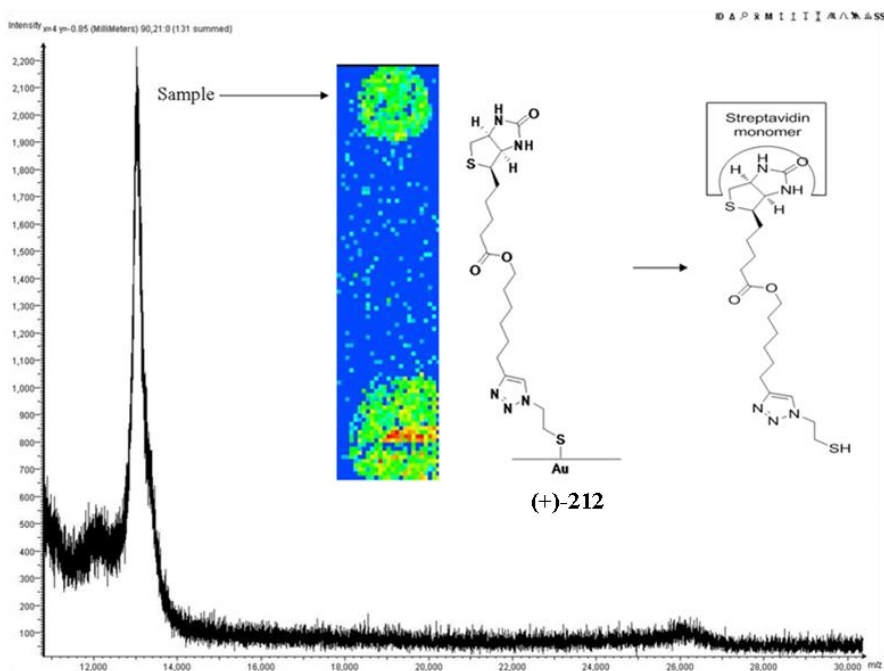


Figure 92 MALDI-TOF image and spectrum of sample (+)-212

The mass spectrum from sample (+)-212 [Figure 92] affords an improvement with a much more intense spectra acquired and a clear peak at ~13 kDa and a clearer ‘hump’ at 26 kDa compared to the previous sample using (+)-208. The intensity for the streptavidin monomer is ~2200 and a signal to noise ratio of ~15:1. This would suggest that this sample has more streptavidin bound to it than the previous example (+)-208. The increase in chain length here appears to have improved binding efficiency of the streptavidin and the (+)-biotin.

With another promising result, the next to face the LASER bombardment was (+)-216, where n=19, an increase of 8 atoms on the linker length. The spot below the sample is, again, the control streptavidin.

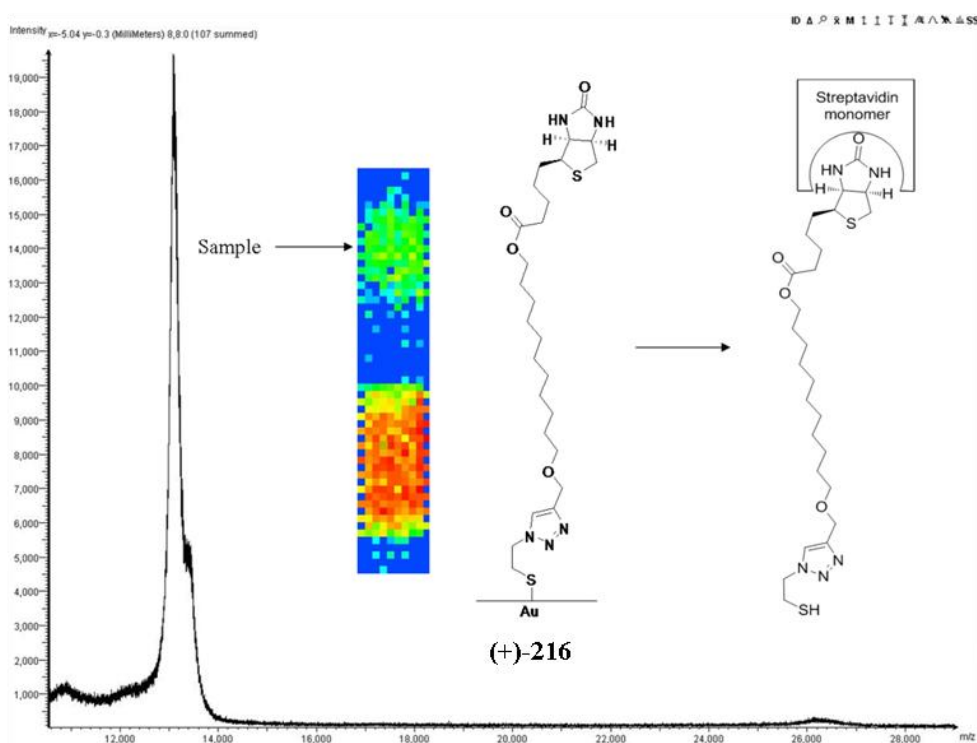


Figure 93 MALDI-TOF image and spectrum of sample (+)-216

For sample (+)-216 there was another improvement in intensity of ~19,500 and an improvement in the signal to noise ratio ~39:1 seen on this sample compared to both previous samples (+)-208 and (+)-212. This affords a strong indication that the (+)-biotin/streptavidin binding events were occurring on the CD surface. The strongest intensity peak at ~13 kDa and an indisputable signal at ~26 kDa seem to confirm mass ions for both monomer and dimer of streptavidin.

With an excellent result in hand the next sample (+)-222 was subjected to MALDI-TOF analysis. Here sample (+)-222 thus, n=19, but with a *tetra*-ethylene glycol linker rather than the alkyl chain as previously seen.

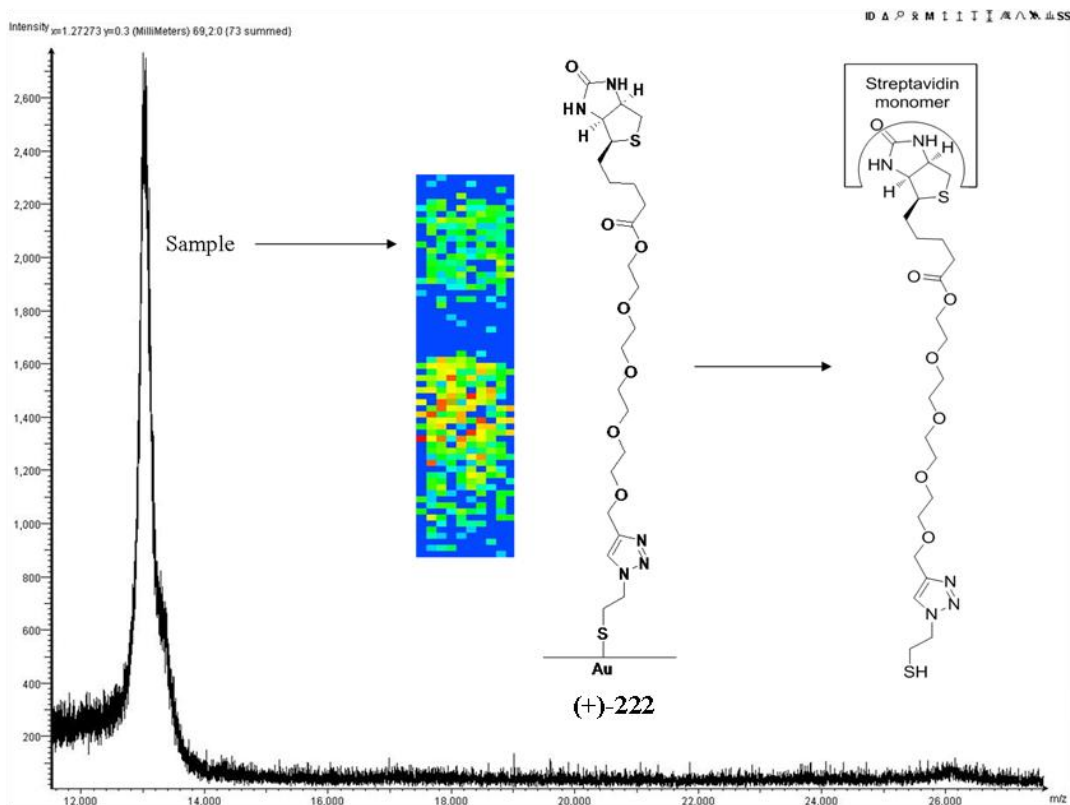


Figure 94 MALDI-TOF image and spectrum of sample (+)-222

From sample (+)-222 [Figure 94] a clear peak is observed at ~13 kDa and a small broad peak at ~26 kDa, suggesting that this has also got potential, however, this doesn't appear to be as successful as the previous sample. The intensity was ~2800 and the signal to noise ratio was ~28:1.

Sample	n=	Intensity	Signal to noise ratio streptavidin monomer
Reference	x	250	2:1
(+)-208	6	340	4:1
(+)-212	11	2200	15:1
(+)-216	19	19500	39:1
(+)-222	19PEG	2800	28:1

Table 13 Intensity and signal to noise ratio for MALDI-TOF analysis

From the data in table 13 above it was clear that the length of the linker on (+)-biotin plays a hugely important role in the detection of streptavidin on a surface. Where the linker is very short *i.e.* n = 6, (+)-208 barely any streptavidin is detected, from this we can infer the (+)-biotin analogue (+)-208 has not bound very much streptavidin. This could be because: a) the linker has not packed very well onto the surface, reducing the density of the SAM and therefore less (+)-biotin is present on the surface for binding to streptavidin. b) the linker has bound to the surface and has a high density SAM but the linker is too short for the (+)-biotin to interact with the streptavidin binding sites. The increase in linker length to n = 11 (+)-212 has made a great improvement in the intensity and the

signal to noise ratio. The increase in the length of the linker could have increased the density of the SAM or made the (+)-biotin more available to the binding pockets of the streptavidin, therefore affording a stronger signal. When $n = 19$ via an alkane chain (+)-**216** a vastly improved spectrum was afforded. The intensity has been increased to a huge 19,500 and a signal to noise ratio of nearly 40:1 affording a very strong indication that the (+)-biotin and streptavidin were interacting at easily detectable concentrations on the compact disc. Sample (+)-**222** where $n = 19$ via a PEG chain the intensity and signal to noise ratios are still very good but not as conclusive as the previous sample (+)-**216**. The data in Table 13 gives a very strong indication that the best performing ligand in the series of compounds (+)-**208**, (+)-**212**, (+)-**216** and (+)-**222** was (+)-**216** where $n = 19$ via an aliphatic chain

This was probably indicative of the interactions of the alkyl chains between neighbouring SAMs, as described by Perez-Luna *et al*, the longer linker allows them to pack more tightly.⁷⁰ Thus, affording more (+)-biotin tail groups for the streptavidin to bind to, resulting in increased quantities of streptavidin on the surface and a stronger signal under MALDI-TOF analysis.

4.18 Tröger's Base Scaffolds for SAMs

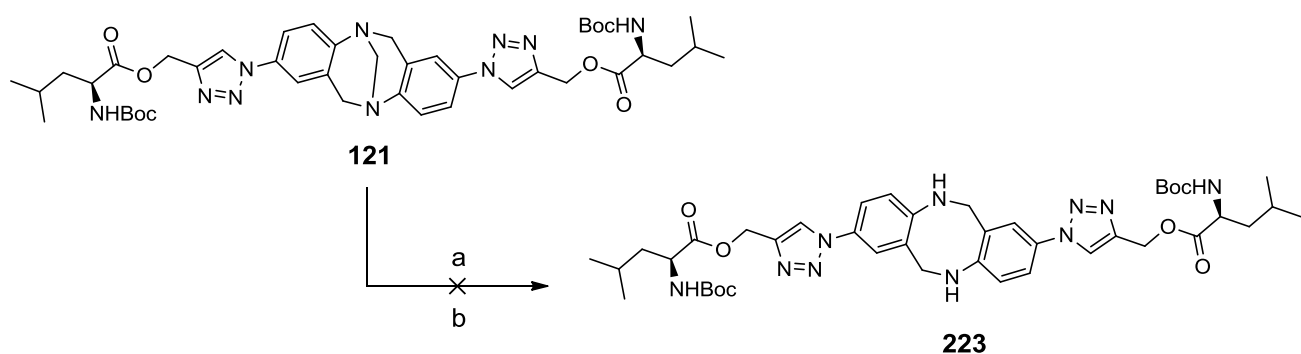
With some excellent results in hand, we postulated the idea that doubling the available (+)-biotin motifs on the SAMs, may allow more streptavidin to bind to the gold surface. If this was successful it would have the potential to increase the signal observed by the mass analysis or allow the spectra to be run for a shorter amount of time.

The Tröger's base scaffold, with its right angled shape, rigid structure and 3-fold functionality would be ideal scaffold for this purpose. Utilising the right angled shape and directing properties of Tröger's base, in conjunction with the 1,4 *bis*-substituted-1,2,3-triazole at the 2- and 8- position, would 'push' the (+)-biotin motifs away from each other. This would potentially allow twice the number of (+)-biotin motifs to be available for binding to the streptavidin protein. With the chemistry for functionalisation at the 2- and 8- position already in place, modification of the C13 methylene bridge could be attempted.

4.19 Methylene bridge removal from Tröger's base

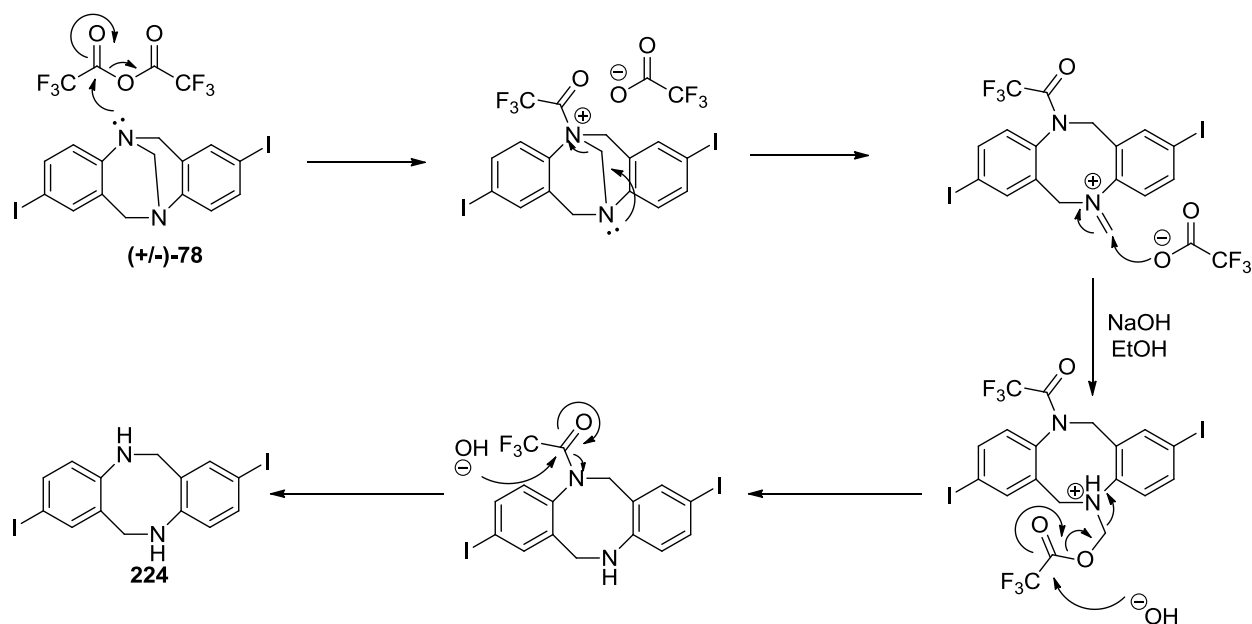
Insertion, modification or replacement of the methylene bridge (C13) of Tröger's base has been previously reported. These include total removal with acids and anhydrides,¹⁷ insertion of activated alkynes¹⁶ and replacement with aldehydes and di-bromo alkanes.¹⁹ The method as described by Mahon *et al*, total removal of the methylene bridge using trifluoroacetic anhydride, followed by

ethanolysis with sodium hydroxide in ethanol, was employed on a 2,8-*bis*-1,2,3-triazole-*N*-Boc-L-leucine Tröger's base derivative **121**.

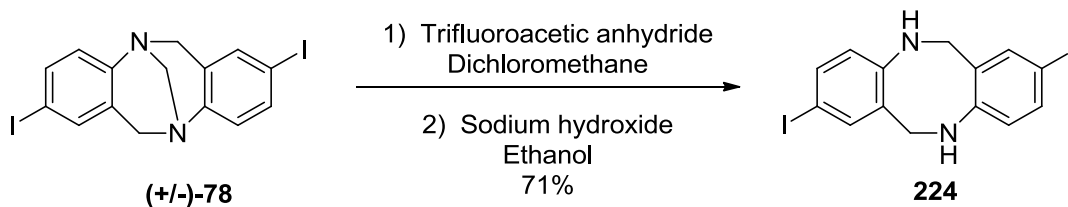


Scheme 55 Attempted removal of C13 bridgehead methylene from **121**. a) trifluoroacetic anhydride, DCM, 16 hours. b) Sodium hydroxide and ethanol.

This was unsuccessful and resulted in the efficient recovery of the starting material **121**. Undeterred, the much simpler 2,8-*bis*-iodo-Tröger's base (+/-)-**78** was submitted to the same procedure. Gratifyingly this afforded the desired diazocine **224** in a 71% yield. The reaction mechanism for the synthesis of **224** from (+/-)-**78** [Scheme 56] proceeds *via* nucleophilic attack of the tertiary amine of (+/-)-**78** on trifluoroacetic anhydride thus affording an amide salt. This was followed by imine formation of the remaining amine to the C13 methylene thus ring opening the structure. The resulting imine is attacked by the carboxylate ion of trifluoroacetic acid to give the corresponding ester. The resulting amide and ester are then hydrolysed *via* ethanolysis to give the diamine **224**.



Scheme 56 Proposed mechanism for the C13 bridgehead methylene removal using trifluoroacetic anhydride followed by ethanolysis.



Scheme 57 Reaction scheme for the removal of C13 bridgehead methylene of 2,8-*bis*-iodo Tröger's base (+/-)-**78**

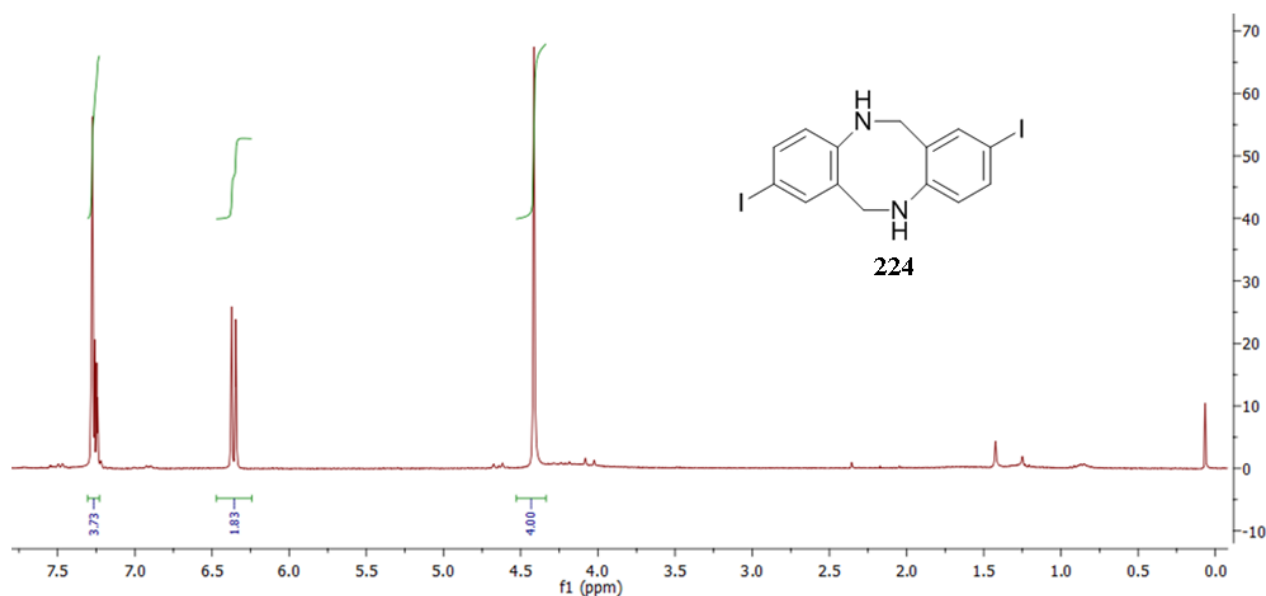


Figure 95 $^1\text{H-NMR}$ (400MHz) spectrum of 2,8-*bis*-iodo-5,6,11,12-tetrahydrodibenzo[b,f][1,5]diazocine **224**

The $^1\text{H-NMR}$ (400MHz) spectra of **224** [Figure 96] has dramatically changed, the aliphatic doublets from (+/-)-**78** have been replaced by a singlet at δ 4.41 integrating to 4 protons. Thus the singlet originating from the C13 bridgehead group is no longer observed and a shift can be seen in the aromatic region.

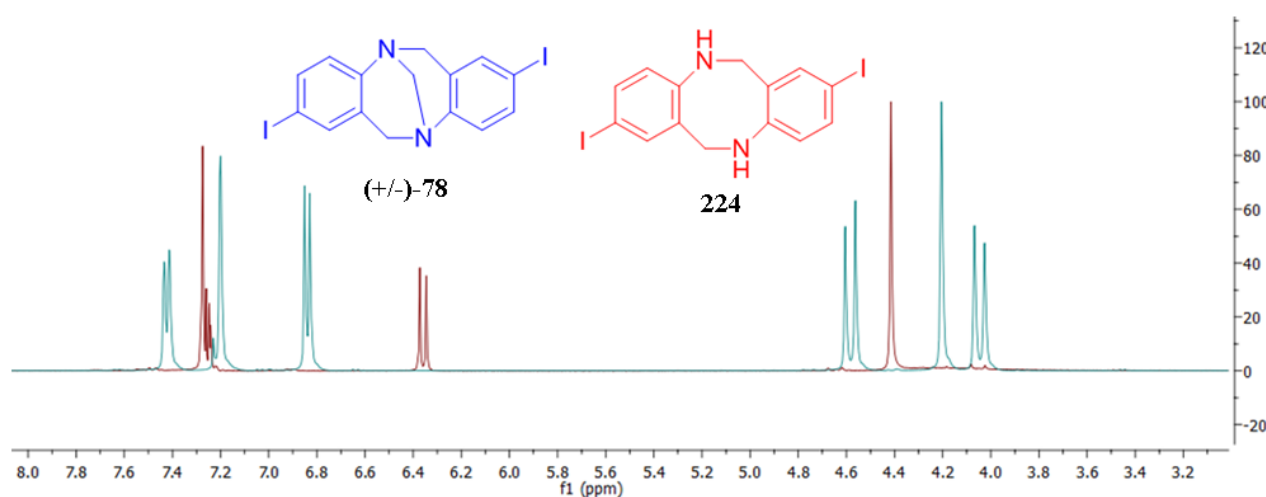


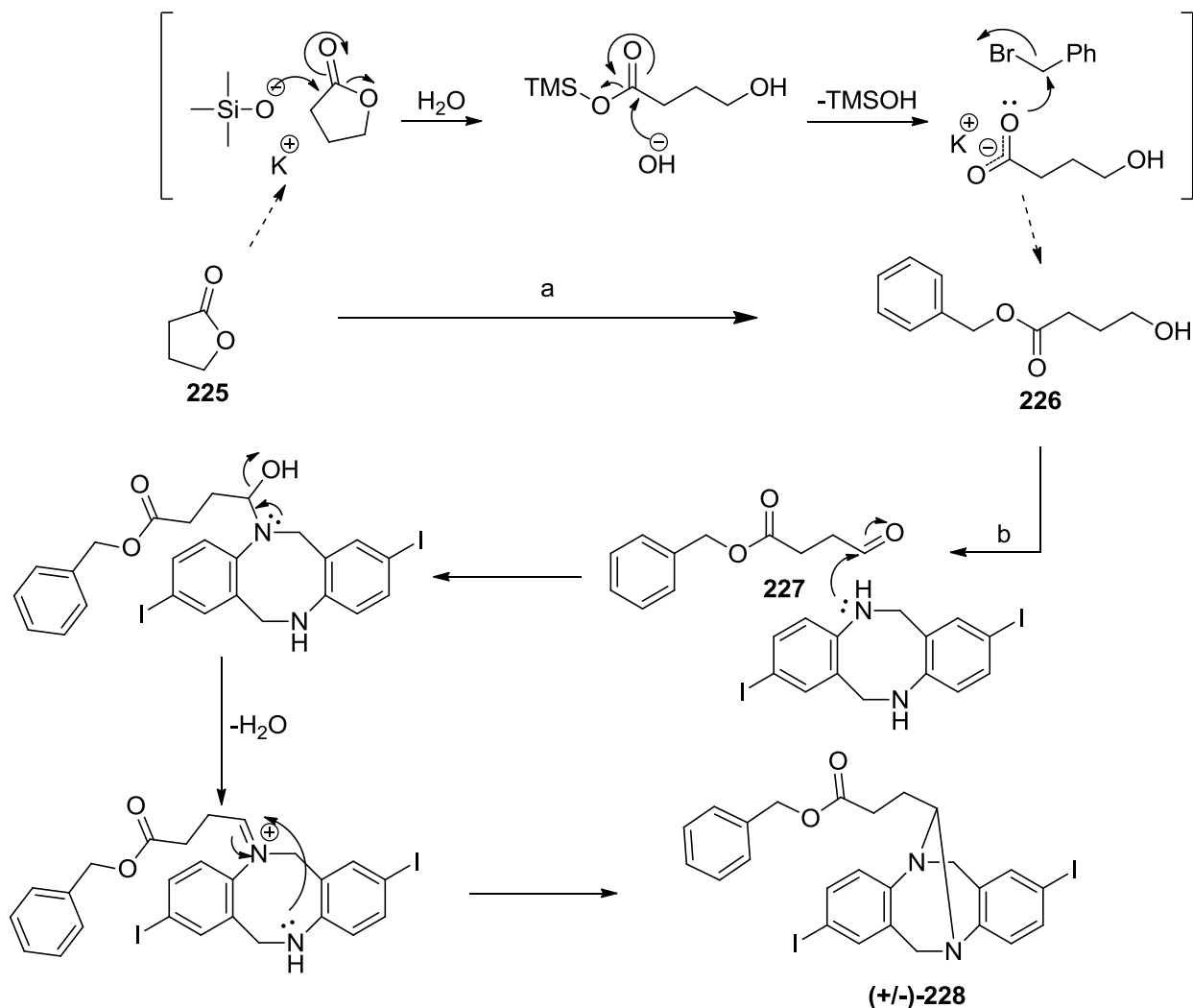
Figure 96 Superimposed $^1\text{H-NMR}$ spectra of 2,8-*bis*-iodo Tröger's base (+/-)-**78** and 2,8-*bis*-iodo-5,6,11,12-tetrahydrodibenzo[b,f][1,5]diazocine **224**

The diagnostic peak for the carbon-iodine bond, in the ^{13}C -NMR (100 MHz) of **224**, was located at $\delta 79.75$ confirming that the procedure employed had not interfered with this substituent. Analysis *via* mass spectrometry afforded a mass ion at m/z $[\text{ES}]^+$ $\text{M}+\text{H}$ 462.8 this with full physiochemical analysis afforded a strong indication the desired compound had been generated.

4.20 Tröger's base C13 modification

A procedure reported by Mahon *et al.* has demonstrated that aldehydes can be used to replace the C13 methylene bridge.¹⁷ The re-insertion of the methylene bridge for subsequent attachment to the gold CD surface would need to be equipped with an aldehyde and another suitably protected functional group, such as a benzyl ester. A short alkyl chain would be required to allow room for insertion and further coupling later. The functional group of choice was a carboxylic acid as further alkyl chains could be added by utilising the nucleophilicity of the carboxylate anion, which can be formed using a weak base. Protecting groups which require a strong base to deprotect such as methyl or ethyl esters were avoided as other ester groups added 'downstream' in the synthesis could be competitively hydrolysed. The ring opening of γ -butyrolactone **225** with sodium hydroxide as a base¹⁴¹ in the presence of benzyl alcohol or bromide have been reported but was found to be quite poor yielding 35%. An alternative route was necessary, and we considered using potassium trimethylsilanolate and benzyl bromide in *N-N*-dimethylformamide. The lactone **225** was dissolved in *N-N*-dimethylformamide and potassium trimethylsilanolate added, resulting almost immediately in a precipitate forming. Stirring the reaction for 16 hours, allowed the precipitate to re dissolve. Following an aqueous work up and flash chromatography on silica gel, eluting with 25% ethyl acetate in hexane afforded a colourless liquid in a 69% yield. Subsequent physiochemical analysis was in agreement with the literature values for **226**.¹⁴¹

226 was subsequently oxidised *via* Swern oxidation to give the necessary aldehyde **227**, again the data corresponded with the literature values,¹⁴² in a 54% yield over two steps.



Scheme 58 Proposed reaction mechanism for the potassium trimethylsilanoate mediated ring opening of γ -butyrolactone **225** and subsequent esterification with benzyl bromide. Followed by proposed mechanism of Tröger's base C13 insertion with benzyl 4-oxobutanoate **227**. a) TMSOK, benzyl bromide, DMF, 75%. b) Oxalyl chloride, DMSO, DCM, triethylamine, -60°C, 89%.

The benzyl 4-oxobutanoate linker **227** was then refluxed in toluene with the diazocine **224** affording, presumably an imine followed by immediate intramolecular cyclisation *via* the favoured 6 *endo*-trig cyclisation, driven by the evolution of water, to afford the unreported new modified Tröger's base substrate (+/-)-**228**.

The ¹H-NMR (500MHz) [Figure 97] spectrum outlines the splitting of the protons at C6 and C12, with each of the protons split into doublets δ 4.55 (d, *J*16.7 Hz) and δ 4.46 (d, *J*17.4 Hz) corresponding to the *exo* protons, δ 4.07 (d, *J*16.7 Hz) and δ 3.95 (d, *J*17.4 Hz) the *endo* protons and the C13 proton can be observed as a doublet of doublets δ 4.05 (dd, *J*6.5, 8.1 Hz) nestled between two doublets. The aromatic peaks of both the Tröger's base and benzyl ester were observed, along with the benzyl methylene at δ 5.10 and the aliphatic linker methylenes further upfield, δ 2.57 (t, 7.3

Hz) and δ 1.96. Mass spectrometry afforded a mass ion m/z $[ES]^+ M+H$ 637.0 which further indicated the desired compound (+/-)-**228** had been generated.

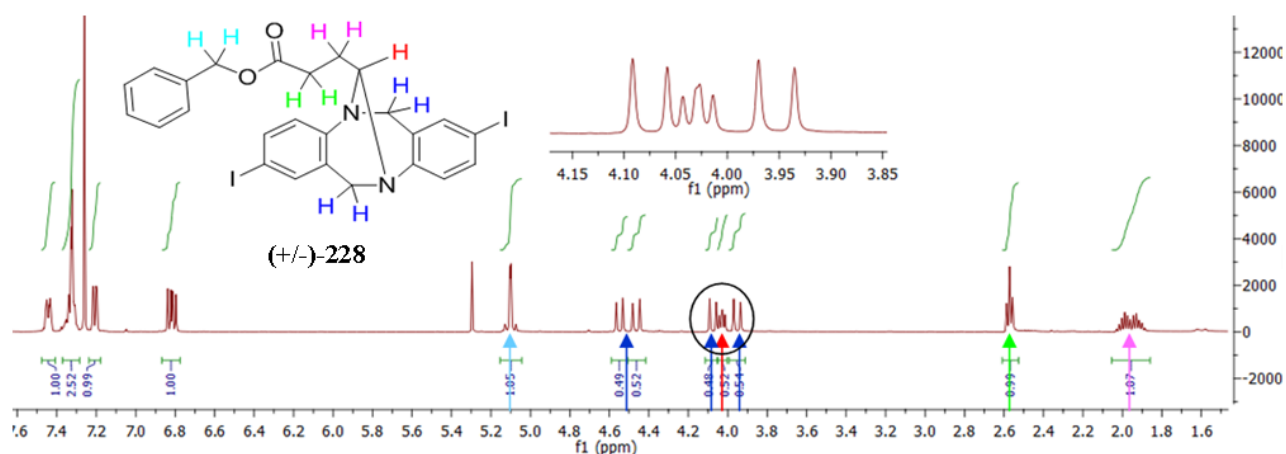
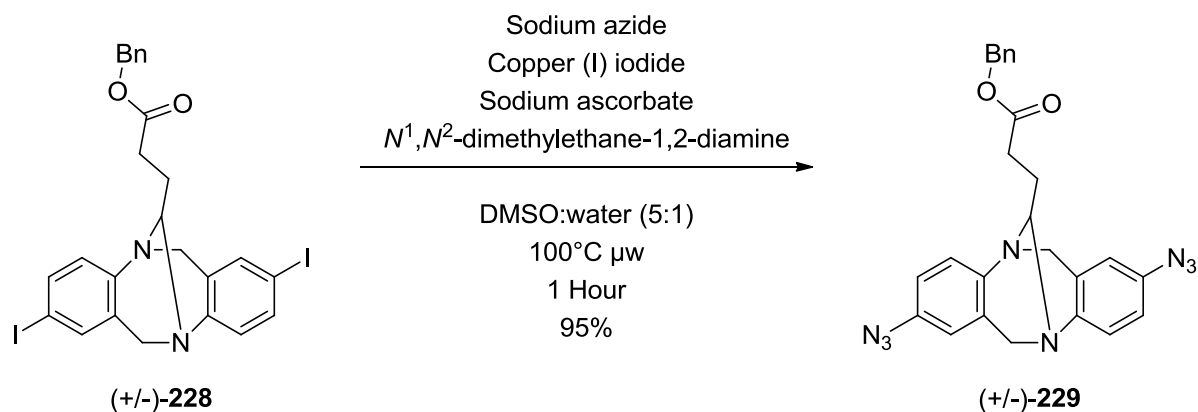


Figure 97 $^1\text{H-NMR}$ (500MHz) of (+/-)-**228** affording a new doublet of doublets at δ 4.05 corresponding to the newly inserted C13 proton.

The $^{13}\text{C-NMR}$ (500MHz) spectrum affords a peak at δ 87.57 confirming the carbon-iodine bond is still intact. A signal at δ 172.91 indicating the presence of a carbonyl peak, associated with the ester group is still present which, is also confirmed by its characteristic FT-IR peak at 1730cm^{-1} . (+/-)-**228** was then converted to the *bis*-azide Tröger's base (+/-)-**229** via the copper catalysed protocol employed earlier. (sodium azide, copper(I) iodide, sodium ascorbate, N^1,N^2 -dimethylethane-1,2-diamine, DMSO / water (5:1), 100°C μw , 1 hour) Once again this employed procedure worked very well affording the desired substrate (+/-)-**229** in a 95% yield after flash column chromatography on silica gel, eluting with 25% ethyl acetate in hexanes.



Scheme 59 Synthesis of benzyl 3-(2,8-*bis*-azido-6,12-dihydro-5,11-methanodibenzo[b,f][1,5]diazocin-13-yl)propanoate (+/-)-**229**

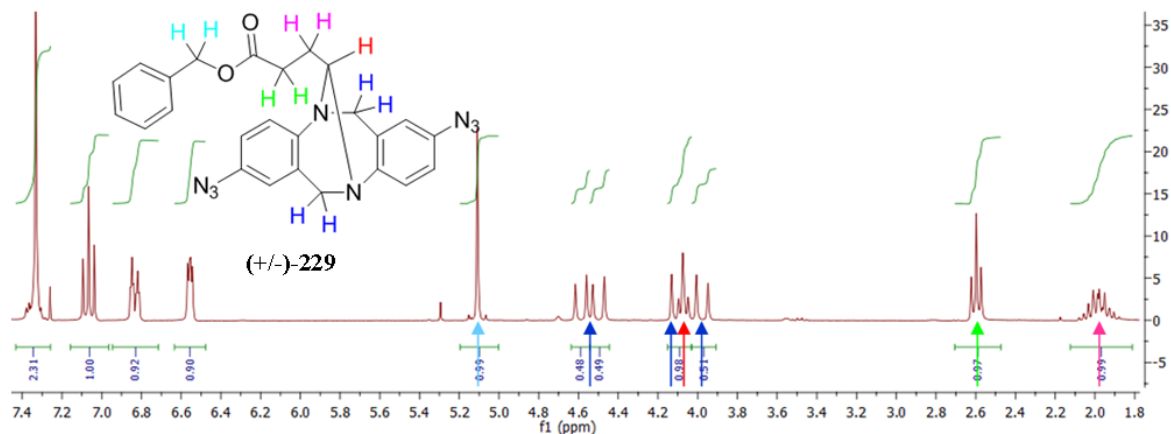


Figure 98 The $^1\text{H-NMR}$ (500MHz) spectra of (+/-)-229

The $^1\text{H-NMR}$ (500MHz) spectra of (+/-)-229 [Figure 98] clearly affords an upfield shift in the aromatic peaks of the Tröger's base with all the other peaks remaining at approximately the same chemical shift. The $^{13}\text{C-NMR}$ (100MHz) of (+/-)-229 [Figure 99] indicates the diagnostic carbon-iodine bond at $\delta 87.57$ has gone with new peaks observed at $\delta 118.77$, 118.36, 116.97 and 116.72. These correspond to the carbon-azide bond located at C2 and C8 of the Tröger's base and four signals are evident, a consequence of the diastereoisomerism of Tröger's base, and the resonance structures of the azide functionality. The FT-IR spectrum afforded a strong signal at 2105 cm^{-1} , a diagnostic peak of the azide functional group.

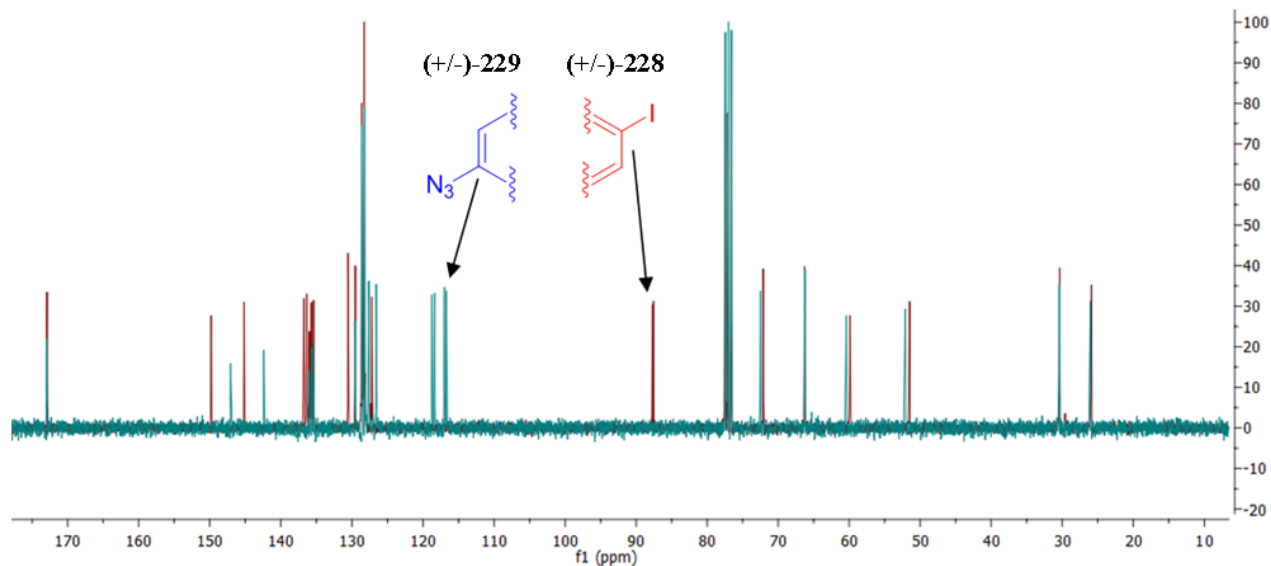
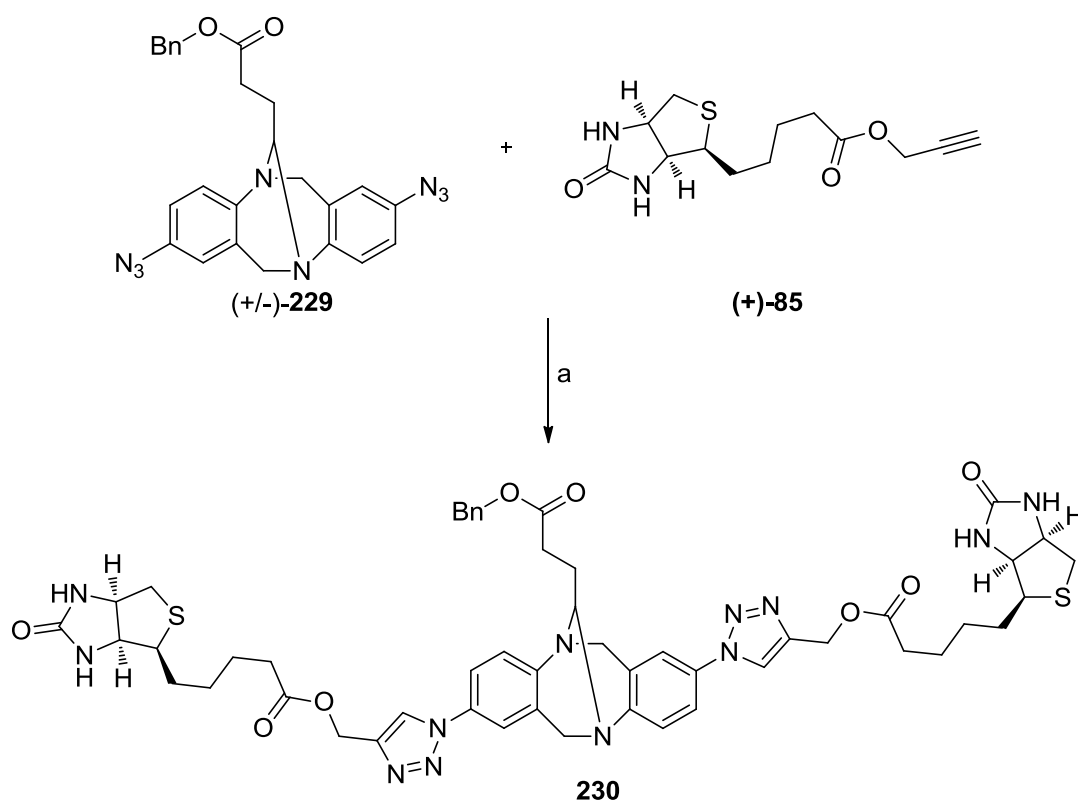


Figure 99 Superimposed $^{13}\text{C-NMR}$ spectra of (+/-)-229 (blue) and (+/-)-228 (red) indicating the shift of the substituted aromatic carbon.

4.21 Synthesis of (+)-biotin incorporated Tröger's bases

With the scaffold successfully synthesised, allowing for functionalisation at the 2- and 8- positions as well as the modified bridgehead, the simplest propargyl (+)-biotin (+)-85 was 'clicked'

symmetrically to the Tröger's base scaffold (+/-)-**229**, using the standard procedure (CuSO₄•5H₂O, TBTA, sodium ascorbate, DMF, 70°C μW, 1 hour). Following an aqueous workup and flash column chromatography on silica gel eluting with a gradient of 5-10% methanol in dichloromethane the required compound was produced in an 85% yield.



Scheme 60 Synthesis of **230** a) CuSO₄•5H₂O, TBTA, sodium ascorbate, DMF, 70°C μW, 1 hour, 82%.

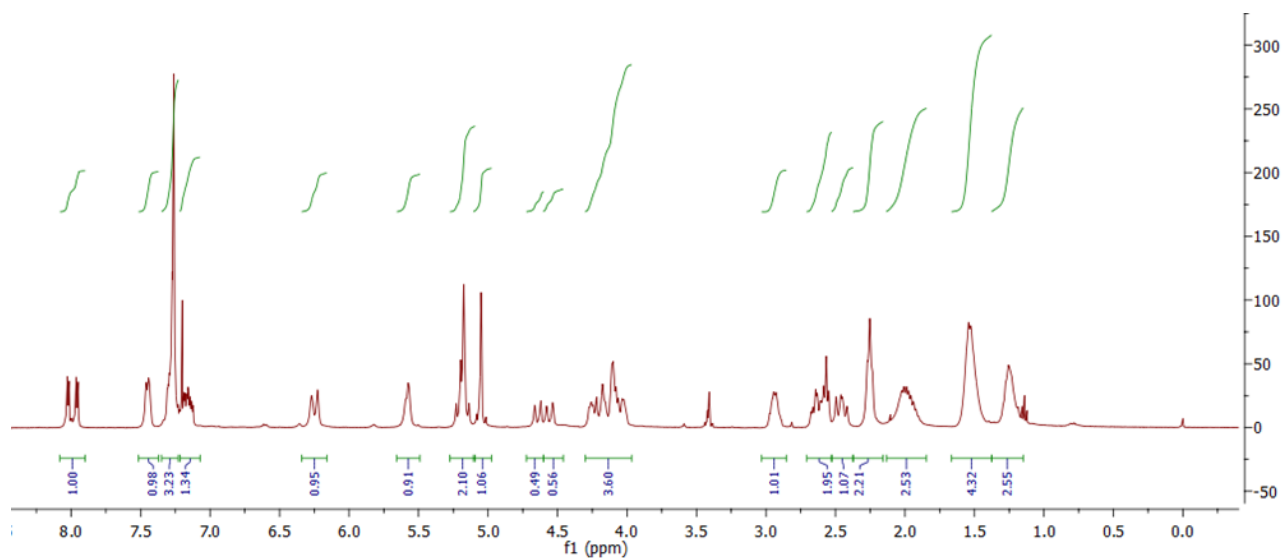


Figure 100 ¹H-NMR (400MHz) spectrum of **230**

The ¹H-NMR (400MHz) of **230** was a little broad most probably due to the poor solubility of **230** in many deuterated solvents, however, the Tröger's base *exo* protons were observed as doublets at

δ 4.64 and δ 4.56, the four NHs' and aliphatic methylenes of the (+)-biotin substrate (+)-**85** at δ 6.25 and δ 5.58, δ 1.48 and δ 1.27 respectively. The two 1,2,3-C₅-triazole peaks, are split into a doublet of doublets, and can be observed at δ 7.99. Together with a mass ion m/z [ES]⁺ M+H 1031.6 and the loss of the azide functionality as determined by FT-IR, the signal at 2105 cm⁻¹ was no longer observed, indicated the substrates had been successfully 'clicked'.

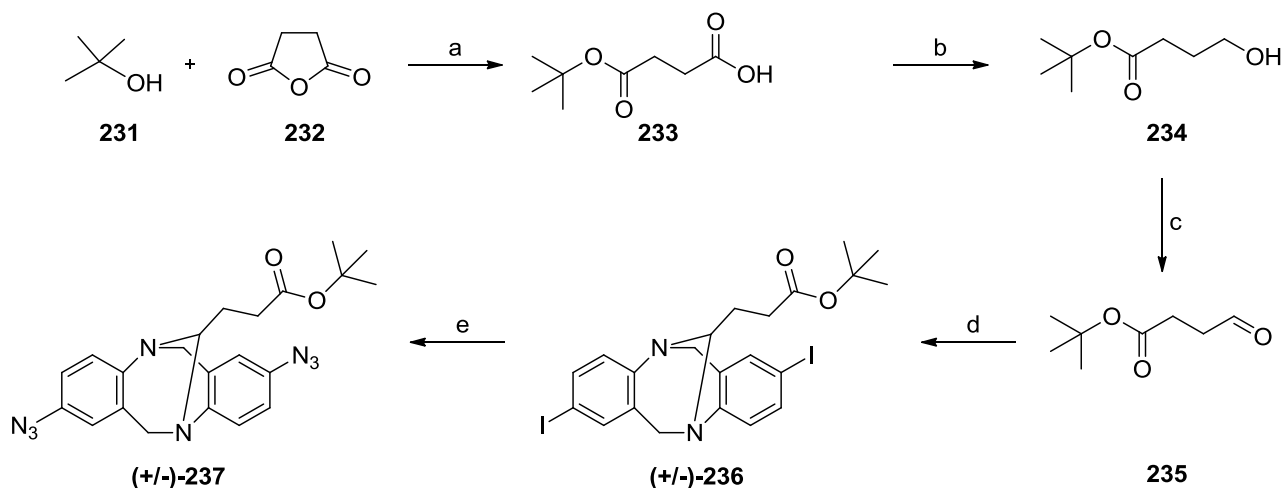
With the symmetrical, *O*-benzyl ester protected, Tröger's base *bis*-biotin **230** in hand deprotection of the benzyl ester was investigated. Routinely removed by hydrogenation over a palladium catalyst, however, **230** was resistant to this treatment see Table 14. A range of *O*-deprotection methods were attempted, however these resulted in very poor yields <10%, recovered start material **230** and/or decomposition of the compound **230**.

Conditions	Yield %	Conditions	Yield %
Pd/C, H ₂ , methanol, 50psi	< 5	Pt/C, H ₂ , Methanol, 50psi	< 10
NiCl ₂ , NaBH ₄ , DCM	s/m recovered	Pd black, 1,4 cyclohexadiene, acetic acid	s/m recovered
PtO ₂ /C, H ₂ , ethanol, 50 psi	< 10	Hydrobromic acid, acetic acid	0

Table 14 Reaction conditions for the attempted *O*-benzyl-deprotection.

Searching the literature, an explanation was found. Palladium catalysts are poisoned by sulfur and amines,¹⁴³ it is presumed that the combination of the sulfurs from the (+)-biotin and the imines from the triazoles and amines from the Tröger's base were co-ordinating on the metal surface inhibiting hydrogenolysis from taking place. Adams catalyst, platinum dioxide, is sometimes employed to negate this problem,¹⁴³ however, this was also ineffective. A procedure reported by Khurana *et al.* using nickel(II) chloride and sodium borohydride¹⁴⁴ was attempted but this also returned start material **230**. An alternative, but much harsher, *O*-deprotection using hydrobromic acid in acetic acid didn't return any product or start material. After many attempts this pathway was abandoned and another was devised and investigated.

The *tert*-butyl ester protecting group was considered a suitable alternative for this protection; this would require deprotection by trifluoroacetic acid, which is compatible with both (+)-biotin and the Tröger's base scaffold, as Tröger's base was synthesised in neat trifluoroacetic acid.



Scheme 61 Reaction scheme for the synthesis of (+/-)-**237**. a) *N*-hydroxysuccinamide, DMAP, triethylamine in toluene, reflux 24 hours, 75%. b) borane dimethyl sulfide complex, THF, 0°C – ambient temperature, 24 hours, 96%. c) oxalyl chloride, dimethylsulfoxide, dichloromethane, -60°C, 15 minutes, 92%. d) **224**, reflux, toluene 16 hours, Dean-Stark trap, 95%. e) Sodium azide, copper(I) iodide, *N*¹,*N*²-dimethylethane-1,2-diamine, DMSO:water 5:1, 100°C μ W, 1 hour, 81%.

This was achieved using a procedure reported by Srinivasan *et al*, employing succinic anhydride **232** was ring-opened and activated by *N*-hydroxy succinamide. This was subsequently esterified with *tert*-butanol, affording a mono-protected 1,4 dicarboxylic acid **233**.¹⁴⁵ Subsequent reduction using borane-dimethylsulfide, afforded the corresponding alcohol **234**. Oxidation of the primary alcohol to the aldehyde **235** via Swern oxidation generated the desired linker for subsequent insertion into the diazocine **224**. This was accomplished, in 95% yield, by refluxing **224** and **235** in toluene followed by the copper(I) catalysed, azide formation (sodium azide, copper(I) iodide, sodium ascorbate, *N*¹,*N*²-dimethylethane-1,2-diamine, DMSO / water (5:1), 100°C μ w, 1 hour) afforded the *bis*-azide (+/-)-**237** once again in excellent yield 81%.

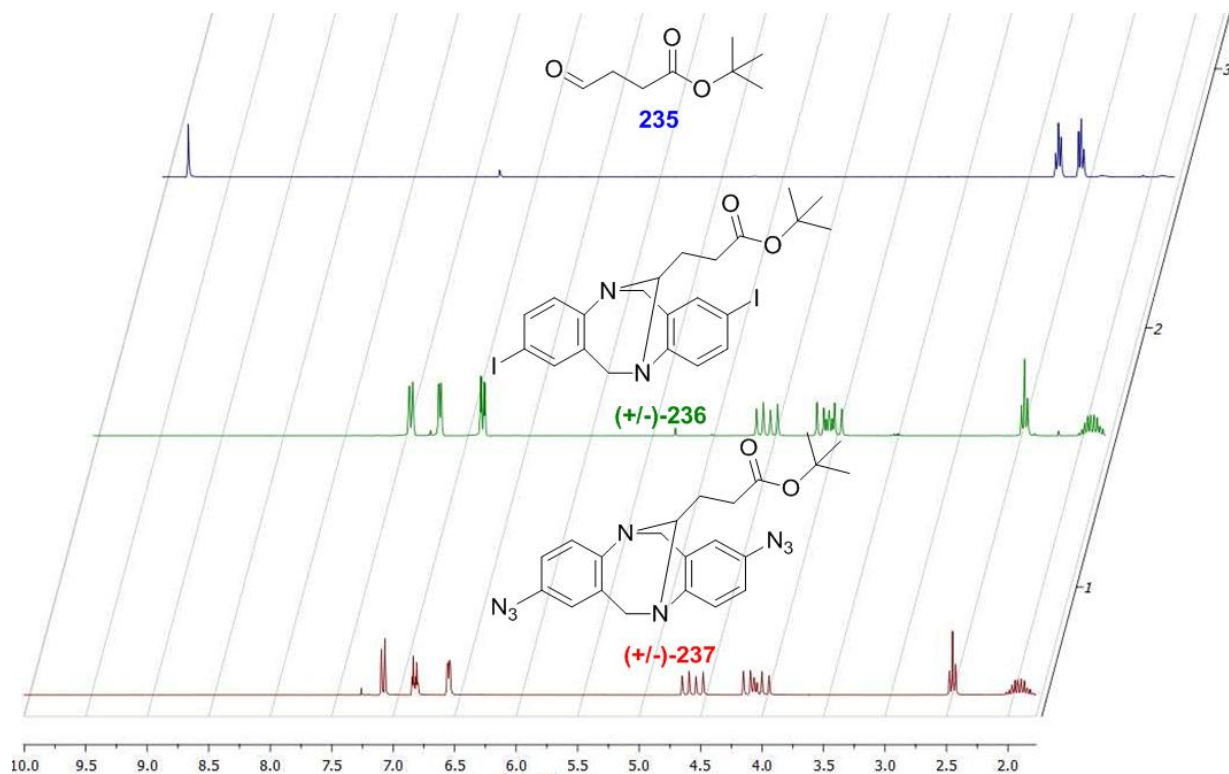


Figure 101 Stacked $^1\text{H-NMR}$ spectra of **235**(blue), (+/-)-**236** (green) and (+/-)-**237** (red).

The $^1\text{H-NMR}$ (400MHz) spectra [Figure 101] (blue) outlines the aldehyde peak of **235** at δ 9.79, two triplets from the methylenes at δ 2.72 and δ 2.53 with a coupling constant of J 6.7 Hz and a sharp singlet at δ 1.43 for the *tert*-butyl protons. In the spectra of (+/-)-**236** (green) the aldehyde peak had disappeared and aromatic peaks at δ 7.42, 7.18, 6.84 corresponding to the Tröger's base section of the scaffold are clearly identifiable. The methylene protons found at C6 and C12 were located at δ 4.58 (J 16.7 Hz), δ 4.47 (J 17.4 Hz), δ 4.09 (J 16.7 Hz) and δ 3.94 (J 17.5 Hz), demonstrating the *exo* and *endo* couplings. The triplet at δ 4.02 is the proton at the newly inserted C13 bridgehead. The methylene next to the *tert*-butyl ester of the linker has moved slightly upfield to δ 2.43 ppm, however, the methylene closest to the scaffold has shifted dramatically upfield to δ 1.90 and has been split into a multiplet. Conversion of (+/-)-**236** to (+/-)-**237** affords a shift of the aromatic protons upfield to δ 7.08, δ 6.82 and δ 6.55 due to a change in chemical environment of the aromatic protons, as would be expected when converting from a carbon-iodine bond to a carbon-azide bond. The FT-IR spectra afforded a strong peak at 2104 cm^{-1} further indicating that the azide group had been introduced.

With the new *tert*-butyl protected scaffold (+/-)-**237** in hand, 'clicking' of the (+)-biotin substrate (+)-**85** was the next task. Using the same procedure as employed for the synthesis of (+/-)-**230**, the reagents ($\text{CuSO}_4 \cdot 5\text{H}_2\text{O}$, TBTA, sodium ascorbate, DMF) were sealed in a microwave vial and heated to 70°C for 1 hour. Following an aqueous work up and column chromatography on silica

gel eluting with a gradient of 5-10% methanol in dichloromethane a white amorphous powder was collected in a 92% yield.

238 was submitted for physicochemical analysis, this suggested that this was the expected product. The $^1\text{H-NMR}$ (400MHz) spectrum [Figure 103] afforded a 1,2,3- C_5 -triazole peaks as two singlets δ 8.04 and 8.01. The Tröger's base *exo* protons have remained intact at δ 4.74 (J 16.8 Hz) and 4.62 (J 17.8 Hz), the diagnostic (+)-biotin NHs at δ 6.33 and 5.70 and the *tert*-butyl protecting group can be seen at δ 1.41. The FT-IR spectra affords no azide peak, usually observed at 2106 cm^{-1} , in compound (+/-)-**237** this was no longer present, indicating the azide has reacted as expected.

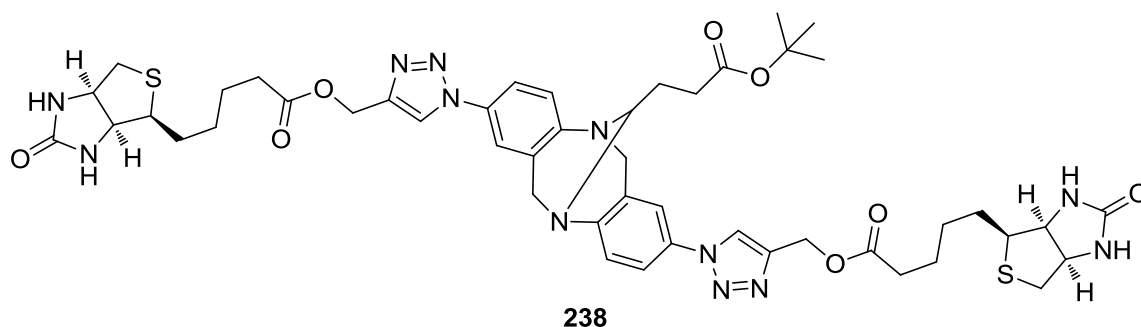


Figure 102 Structure of **238**, product of the reaction between (+/-)-**237** and (+)-**85**

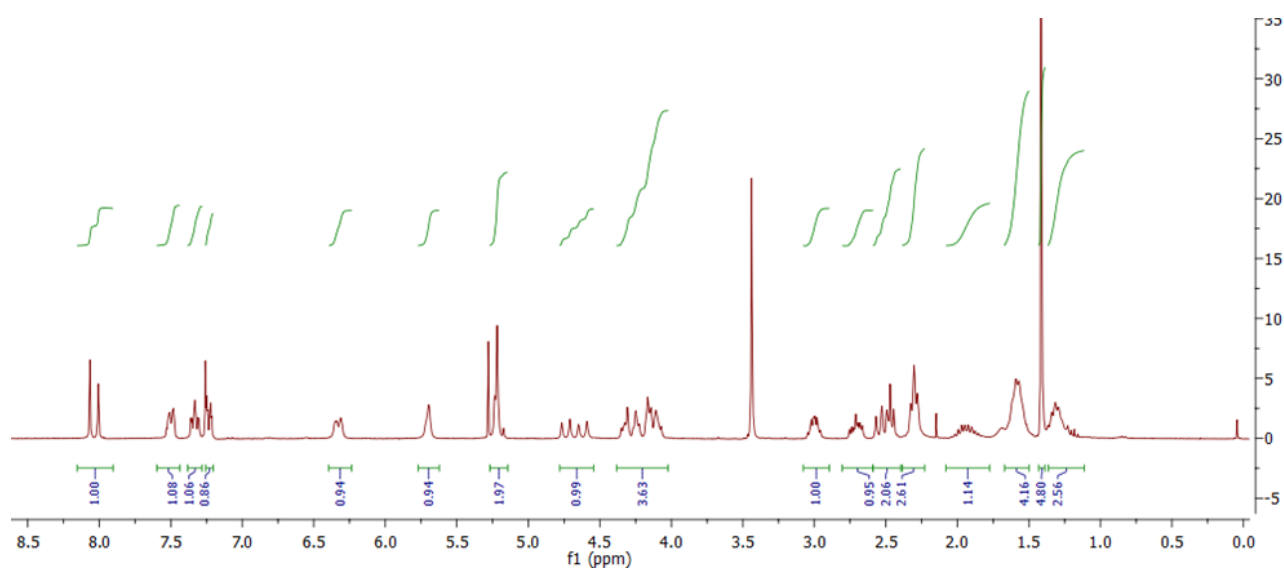
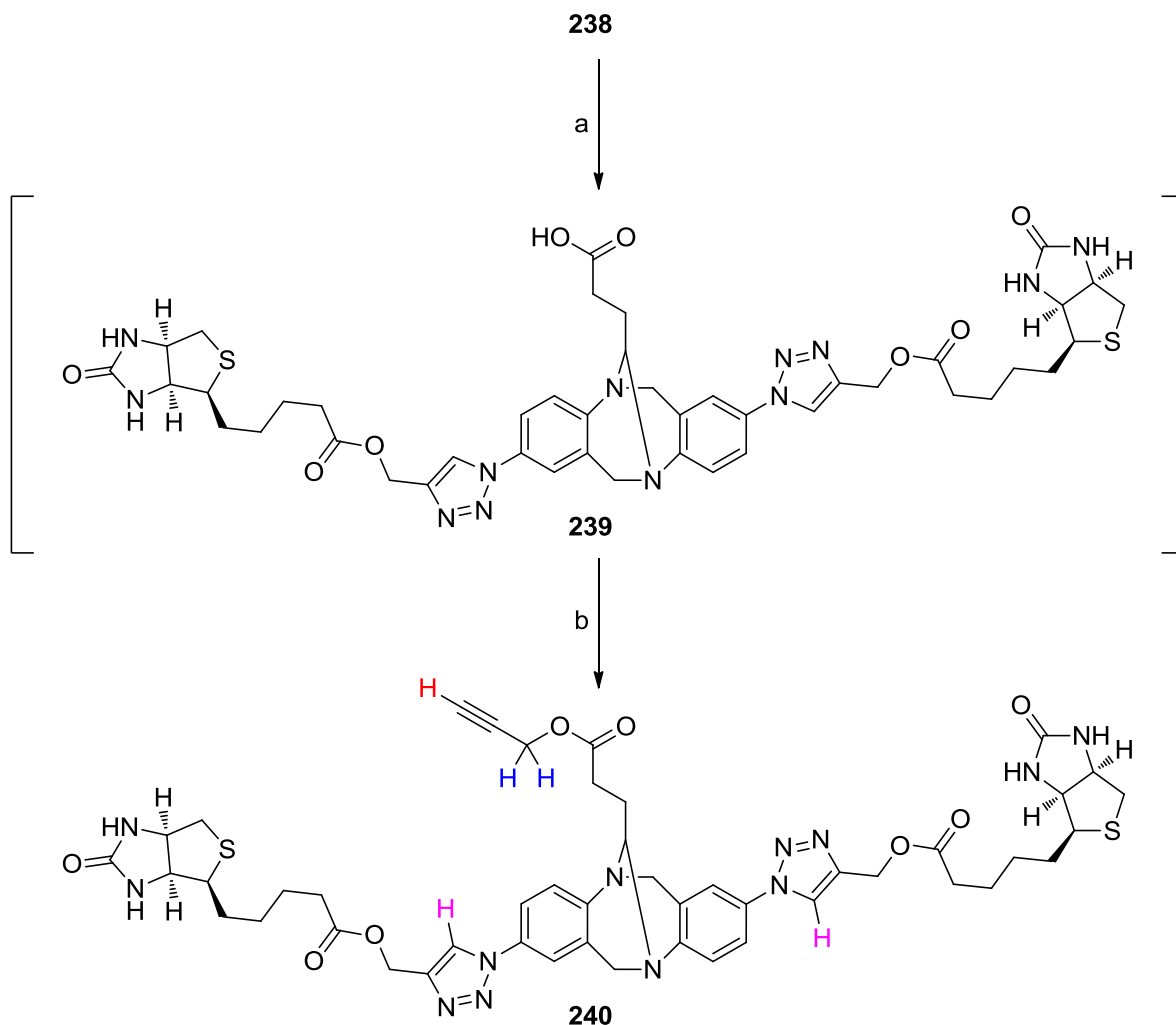


Figure 103 $^1\text{H-NMR}$ (400MHz) spectrum of **238**

With **238** in hand the deprotection was, once again, attempted in this case **238** was dissolved in dichloromethane and sealed in a 2.5 mL microwave vial. One equivalent of trifluoroacetic acid was added via syringe and left to stir at room temperature. Thin layer chromatography was used to monitor the *tert*-butyl ester deprotection and after 12 hours start material **238** had been consumed and all material was on the baseline. The solvent and trifluoroacetic acid were removed under reduced pressure and the residue redissolved in the minimum amount of dichloromethane and diethyl ether was added resulting in the formation of a precipitate. This was filtered off and taken

straight through to the next step. Using **239** it was submitted to the mild conditions (potassium carbonate and propargyl bromide in dimethylformamide, as described by Bew and Hiatt-Gipson, for the synthesis of propargyl esters,¹⁰⁵) gratifyingly **240** was afforded in an excellent 88% yield.



Scheme 62 Synthesis of **240** from **238**. *tert*-butyl deprotection with a) trifluoroacetic acid, dichloromethane, 12 hours, affording intermediate **239** followed by propargyl ester formation b) potassium carbonate, propargyl bromide in *N,N*-dimethylformamide afforded **240** in 88% yield.

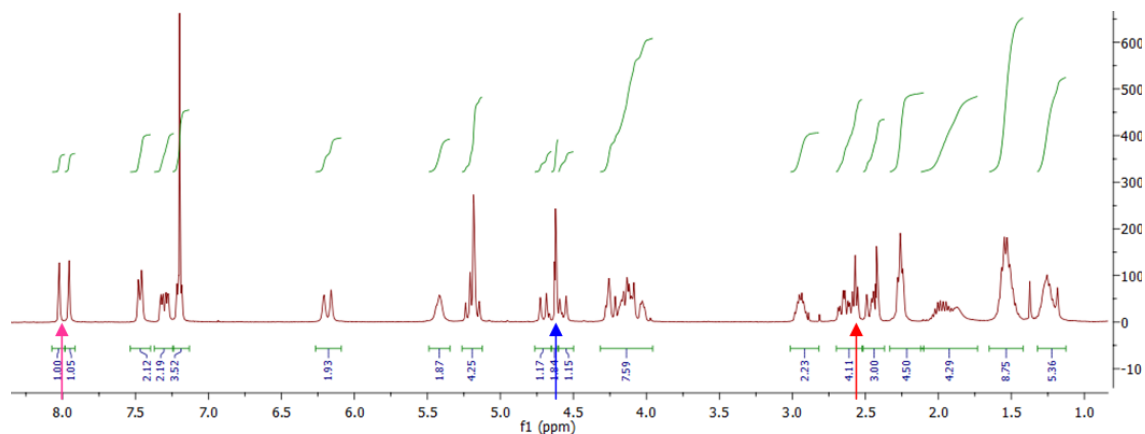


Figure 104 ¹H-NMR (400MHz) spectrum of **240**

$^1\text{H-NMR}$ (400MHz) analysis of **240** [Figure 104] confirmed that a new methylene peak at $\delta 4.63$, corresponding to the propargyl group and the alkynyl proton, usually seen at $\sim\delta 2.50$ cannot be clearly seen as it has merged with other signals found at the same chemical shift. LC-MS [ES] $^+$ confirmed an expected mass ion m/z [ES] $^+\text{M}+\text{Na}1001.4$, offering evidence that compound **240** had been successfully synthesised. With the *O-tert*-butyl ester deprotection of **238** accomplished and a methodology to introduce an alkynyl group on to the Tröger's base scaffold, the (+)-biotin linkers (+)-**211** and **215**, were coupled *via* the same procedure, ($\text{CuSO}_4\cdot 5\text{H}_2\text{O}$, TBTA, sodium ascorbate, DMF, 70°C μW , 1 hour) affording different length (+)-biotin linkers to Tröger's base scaffold **241** and **242**.

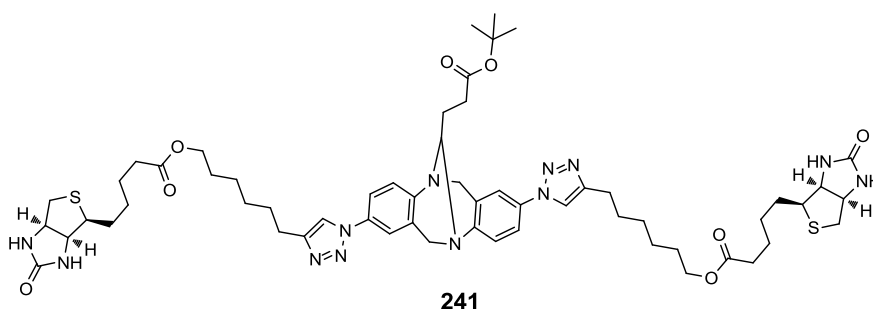


Figure 105 Structure of **241**

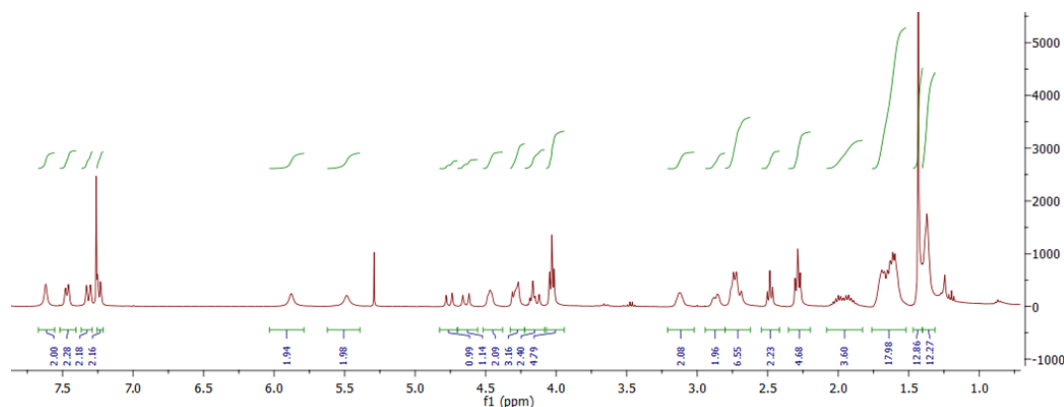


Figure 106 $^1\text{H-NMR}$ (400MHz) of **241**

The $^1\text{H-NMR}$ (400MHz) of **241** was very similar to **240**, however the signals were broader due to the increased degrees of freedom from the extended, more flexible alkyl linker. The 1,2,3- C_5 -triazole peak was observed at $\delta 7.62$, the characteristic (+)-biotin amide protons at $\delta 5.88$ and $\delta 5.49$ and the Tröger's base *exo* methylene doublets at $\delta 4.76$ (d, $J_{16.8}$ Hz) and $\delta 4.64$ (d, $J_{17.5}$ Hz). The aliphatic region displayed broad peaks at $\delta 1.64$ (m) and $\delta 1.37$ (s), as before correspond to the methylene protons from (+)-biotin alkyl chain. The FT-IR azide peak at 2106 cm^{-1} , from (+/-)-**237**, has disappeared suggesting reaction at the azide moiety affording the desired product in 89% yield.

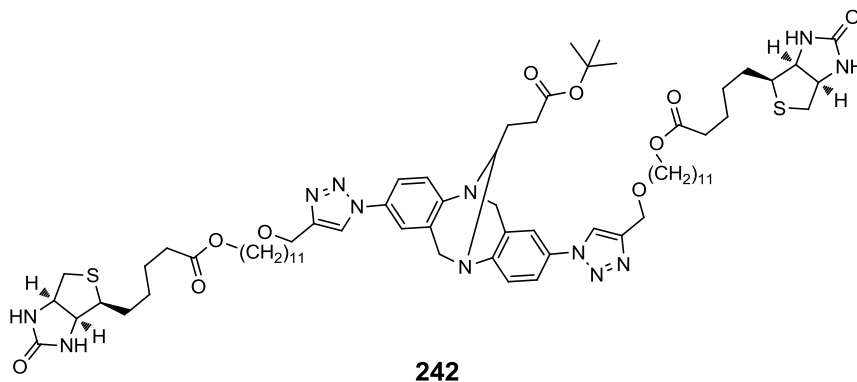


Figure 107 Structure of **242**

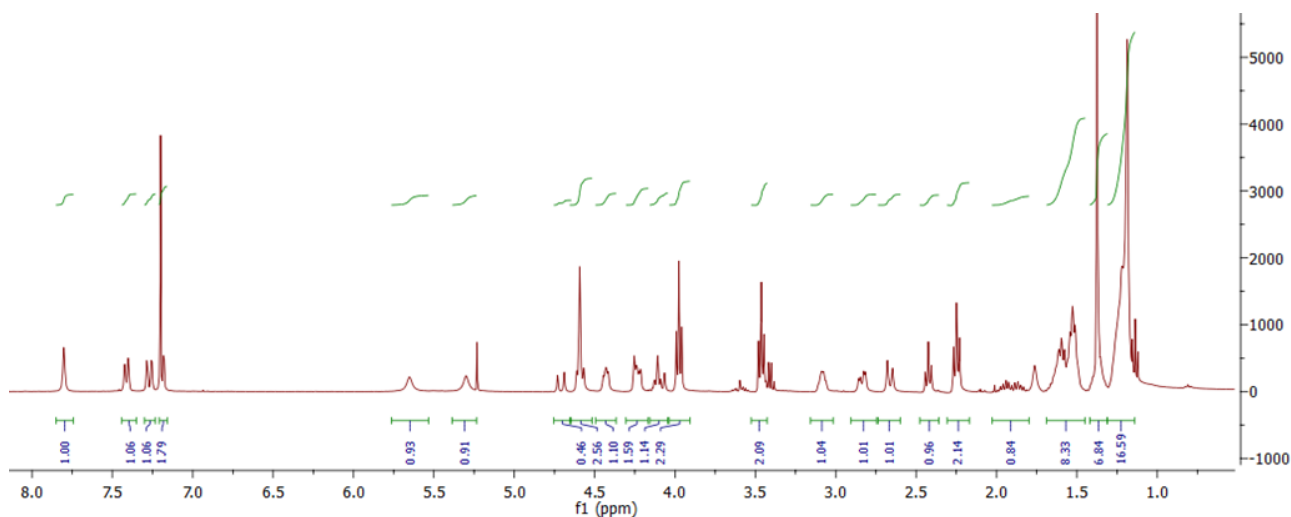
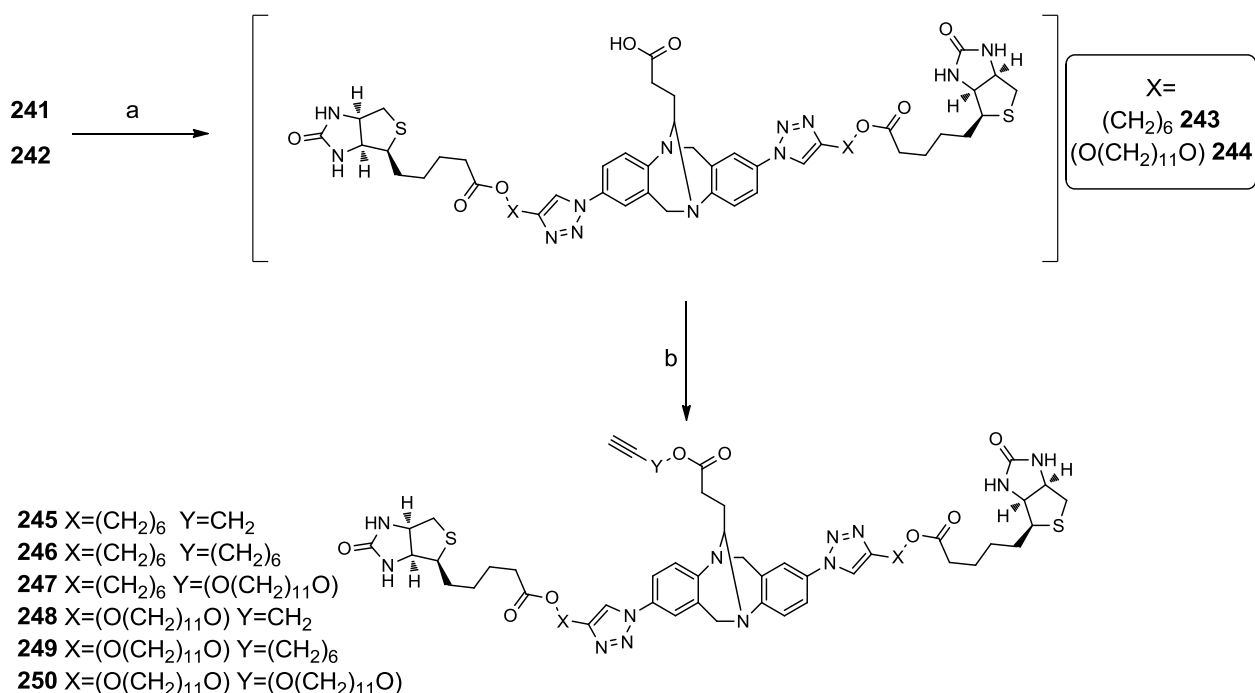


Figure 108 ¹H-NMR (400MHz) spectrum of **242**

The ¹H-NMR (400MHz) spectrum of **242** affords the 1,2,3-*C*₅-triazole peak at δ7.80, the diagnostic amide protons of (+)-biotin at δ5.65 and δ5.30, and one of the *exo* protons of the Tröger's base methylenes is visible as a doublet at δ4.71. The second Tröger's base *exo* proton is obscured by the new signal at δ4.59 corresponding to the methylenes of the (+)-biotin linker next to the triazole ring. Once again there were strong signals in the aliphatic region δ1.56 and δ1.18 corresponding to the methylenes from the (+)-biotin linker. The FT-IR also shows the disappearance of the azide signal at 2106 cm⁻¹ and a mass ion *m/z* [ES]⁺ M+Na 1308.7 afforded a strong indication that the reaction was successful in 85% yield.

With compounds **241** and **242** in hand these were *O*-*tert*-butyl deprotected using trifluoroacetic acid in dichloromethane. After 16 hours of reaction time, the solvent was removed under reduced pressure and redissolved in the minimum amount of dichloromethane. A precipitate was generated upon addition of diethyl ether and the precipitate was filtered off. The free carboxylic acid derivatives were dissolved in *N,N*-dimethylformamide and potassium carbonate added. This was followed by addition of linkers **86**, **210** and **214** and left to stir for 12 hours affording the

corresponding Tröger's base scaffold **245-250** with varying lengths of (+)-biotin linkers and extended linkers for 'clicking' with the disulfide **207**.



Scheme 63 Synthesis of extended linkers for **245-250**. a) TFA, DCM, 12 hours, b) potassium carbonate, **86** or **210** or **214**, DMF, 12 hours.

Compound	Structure	Yield %	¹ H-NMR alkynyl peak
245	X=(CH ₂) ₆ , Y=CH ₂	88	δ2.41
246	X=(CH ₂) ₆ , Y=(CH ₂) ₆	86	δ1.87
247	X=(CH ₂) ₆ , Y=(O(CH ₂) ₁₁ O)	75	δ2.35
248	X=(O(CH ₂) ₁₁ O), Y=CH ₂	66	δ2.41
249	X=(O(CH ₂) ₁₁ O), Y=(CH ₂) ₆	85	δ1.87
250	X=(O(CH ₂) ₁₁ O), Y=(O(CH ₂) ₁₁ O)	83	δ2.35

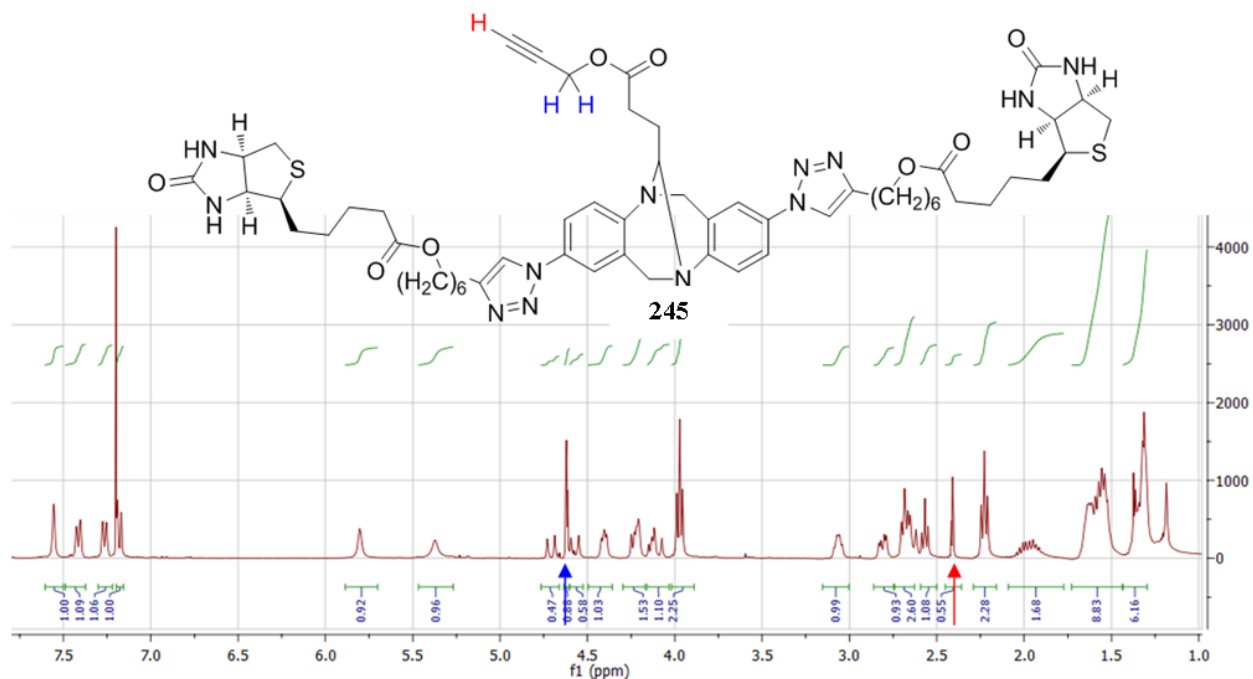


Figure 109 $^1\text{H-NMR}$ (400MHz) of **245**

In the $^1\text{H-NMR}$ (400MHz) of **245** [Figure109] the propargyl methylene was observed at $\delta 4.62$ (t, $J_{2.4}\text{Hz}$) and the alkynyl proton was observed at $\delta 2.41$ (t, $J_{2.5}\text{Hz}$).

The $^1\text{H-NMR}$ (500MHz) spectra of **250** [Figure 110] afforded a propargyl methylene signal at $\delta 4.12$ (d, $J_{2.4}\text{Hz}$), slightly upfield of **245**, due to less shielding from the ether bond, and the signal from the alkynyl proton was observed at $\delta 2.35$ (t, $J_{2.4}\text{Hz}$).

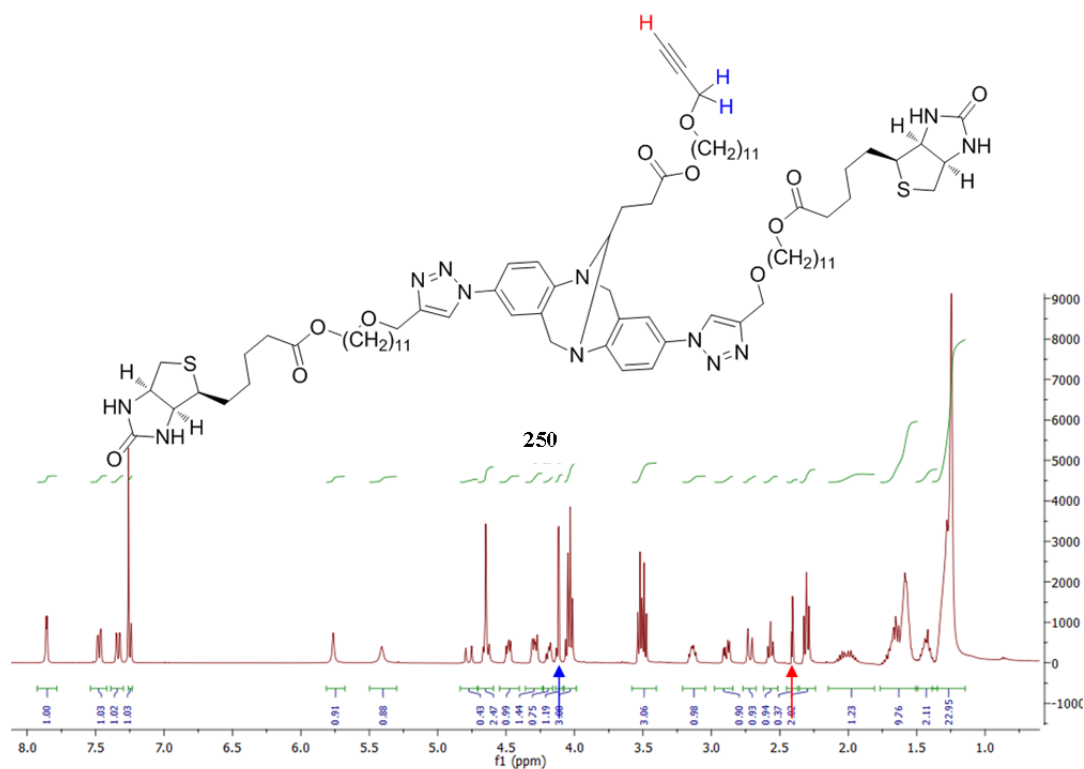
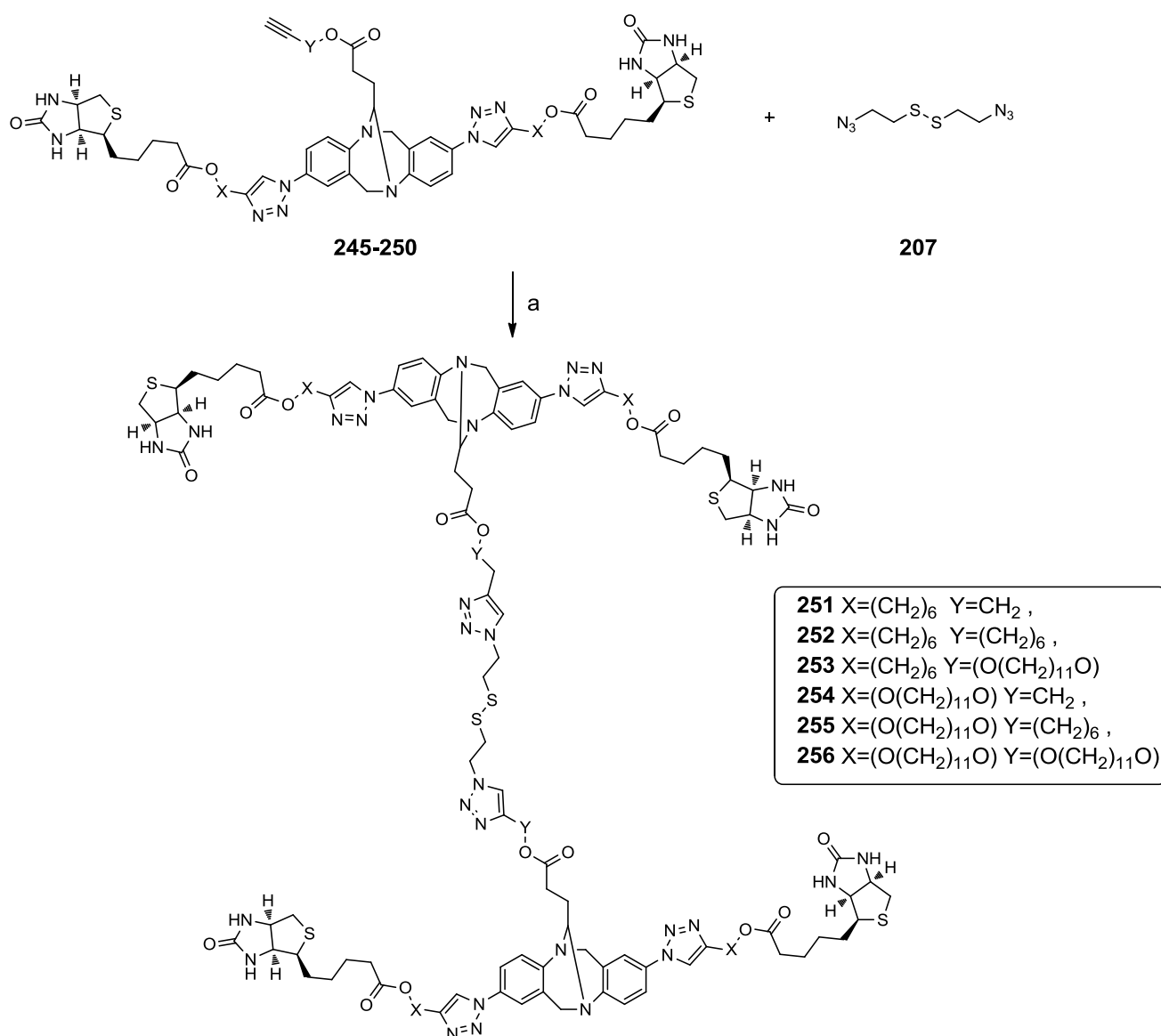


Figure 110 Structure and $^1\text{H-NMR}$ (500MHz) of **250**

4.22 Synthesis of symmetrical 2,8-1,2,3-triazole Tröger's base C13 disulfide dimers

The next step in this project will be the synthesis of the disulfide dimers of the Tröger's base analogues **251-256**. This was already attempted and purification of the large analogues was far from facile. The reaction appeared to proceed under the reaction conditions [Scheme 64] the consumption of both start materials **245** and **207**, however upon aqueous work up of the reaction mixture less than 10% of mass balance was recovered and $^1\text{H-NMR}$ analysis afforded a complex spectrum with minimal structural information acquired. MALDI-TOF mass spectrometry afforded mass ions of the expected mass, however this was far from conclusive. Efforts are ongoing to resolve this problem and semi-preparative reverse phase chromatography will be attempted. Another option that is currently under investigation is to perform the 'click' reaction on the surface of the gold compact disc *in situ* by forming SAMs of the di-sulfide di-azido linker **207** and then coupling the Tröger base analogues **245-250**.



Scheme 64 Proposed synthesis of Tröger's base dimers **251-256** from **245-250**. a) $\text{CuSO}_4 \cdot 5\text{H}_2\text{O}$, TBTA, sodium ascorbate, DMF, 70°C μW , 1 hour

Once these have been successfully synthesised and characterised they will be bound to the gold CD surface as previously reported *via* the hanging drop method. They will then be treated with a solution of streptavidin and submitted for MALDI-TOF mass spectrometry analysis.

5.0 Discussion

During the course of this project a plethora of novel Tröger's base analogues have been synthesised, including symmetrical and unsymmetrical 2,8-(1,2,3,-triazole)-1,4 substituted Tröger's bases'. ^2H , ^{15}N and ^{13}C isotopically enriched Tröger's bases' have been synthesised as well as many novel propargyl compounds. A procedure has been discovered and applied for the mild deuteration of terminal alkynes and their use as a building block for organic synthesis has been explored.

The binding of biotinylated linkers to a compact disc, *via* self assembled monolayers, and their ability to subsequently bind streptavidin to the surface of the disc has been investigated and probed by MALDI-TOF spectroscopy affording positive results. This ability to detect proteins on a compact disc by MALDI-TOF has afforded a proof of concept and work will continue to discover further ligands and proteins, for example the detection of cholera and anthrax proteins, that can be incorporated into this design.

The use of Tröger's base as a scaffold for these interactions, is still ongoing and although the chemistry has been successful, the analysis of their ability to bind proteins more efficiently than (+)-**208**, (+)-**212**, (+)-**216** and (+)-**222** is still unknown. The confirmation that these complex Tröger's base analogues **251-256** have the ability to form self assembled monolayer on the surface of the compact disc will be discovered when a suitable protocol for their purification is developed.

This work has currently afforded two peer reviewed publications (included in the appendix) and there are currently two more awaiting submission.

5.1 Further work

With successful results of the detection of proteins on a compact disc by MALDI-TOF spectroscopy this work could be used as a model for designing ligands to bind to more interesting proteins. For example work has begun on designing a ligand that can be bound to the compact disc surface for the detection of cholera lethal factor. It is known that the carbohydrates lactose and galactose have been used to detect the cholera lethal factor on gold nano-particles.¹⁴⁶ These ligands are currently being synthesised to bind to the compact disc, using the same procedures as seen in this report. Should this be successful then the detection of cholera contaminated water could be analysed in minutes or hours, rather than the days it currently takes and has the potential for saving

lives in developing countries. There has been interest from the DSTL who provided some of the funding for this project and steps are being taken to design a scaffold to bind to the compact disc for the detection of anthrax toxin. It is envisaged that this could be used in the field on military operations for the rapid detection of this toxin and others.

Interestingly, with the compounds being bound to a compact disc and reports in the literature that a CD-player has been adapted to be used as a LASER spectrometer.¹⁰³ It could be possible to make the procedure of protein detection even easier and more compact by simply placing the compact disc into a laptop and running a scan of the surface. Early efforts to investigate this possibility were undertaken with some interesting but not conclusive results. A series of compounds were generated containing modified LASER dyes and di-sulfide bonds. These compounds were bound to the surface of the compact disc and analysed by physical chemists to see if any fluorescence could be detected from the SAMs when they were irradiated with light of 405nm. Interestingly small amounts of light emitted from the compounds on the compact disc were observed.

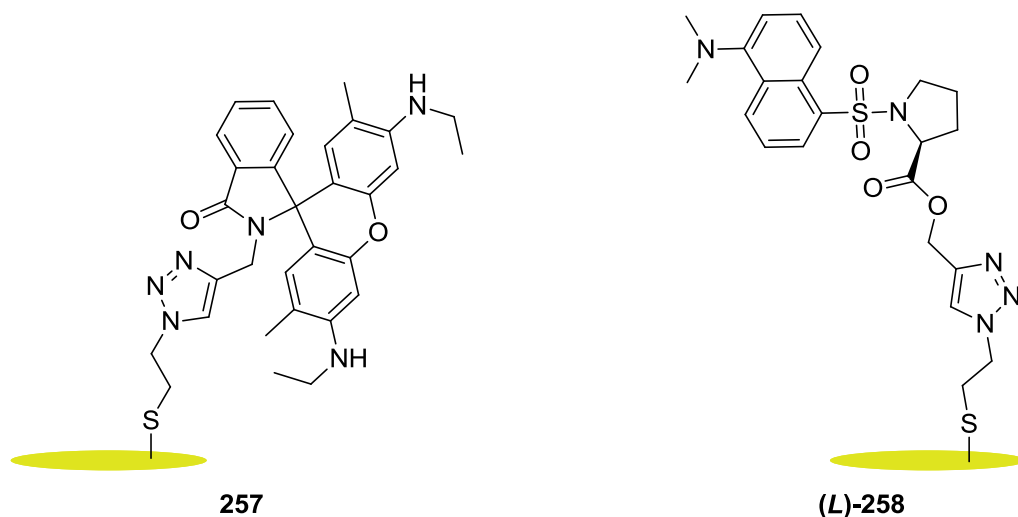


Figure 111 Representation of a rhodamine 6G analogue **257** and the dansyl fluorophore analogue (*L*)-**258** bound to the surface of a gold CD *via* self assembled monolayer formation.

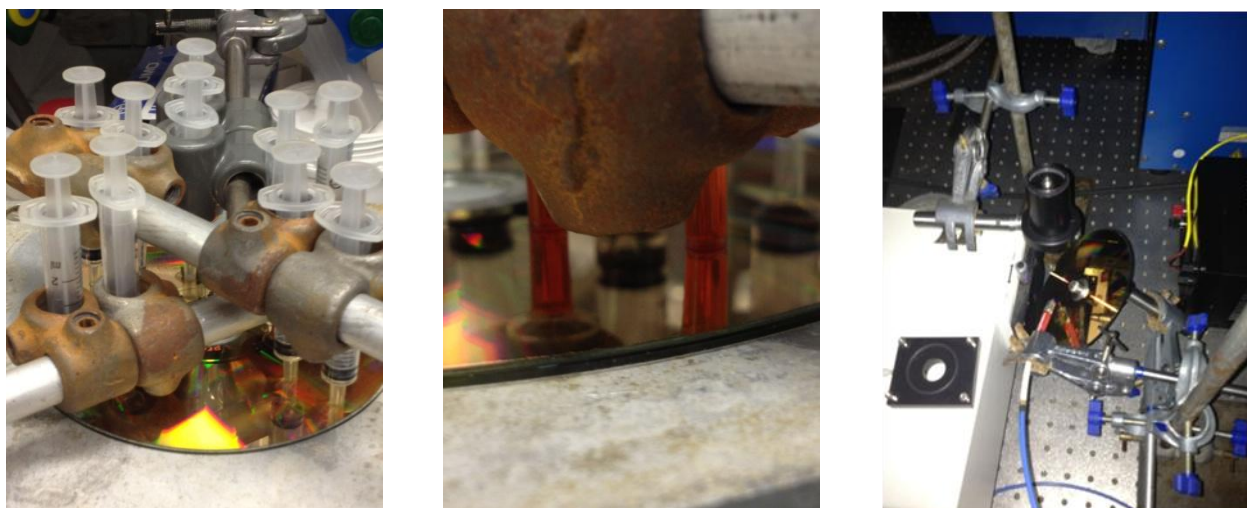


Figure 112 Image of rig used to bind **257** and (*L*)-**258** to gold CD surface (left). Close up image of applicator syringe applying **257** and (*L*)-**258** to gold CD surface (centre). Image of LASER detector set up for analysing the emission of **257** and (*L*)-**258** on gold CD surface (right).

The compounds **257** and (*L*)-**258** were bound to the disk using the rig shown in Figure 112 and analysed using the set up in figure 112. A gold CD with **257** and (*L*)-**258** bound to its surface was installed on a light table. A fibre optic detector (blue lead) was placed near to the surface of the CD at a suitable angle to detect / capture reflected light off the CD surface. The compact disk was rotated, to ‘scan’ over the surface in alignment with the bound samples.

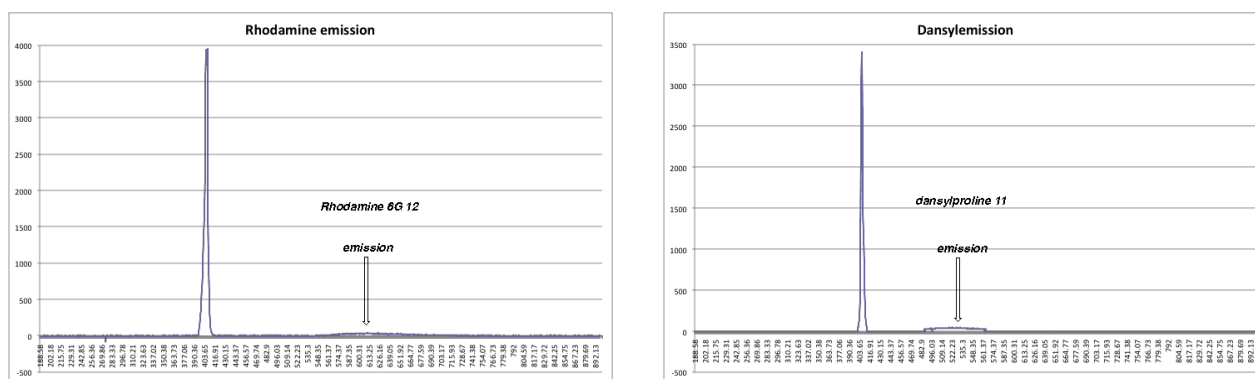


Figure 113 Emission spectra of **257** and (*L*)-**258** on a gold compact disc when illuminated with a light of 405 nm

Gratifyingly when the light passed over the SAMs a small amount of emission, at different wavelengths ~560-650nm for **257**, ~480-560nm for (*L*)-**258** was detected for both, Figure 113. It is unknown whether this emission would be strong enough or change enough to observe a binding event on the CD surface. The next step would be to design a ligand that incorporates the (+)-biotin and LASER dye moieties. This is currently under investigation by utilising the unsymmetrical Tröger’s base ‘click’ reaction described in this work.

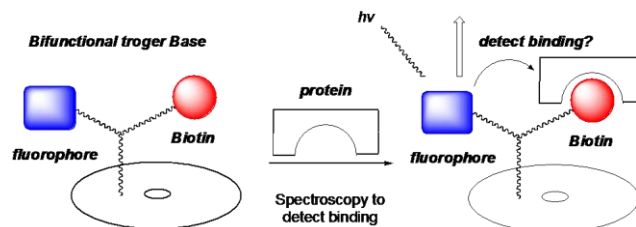


Figure 114 Schematic of how this project could be incorporated into a CD-player spectrometer.

Efforts to convert a CD drive into a CD spectrometer was also briefly investigated. Using a reported method by Potyralio *et al.* a CD drive was converted to intercept the analogue signal from the drive before it was converted to a digital signal by the onboard micro processor.¹⁰³ The drive was opened and the connection from the LASER diode detector was intercepted by soldering a wire to the Rf connection found on the main circuit board figure 115.



Figure 115 A standard CD-drive has been modified to intercept the analogue signal *via* the soldering of a wire to the output of the detector diode.

To test whether the signal could be detected a standard compact disc was defaced using a black marker and placed in the drive. The soldered wire was connected to a high end oscilloscope and the surface was scanned using a CD error diagnostics program. Interestingly the oscilloscope picked up the errors more rapidly than the diagnostics tool. This was thought to be a good indication that the analogue signal was being intercepted as the time lag between the signal from the detector and the time taken convert this to digital signal was observed. The results were collected and produced 30 million data points, it was necessary to thin out these results to process the data as MS Excel and Origin pro found it difficult to work with data of this volume. Once the data had been processed a clear change in observed voltages from the detector, matched that from the pattern that defaced the CD. This afforded a strong indication that the analogue signal had been intercepted.

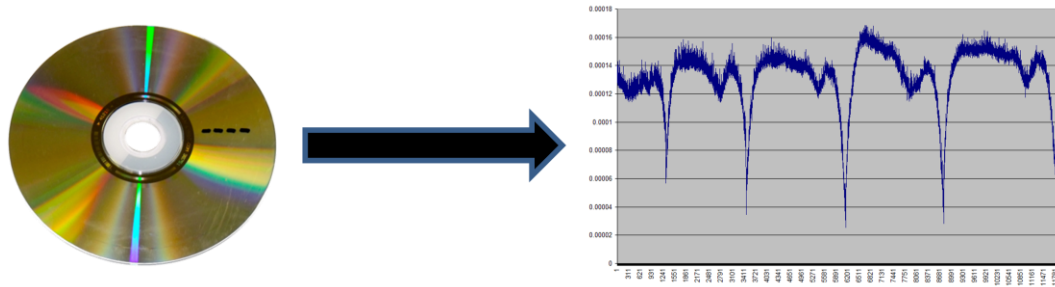


Figure 116 A defaced compact disc was used to test whether the analogue signal had been successfully intercepted.

Unfortunately this couldn't be investigated further as the computing knowledge needed to make the CD drive spin and record data without the header of the CD being present was far too complicated to design without outside help. Attempts to find a collaborator both within the university, from the School of Computer Science, and from industry was not possible and this aspect of the project was postponed until a suitable collaborator could be found.

6.0 Experimental

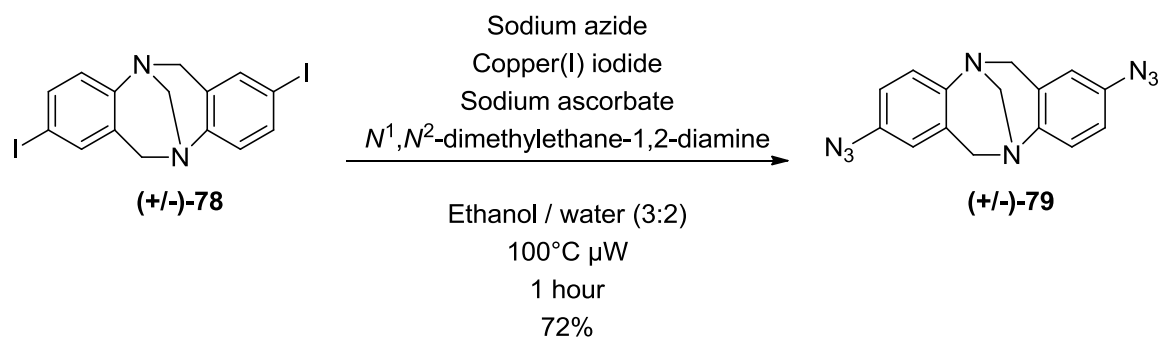
6.1 General Directions

Reactions described as under an argon or nitrogen atmosphere were conducted in flame dried apparatus. Reactions carried out at 0°C were cooled using a water / ice bath, those at -78°C were cooled in an acetone / cardice bath. Tetrahydrofuran and diethyl ether were freshly distilled from sodium benzophenone ketyl under argon. Dichloromethane and triethylamine were freshly distilled from calcium hydride under argon. Toluene and acetonitrile were freshly distilled from sodium under argon. Anhydrous dimethylformamide was purchased from Sigma Aldrich. All commercially available reagents were used as supplied. Petroleum ether refers to the fraction that boils between 40 and 60°C. Column chromatography was carried out on silica gel (Fluka Silica gel 60 70-230 mesh) TLC was performed on Merck plates (aluminium coated with 0.2mm silica gel 60 F₂₅₄). NH₂ loaded silica refers to pre-packed Isolute flash chromatography cartridges. 24 carat gold coated compact discs (Sony Gold CD-R pro 24k Gold 4 – 16x – 700) were purchased from a variety of vendors.

6.2 Characterisation

Melting points were recorded using open capillary tubes on melting point apparatus and are uncorrected. Infrared spectra were recorded either as a thin film or neat sample. ¹H and ¹³C-NMR spectra were recorded in Fourier transform mode on an Oxford Gemini 300 MHz, 400 MHz, Bruker Ultrashield 400MHz or Bruker Ascend 500 MHz at the field strength indicated and unless otherwise stated deuterated chloroform was used as solvent. ¹⁵N and ²H-NMR were run, unlocked, on a Bruker Ascend 500MHz. The ¹H-spectra were recorded in ppm and referenced to the residual CHCl₃ signal located at δ 7.26 ppm. ¹³C-NMR spectra were recorded in ppm and referenced to the residual CHCl₃ signal found at δ 77.00. Multiplicities in the NMR spectra are described as: s = singlet, d = doublet, t = triplet, q = quartet, m = multiplet, br = broad; coupling constants are reported in Hz. Ion mass/charge (*m/z*) ratios are reported as values in atomic mass units and carried out on a Shimadzu LCMS or Shimadzu Kratos MALDI-TOF. Microwave reactions were carried out in sealed vials in a Biotage Optimizer or Emerys Creator. Optical rotation values were measured on a Perkin Elmer 241 polarimeter. FT-IR spectra were recorded on a Perkin-Elmer 298 spectrometer. HRMS was carried out by the EPSRC at the National Mass Spectrometry Service, University of Wales, Swansea

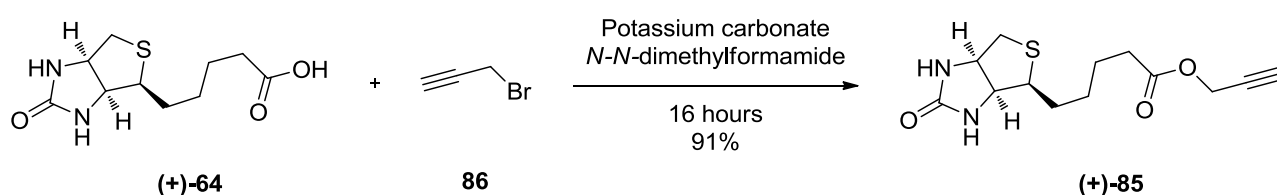
Synthesis of 2,8-Diazo-6H,12H-5,11-methandibenzo[b,f][1,5]diazocine (+/-)-79



(+/-)-79 A 5 mL microwave vial was charged with 2,8-*bis*-iodo-6H,12H-5,11-methandibenzo[b,f][1,5]diazocine **(+/-)-78** (1.5 g, 3.16 mmol), sodium ascorbate (0.063 g, 0.319 mmol), copper(I) iodide (0.122 g, 0.638 mmol) and sodium azide (0.830 g, 12.76 mmol) in ethanol (5 mL) and water (2.143 mL). The reaction vessel was sealed and to this N^1,N^2 -dimethylethane-1,2-diamine (59 μ L, 0.957 mmol) was added and the reaction mixture heated to 100°C for 1 hour by microwave irradiation. The reaction mixture was diluted with water (5 mL) and extracted with dichloromethane (2 x 10 mL). The combined organic extracts were washed with brine (5 mL) and dried with magnesium sulfate. This was filtered and solvent removed under reduced pressure. The reaction mixture was absorbed onto silica and purified by flash chromatography (hexane : ethyl acetate 4 : 1). Subsequent physiochemical analysis confirmed this to be the title compound **(+/-)-79** (702 mg, 2.307 mmol, 72.3 % yield)

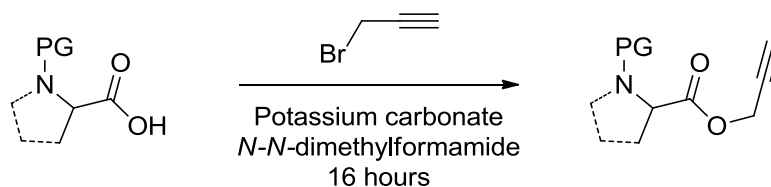
Pale orange solid. *R_f* 0.6 (hexane : ethyl acetate 4 : 1). MP : 120-122°C (diethyl ether); $^1\text{H-NMR}$ (400MHz, CDCl_3) δ 7.08 (d, *J*8.5 Hz, 2H, ArH), 6.81 (d, *J*8.4 Hz, 2H, ArH), 6.55 (s, 2H, ArH), 4.62 (d, *J*16.8 Hz, 2H, CHH), 4.25 (s, 2H, CH_2), 4.07 (d, *J*16.8 Hz, 2H, CHH); $^{13}\text{C-NMR}$ (100MHz, CDCl_3) δ 145.02, 135.78, 129.36, 126.62, 118.68, 117.23, 67.13, 58.88 ppm; FT-IR (KBr neat) 2112 azide cm^{-1} ; m/z $[\text{ES}]^+$ M+H (found) 305.1, (calc): 305.1, HRMS (NSI) Calcd for $\text{C}_{15}\text{H}_{13}\text{N}_8$, M+H, 305.1258; Found 305.1260.

Synthesis of prop-2-ynyl 5-((3*aS*,4*S*,6*aR*)-2-oxohexahydro-1*H*-thieno[3,4-*d*]imidazol-4-yl)pentanoate (+)-**85**



A flame-dried 25 mL round-bottomed flask was charged with (+)-biotin (+)-**64** (500 mg, 2.047 mmol) and potassium carbonate (424 mg, 3.07 mmol) in *N,N*-dimethylformamide (10 mL) and left to stir under an argon atmosphere for 30 minutes. Following this propargyl bromide **86** (331 μ L, 3.07 mmol) was added slowly and left to stir for 16 hours at room temperature. The resulting solution was diluted with ethyl acetate (10 mL), water (10 mL) and transferred to a 50 mL separating funnel. The solution was extracted with ethyl acetate (2 x 10 mL) and the combined organic extracts were washed with water (5 x 10 mL), washed with brine (10 mL) and dried over magnesium sulfate. The solution was filtered and the solvent removed under reduced pressure. The residue was purified by flash chromatography on silica eluting with 3% methanol in dichloromethane affording a white solid. Subsequent physicochemical analysis confirmed this to be the title compound *O*-propargyl (+)-biotin (+)-**85** (525 mg, 1.859 mmol, 91 % yield)

White solid *R*_f 0.45 (3% methanol in dichloromethane). MP 87-88°C (methanol/ether). ¹H-NMR (400 MHz, CDCl₃) δ 6.34 (s, 1H, NH), 5.96 (s, 1H, NH), 4.61 (d, *J* 2.5 Hz, 2H, CH₂), 4.44 (dd, *J* 7.7, 4.8 Hz, 1H, CH), 4.24 (dd, *J* 7.7, 4.7 Hz, 1H, CH), 3.20 – 2.97 (m, 1H, CH), 2.84 (dd, *J* 12.8, 4.9 Hz, 1H, CH), 2.69 (d, *J* 12.7 Hz, 1H, CH), 2.45 (t, *J* 2.5 Hz, 1H, CH), 2.33 (t, *J* 7.5 Hz, 2H, CH₂), 1.76 – 1.51 (m, 4H, 2CH₂), 1.46 – 1.29 (m, 2H, CH₂). ¹³C-NMR (101 MHz, CDCl₃) δ 173.08, 164.34, 77.98, 75.16, 62.16, 60.34, 55.76, 52.06, 40.77, 33.80, 28.52, 28.38, 24.83 ppm. ATR-IR 3214 CH alkyne, 2135 C-C alkyne, 1759 C=O, 1678 C=O cm⁻¹ *m/z* [ES]⁺ M+Na 305.1. HRMS (NSI) Calcd for, C₁₃H₂₂N₃O₃S, M+NH₄, 300.1390; Found 300.1392

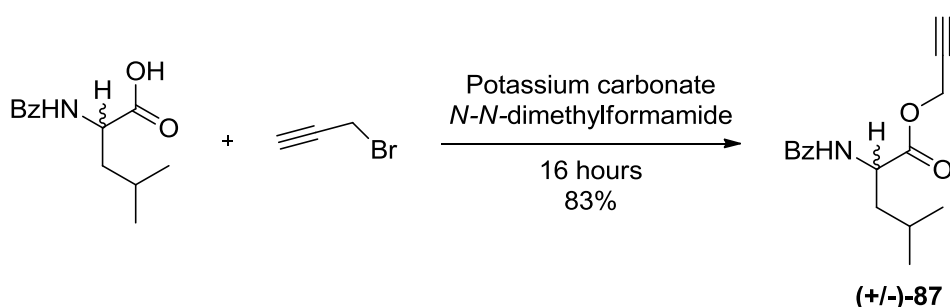


General procedure for propargylation of terminal alkynes

A flame dried 25 mL round bottomed flask was charged with carboxylic acid (1eq), potassium carbonate (1.5 eq) in dimethylformamide (10 mL). This was left to stir under an inert atmosphere

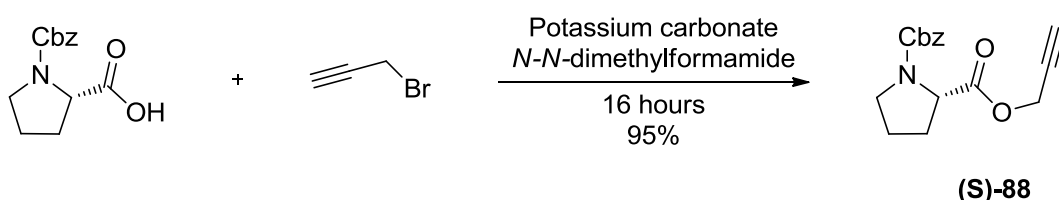
of argon for 30 minutes. To this propargyl bromide (80% in toluene, 1.5 eq) was added drop wise and left to stir for 16 hours at room temperature. The reaction mixture was diluted with dichloromethane (5 mL) and water (10 mL), transferred to a separating funnel and extracted with dichloromethane (2 x 5 mL). The combined organic extracts were washed with water (5 x 10 mL), saturated sodium bicarbonate (2 x 10 mL), brine (10 mL), dried with magnesium sulfate and filtered through a NH₂ loaded silica column (Isolute prepacked flash chromatography cartridge), eluted with dichloromethane and the solvent removed under reduced pressure to afford the corresponding *O*-propargylated compound.

Prop-2-ynyl 2-benzamido-4-methylpentanoate (+/-)-87



(+/-)-87 (54 mg, 0.198 mmol, 83%) orange oil. No further purification necessary. *R_f* 0.6 (1:5, ethyl acetate : hexane). ¹H-NMR (400MHz, CDCl₃) δ7.72 (dd, *J*1.3, 8.3Hz, 2H, ArH), 7.43 (m, 1H, ArH), 7.35 (m, 2H, ArH), 6.56 (d, *J*8.1Hz, 1H, NH), 4.82 (ddd, *J*5.1, 8.6 Hz, 1H, CH), 4.68 (m, 2H, CH₂), 2.43 (t, *J*2.1Hz, 1H, CH), 1.50 – 1.78 (m, 3H, CH₂, CH), 0.91 (t, *J*5.7Hz, 6H, (CH₃)₂); ¹³C-NMR (100 MHz, CDCl₃) δ172.7, 167.4, 134.0, 132.0, 128.8, 127.3, 77.5, 75.6, 52.9, 51.2, 41.7, 25.1, 23.1, 22.2 ppm; FT-IR(KBr neat) 3298 CH alkyne, 2129 C-C alkyne, 1747 C=O, 1643 C=O cm⁻¹; *m/z* [ES]⁺ M+H (found) 274.1, M+Na (found) 296.1, M+H (calc) 274.14, M+Na (calc) 296.13. HRMS (NSI) Calcd for C₁₆H₂₀NO₃, M+NH₄. 274.1438; Found, 274.1440.

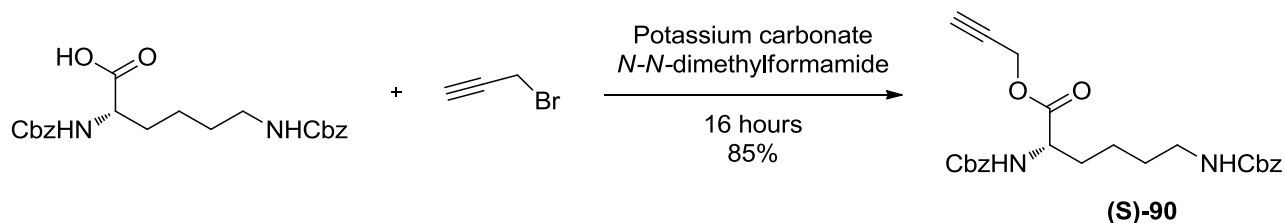
(S)-1-benzyl 2-prop-2-ynyl pyrrolidine-1,2-dicarboxylate (S)-88



(S)-88 (1.1g, 3.8 mmol, 95%) yellow oil. No further purification necessary. *R_f* 0.5 (1:5, ethyl acetate : hexane). ¹H-NMR (400MHz, CDCl₃) δ7.23 (m, 5H, ArH), 5.03 (m, 2H, CH₂) 4.62 (m, 1H, CH), 4.45 (s, 1H, βCHH), 4.28 (m, 1H, βCHH), 3.41 (m, 2H, CH₂), 2.41 (t, *J*2.4Hz, 1H, CH_(yne)), 2.12 (d, *J*7.4Hz, 1H, CHH), 1.85 (m, 3H, CH₂, CHH); ¹³C-NMR (75MHz, CDCl₃) δ172.1, 171.9, 154.9, 154.2, 136.7, 136.6, 128.5, 128.4, 128.0, 127.9, 127.9, 127.8, 77.2, 75.3, 66.9, 66.9,

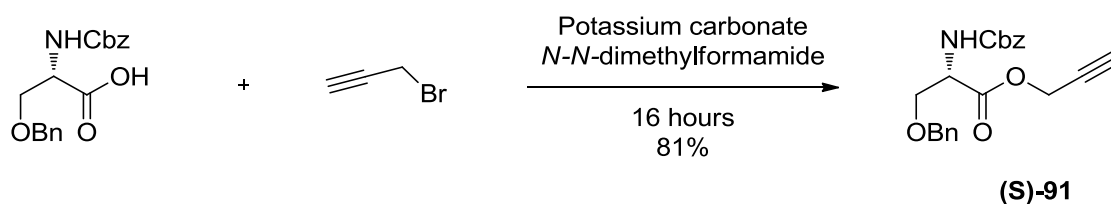
58.9, 58.6, 52.4, 52.3, 46.8, 46.3, 30.6, 29.6, 24.1, 23.3 ppm; FT-IR (KBr neat) 3285 CH alkyne, 1753 C=O, 1704 C=O cm^{-1} ; m/z [ES]⁺ M+Na (found) 310.0, (calc): 310.11; HRMS (NSI) Calcd for C₁₆H₂₁N₂O₄, M+NH₄, 305.1496; Found 305.1496. $[\alpha]_D^{25}$ -80.3 (c 1.0, CHCl₃).

(S)-Prop-2-ynyl 3,11-dioxo-1,13-diphenyl-2,12-dioxa-4,10-diazatridecane-5-carboxylate (S)-90



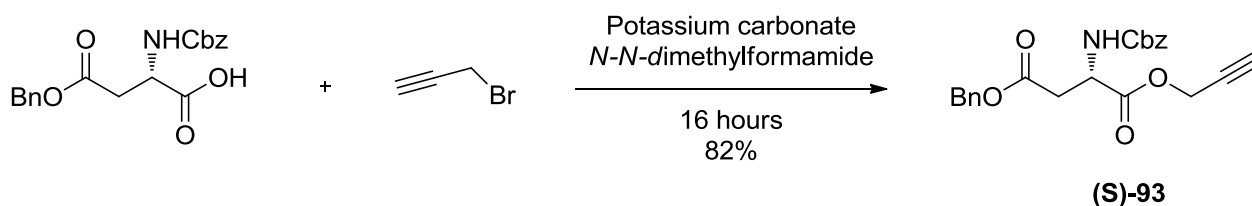
(S)-90 (93 mg, 0.205 mmol, 85%) orange oil. No further purification necessary. *R_f* 0.45 (1:5, ethyl acetate : hexane). ¹H-NMR (300 MHz, CDCl₃) δ 7.33 (s, 10H, ArH), 5.48 (d, *J*7.4Hz, 1H, NH), 5.08 (d, *J*7.7Hz, 4H, (CH₂)₂), 4.89 (m, 1H, NH), 4.72 (m, 2H, CH₂), 4.39 (m, 1H, α CH), 3.17 (dd, *J*6.2, 12.5Hz, 2H, β CH₂), 2.49 (t, *J*2.2Hz, 1H, CH), 1.75 (m, 2H, CH₂), 1.41 (m, 4H, (CH₂)₂); ¹³C-NMR (75 MHz, CDCl₃) δ 171.8, 156.6, 156.1, 136.6, 136.2, 128.6, 128.5, 128.2, 128.2, 128.2, 77.3, 75.5, 67.0, 66.6, 53.5, 52.6, 40.3, 31.7, 29.2, 22.0 ppm; KBr neat 3298 CH alkyne, 2129 C-C alkyne, 1703, br, C=O cm^{-1} . m/z [ES]⁺ M+Na (found) 475.2 M+Na (calc) 475.18; HRMS (NSI) Calcd for C₂₅H₃₂N₃O₆, M+NH₄, 470.2286; Found 470.2282. $[\alpha]_D^{25}$ -8.0 (c1.0, CHCl₃)

(S)-prop-2-ynyl-3-(benzyloxy)-2-(benzyloxycarbonylamino) propanoate (S)-91



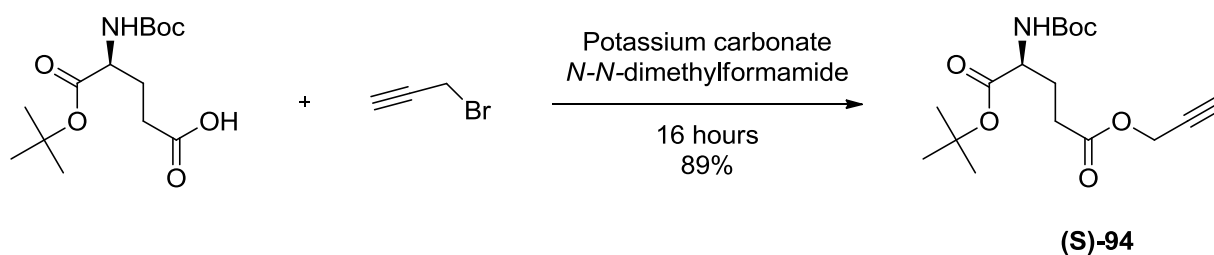
(S)-91 (90 mg, 0.245 mmol, 81%) yellow oil. No further purification necessary. *R_f* 0.55 (1:5, ethyl acetate : hexane). ¹H-NMR (300MHz, CDCl₃) δ 7.31 (m, 10H, ArH), 5.72 (d, *J*8.4Hz, 1H, NH), 5.14 (s, 2H, CH₂), 4.74 (d, *J*2.1Hz, 2H, CH₂), 4.57 (m, 1H, α CH), 4.52 (d, *J*5.5Hz, 2H, CH₂), 3.94 (dd, *J*2.9, 9.4Hz, 1H, β CHH), 3.72 (dd, *J*2.9, 9.4Hz, 1H, β CHH), 2.49 (t, *J*2.4Hz, 1H, CH); ¹³C-NMR (75 MHz, CDCl₃) δ 169.5, 156.1, 137.4, 136.3, 128.6, 128.5, 128.2, 128.1, 127.9, 127.7, 75.4, 73.3, 69.6, 67.0, 54.4, 52.9 ppm; FT-IR (KBr neat) 3291 CH alkyne, 2130 C-C alkyne, 1755 C=O, 1736 C=O cm^{-1} ; m/z [ES]⁺ (found) M+H 368.1, M+Na 390.0 (calc) M+H 368.2, M+Na 390.13; HRMS (NSI) Calcd for C₂₁H₂₂NO₅, M+H, 368.1492; Found 368.1497. $[\alpha]_D^{25}$ +19 (c1.0, CHCl₃).

(S)-4-benzyl-1-prop-2-ynyl 2-(benzyloxycarbonylamino) succinate (S)-93



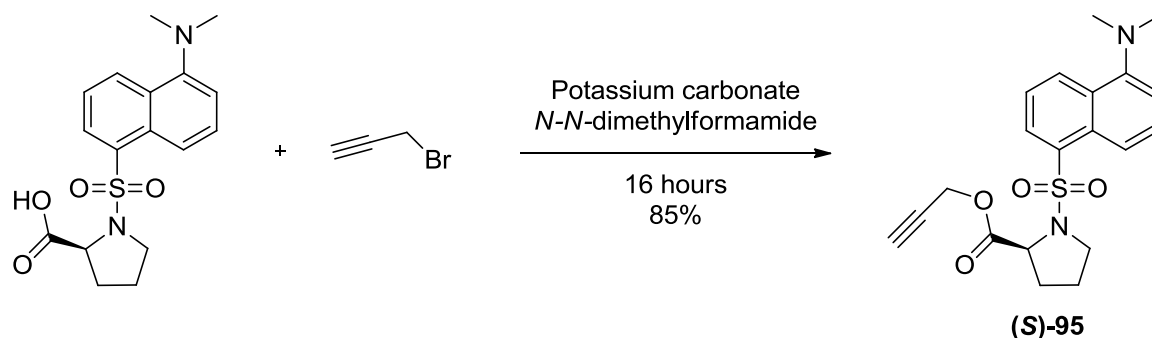
(S)-93 (91 mg, 0.23 mmol, 82%) yellow oil. No further purification necessary. *R_f* 0.3 (1:5, ethyl acetate : hexane). ¹H-NMR (400MHz, CDCl₃) δ7.24 (m, 10H, ArH), 5.74 (d, *J*8.5 Hz, 1H, NH), 5.03 (s, 4H, (CH₂)₂), 4.59 (m, 3H, CH₂, αCH), 3.00 (dd, *J*4.7 Hz, 1H, βCHH), 2.83 (dd, *J*4.5 Hz, 1H, βCHH), 2.38 (t, *J*2.5, 1H, CH); ¹³C-NMR (100 MHz, CDCl₃) δ170.7, 170.2, 156.1, 136.3, 135.4, 128.9, 128.7, 128.7, 128.6, 128.4, 128.3, 77.1, 75.8, 67.4, 67.2, 53.4, 50.6, 36.9 ppm; FT-IR (KBr neat) 3290 CH alkyne, 2130 C-C alkyne, 1731 C=O cm⁻¹; *m/z* [ES]⁺ (found) M+Na 418.1 (calc) M+Na 418.13. HRMS (NSI) Calcd for C₂₂H₂₅N₂O₆, M+NH₄, 413.1707; Found 413.1701. [α]²⁵_D +21.2 (c1.0, CHCl₃).

(S)-1-tert-butyl 5-prop-2-ynyl 2-(tert-butoxycarbonylamino) pentanedioate (S)-94



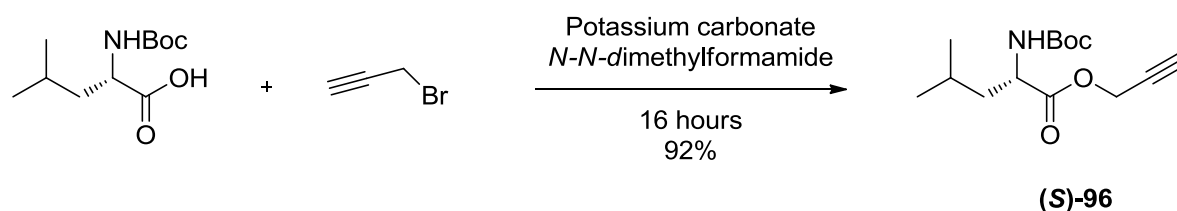
(S)-94 (998mg, 2.93 mmol, 89%) pale yellow solid. No further purification necessary. *R_f* 0.7 (1:5, ethyl acetate : hexane). MP 37-39°C (hexane). ¹H-NMR (300 MHz, CDCl₃) δ5.09 (d, *J*8.1 Hz, 1H, NH), 4.63 (d, *J*2.5 Hz, 2H, CH₂), 4.15 (d, *J*4.9 Hz, 1H, αCH), 2.40 (m, 3H, CH₂, CH), 2.12 (m, 1H, CHH), 1.87 (m, 1H, CHH), 1.41 (s, 9H, (CH₃)₃), 1.38 (s, 9H, (CH₃)₃); ¹³C-NMR (75 MHz, CDCl₃) δ172.1, 171.3, 155.4, 82.1, 79.7, 74.9, 53.1, 51.9, 29.9, 28.1, 27.8 ppm; FT-IR (KBr neat) 3293 C-H alkyne, 1713 C=O cm⁻¹; *m/z* [ES]⁺ (found) M+Na 364.1 (calc) M+Na 364.17. HRMS (NSI) Calcd for C₁₇H₂₈NO₆, M+NH₄, 342.1911; Found 342.1913. [α]²⁵_D 10.4 (c 1.0, CHCl₃).

(S)-prop-2-ynyl-1-(5-(dimethylamino)naphthalen-1-ylsulfonyl) pyrrolidine-2-carboxylate (S)-95



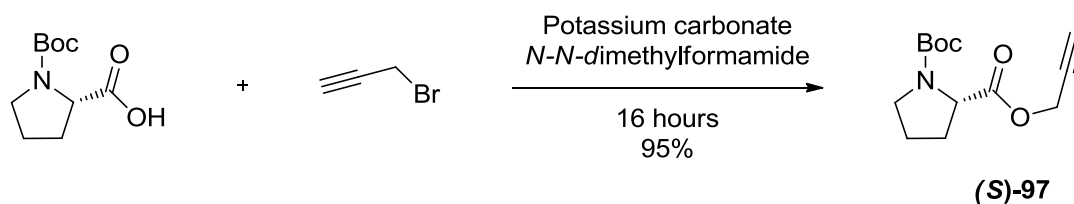
(S)-95 (47 mg, 0.122 mmol, 85%) bright yellow oil. No further purification necessary. *R_f* 0.3 (1:5, ethyl acetate : hexane). ¹H-NMR (300 MHz, CDCl₃) δ8.54 (dt, *J*7.5, 1.3 Hz, 1H, ArH), 8.45 (dt, *J*0.9, 8.7 Hz, 1H, ArH), 8.27 (dd, *J*1.3, 7.4 Hz, 1H, ArH), 7.54 (ddd, *J*7.5, 8.61, 13.3 Hz, 2H, ArH), 7.18 (dd, *J*0.8, 7.6 Hz, 1H, ArH), 4.55 (d, *J*8.5 Hz, 1H, αCH), 4.50 (t, *J*2.5 Hz, 2H, CH₂), 3.51 (m, 2H, CH₂), 2.87 (s, 6H, (CH₃)₂), 2.44 (t, *J*2.5 Hz, 1H, CH), 1.75 – 2.30 (m, 4H, (CH₂)₂); ¹³C-NMR (75 MHz, CDCl₃) δ171.3, 151.7, 134.4, 130.7, 130.7, 130.4, 130.0, 128.2, 123.2, 119.7, 115.3, 77.2, 75.2, 59.8, 52.4, 48.4, 45.3, 30.9, 24.6 ppm; FT-IR (KBr neat) 3276 C-H alkyne, 2129 C-C alkyne, 1754 C=O, 1335 O=S=O, 1143 O=S=O cm⁻¹; *m/z* [ES]⁺ (found) M+H 387.1, M+Na 409.1, (calc) M+H 387.14, M+Na 409.12. HRMS (NSI) Calcd for C₂₀H₂₃N₂O₄S, M+H, 387.1373; Found 387.1373. [α]_D²⁵ -65 (c 1.0, CHCl₃).

(S)-prop-2-ynyl-2-(tert-butoxycarbonylamino)-4-methyl pentanoate (S)-96



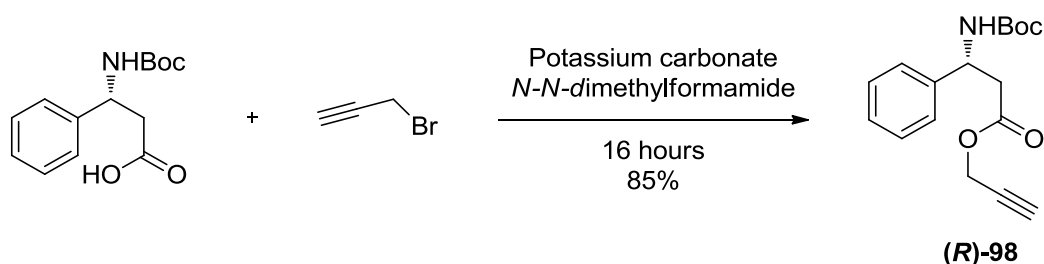
(S)-96 (1.07 g, 3.98 mmol, 92%) yellow oil. No further purification necessary. *R_f* 0.7 (1:5, ethyl acetate : hexane). ¹H-NMR (300MHz CDCl₃) δ4.90 (d, *J*8.3 Hz, 1H, NH), 4.71 (q, *J*15.8 Hz, 2H, CH₂), 4.33 (t, *J*8.2 Hz, 1H, αCH), 2.47 (s, 1H, CH), 1.61 (m, 3H, CH₂ and CH), 1.42 (s, 9H, (CH₃)₃), 0.93 (d, *J*6.2 Hz, 6H, (CH₃)₂). ¹³C-NMR (75 MHz CDCl₃) 172.86, 155.45, 79.90, 77.15, 75.15, 52.40, 51.90, 41.41, 28.15, 24.59, 22.67, 21.66 ppm. FT-IR (KBr neat) 3363 C-H alkyne, 1750 C=O, 1713 C=O cm⁻¹. *m/z* [ES]⁺ (found) M+Na 292.1 (calc) M+Na 292.15 HRMS (NSI) Calcd for C₁₄H₂₄NO₄, M+H, 270.1700; Found 270.1701. [α]_D²⁵ -17.8 (c 1.0, CHCl₃).

(S)-1-tert-butyl 2-prop-2-ynyl pyrrolidine-1,2-dicarboxylate (S)-97



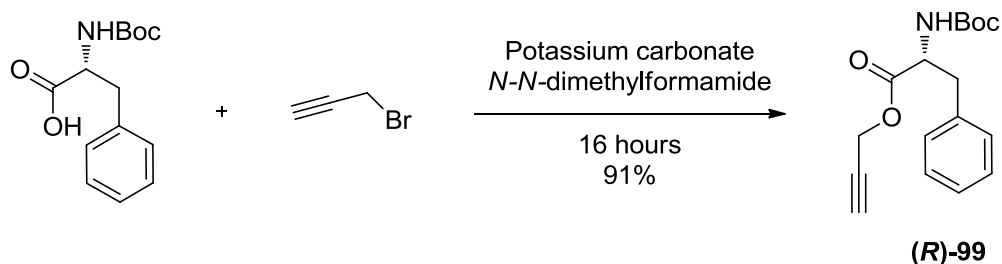
(S)-97 (1.1 g, 4.42 mmol, 95%), white solid. No further purification necessary. *R_f* 0.6 (1:5, ethyl acetate : hexane). MP 52-54°C (hexane), ¹H-NMR (300MHz, CDCl₃) δ4.70 (m, 2H, CH₂), 4.27 (m, 1H, αCH), 3.45 (m, 2H, CH₂), 2.45 (m, 1H, CH), 2.21 (m, 1H, CHH), 1.90 (m, 3H, CH₂, CHH), 1.41 (d, *J*11.89 Hz, 9H, (CH₃)₃); ¹³C-NMR (75 MHz, CDCl₃) δ175.5, 172.2, 153.7, 150.5, 79.9, 79.8, 77.3, 75.0, 74.9, 58.8, 58.5, 52.3, 52.1, 46.4, 46.2, 30.6, 29.6, 28.2, 28.1, 24.1, 23.4 ppm; FT-IR (KBr neat) 3509, 3242 C-H alkyne, 2127 C-C alkyne, 1755 C=O, 1700 C=O cm⁻¹; *m/z* [ES]⁺ M+Na (found)276.0, calc(276.12) HRMS (NSI) Calcd for C₁₃H₂₀NO₄, M+H, 254.1387; Found 254.1381. [α]²⁵_D -68.5 (c 1.0, CHCl₃).

(R)-prop-2-yn-1-yl-3-(tert-butoxycarbonylamino)-3-phenyl propanoate (R)-98



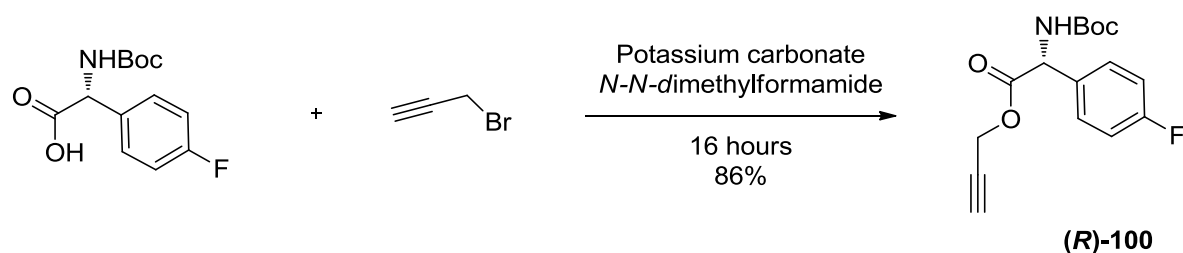
(S)-98 (43 mg, 0.142 mmol, 75%) white solid. No further purification necessary. *R_f* 0.7 (1:5, ethyl acetate : hexane). MP 47-49°C, ¹H-NMR (300 MHz, CDCl₃) δ7.29 (m, 5H, ArH), 5.40 (s, 1H, NH), 5.13 (s, 1H, αCH), 4.60 (d, *J*2.5 Hz, 2H, CH₂), 2.89 (qd, *J*6.5, 15.6 Hz, 2H, βCH₂), 2.43 (t, *J*2.5 Hz, 1H, CH), 1.41 (s, 9H, (CH₃)₃); ¹³C-NMR (75 MHz, CDCl₃) δ170.2, 155.1, 128.7, 127.7, 126.2, 79.7, 77.2, 75.0, 52.0, 51.2, 40.6, 28.2 ppm; FT-IR (KBr neat) 3354 C-H alkyne, 2130 C-C alkyne, 1742 C=O, 1711 C=O cm⁻¹; *m/z* [ES]⁺ (found) M+Na 326.0 (calc) M+Na 326.14. HRMS (NSI) Calcd for C₁₇H₂₂NO₄, M+H, 304.1543; Found 304.1545. [α]²⁵_D 23.3 (c1.0, CHCl₃).

(R)-prop-2-ynyl-2-(tert-butoxycarbonylamino)-3-phenyl propanoate (R)-99



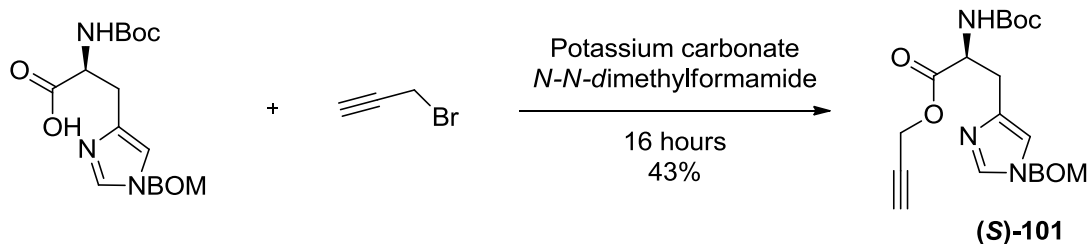
(R)-99 (1.04g, 3.43 mmol, 91%) colourless oil. No further purification necessary. *R_f* 0.7 (1:5, ethyl acetate : hexane). ¹H-NMR (300 MHz, CDCl₃) δ7.29 (m, 3H, ArH), 7.16 (m, 2H, ArH), 4.96 (s, 1H, NH), 4.72 (m, 3H, αCH, CH₂), 3.11 (m, 2H, CH₂), 2.51 (t, *J*1.9 Hz, 1H, CH), 1.41 (s, 9H, (CH₃)₃); ¹³C-NMR (75 MHz, CDCl₃) δ171.3, 155.2, 135.8, 129.4, 128.6, 127.2, 80.0, 75.4, 54.2, 52.5, 38.0, 28.1 ppm; FT-IR (KBr neat) 3383 C-H alkyne, 2129 C-C alkyne, 1750C=O, 1713 C=O cm⁻¹; *m/z* [ES]⁺ (found) M+Na 326.1, (calc) M+Na 326.14. HRMS (NSI) Calcd for C₁₇H₂₂NO₄, M+H, 304.1543; Found 304.1546. [α]_D²⁵ -13.5 (c 1.0, CHCl₃).

(R)-prop-2-ynyl 2-(tert-butoxycarbonylamino)-2-(4-fluorophenyl) acetate (R)-100



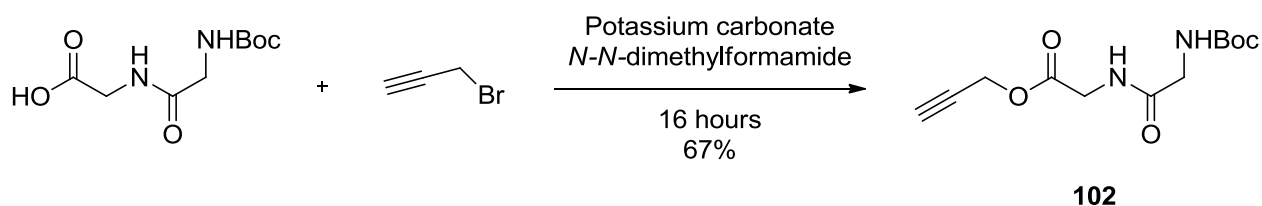
(R)-100 (49mg, 0.16 mmol, 86%) yellow oil. No further purification necessary. *R_f* 0.7 (1:5, ethyl acetate : hexane). ¹H-NMR (300 MHz, CDCl₃) δ7.35 (m, 2H, ArH), 7.04 (m, 2H, ArH), 5.51 (s, 1H, NH), 5.34 (d, *J*7.1 Hz, 1H, αCH), 4.68 (ddd, *J*2.4, 5.3, 8.3 Hz, 2H, CH₂), 2.45 (t, *J*2.5 Hz, 1H, CH), 1.42(s, 9H, (CH₃)₃); ¹³C-NMR (75 MHz, CDCl₃) δ162.9 (d, *J*_{C-F} 246.0 Hz), 129.0 (d, *J*_{C-F} 8.4 Hz), 115.9 (d, *J*_{C-F} 21.0 Hz), 80.4, 76.6, 75.5, 56.8, 53.0, 28.1 ppm; FT-IR (KBr neat) 3301C-H alkyne, 2130 C-C alkyne, 1752 C=O, 1712C=O cm⁻¹; *m/z* [ES]⁺ (found) M+Na 330.1(calc) M+Na 330.11. HRMS (NSI) Calcd for C₁₆H₁₉FNO₄, M+H, 308.1293; Found 308.1294. [α]_D²⁵ -49.4 (c1.0, CHCl₃).

(S)-prop-2-ynyl 3-(1-(benzyloxymethyl)-1H-imidazol-4-yl)-2-(tert-butoxycarbonyl amino) propanoate (S)-101



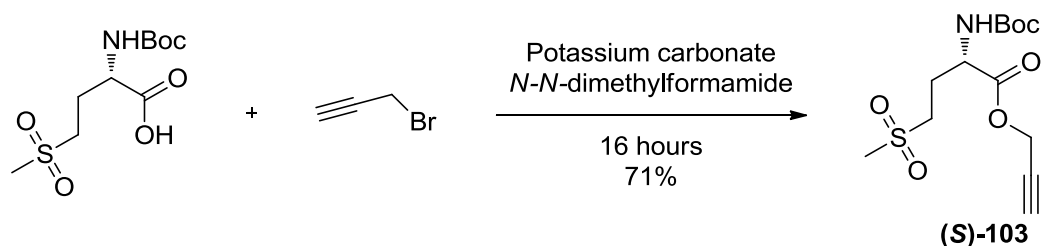
(S)-101 (47 mg, 0.11 mmol, 43%) orange oil. No further purification necessary. *R_f* 0.3 (1:5, ethyl acetate : hexane). ¹H-NMR (300 MHz, CDCl₃) δ7.48 (s, 1H, CH), 7.32 (m, 5H, ArH), 6.90 (s, 1H, CH), 5.27 (m, 3H, NH, CH₂), 4.70 (m, 2H, CH₂), 4.59 (m, 1H, αCH), 4.44 (s, 2H, CH₂), 3.16 (m, 2H, βCH₂), 2.49 (t, *J*2.5 Hz, 1H, CH), 1.39 (s, 9H, (CH₃)₃); ¹³C-NMR (75 MHz, CDCl₃) δ170.8, 155.2, 138.5, 136.1, 129.7, 128.7, 128.4, 128.1, 126.4, 80.2, 76.8, 75.6, 73.0, 69.7, 52.9, 52.8, 28.1, 26.5 ppm; FT-IR (KBr neat) 3287 C-H alkyne, 2128 C-C alkyne, 1750 C=O, 1710C=O cm⁻¹; *m/z* [ES]⁺ (found) M+H 414.3, M+Na 436.2 (calc) M+H 414.20, M+Na 436.18. HRMS (NSI) Calcd for C₂₂H₂₈N₃O₅, M+H, 414.2023; Found 414.2014. [α]_D²⁵ -3.5 (c 1.0, CHCl₃).

Prop-2-ynyl-2-(2-(tert-butoxycarbonylamino)acetamido) acetate 102



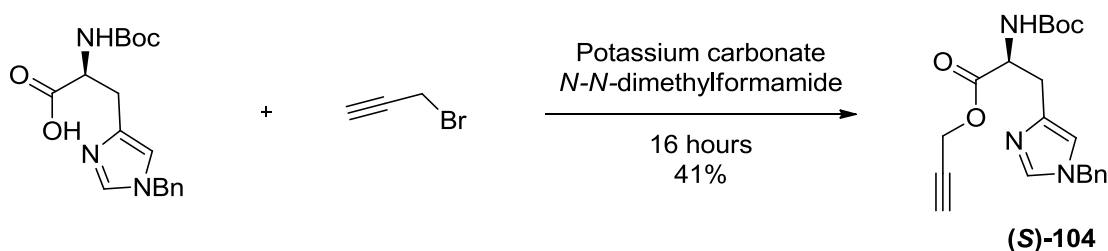
102 (780 mg, 2.89 mmol, 67%) white solid. No further purification necessary. *R_f* 0.7 (1:5, ethyl acetate : hexane). MP : 93-95°C (hexane), ¹H-NMR (400MHz, CDCl₃) δ7.08 (s, 1H, NH), 5.52 (s, 1H, NH), 4.67 (dd, *J*1.1, 2.5Hz, 2H, CH₂), 4.03 (d, *J*5.2 Hz, 2H, CH₂), 3.80 (d, *J*5.2 Hz, 2H, CH₂), 2.47 (t, *J*2.45Hz, 1H, CH); ¹³C-NMR (75 MHz, CDCl₃) δ170.4, 169.3, 156.3, 80.2, 76.9, 75.5, 52.7, 43.9, 40.9, 28.1 ppm; FT-IR (KBr neat) 3251 C-H alkyne, 1747 C=O, 1671C=O, cm⁻¹; *m/z* [ES]⁺ M+Na (found)293.0, (calc): 293.11. HRMS (NSI) Calcd for C₁₂H₁₉N₂O₅, M+H, 271.1288; Found 271.1291.

(S)-prop-2-ynyl 2-(tert-butoxycarbonylamino)-4-(methylsulfonyl)butanoate (S)-103



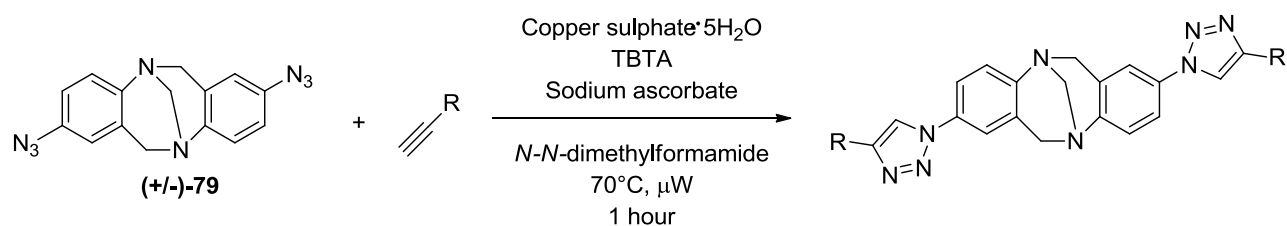
(S)-103 (86 mg, 0.269 mmol, 71%) white solid. No further purification necessary. *R_f* 0.5 (1:5, ethyl acetate : hexane). MP 85-87°C (hexane), ¹H-NMR (300 MHz, CDCl₃) δ5.33 (d, *J*8.2 Hz, 1H, NH), 4.70 (qd, *J*2.5, 15.5 Hz, 2H, CH₂), 4.37 (s, 1H, αCH), 3.08 (m, 2H, βCH₂), 2.88 (s, 3H, CH₃), 2.49 (t, *J*2.5 Hz, 1H, CH), 2.37 (m, 1H, CHH), 2.13 (m, 1H, CHH), 1.38 (s, 9H, (CH₃)₃); ¹³C-NMR (75 MHz, CDCl₃) δ170.7, 155.4, 80.6, 76.7, 75.9, 53.1, 51.9, 50.8, 40.6, 28.1, 25.3 ppm; FT-IR (KBr neat) 3356 C-H alkyne, 2129 C-C alkyne, 1748 C=O, 1712 C=O, 1368 O=S=O cm⁻¹; *m/z* [ES]⁺ M+Na (found)342.1, (calc)342.1. HRMS (NSI) Calcd for C₁₃H₂₅N₂O₆S, M+NH₄, 337.1428; Found 337.1432. [α]_D²⁵ +12.5 (c 1.0, CHCl₃).

(S)-prop-2-ynyl-3-(1-benzyl-1H-imidazol-4-yl)-2-(tert-butoxycarbonylamino) propanoate (S)-104



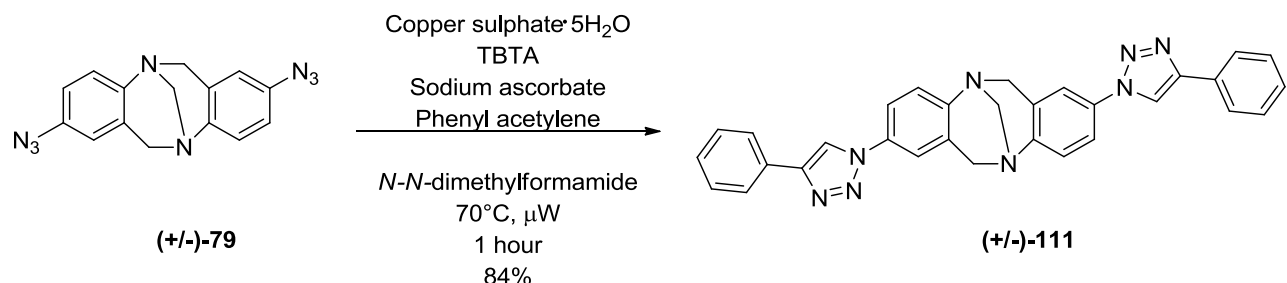
(S)-104 (45 mg, 0.12 mmol, 41%) yellow oil. No further purification necessary. *R_f* 0.3 (1:5, ethyl acetate : hexane) ¹H-NMR (300 MHz, CDCl₃) δ7.46 (d, *J*1.2 Hz, 1H, CH), 7.3 (m, 3H, ArH), 7.12 (m, 2H, ArH), 6.68 (s, 1H, CH), 6.02 (d, *J*8.2 Hz, 1H), 5.03 (s, 2H, CH₂), 4.63 (m, 3H, αCH, CH₂), 3.05 (m, 2H, βCH₂), 2.32 (t, *J*2.4 Hz, 1H, CH), 1.42 (s, 9H, (CH₃)₃); ¹³C-NMR (75 MHz, CDCl₃) δ171.4, 155.7, 137.7, 136.0, 129.0, 128.3, 127.3, 117.2, 79.6, 77.2, 74.9, 53.5, 52.3, 50.7, 29.9, 28.2 ppm. FT-IR (KBr neat) 3290 C-H alkyne, 2128 C-C alkyne, 1754 C=O, 1711 C=O cm⁻¹; *m/z* [ES]⁺ M+H (found) 384.2, (calc): 384.19. HRMS (NSI) Calcd for C₂₁H₂₆N₃O₄, M+H, 384.1918; Found 384.1911. [α]_D²⁵ -5.6 (c 1.0, CHCl₃).

General procedure for *bis*-functionalisation of 2,8-diazo-6H,12H-5,11-methanodibenzo [b,f][1,5]diazocine



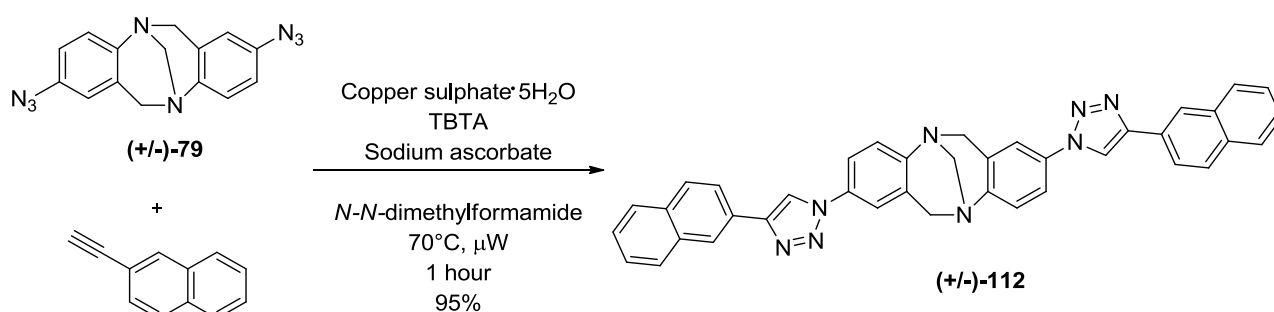
A microwave vial was charged with 2,8-diazo-6H,12H-5,11-methanodibenzo[b,f][1,5]diazocine (+/-)-**79** (1 eq), alkyne (2.2 eq), copper(II) sulfate pentahydrate (0.3 eq), sodium-*L*-ascorbate (0.8 eq) and TBTA (0.3 eq) in *N,N*-dimethylformamide. The reaction mixture was heated to 70°C, in a sealed vial, by microwave radiation for 1 hour. The reaction mixture was then diluted with dichloromethane (5 mL), washed with water (5 x 10 mL), brine (5 mL) and dried with magnesium sulfate. The suspension was filtered and the solvent removed under reduced pressure. The reaction mixture was purified by flash column chromatography on silica gel 1:1 ethyl acetate : petroleum ether unless otherwise stated.

2, 8 *bis*-(4-phenyl-1H-1,2,3-triazole)-6H, 12H-5, 11-methanodibenzo [b,f][1,5]diazocine (+/-)-**111**



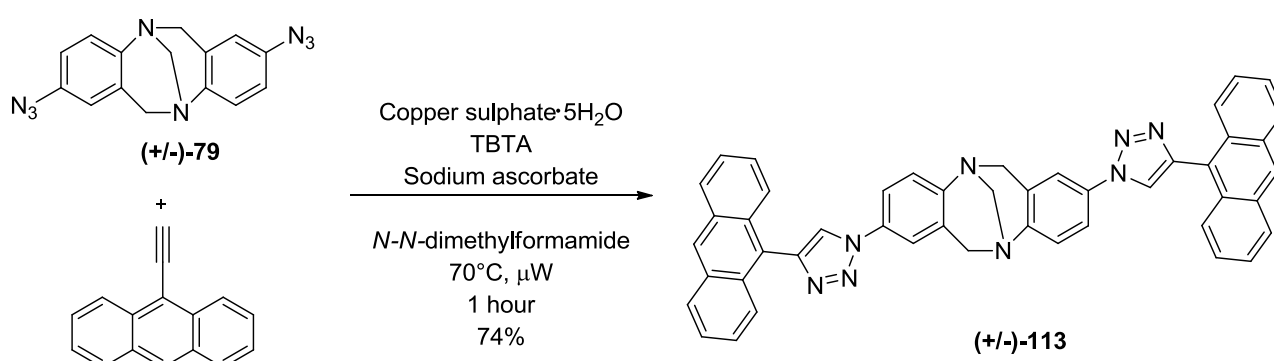
(+/-)-**111** Purified by flash chromatography on silica eluting with 1:1 ethyl acetate : petroleum ether to afford an of white solid (28 mg, 0.06 mmol, 84%) *R_f* 0.6 (1:1 ethyl acetate : petroleum ether), MP : 268-270°C (DCM); ¹H-NMR (300MHz, CDCl₃) δ 8.08 (s, 2H, (CH)₂), 7.87 (dd, *J*1.4, 8.4 Hz, 4H, ArH), 7.56 (dd, *J*2.5, 8.7 Hz, 2H), 7.45 (m, 6H, ArH), 7.37 (m, 2H, ArH), 7.33 (m, 2H, ArH), 4.83 (d, *J*16.8 Hz, 2H, 2(CHH)), 4.40 (s, 2H, CH₂), 4.32 (d, *J*16.8 Hz, 2H, (2CHH)); ¹³C-NMR (75MHz, CDCl₃) δ 148.46, 148.42, 133.19, 130.21, 129.22, 128.96, 128.48, 126.38, 125.84, 120.05, 119.05, 119.44, 117.54, 66.78, 58.77, 29.56 ppm; ATR-IR-IR 3052, 2161, 1975, 1610, 1498, 1482, 1329, 1230 cm⁻¹; *m/z* [ES]⁺ M+1 (found) 509.5, (calc): 509.6. HRMS (NSI) Calcd for C₃₁H₂₅N₈, M+H, 509.2197; Found 509.2190.

**2, 8 bis-(4-(naphthalen-2-yl)-1H-1,2,3-triazole)-6H, 12H-5, 11-methanodibenzo [b,f]
[1,5]diazocine (+/-)-112**



(+/-)-**112** (19 mg, 0.03 mmol, 95%) Precipitated from dichloromethane with hexane to afford a cream solid. *R_f* 0.4 (1:1 ethyl acetate : petroleum ether). MP : 226-228°C (ether); ¹H-NMR (400MHz, CDCl₃) δ 8.32 (s, 2H, 2CH), 8.14 (s, 2H, ArH), 7.93-7.74 (m, 8H, ArH), 7.25 (dd, *J*2.5, 8.6 Hz, 2H, ArH), 7.48-7.38 (m, 6H, ArH), 7.32 (d, *J*8.7 Hz, 2H, ArH), 4.80 (d, *J*17.0 Hz, 2H, 2(CHH)), 4.38 (s, 2H, CH₂), 4.29 (d, *J*17.0 Hz, 2H, (2CHH)); ¹³C-NMR (75MHz, CDCl₃) δ148.50, 147.31, 133.30, 132.86, 132.43, 129.73, 128.80, 128.17, 127.91, 126.87, 126.44, 123.80, 120.10, 119.43, 118.95, 66.05, 58.25 ppm; FT-IR (ATR) 2936, 1605, 1495, 1433, 1338, 1230, 1213, 1112, 1035, 965, 937, 824, 782, 759 cm⁻¹; *m/z* [CI] M+H (found) 609.2, (calc): 609.3. HRMS (NSI) Calcd for C₃₉H₂₉N₈, M+H, 609.2510; Found 609.2505.

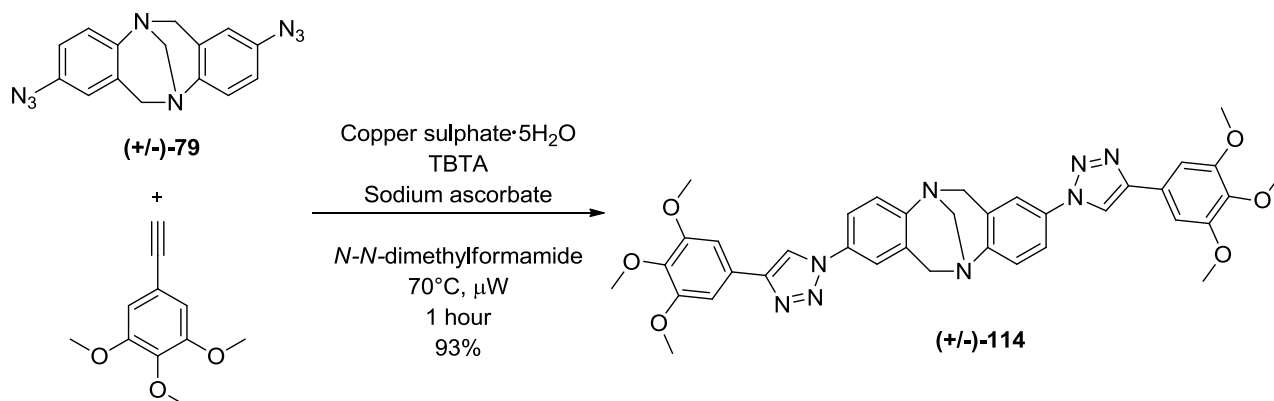
**2, 8 bis -4-(anthracen-9-yl) -1H-1,2,3-triazole-6H, 12H-5, 11-methanodibenzo[b,f]
[1,5]diazocine (+/-)-113**



(+/-)-**113** (52 mg, 0.07 mmol, 74%) Purified by flash chromatography on silica eluting with diethyl ether to afford a red solid. *R_f* 0.6 (diethyl ether) MP :256-259°C (diethyl ether); ¹H-NMR (400MHz, CDCl₃) δ8.53 (s, 2H, 2CH), 8.10 (s,2H, ArH), 8.02 (d, *J*8.4 Hz, 4H, ArH), 7.84 (dd, *J*0.9, 8.7 Hz, 4H, ArH), 7.65 (dd, *J*2.5, 8.6 Hz, 2H, ArH), 7.5 (d, *J*2.5 Hz, 2H, ArH), 7.44 (m, 4H, ArH), 7.38 (m, 4H, ArH), 7.33 (d, *J*8.7 Hz, 2H, ArH), 4.82 (d, *J*17.0Hz, 2H, 2(CHH)), 4.41 (s, 2H, CH₂), 4.33 (d, *J*17.0 Hz, 2H, (2CHH)); ¹³C-NMR (75MHz, CDCl₃) δ148.58, 144.83, 133.32,

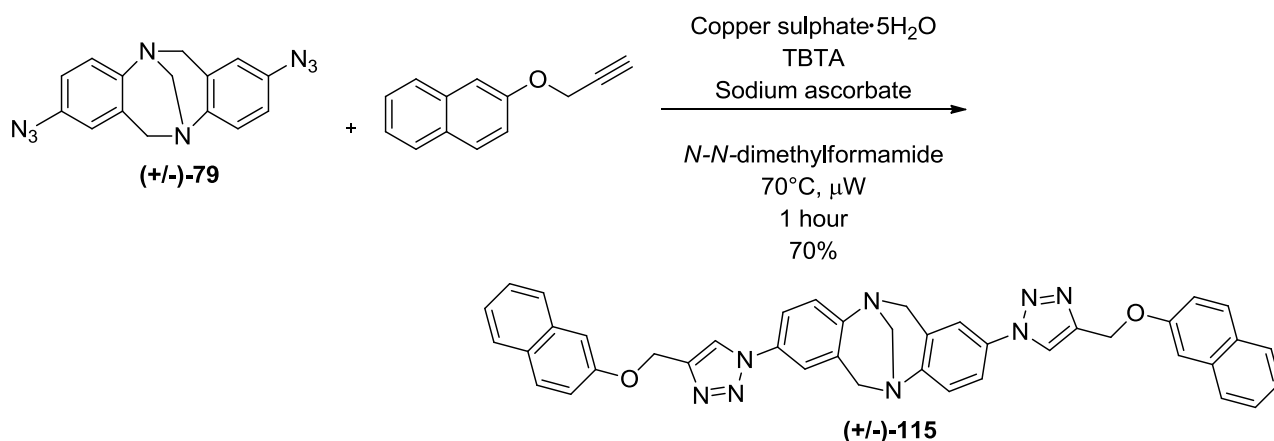
131.48, 131.46, 129.49, 128.74, 126.61, 126.45, 126.03, 125.49, 124.16, 122.90, 120.16, 119.55, 67.12, 59.15 ppm; FT-IR (KBr neat), 3049, 2970, 2949, 2241, 1739, 1498, 1365, 1227, 1217, 1046, 920, 734 cm^{-1} ; m/z [CI] M+H (found) 709.3, (calc): 709.3. HRMS (NSI) Calcd for $\text{C}_{47}\text{H}_{33}\text{N}_8\text{O}_4$, M+H, 709.2823; Found 709.2820.

2,8-bis(4-(3,4,5-trimethoxyphenyl)-1H-1,2,3-triazol-1-yl)-6,12-dihydro-5,11-methanodibenzo [b,f][1,5]diazocine (+/-)-114



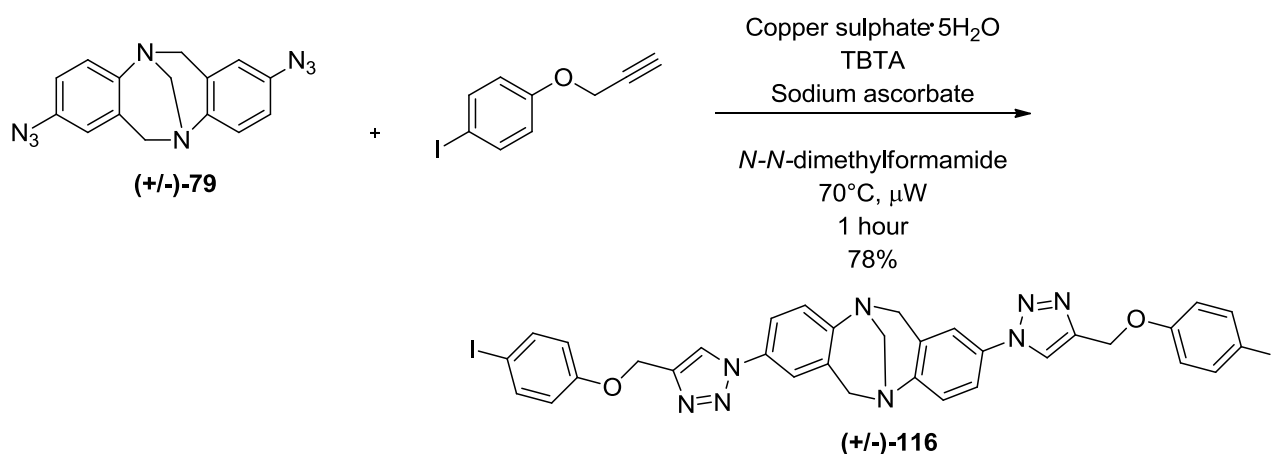
(+/-)-**114** (21 mg, 0.03 mmol, 93%) Purified by flash chromatography on silica eluting with 1:1 ethyl acetate : petroleum ether to afford an off white solid. R_f 0.5 (1:1 ethyl acetate : petroleum ether) MP : 170-172 °C (hexane); $^1\text{H-NMR}$ (300MHz, CDCl_3) δ 8.06 (s, 2H, 2(CH)), 7.55 (dd, J 2.5, 8.7 Hz, 2H, ArH), 7.42 (d, J 2.3 Hz, 2H, ArH), 7.30 (d, J 8.7 Hz, 2H, ArH), 7.09 (s, 4H, ArH), 4.81 (d, J 17.0 Hz, 2H, 2(CHH)), 4.39 (s, 2H, CH_2), 4.30 (d, J 17.0 Hz, 2H, 2(CHH)), 3.91(s, 12H, 4(CH_3)), 3.87 (s, 6H, 2(CH_3)); $^{13}\text{C-NMR}$ (75MHz, CDCl_3) δ 153.86, 148.54, 148.39, 138.40, 133.20, 129.36, 126.49, 125.92, 120.16, 119.53, 117.61, 103.02, 61.20, 59.02, 56.42 ppm; FT-IR (KBr neat) 3133, 2935, 2840, 1589, 1495, 1352, 1239, 1125, 1046, 1003, 863, 735 cm^{-1} ; m/z [ES]⁺ M+Na (found) 711.5, (calc): 711.7. HRMS (NSI) Calcd for $\text{C}_{37}\text{H}_{37}\text{N}_8\text{O}_6$, M+H, 689.2831; Found 689.2826.

2, 8 bis -4-((naphthalen-2-yloxy)methyl)-1H-1,2,3-triazole -6H, 12H-5, 11-methanodibenzo [b,f][1,5]diazocine (+/-)-115



(+/-)-115 (75 mg, 0.11 mmol, 70%) Purified by flash chromatography on silica eluting with 1:1 ethyl acetate : petroleum ether to afford yellow solid. *R_f* 0.5 (1:1 ethyl acetate : petroleum ether) MP : 162-164°C (hexane); ¹H-NMR (300MHz, CDCl₃) 7.95 (s, 2H, 2(CH)), 7.75 (m, 6H, ArH), 7.46 (ddd, *J*4.6, 8.4, 13.4 Hz, 4H, ArH), 7.35 (m, 4H, ArH), 7.26 (d, *J*8.6 Hz, 4H, ArH), 7.18 (dd, *J*2.6, 8.9 Hz, 2H, ArH), 5.37(s, 4H, 2(CH₂)), 4.76 (d, *J*17.0, 2H, 2(CHH)), 4.35 (s, 2H, CH₂), 4.24 (d, *J*17.0Hz, 2H, (CHH)); ¹³C-NMR (75MHz, CDCl₃) δ156.10, 148.44, 144.88, 134.42, 133.03, 129.69, 129.23, 129.15, 127.69, 126.96, 126.58, 126.34, 124.02, 120.93, 120.11, 119.47, 118.74, 107.19, 66.69, 61.92, 58.67 ppm; FT-IR (KBr neat) 3853, 3744, 3649, 3056, 2923, 2322, 1627, 1599, 1500, 1257, 1214, 1179, 1119, 1013, 836, 735 cm⁻¹; *m/z* [ES]⁺ M+1 (found) 669.2, (calc): 669.3. HRMS (NSI) Calcd for C₄₁H₃₃N₈O₂, M+H, 669.2721; Found 669.2719.

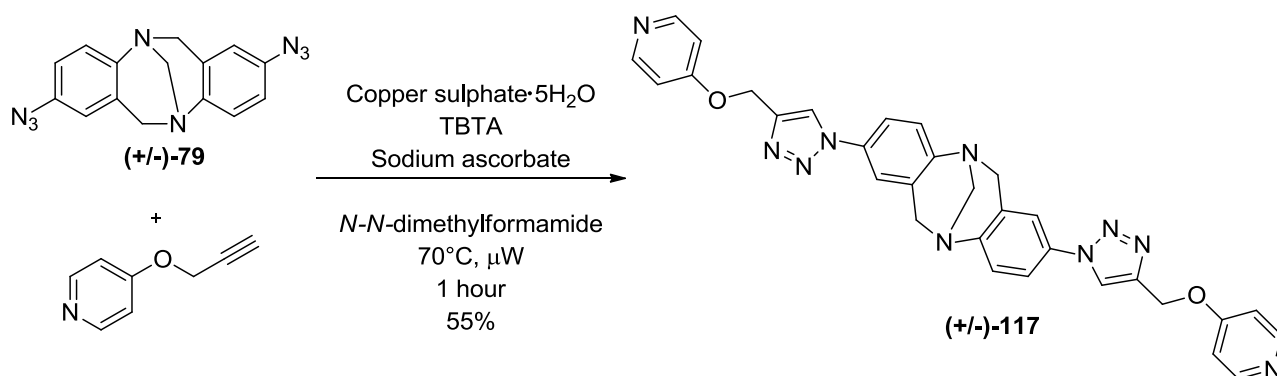
2, 8 bis (4-((4-iodophenoxy)methyl)-1H-1,2,3-triazole-6H), 12H-5, 11-methanodibenzo [b,f][1,5]diazocine (+/-)-116



(+/-)-116 (42 mg, 0.05 mmol, 78%) Precipitated from dichloromethane with diethyl ether to afford a white solid. *R_f* 0.4 (1:1 ethyl acetate : petroleum ether), MP : 224-226°C (diethyl ether); ¹H-NMR (400MHz, CDCl₃) δ7.88 (s, 2H, 2(CH)), 7.53 (m, 4H, ArH), 7.47 (dd, *J*2.5, 8.7 Hz, 2H, ArH), 7.34 (d, *J*2.4 Hz, 2H, ArH), 7.29 (d, *J*8.7 Hz, 2H, ArH), 6.74 (m, 4H, ArH), 5.19 (s, 4H, 2(CH₂)), 4.78

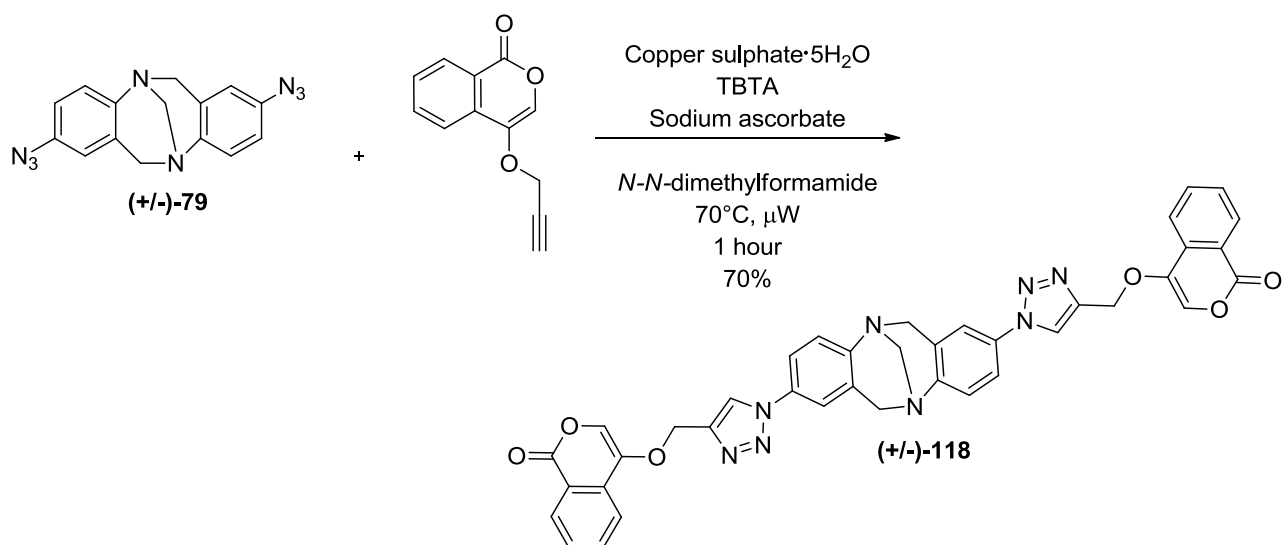
(d, J 17.0 Hz, 2H, 2(CHH)), 4.37 (s, 2H, CH₂), 4.26 (d, J 17.0 Hz, 2H, 2(CHH)); ¹³C-NMR (75 MHz, CDCl₃) δ 158.05, 144.58, 138.43, 133.28, 128.94, 126.39, 120.88, 120.21, 119.63, 119.51, 117.19, 83.57, 66.70, 61.91, 58.57 ppm; ATR-IR 2158, 1571, 1497, 1483, 1401, 1329, 1235, 1208, 1178, 1047, 995, 821, 804 cm⁻¹; m/z [ES]⁺ M+H (found) 821.1, (calc): 821.0. HRMS (NSI) Calcd for C₃₃H₂₇I₂N₈O₂, M+H, 821.0341; Found 821.0339.

2, 8 bis-4-((1H-1,2,3-triazol-4-yl)methoxy)pyridine-6H, 12H-5, 11-methanodibenzo[b,f][1,5] diazocine (+/-)-117



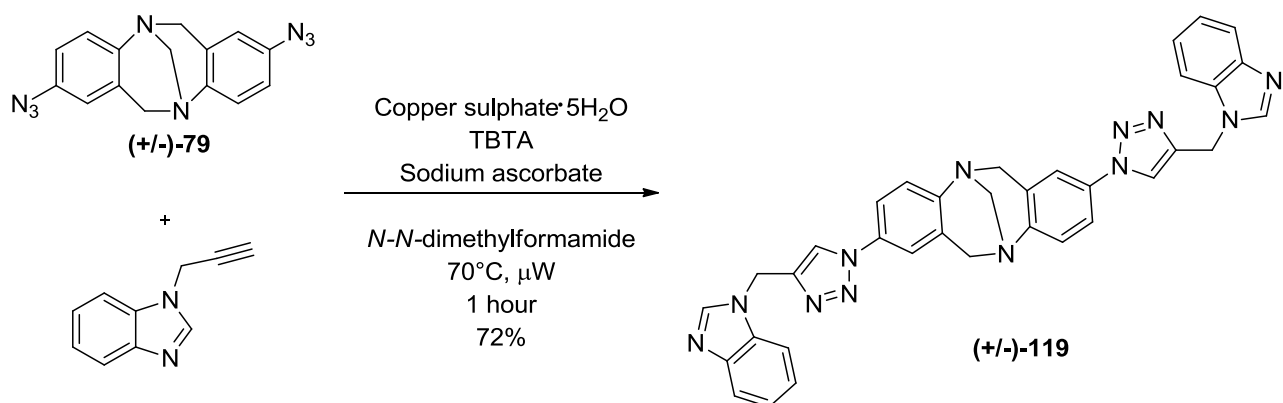
(+/-)-**117** (83 mg, 0.15 mmol, 55%) Purified by flash chromatography on silica eluting with 5-20% methanol in dichloromethane affording an off white solid. R_f 0.5 (20% methanol in dichloromethane), MP : <300°C (methanol); ¹H-NMR (300 MHz, DMSO) δ 8.66 (s, 2H, 2CH), 7.73 (d, J 7.6 Hz, 4H, ArH), 7.62 (dd, J 8.6, 2.4 Hz, 2H, ArH), 7.49 (d, J 2.3 Hz, 2H, ArH), 7.33 (d, J 8.7 Hz, 2H, ArH), 6.08 (d, J 7.6 Hz, 4H, ArH), 5.20 (s, 4H, 2CH₂), 4.72 (d, J 16.9 Hz, 2H, 2CHH), 4.27 (d, J 20.6 Hz, 4H, 2CHH, CH₂). ¹³C-NMR (75 MHz, DMSO) δ 177.52, 148.56, 143.48, 141.12, 132.16, 129.67, 126.34, 126.16, 122.47, 122.15, 119.63, 119.31, 119.14, 117.80, 65.96, 58.33, 49.82 ppm; FT-IR (KBr neat) 1635, 1540, 1182, 1101, 616 cm⁻¹; m/z [CI] M+H (found) 571.3, (calc): 571.2. HRMS (NSI) Calcd for C₃₁H₂₇N₁₀O₂, M+H, 571.2313; Found 571.2306.

2, 8 bis -(4-((1H-1,2,3-triazol-4-yl)methoxy)-2H-chromen-2-one) 6H, 12H-5, 11-methano-dibenzo[b,f][1,5]diazocine (+/-)-118



(+/-)-**118** (40 mg, 0.06 mmol, 86%) Purified by flash chromatography on silica eluting with 1 : 1 ethyl acetate : petroleum ether to afford a white solid. *R_f* 0.6 (1 : 1 ethyl acetate : petroleum ether), MP : decomposed 245°C (hexane); ¹H-NMR (400MHz, CDCl₃) δ 7.98 (s, 2H), 7.70 (dd, *J*1.6, 7.9 Hz, 2H), 7.52-7.42 (m, 4H), 7.33 (d, *J*2.3 Hz, 2H), 7.26 (d, *J*8.7 Hz, 2H), 7.23 (m, 2H), 7.16 (m, 2H), 5.79 (s, 2H), 5.32 (s, 4H), 4.75 (d, *J*17.0Hz, 2H), 4.33 (s, 2H), 4.24 (d, *J*17.0Hz, 2H); ¹³C-NMR (75MHz, CDCl₃) δ 165.00, 162.61, 153.43, 148.57, 142.17, 132.88, 132.67, 129.23, 126.46, 123.97, 123.12, 121.66, 120.24, 119.66, 116.8, 115.41, 91.24, 66.72, 62.48, 58.68 ppm; FT-IR (KBr neat) 3442, 3089, 2949, 2245, 1712 C=O, 1621, 1565, 1500, 1238, 1106, 1048, 937, 730 cm⁻¹; *m/z* [ES]⁺ M+Na (found) 727.6, (calc): 727.7. HRMS (NSI) Calcd for C₃₉H₂₉N₈O₆, M+H, 705.2210; Found 705.2223.

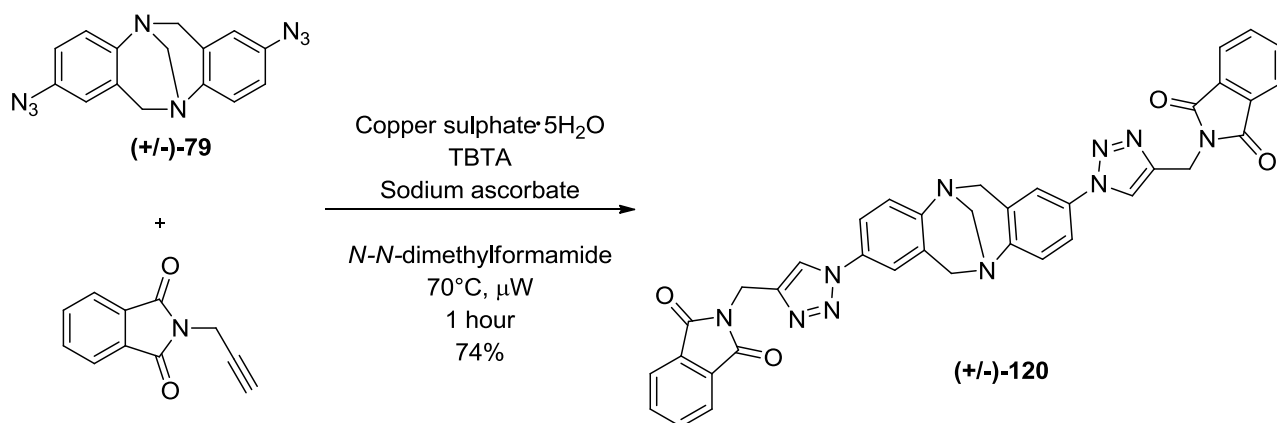
2, 8 bis (1-((1H-1,2,3-triazol-4-yl)methyl)-1H-benzo[d]imidazole)-6H, 12H-5, 11-methanodibenzo[b,f][1,5]diazocine (+/-)-119



(+/-)-**119** (51 mg, 0.08mmol, 72%) Purified by flash chromatography on silica eluting with 1 : 1 ethyl acetate : petroleum ether to afford a white solid. *R_f* 0.4 (1 : 1 ethyl acetate : petroleum ether).

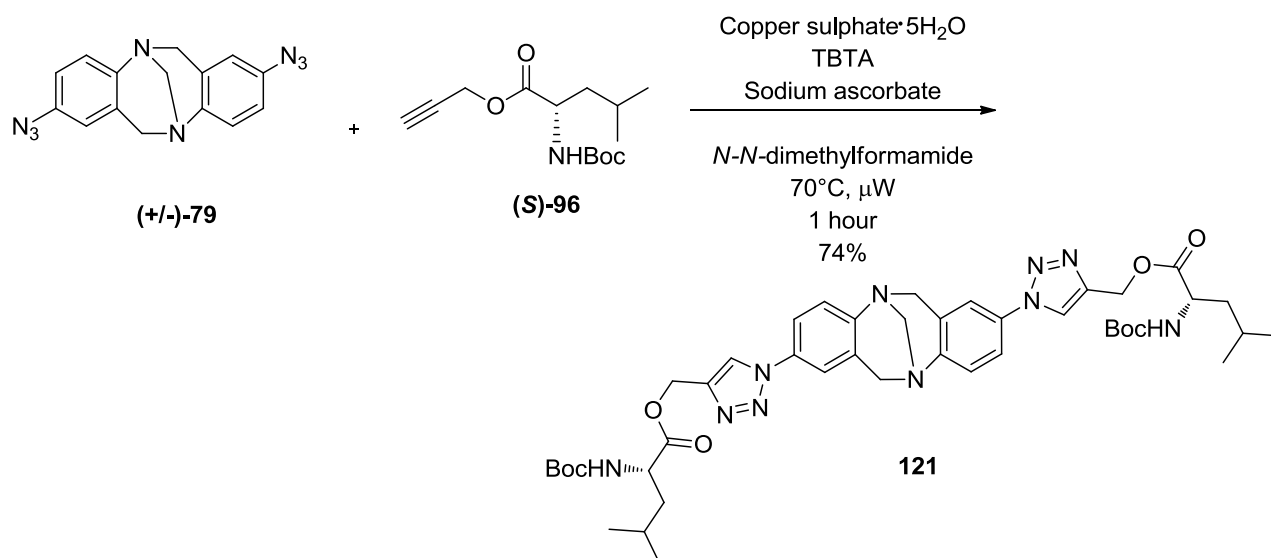
MP : Decomposed 210°C (diethyl ether); ¹H-NMR (300MHz, CDCl₃) δ8.02 (s, 2H, 2CH), 7.79 (d, *J*5.2 Hz, 2H, ArH), 7.57 (s, 2H, 2CH), 7.41 (d, *J*3.5 Hz, 2H, ArH), 7.36 (dd, *J*2.4, 8.7 Hz, 2H, ArH), 7.27 (dd, *J*2.9, 6.2 Hz, 4H, ArH), 7.19 (m, 4H, ArH) 5.52 (s, 4H, 2CH₂), 4.69 (d, *J*17.0 Hz, 2H, 2CHH), 4.29 (s, 2H, CH₂), 4.16 (d, *J*17.0 Hz, 2H, 2CHH); ¹³C-NMR (75MHz, DMSO) δ148.46, 143.19, 132.15, 129.59, 126.17, 123.11, 122.19, 119.53, 119.09, 79.26, 65.94, 58.11 ppm; FT-IR (ATR) 3200, 1673, 1410, 1177, 1103, 1078, 1045, 983 cm⁻¹; *m/z* [CI] M+H (found) 617.4, (calc): 617.3. HRMS (NSI) Calcd for C₃₅H₂₉N₁₂, M+H, 617.2633; Found 617.2624.

2, 8 bis -(2-((1H-1,2,3-triazol-4-yl)methyl)isoindoline-1,3-dione) -6H, 12H-5, 11-methanodibenzo[b,f][1,5]diazocine (+/-)-120



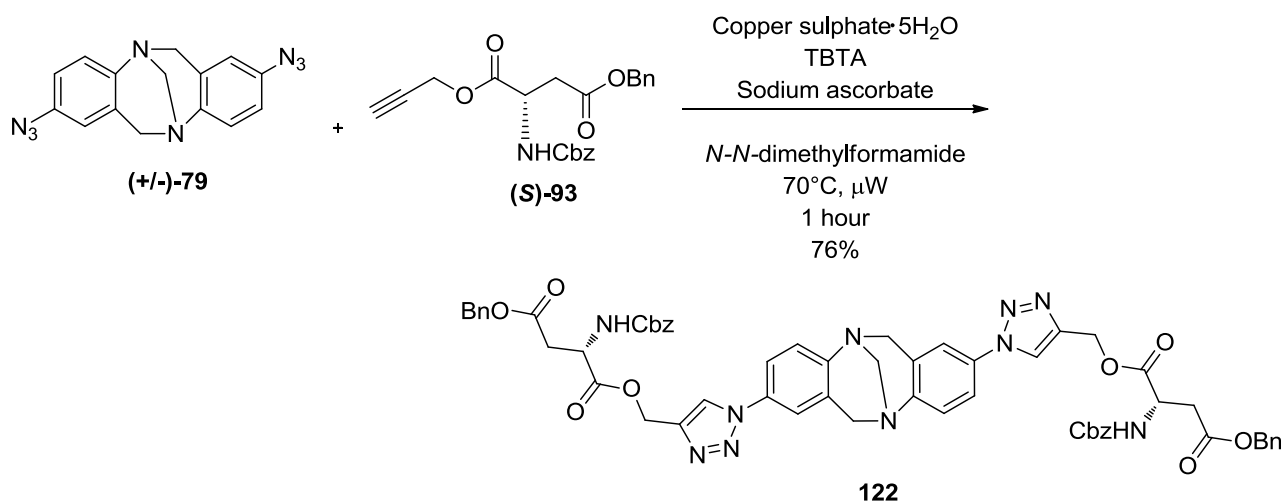
(+/-)-**120** (33 mg, 0.05 mmol, 74%) Purified by flash chromatography on silica eluting with 1 : 1 ethyl acetate : petroleum ether to afford a white solid. *R_f* 0.5 (1 : 1 ethyl acetate : petroleum ether), MP : 300+°C (hexane); ¹H-NMR (300MHz, CDCl₃) δ7.90 (s, 2H, 2CH), 7.84 (dd, *J*3.0, 5.5 Hz, 4H, ArH), 7.71 (dd, *J*3.1, 5.4 Hz, 4H, ArH), 7.44 (dd, *J*2.5, 8.6 Hz, 2H, ArH), 7.28 (d, *J*2.4 Hz, 2H, ArH), 7.23 (d, *J*8.7 Hz, 2H, ArH), 5.03 (s, 4H, 2CH₂), 4.74 (d, *J*16.8 Hz, 2H, 2CHH), 4.33 (s, 2H, CH₂), 4.22 (d, *J*16.9 Hz, 2H, 2CHH); ¹³C-NMR (75MHz, CDCl₃) 167.76, 148.32, 143.42, 134.22, 132.98, 132.02, 129.05, 126.26, 123.51, 121.23, 120.10, 119.43, 66.67, 58.62, 53.38, 52.85, 29.56 ppm; FT-IR (KBr neat) 2925, 1771 C=O, 1713 C=O, 1500, 1395, 1331, 1045, 939, 731, 713, 529 cm⁻¹; *m/z* [ES]⁺ M+Na (found) 697.2, (calc): 697.2. HRMS (NSI) Calcd for C₃₇H₂₇N₁₀O₄, M+H, 675.2211; Found 675.2207.

2, 8 bis-4-((S)-(1H-1,2,3-triazol-4-yl)methyl 2-(tert-butoxycarbonylamino)-4-methyl pentanoate)-6H, 12H-5, 11-methanodibenzo[b,f][1,5]diazocine 121



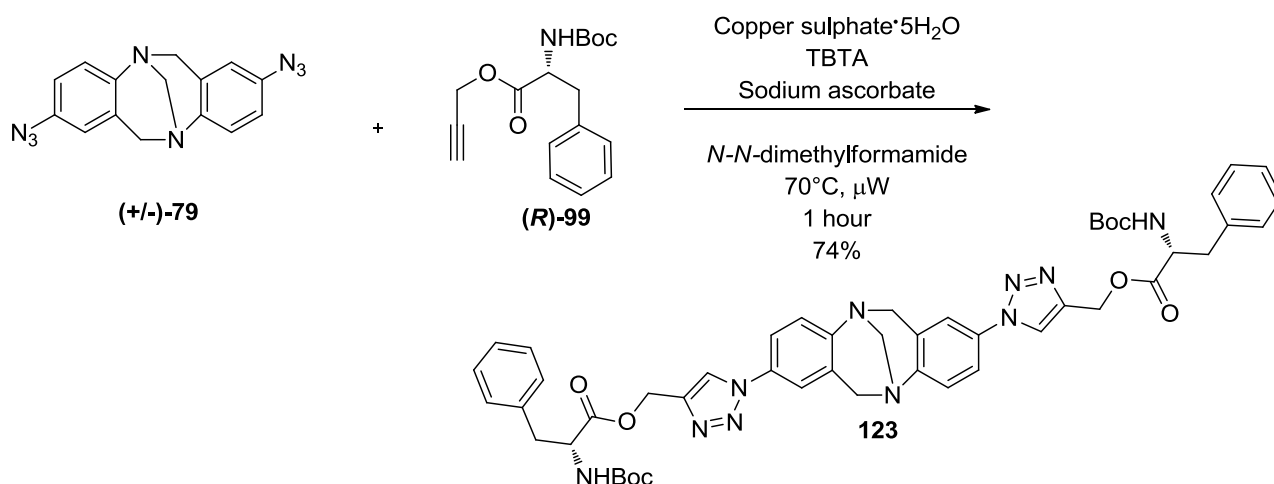
121 (100 mg, 0.12 mmol, 74%) Purified by flash chromatography on silica eluting with 1 : 1 ethyl acetate : petroleum ether to afford a white solid. *R_f* 0.6 (1 : 1 ethyl acetate : petroleum ether) MP : 92 - 94°C (hexane); ¹H-NMR (300MHz, CDCl₃) δ 7.97 (s, 2H, 2CH), 7.50(d, *J*8.7 Hz, 2H, ArH), 7.35 (s, 2H, ArH), 7.28 (d, *J*9.1 Hz, 2H, ArH), 5.32 (q, *J*12.9 Hz, 4H, 2CH₂), 4.87 (d, *J*8.3 Hz, 2H, 2NH), 4.78 (d, *J*16.9 Hz, 2H, CHH), 4.36 (s, 2H, CH₂), 4.28 (m, 3H, CHH, 2 α CH), 1.58 (m, 6H, 2 β CH₂, 2CH), 1.38 (s, 18H, (CH₃)₆), 0.89 (dd, *J*2.3, 6.4, 12H, (CH₃)₄); ¹³C-NMR (75MHz, CDCl₃) δ 173.69, 155.73, 148.57, 143.54, 133.09, 129.29, 126.49, 122.14, 120.19, 119.51, 80.18, 66.95, 58.95, 58.50, 52.41, 41.41, 28.48, 24.94, 23.05, 21.89 ppm; FT-IR (KBr neat) 3360, 3145, 2960, 1707 C=O, 1501, 1367, 1234, 1047, 756 cm⁻¹; *m/z* [ES]⁺ M+Na (found) 865.5, (calc): 865.43. HRMS (NSI) Calcd for C₄₃H₅₉N₁₀O₈, M+H, 843.4512; Found 843.4516. [α]_D²⁶ +10.5 (c 1.0, CHCl₃).

2, 8-bis-((S)-4-benzyl 1-(1H-1,2,3-triazol-4-yl)methyl 2-(benzyloxycarbonylamino)succinate)-6H, 12H-5, 11-methanodibenzo[b,f][1,5]diazocine 122



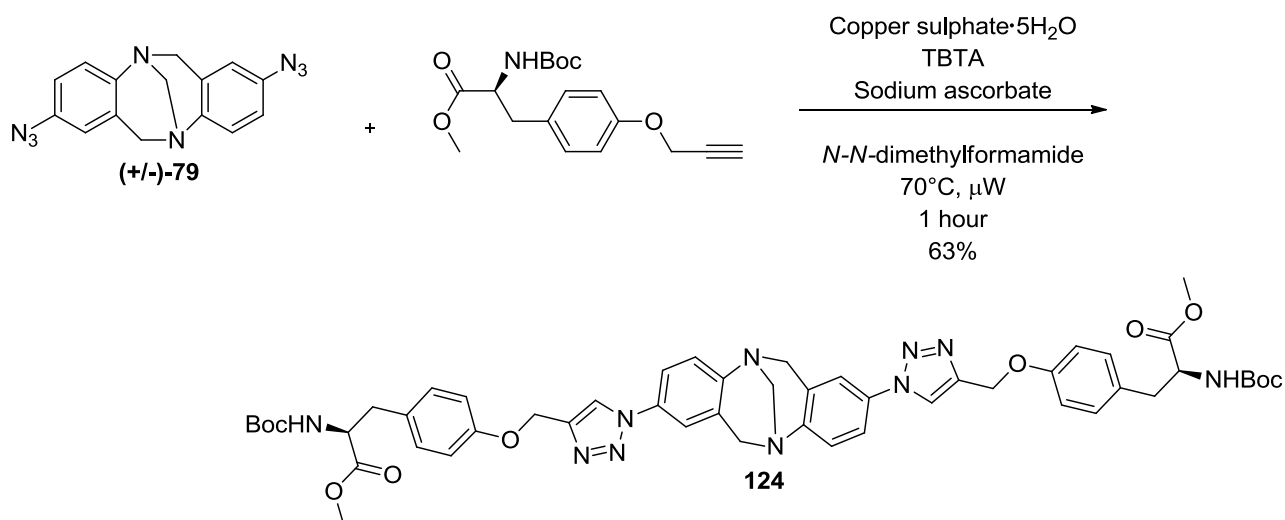
122 (19 mg, 0.02 mmol, 76%) Purified by flash chromatography on silica eluting with 8 : 2 ethyl acetate : dichloromethane affording a yellow solid. *R_f* 0.5 (8 : 2 ethyl acetate : dichloromethane), MP : 70-72 °C diethyl ether; ¹H-NMR (300MHz, CDCl₃) δ7.82 (s, 2H, 2CH), 7.40 (dt, *J*2.2, 9.1 Hz, 2H, ArH), 7.30-7.14 (m, 24H, ArH), 5.70 (d, *J*8.6 Hz, 2H, 2NH), 5.26 (s, 4H, 2CH₂), 5.03 (s, 4H, 2CH₂), 4.95 (d, *J*2.1 Hz, 4H, 2CH₂), 4.71 (d, *J*17.0 Hz, 2H, CHH), 4.60 (m, 2H, 2αCH), 4.29 (s, 2H, CH₂), 4.19 (d, *J*17.0Hz, 2H, CHH), 3.02 (dd, *J*4.4, 17.3 Hz, 2H, 2βCHH), 2.82 (dd, *J*4.5, 17.3 Hz, 2H, 2βCHH); ¹³C-NMR (75MHz, CDCl₃) δ170.87, 156.08, 148.59, 143.04, 136.15, 135.27, 133.05, 128.82, 128.76, 128.69, 128.48, 128.30, 126.48, 122.42, 120.22, 119.57, 67.40, 67.10, 59.05, 58.92, 50.54, 36.87 ppm; FT-IR (KBr neat) 3357, 2338, 1729 C=O, 1502, 1206, 1046, 753, 698 cm⁻¹; *m/z* [ES]⁺ M+Na (found) 1118.0, (calc): 1118.1. HRMS (NSI) Calcd for C₅₉H₅₅N₁₀O₁₂, M+H, 1095.3995; Found 1095.3979. [α]_D²⁶ +12.0 (c 1.0, CHCl₃).

2, 8 bis-((R)-(1H-1,2,3-triazol-4-yl)methyl 2-(tert-butoxycarbonylamino)-3-phenylpropanoate)-6H, 12H-5, 11-methanodibenzo[b,f][1,5]diazocine 123



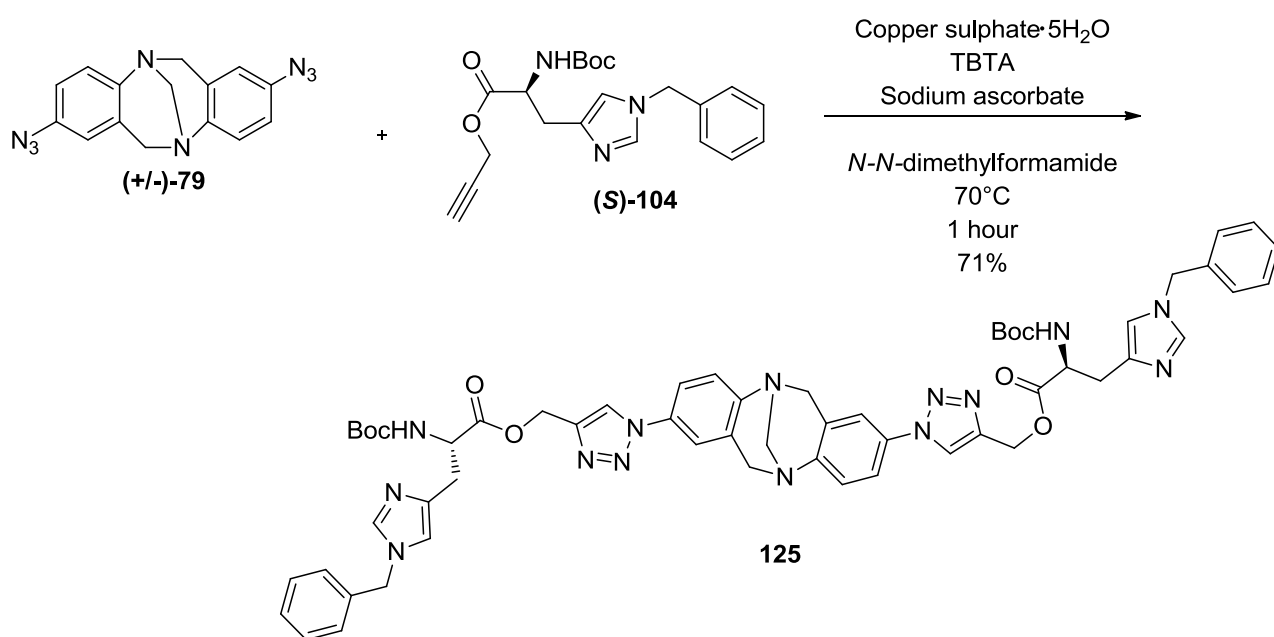
123 (44mg, 0.05 mmol, 74%) Purified by flash chromatography on silica gel eluting with 1-3% methanol in dichloromethane to afford a pale yellow solid. *R_f* 0.7 (3% methanol in dichloromethane), MP : 102-104°C (hexane); ¹H-NMR (300MHz, CDCl₃) δ7.82 (s, 2H), 7.48 (dt, *J*2.9, 8.6 Hz, 2H), 7.34 (t, *J*2.4 Hz, 2H), 7.30 (d, *J*8.7 Hz, 2H), 7.14 (m, 6H), 7.02 (m, 4H), 5.29 (d, *J*3.1 Hz, 4H), 5.00 (d, *J*8.1 Hz, 2H), 4.80 (d, *J*15.2 Hz, 2H), 4.57 (dd, *J*6.2, 14.0 Hz, 2H), 4.37 (s, 2H), 4.28 (d, *J*17.1 Hz, 2H), 3.05 (m, 4H), 1.38 (s, 18H); ¹³C-NMR (75MHz, CDCl₃) δ171.97, 155.21, 148.48, 143.09, 135.75, 132.92, 129.34, 129.17, 128.51, 127.04, 126.35, 122.25, 119.99, 119.37, 80.03, 66.69, 58.68, 58.28, 54.34, 37.89, 28.14 ppm; FT-IR (KBr neat) 3362, 2976, 2929, 1743C=O, 1706 C=O, 1500,1366, 1165, 1047, 733 cm⁻¹; *m/z* [ES]⁺ M+Na (found) 933.0, (calc): 933.4. HRMS (NSI) Calcd for C₄₉H₅₅N₁₀O₈, M+H, 911.4199; Found 911.4201. [α]_D²⁷ -38.8 (c 1.0, CHCl₃).

2, 8 bis-((*S*)-methyl 2-(*tert*-butoxycarbonylamino)-3-(4-((1*H*-1,2,3-triazol-4-yl)methoxy)phenyl)propanoate)-6*H*, 12*H*-5, 11-methanodibenzo[*b,f*][1,5]diazocine 124



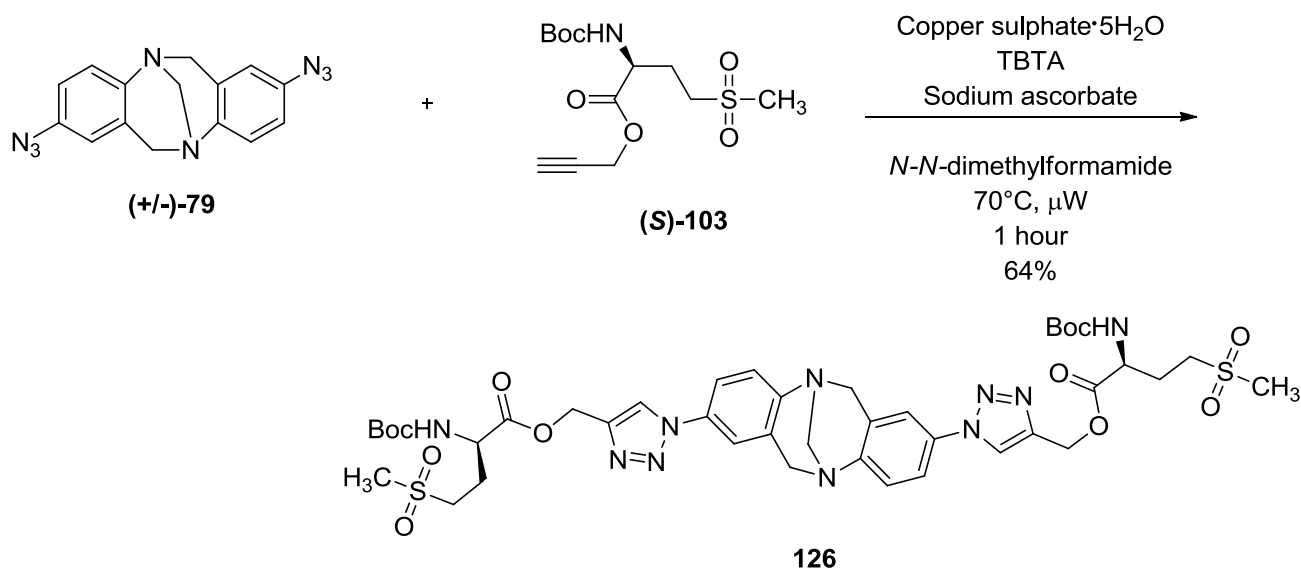
124 (50.3 mg, 0.052 mmol, 63 %) Purified by flash chromatography on silica gel eluting with 4 : 1 ethyl acetate : dichloromethane to afford a pale red solid. *R_f* 0.5 (4 : 1 ethyl acetate : dichloromethane), MP : 98-100°C (diethyl ether); ¹H-NMR (400MHz, CDCl₃) δ7.91 (s, 2H, 2CH), 7.48 (dd, *J*2.5, 8.6 Hz, 2H, 2ArH), 7.33 (d, *J*2.4 Hz, 2H, 2ArH), 7.27 (d, *J*8.7 Hz, 2H, 2ArH), 7.03 (d, *J*8.7 Hz, 4H, 4ArH), 6.90 (d, *J*8.7 Hz, 4H, 4ArH), 5.21 (s, 4H, 2CH₂), 4.99 (d, *J*8.4 Hz, 2H, 2NH), 4.76 (d, *J*16.9 Hz, 2H, CHH), 4.52 (dd, *J*6.1, 13.8 Hz, 2H, 2αCH), 4.35 (s, 2H, CH₂), 4.25 (d, *J*16.9 Hz, 2H, CHH), 3.69 (s, 6H, 2CH₃), 3.00 (m, 4H, 2βCH₂), 1.39 (s, 18H, 2(CH₃)₃); ¹³C-NMR (100MHz, CDCl₃) δ172.49, 157.31, 148.33, 144.95, 133.08, 130.47, 129.11, 128.80, 126.35, 120.88, 120.10, 119.44, 114.83, 79.89, 66.66, 61.90, 58.64, 54.41, 53.37, 52.15, 37.35, 28.16 ppm; FT-IR (KBr neat) 3363, 3144, 2977, 2953, 2930, 2250, 1742 C=O, 1705 C=O, 1611, 1505, 1439, 1366, 1241, 1166, 1046, 1016, 731 cm⁻¹; *m/z* [CI] M+H -2boc (found) 771.4, (calc): 771.3. HRMS (NSI) Calcd for C₅₁H₅₉N₁₀O₁₀, M+H, 971.4410; Found 971.4421. [α]²⁷_D +26.4 (c 1.0, CHCl₃).

2, 8 bis-((S)-(1H-1,2,3-triazol-4-yl)methyl 3-(1-benzyl-1H-imidazol-4-yl)-2-(tert-butoxycarbonylamino)propanoate)-6H, 12H-5, 11-methanodibenzo [b,f][1,5]diazocine 125



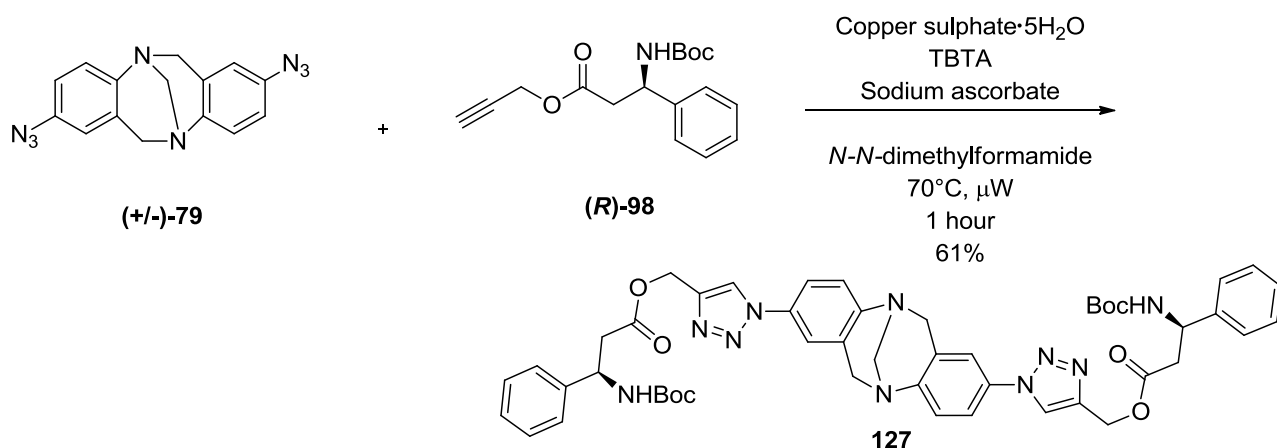
125 (62 mg, 0.06 mmol, 71%) Purified by flash chromatography on silica eluting with 1-3% methanol in dichloromethane to afford a yellow solid. *R_f* 0.8 (3% methanol in dichloromethane) MP : 96-98°C (diethyl ether); ¹H-NMR (300MHz, CDCl₃) δ7.99 (d, *J*3.9 Hz, 2H, ArH), 7.50 (d, *J*8.6 Hz, 2H, ArH), 7.42-7.18 (m, 12H, ArH), 7.02 (d, *J*3.8 Hz, 2H, ArH), 6.56 (s, br, 2H), 6.05 (s, br, 2H), 5.24 (m, 4H, 2CH₂), 4.89 (d, *J*11.0 Hz, 4H, 2CH₂), 4.75 (d, *J*16.8 Hz, 2H, CHH), 4.52 (s, br, 2H, αCH), 4.34 (s, 2H, CH₂), 4.24 (d, *J*16.8 Hz, 2H, CHH), 2.98 (s, br, 4H, 2βCH₂), 1.39 (s, 18H, 2(CH₃)₃); ¹³C-NMR (100MHz, CDCl₃) δ172.23, 155.88, 148.52, 143.76, 136.11, 133.08, 129.29, 129.12, 128.45, 127.38, 126.48, 122.20, 120.00, 119.25, 79.82, 77.59, 77.28, 76.96, 66.96, 58.94, 58.42, 53.88, 53.66, 50.94, 30.17, 28.52 ppm; FT-IR (ATR) 2937, 2490, 2159, 2029, 1976, 1738 C=O, 1500, 1436, 1367, 1212, 1135, 1040, 974, 729 cm⁻¹; *m/z* [ES]⁺ M+H (found) 1071.6, (calc): 1071.5. HRMS (NSI) Calcd for C₅₇H₆₃N₁₄O₈, M+H, 1071.4948; Found 1071.4936. [α]_D²³ +5.0 (c 1.0, CHCl₃).

2, 8 bis-((S)-(1H-1,2,3-triazol-4-yl)methyl 2-(tert-butoxycarbonylamino)-4-(methylsulfonyl)butanoate)-6H, 12H-5, 11-methanodibenzo[b,f][1,5] diazocine 126



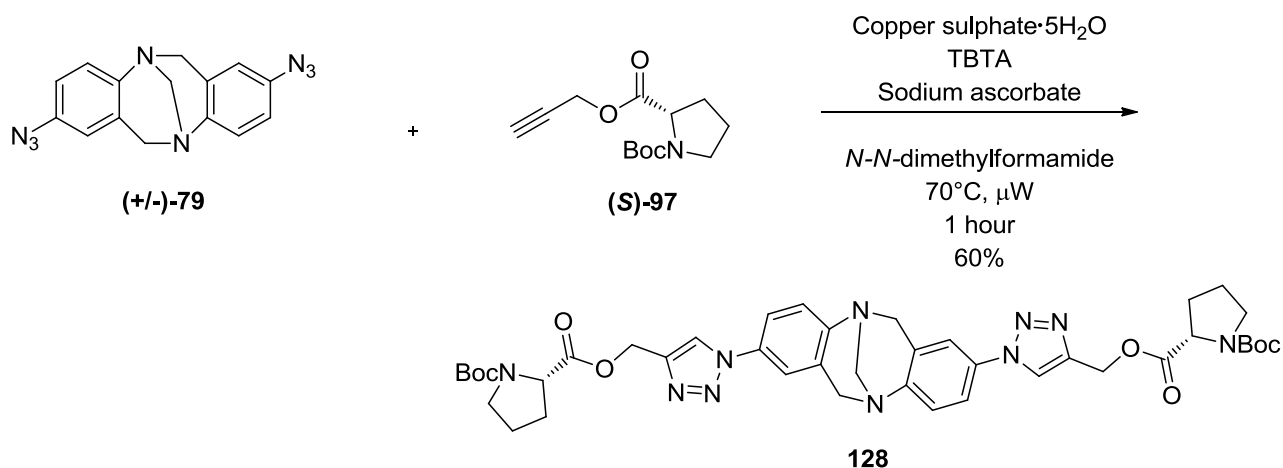
126 (14 mg, 0.02 mmol, 64%) yellow solid. Purified by flash chromatography on silica eluting with 2-5% methanol in dichloromethane. *R_f* 0.8 (5% methanol in dichloromethane). MP : 154-156°C (diethyl ether); ¹H-NMR (300MHz, CDCl₃) δ 7.96 (s, 2H, ArH), 7.50 (dt, *J*2.8, 8.4 Hz, 2H, ArH), 7.35 (t, *J*2.5 Hz, 2H, ArH), 7.29 (d, *J*8.7 Hz, 2H, ArH), 5.36 (dd, *J*12.8 Hz, 4H, 2CH₂), 5.25 (d, *J*7.8 Hz, 2H, 2NH), 4.79 (d, *J*16.9 Hz, 2H, CHH), 4.41 (m, 4H, CH₂, 2 α CH), 4.28 (d, *J*16.9 Hz, 2H, CHH), 3.21 – 2.94 (m, 4H, 2 β CH₂), 2.89 (s, 6H, 2CH₃), 2.47 – 2.27 (m, 2H, CH₂), 2.27 – 2.07 (m, 2H, CH₂), 1.41 (s, 18H, 2(CH₃)₃); ¹³C-NMR (75MHz, CDCl₃) δ 171.24, 155.52, 148.72, 142.75, 132.93, 126.36, 126.55, 122.35, 120.31, 119.77, 94.62, 80.88, 66.97, 58.97, 58.49, 52.22, 51.04, 40.98, 28.44, 25.61 ppm; FT-IR (KBr neat) 2367, 1750, 1710 C=O, 1676 C=O, 1636, 1508, 1367 O=S=O, 1299, 1164, 1050, 764 cm⁻¹; *m/z* [CI]⁺ M+H -2Boc (found)743.3, (calc): 743.2. HRMS (NSI) Calcd for C₄₁H₅₅N₁₀O₁₂S₂, M+H, 943.3437; Found 943.3437. [α]_D²⁷ +4.6 (c 1.0, CHCl₃).

2, 8-bis-((*R*)-(1*H*-1,2,3-triazol-4-yl)methyl 3-(*tert*-butoxycarbonylamino)-3-phenylpropanoate)-6*H*, 12*H*-5, 11-methanodibenzo[*b,f*][1,5]diazocine 127



127 (18 mg, 0.02 mmol, 61%) white solid. Purified by flash chromatography on silica gel eluting with 1 – 3% methanol in dichloromethane. *R_f* 0.8 (3% methanol in dichloromethane) MP : 90-92°C (diethyl ether); ¹H-NMR (300MHz, CDCl₃) 7.72 (s, 2H, ArH), 7.46 (dd, *J*2.4, 8.6 Hz, 2H, ArH), 7.30 (m, 2H, ArH), 7.23 (d, *J*4.4 Hz, 8H, ArH), 7.13 (dd, *J*4.6, 8.9 Hz, 2H, ArH), 5.29 (s, 2H, 2NH), 5.21 (s, 4H, 2CH₂), 5.10 (s, br, 2H, 2 α CH), 4.80 (d, *J*16.9 Hz, 2H, *CHH*), 4.38 (s, 2H, CH₂), 4.28 (d, *J*16.9 Hz, 2H, *CHH*), 2.86 (m, 4H, 2 β CH₂), 1.38 (s, 18H, 2(CH₃)₃); ¹³C-NMR (75MHz, CDCl₃) δ 170.91, 155.17, 148.61, 143.45, 133.06, 129.28, 128.79, 127.75, 126.45, 126.35, 122.04, 120.23, 119.57, 67.00, 58.98, 58.03, 41.04, 28.50 ppm; FT-IR (KBr neat) 3340, 2976, 2928, 2247, 1704 C=O, 1506, 1366, 1239, 1164, 1046, 732 cm⁻¹; *m/z* [ES]⁺ M+H (found) 911.4, (calc): 911.3. HRMS (NSI) Calcd for C₄₉H₅₅N₁₀O₈, M+H, 911.4199; Found 911.4201. [α]_D²⁷ +11.0 (c 1.0, CHCl₃).

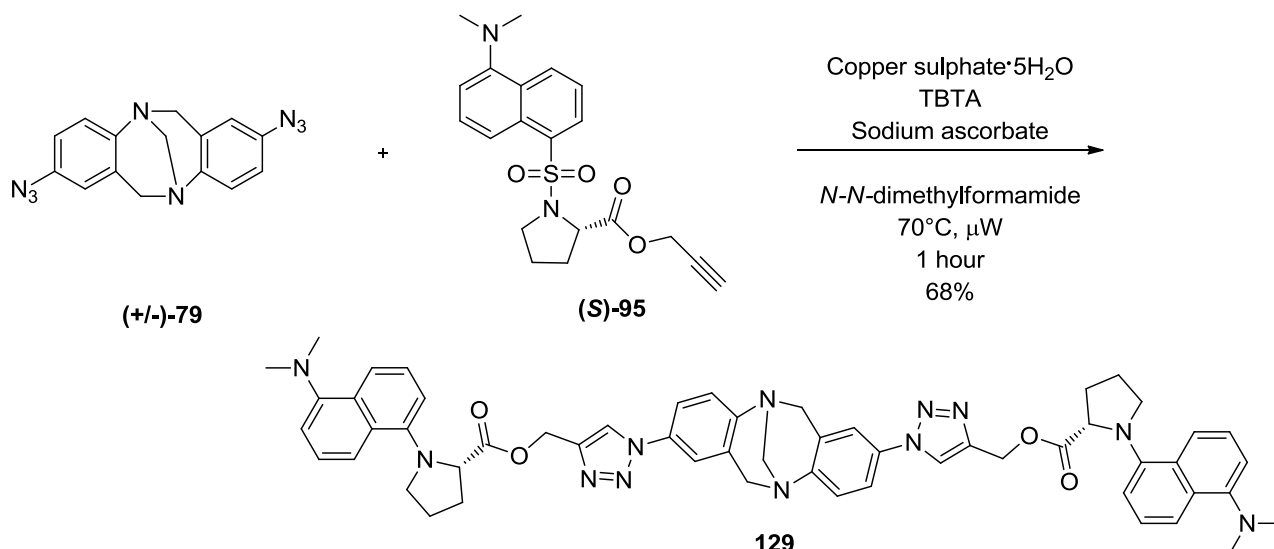
2, 8-bis-((*S*)-1-*tert*-butyl 2-(1*H*-1,2,3-triazol-4-yl)methyl pyrrolidine-1,2-dicarboxylate)-6*H*, 12*H*-5, 11-methanodibenzo[*b,f*][1,5]diazocine 128



128 (32 mg, 0.07 mmol, 60%) white solid. Purified by flash chromatography on silica eluting with

3 : 2, ethyl acetate : petroleum ether. *R_f* 0.6 (3 : 2, ethyl acetate : petroleum ether) MP : 100-102°C (diethyl ether); ¹H-NMR (300MHz, CDCl₃) δ8.08 (s, 1H, ArH), 7.94 (s, 1H, ArH), 7.51 (m, 2H, ArH), 7.35 (m, 2H, ArH), 7.27 (m, 2H, ArH), 5.35 (d, *J*3.5 Hz, 2H, CH₂), 5.28 (s, 2H, CH₂), 4.78 (d, *J*16.7 Hz, 2H, CHH), 4.36(s, 2H, CH₂), 4.31 (dd, *J*3.4, 8.6 Hz, 2H, CH₂). 4.22 (m, 2H, CHH), 3.44 (m, 4H, 2CH₂), 2.19 (m, 2H, CHH), 1.87 (m, 6H, 2CH₂, CHH), 1.41 (d, *J*4.9 Hz, 9H, 3(CH₃)), 1.28 (s, 9H, 3(CH₃)); ¹³C-NMR (75MHz, CDCl₃) δ173.4, 173.2, 154.6, 153.7, 148.1, 143.9, 143.2, 133.1, 132.8, 129.2, 128.9, 126.3, 126.2, 122.2, 121.8, 119.9, 119.3, 119.1, 79.8, 66.6, 58.8, 58.6, 58.2, 57.8, 53.3, 46.5, 46.2, 30.6, 30.1, 29.7, 29.5, 28.2, 28.0, 24.2, 23.4 ppm; FT-IR (KBr neat) 3483, 3139, 2974, 2927, 2247, 1748 C=O, 1692 C=O, 1500, 1401, 1366, 1159, 1124, 73 cm⁻¹; *m/z* [ES]⁺ M+Na (found) 833.4, (calc): 833.4. HRMS (NSI) Calcd for C₄₁H₅₁N₁₀O₈, 811.3886; M+H, Found 811.3892. [α]_D²⁶ -13.3 (c 1.0, CHCl₃).

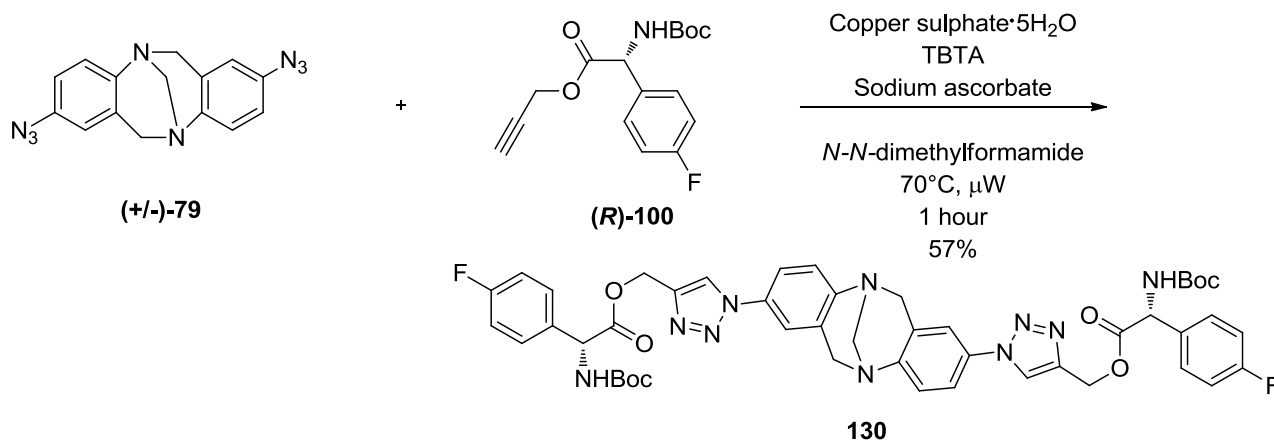
2, 8 bis -((S)-(1H-1,2,3-triazol-4-yl)methyl 1-(5-(dimethylamino)naphthalen-1-ylsulfonyl)pyrrolidine-2-carboxylate)-6H, 12H-5, 11-methanodibenzo[b,f][1,5]diazocine129



129 (12 mg, 0.01 mmol, 68%) yellow solid. Purified by flash chromatography on silica gel eluting with ethyl acetate. *R_f* 0.7 (ethyl acetate). MP : 98-100°C (diethyl-ether); ¹H-NMR (300MHz, CDCl₃) δ8.46 (dd, *J*8.4 Hz, 4H, ArH), 8.20 (dd, *J*1.2, 7.4 Hz, 2H, ArH), 7.97 (d, *J*1.6 Hz, 2H, ArH), 7.49 (m, 6H, ArH), 7.31 (d, *J*2.4 Hz, 2H, ArH), 7.23 (d, *J*6.9 Hz, 2H, ArH), 7.13 (d, *J*7.6 Hz, 2H, ArH), 5.22 (q, *J*12.9 Hz, 4H, 2CH₂), 4.74 (d, *J*16.6 Hz, 2H, 2CHH), 4.50 (d, *J*5.9 Hz, 2H, 2 α CH), 4.33 (s, 2H, CH₂), 4.22 (d, *J*16.8 Hz, 2H, 2CHH), 3.43 (m, 4H, 2CH₂), 2.83 (s, 12H, 4(CH₃)), 2.17-1.71 (m, 8H, 4(CH₂)); ¹³C-NMR (100MHz, CDCl₃) δ172.24, 148.52, 143.50, 134.41, 133.10, 130.82, 130.46, 130.13, 130.07, 129.23, 128.35, 126.50, 123.37, 122.03, 120.16, 119.66, 119.44, 115.44, 77.42, 66.96, 60.36, 58.92, 58.79, 48.69, 45.58, 31.15, 24.95 ppm; FT-IR (KBr neat) 2947, 1653C=O, 1571, 1500, 1404, 1329 O=S=O, 1142, 1075, 1046, 791, 731 cm⁻¹; *m/z* [ES]⁺ M+H

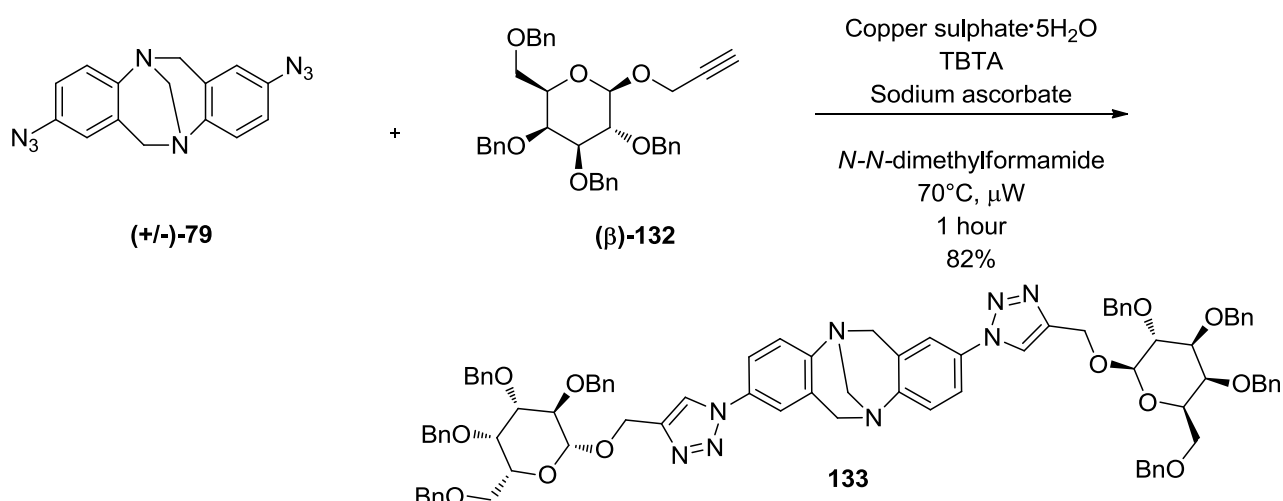
(found) 1077.5, (calc): 1077.4. HRMS (NSI) Calcd for C₅₅H₅₇N₁₂O₈S₂, M+H, 1077.3858; Found 1077.3859. $[\alpha]_D^{27}$ -22.2 (c 1.0, CHCl₃).

2, 8 bis-((R)-(1H-1,2,3-triazol-4-yl)methyl 2-(tert-butoxycarbonylamino)-2-(4-fluorophenyl) acetate)-6H, 12H-5, 11-methandibenzo[b,f] [1,5]diazocine 130



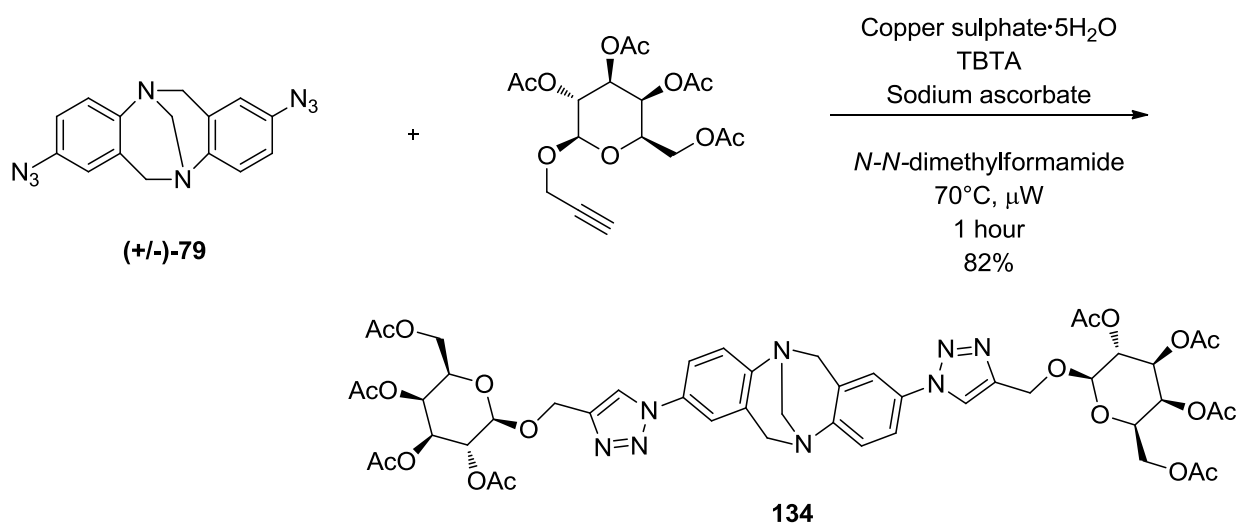
130 (12 mg, 0.01 mmol, 57%) off white solid. Purified by flash chromatography eluting with 1 : 1 ethyl acetate : petroleum ether. *R_f* 0.5 (1 : 1 ethyl acetate : petroleum ether). MP : 88-90°C (diethyl ether); ¹H-NMR (300MHz, CDCl₃) δ 7.73 (s, 2H, ArH), 7.45 (d, *J*9.1 Hz, 2H, ArH), 7.36-7.26 (m, 8H, ArH), 7.00 (t, *J*8.6 Hz, 4H, ArH), 5.49 (d, *J*6.3 Hz, 2H, 2NH), 5.32 (m, 6H, 2 α CH, 2CH₂), 4.79 (d, *J*16.7 Hz, 2H, CHH), 4.37 (s, 2H, CH₂), 4.27 (d, *J*17.0 Hz, 2H, CHH), 1.40 (s, 18H, 2(CH₃)₃); ¹³C-NMR (75MHz, CDCl₃) δ 171.00, (C-F resonance too small to observe), 148.69, 143.21, 133.01, 129.2 (d, *J*_{C-F} 8.0 Hz), 126.53, 121.73, 120.17, 119.50, 116.11 (d, *J*_{C-F} 21.6 Hz), 80.65, 66.96, 58.95, 57.33, 28.45 ppm; FT-IR (KBr neat) 3444, 2970, 1738 C=O, 1604 C=O, 1506, 1365, 1228, 1217, 1160, 1049 cm⁻¹; *m/z* [ES]⁺ M+Na (found) 941.6, (calc): 941.4. HRMS (NSI) Calcd for C₄₇H₅₂F₂N₁₁O₈, M+NH₄, 936.3663; Found 936.3673. $[\alpha]_D^{26}$ -8.6 (c 1.0, CHCl₃).

2, 8 bis-(4-(((3*R*,4*S*,5*R*,6*R*)-3,4,5-tris(benzyloxy)-6-(benzyloxymethyl)tetrahydro-2*H*-pyran-2-yloxy)methyl)-1*H*-1,2,3-triazole)-6*H*, 12*H*-5, 11-methanodibenzo[*b*,*f*][1,5] diazocine 133



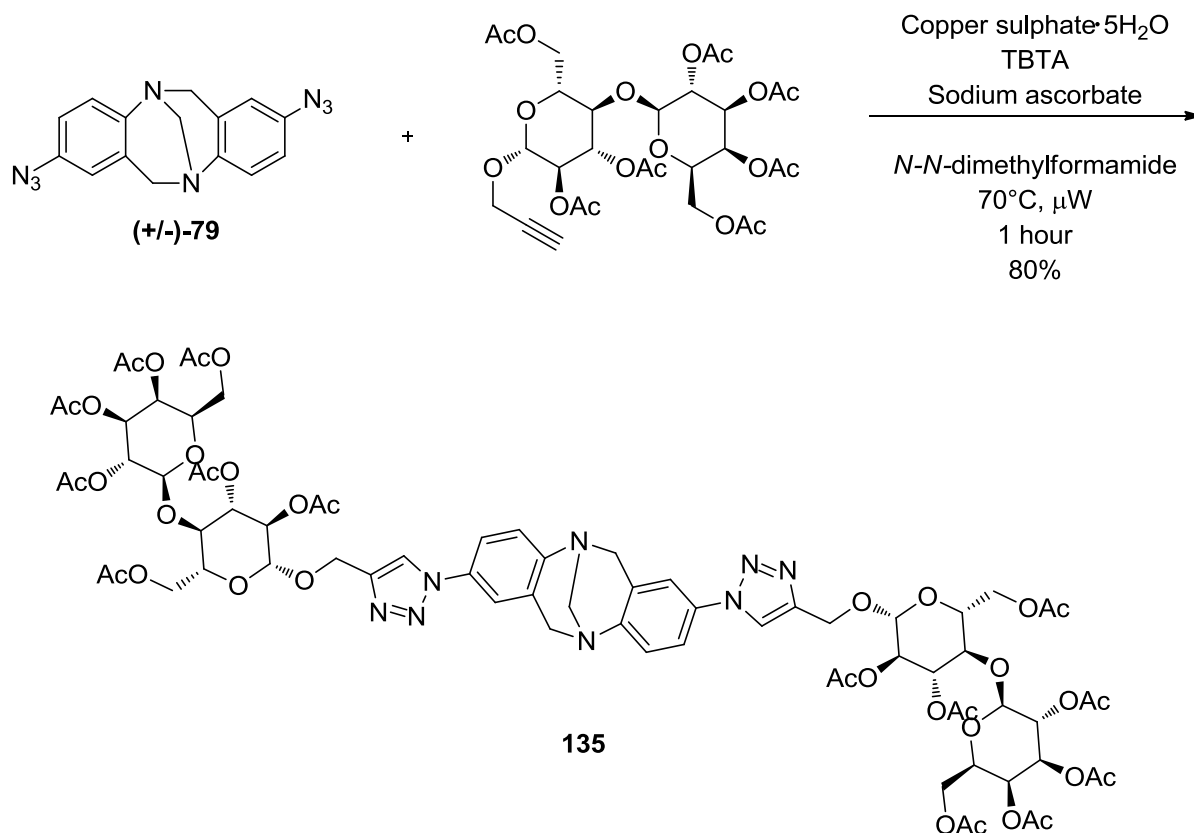
133 (98 mg, 0.07 mmol, 82%) yellow solid. Purified by flash chromatography eluting with ethyl acetate. *R_f* 0.7 (ethyl acetate). MP : 84-86°C (ether); ¹H-NMR (300MHz, CDCl₃) δ7.76 (d, *J*2.5 Hz, 2H), 7.17 (m, 40H), 7.10 (s, 2H), 7.05 (m, 4H), 4.97 (d, *J*13.1 Hz, 2H), 4.88 (d, *J*13.2 Hz, 2H), 4.82 (d, *J*11.0 Hz, 4H), 4.71 (t, *J*10.4 Hz, 4H), 4.63 (dd, *J*9.1, 14.0 Hz, 4H), 4.50 (d, *J*12.2 Hz, 2H), 4.43 (m, 6H), 4.23 (s, 2H), 4.09 (d, *J*17.0 Hz, 2H), 3.62 (m, 4H), 3.53 (m, 4H), 3.41 (m, 4H); ¹³C-NMR (75MHz, CDCl₃) δ148.29, 145.67, 138.61, 138.15, 138.11, 133.12, 129.06, 128.48, 128.01, 127.98, 127.94, 127.86, 127.83, 127.76, 127.73, 127.68, 126.25, 121.02, 119.85, 119.16, 102.70, 84.68, 82.27, 77.77, 75.69, 74.98, 74.77, 73.45, 68.89, 66.71, 62.96, 58.68 ppm; FT-IR (KBr neat) 2903, 2867, 1498, 1453, 1360, 1208, 1070, 1044, 735, 697 cm⁻¹; *m/z* [ES]⁺ M+Na (found) 1484.8, (calc): 1484.7. HRMS (NSI) Calcd for C₈₉H₉₀N₈O₁₂, M+H, 1462.6626; Found 1462.6630. [α]_D²³ -12.7(c 1.0, CHCl₃).

2, 8 bis-((2R,3S,4S,5R)-2-(acetoxymethyl)-6-((1H-1,2,3-triazol-4-yl)methoxy)tetrahydro-2H-pyran-3,4,5-triyl triacetate) -6H, 12H-5, 11-methandibenzo[b,f] [1,5]diazocine 134



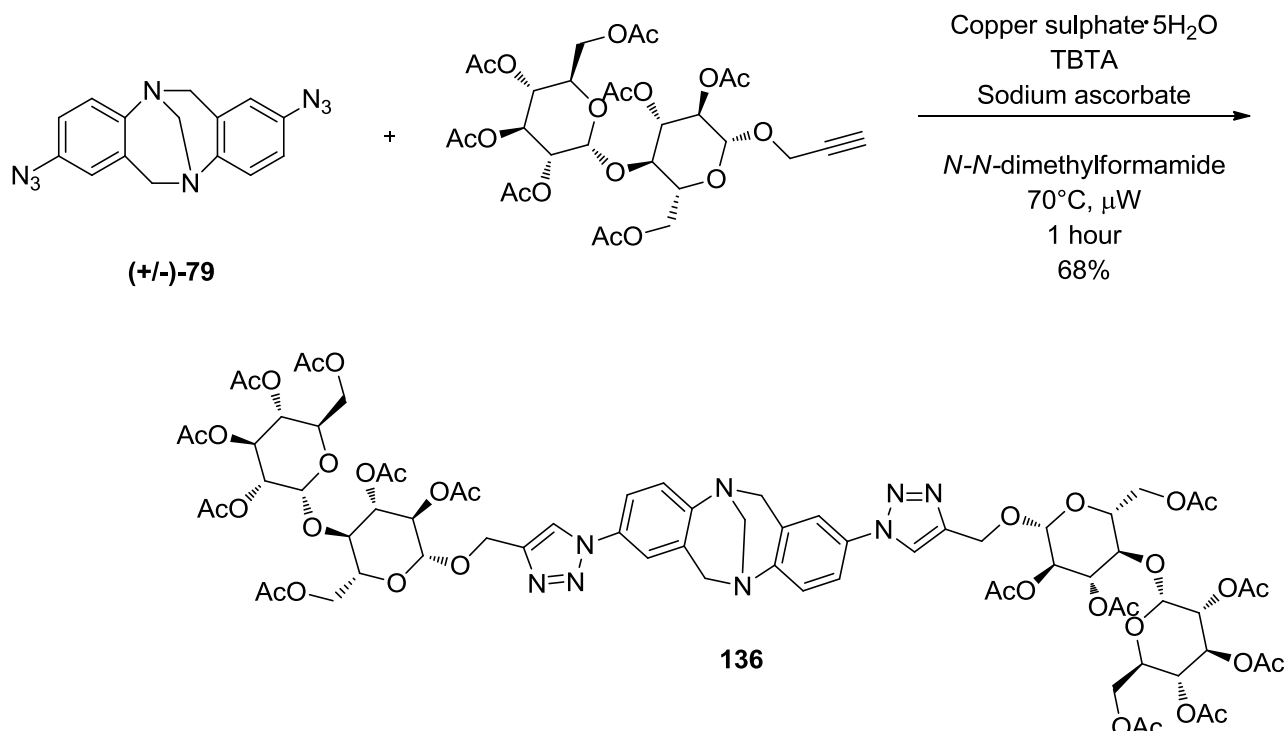
134 (58 mg, 0.05mmol,82%) pale yellow solid. Purified by flash chromatography on silica eluting with 1 – 5% methanol in dichloromethane. *R_f* 0.7 (5% methanol in dichloromethane) MP : 92-94°C (diethyl ether); ¹H-NMR (300MHz, CDCl₃) δ7.88 (t, *J*11.6 Hz, 2H), 7.51 (d, *J*8.6 Hz, 2H), 7.38 (s, 2H), 7.31 (d, *J*8.6 Hz, 2H), 5.41 (dd, *J*2.9, 14.8 Hz, 2H), 5.33 (dd, *J*3.6, 10.6 Hz, 2H), 5.26 (d, *J*3.6 Hz, 2H), 5.13 (dd, *J*3.6, 10.9 Hz, 2H), 5.04 (dd, *J*7.0, 14.9 Hz, 2H), 4.88 (d, *J*12.4 Hz, 2H), 4.78 (s, 2H), 4.71 (d, *J*12.5 Hz, 2H), 4.38 (s,2H), 4.32 (s, 2H), 4.26 (t, *J*7.0 Hz, 2H), 4.09 (d, *J*6.2 Hz, 2H), 2.13 (d, *J*2.5 Hz, 6H), 2.06 (m, 6H), 2.01 (d, *J*4.0 Hz, 6H), 1.96 (d, *J*1.3 Hz, 6H); ¹³C-NMR (75MHz, CDCl₃) δ170.74, 170.56, 170.42, 170.23, 144.53, 133.23, 126.55, 121.13, 120.37, 119.59, 95.87, 77.44, 68.11, 68.06, 67.63, 66.97, 66.69, 61.83, 61.50, 58.93, 21.02, 20.97, 20.87 ppm; FT-IR (ATR) 2934, 2490, 2159, 2029, 1977, 1738 C=O, 1500, 1437, 1368, 1214, 1133, 1039, 832, 729 cm⁻¹; *m/z* [ES]⁺ M+Na (found) 1100.6, (calc): 1100.0. HRMS (NSI) Calcd for C₄₉H₅₇N₈O₂₀, M+H, 1077.3689; Found 1077.3692. [α]_D²³ +25.4 (c 1.0, CHCl₃).

2, 8 -bis-((2*S*,3*R*,4*S*,5*S*,6*R*)-2-((2*R*,3*R*,4*S*,5*R*)-6-((1*H*-1,2,3-triazol-4-yl)methoxy)-4,5-diacetoxy-2-(acetoxymethyl) tetrahydro-2*H*-pyran-3-yloxy)-6-(acetoxymethyl)tetrahydro-2*H*-pyran-3,4,5-triyl triacetate)-6*H*, 12*H*-5, 11-methandibenzo[*b*,*f*][1,5] diazocine 135



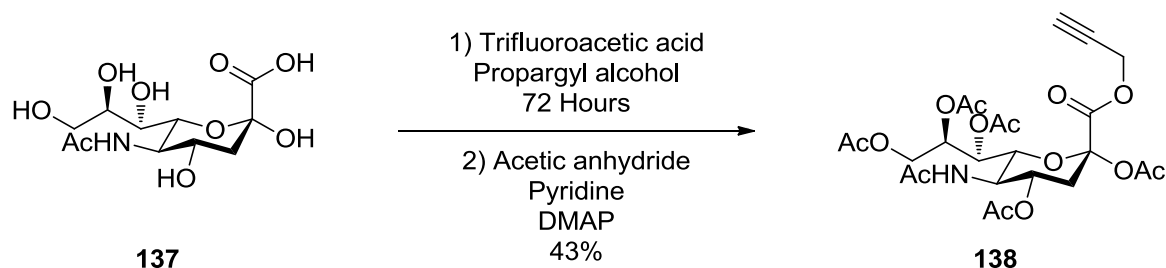
135 (65 mg, 0.04 mmol, 80%) Yellow translucent solid. Purified by flash chromatography on silica eluting with 1 – 10% methanol in dichloromethane. *R_f* 0.8 (10% methanol in dichloromethane). MP : 150-152°C (diethyl-ether); ¹H-NMR (400MHz, CDCl₃) δ 7.78 (s, 2H), 7.43 (dd, *J*1.7, 8.6 Hz, 2H), 7.30 (d, *J*2.4 Hz, 2H), 7.23 (d, *J*8.7, Hz, 2H), 5.28 (d, *J*3.3 Hz, 2H), 5.12 (t, *J*9.2 Hz, 2H), 5.04 (dd, *J*7.9, 10.4 Hz, 2H), 4.88 (ddd, *J*2.6, 4.8, 9.4 Hz, 6H), 4.77 (dd, *J*17.8, 30.8 Hz, 4H), 4.60 (dd, *J*1.6, 7.9 Hz, 2H), 4.45 (m, 2H), 4.31 (s, 2H), 4.23 (d, *J*17.0 Hz, 2H), 4.04 (m, 8H), 3.75 (t, *J*7.2 Hz, 2H), 3.75 (t, *J*9.4 Hz, 2H), 3.59 (m, 2H), 2.09 (s, 6H), 2.03 (d, *J*2.7 Hz, 6H), 1.99 (s, 6H), 1.98 (s, 6H), 1.97 (s, 6H), 1.91 (m, 12H); ¹³C-NMR (100 MHz, CDCl₃) δ 170.54, 170.52, 170.32, 170.24, 169.89, 169.84, 169.22, 148.59, 144.97, 133.12, 129.33, 126.50, 121.11, 120.14, 119.58, 119.55, 101.17, 99.99, 76.26, 72.99, 72.84, 71.71, 71.11, 70.83, 69.25, 66.78, 63.13, 62.02, 60.96, 58.59, 21.04, 20.95, 20.90, 20.81, 20.69 ppm; FT-IR (KBr neat) 2970, 2946, 1746 C=O, 1504, 1370, 1228, 1217, 1057, 1046, 732 cm⁻¹; *m/z* [ES]⁺ M+Na (found) 1676.6, (calc): 1676.5. HRMS (NSI) Calcd for C₇₃H₉₀N₈O₃₆, M+H, 1654.5406; Found 1654.5372. [α]_D²³ -27.8 (c 1.0, CHCl₃).

2, 8 bis-((2*R*,3*R*,4*S*,5*R*,6*R*)-2-(acetoxymethyl)-6-((2*R*,3*R*,4*S*,5*R*)-4,5-diacetoxy-2-(acetoxymethyl)-6-((1*H*-1,2,3-triazol-4-yl)methoxy)tetrahydro-2*H*-pyran-3-yloxy)tetrahydro-2*H*-pyran-3,4,5-triyl triacetate)-6*H*, 12*H*-5, 11-methandibenzo[*b*,*f*][1,5]diazocine 136



136 (74 mg, 0.05 mmol, 68%) white solid. Purified by flash chromatography on silica gel eluting with 1 – 10% methanol in dichloromethane. *R_f* 0.8 (10% methanol in dichloromethane). MP : 112–114°C; ¹H-NMR (300MHz, CDCl₃) δ7.85 (d, *J*7.8 Hz, 2H), 7.48 (t, *J*7.3 Hz, 2H), 7.31 (m, 4H), 5.45 (m, 2H), 5.18 (dd, *J*6.5, 12.4 Hz, 4H), 5.07 (dd, *J*5.6, 9.7 Hz, 4H), 4.99 (m, 2H), 4.85 (m, 6H), 4.76 (s, 2H), 4.71 (d, *J*5.4 Hz, 2H), 4.67 (s, 2H), 4.36 (s, 2H), 4.25 (m, 6H), 4.09 (t, *J*14.0 Hz, 4H), 3.74 (s, 2H), 2.06 (s, 6H), 2.03 (s, 6H), 2.00 (s, 6H), 1.98 (d, *J*1.0 Hz, 9H), 1.97 (d, *J*1.0 Hz, 9H), 1.94 (d, *J*1.5 Hz, 6H); ¹³C-NMR (100MHz, CDCl₃) δ169.68, 169.64, 169.18, 169.11, 169.07, 168.56, 168.44, 168.39, 147.30, 143.81, 143.17, 131.96, 128.11, 125.34, 120.05, 119.93, 119.13, 118.98, 118.54, 118.36, 99.02, 94.27, 71.64, 70.89, 70.16, 69.55, 68.94, 67.38, 67.21, 66.50, 65.73, 61.99, 60.80, 60.70, 60.37, 57.71, 19.76, 19.73, 19.69, 19.61 ppm; FT-IR (KBr neat) 3474, 3145, 2959, 1753 C=O, 1501, 1436, 1368, 1331, 1227, 1041, 834, 735 cm⁻¹; *m/z* [ES]⁺ M+Na (found) 1675.7, (calc): 1675.5. HRMS (NSI) Calcd for C₇₃H₈₉N₈O₃₆, M+H, 1653.5379; Found 1653.5401. [α]_D²⁶ -8.6 (c 1.0, CHCl₃).

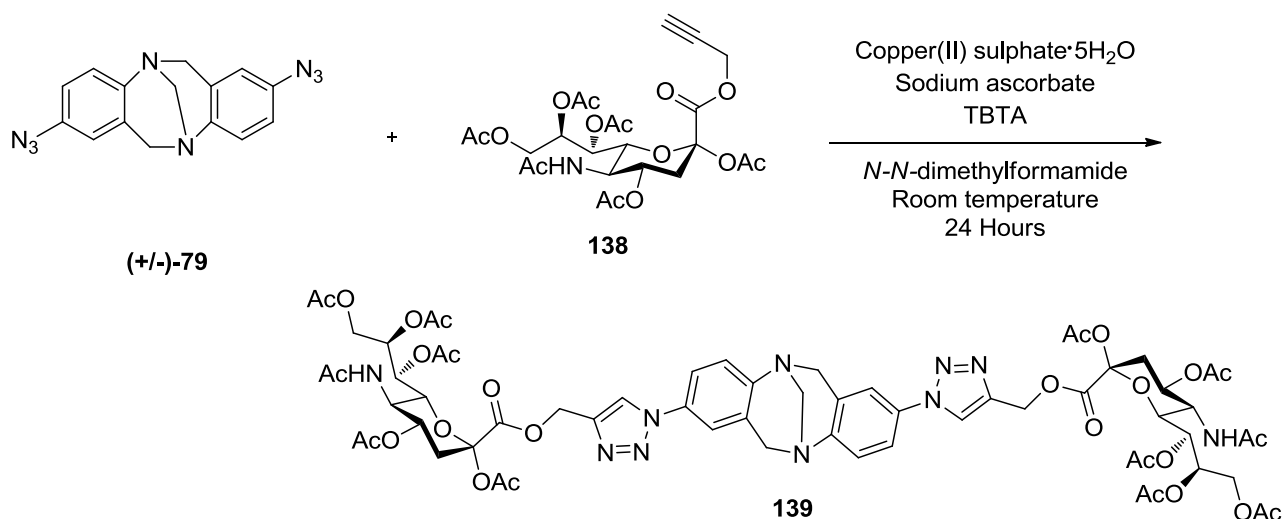
Synthesis of (1*S*,2*R*)-1-((2*R*,3*R*,4*S*,6*R*)-3-acetamido-4,6-diacetoxy-6-((prop-2-ynyloxy)carbonyl)tetrahydro-2*H*-pyran-2-yl)propane-1,2,3-triyl triacetate **138**



A flame-dried 25 mL, round-bottomed flask was charged with Neu5Ac (100 mg, 0.323 mmol) in propargyl alcohol (6 mL). To this TFA (37 μ L, 0.485 mmol) was added and left to stir for 3 days at 40°C. The solvent was removed under reduced pressure and azeotroped with toluene (3 x 10mL). The resulting oil was dissolved in acetic anhydride (5 mL), pyridine (2 mL) and *N,N*-dimethylaminopyridine (5 mg) was added. The solution was left to stir at room temperature for 3 days. The solvent was removed under reduced pressure and the resulting residue was azeotroped with toluene (3 x 10 mL). The reaction mixture was then absorbed onto silica and subjected to flash chromatography, eluting with ethyl acetate affording an off white solid. Subsequent physicochemical analysis confirmed this to be the title compound **138** (78 mg, 0.14 mmol, 43%)

138 (78 mg, 0.14mmol, 43%) white solid. *R_f* 0.4 (ethyl acetate). MP : 60-62°C (ethyl acetate); ¹H-NMR (300MHz, CDCl₃) δ 5.57 (d, *J*9.5 Hz, 1H), 5.35 (d, *J*4.8 Hz, 1H), 5.23 (dt, *J*6.5, 10.6 Hz, 1H), 5.04 (m, 1H), 4.74 (t, *J*2.4 Hz, 2H), 4.46 (dd, *J*2.0, 12.5 Hz, 1H), 4.11 (m, 3H), 2.52 (m, 2H), 2.12 (dd, *J*0.8, 4.6 Hz, 7H), 2.03 (d, *J*0.8 Hz, 3H), 2.01 (m, 6H), 1.86 (d, *J*0.8 Hz, 3H); ¹³C-NMR (75MHz, CDCl₃) δ 171.17, 170.80, 170.52, 170.74, 168.42, 165.23, 97.37, 76.69, 75.94, 73.11, 71.62, 68.38, 68.05, 62.26, 53.82, 49.43, 35.99, 23.37, 21.12, 21.05, 21.00, 20.99, 20.89 ppm; FT-IR (KBr neat) 3277 CH alkyne, C-Calkyne, 1748 C=O, 1664 C=O cm⁻¹; *m/z* [ES]⁺ M+Na (found) 580.3, (calc): 580.2. HRMS (NSI) Calcd for C₂₄H₃₂NO₁₄, M+H, 558.1823; Found 558.1798. $[\alpha]_D^{23}$ -17 (c 1.0, CHCl₃).

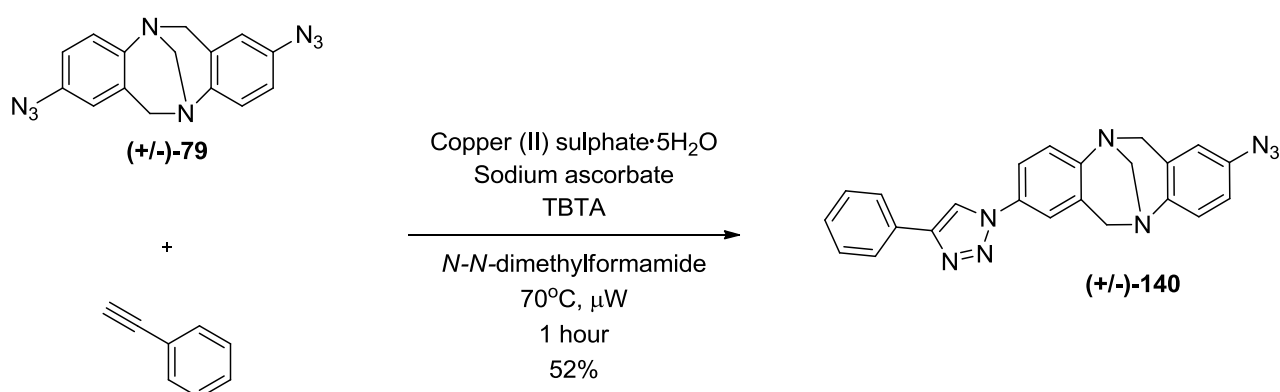
Synthesis of 2, 8 bis-(((1*S*,2*R*)-1-(((2*R*,3*R*,4*S*,6*R*)-3-acetamido-4,6-diacetoxy-6-(((1*H*-1,2,3-triazol-4-yl)methoxy)carbonyl) tetrahydro-2*H*-pyran-2-yl)propane-1,2,3-triyl triacetate))-6*H*, 12*H*-5, 11-methanodibenzo[*b*,*f*] [1,5]diazocine **139**



A flame dried 5 mL round bottomed flask was charged with 2,8-*bis*-azido-6*H*,12*H*-5,11-methandibenzo[*b*,*f*][1,5]diazocine (+/-)-**79** (4.5 mg, 0.015 mmol), **138** (17 mg, 0.03 mmol), TBTA (616 μg, 1.162 μmol), copper(II) sulfate pentahydrate (290 μg, 1.161 μmol) and sodium ascorbate (2.3 mg, 0.012 mmol) in *N,N*-dimethylformamide (1 mL). The resulting solution was stirred at ambient temperature, under an atmosphere of nitrogen for 24 hours. The reaction mixture was diluted with ethyl acetate (2 mL) and transferred to a 10 mL separating funnel, washed with water (3 x 5 mL), brine (5 mL) and dried with magnesium sulfate. The suspension was filtered and the solvent removed under reduced pressure. The resulting residue was columned under gravity (ethyl acetate, acetone, 9:1) affording a white solid. Subsequent physicochemical analysis confirmed this to be the title compound **139** (12 mg, 8.45 μmol, 58%)

139 (12 mg, 8.45 μmol, 58%) white solid. *R_f* 0.5 (ethyl acetate, acetone, 9:1). MP : 122-124°C (ethyl acetate); ¹H NMR (400 MHz, CDCl₃) δ 8.03 (d, *J* 3.1 Hz, 2H), 7.52 (t, *J* 7.9 Hz, 2H), 7.37 (d, *J* 5.4 Hz, 2H), 7.23 (d, *J* 8.7 Hz, 2H), 4.99 (t, *J* 7.2 Hz, 2H), 4.73 (d, *J* 16.9 Hz, 2H), 4.37 (d, *J* 10.0 Hz, 2H), 4.31 (s, 2H), 4.24 (d, *J* 17.1 Hz, 2H), 4.03 (t, *J* 8.5 Hz, 6H), 2.46 (dd, *J* 13.4, 5.0 Hz, 2H), 2.05 (d, *J* 1.4 Hz, 6H), 2.01 (d, *J* 1.1 Hz, 6H), 1.95 (t, *J* 3.1 Hz, 12H), 1.91 (d, *J* 4.8 Hz, 6H), 1.82 (s, 6H); ¹³C-NMR (75 MHz, CDCl₃) δ 171.04, 170.70, 170.40, 170.28, 170.15, 168.29, 165.84, 148.00, 142.70, 133.24, 128.97, 126.32, 122.29, 120.15, 119.38, 97.38, 77.17, 72.56, 70.65, 68.08, 67.38, 66.73, 61.78, 59.44, 58.58, 49.20, 35.77, 29.56, 23.03, 20.76, 20.67, 20.64, 20.54 ppm; FT-IR (KBr neat) 1745 C=O, 1671 C=O cm⁻¹; *m/z* [ES]⁺ M+Na (found) 1442.9, calc (1442.3). HRMS (NSI) Calcd for C₆₃H₇₅N₁₀O₂₈, M+H, 1419.4752; Found 1419.4746. [α]_D²³ -27 (c 1.0, CHCl₃).

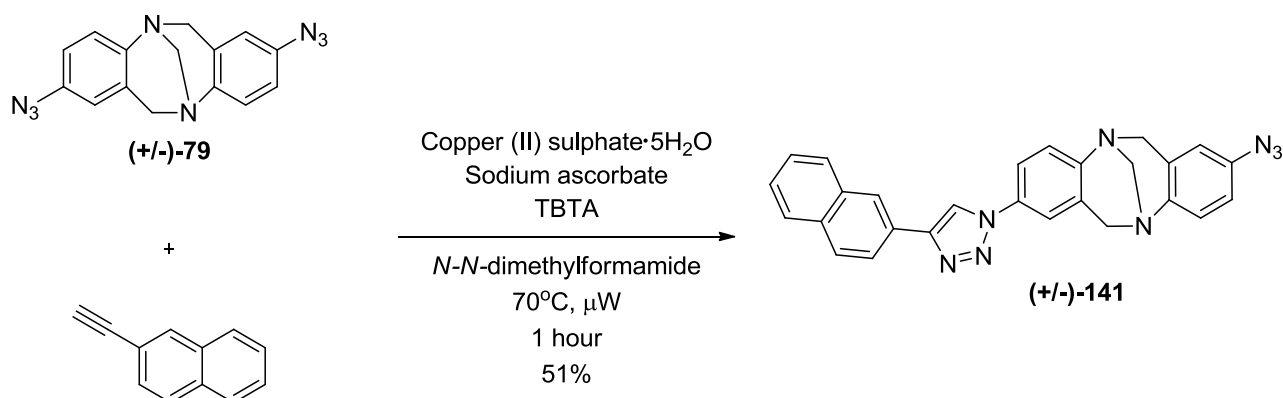
Synthesis of 2-(4-phenyl-1H-1,2,3-triazole)-8-azo -6H, 12H-5, 11-methandibenzo[b,f][1,5] diazocine (+/-)-140



A 10 mL microwave vial was charged with 2,8-*bis*-azido-6H,12H-5,11-methandibenzo[b,f][1,5]diazocine (+/-)-**79** (100mg, 0.329 mmol), copper sulfate pentahydrate (1.641 mg, 6.57 μmol), TBTA (3.49 mg, 6.57 μmol), sodium ascorbate (13.02 mg, 0.066mmol) in *N,N*-dimethylformamide (7 mL). The vial was sealed with a Teflon cap and phenyl acetylene (33.6 mg, 0.329 mmol) was added *via* syringe. The reaction mixture was heated to 70°C in a microwave reactor for 1 hour. The reaction mixture was diluted with dichloromethane (5 mL), transferred to a 50 mL separating funnel, washed with water (5 x 10 mL), brine (5 mL) and dried with magnesium sulfate. The resulting suspension was filtered and the solvent removed under reduced pressure. The impure material was submitted to flash column chromatography on silica gel eluting with diethyl ether affording an off white solid. Subsequent physicochemical analysis confirmed this to be the desired product. (70 mg, 0.171 mmol, 52%).

(+/-)-**140** (70 mg, 0.171, 52%). *R_f* 0.6 (diethyl ether) ¹H-NMR (300MHz, CDCl₃) δ 8.07 (s, 1H, ArH), 7.87 (d, *J*7.1 Hz, 2H, ArH), 7.54 (dd, *J*2.4, 8.6 Hz, 1H, ArH), 7.44 (t, *J*7.4 Hz, 1H, ArH), 7.37 (m, 2H, ArH), 7.28 (d, *J*8.7 Hz, 1H, ArH), 7.14 (d, *J*8.6 Hz, 1H, ArH), 6.86 (dd, *J*2.5, 8.6 Hz, 1H, ArH), 6.60 (d, *J*2.5 Hz, 1H, ArH), 4.73 (dd, *J*8.9, 16.8 Hz, 2H, CH₂), 4.33 (s, 2H, CH₂), 4.20 (dd, *J*8.3, 16.9 Hz, 2H, CH₂). ¹³C-NMR (75 MHz, CDCl₃) δ 148.56, 148.35, 144.63, 135.85, 133.04, 130.22, 129.35, 128.97, 128.47, 126.53, 126.30, 125.83, 119.91, 119.36, 118.68, 117.58, 117.06, 66.80, 58.69, 58.6. FT-IR KBr neat : 3411, 2359, 2113 N₃, 1614, 1504, 1488, 1210, 912, 732. *m/z* [ES]⁺ M-N₂+Na (found) 401.5, calc (401.42). HRMS (NSI) Calcd for C₂₃H₂₂N₉, M+NH₄, 424.1992; Found 424.1996.

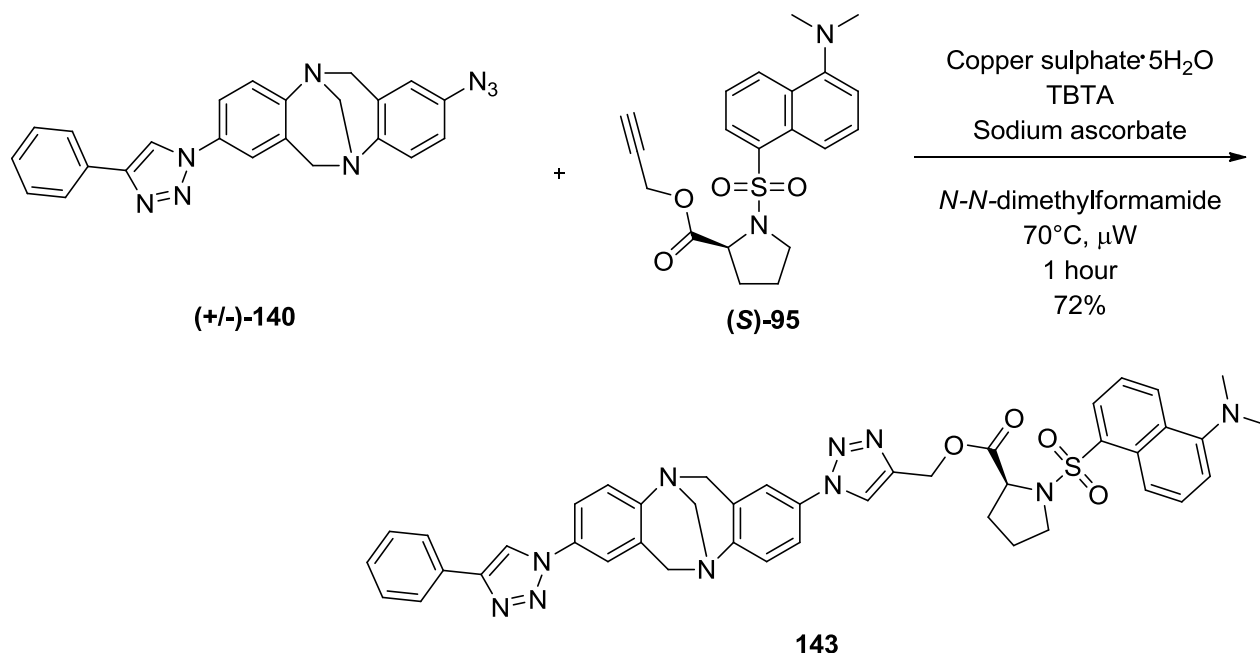
Synthesis of 2-azido-8-(4-(naphthalen-2-yl)-1H-1,2,3-triazol-1-yl)-6,12-dihydro-5,11-methanodibenzo[b,f][1,5]diazocine (+/-)-141



A 10 mL microwave vial was charged with 2,8-*bis*-azido-6H,12H-5,11-methandibenzo[b,f][1,5]diazocine (+/-)-**79** (100mg, 0.329 mmol), 2-ethynynaphthalene (50 mg, 0.329 mmol), copper(II) sulfate pentahydrate (1.641 mg, 6.57 μmol), TBTA (3.49 mg, 6.57 μmol), sodium ascorbate (13.02 mg, 0.066mmol) in *N,N*-dimethylformamide (7 mL). The vial was sealed with a Teflon cap and the reaction mixture was heated to 70°C in a microwave reactor for 1 hour. The reaction mixture was diluted with dichloromethane (5 mL), transferred to a 50 mL separating funnel, washed with water (5 x 10 mL), brine (5 mL) and dried with magnesium sulfate. The resulting suspension was filtered and the solvent removed under reduced pressure. The impure material was submitted to flash column chromatography on silica gel eluting with diethyl ether affording a yellow solid. Subsequent physicochemical analysis confirmed this to be the desired product (+/-)-**141**. (76 mg, 0.165, 51%).

(+/-)-**141** (76 mg, 0.165, 51%) *R_f* 0.4 (diethyl ether), ¹H-NMR (400 MHz, CDCl₃) δ 8.38 (s, 1H, ArH), 8.18 (s, 1H), 7.87 (dd, *J*1.7, 8.5 Hz, 1H, ArH), 7.78 (m, 3H, ArH), 7.47 (dd, *J*2.5, 8.6 Hz, 1H, ArH), 7.40 (m, 2H, ArH), 7.30 (d, *J*2.4 Hz, 1H, ArH), 7.19 (d, *J*8.6 Hz, 1H, ArH), 7.06 (d, *J*8.6 Hz, 1H), 6.77 (dd, *J*2.6, 8.6 Hz, 1H), 6.51 (d, *J*2.5 Hz, 1H), 4.72 (dd, *J*9.3, 16.8 Hz, 2H, CH₂), 4.32 (s, 2H, CH₂), 4.19 (dd, *J*10.4, 16.9 Hz, 2H, CH₂). FT-IR KBr neat : 2112 N₃. *m/z* [ES]⁺ M-N₂+Na (found) 451.3, calc (451.1). HRMS (NSI) Calcd for C₂₇H₂₄N₉, M+NH₄, 474.2161; Found 474.2156.

Synthesis of 2, - (4-phenyl-1H-1,2,3-triazole), 8,-((S)-(1H-1,2,3-triazol-4-yl)methyl 1-(5-(dimethylamino)naphthalen-1-ylsulfonyl)pyrrolidine-2-carboxylate)-6H, 12H-5, 11-methanodibenzo [b,f][1,5]diazocine (+/-)-145

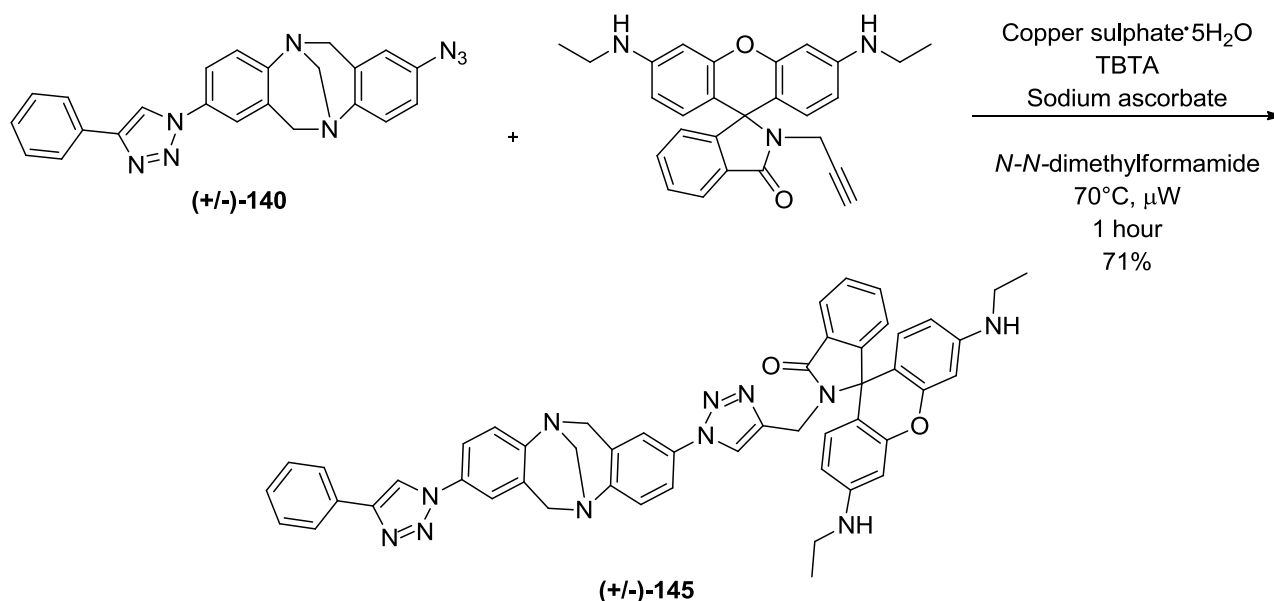


A 2.5 mL microwave vial was charged with 2-(4-phenyl-1H-1,2,3-triazole)-8-azo-6H, 12H-5, 11-methanodibenzo[b,f][1,5]diazocine (+/-)-**140** (10mg, 0.025 mmol), (S)-prop-2-ynyl 1-(5-(dimethylamino)naphthalen-1-ylsulfonyl)pyrrolidine-2-carboxylate (10.46 mg, 0.027 mmol), copper(II) sulfate pentahydrate (0.49 mg, 1.968 μmol), TBTA (1.04mg, 1.968 μmol) and sodium ascorbate (3.9 mg, 0.02 mmol) in *N-N*-dimethylformamide (1mL). The vial was sealed with a Teflon cap and heated to 70°C in a microwave reactor for 1 hour. The reaction mixture was diluted with ethyl acetate (2mL) and transferred to a 25 mL separating funnel, washed with water (5 x 5 mL), brine (2 mL) and dried with magnesium sulfate. The resulting suspension was filtered and the solvent removed under reduced pressure. The resulting solid was columned by flash chromatography (dichloromethane:methanol 1-5%) affording a yellow solid. Subsequent physiochemical analysis confirmed this to be the title compound (+/-)-**143** (14 mg, 0.02 mmol, 72%)

(+/-)-**143** (14mg, 0.02 mmol, 72%) Dark yellow solid. *R_f* 0.6 (dichloromethane:methanol 5%) MP : 162-164°C (diethyl ether); ¹H-NMR (300MHz, CDCl₃) 8.51 (d, *J*8.6 Hz, 1H), 8.40 (d, *J*8.7 Hz, 1H), 8.20 (dd, *J*1.2, 7.4 Hz, 1H), 8.07 (s, 1H), 8.01 (s, 1H), 7.86 (dd, *J*1.3, 8.3 Hz, 2H), 7.57 – 7.24 (m, 11H), 7.14 (d, *J*7.6, 1H), 5.25 (q, *J*13.0, 12.9 Hz, 2H), 4.78 (dd, *J*17.6, 8.4 Hz, 2H), 4.51 (ddd, *J*1.7, 3.7, 8.5 Hz, 1H), 4.37 (s, 2H), 4.27 (dd, *J*7.4, 16.9 Hz, 2H), 3.52 (m, 1H), 3.36 (m, 1H), 2.84 (d, *J*0.6 Hz, 6H), 2.04 (m, 3H), 1.80 (m, 1H); ¹³C-NMR (75MHz, CDCl₃) δ 172.18, 148.41, 143.44, 133.16, 133.00, 130.66, 130.32, 130.22, 129.92, 129.17, 129.10, 128.94, 128.44, 128.19, 126.35,

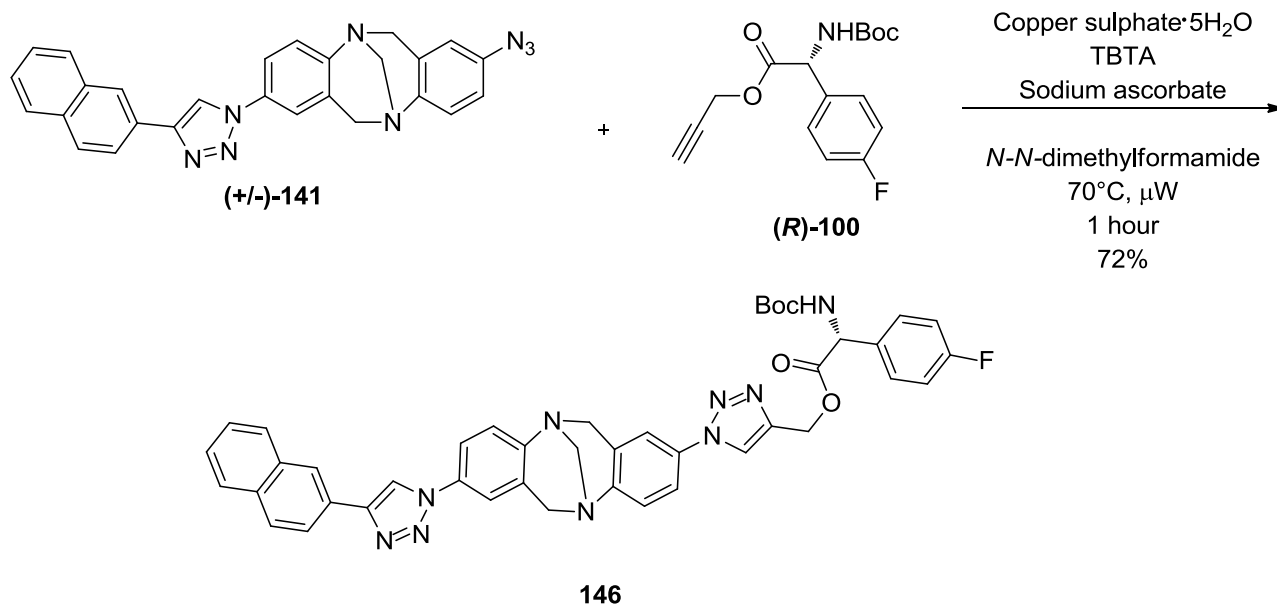
125.83, 123.23, 121.89, 120.03, 119.37, 119.32, 117.56, 115.31, 66.74, 60.11, 58.70, 58.54, 48.40, 45.29, 31.44, 30.82, 29.55, 24.60, 22.49, 13.94 ppm; FT-IR (KBr neat) 1747 C=O, 1675 C=O, 1331 O=S=O cm⁻¹; *m/z* [ES]⁺ M+H (found) 793.4, (calc): 793.3. HRMS (NSI) Calcd for C₄₃H₄₁N₁₀O₄S, M+H, 793.3027; Found 793.3028. [α]_D²⁸ -8.8 (c 1.0, CHCl₃).

2,-(4-phenyl-1H-1,2,3-triazole),-8 (3',6'-bis(ethylamino)-2',7'-dimethyl-2-((1H-1,2,3-triazol-4-yl)methyl)spiro [isoindoline-1,9'-xanthen]-3-one)-6H, 12H-5, 11-methanodibenzo[b,f][1,5] diazocine (+/-)-145



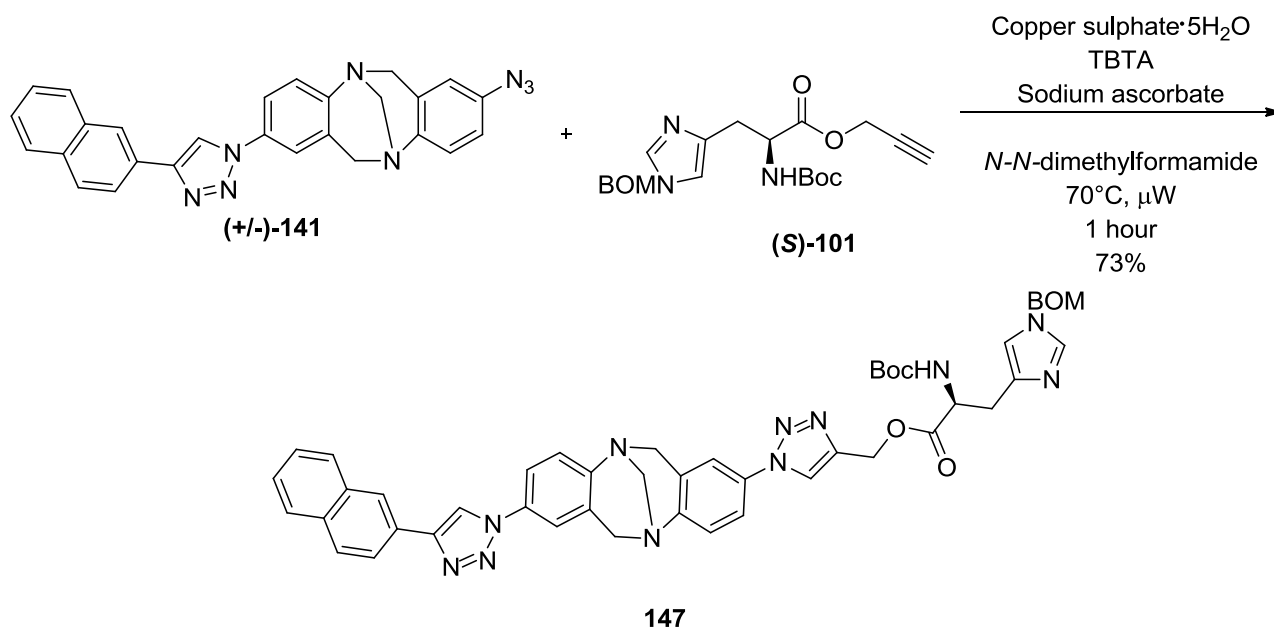
(+/-)-145 Purified *via* flash chromatography on silica gel eluting with 1-5% methanol in dichloromethane (15 mg, 0.02 mmol, 71%) pink solid. *R_f* 0.4 (5% methanol in dichloromethane). MP : 210-212°C (diethyl ether); ¹H-NMR (300MHz, CDCl₃) δ 8.08 (s,1H), 7.95 (m, 1H), 7.87 (d, *J*7.0 Hz, 2H), 7.54 (dd, *J*2.5, 8.5 Hz, 2H), 7.44 (dd, *J*6.2, 8.5 Hz, 6H), 7.36 (d, *J*7.3 Hz, 1H), 7.30 (d, *J*8.7 Hz, 1H), 7.22 (d, *J*4.4 Hz, 2H), 7.18 (d, *J*3.9 Hz, 2H), 7.05 (dd, *J*2.8, 5.8 Hz, 1H), 6.29 (d, *J*2.9 Hz, 2H), 6.08 (s, 2H), 4.78 (dd, *J*13.2, 16.6 Hz, 2H), 4.49 (s, 2H), 4.37 (s, 2H), 4.26 (dd, *J*7.9, 16.9 Hz, 2H), 3.13 (qd, (*J*3.0, 7.5, 7.7 Hz, 4H), 1.74 (d, *J*3.6 Hz, 6H), 1.25 (m, 6H) ¹³C-NMR (75MHz, CDCl₃) δ 168.01, 153.54, 151.92, 148.46, 148.41, 147.86, 147.39, 144.84, 133.21, 133.15, 132.71, 130.90, 130.20, 129.22, 128.95, 128.84, 128.56, 128.47, 128.15, 126.31, 125.93, 125.84, 123.89, 123.01, 120.44, 119.96, 119.56, 119.41, 118.91, 117.66, 117.55, 105.71, 105.66, 96.53, 77.39, 77.17, 76.97, 76.54, 66.77, 65.02, 58.73, 38.18, 34.91, 29.56, 16.45, 16.42, 14.57 ppm; FT-IR (KBr neat) 3420, 2925, 2324, 1684C=O, 1620, 1504, 1422, 1268, 1207, 1092 cm⁻¹; *m/z* [CI]⁺ M+H (found) 858.5, (calc): 858.4. HRMS (NSI) Calcd for C₅₂H₄₈N₁₁O₂, M+H, 858.3987; Found 858.3986

2,-(4-(naphthalen-2-yl)-1H-1,2,3-triazole),-8-((1H-1,2,3-triazol-4-yl)methyl 2-(*tert*-butoxy carbonylamino)-2-(4-fluorophenyl)acetate),-6H,12H-5,11-methanodibenzo[b,f] [1,5]diazocine 146



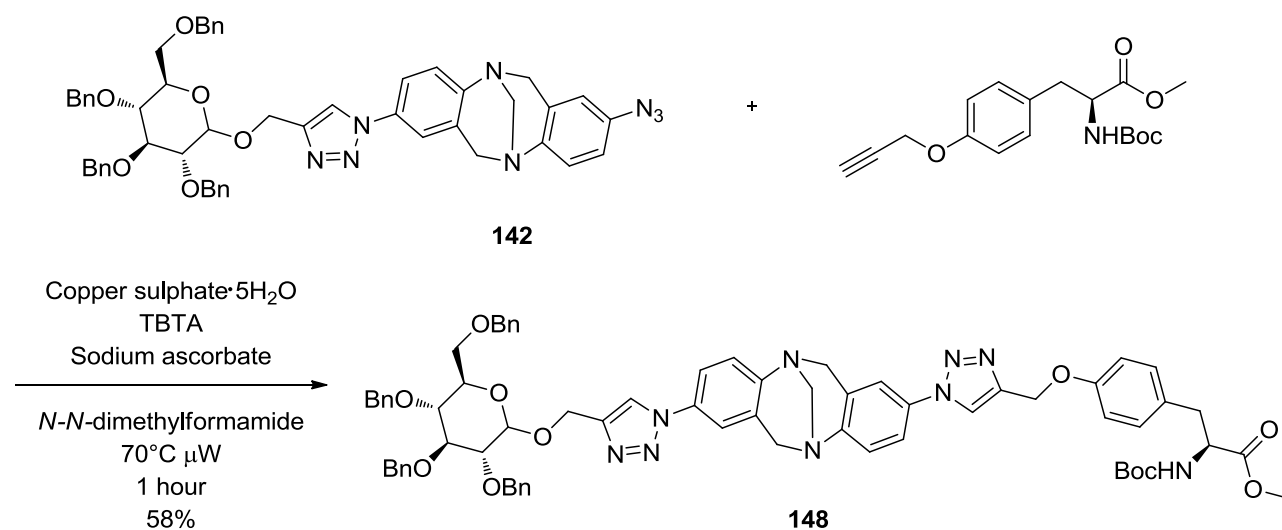
146 Purified *via* flash chromatography eluting with 1-5% methanol in dichloromethane (12 mg, 0.02mmol, 72%) white solid. *R_f* 0.7 (5% methanol in dichloromethane). MP : 106-108°C (diethyl ether); ¹H-NMR (300MHz, CDCl₃) δ8.39 (s, 1H), 8.20 (s,1H), 7.95 (d, *J*1.6 Hz, 1H), 7.93 (s, 1H), 7.88 (m, 2H), 7.75 (s, 1H), 7.59 (dd, *J*2.4, 8.7 Hz, 1H), 7.54-7.43 (m, 4H), 7.38-7.28 (m, 5H), 7.02 (d, *J*8.5 Hz, 2H), 5.49 (d, *J*7.8 Hz, 1H), 5.33 (dd, *J*9.4,Hz, 3H), 4.82 (dd, *J*6.7, 16.7 Hz, 2H), 4.40 (s, 2H), 4.31 (dd, *J*5.8, 16.1 Hz, 2H), 1.40 (s, 9H); ¹³C-NMR (75MHz, CDCl₃) δ170.84,(C-F resonance too small to observe) 148.62, 148.46, 133.57, 133.32, 133.19, 132.87, 129.02 (d, *J*_{C-F} 8.3 Hz) 128.97, 128.73, 128.26, 127.83, 127.51, 126.58, 126.38, 124.66, 123.80, 121.58, 120.05, 119.44, 119.35, 117.82, 116.06, 115.92 (d, *J*_{C-F} 21.8 Hz), 77.16, 66.75, 58.76, 29.55, 28.12 ppm; FT-IR (KBr neat) 2924, 2853, 1745C=O, 1706 C=O, 1500, 1367, 1229,1159, 1044 cm⁻¹; *m/z* [CI] M+H – boc (found) 664.3, (calc): 664.3. HRMS (NSI) Calcd for C₄₃H₃₉FN₉O₄, M+H, 764.3104; Found 764.3102. [α]_D²⁷ -4.5 (c 1.0, CHCl₃).

2-(4-(naphthalen-2-yl)-1H-1,2,3-triazole), 8-((R)-(1H-1,2,3-triazol-4-yl)methyl 3-(1-(benzyloxymethyl)-1H-imidazol-4-yl)-2-(tert-butoxycarbonyl amino)propanoate),-6H, 12H-5, 11-methandibenzo[b,f][1,5]diazocine 147



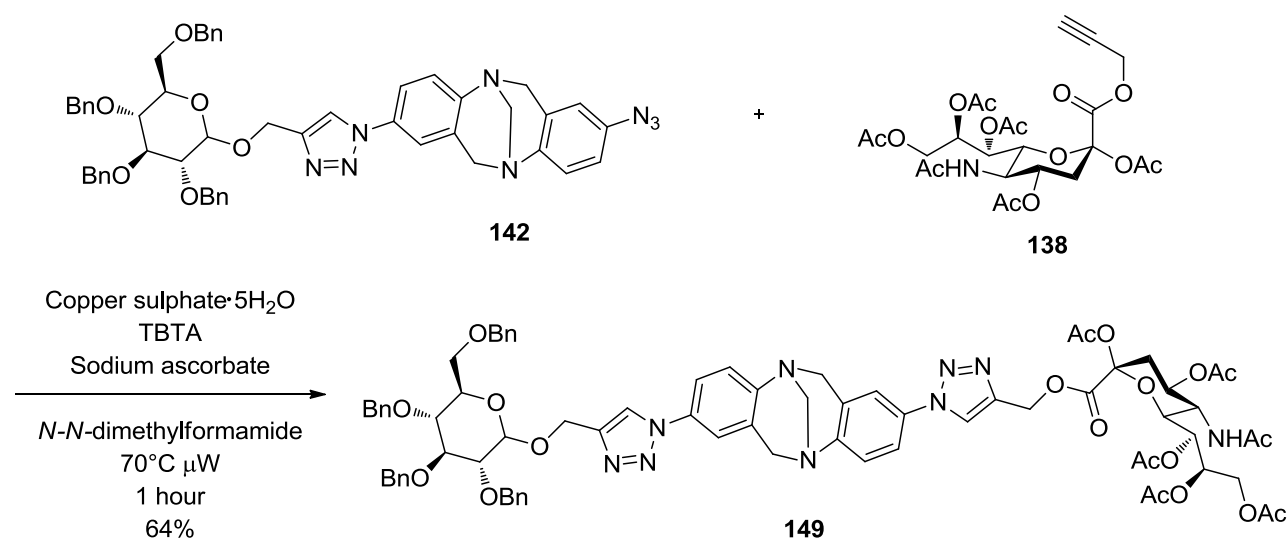
147 Purified *via* flash chromatography eluting with 5% methanol in dichloromethane. (14 mg, 0.02 mmol, 73%) dark yellow solid. *R_f* 0.6 (5% methanol in dichloromethane). MP : 114-116 °C (diethyl ether); ¹H-NMR (300MHz, CDCl₃) δ 8.39 (s, 1H, ArH), 8.20 (s, 1H, ArH), 7.99-7.82 (m, 5H, ArH), 7.63-7.44 (m, 5H, ArH), 7.41-7.20 (m, 9H, ArH), 5.38 (s, 3H), 5.21 (s, 2H), 4.82 (dd, *J*6.0, 17.1 Hz, 2H, 2CHH), 4.58 (dd, *J*6.9, 13.3 Hz, 1H, α CH), 4.34 (m, 6H), 3.13 (m, 2H, β CH₂), 1.37 (s, 9H, 3(CH₃)); ¹³C-NMR (75MHz, CDCl₃) δ 171.42, 148.63, 148.45, 135.95, 133.58, 133.32, 133.19, 132.90, 129.22, 128.73, 128.37, 128.25, 128.03, 127.83, 127.54, 126.57, 126.39, 126.33, 124.66, 123.80, 122.22, 120.17, 120.06, 119.51, 119.43, 117.83, 77.15, 69.75, 66.76, 58.73, 58.42, 29.55, 28.11 ppm; FT-IR (KBr neat) 3300, 2928, 1705C=O, 1500, 1366, 1162, 1046 cm⁻¹; *m/z* [ES]⁺ M+H (found) 870.5, (calc): 870.4. HRMS (NSI) Calcd for C₄₉H₄₈N₁₁O₅, M+H, 870.3834; Found 870.3831. [α]_D²⁷ +2.2 (c 1.0, CHCl₃).

2,-(4-(((2R,3R,4S,5R,6R)-3,4,5-tris(benzyloxy)-6-(benzyloxymethyl)tetrahydro-2H-pyran-2-yloxy)methyl)-1H-1,2,3-triazole),- 8- ((methyl 2-(tert-butoxycarbonylamino)-3-(4-((1H-1,2,3-triazol-4-yl)methoxy)phenyl)propanoate),-6H,12H-5,11-methandibenzo[b,f][1,5] diazocine
148



148 Purified *via* flash chromatography eluting with 5% methanol in dichloromethane. (8 mg, 6.58 μmol, 58%) white solid. *R_f* 0.6 (5% methanol in dichloromethane). MP :64-66°C (diethyl ether); ¹H-NMR (300MHz, CDCl₃) δ7.93 (s, 1H), 7.87 (s,1H), 7.54 (d, *J*7.5 Hz, 2H), 7.40(d, *J*8.0 Hz, 2H), 7.34 – 7.20 (m, 20H), 7.14 (m, 2H), 7.04 (d, *J*7.9 Hz, 2H), 6.91 (d, *J*8.6 Hz, 2H), 5.23 (s, 2H), 5.10 – 4.91 (m, 4H), 4.88(s, 2H), 4.81 (d, *J*5.2 Hz, 3H), 4.73 (d, *J*11.2 Hz, 2H), 4.59 (d, *J*11.6 Hz, 2H), 4.51 (d, *J*10.9 Hz, 4H), 4.44 (s, 2H), 4.35 (t, *J*15.3 Hz, 2H), 3.71 (m, 3H), 3.61 (m, 2H), 3.49 (m, 2H), 3.01 (m, 2H), 1.40 (s, 9H); ¹³C-NMR (75MHz, CDCl₃) δ172.46, 157.35, 148.52, 148.20, 145.66, 144.97, 138.52, 138.05, 133.10, 133.05, 130.46, 129.18, 128.98, 128.82, 128.42, 127.97, 127.89, 127.77, 127.70, 127.63, 126.33, 126.21, 120.95, 120.79, 120.05, 119.86, 119.44, 119.16, 114.85, 102.66, 84.62, 82.22, 79.86, 77.70, 75.66, 74.94, 74.72, 73.40, 68.80, 66.71, 62.96, 61.96, 58.66, 52.10, 29.55, 28.14 ppm; FT-IR (KBr neat) 2924, 2862, 1747 C=O, 1713 C=O, 1500, 1454, 1365, 1246, 1209, 1164, 1070 cm⁻¹; *m/z* [CI] M+Na (found) 1239.8, (calc): 1239.4 HRMS (NSI) Calcd for C₇₀H₇₄N₉O₁₁, M+H, 1216.5508; Found 1216.5523. [α]_D²³ 15.0 (c 1.0, CHCl₃).

Synthesis of 2-(4-(((2*R*,3*R*,4*S*,5*R*,6*R*)-3,4,5-*tris*(benzyloxy)-6-(benzyloxymethyl)tetrahydro-2*H*-pyran-2-yloxy)methyl)-1*H*-1,2,3-triazole)-8-(((1*S*,2*R*)-1-(((2*R*,3*R*,4*S*,6*R*)-3-acetamido-4,6-diacetoxy-6-(((1*H*-1,2,3-triazol-4-yl)methoxy)carbonyl)tetrahydro-2*H*-pyran-2-yl)propane-1,2,3-triyl triacetate)) -6*H*, 12*H*-5, 11-methanodibenzo [b,f][1,5]diazocine **149**

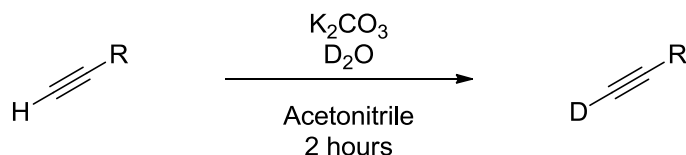


A flame-dried 5 mL round-bottomed flask was charged with 2-(4-(((2*R*,3*R*,4*S*,5*R*,6*R*)-3,4,5-*tris*(benzyloxy)-6-(benzyloxymethyl)tetrahydro-2*H*-pyran-2-yloxy)methyl)-1*H*-1,2,3-triazole)-8-azo-6*H*, 12*H*-5, 11-methandibenzo [b,f][1,5]diazocine **142** (8.64 mg, 9.78 μmol), (1*S*,2*R*)-1-(((2*R*,3*R*,4*S*,6*R*)-3-acetamido-4,6-diacetoxy-6-((prop-2-ynoxy)carbonyl)tetrahydro-2*H*-pyran-2-yl)propane-1,2,3-triyl triacetate **138** (6 mg, 10.76 μmol), TBTA (0.42 mg, 0.783 μmol), sodium ascorbate (1.6 mg, 7.83 μmol) and copper(II) sulfate pentahydrate (0.195 mg, 0.783 μmol) in *N-N*-dimethylformamide (1 mL). The solution was left to stir under an atmosphere of nitrogen for 24 hours. The reaction mixture was diluted with ethyl acetate (2 mL) and transferred to a separating funnel, washed with water (5 x 5mL), brine (3 mL) and dried with magnesium sulfate. The resulting suspension was filtered and the solvent removed under reduced pressure. The resulting mixture was absorbed onto silica and columned under gravity, eluting with ethyl acetate: acetone (9:1) affording a white solid. Subsequent physiochemical analysis confirmed this to be the title compound **149** (9mg, 6.25 μmol, 64%)

149 (9mg, 6.25 μmol, 64%) white solid. *R_f* 0.6 (ethyl acetate: acetone (9:1)). MP : 108-110°C (diethyl ether); ¹H-NMR (300MHz, CDCl₃) 8.08 (d, *J*2.5 Hz, 1H), 7.84 (d, *J*2.7 Hz, 2H), 7.56 (m, 2H), 7.43 (m, 1H), 7.36 – 7.19 (m, 21H), 7.14 (m, 2H), 5.38(m, 3H), 5.22 (d, *J*9.3 Hz, 2H), 5.04 (m, 3H), 4.90 (d, *J*11.0 Hz, 2H), 4.81 (d, *J*7.2 Hz, 2H), 4.73 (d, *J*17.2 Hz, 3H), 4.55 (d, *J*15.3 Hz, 3H), 4.44 (m, 2H), 4.33 (d, *J*14.9 Hz, 3H), 4.21 (d, *J*17.2 Hz, 2H), 4.08 (t, *J*6.1 Hz, 2H), 3.70 (d, *J*7.1 Hz, 2H), 3.62 (d, *J*5.6 Hz, 2H), 3.48 (s, 2H), 2.52 (dd, *J*5.0, 13.4 Hz, 1H), 2.10 (d, *J*1.1 Hz,

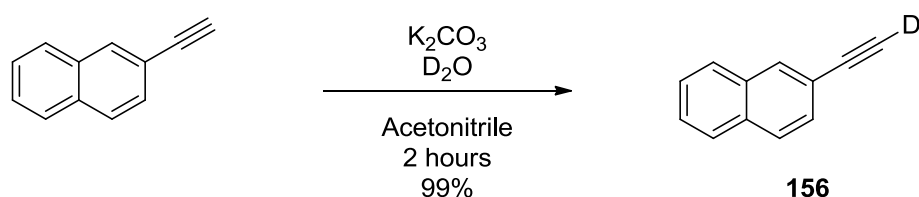
4H), 2.06 (s, 3H), 2.00 (s, 6H), 1.96 (d, $J_{5.9}$ Hz, 3H), 1.88 (s, 3H); ^{13}C -NMR (75MHz, CDCl_3) δ 171.07, 170.67, 170.35, 170.29, 168.27, 165.82, 148.43, 145.66, 142.64, 138.52, 138.05, 133.07, 129.11, 129.00, 128.44, 127.99, 127.91, 127.78, 127.71, 126.23, 122.27, 97.39, 84.63, 82.22, 75.68, 74.96, 72.73, 73.41, 72.60, 70.98, 70.65, 68.79, 68.04, 67.35, 66.72, 58.64, 35.75, 29.55, 23.06, 20.67, 20.55 ppm; FT-IR (KBr neat) 2967, 2925, 2862, 2253, 1747 C=O, 1683 C=O, 1500, 1454, 1369, 1229, 1070cm^{-1} ; m/z $[\text{ES}]^+$ M+Na (found) 1463.5, calc (1463.5). HRMS (NSI) Calcd for $\text{C}_{76}\text{H}_{82}\text{N}_9\text{O}_{20}$, M+H, 1440.5676; Found 1440.5678. $[\alpha]_D^{23}$ -7.2(c 1.0, CHCl_3).

General procedure for the deuteration of terminal alkynes



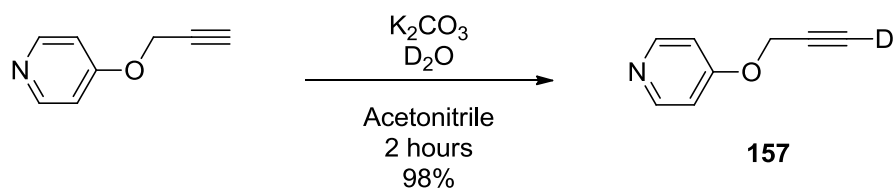
A flame-dried 10 mL round-bottomed flask was charged with an alkyne (1 eq) and potassium carbonate (1.5 eq) in acetonitrile (2mL). This was left to stir under an atmosphere of nitrogen gas for 30 minutes. To this deuterium oxide (500 μL , $\sim 50\text{eq}$) was added *via* syringe and left to stir for 1 hour. The resulting reaction mixture was diluted with dichloromethane (5 mL) and transferred to a 25 mL separating funnel. The organic layer was separated and dried with magnesium sulfate, filtered and the solvent removed under reduced pressure. Subsequent physicochemical analysis confirmed the alkyne had been deuterated. No further purification was necessary unless otherwise stated

2-ethynyl-(1-D)-naphthalene **156**



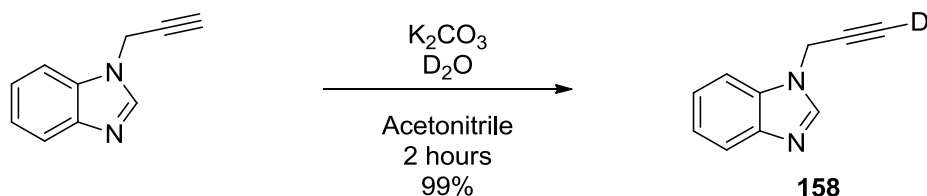
156 99% yield, 98% deuterium incorporation. Off white solid. No further purification necessary. *Rf* 0.7 (10% diethyl ether in hexane) MP 30-32°C (hexane). ^1H -NMR (400 MHz, CDCl_3) δ 8.37 (d, $J_{8.2}$ Hz, 1H, ArH), 7.87 (d, $J_{8.3}$ Hz, 2H, ArH), 7.75 (d, $J_{7.2}$ Hz, 1H, ArH), 7.57 (dt, $J_{7.0}$ Hz, 2H, ArH), 7.47 – 7.39 (m, 1H, ArH). ^{13}C -NMR (101 MHz, CDCl_3) δ 133.24, 133.03, 132.54, 128.78, 128.26, 128.01, 127.14, 126.85, 119.59, 83.78 (t, $J_{\text{C-D}}$ 7.1 Hz), 77.40 (t, $J_{\text{C-D}}$ 25.3 Hz) ppm. ATR-IR 3291 C-D, 2111 C-C cm^{-1} ; m/z LCMS $[\text{ES}]^+$ M+H, 154.0, HRMS calc for $\text{C}_{12}\text{H}_8\text{D}$, M+H, (154.0767) found (154.0765).

4-(prop-1-deuteronyloxy)pyridine 157



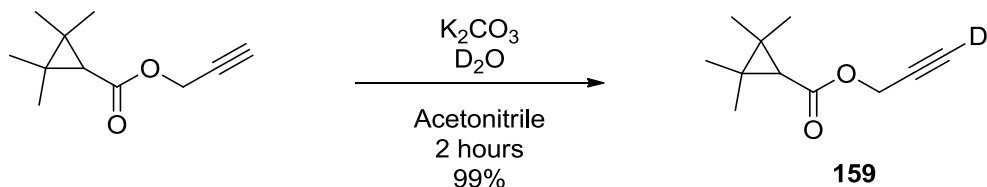
157 98% yield, 99% deuterium incorporation. Yellow solid. No further purification necessary. *R_f* 0.3 (10% diethyl ether in hexane). MP 162-163°C (hexane) ¹H-NMR (300 MHz, CDCl₃) δ 7.42 (d, *J*7.6 Hz, 2H, ArH), 6.35 (d, *J*7.7 Hz, 2H, ArH), 4.57 (s, 2H, CH₂). ¹³C-NMR (75 MHz, CDCl₃) δ 179.0, 139.23, 137.00, 118.97, 76.75 (t, *J*_{C-D}39.8 Hz), 74.90 (t, *J*_{C-D}7.5 Hz), 45.32 ppm; FT-IR [ATR] 2935 C-D, 2602 C-C cm⁻¹; *m/z* LCMS [ES]⁺ M+H 135.0, 2M+1 269.1, 2M+Na 291.1. HRMS calc for C₈H₆DNNaO, M+Na, (157.0488) found (157.0483)

1-(prop-1-deutero-ynyl)-1H-benzo[d]imidazole 158



158 99% yield, 99% deuterium incorporation. Pale yellow oil. No further purification necessary. *R_f* 0.2 (10% diethyl ether in hexane). ¹H-NMR (300 MHz, CDCl₃) δ 8.02 (s, 1H, CH), 7.82 (d, *J*5.8 Hz, 1H, ArH), 7.46 (d, *J*5.8 Hz, 1H, ArH), 7.39 – 7.18 (m, 2H, ArH), 4.86 (s, 2H, CH₂). ¹³C-NMR (101 MHz, CDCl₃) δ 142.24, 123.42, 122.74, 120.47, 109.74, 75.41 (t, *J*_{C-D}8.1 Hz), 74.78 (t, *J*_{C-D}39.4 Hz), 34.71 ppm. ATR-IR 3286 C-D cm⁻¹; *m/z* LCMS [ES]⁺ M+1 158.0, HRMS calc for C₁₀H₈DN₂, M+H, (158.0823), found (158.0822).

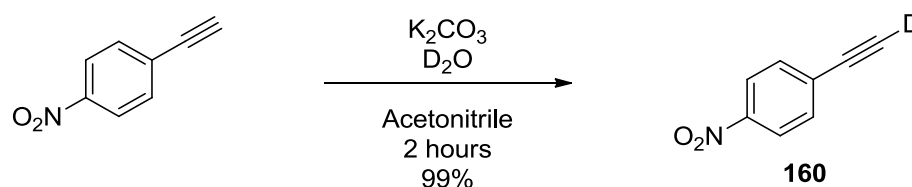
1-deutero-prop-2-ynyl 2,2,3,3-tetramethylcyclopropanecarboxylate 159



159 99% yield, 99% deuterium incorporation. Colourless oil. No further purification necessary. *R_f* 0.5 (10% diethyl ether in hexane). ¹H-NMR (300 MHz, CDCl₃) δ 4.60 (s, 2H, CH₂), 1.21 (s, 7H, 2CH₃, CH), 1.16 (s, 6H, 2CH₃). ¹³C-NMR (75 MHz, CDCl₃) δ 171.23, 77.78 (t, *J*_{C-D}7.5 Hz), 74.13 (t, *J*_{C-D}38.3 Hz), 51.07, 35.20, 30.63, 23.29, 16.32 ppm. FTIR [ATR] 2926 C-D, 2159 C-C, 1595

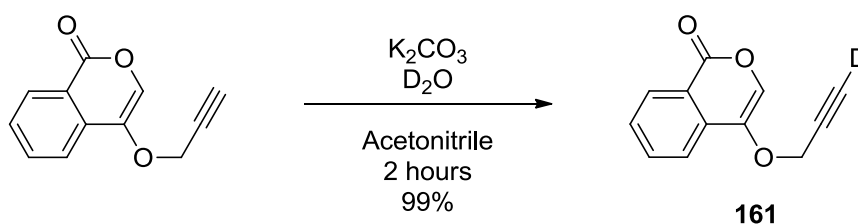
C=O cm^{-1} . m/z LCMS $[\text{ES}]^+$ M+H 181.1. HRMS calc for $\text{C}_{11}\text{H}_{16}\text{NaO}_2$, M+Na, (203.1048) found (203.1052)

1-deutero-ethynyl-4-nitrobenzene 160



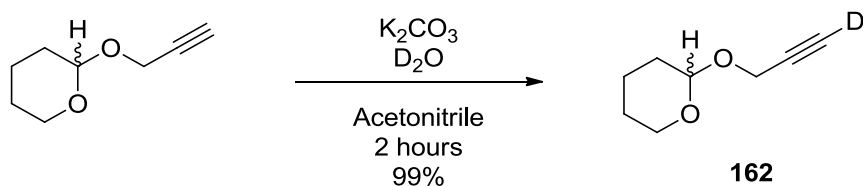
160 99% yield, 99% deuterium incorporation. Yellow solid. No further purification necessary. R_f 0.5 (10% diethyl ether in hexane). MP 130-131°C (hexane) $^1\text{H-NMR}$ (400 MHz, CDCl_3) δ 8.12 (d, $J_{8.9}$ Hz, 2H, ArH), 7.56 (d, $J_{8.9}$ Hz, 2H, ArH); $^{13}\text{C-NMR}$ (101 MHz, CDCl_3) δ 146.53, 131.95, 127.91, 122.54, 81.03 (t, $J_{\text{C-D}}$ 38.4 Hz) 80.15 (t, $J_{\text{C-D}}$ 8.1 Hz) ppm. FTIR [ATR] 3106 C-D, 2921, 2846, 2562 C-C, NO_2 , 1341 NO_2 cm^{-1} . m/z LCMS $[\text{ES}]^+$ 2M- NO_2 251.2. HRMS calc for $\text{C}_8\text{H}_4\text{DNNO}_2$, M+Na, (171.0281) found (171.0285)

4-(prop-1-deutero-ynoxy)-1H-isochromen-1-one 161



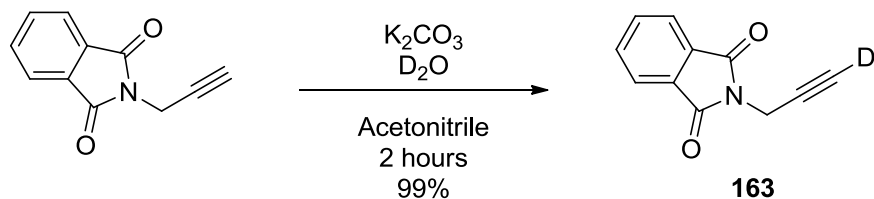
161 99% yield, 99% deuterium incorporation. White solid. No further purification necessary. R_f 0.7 (10% diethyl ether in hexane). MP 142-143°C (hexane). $^1\text{H-NMR}$ (300 MHz, CDCl_3) δ 7.82 (dd, $J_{7.9}$, 1.6 Hz, 1H, ArH), 7.65 – 7.47 (m, 1H, ArH), 7.39 – 7.20 (m, 2H, ArH), 5.82 (s, 1H, CH), 4.86 (s, 2H, CH_2). $^{13}\text{C-NMR}$ (101 MHz, CDCl_3) δ 163.24, 161.43, 152.34, 131.56, 122.99, 122.06, 115.77, 114.38, 90.70, 76.63 (t, $J_{\text{C-D}}$ 39.4 Hz), 74.25 (t, $J_{\text{C-D}}$ 7.6 Hz), 55.82 ppm. ATR-IR 3076 C-D, 2583, 2566, 1982, 1708 C=O cm^{-1} . m/z LCMS $[\text{ES}]^+$ M+Na 223.9. HRMS calc for $\text{C}_{12}\text{H}_7\text{DNNO}_3$, M+Na, (224.0434) found (224.0429)

2-(prop-1-deutero-ynoxy)tetrahydro-2H-pyran **162**



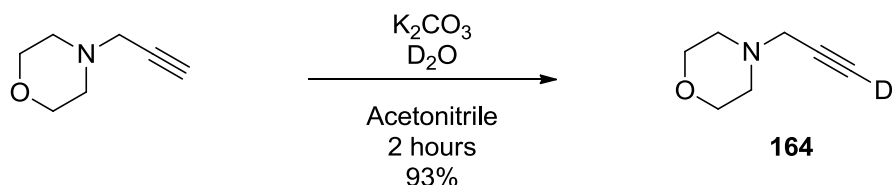
162 99% Yield, 95% deuterium incorporation. Colourless liquid. No further purification necessary. *R_f* 0.9 (10% diethyl ether in hexane) ¹H-NMR (300 MHz, CDCl₃) δ 4.74 (t, *J*3.1 Hz, 1H, CH), 4.33 – 4.00 (m, 2H, CH₂), 3.88 – 3.64 (m, 1H, CHH), 3.57 – 3.29 (m, 1H, CHH), 1.87 – 1.28 (m, 6H, (CH₂)₃). ¹³C-NMR (101 MHz, CDCl₃) δ 96.83, 79.41(t, *J*_{C-D}7.1 Hz), 73.95 (t, *J*_{C-D}38.4 Hz), 62.00, 54.03, 30.30, 25.46, 19.09 ppm. FTIR [ATR] 2946 C-D, 1120 cm⁻¹. *m/z* LCMS [ES]⁺ M+H 142.9. HRMS calc for C₈H₁₁DNaO₂, M+Na, (164.0798) found (164.0795).

2-(prop-1-deutero-ynyl)isoindoline-1,3-dione **163**



163 99% yield, 99% deuterium incorporation. White solid. No further purification necessary. *R_f* 0.6 (10% diethyl ether in hexane) MP 135-136°C (diethyl ether). ¹H-NMR (400 MHz, CDCl₃) δ 7.82 (dd, *J*5.5, 3.0 Hz, 2H, ArH), 7.68 (dd, *J*5.4, 3.1 Hz, 2H, ArH), 4.39 (s, 2H, CH₂). ¹³C-NMR (101 MHz, CDCl₃) δ 167.17, 134.43, 132.13, 123.77, (alkyne carbon resonances obscured by CDCl₃ peak), 71.69 (t, *J*_{C-D}6.1 Hz), 27.16 ppm. ATR-IR 2967 C-D, 2591, 1989, 1770C=O, 1703 C=O cm⁻¹. *m/z* LCMS [ES]⁺ M+H 141.9. HRMS calc for C₁₁H₆DNNaO₂, M+Na, (209.0437) found (209.0439).

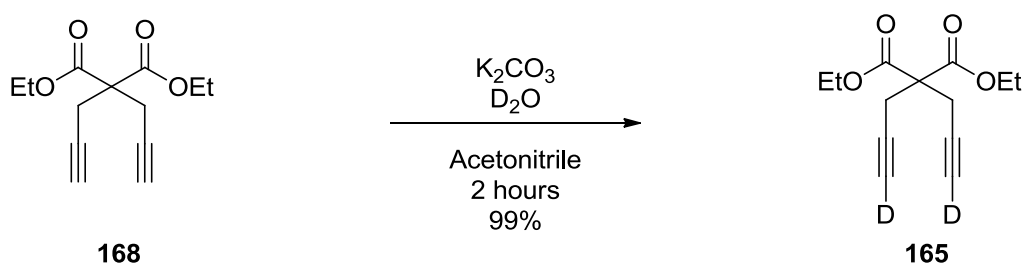
4-(prop-1-deutero-ynyl)morpholine **164**



164 93% yield, 95% deuterium incorporation. Red liquid. No further purification necessary. *R_f* 0.9 (10% diethyl ether in hexane) ¹H-NMR (300 MHz, CDCl₃) δ 3.77 – 3.61 (m, 4H, 2CH₂), 3.25 (s, 2H, CH₂), 2.64 – 2.43 (m, 4H, 2CH₂). ¹³C-NMR (75 MHz, CDCl₃) δ 78.11 (t, *J*_{C-D}7.1 Hz), 73.40 (t, *J*_{C-D}38.4 Hz) 66.74, 52.07, 47.05 ppm. FTIR-[ATR] 2857 C-D, 2582C-C, 1454, 1289, 1113,

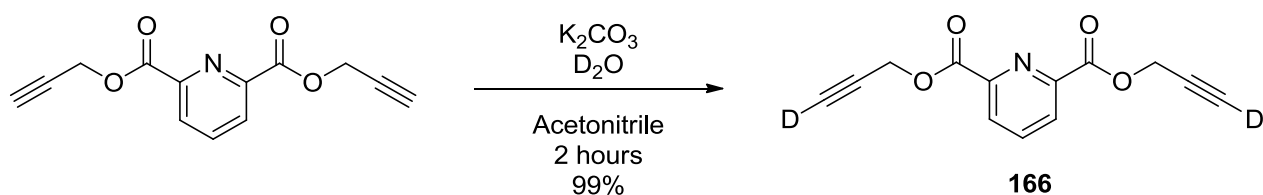
1005, 860 cm^{-1} . m/z LCMS $[\text{ES}]^+$ $\text{M}+\text{H}$ 127.1. HRMS calc for $\text{C}_7\text{H}_{10}\text{DNNaO}$, $\text{M}+\text{Na}$, (149.0801) found (149.0800)

Diethyl 2,2-di(deutero-prop-1-ynyl)malonate 165



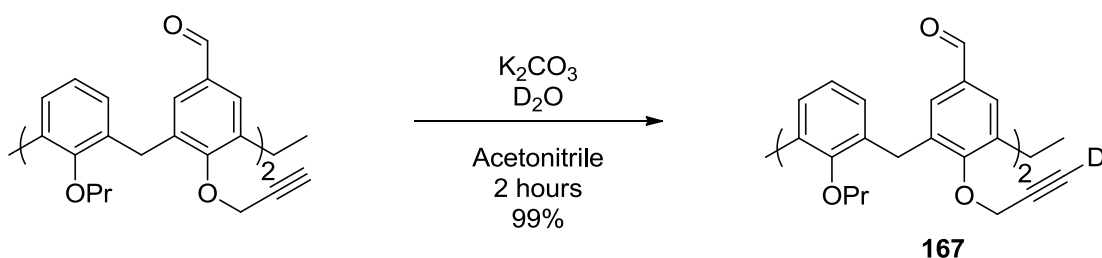
165 99% yield, 99% deuterium incorporation. White solid. No further purification necessary. R_f 0.2 (10% diethyl ether in hexane). MP 28-30°C (diethyl ether). $^1\text{H-NMR}$ (400 MHz, CDCl_3) δ 4.15 (q, $J_{7.1}$ Hz, 4H, $(\text{CH}_2)_2$), 2.90 (s, 4H, $(\text{CH}_2)_2$), 1.19 (t, $J_{7.1}$ Hz, 6H, $(\text{CH}_3)_2$). $^{13}\text{C-NMR}$ (101 MHz, CDCl_3) δ 168.73, 78.08 (t, $J_{\text{C-D}}$ 7.2 Hz), 71.66 (t, $J_{\text{C-D}}$ 38.4 Hz), 62.23, 56.37, 22.59, 14.16 ppm. ATR-IR 2983 C-D, 2587, 2118 C-C, 1732 C=O, 1288, 1188 cm^{-1} . m/z LCMS $[\text{ES}]^+$ $\text{M}+\text{Na}$ 261.1. HRMS calc for $\text{C}_{13}\text{H}_{14}\text{D}_2\text{NaO}_4$, $\text{M}+\text{Na}$, (261.1072) found (261.1068)

Di-prop-1-deutero-ynyl pyridine-2,6-dicarboxylate 166



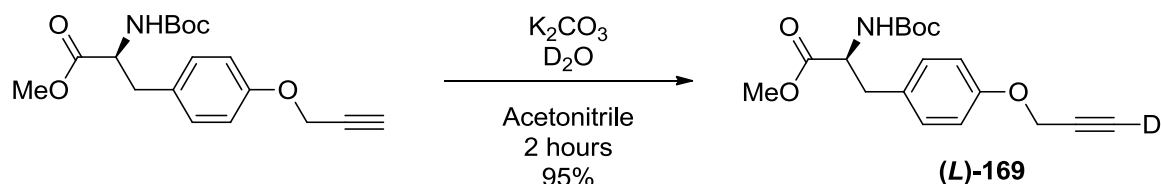
166 99% yield, 96% deuterium incorporation. White solid. No further purification necessary. R_f 0.2 (10% diethyl ether in hexane). MP 108-109°C (diethyl ether). $^1\text{H-NMR}$ (300 MHz, CDCl_3) δ 8.33 (d, $J_{8.1}$ Hz, 2H, ArH), 8.21 – 7.90 (m, 1H, ArH), 5.00 (s, 4H, $(\text{CH}_2)_2$). $^{13}\text{C-NMR}$ (101 MHz, CDCl_3) δ 162.69, 146.82, 137.46, 127.49, 77.45 (t, $J_{\text{C-D}}$ 7.1 Hz), 74.77 (t, $J_{\text{C-D}}$ 39.4 Hz), 52.54 ppm. ATR-IR 2574 C-D, 1979, 1729 C=O, 1446, 1384, 1368, 1133 cm^{-1} . m/z LCMS $[\text{ES}]^+$ $\text{M}+\text{H}$ 246.1, $\text{M}+\text{Na}$ 268.1, $2\text{M}+\text{Na}$ 513.3. HRMS Calc $\text{C}_{13}\text{H}_8\text{D}_2\text{NO}_4$, $\text{M}+\text{H}$, (246.0730), found (246.0732)

1,3 dipropyl, 2,4- di-deutero-propynyl-para-di-formyl-calix[4]arene 167



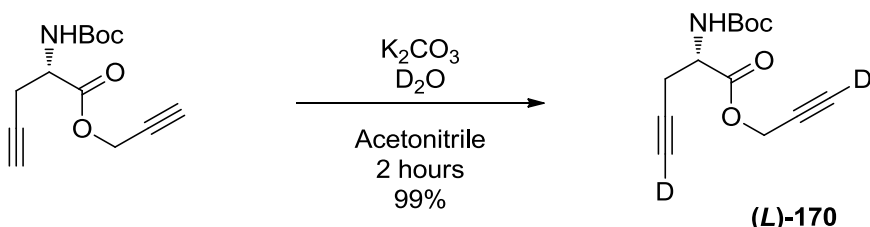
167 99% yield, 97% deuterium incorporation. Off white solid. No further purification necessary. *Rf* 0.5 (25% diethyl ether in hexane). MP 176-178°C (diethyl ether). ¹H-NMR (400 MHz, CDCl₃) δ 9.91 (d, *J* 2.7 Hz, 2H, 2CH), 7.64 (s, 4H, ArH), 6.25 (dd, *J* 8.4, 6.6 Hz, 2H, ArH), 6.17 (d, *J* 7.5 Hz, 4H, ArH), 5.01 (s, 4H, 2CH₂), 4.51 (d, *J* 13.5 Hz, 4H, 4CH), 3.67 (t, *J* 6.9 Hz, 4H, 2CH₂), 3.27 (d, *J* 13.6 Hz, 4H, 2CH), 1.88 (m, 4H, 2CH₂), 1.09 – 0.94 (m, 6H, 2CH₃). ¹³C-NMR (101 MHz, CDCl₃) δ 191.75, 160.97, 155.40, 138.92, 132.25, 132.06, 130.49, 127.87, 122.65, 79.26 (t, *J*_{C-D}4.0 Hz) 77.12 (t, *J*_{C-D}31.3 Hz), 60.19, 31.25, 23.59, 10.86 ppm. ATR-IR 2924.29 C-D, 1681.41 C=O, 1126.40 cm⁻¹. *m/z* LCMS [ES]⁺ M+Na 665.2. HRMS calc for C₄₂H₃₈D₂NaO₆, M+Na, (665.2848) found (665.2852)

(S)-methyl 2-(tert-butoxycarbonylamino)-3-(4-(prop-1-deutero-nyloxy)phenyl) propanoate (L)-169



(L)-169 95% yield, 99% deuterium incorporation. Red oil. No further purification necessary. *Rf* 0.6 (50% diethyl ether in hexane). ¹H-NMR (400 MHz, CDCl₃) δ 6.98 (d, *J*8.4 Hz, 2H, ArH), 6.83 (d, *J*8.6 Hz, 2H, ArH), 4.90 (d, *J*7.7 Hz, 1H, NH), 4.60 (s, 2H, CH₂), 4.48 (dd, *J*13.5, 5.8 Hz, 1H, αCH), 3.64 (s, 3H, CH₃), 2.96 (qd, *J*13.9, 6.1 Hz, 2H, βCH₂), 1.35 (s, 9H, (CH₃)₃). ¹³C-NMR (101 MHz, CDCl₃) δ 172.59, 156.81, 155.28, 130.51, 130.42, 129.13, 121.51, 115.12, 80.12, 78.29 (t, *J*_{C-D}7.1 Hz), 75.46 (t, *J*_{C-D}44.4 Hz), 55.96, 54.65 ppm; *m/z* LCMS [ES]⁺ M+Na 357.3. HRMS calc for C₁₈H₂₂DNaO₅, M+Na, (357.1537) found (357.1541). [α]²⁴_D +42.9 (c 1.0, CHCl₃)

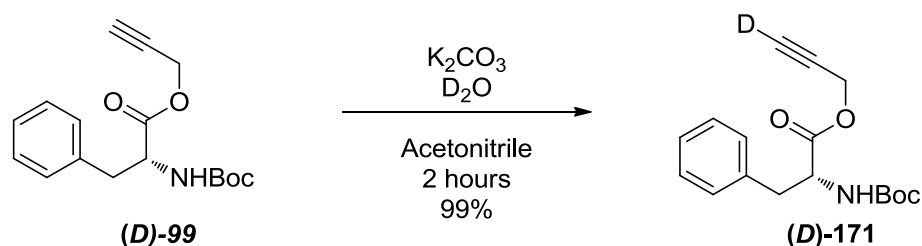
(S)-prop-1-deutero-ynyl 2-(tert-butoxycarbonylamino)pent-4-deutero-ynoate (L)-170



(L)-170 99% yield, 99% deuterium incorporation. Colourless oil. No further purification necessary. *Rf* 0.8 (50% diethyl ether in hexane). ¹H-NMR (400 MHz, CDCl₃) δ 5.28 (d, *J*8.0 Hz, 1H, NH), 4.70 (s, 2H, CH₂), 4.53 – 4.38 (m, 1H, αCH), 2.70 (qd, *J*4.8 Hz, 2H, CH₂), 1.39 (s, 9H, (CH₃)₃). ¹³C-NMR (101 MHz, CDCl₃) δ 79.36, 76.60 (t, *J*_{C-D}7.1 Hz), 75.40 (t, *J*_{C-D}8.1 Hz), 74.28 (t, *J*_{C-D}38.4 Hz), 70.64 (t, *J*_{C-D}38.4 Hz) 52.06, 50.86, 27.26, 21.71 ppm. FTIR [ATR] 3387 C-D, 2978, 2593 C-

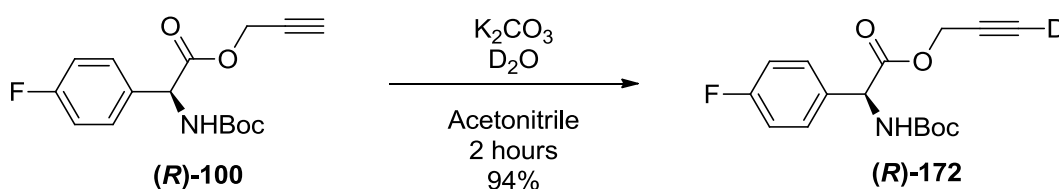
C, 1753 C=O, 1713 C=O cm^{-1} . m/z LCMS [ES]⁺ M+Na 276.0. HRMS calc for $\text{C}_{13}\text{H}_{15}\text{D}_2\text{NNaO}_4$, M+Na, (276.1181) found (276.1184). $[\alpha]_{\text{D}}^{29} +10.6$ (c 1.0, CHCl_3).

(R)-prop-1-deutero-ynyl 2-(tert-butoxycarbonylamino)-3-phenylpropanoate (D)-171



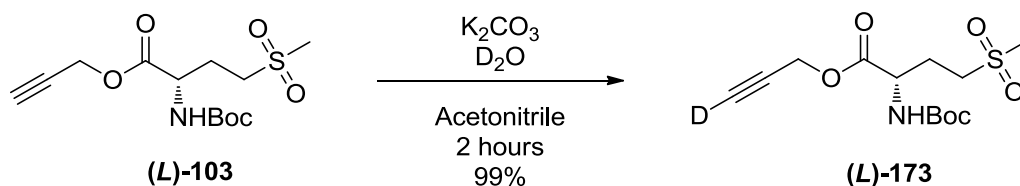
(D)-171 99% yield, 99% deuterium incorporation. Colourless oil. No further purification necessary. R_f 0.7 (1:5, ethyl acetate : hexane). $^1\text{H-NMR}$ (300 MHz, CDCl_3) δ 7.34 – 7.20 (m, 3H, ArH), 7.15 (dd, $J_{7,8}$, 1.7 Hz, 2H, ArH), 4.94 (d, $J_{8,2}$ Hz, 1H, NH), 4.72 (m, 2H, CH_2), 4.66 – 4.57 (m, 1H, αCH), 3.25 – 2.92 (m, 2H, βCH_2), 1.41 (s, 9H, $(\text{CH}_3)_3$). $^{13}\text{C-NMR}$ (101 MHz, CDCl_3) δ 171.15, 155.06, 135.69, 129.41, 128.60, 127.13, 80.06, (alkyne carbon resonances obscured by CDCl_3 peak), 75.18 (t, $J_{\text{C-D}}$ 38.4 Hz), 54.30, 52.63, 38.10, 28.28 ppm. FTIR [ATR] 2979 C-D, 1748 C=O, 1701C=O, 1411, 1162, 906 cm^{-1} . m/z LCMS [ES]⁺ M+Na 327.0 HRMS Calc for $\text{C}_{17}\text{H}_{20}\text{DNO}_4\text{Na}$, M+Na, 327.1426, found: 327.1435. $[\alpha]_{\text{D}}^{27} -12.9$ (c 1.0, CHCl_3)

(R)-prop-1-deutero-ynyl 2-(tert-butoxycarbonylamino)-2-(4-fluorophenyl)acetate. (R)-172



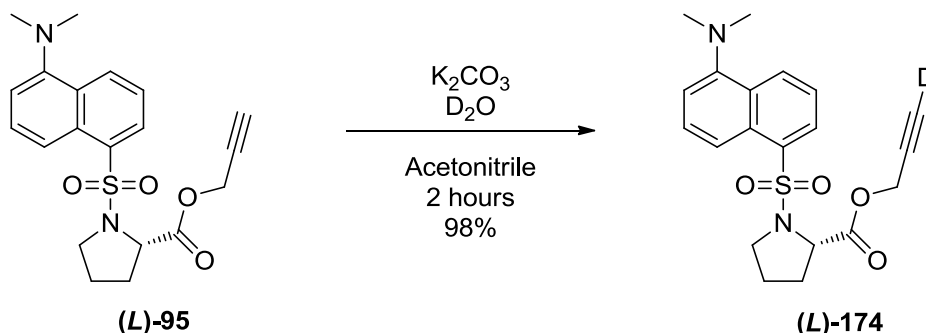
(R)-172 94% yield, 96% deuterium incorporation. Yellow oil. No further purification necessary. R_f 0.7 (1:5, ethyl acetate : hexane). $^1\text{H-NMR}$ (400 MHz, CDCl_3) δ 7.34 – 7.29 (m, 2H, ArH), 7.02 (m, 2H, ArH), 5.28 (d, $J_{2,4}$ Hz, 1H, NH), 4.80 – 4.58 (m, 3H, CH_2 , αCH), 1.40 (s, 9H, $(\text{CH}_3)_3$). $^{13}\text{C-NMR}$ (101 MHz, CDCl_3) δ 170.46, 162.76 (d, $J_{\text{C-F}}$ 248.5 Hz), 132.31, 128.98 (d, $J_{\text{C-F}}$ 9.1 Hz), 115.90 (d, $J_{\text{C-F}}$ 21.2 Hz), 80.64, 76.24 (t, $J_{\text{C-D}}$ 7.1 Hz), 75.34 (t, $J_{\text{C-D}}$ 38.4 Hz), 56.93, 53.34, 28.47 ppm. FTIR [ATR] 2979 C-D, 2593C-C, 1747 C=O, 1702 C=O cm^{-1} . m/z LCMS [ES]⁺ M+Na 330.9. HRMS calc for $\text{C}_{16}\text{H}_{17}\text{DFNNaO}_4$, M+Na, (331.1180) found (331.1177). $[\alpha]_{\text{D}}^{27} -47.5$ (c1.0, CHCl_3).

(S)-prop-1-deutero-ynyl 2-(tert-butoxycarbonylamino)-4-(methylsulfonyl) butanoate (L)-173



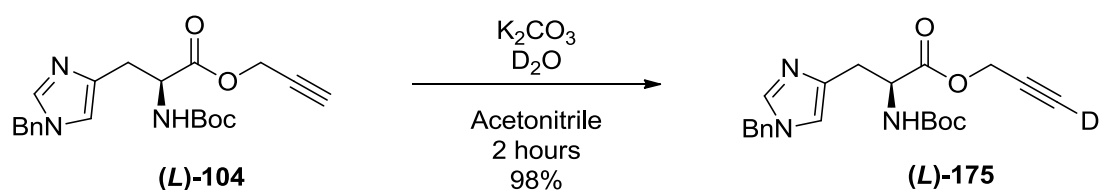
(L)-173 99% yield, 95% deuterium incorporation. White solid. No further purification necessary. *R_f* 0.5 (1:5, ethyl acetate : hexane). MP 86-88°C (hexane) ¹H-NMR (400 MHz, CDCl₃) δ 5.13 (s, 1H, NH), 4.70 (m, 2H, CH₂), 4.38 (s, 1H, αCH), 3.07 (m, 2H, βCH₂), 2.87 (s, 3H, CH₃), 2.40 (m, 1H, CHH), 2.20 – 2.01 (m, 1H, CHH), 1.38 (s, 9H, (CH₃)₃). ¹³C-NMR (101 MHz, CDCl₃) δ 170.47, 155.30, 80.78, (alkyne carbon resonances obscured by CDCl₃ peak), 53.24, 51.98, 50.98, 40.80, 28.25, 25.74 ppm. FTIR [ATR] 3355 C-D, 2160 C-C, 1977, 1749 C=O, 1707 C=O, 1367 O=S=O cm⁻¹; *m/z* LCMS [ES]⁺ M+Na 343. HRMS calc for C₁₃H₂₀DNNaO₆S, M+Na, (343.1050) found (343.1047). [α]²⁷_D +13.6 (c 1.0, CHCl₃)

(S)-prop-1-deutero-ynyl 1-(5-(dimethylamino)naphthalen-1-ylsulfonyl) pyrrolidine-2-carboxylate (L)-174



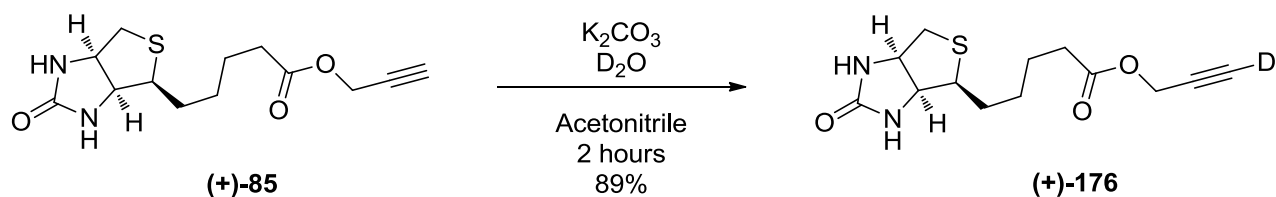
(L)-174 98% yield, 98% deuterium incorporation. Yellow oil. No further purification necessary. *R_f* 0.3 (1:5, ethyl acetate : hexane). ¹H-NMR (300 MHz, CDCl₃) δ 8.58 – 8.51 (m, 1H, ArH), 8.46 (d, *J*8.7 Hz, 1H, ArH), 8.27 (dd, *J*7.4, 1.3 Hz, 1H, ArH), 7.54 (m, 2H, ArH), 7.18 (dd, *J*7.6, 0.8 Hz, 1H, ArH), 4.59 – 4.52 (m, 1H, αCH), 4.50 (d, *J*2.5 Hz, 2H, CH₂), 3.59 – 3.42 (m, 2H, CH₂), 2.87 (s, 6H, (CH₃)₂), 2.23 – 2.13 (m, 1H, CHH), 2.12 – 2.00 (m, 2H, CHH, CH'H'), 1.95 – 1.80 (m, 1H, CH'H'). ¹³C-NMR (101 MHz, CDCl₃) δ 171.39, 151.82, 134.49, 130.86, 130.52, 130.19, 128.34, 123.37, 119.86, 115.45, (alkyne carbon resonances obscured by CDCl₃ peak), 60.03, 52.72, 48.72, 45.63, 31.20, 24.91 ppm. FTIR [ATR] 2944 C-D, 2583, 1755 C=O, 1574, 1332 O=S=O, 1142 O=S=O cm⁻¹. *m/z* LCMS [ES]⁺ M+1 388.1, M+Na 410.3. HRMS calc for C₂₀DH₂₁N₂NaO₂, M+Na, (346.1579) found (346.1575) [α]²⁷_D -64.2 (c 1.0, CHCl₃).

(S)-prop-1-deutero-ynyl-3-(1-benzyl-1H-imidazol-4-yl)-2-(tert-butoxycarbonyl amino) propanoate (L)-175



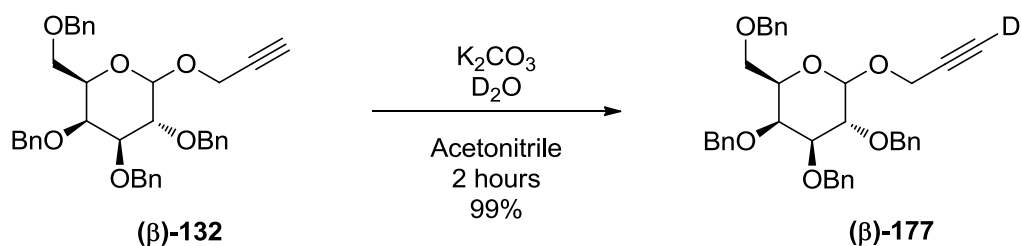
(L)-175 98% yield, 98% deuterium incorporation. Brown oil. No further purification necessary. *R_f* 0.3 (1:5, ethyl acetate : hexane). ¹H-NMR (300 MHz, CDCl₃) δ 7.77 (s, 1H, CH), 7.36 (d, *J*_{6.8} Hz, 3H, ArH), 7.16 (dd, *J*_{7.5}, 1.9 Hz, 2H, ArH), 6.74 (s, 1H, CH), 5.99 (d, *J*_{9.5} Hz, 1H, NH), 5.09 (s, 2H, CH₂), 4.78 – 4.43 (m, 3H, CH₂, αCH), 3.12 (m, 2H, βCH₂), 1.41 (s, 9H, (CH₃)₃). ¹³C-NMR (75 MHz, CDCl₃) δ 171.32, 155.61, 137.59, 137.32, 136.22, 128.94, 128.20, 127.29, 117.15, 79.89 (t, *J*_{C-D}6.1 Hz) 79.43, 74.83 (t, *J*_{C-D}38.3 Hz), 53.40, 52.16, 50.56, 29.72, 28.13 ppm. ATR-IR: 1707.90 C=O cm⁻¹. *m/z* LCMS [ES]⁺ M+H 385.3, M+Na 407.1. HRMS calc for C₂₁H₂₄DN₃NaO₄, M+Na, (407.1806) found (407.1810). [α]_D²⁷ -6.2 (c 1.0, CHCl₃).

Prop-1-deutero-ynyl 5-((3a*S*,4*S*,6a*R*)-2-oxohexahydro-1H-thieno[3,4-*d*]imidazol-4-yl)pentanoate (+)-176



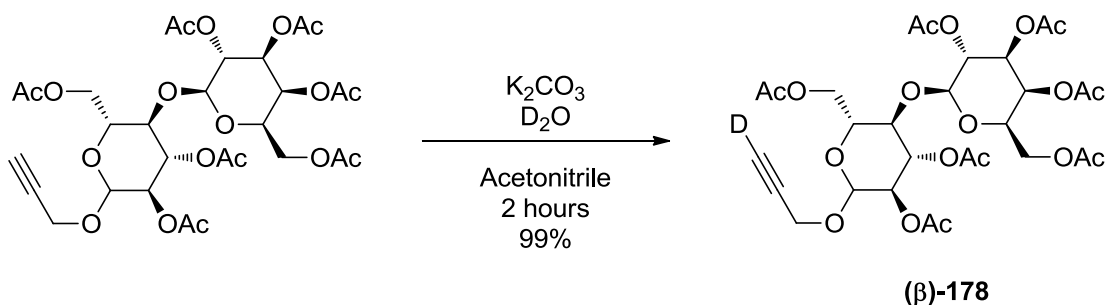
(+)-176 89% yield, 98% deuterium incorporation. Purified by column chromatography on silica and eluted with 3% methanol in dichloromethane. White solid. *R_f* 0.45 (3% methanol in dichloromethane). MP 58-60°C. ¹H-NMR (300 MHz, CDCl₃) δ 5.94 (s, 1H, NH), 5.41 (s, 1H, NH), 4.67 (s, 2H, CH₂), 4.50 (dd, *J*_{7.3}, 5.4 Hz, 1H, CH), 4.30 (dd, *J*_{7.8}, 4.6 Hz, 1H, CH), 3.14 (dd, *J*_{12.0}, 7.3 Hz, 1H, CH), 2.98 – 2.64 (m, 2H, CH₂), 2.38 (t, *J*_{7.5} Hz, 2H, CH₂), 1.78 – 1.60 (m, 4H, (CH₂)₂), 1.46 (m, 2H, CH₂). ¹³C-NMR (101 MHz, CDCl₃) δ 171.62, 161.75, (alkyne carbon resonances obscured by CDCl₃ peak), 60.82, 59.04, 54.11, 50.87, 39.53, 32.51, 28.69, 27.21, 23.56 ppm. FT-IR [ATR] 3219 C-D, 2929, 1732C=O, 1698 C=O, 1464, 1165 cm⁻¹. *m/z* LCMS [ES]⁺ M+Na 306.1. HRMS calc for C₁₃H₁₇DN₂NaO₃S, M+Na, (306.0999) found (306.1001). [α]_D²⁴ 36.8 (c 1.0, CHCl₃).

(2R,3R,4S,5R,6S)-3,4,5-tris(benzyloxy)-2-(benzyloxymethyl)-6-(prop-1-deutero-ynyloxy)tetrahydro-2H-pyran (β)-177



(β)-177 99% yield, 99% deuterium incorporation. White solid. No further purification necessary. *R_f* 0.3 (1:5, ethyl acetate : hexane). MP: 72-73°C (diethyl ether), ¹H-NMR (300 MHz, CDCl₃) δ 7.54 – 7.07 (m, 20H, ArH), 5.02 (d, *J*10.8 Hz, 1H, CH), 4.97 (d, *J*10.9 Hz, 1H, CH), 4.84 (t, *J*11.2 Hz, 2H, CH₂), 4.73 (d, *J*10.8 Hz, 1H, CH), 4.66 (t, *J*4.5 Hz, 1H, CH), 4.63 (s, 1H, CH), 4.58 (d, *J*3.4 Hz, 1H, CH), 4.54 (d, *J*2.2 Hz, 1H, CH), 4.48 (d, *J*6.0 Hz, 2H,), 3.82 – 3.60 (m, 4H), 3.52 (dd, *J*14.2, 5.3 Hz, 2H). ¹³C-NMR (101 MHz, CDCl₃) δ 138.62, 138.41, 138.12, 128.54 – 128.19 (m), 128.05 – 127.43 (m), 101.47, 84.63, 82.00, 78.59 (t, *J*_{C-D}7.1 Hz) 77.67, 75.73, 74.90 (t, *J*_{C-D}11.1 Hz), 73.52, 68.81, 55.97 ppm. FTIR [ATR] 3029 C-D, 2865, 1604, 1496, 1452, 1360 cm⁻¹. *m/z* LCMS [ES]⁺ M+Na 602.4. HRMS calc for C₃₇H₃₇DNaO₆, M+Na, (602.2629) found (602.2628). [α]_D²⁴ -6.0 (c 1.0, CHCl₃).

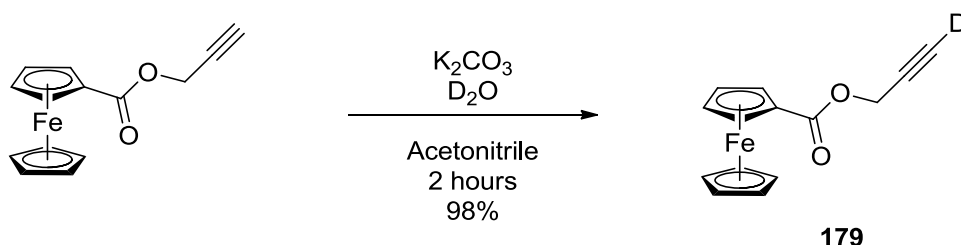
(2R,3S,4S,5R,6S)-2-(acetoxymethyl)-6-((2R,3R,4S,5R)-4,5-diacetoxy-2-(acetoxymethyl)-6-(prop-1-deutero-ynyloxy)tetrahydro-2H-pyran-3-yloxy)tetrahydro-2H-pyran-3,4,5-triyl triacetate (β)-178



(β)-178 99% yield, 99% deuterium incorporation. White solid. No further purification necessary. *R_f* 0.35 (1:5, ethyl acetate : hexane). MP 77-78°C (diethyl ether). ¹H-NMR (300 MHz, CDCl₃) δ 5.33 (d, *J*3.3 Hz, 1H, CH), 5.30 – 5.22 (m, 1H, CH), 5.20 (d, *J*9.4 Hz, 1H, CH), 5.09 (dd, *J*10.4, 7.9 Hz, 1H, CH), 4.92 (ddd, *J*11.4, 8.6, 5.7 Hz, 2H, CH₂), 4.72 (d, *J*7.9 Hz, 1H, CH), 4.52 – 4.43 (m, 2H, CH₂), 4.33 (d, *J*6.3 Hz, 2H, CH₂), 4.15 – 3.99 (m, 3H, (CH)₃), 3.93 – 3.82 (m, 1H, CH), 3.78 (d, *J*9.4 Hz, 1H, CH), 3.62 (ddd, *J*9.9, 4.8, 2.0 Hz, 1H, CH), 2.17 – 2.12 (m, 3H, CH₃), 2.10 (d, *J*4.3 Hz, 4H, CH₃, CHHH), 2.08 – 2.01 (m, 11H), 1.99 (t, *J*3.7 Hz, 1H), 1.94 (s, 2H). ¹³C-NMR (101

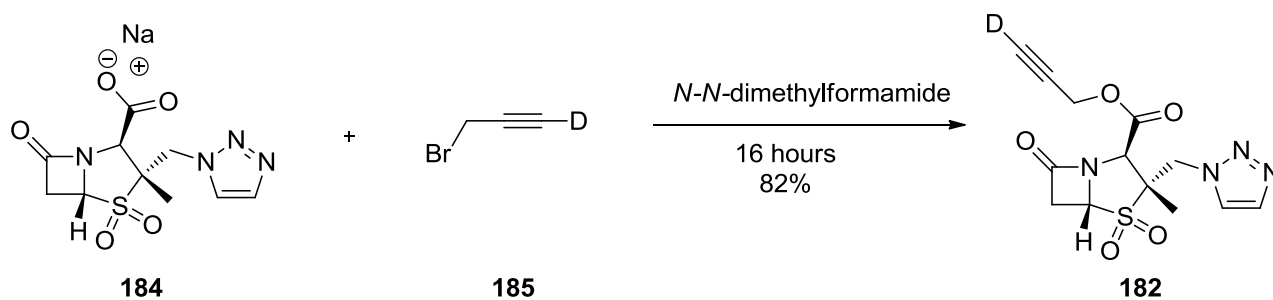
MHz, CDCl₃) δ 170.54, 170.34, 170.26, 169.93, 169.24, 101.20, 98.04, (alkyne carbon resonances obscured by CDCl₃ peak), 76.30, 72.92, 72.85, 71.46, 71.15, 70.86, 69.26, 66.78, 62.00, 61.00, 56.05, 21.06, 20.99, 20.92, 20.84, 20.71 ppm. ATR-IR: 1743 C=O, 1368, 1218, 1053, 901 cm⁻¹; *m/z* LCMS [ES]⁺ M+Na 336.9. HRMS calc for C₂₉H₃₈NaO₁₈, M+Na, (697.1956) found (697.1959). $[\alpha]_D^{24}$ -24.5 (c 1.0, CHCl₃).

1-deutero-propynyl-1-ferrocenoate **179**



179 98% yield, 98% deuterium incorporation. Orange solid. No further purification necessary. *R_f* 0.7 (1:5, ethyl acetate : hexane). MP 76-76°C. ¹H-NMR (300 MHz, CDCl₃) δ 4.87 – 4.83 (m, 2H, ArH), 4.82 (s, 2H, CH₂), 4.45 – 4.39 (m, 2H, ArH), 4.25 (s, 5H, ArH). ¹³C-NMR (101 MHz, CDCl₃) δ 170.06, 77.08(t, *J*_{C-D}7.1 Hz), 73.26 (t, *J*_{C-D}39.4 Hz), 70.61, 69.25, 68.83, 50.47 ppm. ATR-IR 2578 C-D, 1980, 1712 C=O cm⁻¹. *m/z* LCMS [ES]⁺ M+K 297.1. HRMS calc for C₁₄H₁₃DFeNO₂, M+NH₄, (285.0515) found (285.0510).

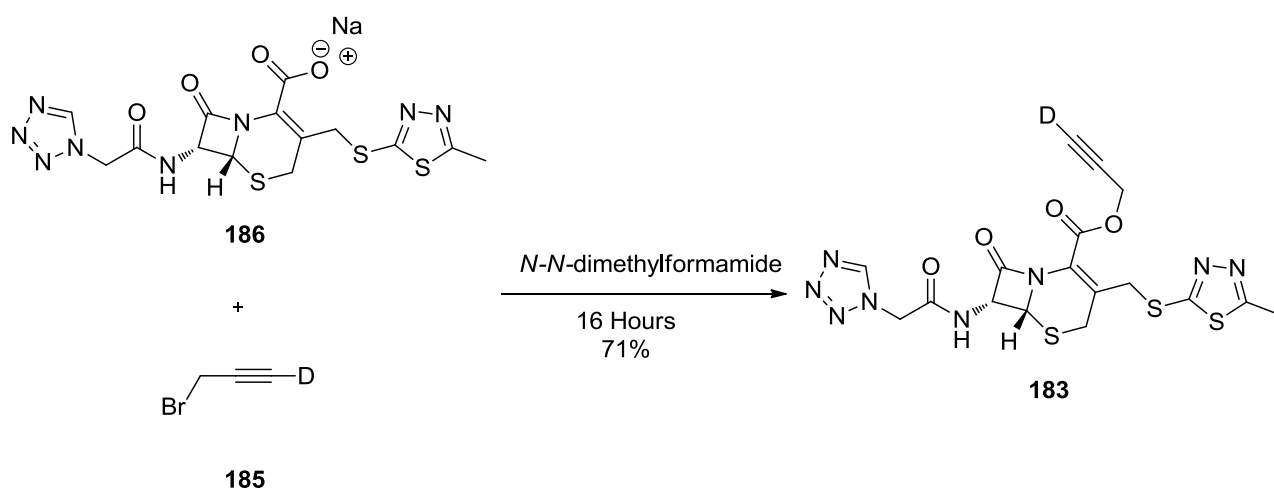
Synthesis of deuterio-1-propargyl tazobactam **182**



A flame-dried 10 mL round-bottomed flask was charged with tazobactam sodium salt **184** (30 mg, 0.093 mmol) in *N,N*-dimethylformamide (2 ml). To this *d*-1-propargyl bromide **185** (0.012 ml, 0.140 mmol) was added and left to stir under an atmosphere of argon gas at ambient temperature for 16 hours. The solvent was removed under reduced pressure and the residue was transferred to a silica column and eluted with 1-5% methanol in dichloromethane. This afforded a white solid and subsequent physicochemical analysis confirmed this was the title compound (**182**) (26 mg, 0.077 mmol, 82 % yield, 96% deuterium incorporation).

182 White solid. *R_f* 0.6 (5% methanol in dichloromethane). MP 140-142°C (diethyl ether) ¹H-NMR (300 MHz, CDCl₃) δ 7.82 (d, *J*_{1.1} Hz, 1H, CH), 7.76 (d, *J*_{1.0} Hz, 1H, CH), 5.09 (q, *J*_{15.0} Hz, 2H, CH₂), 4.85 (q, *J*_{15.4} Hz, 2H, CH₂), 4.67 (dd, *J*_{4.2}, 2.0 Hz, 1H, CH), 4.60 (s, 1H, CH), 3.56 (qd, *J*_{16.3}, 3.1 Hz, 2H, CH₂), 1.41 (s, 3H, CH₃). ¹³C-NMR (101 MHz, CDCl₃) δ 169.62, 165.37, 134.38, 125.76, 75.32 (t, *J*_{C-D}7.1 Hz), 65.29, 62.58, 60.28, 54.01, 53.43, 50.52, 39.22, 16.13 ppm. ATR-IR 3019 C-D, 2968, 2579, 1983, 1792 C=O, 1756 C=O, 1404, 1376 O=S=O, 1322, 1274, 1187 O=S=O cm⁻¹. *m/z* LCMS [ES]⁺ M+Na 362.0 HRMS calc for C₁₃H₁₃DN₄NaO₅S, M+Na, (362.0645) found (362.0649). [α]_D²⁴ +27.4 (c 1.0, CHCl₃).

Synthesis of deuterio-1-propargyl cefazolin **183**

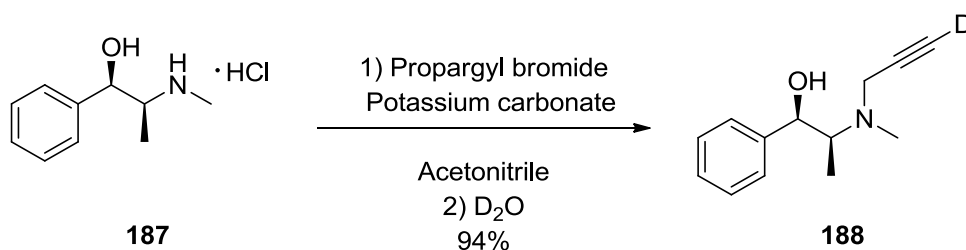


A flame-dried 10 mL round-bottomed flask was charged with cefazolin sodium salt **186** (30 mg, 0.063 mmol) in *N,N*-dimethylformamide (2 ml). To this 1-deutero-propargyl bromide **185** (8.14 μl, 0.094 mmol) was added and left to stir under an atmosphere of argon gas at ambient temperature for 16 hours. The solvent was removed under reduced pressure and transferred to a silica column eluting with 1-5% methanol in dichloromethane to afford a white solid. Subsequent physicochemical analysis confirmed this to be the title compound **183** (22 mg, 0.045 mmol, 70.8 % yield, 96% deuterium incorporation).

183 White solid. *R_f* 0.3 (5% methanol in dichloromethane) MP 128-130°C (diethyl ether). ¹H-NMR (300 MHz, CDCl₃) δ 8.90 (s, 1H, CH), 7.76 (d, *J*_{8.9} Hz, 1H, NH), 5.82 (dd, *J*_{8.7}, 4.8 Hz, 1H, CH), 5.32 (dd, *J*_{41.0}, 16.6 Hz, 2H, CH₂), 5.00 (d, *J*_{4.9} Hz, 1H, CH), 4.88 (q, *J*_{15.6} Hz, 2H, CH₂), 4.60 (d, *J*_{13.8} Hz, 1H, CH), 4.23 (d, *J*_{13.8} Hz, 1H, CH), 3.76 (s, 2H, CH₂), 2.75 – 2.71 (m, 3H, CH₃). ¹³C-NMR (101 MHz, CD₃OD, CDCl₃) δ 167.15, 165.49, 164.72, 164.30, 160.95, 144.47, 130.06, 124.72, 76.64 (t, *J*_{C-D}7.1 Hz), 75.98 (t, *J*_{C-D}41.4 Hz) 59.36, 57.52, 53.60, 49.79, 35.64 ppm. ATR-IR 1775 C=O, 1699 C=O, 1553, 1381, 1242, 1168, 1098, 1023 cm⁻¹. *m/z* LCMS [ES]⁺

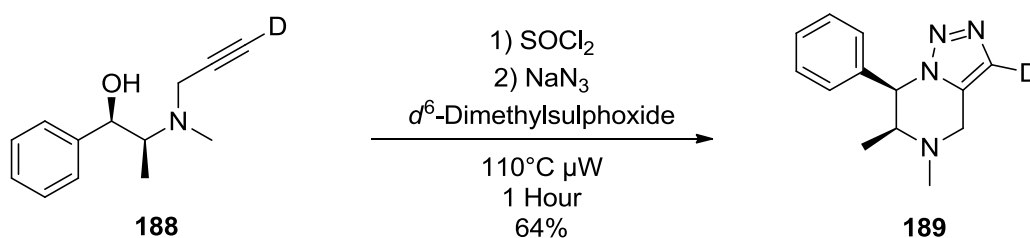
M+Na516.0. HRMS calc for C₁₇H₁₅DN₈NaO₄S₃, M+Na, (516.0417) found (516.0414). $[\alpha]_D^{24}$ -19.0 (c 1.0, CHCl₃)

Synthesis of (1*R*,2*S*)-2-(methyl(prop-1-deutero-ynyl)amino)-1-phenylpropan-1-ol **188**



A 25 mL round-bottomed flask was charged with (+) ephedrine hydrochloride **187** (250 mg, 1.240 mmol) and potassium carbonate (377 mg, 2.73 mmol) in acetonitrile (4 ml). This was left to stir for 30 minutes. To this propargyl bromide (0.147 ml, 1.363 mmol) was added and left to stir under an atmosphere of argon gas at ambient temperature for 16 hours. After 16 hours potassium carbonate (171 mg, 1.24 mmol) was added and deuterium oxide (2 mL) was added and left to stir for 2 hours. The reaction mixture was transferred to a 25 mL separating funnel and extracted with dichloromethane (2 x 5 mL). The organic extracts were dried with magnesium sulfate, filtered and the solvent removed under reduced pressure to afford a yellow oil. 234 mg. Subsequent physicochemical analysis confirmed this to be the titled compound **188**. 94% yield, 99% deuterium incorporation. Yellow Oil. No further purification necessary. *R_f* 0.5(ethyl acetate). ¹H-NMR (CDCl₃, 400 MHz) δ 7.24-7.17 (m, 5H, ArH), 4.15 (d, *J*_{9.6} Hz, 1H, CH), 3.53-3.19 (m, 2H, CH₂), 2.88-2.59 (m, 1H, CH). 2.32 (s, 3H, CH₃), 0.74 (d, *J*_{6.7}, 3H, CH₃). ¹³C-NMR (CDCl₃, 100 MHz) δ 141.84, 128.47, 128.02, 127.60, 80.01 (t, *J*_{C-D}7.1 Hz), 75.04, 72.93 (t, *J*_{C-D}38.4 Hz), 44.04, 35.41, 8.4 ppm. FT-IR (ATR) 3366 OH, 2970, 2588, 1454, 1037 cm⁻¹. *m/z* LCMS [ES]⁺ M+H 205.0, HRMS calc for C₁₃H₁₇DNO, M+H (205.1451) found (205.1455). $[\alpha]_D^{24}$ +36 (c 1.0, CHCl₃).

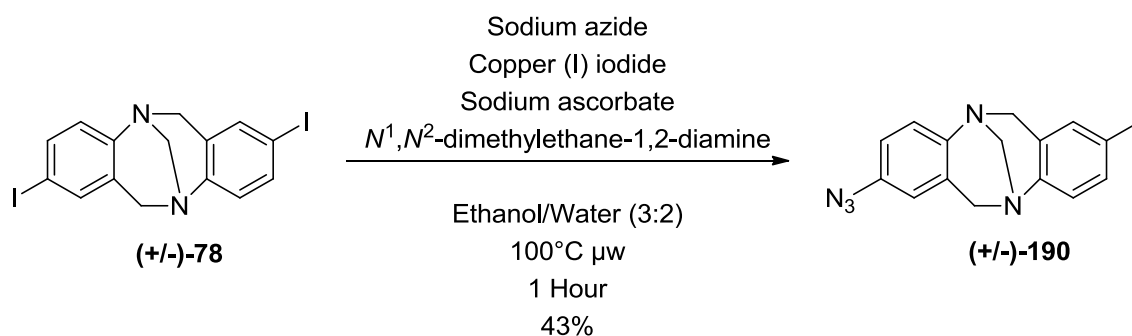
Synthesis of (6*S*,7*R*)-5,6-dimethyl-7-phenyl-4,5,6,7-tetrahydro-[1,2,3]triazolo[1,5-*d*]-pyrazine **189**



A 10 mL flame-dried round-bottomed flask was charged with (1*R*,2*S*)-2-(methyl(prop-2-deutero-ynyl)amino)-1-phenylpropan-1-ol **188** (46 mg, 0.224 mmol) and dissolved in dry dichloromethane

(2 mL). To this thionyl chloride (1 mL) was added slowly with stirring. This was left to stir for 2 hours. The reaction mixture was concentrated under vacuum to afford a brown oil. This was dissolved in deuterated dimethylsulfoxide (2 mL) and transferred to a 2.5 mL microwave vial. To this sodium azide (15mg, 0.224 mmol) was added, the vial was sealed with a Teflon cap and heated to 110 °C in a microwave reactor for 1 hour. The resulting solution was diluted with ethyl acetate (5 mL), transferred to 25 mL separating funnel and washed with saturated sodium bicarbonate solution (5mL), water (5 x 5mL) and with brine. The organic extracts were dried with magnesium sulfate, filtered and the solvent removed under reduced pressure. The resulting oil was further purified by chromatography (Et₂O : EtOH, 8:2) to afford a yellow/brown oil. Subsequent physiochemical analysis confirmed this to be the title compound **189**. 33mg, 64% yield, 95% deuterium incorporation. *R_f* 0.4 (Et₂O : EtOH, 8:2) ¹H-NMR (300 MHz, CDCl₃) δ 7.29 (dd, *J*6.6, 3.6 Hz, 3H, ArH), 7.19 (dd, *J*6.8, 3.0 Hz, 2H, ArH), 5.54 (d, *J*4.0 Hz, 1H, CH), 4.20 (d, *J*15.3 Hz, 1H, CHH), 3.59 (d, *J*15.3 Hz, 1H, CHH), 3.22 – 2.95 (m, 1H, CH), 2.42 (s, 3H, CH₃), 0.96 (d, *J*6.7 Hz, 3H, CH₃). ¹³C-NMR (101 MHz, CDCl₃) δ (carbon deuterium resonances too weak to be observed), 127.57, 127.30, 127.11, 63.57, 57.77, 48.47, 40.34, 28.68 ppm. FTIR [ATR] 2786, 2336, 1655, 1454, 1355, 1245, 998 cm⁻¹. *m/z* LCMS [ES]⁺ M+H 230.1. HRMS calc for C₁₃H₁₅DN₄Na, M+Na, (252.1335) found (252.1335). [α]_D²⁴ +24 (c 1.0, CHCl₃)

Synthesis of 2-azido-8-iodo-6H,12H-5,11-methanodibenzo[b,f][1,5]diazocine (+/-)-190

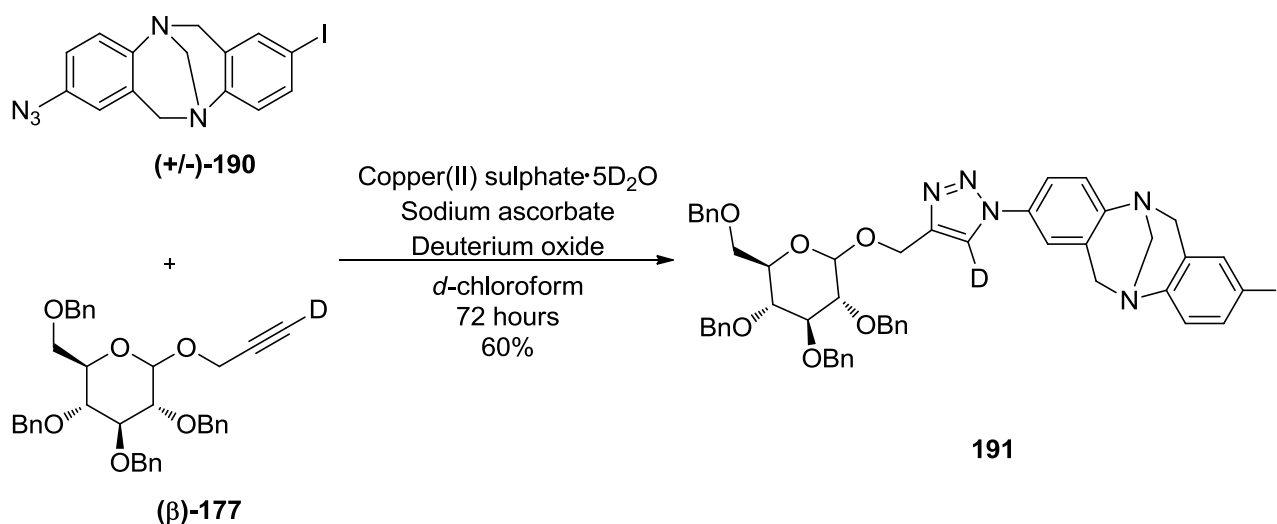


A 10 mL microwave vial was charged with 2,8-bis-iodo-6H,12H-5,11-methanodibenzo[b,f][1,5]diazocine (+/-)-**78** (700mg, 1.47 mmol), sodium ascorbate (29mg, 0.148 mmol), copper(I) iodide (28mg, 0.148 mmol) and sodium azide (86mg, 1.329 mmol) in a 1 : 1 ethanol : water mixture (7 mL). The reaction vessel was sealed with a Teflon cap and to this N^1,N^2 -dimethylethane-1,2-diamine (13mg, 0.148 mmol) was added *via* syringe and the reaction mixture was heated to 100 °C for 1 hour by microwave irradiation. The reaction mixture was diluted with water (5 mL) and transferred to a 25 mL separating funnel, extracted with dichloromethane (2 x 10 mL). The combined organic extracts were washed with brine (5 mL) and dried with magnesium sulfate. The suspension was filtered and the solvent removed under reduced

pressure. The resulting solid was purified by flash chromatography on silica gel eluting with (hexane : ethyl acetate 4 : 1) affording an off white solid. Subsequent physicochemical analysis confirmed this was the title compound. 2-azido-8-iodo-6H,12H-5,11-methanodibenzo[b,f][1,5]diazocine (+/-)-**190** (193mg, 0.643mmol, 43%)

R_f 0.6 (hexane : ethyl acetate ,1:1) ¹H-NMR (500 MHz, CDCl₃) δ 7.39 (d, *J* 8.6 Hz, 1H), 7.17 (d, *J* 2.0 Hz, 1H), 7.03 (d, *J* 8.6 Hz, 1H), 6.88 – 6.71 (m, 2H), 6.50 (d, *J* 2.5 Hz, 1H), 4.57 (dd, *J* 16.7, 12.4 Hz, 2H), 4.23 – 4.14 (m, 2H), 4.09 – 3.93 (m, 2H). ¹³C-NMR (126 MHz, CDCl₃) δ 147.70, 144.76, 135.78, 130.26, 129.12, 126.45, 118.56, 117.04, 87.60, 66.75, 58.66, 58.18 ppm; FT-IR (KBr neat) 2112 N₃, 1488, 1209 cm⁻¹. *m/z* [MALDI]⁺ M-N₂ 362.05, HRMS (NSI) Calcd for C₁₅H₁₆IN₆, M+N₄, 407.0481; Found 407.0477

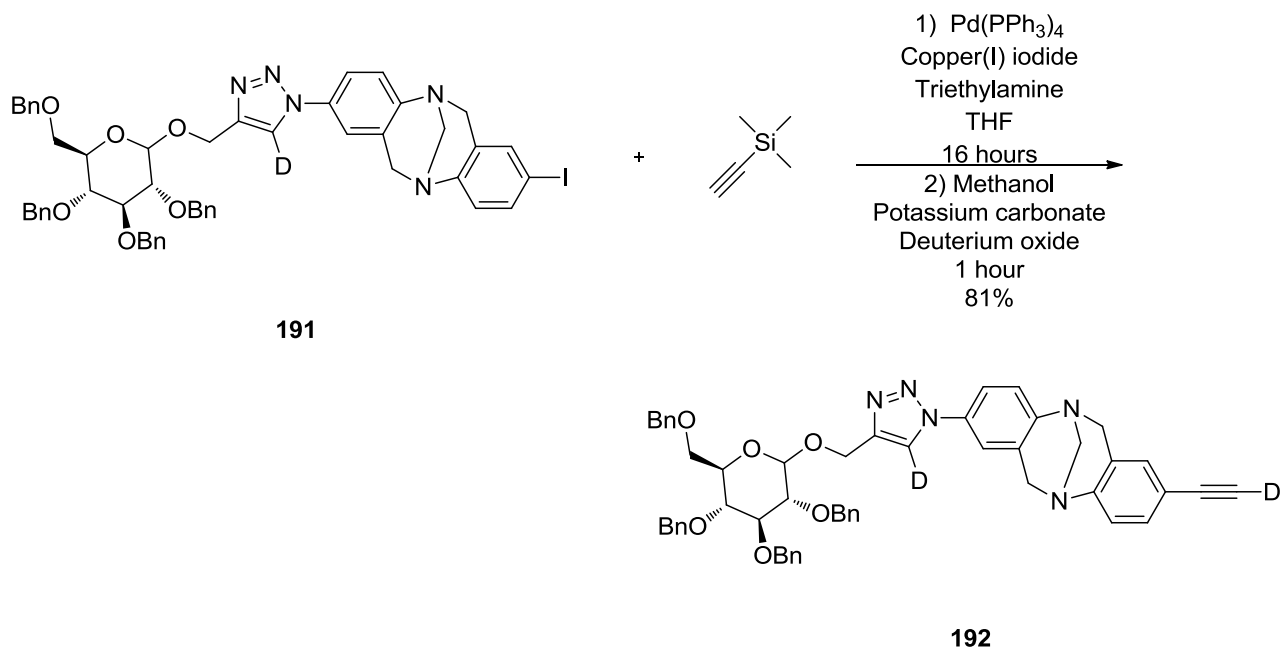
Synthesis of 2-iodo-8-(5-deutero-4-(((3R,4S,5R,6R)-3,4,5-tris(benzyloxy)-6-((benzyloxy)methyl)tetrahydro-2H-pyran-2-yl)oxy)methyl)-1H-1,2,3-triazol-1-yl)-6,12-dihydro-5,11-methanodibenzo[b,f][1,5]diazocine **191**



A 25 mL round-bottomed flask was charged with 2-azido-8-iodo-6H,12H-5,11-methanodibenzo[b,f][1,5]diazocine (44.7 mg, 0.077 mmol) and deuterated propargyl-*O*-benzyl glucose (30 mg, 0.077 mmol) in *d*-chloroform (1 mL). To this a solution of copper(II) sulfate pentadeuterate (1.230 mg, 7.71 μmol) and sodium ascorbate (15.27 mg, 0.077 mmol) in deuterium oxide (1 mL) was added and stirred vigorously for 72 hours at room temperature. The solution was transferred to a 25 mL separating funnel and the organic layer was collected. The impure reaction mixture was dried with magnesium sulfate, filtered and the solvent removed under reduced pressure. The resulting mixture was purified *via* flash chromatography eluting with 50% ethyl acetate : petrol. Subsequent physicochemical analysis confirmed this to be the title compound. **191** (45 mg, 0.046 mmol, 60.3 % yield)

191 *Rf* 0.3 (hexane : ethyl acetate, 1:1) $^1\text{H-NMR}$ (400 MHz, CDCl_3) δ 7.40 (d, J 8.5 Hz, 1H), 7.28 – 7.02 (m, 23H), 6.83 (d, J 8.5 Hz, 1H), 4.94 (dd, J 34.6, 13.5 Hz, 2H), 4.84 (d, J 11.0 Hz, 2H), 4.73 (t, J 10.3 Hz, 2H), 4.66 (d, J 11.1 Hz, 1H), 4.60 (d, J 16.9 Hz, 2H), 4.53 (dd, J 12.1, 1.8 Hz, 1H), 4.48 – 4.41 (m, 3H), 4.23 (s, 2H), 4.06 (d, J 17.9 Hz, 2H), 3.57 (m, 6H). $^{13}\text{C-NMR}$ (126 MHz, CDCl_3) δ 147.17, 146.44, 144.42, 137.57 – 137.32, 137.11 – 136.87, 135.52, 134.70, 131.92, 128.97, 128.04, 127.69, 127.47 (t, $J_{\text{C-D}}$ 27.7 Hz), 127.37 – 127.13, 127.01 – 126.48, 126.01, 125.10, 119.69 (t, $J_{\text{C-D}}$ 30.2 Hz), 118.73, 118.06, 101.61, 86.71, 83.65, 81.24, 76.74, 74.69, 73.97, 73.76, 72.45, 67.86, 65.60, 64.83, 61.98, 57.58, 57.20 ppm. FT-IR (KBr neat) 1503, 1474, 1454, 1211, 1070 cm^{-1} ; m/z [MALDI] $^+$ $\text{M}+\text{Na}$ 991.25, HRMS (NSI) Calcd for $\text{C}_{52}\text{H}_{53}\text{DIN}_6\text{O}_6$, $\text{M}+\text{NH}_4$, 986.3212; Found 986.3215.

Synthesis of 2-deutero-ethynyl-8-(4-(((3*R*,4*S*,5*R*,6*R*)-3,4,5-tris(benzyloxy)-6-((benzyloxy)methyl)tetrahydro-2*H*-pyran-2-yl)oxy)methyl)-1*D*-1,2,3-triazol-1-yl)-6,12-dihydro-5,11-methanodibenzo[*b,f*][1,5]diazocine **192**

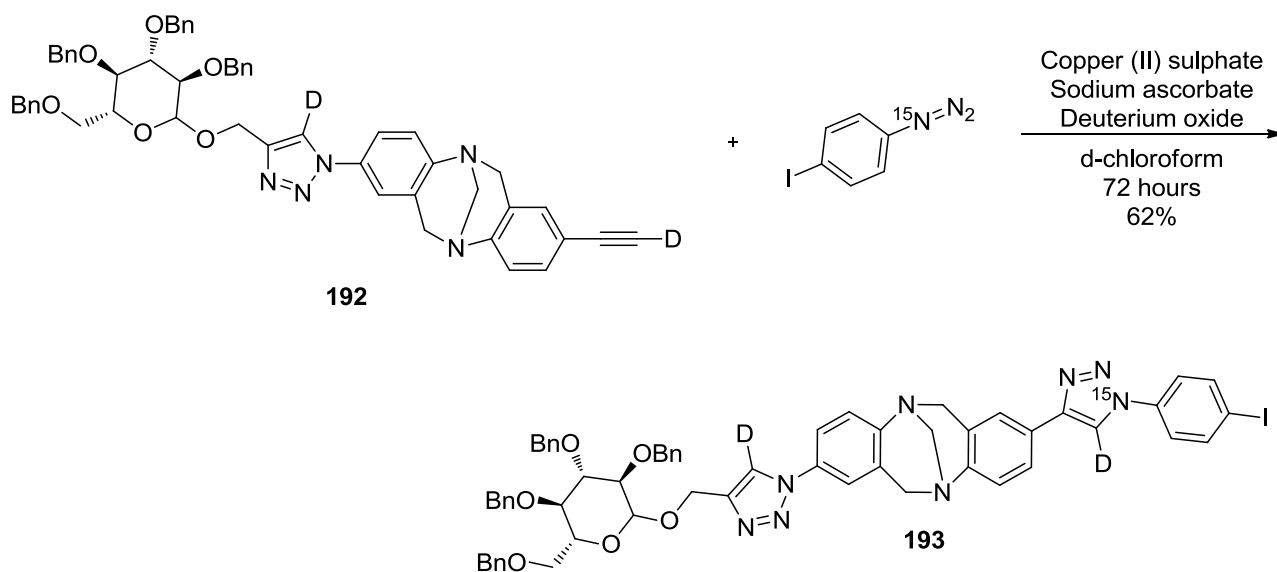


A flame dried 25 mL round bottomed flask was charged with **191** (40 mg, 0.041 mmol), tetrakis(triphenylphosphine) palladium(0) (4.77 mg, 4.13 μmol), copper(I) iodide (1.573 mg, 8.26 μmol) in tetrahydrofuran (2 mL). To this trimethylsilylacetylene (0.018 mL, 0.124 mmol) was added and left to stir for 20 minutes. This was followed by the addition of triethylamine (0.023 mL, 0.165 mmol) and the resulting solution was left to stir for 24 hours at ambient temperature under an atmosphere of argon gas. The reaction mixture was transferred into a 25 mL separating funnel and extracted with ethyl acetate (2 x 5 mL). The combined extracts were washed with brine (5 mL) and dried with magnesium sulfate. The suspension was filtered and the solvent removed under reduced pressure. The resulting solid mixture was dissolved in methanol (2 mL) and potassium carbonate

(11.41 mg, 0.083 mmol) was added and left to stir for 1 hours. The solution was transferred to a 25mL separating funnel, diluted with ethyl acetate and washed with water (5 mL) and brine (5 mL). The solution was dried with magnesium sulfate, filtered and the solvent removed under reduced pressure. The impure solid was dissolved in acetonitrile (1 mL) and potassium carbonate (11.41 mg, 0.083 mmol) was added followed by deuterium oxide (1 mL) and left to stir for 1 hour. The solution was diluted with dichloromethane (5 mL), transferred to a 25 mL separating funnel and the organic layer was collected, dried with magnesium sulfate, filtered and the solvent removed under reduced pressure. The impure solid was purified *via* flash chromatography on silica gel eluting with 1:1 ethyl acetate : petrol to afford a yellow solid. Subsequent physiochemical analysis confirmed this was the title product. **192** (29 mg, 0.033 mmol, 81 % yield)

192 *Rf* 0.4 (hexane : ethyl acetate, 1:1) ^1H NMR (500 MHz, CDCl_3) δ 7.29 – 7.09 (m, 20H), 7.09 – 7.05 (m, 4H), 7.01 (d, J 7.4 Hz, 2H), 4.98 (dd, J 13.2, 1.7 Hz, 1H), 4.90 (dd, J 13.2, 1.1 Hz, 1H), 4.83 (d, J 11.0 Hz, 2H), 4.72 (t, J 11.6 Hz, 2H), 4.67 (s, 1H), 4.65 – 4.61 (m, 1H), 4.60 (d, J 5.5 Hz, 1H), 4.52 (dd, J 12.2, 2.0 Hz, 1H), 4.45 (d, J 7.8 Hz, 3H), 4.24 (s, 2H), 4.09 (t, J 15.6 Hz, 2H), 3.69 – 3.59 (m, 2H), 3.59 – 3.50 (m, 2H), 3.45 – 3.37 (m, 2H). ^{13}C NMR (126 MHz, CDCl_3) δ 147.27, 147.19, 144.43, 137.48, 137.43, 137.42, 137.02, 136.98, 131.91, 130.37, 129.85, 128.10, 127.53 (t, $J_{\text{C-D}}$ 20.2Hz), 127.37, 127.35, 126.92, 126.89, 126.85, 126.76, 126.72, 126.65, 126.63, 126.58, 126.50, 119.70 (t, $J_{\text{C-D}}$ 29.1 Hz), 118.74, 118.04, 116.87, 101.61, 83.65, 81.71 (t, $J_{\text{C-D}}$ 6.3 Hz), 81.25, 76.75, 76.41 (t, $J_{\text{C-D}}$ 20.2 Hz), 74.70, 73.98, 73.76, 72.46, 67.86, 65.70, 62.01, 57.57 ppm. ^2H -NMR (77 MHz, DCM) δ 7.86 (s, 1D), 2.93 (s, 1D). m/z [MALDI] $^+$ M+Na 890.4.

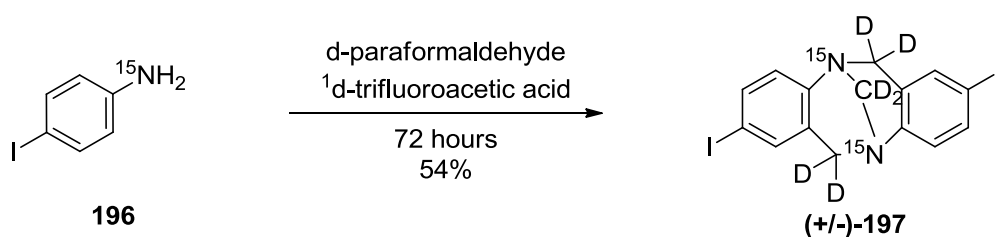
Synthesis of 2-(1-(4-iodophenyl)-1D-1 ^{15}N ,2,3-triazol-4-yl)-8-(4-(((3R,4S,5R,6R)-3,4,5-tris(benzyloxy)-6-((benzyloxy)methyl)tetrahydro-2H-pyran-2-yl)oxy)methyl)-1D-1,2,3-triazol-1-yl)-6,12-dihydro-5,11-methanodibenzo[b,f][1,5]diazocine 193



A 25 mL round-bottomed flask was charged with **192** (15mg, 0.017 mmol) and ^{15}N - α -1-azido-4-iodobenzene (6mg, 0.024mmol) in deuterated chloroform (2 mL). To this a premixed solution of copper (II) sulfate pentadeuterate (0.25mg, 0.0017 mmol) and sodium ascorbate (0.3 mg, 0.0017 mmol) in deuterium oxide (2 mL) was added and left stirring vigorously for 72 hours. The resulting biphasic mixture was transferred to a 25 mL separating funnel and extracted with dichloromethane (3 x 5mL). The organic extracts were washed with brine (5 mL) and dried with magnesium sulfate. The suspension was filtered and the solvent removed under reduced pressure. The impure mixture was purified *via* flash chromatography on silica gel eluting with 50 – 100% ethyl acetate in petroleum ether to afford an off white solid. Subsequent physiochemical analysis confirmed this to be the title compound **193** (12 mg, 10.8 μmol , 62% yield, 95% ^2H)

193 *Rf* 0.6 (ethyl acetate) ^1H -NMR (500 MHz, CDCl_3) δ 7.78 (t, J 8.7 Hz, 2H), 7.57 (d, J 8.3 Hz, 2H), 7.45 (ddd, J 24.2, 15.6, 8.5 Hz, 3H), 7.30 – 7.11 (m, 21 H), 7.11 – 7.00 (m, 2H), 4.94 (ddd, J 13.2, 1.5 Hz, 2H), 4.82 (dd, J 11.0, 2.6 Hz, 2H), 4.72 (dd, J 13.2, 11.2 Hz, 2H), 4.68 – 4.61 (m, 2H), 4.54 – 4.49 (m, 2H), 4.47 – 4.39 (m, 2H), 4.35 – 4.23 (m, 2H), 4.18 (t, J 16.2 Hz, 2H), 3.69 – 3.49 (m, 4H), 3.40 (dt, J 9.5, 5.8 Hz, 2H). ^{13}C -NMR (126 MHz, CDCl_3) δ 147.46, 147.09, 144.41, 137.86 (d, $J_{\text{C-N}}$ 1.9 Hz), 137.43(t, $J_{\text{C-D}}$ 5.0 Hz), 136.99 (d, $J_{\text{C-N}}$ 5.6 Hz), 131.84, 128.24, 127.37, 126.92, 126.85, 126.73, 126.65, 126.58, 125.16, 124.53, 124.23, 123.44, 120.88, 118.70, 118.10, 101.60 (d, $J_{\text{C-N}}$ 2.8 Hz), 92.54, 83.65, 81.24, 74.70, 73.98, 73.76, 72.46, 67.85, 65.85, 61.98, 57.86, 57.66, 52.40, 28.68 ppm. ^{15}N -NMR (51 MHz, CDCl_3) δ -127.18 (wrt CH_3NO_2). ^2H -NMR (77 MHz, DCM) δ 8.13, 7.89. FT-IR (KBr neat) 2925, 1499, 1465, 1260, 1106, 1069 cm^{-1} . m/z [ES] $^+$ M+H 1115.1, HRMS (NSI) Calcd for $\text{C}_{60}\text{H}_{57}\text{D}_2\text{IN}_8^{15}\text{NO}_6$, M+ NH_4 , 1131.3729; Found 1131.3724.

Synthesis of 2,8-bis-iodo-6,12-dideutero-5,11-deutero methanodibenzo[b,f][1,5] ^{15}N diazocine (+/-)-**197**

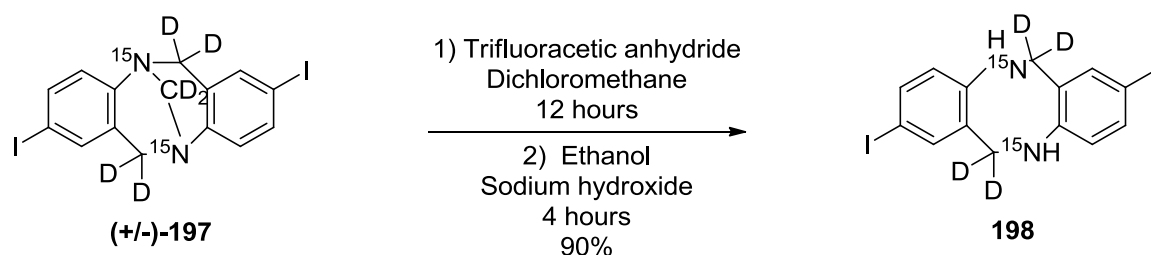


A flame-dried 25 mL round-bottomed flask was charged with ^{15}N -4-iodoaniline (75mg, 0.34 mmol) and d_2 -paraformaldehyde (16mg, 0.51 mmol). This was cooled 0°C in an ice bath and stirred vigorously with a magnetic stirrer. To this d_3 -trifluoroacetic acid (1 mL) was added slowly over 5 minutes. The reaction mixture was allowed to warm to ambient temperature and kept in the dark by covering the flask in tin foil for 72 hours. The reaction mixture was diluted with water (2 mL) and

neutralised with ammonia solution (aqueous 35%) until the mixture had changed from red to bright yellow. The resulting slurry was transferred to a 25 mL separating funnel and extracted with chloroform (3 x 5mL). The combined organic extracts were washed with brine (5 mL) and dried with magnesium sulfate. The suspension was filtered and the solvent was removed under reduced pressure. The resulting yellow solid was purified by flash chromatography eluting with ethyl acetate : petrol (1 : 5) affording an off white solid. Subsequent physiochemical analysis confirmed this to be the title compound (+/-)-**197** (45mg, 0.09 mmol, 54%)

(+/-)-**197** *Rf* 0.3 (ethyl acetate : hexane, 1 : 5) ¹H-NMR (400 MHz, CDCl₃) δ 7.37 (dd, *J*_{8.5}, 2.0 Hz, 2H), 7.15 (d, *J*_{2.0} Hz, 2H), 6.79 (dd, *J*_{8.5}, 1.2 Hz, 2H). ¹³C-NMR (101 MHz, CDCl₃) δ 147.55 (d, *J*_{C-N}6.6 Hz), 136.49, 135.76, 130.03, 127.04, 87.66, 65.79 (t, *J*_{C-D}22.2 Hz), 57.35 (quintet, *J*_{C-D}20.2 Hz) ppm. ²H-NMR (77 MHz, DCM) δ 3.69 (s, 2D), 3.31 (s, 2D), 3.16 (s, 2D). ¹⁵N-NMR (51 MHz, DCM) δ -341.00 (s). wrt CH₃NO₂. FT-IR (KBr neat) 1470, 1389, 1265, 1242 cm⁻¹; *m/z* [MALDI]⁺ M+H(found) 481.87, (calc) 481.94. HRMS (NSI) Calcd for C₁₅H₇D₆I₂¹⁵N₂, M+H, 482.9485; Found 482.9479

Synthesis of 2,8-bis-iodo-5,6,11,12-tetradeuterodibenzo[b,f][1,5]di-¹⁵N-azocine **198**

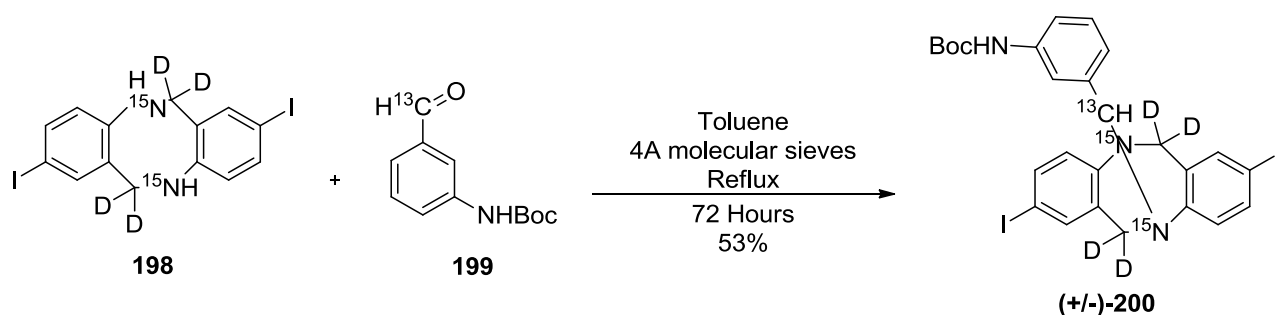


A flame-dried 25 mL round-bottomed flask was charged with (+/-)-**197** (40 mg, 0.083 mmol) in anhydrous dichloromethane (1 mL) with stirring. To this trifluoroacetic anhydride (115μL, 0.83mmol) was added and left to stir under argon gas for 16 hours. The reaction mixture was diluted with water (2 mL) and neutralised with the drop wise addition of an aqueous saturated sodium bicarbonate solution until bubbling stopped. The reaction mixture was transferred to a 25 mL separating funnel and extracted with dichloromethane (3 x 5 mL). The combined organic extracts were washed with brine (5 mL) and dried with magnesium sulfate, filtered and the solvent removed under reduced pressure. The resulting solid was dissolved in ethanol (2 mL) and sodium hydroxide (100mg) was added and the resulting cloudy solution was left to stir for 4 hours at ambient temperature under an atmosphere of argon. This was then diluted with water (5 mL) and transferred to a 25 ml separating funnel and extracted with dichloromethane (3 x 5 mL). The combined organic extracts were washed with brine (5 mL) and dried with magnesium sulfate, filtered and the solvent removed under reduced pressure. The impure mixture was purified by flash

chromatography on silica gel eluting with dichloromethane to afford a pale yellow solid. Subsequent physicochemical analysis confirmed this to be the title compound **198**. (35 mg, 0.075mmol, 90%)

198 *Rf* 0.5 (dichloromethane) $^1\text{H-NMR}$ (400 MHz, $\text{CD}_3\text{OD}/\text{CDCl}_3$) δ 7.25 (dd, $J_{12.4}$, 11.0 Hz, 4H), 6.53 – 6.36 (m, 2H). $^{13}\text{C-NMR}$ (101 MHz, CD_2Cl_2) δ 148.10 (d, $J_{\text{C-N}}$ 13.1 Hz), 140.28, 137.24, 127.78 (d, $J_{\text{C-N}}$ 4.0 Hz), 120.18 (d, $J_{\text{C-D}}$ 3.0 Hz), 79.58, 48.87 (ddd, $J_{\text{C-D}}$ 26.3, 20.6, 4.9 Hz). $^2\text{H-NMR}$ (77 MHz, None) δ 4.60 (s, 4D). $^{15}\text{N-NMR}$ (51 MHz, None) δ -310.74. wrt CH_3NO_2 . FT-IR (KBr neat) 1475, 1394, 1260, 1189 cm^{-1} ; m/z [MALDI] $^+$ M+K (found) 508.97, (calc) 508.18. HRMS (NSI) Calcd for $\text{C}_{14}\text{H}_{11}\text{D}_5\text{I}_2\text{N}^{15}\text{N}_2$, M+ NH_4 , 486.9679; Found 486.9688.

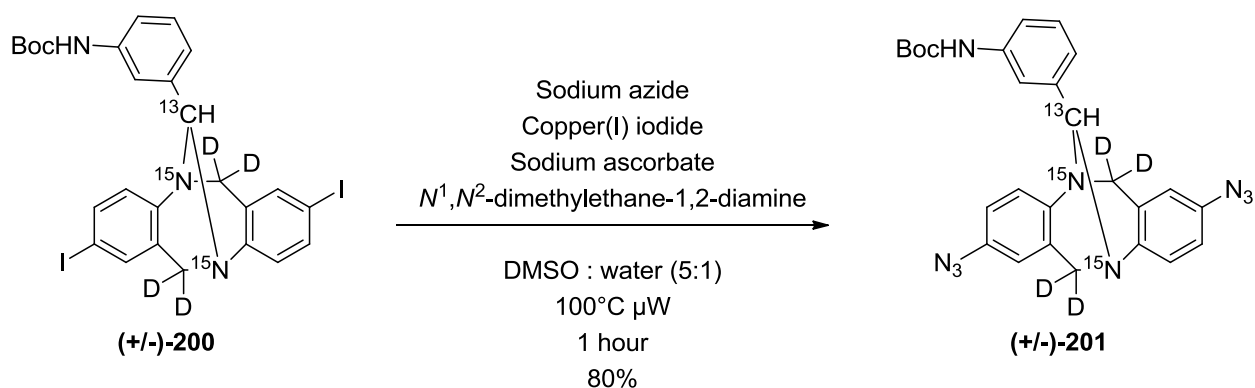
Synthesis of *tert*-butyl (3-((5*R*,11*S*)-2,8-bis-iodo-6,12-di-deutero-5,11- ^{13}C -methanodibenzo[*b,f*] [1,5]- ^{15}N -diazocin-13-yl)phenyl)carbamate (+/-)-**200**



A flame-dried 25 mL round-bottomed flask was charged with **198** (30mg, 0.064 mmol) and ^{13}C - α -3-*boc* amino benzaldehyde **199** (14mg, 0.064mmol) and pre-dried 4Å molecular sieves in toluene (5 mL). The reaction mixture was heated to reflux for 24 hours. After this time the solvent was removed under reduced pressure and the resulting mixture was purified by flash chromatography on silica gel eluting with diethyl ether : petroleum ether (1 : 5) to afford a waxy solid. Subsequent physicochemical analysis confirmed this to be the title compound (+/-)-**200**. (23mg, 0.034mmol, 53%)

(+/-)-**200** *Rf* 0.4 (diethyl ether : hexane (1 : 5)). $^1\text{H-NMR}$ (500 MHz, CDCl_3) δ 7.36 (ddd, $J_{13.2}$, 8.5, 2.0 Hz, 2H), 7.29 (d, $J_{8.4}$ Hz, 2H), 7.18 (d, $J_{2.0}$ Hz, 1H), 7.12 – 7.04 (m, 2H), 6.91 (dd, $J_{8.5}$, 1.6 Hz, 1H), 6.88 (d, $J_{2.0}$ Hz, 1H), 6.86 (dd, $J_{8.5}$, 1.2 Hz, 1H), 6.33 (s, 1H), 5.13 (m, 1H), 1.38 (s, 9H). ^{13}C NMR (126 MHz, CDCl_3) δ 152.71, 138.61, 136.65 (d, $J_{\text{C-N}}$ 36.5 Hz), 135.65 (d, $J_{\text{C-D}}$ 37.8 Hz), 129.25, 127.59, 127.47 (ddd, $J_{\text{C-D}}$ 22.4, 6.3, 2.2 Hz), 122.01, 118.14, 117.55, 87.84, 80.64, 74.13, 73.24, 28.41 ppm. $^{15}\text{N-NMR}$ (51 MHz, DCM) δ -335.12, -338.22 with respect to CH_3NO_2 . $^2\text{H-NMR}$ (77 MHz, DCM) δ 4.71 (s, 1D), 3.69 (d, 3D). FT-IR (KBr neat) 1714 C=O, 1610, 1531, 1470, 1159 cm^{-1} . m/z [MALDI] $^+$ M+Na (found) 695.01, (calc) 695.02. HRMS (NSI) Calcd for $\text{C}_{25}^{13}\text{CH}_{25}\text{D}_4\text{I}_2\text{N}_2^{15}\text{N}_2\text{O}_2$, M+ NH_4 , 690.0605; Found 690.0600

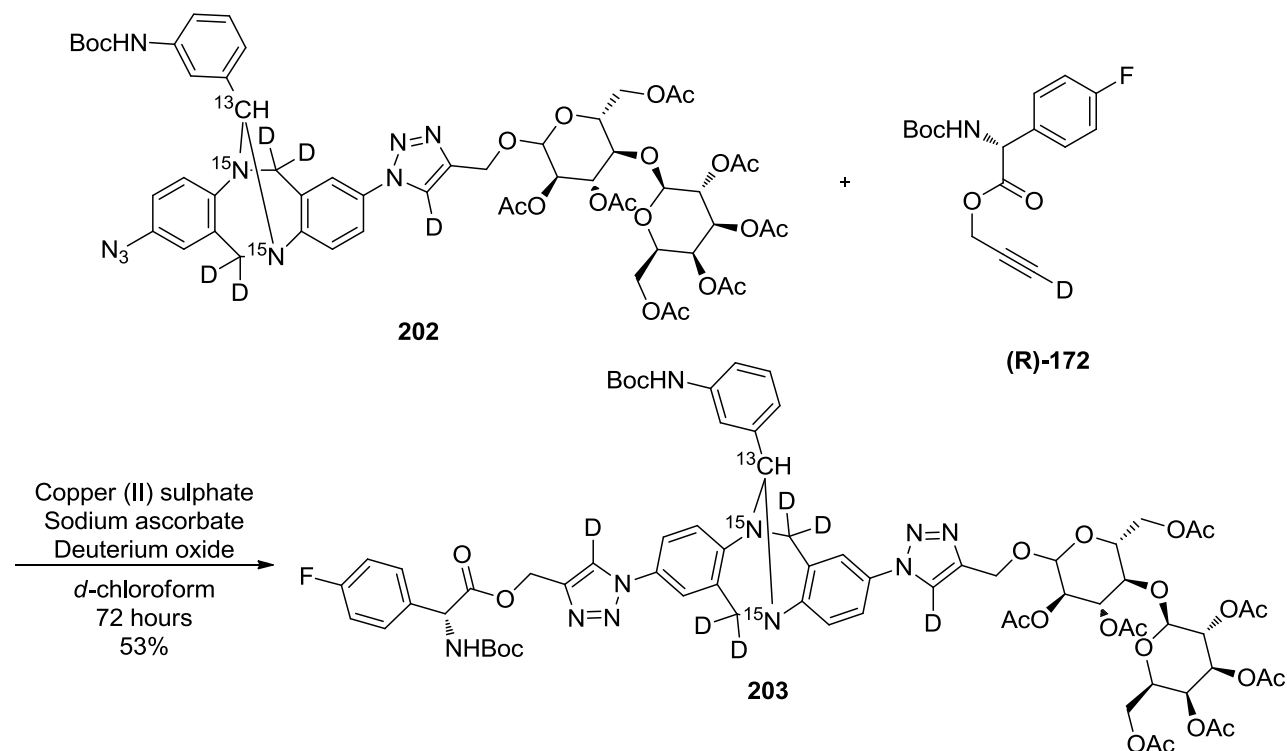
Synthesis of *tert*-butyl (3-((5*R*,11*S*)-2,8-*bis*-azido-6,12-di-deutero-5,11-¹³C-methanodibenzo [b,f][1,5]-¹⁵N-diazocin-13-yl)phenyl)carbamate (+/-)-201



A 10 mL microwave vial was charged with (+/-)-**200** (50 mg, 0.074 mmol), sodium azide (19.34 mg, 0.297 mmol), copper(I) iodide (1.416 mg, 7.44 μ mol), sodium ascorbate (2.95 mg, 0.015 mmol) and N^1,N^2 -dimethylethane-1,2-diamine (1.967 mg, 0.022 mmol) in a 5 : 1 dimethylsulfoxide, water mixture. The vial was sealed with a Teflon stopper and heated *via* microwave irradiation at 100 °C for 1 hour. The reaction mixture was diluted with dichloromethane (10 mL) and transferred to a 50 mL separating funnel and washed with water (5 x 20mL). The organic extract was washed with brine (10 mL) and dried with magnesium sulfate. The suspension was filtered and the solvent removed under reduced pressure. The remaining solid purified *via* flash chromatography eluting with 20% diethyl ether in petrol to afford a yellow solid. Subsequent physicochemical analysis confirmed this to be the title compound. (+/-)-**201** (30 mg, 0.060 mmol, 80 %)

(+/-)-**201** *Rf* 0.5(diethyl ether : petrol, 1 : 5) ¹H-NMR (500 MHz, CDCl₃) δ 7.41 (s, 2H), 7.27 – 7.25 (m, 2H), 7.23 – 7.17 (m, 3H), 6.87 (ddd, *J* 14.6, 8.6, 2.6 Hz, 2H), 6.65 (d, *J* 2.6 Hz, 1H), 6.44 (s, 1H), 6.35 (d, *J* 2.6 Hz, 1H), 5.26 (d, 1H), 1.51 (s, 9H). ¹³C NMR (126 MHz, CDCl₃) δ 165.28, 151.64, 145.83, 142.07, 137.76, 137.49, 137.34, 134.40 (d, *J*_{C-N}42.8 Hz), 128.68 (d, *J*_{C-N}6.4 Hz), 128.24 (d, *J*_{C-N}5.8 Hz), 128.04, 125.83 (ddd, *J*_{C-D}26.3, 6.5, 2.4 Hz), 121.01, 117.69, 117.38, 116.88, 116.56, 115.97, 115.73, 79.51, 73.26, 27.32 ppm. ¹⁵N-NMR (51 MHz, CDCl₃) δ -335.25 (s), -338.35 (s). ²H-NMR (77 MHz, None) δ 4.72 (s, 1D), 4.18 (d, *J* 5.1 Hz, 2D), 3.81 (s, 1D). FT-IR (KBr neat) 2977, 2110 C-N₃, 1715 C=O, 1486, 1159 cm⁻¹. *m/z* [MALDI]⁺ M+H 503.35, HRMS (NSI) Calcd for C₂₅¹³CH₂₁D₄N₇¹⁵N₂NaO₂, M+Na, 525.2254; Found 525.2263.

Synthesis of (2*R*,3*S*,4*S*,5*R*,6*S*)-2-(acetoxymethyl)-6-(((2*R*,3*R*,4*S*,5*R*)-4,5-diacetoxy-2-(acetoxymethyl)-6-((1-((5*R*,11*S*)-8-(4-(((*R*)-2-((*tert*-butoxycarbonyl)amino)-2-(4-fluorophenyl)acetoxymethyl)-1*D*-1,2,3-triazol-1-yl)-13-(3-((*tert*-butoxycarbonyl)amino)phenyl)-6,12-dihydro-5,11-¹³C-methanodibenzo[*b,f*][1,5]-¹⁵N-diazocin-2-yl)-1*D*-1,2,3-triazol-4-yl)methoxy)tetrahydro-2*H*-pyran-3-yl)oxy)tetradeutero-2*H*-pyran-3,4,5-triyl triacetate. 203

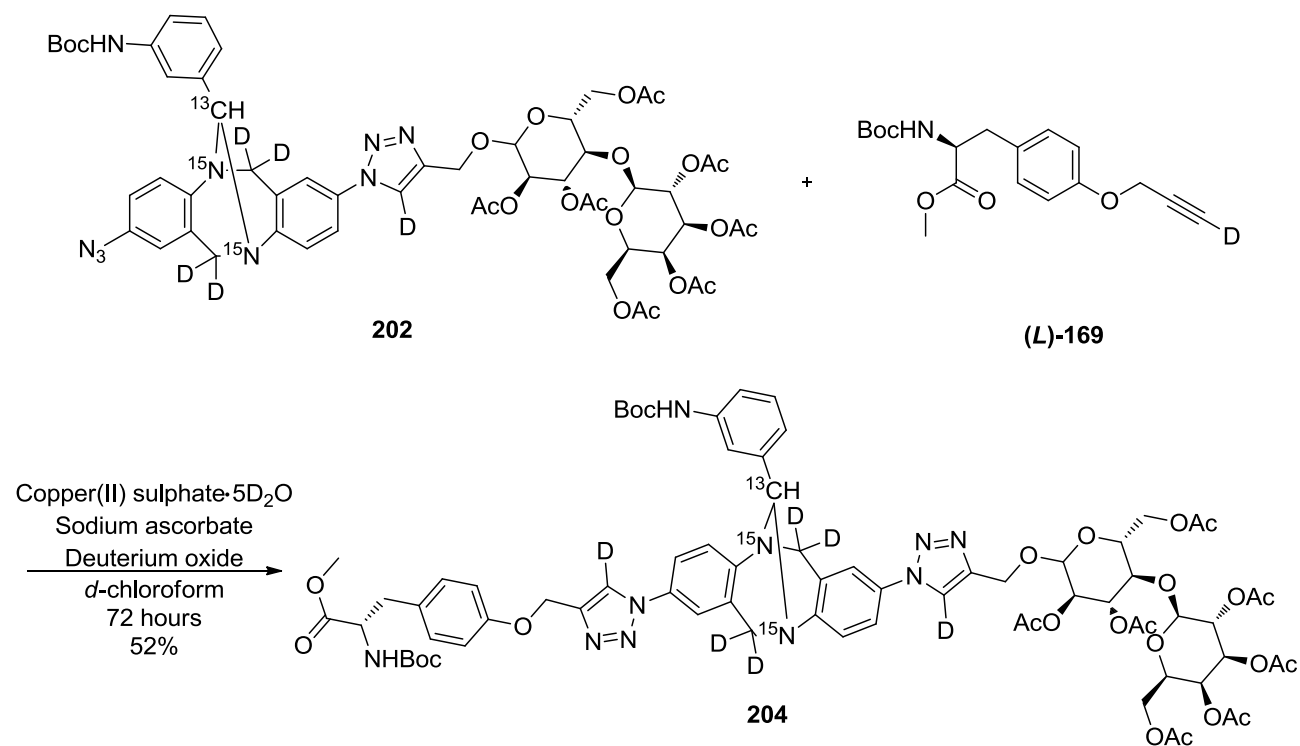


A 2.5 mL microwave vial was charged with **202** (6mg, 5.09 μ mol) and **(R)-172** (3.14mg, 10.18 μ mol) in deuterated chloroform (1 mL). To this a premixed solution of copper (II) sulfate pentadeuterate (0.5mg, 0.0034 mmol) and sodium ascorbate (0.7 mg, 0.0034 mmol) in deuterium oxide (1 mL) was added and left stirring vigorously for 72 hours under an argon gas atmosphere. The resulting biphasic mixture was transferred to a 25 mL separating funnel and extracted with dichloromethane (3 x 5 mL). The organic extracts were washed with brine (5 mL) and dried with magnesium sulfate. The suspension was filtered and the solvent removed under reduced pressure. The impure mixture was purified *via* flash chromatography on silica gel eluting with 2-4% methanol in dichloromethane to afford an off white amorphous solid. Subsequent physiochemical analysis confirmed this to be the titled compound **203** (4mg, 2.69 μ mol, 53%)

203 *R_f* 0.6 (4% methanol in dichloromethane) ¹H-NMR (500 MHz, CDCl₃) δ 7.51 – 7.41 (m, 2H), 7.38 (dd, *J*12.6, 6.0 Hz, 2H), 7.19 (s, 2H), 7.01 – 6.86 (m, 4H), 6.38 (s, 1H), 5.34 – 5.19 (m, 4H), 5.06 (ddt, *J* 10.5, 7.9, 7.4 Hz, 4H), 4.93 – 4.70 (m, 4H), 4.67 – 4.54 (m, 2H), 4.48 – 4.37 (m, 2H), 4.11 – 3.96 (m, 4H), 3.84 – 3.68 (m, 4H), 3.58 (d, *J* 12.3 Hz, 2H), 2.09 – 2.05 (m, 3H), 2.05 – 2.00 (m, 3H), 2.00 – 1.93 (m, 9H), 1.93 – 1.86 (m, 6H), 1.51 (d, *J* 18.4 Hz, 18H). ¹³C-NMR (126 MHz,

CDCl₃) δ 74.23 ppm. ¹⁹F-NMR (471 MHz, CDCl₃) δ -107.23. FT-IR (KBr neat) 2928, 1755 C=O, 1495, 1229, 1060 cm⁻¹. *m/z* [ES]⁺ M+K 1526.0. HRMS (NSI) Calcd for C₇₀¹³CH₇₇D₈FN₉¹⁵N₂O₂₄, M+NH₄, 1505.6229; Found 1505.6237.

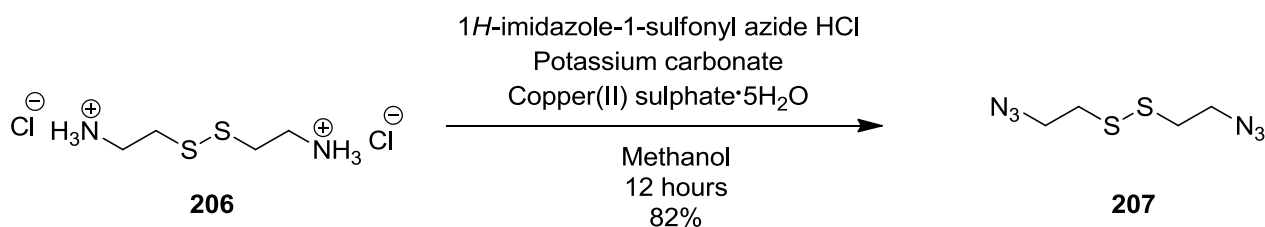
Synthesis of (2*R*,3*S*,4*S*,5*R*,6*S*)-2-(acetoxymethyl)-6-(((2*R*,3*R*,4*S*,5*R*)-4,5-diacetoxy-2-(acetoxymethyl)-6-((1-((5*R*,11*S*,13*R*)-8-(4-((4-((*R*)-2-((*tert*-butoxycarbonyl)amino)-3-methoxy-3-oxopropyl)phenoxy)methyl)-1*D*-1,2,3-triazol-1-yl)-13-(3-((*tert*-butoxycarbonyl)amino)phenyl)-6,12-dideutero-5,11-¹³C-methanodibenzo[*b,f*][1,5]-¹⁵N-diazocin-2-yl)-1*D*-1,2,3-triazol-4-yl)methoxy)tetrahydro-2*H*-pyran-3-yl)oxy)tetrahydro-2*H*-pyran-3,4,5-triyl triacetate. 204



A 2.5 mL microwave vial was charged with **202** (6mg, 5.09 μmol) and **(L)-169**(3.40mg, 10.18μmol) in deuterated chloroform (1 mL). To this a premixed solution of copper(II) sulfate pentadeuterate (0.5mg, 0.0034 mmol) and sodium ascorbate (0.7 mg, 0.0034 mmol) in deuterium oxide (1 mL) was added and left stirring vigorously for 72 hours. The resulting biphasic mixture was transferred to a 25 mL separating funnel and extracted with dichloromethane (3 x 5 mL). The organic extracts were washed with brine (5 mL) and dried with magnesium sulfate. The suspension was filtered and the solvent removed under reduced pressure. The impure mixture was purified by flash chromatography on silica gel eluting with 2-4% methanol in dichloromethane to afford an off white amorphous solid. Subsequent physiochemical analysis confirmed this to be the title compound **204** (4mg, 2.64μmol, 52%)

204 *Rf* 0.5 (4% methanol in dichloromethane) $^1\text{H-NMR}$ (500 MHz, CDCl_3) δ 7.50 – 7.43 (m, 3H), 7.40 – 7.34 (m, 2H), 7.32 (dd, J 7.9, 3.6 Hz, 2H), 7.19 – 7.15 (m, 2H), 7.04 – 7.01 (m, 1H), 7.00 – 6.93 (m, 2H), 6.84 (dd, J 17.8, 8.7 Hz, 2H), 6.38 (s, 1H), 5.30 – 5.25 (m, 1H), 5.19 – 4.98 (m, 4H), 4.92 – 4.71 (m, 4H), 4.58 (ddd, J 17.5, 7.9, 1.8 Hz, 2H), 4.49 – 4.38 (m, 2H), 4.11 – 3.96 (m, 4H), 3.82 – 3.69 (m, 4H), 3.62 (t, J 9.7 Hz, 3H), 3.60 – 3.48 (m, 1H), 2.95 (dd, J 15.1, 8.8 Hz, 2H), 2.10 (d, J 6.4 Hz, 2H), 2.09 – 2.06 (m, 4H), 2.02 (dd, J 5.9, 2.8 Hz, 2H), 2.01 – 1.94 (m, 10H), 1.93 – 1.86 (m, 4H), 1.44 (s, 9H), 1.37 – 1.29 (m, 9H). $^{13}\text{C-NMR}$ (126 MHz, CDCl_3) δ 73.21 ppm. $^{15}\text{N-NMR}$ (51 MHz, none) δ -333.47, -336.47 (with respect to CH_3NO_2). FT-IR (KBr neat) 2927, 1752 C=O , 1495, 1368, 1231, 1168, 1160 cm^{-1} . m/z $[\text{ES}]^+$ $\text{M}+\text{K}$ 1552.4. HRMS (NSI) Calcd for $\text{C}_{72}^{13}\text{CH}_{83}\text{D}_7\text{N}_9^{15}\text{N}_2\text{O}_{25}$, $\text{M}+\text{NH}_4$, 1530.6523; Found 1530.6529

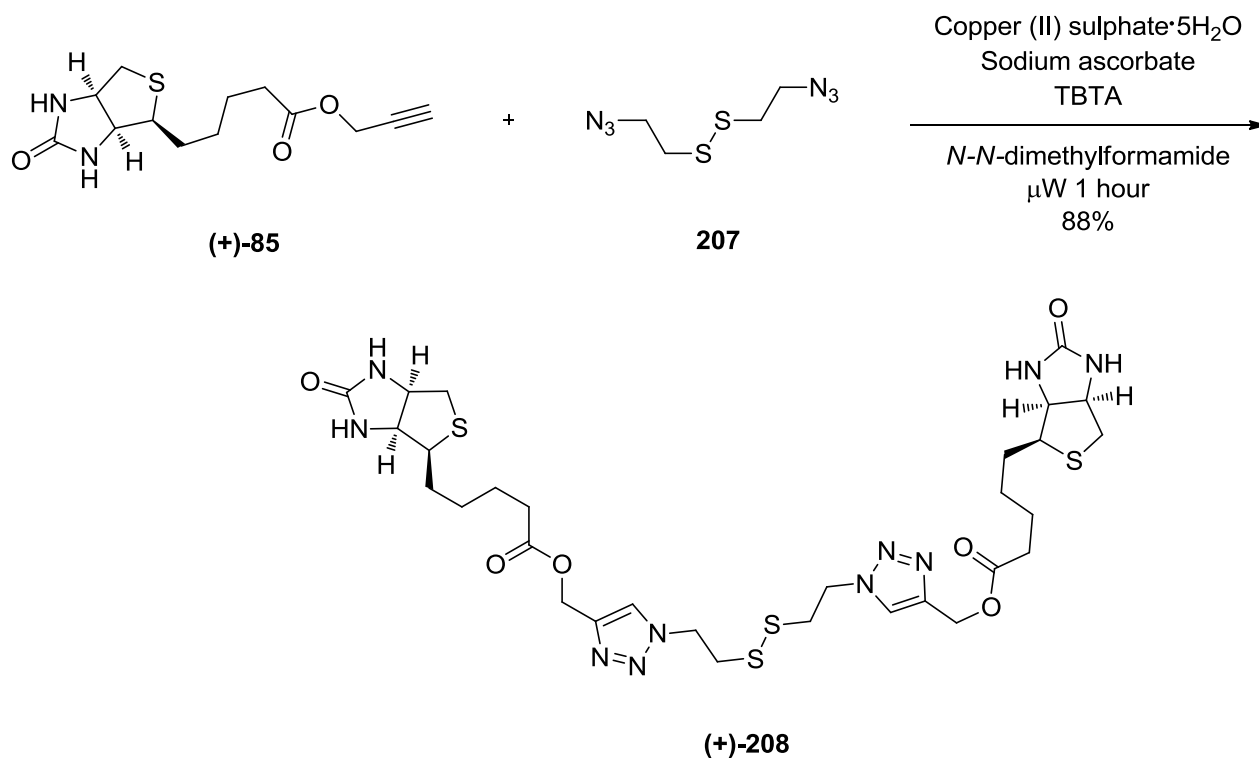
Synthesis of 1,2-bis(2-azidoethyl)disulfane **207**



A 25 mL round-bottomed flask was charged with 2,2'-disulfanediyldiethanaminium chloride **206** (134 mg, 0.596 mmol), potassium carbonate (494 mg, 3.58 mmol) and copper(II) sulfate pentahydrate (1.489 mg, 5.96 μmol) in methanol (10 ml). To this 1H-imidazole-1-sulfonyl azide hydrochloride (250 mg, 1.193 mmol) was added in portions over 5 minutes. The reaction mixture was left to stir for 12 hours under an atmosphere of argon. The impure reaction mixture was transferred to a 25 mL separating funnel and diluted with water (10 mL). 1N aqueous hydrochloric acid (10 mL) was added and pH was checked to ensure the aqueous layer was acidic (pH1). The mixture was extracted with ether (2x10mL) and washed with 1N aqueous hydrochloric acid (10 mL), washed with brine (10 mL) and dried with magnesium sulfate. The suspension was filtered and the solvent was removed under reduced pressure until 1 mL remained. This was filtered through a small plug of silica, washed through with diethyl ether (3 mL) and the solvent was removed under reduced pressure to afford a yellow liquid. Subsequent physicochemical analysis confirmed this to be the title compound **207** (100 mg, 0.490 mmol, 82 % yield)

207 *Rf* 0.8 (diethyl ether) $^1\text{H-NMR}$ (300 MHz, CDCl_3) δ 3.59 (t, J 6.7 Hz, 4H), 2.86 (t, J 6.7 Hz, 4H). $^{13}\text{C-NMR}$ (75 MHz, CDCl_3) δ 49.81, 37.45 ppm. ATR-IR 2101 C-N_3 cm^{-1} .

Synthesis of (*S,S,R*)-(1,1'-(2,2'-disulfaneyldiylbis(ethane-2,1-diyl))bis(1*H*-1,2,3-triazole-4,1-diyl))bis(methylene) bis(5-((3*aS*,4*S*,6*aR*)-2-oxohexahydro-1*H*-thieno[3,4-*d*]imidazol-4-yl)pentanoate) (+)-208****

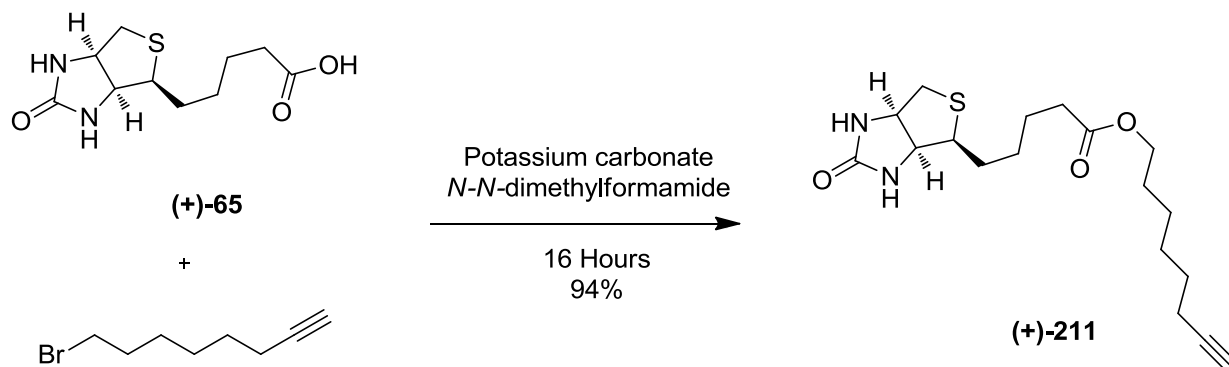


A 2.5 mL microwave vial was charged with propargyl (+)-biotin (**85**) (25 mg, 0.089 mmol), 1,2-*bis*(2-azidoethyl)disulfane **207** (9.04 mg, 0.044 mmol), sodium ascorbate (2.63 mg, 0.013 mmol), copper(II) sulfate pentahydrate (1.105 mg, 4.43 μ mol) and TBTA (4.70 mg, 8.85 μ mol) in *N,N*-dimethylformamide (2 mL). The vial was sealed with a Teflon cap and heated *via* microwave irradiation for 1 hour at 70 °C. The resulting solution was diluted with ethyl acetate (2 mL), water (2 mL) and transferred to a 25 mL separating funnel. The mixture was extracted with ethyl acetate (2 x 5 mL) and the combined organic extracts were washed with water (5 x 10mL) and washed with brine (5 mL) and dried with magnesium sulfate. The suspension was filtered and the solvent removed under reduced pressure. The impure product was purified by flash chromatography on silica gel eluting with 10% methanol in dichloromethane to afford a white solid. Subsequent physiochemical analysis confirmed this was the title compound (**208**) (30 mg, 0.039 mmol, 88 % yield)

208 *R*_f 0.4 (10% methanol in dichloromethane) ¹H NMR (400 MHz, DMSO) δ 8.19 (s, 2H), 6.44 (s, 2H), 6.38 (s, 2H), 5.13 (s, 4H), 4.64 (t, *J* 6.6 Hz, 4H), 4.38 – 4.22 (m, 2H), 4.12 (d, *J* 6.0 Hz, 2H), 3.25 (t, *J* 6.5 Hz, 4H), 3.08 (t, *J* 9.7 Hz, 2H), 2.81 (dd, *J* 12.6, 5.0 Hz, 2H), 2.31 (t, *J* 7.4 Hz, 4H), 1.66 – 1.18 (m, 12H). ¹³C NMR (101 MHz, DMSO) δ 180.04, 176.94, 142.62, 125.63, 61.63, 59.81, 57.65, 56.00, 48.70, 37.55, 28.60, 25.09, 9.39, 9.18. ATR-IR 1748 C=O, 1679 C=O *m/z*

[ES]⁺ M+Na 791.1 HRMS (NSI) Calcd for C₃₀H₄₈N₁₁O₆S₄, M+NH₄, 787.2705; Found 787.2710.
[α]_D²⁷ +39 (c 1.0, CHCl₃).

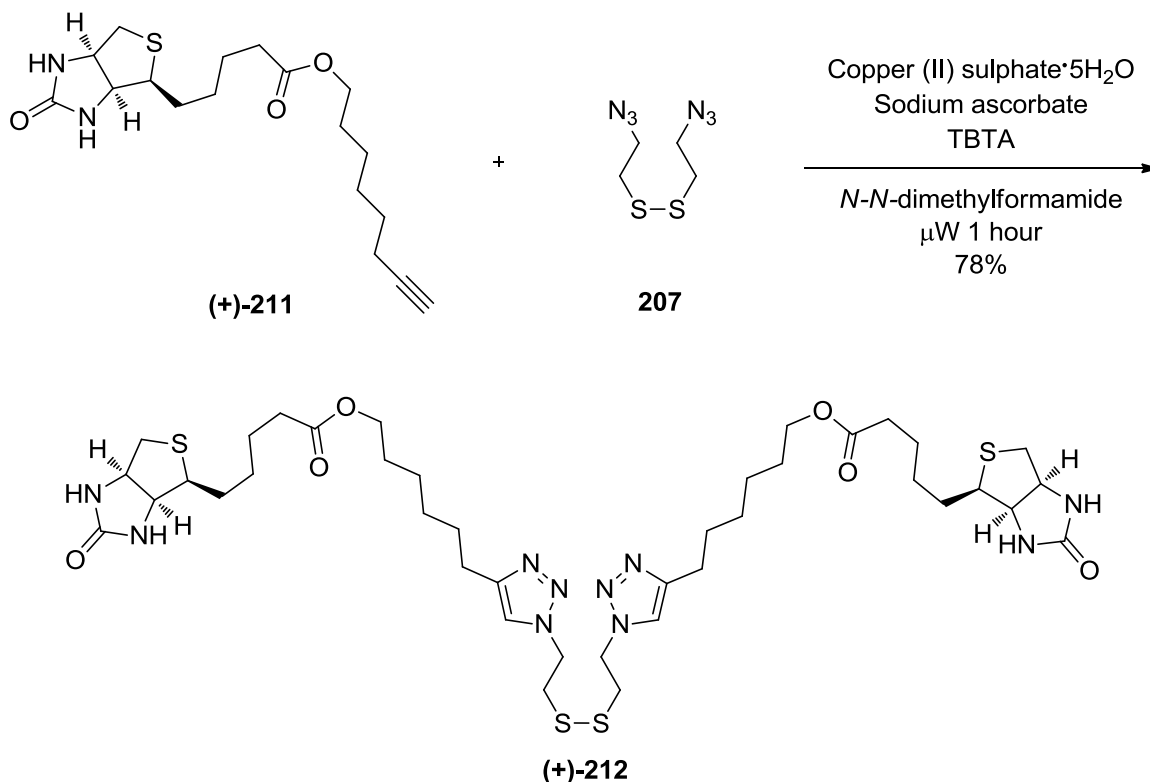
Synthesis of oct-7-ynyl 5-((3a*S*,4*S*,6a*R*)-2-oxohexahydro-1*H*-thieno[3,4-*d*]imidazol-4-yl)pentanoate (+)-**211**



A 25 mL round-bottomed flask was charged with (+)-biotin (+)-**64** (100 mg, 0.409 mmol) and potassium carbonate (85 mg, 0.614 mmol) in *N,N*-dimethylformamide (5 mL). This was left to stir for 30 minutes before addition of 8-bromooct-1-yne (116 mg, 0.614 mmol). The resulting solution was left to stir for 16 hours under an atmosphere of argon. The resulting solution was diluted with ethyl acetate (5 mL), transferred to a 50 mL separating funnel and diluted with water (10 mL). The mixture was extracted with ethyl acetate (2 x 5 mL) and the combined organic extracts were washed with water (5 x 10 mL), brine (10 mL) and dried with magnesium sulfate. The suspension was filtered and the solvent removed under reduced pressure. The impure material was purified by flash chromatography on silica gel eluting with 5% methanol in dichloromethane to afford a waxy solid. Subsequent physicochemical analysis confirmed this to be the title compound. (+)-**211** (135 mg, 0.383 mmol, 94 % yield)

(+)-**211** *R*_f 0.5 (5% methanol in dichloromethane) ¹H-NMR (400 MHz, CDCl₃) δ 6.06 (s, 1H, NH), 5.73 (s, 1H, NH), 4.44 (dd, *J* 7.6, 4.7 Hz, 1H, CH), 4.24 (dd, *J* 7.5, 4.8 Hz, 1H, CH), 3.99 (t, *J* 6.7 Hz, 2H, CH₂), 3.15 – 3.01 (m, 1H, CH), 2.84 (dd, *J* 12.8, 5.0 Hz, 1H, CH), 2.68 (d, *J* 12.7 Hz, 1H, CH), 2.26 (t, *J* 7.5 Hz, 2H, CH₂), 2.13 (td, *J* 7.0, 2.6 Hz, 1H, CH), 1.89 (t, *J* 2.6 Hz, 1H, CH), 1.74 – 1.51 (m, 8H, 4CH₂), 1.42 – 1.21 (m, 6H, 3CH₂). ¹³C-NMR (101 MHz, CDCl₃) δ 173.79, 163.92, 84.49, 68.31, 64.37, 64.24, 61.99, 60.15, 55.51, 40.56, 33.97, 32.59, 28.49, 28.40, 28.28, 25.44, 24.83, 18.30 ppm. FT-IR KBr(neat) 3220 C-H, 2119 C-C, 1729 C=O, 1699 C=O cm⁻¹. *m/z* [ES]⁺ M+Na 375.1 HRMS (NSI) Calcd for C₁₈H₂₉N₂O₃S 353.1893, M+H, Found 353.1898. [α]_D²⁶ +35 (c 1.0, CHCl₃).

Synthesis of 6-(1-(2-((2-(4-(6-(5-((3aR,4R,6aS)-2-oxohexahydro-1H-thieno[3,4-d]imidazol-4-yl)pentanoyloxy)hexyl)-1H-1,2,3-triazol-1-yl)ethyl)disulfanyl)ethyl)-1H-1,2,3-triazol-4-yl)hexyl 5-((3aS,4S,6aR)-2-oxohexahydro-1H-thieno[3,4-d]imidazol-4-yl)pentanoate (+)-212

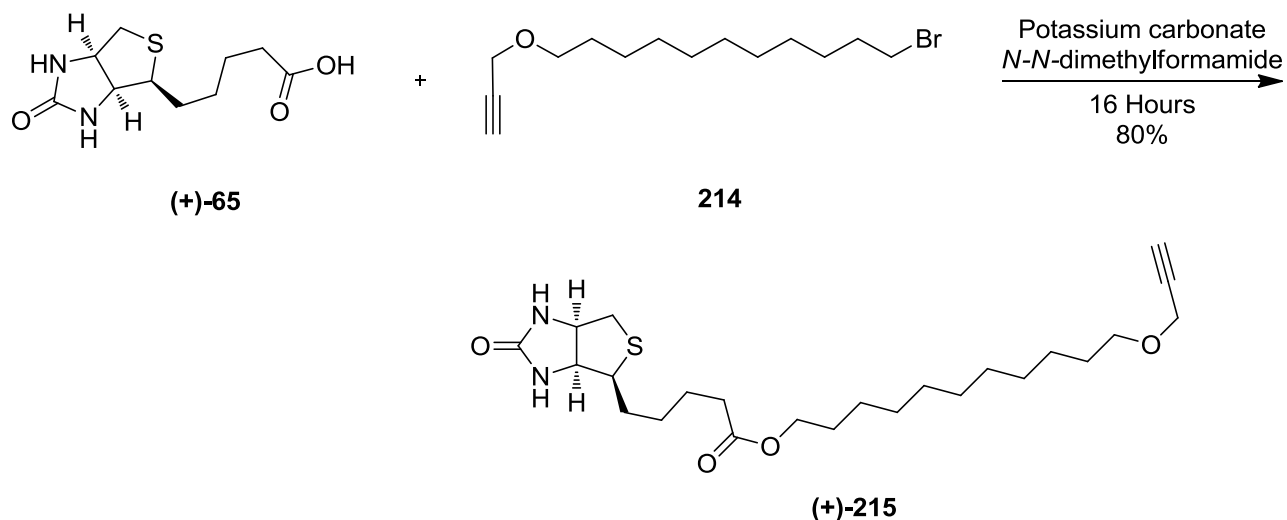


A 3 mL microwave vial was charged with oct-7-ynyl 5-((3aS,4S,6aR)-2-oxohexahydro-1H-thieno[3,4-d]imidazol-4-yl)pentanoate (+)-**211** (40 mg, 0.113 mmol), 1,2-bis(2-azidoethyl)disulfane **207** (11.59 mg, 0.057 mmol), copper (II) sulfate pentahydrate (1.5 mg, 5.67 μ mol), sodium ascorbate (8.99 mg, 0.05 mmol) and TBTA (3 mg, 5.67 μ mol) in *N,N*-dimethylformamide (2 mL). The vial was sealed with a Teflon cap and heated to 70°C *via* microwave irradiation for 1 hour. The resulting solution was transferred to a 50 mL separating funnel and diluted with ethyl acetate (2 mL) and water (5 mL). The solution was extracted with ethyl acetate (2 x 5mL) and the combined organic extracts were washed with water (5 x 10mL), brine (10 mL) and dried with magnesium sulfate. The suspension was filtered and the solvent removed under reduced pressure. The resulting impure product was purified by flash chromatography on silica gel eluting with 10% methanol in dichloromethane to afford an off white solid. Subsequent physicochemical analysis confirmed this to be the title compound (+)-**212** (40 mg, 0.044 mmol, 78 % yield)

(+)-**212** *Rf* 0.4 (10% methanol in dichloromethane). ¹H-NMR (400 MHz, CDCl₃, 10% CD₃OD) δ 7.52 (s, 2H, ArH), 4.59 (s, 4H, 2CH₂), 4.50 – 4.35 (m, 2H, 2CH), 4.34 – 4.17 (m, 2H, 2CH), 4.00 (t, *J* 6.6 Hz, 4H, 2CH₂), 3.13 (t, *J* 5.4 Hz, 6H, 2CH₂, 2CH), 2.68 (d, *J* 12.4 Hz, 6H, 2CH₂, 2CH), 2.27 (t, *J* 7.3 Hz, 4H, 2CH₂), 1.75 – 1.46 (m, 18H, 9CH₂), 1.38 (m, 12H, 6CH₂). ¹³C-NMR (101 MHz,

CDCl₃, 10%CD₃OD) δ 173.97, 163.92, 153.72, 124.24, 64.45, 61.93, 60.10, 55.42, 40.36, 37.58, 33.94, 29.05, 28.66, 28.41, 28.22, 25.59, 25.36, 24.75 ppm. AT-IR 1750 C=O, 1683 C=O *m/z* [ESI]⁺ M+Na 931.2 HRMS (NSI) Calcd for C₄₀H₆₈N₁₁O₆S₄, M+NH₄, 926.4237, found 926.4232. $[\alpha]_D^{26}$ +37 (c 1.0, CHCl₃).

Synthesis of 11-(prop-2-ynyloxy)undecyl 5-((3*aS*,4*S*,6*aR*)-2-oxohexahydro-1*H*-thieno[3,4-*d*]imidazol-4-yl)pentanoate (+)-**215**

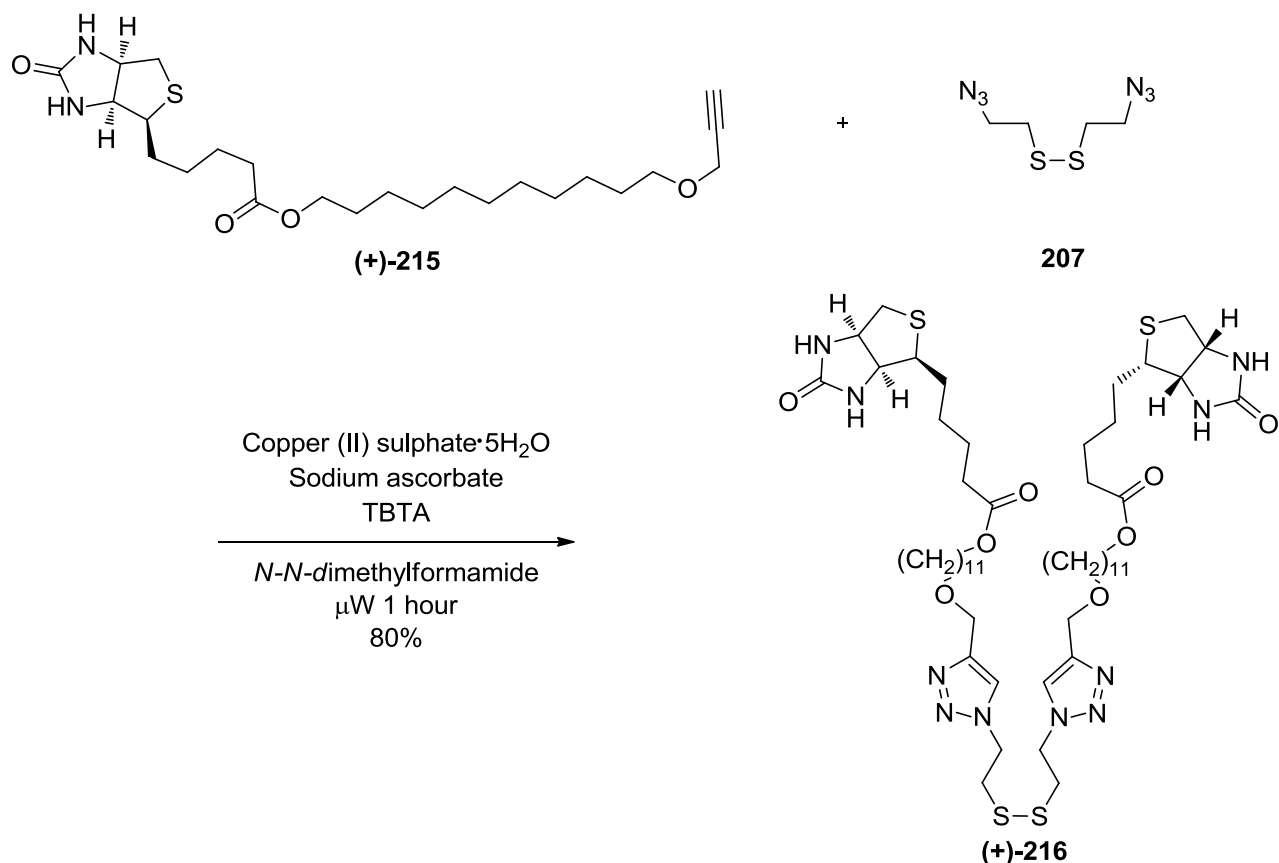


A 25 mL round-bottomed flask was charged with (+)-biotin (+)-**65** (100 mg, 0.409 mmol) and potassium carbonate (85 mg, 0.614 mmol) in *N-N*-dimethylformamide (5 mL). This was stirred for 30 minutes before addition of 1-bromo-11-(prop-2-ynyloxy)undecane **214** (154 mg, 0.532 mmol). The solution was left to stir for 16 hours under an atmosphere of argon and then diluted with ethyl acetate (5 mL), water (5 mL) and transferred to a 50 mL separating funnel. The mixture was extracted with ethyl acetate (2 x 5 mL) and the combined organic extracts were washed with water (5 x 10 mL), brine (5 mL) and dried with magnesium sulfate. The suspension was filtered and the solvent removed under reduced pressure. The impure product was purified by flash chromatography on silica gel eluting with 5-7% methanol in dichloromethane to afford an off white solid. Subsequent physicochemical analysis confirmed this was the title product. (+)-**215** (148 mg, 0.327 mmol, 80 % yield)

(+)-**215** *R_f* 0.5 (7% methanol in dichloromethane) ¹H-NMR (400 MHz, CDCl₃) δ 5.57 (d, br, 1H, NH), 5.20 (s, br, 1H, NH), 4.62 – 4.45 (m, 1H, CH), 4.34 (dd, *J* 7.5, 4.6 Hz, 1H, CH), 4.15 (d, *J* 2.3 Hz, 2H, CH₂), 4.07 (t, *J* 6.7 Hz, 2H, CH₂), 3.53 (t, *J* 6.6 Hz, 2H, CH₂), 3.19 (s, 1H, CH), 2.95 (d, *J* 12.6 Hz, 1H, CH), 2.76 (d, *J* 12.8 Hz, 1H, CH), 2.44 (t, *J* 2.3 Hz, 1H, CH), 2.35 (t, *J* 7.4 Hz, 2H, CH₂), 1.82 – 1.56 (m, 8H, 4CH₂), 1.54 – 1.42 (m, 2H, CH₂), 1.31 (d, *J* 11.4 Hz, 14H, 7CH₂). ¹³C-NMR (101 MHz, CDCl₃) δ 173.74, 163.30, 80.08, 74.04, 70.32, 64.59, 61.94, 60.13, 58.01, 55.33,

40.55, 33.93, 29.50, 29.42, 29.25, 28.64, 28.34, 28.27, 26.09, 25.93, 24.82 ppm. ATR-IR 3247 C-H, 1727 C=O, 1706 C=O cm^{-1} . m/z [ES]⁺ M+Na475.2, HRMS (NSI) Calcd for C₂₄H₄₁N₂O₄S, M+H, 453.2782; Found 453.2782. $[\alpha]_D^{25} +24$ (c 1.0, CHCl₃)

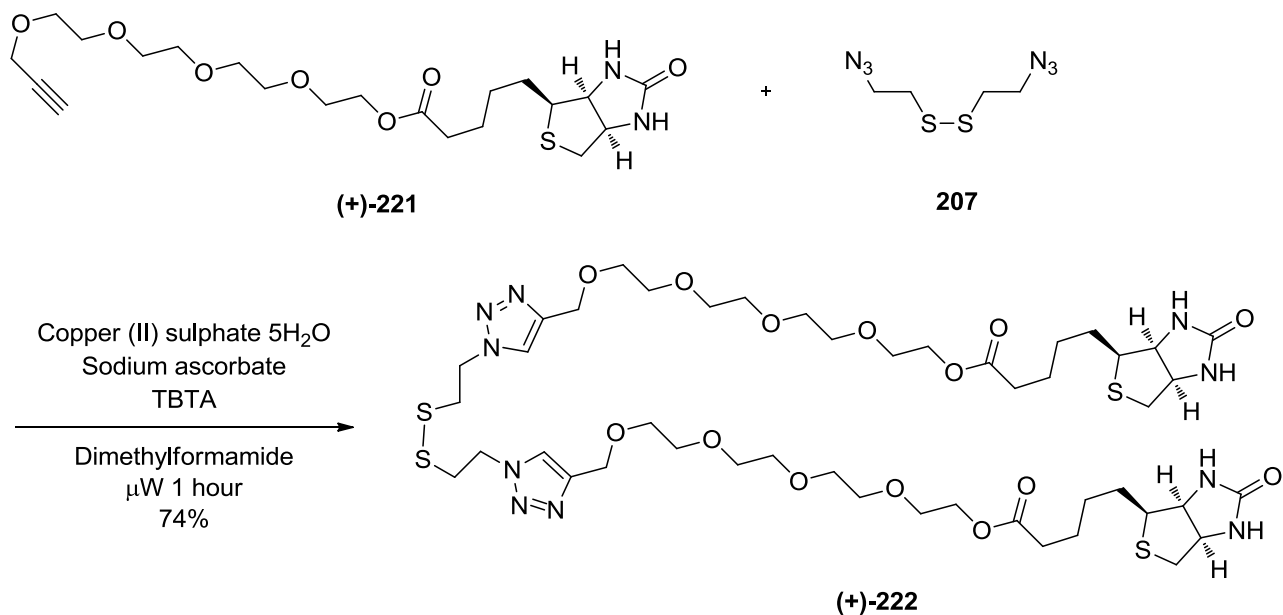
Synthesis of (*S,S,R*)-(((1,1'-(disulfaneyldiyl)bis(ethane-2,1-diyl))bis(1*H*-1,2,3-triazole-4,1-diyl))bis(methylene))bis(oxy))bis(undecane-11,1-diyl) bis(5-((3*aS*,4*S*,6*aR*)-2-oxohexahydro-1*H*-thieno[3,4-*d*]imidazol-4-yl)pentanoate) (+)-216



A 3 mL microwave vial was charged with (+)-**215** (40 mg, 0.088 mmol), 1,2-bis(2-azidoethyl)disulfane **207** (9 mg, 0.044 mmol), copper (II) sulfate pentahydrate (1 mg, 4.42 μmol), sodium ascorbate (7 mg, 0.035 mmol) and TBTA (7 mg, 0.013) in *N,N*-dimethylformamide (2 mL). The vial was sealed with a Teflon cap and heated to 70 °C *via* microwave irradiation for 1 hour. The resulting solution was transferred to a 50 mL separating funnel and diluted with ethyl acetate (2 mL) and water (5 mL). The solution was extracted with ethyl acetate (2 x 5 mL) and the combined organic extracts were washed with water (5 x 10 mL), brine (10 mL) and dried with magnesium sulfate. The suspension was filtered and the solvent removed under reduced pressure. The resulting impure product was purified by flash chromatography on silica gel eluting with 10% methanol in dichloromethane to afford an off white solid. Subsequent physicochemical analysis confirmed this to be the title compound (+)-**216** (39 mg, 0.035 mmol, 80 % yield)

70.58, 70.56, 70.50, 70.39, 69.14, 69.11, 65.83, 63.42, 61.94, 60.11, 58.39, 55.56, 40.53, 33.77, 28.32, 28.22, 24.74, 15.26 ppm. ATR-IR 2112 C-C, 1738 C=O, 1648C=O, 1010 cm⁻¹. *m/z* [ES]⁺ M+H 458.9 HRMS (NSI) Calcd for C₂₁H₃₅N₂O₇S, M+H, 459.2160; found 459.2160. [α]_D²⁶ +28 (c 1.0, CHCl₃).

Synthesis of (*S,S,R*)-1,1'-(1,1'-(disulfaneyldiylbis(ethane-2,1-diyl))bis(1*H*-1,2,3-triazole-4,1-diyl))bis(2,5,8,11-tetraoxatridecane-13,1-diyl) bis(5-((3*aS*,4*S*,6*aR*)-2-oxohexahydro-1*H*-thieno[3,4-*d*]imidazol-4-yl)pentanoate) . (+)-222****

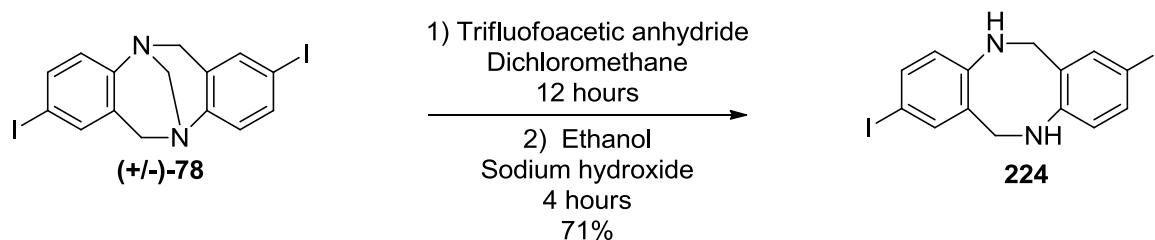


A 3 mL microwave vial was charged with (+)-**221** (30 mg, 0.065 mmol), 1,2-*bis*(2-azidoethyl)disulfane **207** (6.68 mg, 0.033 mmol), copper (II) sulfate pentahydrate (1 mg, 3.27 μmol), sodium ascorbate (5 mg, 0.026 mmol) and TBTA (5.21 mg, 9.81 μmol) in *N,N*-dimethylformamide (2 mL). The vial was sealed with a Teflon cap and heated to 70 °C *via* microwave irradiation for 1 hour. The resulting solution was transferred to a 50 mL separating funnel and diluted with ethyl acetate (2 mL) and water (5 mL). The solution was extracted with ethyl acetate (2 x 5mL) and the combined organic extracts were washed with water (5 x 10mL), brine (10 mL) and dried with magnesium sulfate. The suspension was filtered and the solvent removed under reduced pressure. The resulting impure product was purified by flash chromatography on silica gel eluting with 10% methanol in dichloromethane to afford an off white solid. Subsequent physiochemical analysis confirmed this to be the title compound . (+)-**222** (30 mg, 0.027 mmol, 74 % yield)

¹H-NMR (400 MHz, CDCl₃) δ 7.68 (s, 2H, ArH), 6.08 (s, 2H, 2NH), 5.39 (s, 2H, 2NH), 4.68 – 4.52 (m, 8H, 4CH₂), 4.47 – 4.37 (m, 2H, 2CH), 4.22 (dt, *J*15.3, 7.5 Hz, 2H, 2CH), 4.18 – 4.06 (m, 4H,

2CH₂), 3.69 – 3.49 (m, 24H, 12CH₂), 3.13 (t, *J*6.7 Hz, 4H, 2CH₂), 3.07 (dd, *J*11.8, 7.3 Hz, 2H, 2CH), 2.83 (dd, *J*12.8, 4.9 Hz, 2H, 2CH), 2.67 (d, *J*12.7 Hz, 2H, 2CH), 2.29 (t, *J*7.5 Hz, 4H, 2CH₂), 1.74 – 1.49 (m, 8H, 4CH₂), 1.46 – 1.30 (m, 4H, 2CH₂). ¹³C-NMR (101 MHz, CDCl₃) δ 173.67, 163.67, 123.55, 70.61, 70.56, 70.55, 70.54, 70.53, 69.76, 69.14, 64.62, 63.42, 61.93, 60.11, 55.61, 48.72, 40.57, 37.72, 33.67, 28.31, 28.22, 24.77 ppm. ATR-IR 1740 C=O, 1642C=O, 1012 cm⁻¹. *m/z* [ES]⁺ M+Na 1143.3. HRMS (NSI) Calcd for C₄₆H₈₀N₁₁O₁₄S₄, M+NH₄, 1138.4773; Found 1138.4775. [α]_D²⁵ +27 (c 1.0, CHCl₃)

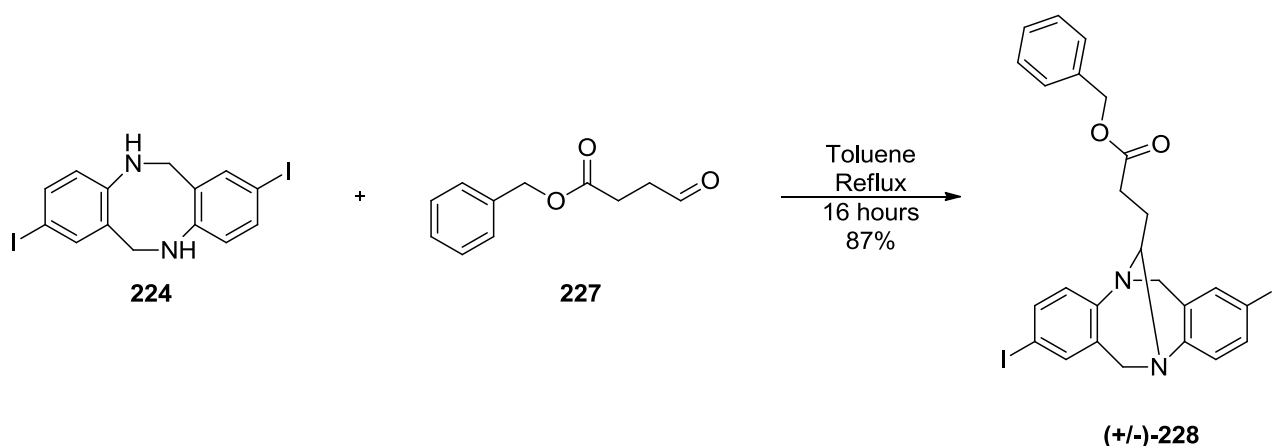
Synthesis of 2,8-bis-iodo-5,6,11,12-tetrahydrobenzo[b,f][1,5]diazocine **224**



A 50 mL round bottomed flask was charged with 2,8-bis-iodo-6H,12H-5,11-methandibenzo[b,f][1,5]diazocine (1.4 g, 2.95 mmol) in dichloromethane (10 mL). To this trifluoroacetic anhydride (1.232 ml, 8.86 mmol) was added and left to stir for 12 hours under an atmosphere of argon gas. The solution was diluted with water (10 mL) and quenched with saturated sodium bicarbonate until fizzing stopped. The reaction mixture was transferred to a 50 mL separating funnel and the layers were separated and extracted with dichloromethane (2 x 10mL) the combined organic extracts were washed with brine (10 mL) and dried with magnesium sulfate. The suspension was filtered and the solvent was removed under reduced pressure and the resulting solid redissolved in ethanol (10 mL). Sodium hydroxide pellets (100mg) were added and left to stir for 4 hours under an atmosphere of argon gas. The reaction mixture was then diluted with water, transferred to a 50 mL separating funnel and extracted with dichloromethane (2 x 10mL). The organic extracts were washed with brine (10 mL) and dried with magnesium sulfate. The solution was filtered and the solvent was removed under reduced pressure. The resulting impure solid was purified by flash chromatography on silica gel eluting with dichloromethane to afford a pale yellow solid. Subsequent physiochemical analysis confirmed this was the title compound 2,8-bis-iodo-5,6,11,12-tetrahydrobenzo[b,f][1,5]diazocine **224** (978 mg, 2.117 mmol, 71.7 % yield)

¹H-NMR (300 MHz, CDCl₃) δ 7.30 – 7.22 (m, 4H), 6.36 (d, *J* 8.0 Hz, 2H), 4.41 (s, 4H). ¹³C-NMR (75 MHz, CDCl₃) δ 147.38, 139.85, 136.99, 127.41, 119.98, 79.75, 49.29 ppm. *m/z* [ES]⁺ M+H, 462.8 HRMS (NSI) Calcd for C₁₄H₁₆I₂N₃, M+NH₄, 479.9434; Found 479.9434

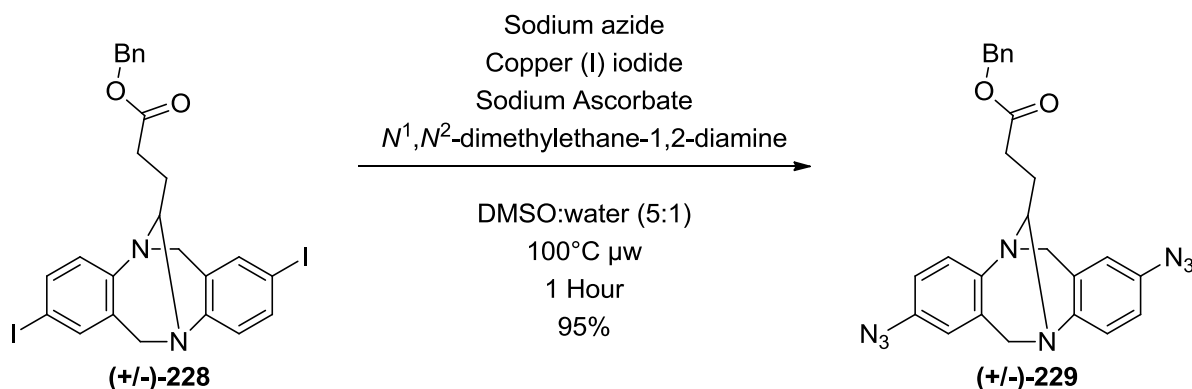
Synthesis of benzyl 3-(2,8-bis-iodo-6,12-dihydro-5,11-methanodibenzo[b,f][1,5]diazocin-13-yl)propanoate (+/-)-228



A flame-dried 25 mL round-bottomed flask was charged with 2,8-bis-iodo-5,6,11,12-tetrahydrodibenzo[b,f][1,5]diazocine **224** (313 mg, 0.676 mmol) and benzyl 4-oxobutanoate **227** (130 mg, 0.676 mmol) in toluene (10 mL). The suspension was heated to 130 °C and refluxed for 16 hours with constant removal of water by Dean-Stark trap. The resulting solution was evaporated to dryness under vacuum and purified *via* flash chromatography silica gel eluting with 20% diethyl ether in petroleum ether affording a waxy solid. Subsequent ¹H-NMR physiochemical analysis confirmed this to be the title compound (+/-)-**228** (374 mg, 0.588 mmol, 87 % yield)

R_f 0.7 (1:5, diethyl ether : hexane) ¹H-NMR (500 MHz, CDCl₃) δ 7.48 – 7.41 (m, 2H, ArH), 7.37 – 7.28 (m, 5H, ArH), 7.21 (dd, *J* 8.4, 1.6 Hz, 2H, ArH), 6.82 (dd, *J* 12.4, 8.5 Hz, 2H, ArH), 5.23 – 4.88 (m, 2H, CH₂), 4.55 (d, *J* 16.7 Hz, 1H, CH), 4.46 (d, *J* 17.4 Hz, 1H, CH), 4.07 (d, *J* 16.7 Hz, 1H, CH), 4.05 (dd, *J* 6.5, 8.1 Hz, 1H, CH), 3.95 (d, *J* 17.4 Hz, 1H, CH), 2.57 (t, *J* 7.3 Hz, 2H, CH₂), 2.05 – 1.86 (m, 2H, CH₂). ¹³C NMR (75 MHz, CDCl₃) δ 172.91, 149.80, 145.17, 136.77, 136.34, 135.97, 135.74, 135.42, 130.56, 129.54, 128.62, 128.32, 128.28, 127.22, 87.57, 72.10, 66.27, 59.87, 51.50, 30.39, 25.92 ppm. ATR-IR 1730 C=O, 1471, 1166, 907, 826, 729 cm⁻¹. *m/z* [ES]⁺ M+H 637.0 HRMS (NSI) Calcd for C₂₅H₂₃I₂N₂O₂, M+H, 636.9843; Found 636.9840.

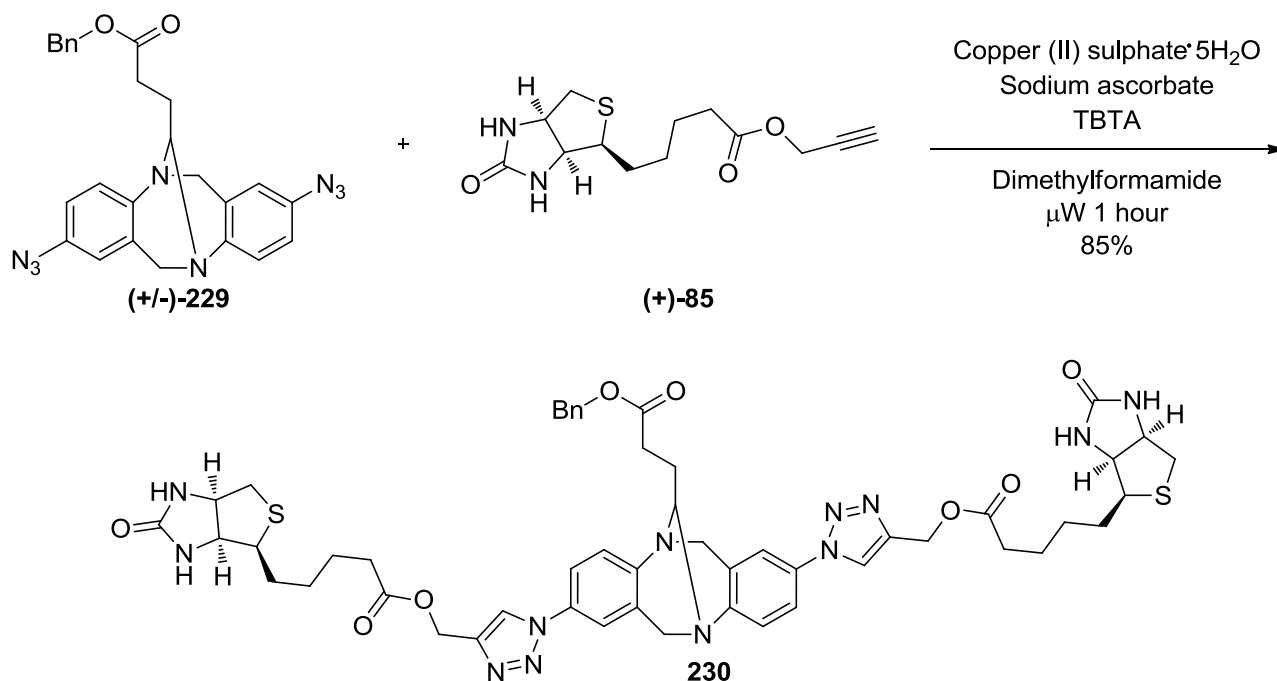
Synthesis of benzyl 3-(2,8-bis-azido-6,12-dihydro-5,11-methanodibenzo[b,f][1,5]diazocin-13-yl)propanoate (+/-)-229



A 5 mL microwave vial was charged with (+/-)-228 (250 mg, 0.393 mmol), sodium azide (102 mg, 1.572 mmol), copper(I) iodide (14.97 mg, 0.079 mmol) and sodium ascorbate (7.78 mg, 0.039 mmol) in dimethylsulfoxide / water mixture (3 mL). The vial was sealed with a Teflon cap and N^1,N^2 -dimethylethane-1,2-diamine (10.39 mg, 0.118 mmol) was added *via* syringe. The suspension was heated to 100 °C for 1 hour *via* microwave irradiation. The reaction mixture was diluted with dichloromethane and transferred to a 50 mL separating funnel and washed with water (3 x 10mL). The combined organic extracts were washed with brine (5 mL) and dried with magnesium sulfate. The suspension was filtered and the solvent removed under reduced pressure. The impure mixture was columned by flash chromatography on silica gel eluting with dichloromethane afforded a thick yellow oil. Subsequent physiochemical analysis confirmed this was the title compound. (+/-)-229 (174 mg, 0.373 mmol, 95 % yield)

Rf 0.6 (dichloromethane) $^1\text{H-NMR}$ (300 MHz, CDCl_3) δ 7.33 (s, 5H, ArH), 7.07 (t, J 8.6 Hz, 2H, ArH), 6.83 (dt, J 8.6, 2.2 Hz, 2H, ArH), 6.56 (dd, J 4.5, 2.6 Hz, 2H, ArH), 5.11 (s, 2H, CH_2), 4.59 (d, J 16.7 Hz, 1H, CH), 4.50 (d, J 17.4 Hz, 1H, CH), 4.09 (m, 2H), 3.98 (d, J 17.5 Hz, 1H, CH), 2.60 (t, J 7.4 Hz, 2H, CH_2), 2.12 – 1.81 (m, 2H, CH_2). $^{13}\text{C-NMR}$ (75 MHz, CDCl_3) δ 173.00, 147.10, 142.40, 135.99, 135.65, 135.48, 129.53, 128.58, 128.49, 128.27, 128.22, 127.64, 126.59, 118.77, 118.36, 116.97, 116.72, 72.50, 66.22, 60.39, 52.09, 30.44, 26.03. ATR-IR (neat) 2105 C-N_3 , 1731 C=O , 1484, 1274, 1165 cm^{-1} . m/z $[\text{ES}]^+$ $\text{M}+\text{H}$ 467.6. HRMS (NSI) Calcd for $\text{C}_{25}\text{H}_{23}\text{N}_8\text{O}_2$, $\text{M}+\text{H}$, 467.1945; Found 467.1946

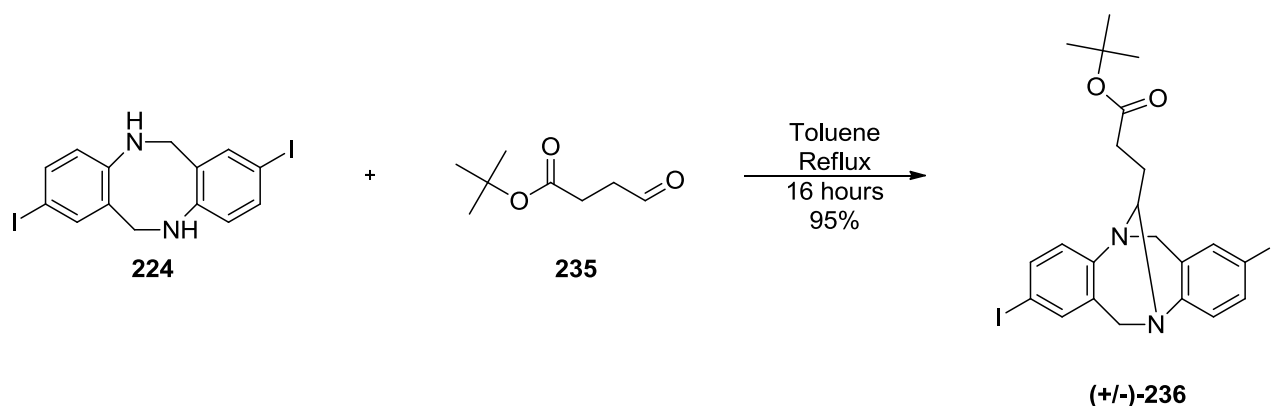
Synthesis of (*S,S,R*)-(1,1'-(13-(3-(benzyloxy)-3-oxopropyl)-6,12-dihydro-5,11-methanodibenzo [b,f][1,5]diazocine-2,8-diyl)bis(1*H*-1,2,3-triazole-4,1-diyl))bis(methylene) bis(5-((3*aS*,4*S*,6*aR*)-2-oxohexahydro-1*H*-thieno[3,4-*d*]imidazol-4-yl)pentanoate) **230**



A 2.5 mL microwave vial was charged with (+/-)-**229** (45 mg, 0.096 mmol), (+/-)-**85** (57.2 mg, 0.203 mmol), copper(II) sulfate pentahydrate (0.3 eq), sodium-*L*-ascorbate (0.8 eq) and TBTA (0.3 eq) in *N,N*-dimethylformamide. The reaction mixture was heated to 70°C, in a sealed vial, by microwave radiation for 1 hour. The reaction mixture was then diluted with ethyl acetate (5 mL) and transferred to a 25mL separating funnel. The solution was extracted with ethyl acetate (2x5mL) and washed with water (5 x 10mL), dried with brine (5 mL) and magnesium sulfate. The extract was filtered and solvent removed under reduced pressure. The reaction mixture was purified by column chromatography on silica eluting with 5-10% methanol in dichloromethane affording a white solid. Subsequent physicochemical analysis confirmed this to be the title compound **230** (85 mg, 0.082 mmol, 85 % yield)

¹H NMR (400 MHz, CDCl₃) δ 7.99 (dd, *J*_{25.5, 5.1} Hz, 2H), 7.45 (d, *J*_{6.4} Hz, 2H), 7.26 (s, 5H), 7.18 – 7.03 (m, 2H), 6.25 (d, *J*_{18.4} Hz, 2H), 5.58 (d, *J*_{6.4} Hz, 2H), 5.30 – 5.11 (m, 4H), 5.12 – 4.95 (m, 2H), 4.64 (d, *J*_{17.1} Hz, 2H), 4.56 (d, *J*_{16.9} Hz, 2H), 4.31 – 3.89 (m, 6H), 2.94 (dd, *J*_{14.7, 8.6} Hz, 4H), 2.60 (dt, *J*_{14.5, 9.5} Hz, 4H), 2.46 (dd, *J*_{17.6, 13.0} Hz, 2H), 2.25 (t, *J*_{6.8} Hz, 4H), 2.13 – 1.71 (m, 4H), 1.48 (m, 8H), 1.27 (m, 4H). ATR-IR (neat) 1745 C=O, 1705 C=O, 1695 C=O cm⁻¹; *m/z* [ES]⁺ M+H 1031.6. HRMS (NSI) Calcd for C₅₁H₆₂N₁₃O₈S₂, M+NH₄, 1048.4284; Found 1048.4284. [α]_D²⁴ +18 (c 1.0, CHCl₃)

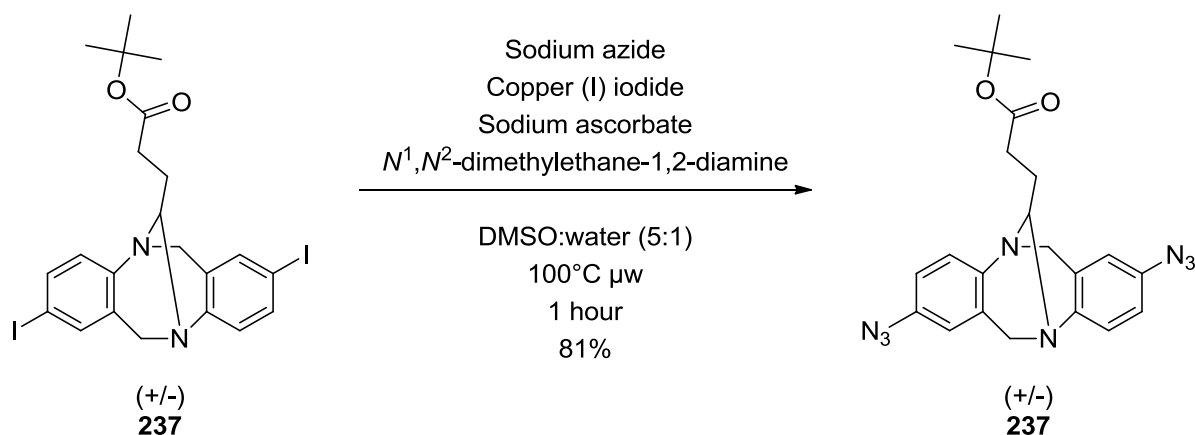
Synthesis of *tert*-butyl 3-(2,8-bis-iodo-6,12-dihydro-5,11-methanodibenzo[b,f][1,5]diazocin-13-yl)propanoate (+/-)-237



A flame-dried 25 mL round-bottomed flask was charged with 2,8-bis-iodo-5,6,11,12-tetrahydrodibenzo[b,f][1,5]diazocine **224** (117 mg, 0.253 mmol) and *tert*-butyl 4-oxobutanoate **235** (40 mg, 0.253 mmol) in toluene (10 mL). The suspension was heated to 130 °C and refluxed for 16 hours with constant removal of the water by Dean-Stark trap. The resulting solution was evaporated to dryness under vacuum and purified *via* flash chromatography on silica gel eluting with 20% diethyl ether in petroleum ether affording a waxy solid. Subsequent physicochemical analysis confirmed this to be the title compound (+/-)-**236** (145 mg, 0.241 mmol, 95 % yield)

R_f 0.8 (1:5, diethyl ether : hexane) ¹H-NMR (300 MHz, CDCl₃) δ 7.42 (dt, *J* 8.5, 1.9 Hz, 2H, ArH), 7.18 (dd, *J* 5.7, 1.8 Hz, 2H, ArH), 6.84 (dd, *J* 8.5, 2.6 Hz, 2H, ArH), 4.58 (d, *J* 16.7 Hz, 1H, CH), 4.47 (d, *J* 17.4 Hz, 1H, CH), 4.09 (d, *J* 16.9 Hz, 1H, CH), 4.05 – 3.99 (m, 1H, CH), 3.94 (d, *J* 17.5 Hz, 1H, CH), 2.43 (t, *J* 7.5 Hz, 2H, CH₂), 2.04 – 1.75 (m, 2H, CH₂), 1.42 (s, 9H, (CH₃)₃). ¹³C-NMR (75 MHz, CDCl₃) δ 172.45, 149.89, 145.26, 136.70, 136.30, 135.71, 135.40, 130.58, 129.65, 128.28, 127.26, 87.72, 87.57, 80.35, 72.19, 59.94, 51.51, 31.50, 28.06, 26.04 ppm. ATR-IR 1748 C=O cm⁻¹. *m/z* [ES]⁺ M+H 603.0. HRMS (NSI) Calcd for C₂₂H₂₅I₂N₂O₂, M+H, 603.0000; Found 602.9996

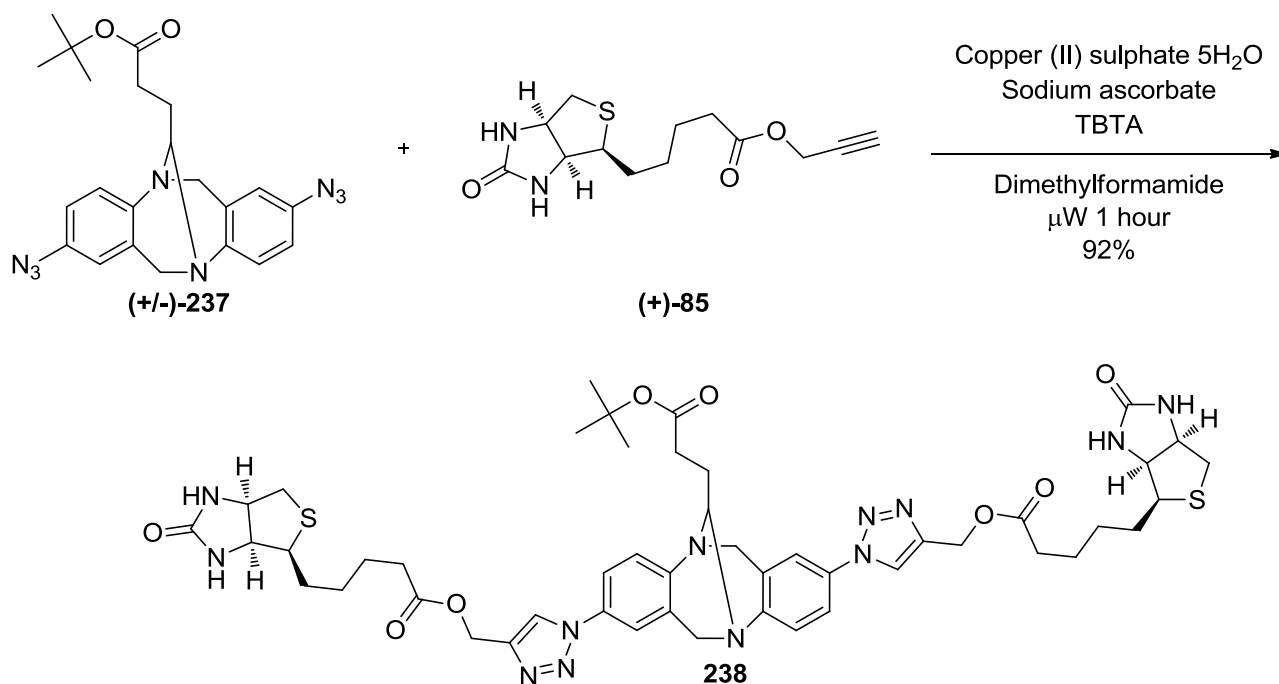
Synthesis of *tert*-butyl 3-(2,8-bis-azido-6,12-dihydro-5,11-methanodibenzo[*b,f*][1,5]diazocin-13-yl)propanoate (+/-)-**237**



A 5 mL microwave vial was charged with (+/-)-**236** (235 mg, 0.390 mmol), sodium azide (101 mg, 1.561 mmol), copper(I) iodide (7.43 mg, 0.039 mmol) and sodium ascorbate (7.73 mg, 0.039 mmol) in a dimethylsulfoxide / water mixture (5:1, 3 mL). The vial was sealed with a Teflon cap and *N*¹,*N*²-dimethylethane-1,2-diamine (5.16 mg, 0.059 mmol) was added *via* syringe. The suspension was heated to 100 °C for 1 hour *via* microwave irradiation. The reaction mixture was diluted with dichloromethane and transferred to a 50 mL separating funnel and washed with water (3 x10mL). The combined organic extracts were washed with brine (5 mL) and dried with magnesium sulfate. The suspension was filtered and the solvent removed under reduced pressure. The impure mixture was purified *via* flash chromatography on silica gel eluting with 20% diethyl ether in petroleum ether affording a yellow oil. Subsequent physicochemical analysis confirmed this was the title compound. (+/-)-**237** (136 mg, 0.314 mmol, 81 % yield)

¹H-NMR (300 MHz, CDCl₃) δ 7.08 (dd, *J* 8.6, 0.7 Hz, 2H), 6.82 (dt, *J* 8.6, 2.5 Hz, 2H), 6.55 (dd, *J* 5.3, 2.5 Hz, 2H), 4.62 (d, *J* 16.7 Hz, 1H), 4.51 (d, *J* 17.4 Hz, 1H), 4.09 (dd, *J* 20.9, 11.9 Hz, 2H), 3.97 (d, *J* 17.4 Hz, 1H), 2.45 (t, *J* 7.5 Hz, 2H), 2.08 – 1.75 (m, 2H), 1.43 (s, 9H). ¹³C-NMR (75 MHz, CDCl₃) δ 172.56, 147.20, 142.51, 135.56, 135.39, 129.54, 128.62, 127.62, 126.59, 118.72, 118.34, 116.96, 116.73, 80.31, 72.63, 60.46, 52.09, 31.57, 27.99, 26.18 ppm. ATR-IR 2104 C-N₃, 1749 C=O cm⁻¹. *m/z* [ES]⁺ M+1 433.1 HRMS (NSI) Calcd for C₂₂H₂₅N₈O₂, M+H, 433.2095; Found 433.2096

Synthesis of (*S,S,R*)-(1,1'-(13-(3-(*tert*-butoxy)-3-oxopropyl)-6,12-dihydro-5,11-methanodibenzo[*b,f*][1,5]diazocine-2,8-diyl)bis(1*H*-1,2,3-triazole-4,1-diyl))bis(methylene)bis(5-((3*aS*,4*S*,6*aR*)-2-oxohexahydro-1*H*-thieno[3,4-*d*]imidazol-4-yl)pentanoate) **238**

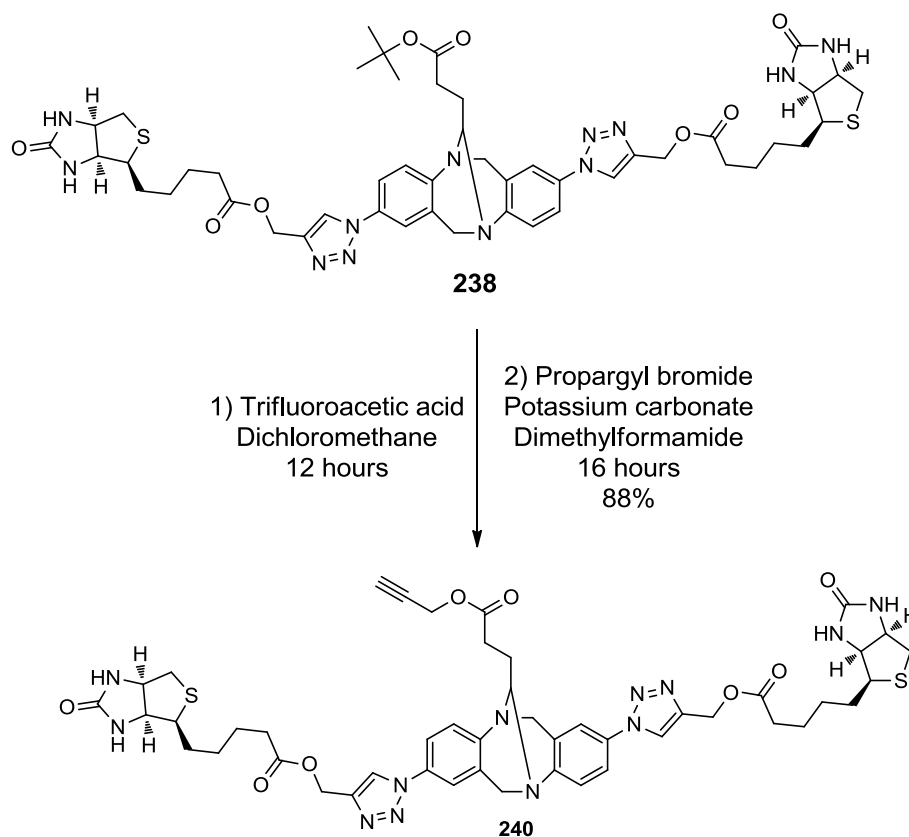


A 5 mL microwave vial was charged with (+/-)-**237** (53 mg, 0.123 mmol), (+)-**85** (73 mg, 0.257 mmol), copper(II) sulfate pentahydrate (3 mg, 0.012 mmol), sodium-*L*-ascorbate (19 mg, 0.098 mmol) and TBTA (13 mg, 0.025 mmol) in *N,N*-dimethylformamide (2 mL). The reaction mixture was heated to 70°C, in a sealed vial, by microwave radiation for 1 hour. The reaction mixture was then diluted with ethyl acetate (5 mL) and transferred to a 25 mL separating funnel. The solution was extracted with ethyl acetate (2 x 5 mL) and washed with water (5 x 10 mL), brine (5 mL) and dried with magnesium sulfate. The suspension was filtered and solvent removed under reduced pressure. The reaction mixture was purified by flash chromatography on silica gel eluting with 5-10% methanol in dichloromethane affording a white solid. Subsequent physicochemical analysis confirmed this was the title product **238** (112 mg, 0.112 mmol, 92 % yield)

*R*_f 0.5 (10% methanol in dichloromethane) ¹H-NMR (300 MHz, CDCl₃) δ 8.01 (s, 2H, ArH), 7.60 – 7.44 (m, 2H, ArH), 7.38 – 7.28 (m, 2H, ArH), 6.33 (d, *J* 8.9 Hz, 2H, NH), 5.70 (s, 2H, NH), 5.27 – 5.14 (m, 4H, 2CH₂), 4.74 (d, *J* 16.8 Hz, 2H, 2CH), 4.62 (d, *J* 17.8 Hz, 2H), 4.38 – 4.02 (m, 5H, 1CH, 2CH₂), 3.08 – 2.90 (m, 2H, 2CH), 2.80 – 2.59 (m, 2H, 2CH), 2.59 – 2.40 (m, 4H, 2CH₂), 2.30 (t, *J* 7.0 Hz, 4H, 2CH₂), 1.94 (qd, *J* 13.9, 6.7 Hz, 2H, 2CH₂), 1.58 (d, *J* 6.8 Hz, 8H, 4CH₂), 1.41 (s, 9H, 3(CH₃)) ¹³C-NMR (75 MHz, CDCl₃) δ 173.66, 172.51, 163.99, 150.61, 146.13, 143.58, 132.82, 132.67, 129.52, 128.61, 127.49, 122.18, 120.23, 119.86, 119.22, 118.89, 80.53, 72.52, 61.74, 60.56, 59.98, 57.30, 55.44, 50.57, 40.32, 33.61, 31.40, 28.06, 27.99, 26.09, 24.60 ppm.

ATR-IR 1744 (br) C=O, 1697 C=O cm^{-1} m/z $[\text{ES}]^+$ $\text{M}+\text{Na}$ 1019.3, HRMS (NSI) Calcd for $\text{C}_{48}\text{H}_{64}\text{N}_{13}\text{O}_8\text{S}_2$, $\text{M}+\text{NH}_4$, 1014.4444; Found 1014.4446. $[\alpha]_{\text{D}}^{25} +19$ (c 1.0, CHCl_3)

Synthesis of (*S,S,R*)-(1,1'-(13-(3-oxo-3-(prop-2-yn-1-yloxy)propyl)-6,12-dihydro-5,11-methanodibenzo[b,f][1,5]diazocine-2,8-diyl)bis(1H-1,2,3-triazole-4,1-diyl))bis(methylene)bis(5-((3*aS*,4*S*,6*aR*)-2-oxohexahydro-1H-thieno[3,4-d]imidazol-4-yl)pentanoate) **240**



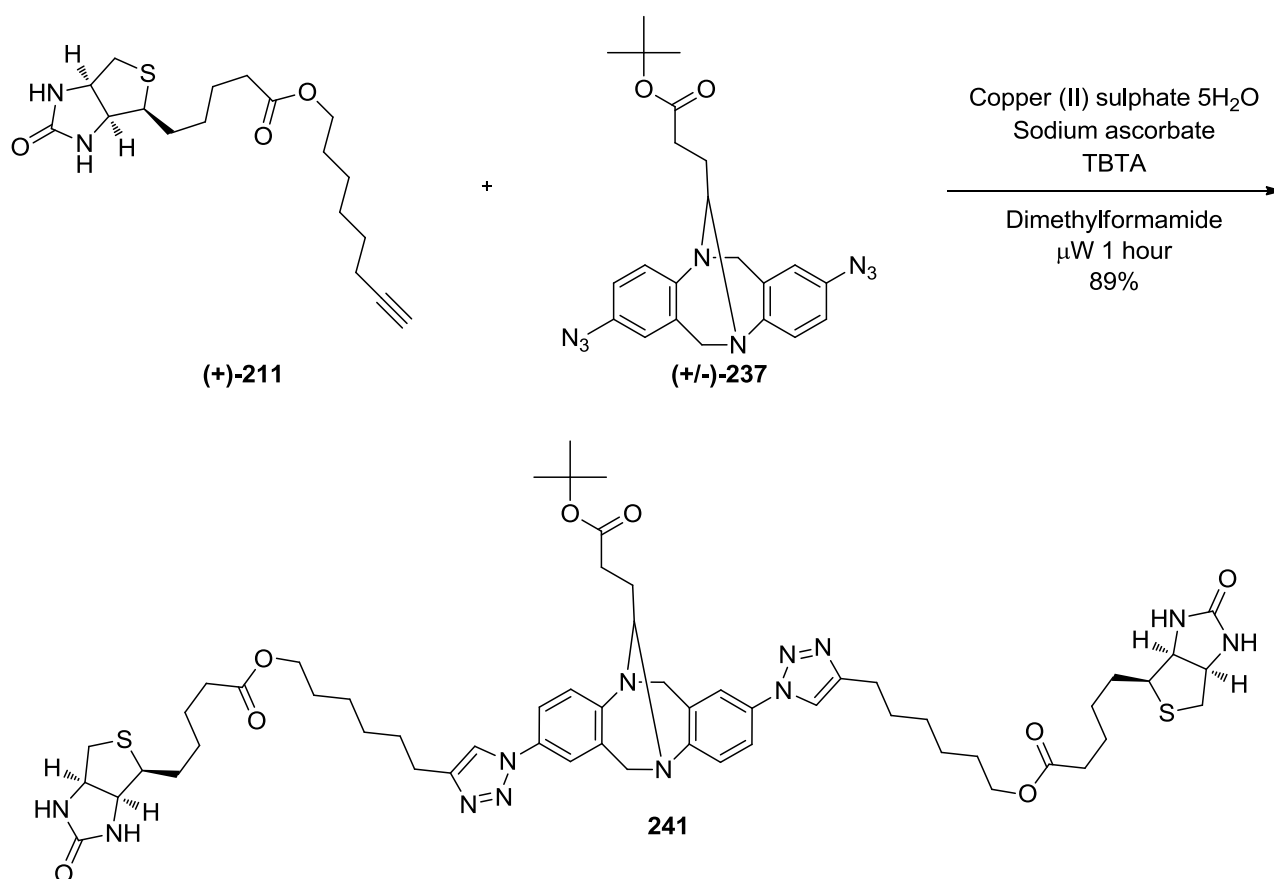
A 2.5 mL microwave vial was charged with **238** (94 mg, 0.094 mmol) in dichloromethane (2 mL). To this trifluoroacetic acid (500 μL , 6.49 mmol) was added, the vial was sealed and left to stir for 12 hours. The solvent was removed under reduced pressure and the residue was dissolved in a minimum amount of dichloromethane (500 μL) followed by addition of diethyl ether (3 mL). The precipitate was filtered off and used without further purification. **239** (85 mg, 0.090 mmol, 96 % yield)

A 25 mL round-bottomed flask was charged with **239** (25 mg, 0.027 mmol) and potassium carbonate (7.34 mg, 0.053 mmol) in *N,N*-dimethylformamide (2 mL) and left to stir for 30 minutes. To this propargyl bromide (4.29 μL , 0.040 mmol) was added and the solution continued to be stirred for 16 hours. The resulting mixture was diluted with water (5 mL) and ethyl acetate (5 mL) then transferred to a 50 mL separating funnel. This was extracted with ethyl acetate (2 x 5 mL) and the combined organic extracts were washed with water (5 x 10 mL), brine and dried with magnesium

sulfate. The suspension was filtered and the solvent removed under reduced pressure. The impure product was purified by flash chromatography on silica eluting with 5-10% methanol in dichloromethane to afford an off white solid. Subsequent physicochemical analysis confirmed this to be the title compound. **240** (23 mg, 0.023 mmol, 88 % yield)

MP 96-98°C (diethyl ether) (Et₂O), ¹H-NMR (400 MHz, CDCl₃) δ 8.02 (s, 1H, ArH), 7.95 (s, 1H, ArH), 7.47 (d, *J* 8.8 Hz, 2H, ArH), 7.30 (dd, *J* 14.1, 6.1 Hz, 2H, ArH), 7.20 (d, *J* 13.0 Hz, 2H), 6.18 (d, *J* 19.5 Hz, 2H, 2NH), 5.41 (s, 2H, 2NH), 5.26 – 5.12 (m, 4H, 2CH₂), 4.71 (d, *J* 16.9 Hz, 1H, CH), 4.63 (d, *J* 2.6 Hz, 2H, CH₂), 4.57 (d, *J* 18.0 Hz, 1H, CH), 4.32 – 3.96 (m, 7H, 3CH₂CH₂), 3.01 – 2.82 (m, 2H, 2CH), 2.70 – 2.52 (m, 4H, 2CH₂), 2.51 – 2.37 (m, 3H, 3CH), 2.26 (t, *J* 6.8 Hz, 4H, 2CH₂), 2.12 – 1.73 (m, 2H, CH₂), 1.65 – 1.42 (m, 8H, 4CH₂), 1.32 – 1.13 (m, 4H, 2CH₂). ¹³C-NMR (101 MHz, CDCl₃/10%CD₃OD) δ 173.82, 172.55, 164.15, 150.50, 146.05, 143.49, 132.99, 132.82, 129.59, 128.51, 127.67, 126.63, 122.44, 120.53, 120.09, 119.42, 119.22, 75.28, 72.51, 61.98, 61.95, 60.64, 60.16, 57.40, 55.59, 52.27, 40.45, 33.81, 30.29, 28.43, 28.20, 26.04, 24.70 ppm. ATR-IR 1749 C=O, 1658 C=O cm⁻¹, *m/z* [ES]⁺ M+Na 1001.4. HRMS (NSI) Calcd for C₄₇H₅₈N₁₃O₈S₂, M+NH₄, 996.3975; Found 996.3971. [α]_D²⁵ +13.4 (c 1.0, CHCl₃/10% MeOH)

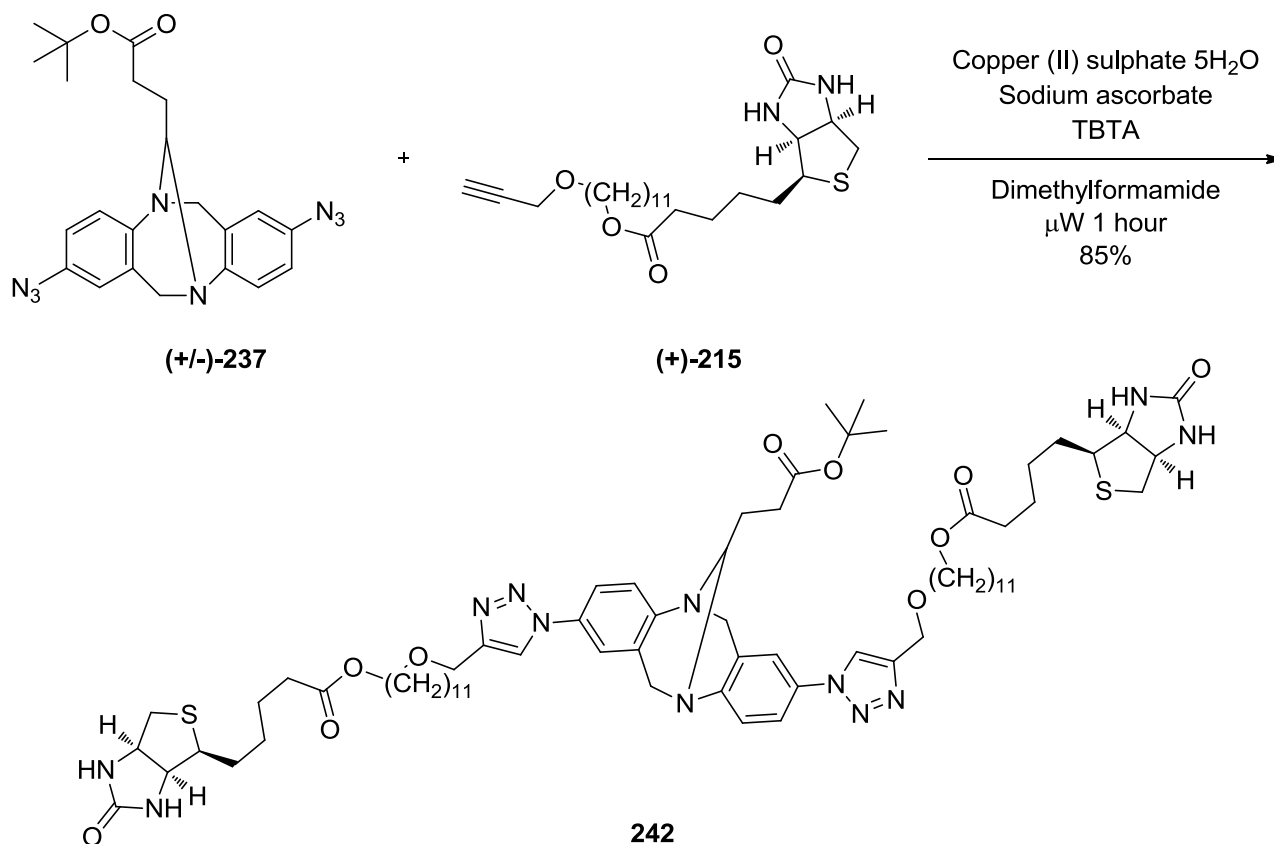
Synthesis of (S,S,R)-(1,1'-(13-(3-(tert-butoxy)-3-oxopropyl)-6,12-dihydro-5,11-methano-dibenzo[b,f][1,5]diazocine-2,8-diyl)bis(1H-1,2,3-triazole-4,1-diyl))bis(hexane-6,1-diyl) bis(5-((3a*S*,4*S*,6a*R*)-2-oxohexahydro-1H-thieno[3,4-*d*]imidazol-4-yl)pentanoate) **241**



A 5 mL microwave vial was charged with (+/-)-**237**(61 mg, 0.142 mmol), (+)-**211** (100 mg, 0.203 mmol), copper(II) sulfate pentahydrate (4 mg, 0.014 mmol), sodium-*L*-ascorbate (22.48 mg, 0.113 mmol) and TBTA (15 mg, 0.028 mmol) in *N,N*-dimethylformamide (3 mL). The reaction mixture was heated to 70°C, in a sealed vial, by microwave radiation for 1 hour. The reaction mixture was then diluted with ethyl acetate (5 mL) and transferred to a 25 mL separating funnel. The solution was extracted with ethyl acetate (2 x 5mL), washed with water (5 x 10mL), brine (5 mL) and dried with magnesium sulfate. The suspension was filtered and solvent removed under reduced pressure. The reaction mixture was purified by flash chromatography on silica gel eluting with 5-10% methanol in dichloromethane affording a white solid. Subsequent physicochemical analysis confirmed this was the title compound **241** (143 mg, 0.126 mmol, 89 % yield)

¹H-NMR (400 MHz, CDCl₃) δ 7.62 (s, 2H, ArH), 7.47 (d, *J* 8.1 Hz, 2H, ArH), 7.32 (d, *J* 11.1 Hz, 2H, ArH), 7.24 (d, *J* 8.7 Hz, 2H, ArH), 5.88 (s, 2H, 2NH), 5.49 (s, 2H, 2NH), 4.76 (d, *J* 16.8 Hz, 1H, CH), 4.64 (d, *J* 17.5 Hz, 1H, CH), 4.52 – 4.38 (m, 2H, 2CH,), 4.33 – 4.22 (m, 3H, 3CH), 4.16 (dd, *J* 16.0, 9.7 Hz, 2H, 2CH), 4.03 (t, *J* 6.5 Hz, 4H, 2CH₂), 3.13 (s, 2H, 2CH), 2.87 (d, *J* 12.2 Hz, 2H, 2CH), 2.80 – 2.62 (m, 6H, 2CH, 2CH₂), 2.48 (t, *J* 7.4 Hz, 2H, CH₂), 2.29 (t, *J* 7.3 Hz, 4H, 2CH₂), 2.08 – 1.83 (m, 2H, CH₂), 1.76 – 1.52 (m, 16H, 8CH₂), 1.43 (s, 9H, 3CH₃), 1.37 (s, 12H, 6CH₂). ¹³C-NMR (101 MHz, CDCl₃) δ 173.76, 172.38, 163.64, 150.19, 145.70, 133.29, 133.13, 129.39, 128.48, 127.38, 126.36, 120.16, 119.73, 119.14, 118.94, 80.54, 72.64, 64.35, 61.97, 60.70, 60.15, 55.45, 52.28, 40.53, 33.97, 31.59, 29.16, 28.66, 28.47, 28.36, 28.26, 28.14, 26.26, 25.68, 25.48, 24.84 ppm. FT-IR KBr(neat) 1703 (br) C=O, *m/z* [ES]⁺ 1159.5. HRMS (NSI) Calcd for C₅₈H₈₄N₁₃O₈S₂, M+NH₄, 1154.6009; Found 1154.6007. [α]_D²⁶ +12 (c 1.0, CHCl₃)

Synthesis of (*S,S,R*)-(((1,1'-(13-(3-(*tert*-butoxy)-3-oxopropyl)-6,12-dihydro-5,11-methano-dibenzo[*b,f*][1,5]diazocine-2,8-diyl)bis(1*H*-1,2,3-triazole-4,1-diyl))bis(methylene))bis(oxy))bis(undecane-11,1-diyl) bis(5-((3*aS*,4*S*,6*aR*)-2-oxohexahydro-1*H*-thieno[3,4-*d*]imidazol-4-yl)pentanoate) 242

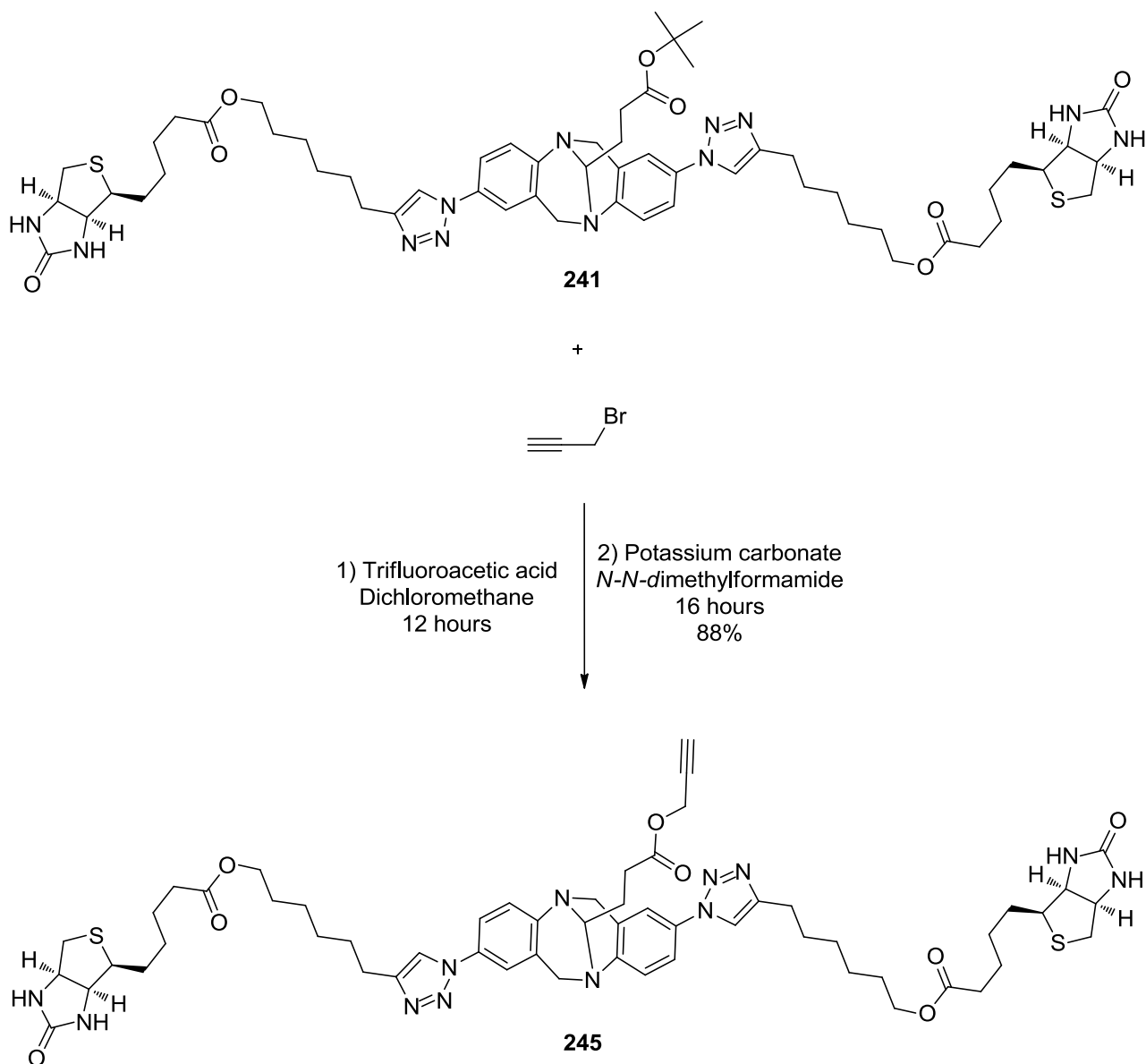


A 5 mL microwave vial was charged with (+)-**237** (50 mg, 0.116 mmol), (+)-**215** (110 mg, 0.243 mmol), copper(II) sulfate pentahydrate (8.66 mg, 0.035 mmol), sodium ascorbate (18.32 mg, 0.092 mmol) and TBTA (18.40 mg, 0.035 mmol) in *N,N*-dimethylformamide (2.5 mL). The reaction mixture was heated to 70°C, in a sealed vial, by microwave radiation for 1 hour. The reaction mixture was then diluted with ethyl acetate (5 mL) and transferred to a 25 mL separating funnel. The solution was extracted with ethyl acetate (2 x 5 mL) and washed with water (5 x 10 mL), brine (5 mL) and dried with magnesium sulfate. The suspension was filtered and the solvent removed under reduced pressure. The reaction mixture was purified by flash chromatography on silica eluting with 5-10% methanol in dichloromethane affording a white solid. Subsequent physicochemical analysis confirmed that this was the title compound **242** (132 mg, 0.099 mmol, 85 % yield)

¹H-NMR (400 MHz, CDCl₃) δ 7.80 (s, 2H, ArH), 7.41 (d, *J* 8.6 Hz, 2H, ArH), 7.27 (dd, *J* 11.1, 2.0 Hz, 2H, ArH), 7.19 (m, 2H, ArH), 5.65 (s, 2H, 2NH), 5.30 (s, 2H, 2NH), 4.71 (d, *J* 16.8 Hz, 1H, CH), 4.65 – 4.52 (m, 5H, CH, 2CH₂), 4.49 – 4.37 (m, 2H, 2CH), 4.31 – 4.17 (m, 3H, 3CH), 4.10 (dd, *J* 15.9, 8.2 Hz, 2H, 2CH), 3.98 (t, *J* 6.7 Hz, 4H, 2CH₂), 3.46 (t, *J* 6.7 Hz, 4H, 2CH₂), 3.08 (dd,

J 11.0, 7.0 Hz, 2H, 2CH), 2.84 (dd, *J* 12.7, 4.5 Hz, 2H, 2CH), 2.66 (d, *J* 12.7 Hz, 2H, 2CH), 2.42 (t, *J* 7.4 Hz, 2H, 2CH), 2.25 (t, *J* 7.4 Hz, 4H, 2CH₂), 2.03 – 1.80 (m, 2H, CH₂), 1.69 – 1.45 (m, 16H, 8CH₂), 1.37 (s, 9H), 1.31 – 1.14 (m, 32H, 16CH₂). FT-IR KBr(neat) 1703(br) C=O cm⁻¹, LCMS [ES]⁺ M+Na 1360.8 HRMS (NSI) Calcd for C₇₆H₁₁₈N₁₃O₁₁S₂, M+NH₄, 1354.7785; Found 1354.7789. [α]_D²⁷ +13 (c 1.0, CHCl₃)

Synthesis of (*S,S,R*)-(1,1'-(13-(3-oxo-3-(prop-2-yn-1-yloxy)propyl)-6,12-dihydro-5,11-methanodibenzo[*b,f*][1,5]diazocine-2,8-diyl)bis(1*H*-1,2,3-triazole-4,1-diyl))bis(hexane-6,1-diyl)bis(5-((3*aS*,4*S*,6*aR*)-2-oxohexahydro-1*H*-thieno[3,4-*d*]imidazol-4-yl)pentanoate) 245



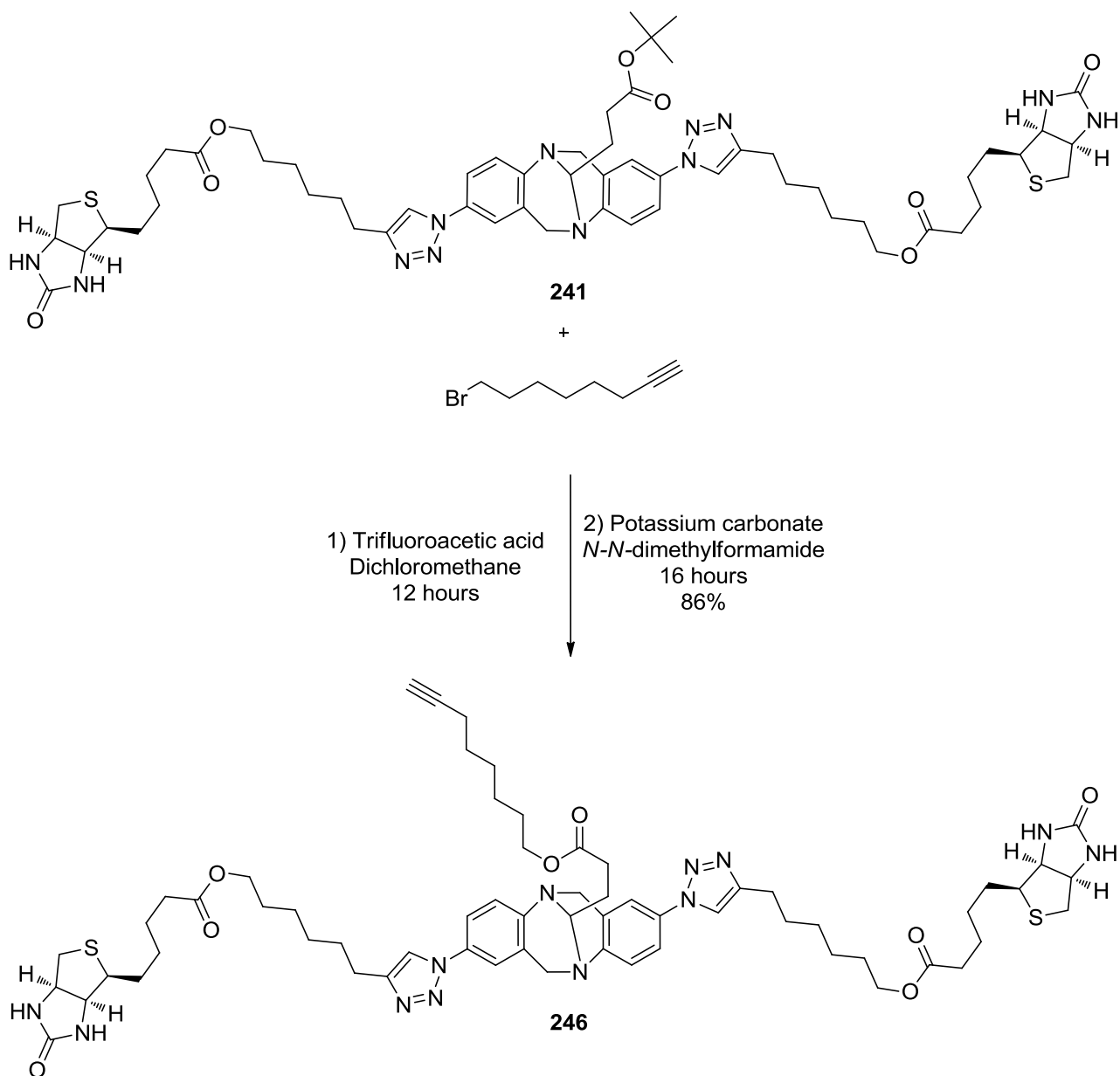
A 5 mL microwave vial was charged with **241** (90 mg, 0.018 mmol) in dichloromethane (2 mL). To this trifluoroacetic acid (50 μ L, 0.649 mmol) was added, the vial was sealed and left to stir for 12 hours. The solvent was removed under reduced pressure and the residue was dissolved in a minimum amount of dichloromethane (500 μ L) followed by addition of ether (3 mL). The

precipitate was filtered off and used without further purification. **243** (74 mg, 0.079 mmol, 86 % yield)

A 25 ml round bottomed flask was charged with **243** (20 mg, 0.018 mmol) and potassium carbonate (5.5 mg, 0.037 mmol) in *N,N*-dimethylformamide (2 mL) and left to stir for 30 minutes. To this propargyl bromide (4 μ l, 0.037 mmol) was added and the solution continued to be stirred for 16 hours. The resulting mixture was diluted with water (5 mL) and ethyl acetate (5 mL) then transferred to a 50 mL separating funnel. This was extracted with ethyl acetate (2 x 5mL) and the combined organic extracts were washed with water (5 x 10mL), brine (10 mL) and dried with magnesium sulfate. The suspension was filtered and the solvent removed under reduced pressure. The impure product was purified by flash chromatography on silica gel eluting with 5-10% methanol in dichloromethane to afford an off white solid. Subsequent physiochemical analysis confirmed this to be the title compound. **245** (18 mg, 0.016 mmol, 88 % yield)

m/p 79-80°C (diethyl ether), ¹H-NMR (400 MHz, CDCl₃) δ 7.55 (s, 2H, ArH), 7.41 (d, *J* 8.6 Hz, 2H, ArH), 7.26 (d, *J* 8.5 Hz, 2H, ArH), 7.18 (d, *J* 8.8 Hz, 2H, ArH), 5.80 (s, 2H, 2NH), 5.37 (s, 2H, 2NH), 4.71 (d, *J* 16.9 Hz, 1H, CH), 4.62 (t, *J* 2.3 Hz, 2H, CH₂), 4.57 (d, *J* 17.6 Hz, 1H, CH), 4.50 – 4.36 (m, 2H, 2CH), 4.23 (dd, *J* 10.8, 6.0 Hz, 3H, 3CH), 4.12 (dd, *J* 17.3, 12.7 Hz, 2H, 2CH), 3.97 (t, *J* 6.6 Hz, 4H, 2CH₂), 3.06 (dd, *J* 12.2, 6.3 Hz, 2H, 2CH), 2.81 (dd, *J* 12.6, 4.6 Hz, 2H, 2CH), 2.68 (m, 6H, 2CH, 2CH₂), 2.57 (t, *J* 7.3 Hz, 2H, 2CH), 2.41 (t, *J* 2.5 Hz, 1H), 2.23 (t, *J* 7.4 Hz, 4H, 2CH₂), 1.98 (m, 2H, CH₂), 1.58 (m, 16H, 8CH₂), 1.44 – 1.30 (m, 12H, 6CH₂). ¹³C-NMR (101 MHz, CDCl₃) δ 173.75, 172.17, 163.62, 149.95, 145.46, 133.40, 133.24, 129.35, 128.30, 127.41, 126.37, 120.22, 119.76, 119.11, 118.94, 77.64, 75.01, 72.50, 64.34, 61.96, 60.62, 60.12, 55.44, 52.28, 52.06, 40.53, 33.97, 30.21, 29.70, 29.15, 28.65, 28.46, 28.35, 28.25, 25.98, 25.67, 25.48, 24.84ppm. ATR-IR 1752 C=O, 1635 C=O cm⁻¹ *m/z* [ES]⁺ M+Na, 1141.5. HRMS (NSI) Calcd for C₅₇H₇₅N₁₂O₈S₂, M+H, 1119.5278; Found 1119.5278, [α]_D²⁵ +14.3 (c 1.0, CHCl₃/10% MeOH)

Synthesis of (*S,S,R*)-(1,1'-(13-(3-(oct-7-yn-1-yloxy)-3-oxopropyl)-6,12-dihydro-5,11-methanodibenzo[*b,f*][1,5]diazocine-2,8-diyl))bis(1*H*-1,2,3-triazole-4,1-diyl))bis(hexane-6,1-diyl)bis(5-((3*aS*,4*S*,6*aR*)-2-oxohexahydro-1*H*-thieno[3,4-*d*]imidazol-4-yl)pentanoate) **246**



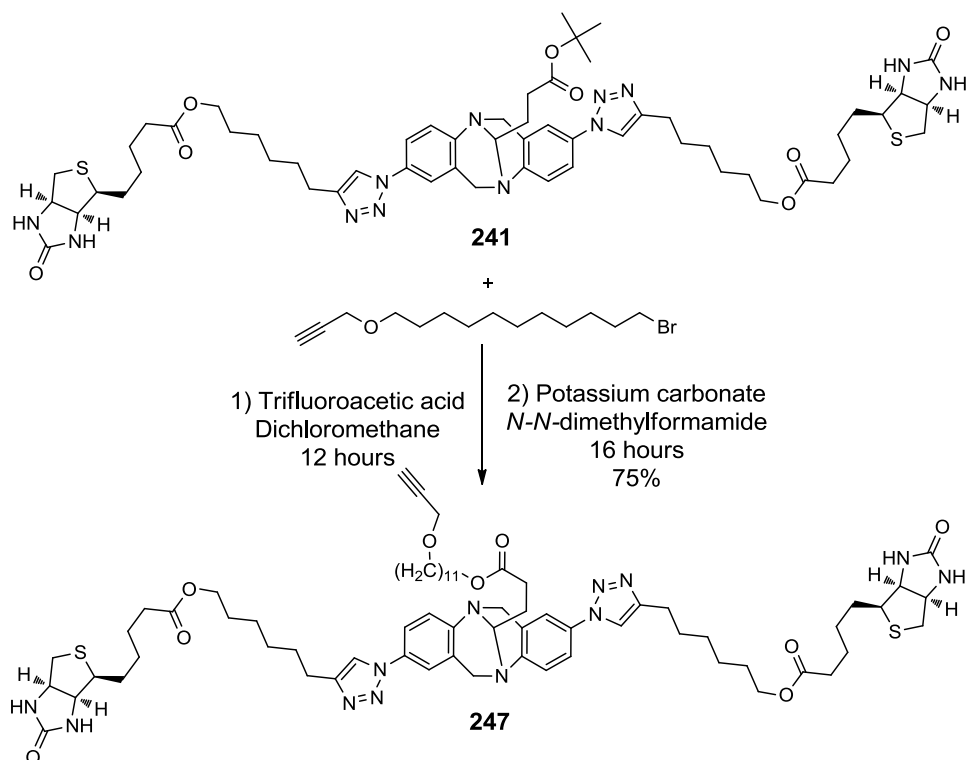
A 5 mL microwave vial was charged with **241** (94 mg, 0.094 mmol) in dichloromethane (2 mL). To this trifluoroacetic acid (500 μ L, 6.49 mmol) was added, the vial was sealed and left to stir for 12 hours. The solvent was removed under reduced pressure and the residue was dissolved in a minimum amount of dichloromethane (500 μ L) followed by addition of ether (3 mL). The precipitate was filtered off and used without further purification. **243** (85 mg, 0.090 mmol, 96 % yield)

A 25 mL round bottomed-flask was charged with **243** (20 mg, 0.018 mmol) and potassium carbonate (5.11 mg, 0.037 mmol) in *N,N*-dimethylformamide (2 mL) and left to stir for 30 minutes. To this 8-bromo-oct-1-yne (7 mg, 0.037 mmol) was added and the solution continued to be stirred for 16

hours. The resulting mixture was diluted with water (5 mL) and ethyl acetate (5 mL) then transferred to a 50 mL separating funnel. This was extracted with ethyl acetate (2 x 5mL) and the combined organic extracts were washed with water (5 x 10mL), brine and dried with magnesium sulfate. The suspension was filtered and the solvent removed under reduced pressure. The impure product was purified by flash chromatography on silica gel eluting with 5-10% methanol in dichloromethane to afford an off white solid. Subsequent physiochemical analysis confirmed this to be the title compound. **246**(19 mg, 0.016 mmol, 86 % yield)

$^1\text{H-NMR}$ (400 MHz, CDCl_3) δ 7.56 (s, 2H, ArH), 7.42 (d, J 8.6 Hz, 2H, ArH), 7.27 (d, J 9.0 Hz, 2H, ArH), 7.19 (d, J 8.6 Hz, 2H, ArH), 5.76 (s, 2H, 2NH), 5.31 (s, 2H, 2NH), 4.71 (d, J 16.9 Hz, 1H, CH), 4.58 (d, J 17.5 Hz, 1H, CH), 4.49 – 4.35 (m, 2H, 2CH), 4.23 (m, 3H, 3CH), 4.12 (m, 2H, 2CH), 3.99 (m, 6H, 2CH, CH_2), 3.07 (d, J 4.2 Hz, 2H, 2CH), 2.81 (dd, J 12.6, 4.3 Hz, 2H, 2CH), 2.73 – 2.60 (m, 6H, 3 CH_2), 2.52 (t, J 7.3 Hz, 2H, CH_2), 2.23 (t, J 7.4 Hz, 4H, 2 CH_2), 2.10 (td, J 6.9, 2.6 Hz, 2H, CH_2), 2.05 – 1.89 (m, 2H, CH_2), 1.87 (t, J 2.6 Hz, 1H, CH_2), 1.58 (m, 18H, 9 CH_2), 1.33 (m, 18H, 9 CH_2). $^{13}\text{C-NMR}$ (101 MHz, CDCl_3) δ 173.74, 173.07, 163.55, 149.97, 145.51, 133.41, 129.33, 128.36, 127.39, 126.36, 120.20, 119.77, 119.13, 118.95, 84.48, 72.61, 68.33, 64.62, 64.49, 64.34, 61.95, 60.66, 60.11, 55.42, 52.28, 40.53, 33.97, 33.74, 32.57, 30.42, 29.15, 28.64, 28.46, 28.35, 28.26, 27.76, 26.14, 25.68, 25.48, 25.16, 24.84, 18.30 ppm. ATR-IR 2152 C-C, 1749 C=O, 1640 C=O cm^{-1} . m/z $[\text{ES}]^+$ M+Na, 1211.5874. HRMS (NSI) Calcd for $\text{C}_{62}\text{H}_{88}\text{N}_{13}\text{O}_8\text{S}_2$, M+ NH_4 , 1206.6320; Found 1206.6323. $[\alpha]_{\text{D}}^{26} +19.5$ (c 1.0, $\text{CHCl}_3/10\%$ MeOH)

Synthesis of (*S,S,R*)-(1,1'-(13-(3-oxo-3-((11-(prop-2-yn-1-yloxy)undecyl)oxy)propyl)-6,12-dihydro-5,11-methanodibenzo[*b,f*][1,5]diazocine-2,8-diyl)*bis*(1*H*-1,2,3-triazole-4,1-diyl))*bis*(hexane-6,1-diyl)-*bis*(5-((3*aS*,4*S*,6*aR*)-2-oxohexahydro-1*H*-thieno[3,4-*d*]imidazol-4-yl)pentanoate) **247**

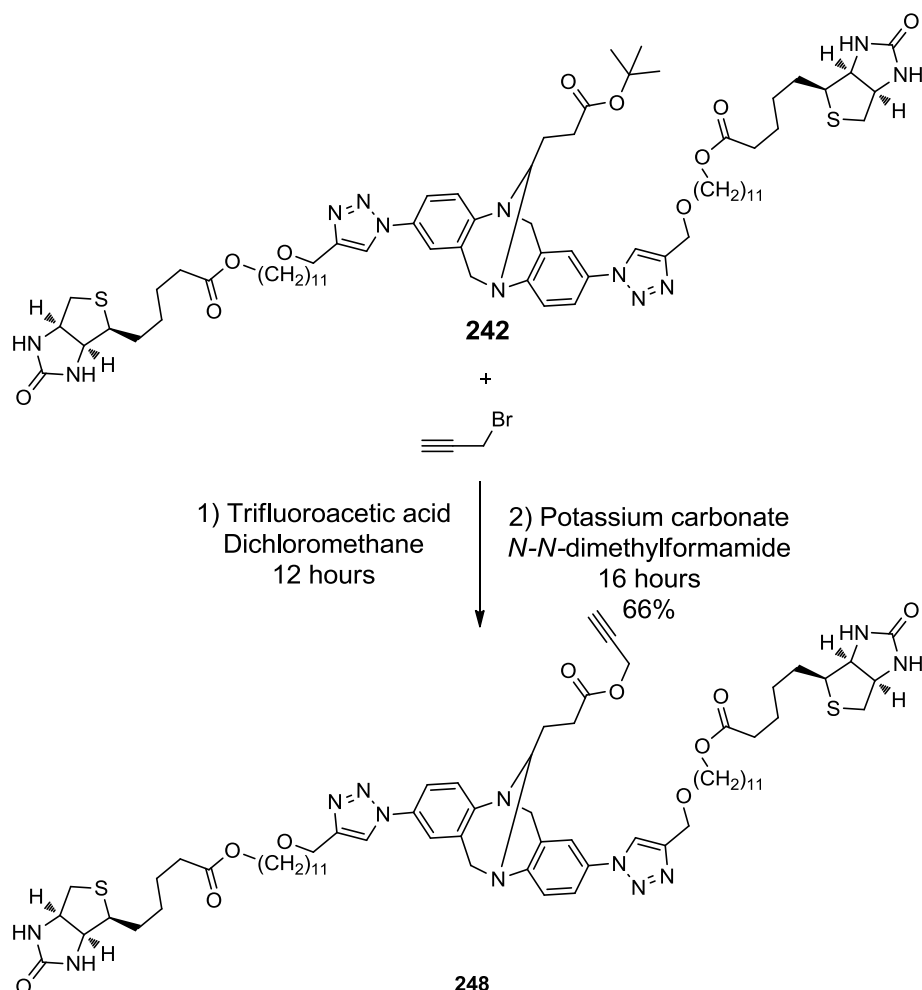


A 2.5 mL microwave vial was charged with **241** (94 mg, 0.094 mmol) in dichloromethane (2 mL). To this trifluoroacetic acid (500 μL , 6.49 mmol) was added, the vial was sealed and left to stir for 12 hours. The solvent was removed under reduced pressure and the residue was dissolved in a minimum amount of dichloromethane (500 μL) followed by addition of diethyl ether (3 mL). The precipitate was filtered off and used without further purification. **243**(85 mg, 0.090 mmol, 96 % yield)

A 25 ml round bottomed flask was charged **243** (20 mg, 0.018 mmol) and potassium carbonate (5.11 mg, 0.037 mmol) in *N,N*-dimethylformamide (2 mL) and left to stir for 30 minutes. To this 1-bromo-11-(prop-2-yn-1-yloxy)undecane (10.70 mg, 0.037 mmol) was added and the solution continued to be stirred for 16 hours. The resulting mixture was diluted with water (5 mL) and ethyl acetate (5 mL) then transferred to a 50 mL separating funnel. This was extracted with ethyl acetate (2 x 5mL) and the combined organic extracts were washed with water (5 x 10mL), brine and dried with magnesium sulfate. The suspension was filtered and the solvent removed under reduced pressure. The impure product was purified by flash chromatography on silica eluting with 5-10% methanol in dichloromethane to afford an off white solid. Subsequent physiochemical analysis confirmed this to be the title compound. **247** (18 mg, 0.014 mmol, 75 % yield)

$^1\text{H-NMR}$ (400 MHz, CDCl_3) δ 7.55 (d, J 2.2 Hz, 2H, ArH), 7.41 (d, J 8.6 Hz, 2H, ArH), 7.26 (d, J 9.2 Hz, 2H, ArH), 7.18 (d, J 8.7 Hz, 2H, ArH), 5.82 (s, 2H, 2NH), 5.38 (s, 2H, 2NH), 4.71 (d, J 16.9 Hz, 1H, CH), 4.58 (d, J 17.5 Hz, 1H, CH), 4.46 – 4.36 (m, 2H, 2CH), 4.27 – 4.18 (m, 3H, 3CH), 4.18 – 4.10 (m, 2H, 2CH), 4.06 (d, J 2.4 Hz, 2H, CH_2), 3.98 (q, J 6.8 Hz, 6H, 3CH_2), 3.43 (t, J 6.6 Hz, 2H, CH_2), 3.07 (dd, J 10.9, 7.9 Hz, 2H, 2CH), 2.81 (dd, J 12.7, 4.7 Hz, 2H, 2CH), 2.73 – 2.58 (m, 6H, 2CH, 2CH_2), 2.51 (t, J 7.4 Hz, 2H, CH_2), 2.35 (t, J 2.4 Hz, 1H, CH), 2.23 (t, J 7.4 Hz, 4H, 2CH_2), 2.05 – 1.82 (m, 2H, CH_2), 1.70 – 1.44 (m, 20H, 10CH_2), 1.30 (m, 26H, 13CH_2). ATR-IR 2158 C-C, 1752 C=O, 1646 C=O cm^{-1} . m/z $[\text{ES}]^+$ $\text{M}+\text{H}$ 1289.7. HRMS (NSI) Calcd for $\text{C}_{68}\text{H}_{100}\text{N}_{13}\text{O}_9\text{S}_2$, $\text{M}+\text{NH}_4$, 1306.7209; Found 1306.7205. $[\alpha]_D^{26} +17$ (c 1.0, CHCl_3).

Synthesis of (*S,S,R*)-(((1,1'-(13-(3-oxo-3-(prop-2-yn-1-yloxy)propyl)-6,12-dihydro-5,11-methanodibenzo[*b,f*][1,5]diazocine-2,8-diyl)bis(1*H*-1,2,3-triazole-4,1-diyl))bis(methylene))bis(oxy))bis(undecane-11,1-diyl)bis(5-((3*aS*,4*S*,6*aR*)-2-oxohexahydro-1*H*-thieno[3,4-*d*]imidazol-4-yl)pentanoate) 248



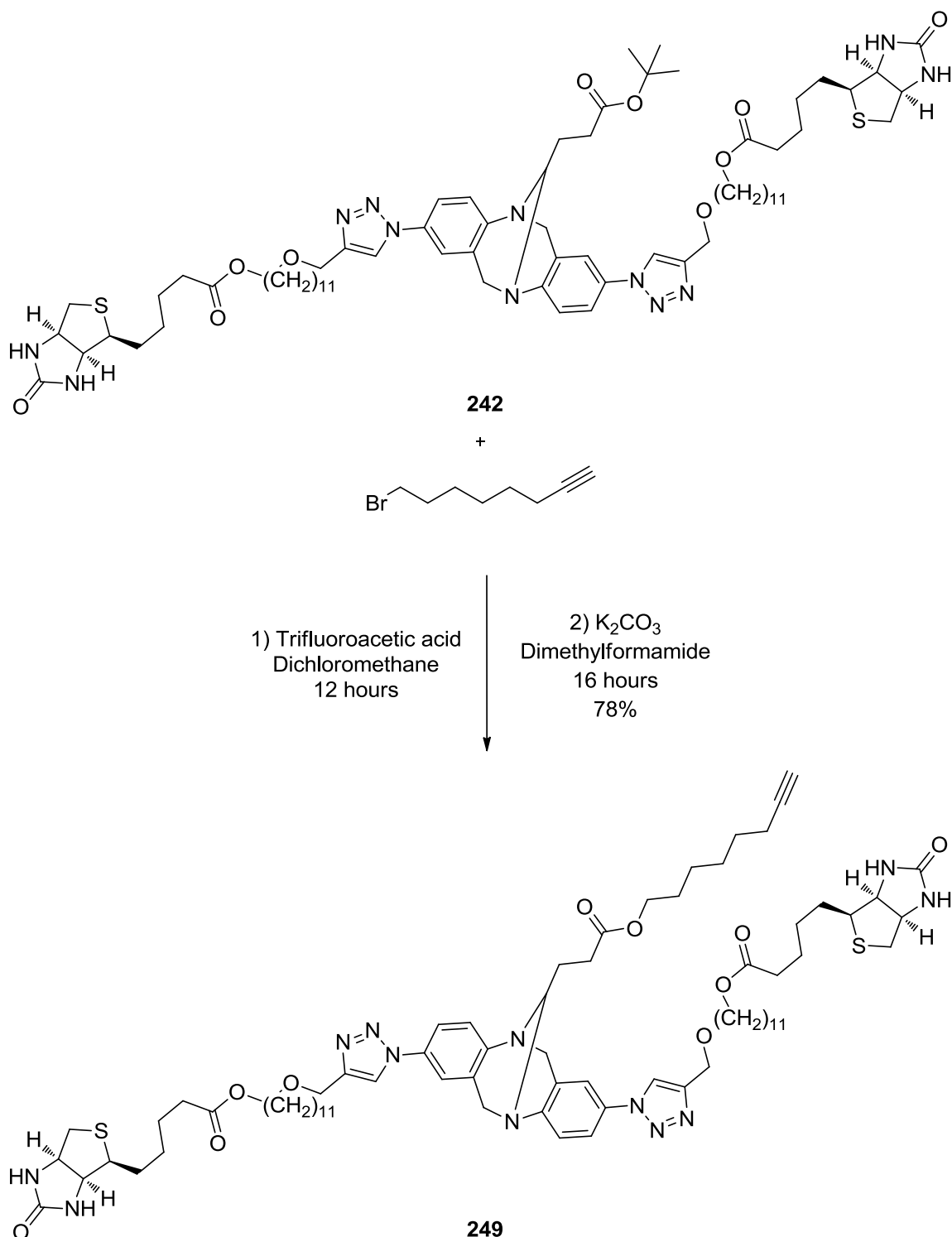
A 5 mL microwave vial was charged with **242** (2 mL). To this trifluoroacetic acid (418 μL , 5.42 mmol) was added, the vial was sealed and left to stir for 12 hours. The solvent was removed under reduced pressure and the residue was dissolved in a minimum amount of dichloromethane (500 μL)

followed by addition of ether (3 mL). The precipitate was filtered off and used without further purification **244** (119 mg, 0.093 mmol, 86 % yield)

A 25 ml round-bottomed flask was charged with **244** (25 mg, 0.020 mmol) and potassium carbonate (4.04 mg, 0.029 mmol) in *N,N*-dimethylformamide (2 mL) and left to stir for 30 minutes. To this propargyl bromide (3.15 μ l, 0.029 mmol) was added and the solution continued to be stirred for 16 hours. The resulting mixture was diluted with water (5 mL) and ethyl acetate (5 mL) then transferred to a 50 mL separating funnel. This was extracted with ethyl acetate (2 x 5mL) and the combined organic extracts were washed with water (5 x 10mL), brine and dried with magnesium sulfate. The suspension was filtered and the solvent removed under reduced pressure. The impure product was purified by flash chromatography on silica gel eluting with 5-10% methanol in dichloromethane to afford an off white solid. Subsequent physicochemical analysis confirmed this to be the title compound. **248** (17 mg, 0.013 mmol, 66.0 % yield)

m/p 64-66°C (Et₂O), ¹H-NMR (400 MHz, CDCl₃) δ 7.80 (s, 2H, ArH), 7.42 (dd, *J* 8.6, 2.1 Hz, 2H, ArH), 7.28 (dd, *J* 8.8, 2.3 Hz, 2H, ArH), 7.18 (s, 2H, ArH), 5.68 (s, 2H, 2NH), 5.34 (s, 2H, 2NH), 4.72 (d, *J* 16.9 Hz, 1H, CH), 4.62 (t, *J* 2.3 Hz, 2H, CH₂), 4.58 (m, 5H, CH, 2CH₂), 4.48 – 4.36 (m, 2H, 2CH), 4.30 – 4.19 (m, 3H, 3CH), 4.17 – 4.05 (m, 2H, 2CH), 3.97 (t, *J* 6.7 Hz, 4H, 2CH₂), 3.46 (t, *J* 6.7 Hz, 4H, 2CH₂), 3.08 (dd, *J* 11.8, 7.1 Hz, 2H, 2CH), 2.83 (dd, *J* 12.8, 4.8 Hz, 2H, 2CH), 2.66 (d, *J* 12.7 Hz, 2H, 2CH), 2.57 (t, *J* 7.3 Hz, 2H, 2CH), 2.41 (t, *J* 2.5 Hz, 1H, CH), 2.25 (t, *J* 7.4 Hz, 4H, 2CH₂), 1.98 (m, 2H, CH₂), 1.73 – 1.43 (m, 16H, 8CH₂), 1.20 (s (br), 32H, 16CH₂). ¹³C-NMR (101 MHz, CDCl₃) δ 173.77, 172.16, 163.54, 150.27, 145.77, 133.22, 133.07, 129.42, 128.39, 127.50, 126.46, 120.63, 120.37, 119.89, 119.30, 119.12, 77.62, 75.01, 72.44, 71.04, 64.56, 64.28, 61.94, 60.57, 60.13, 55.41, 52.24, 52.07, 40.55, 33.96, 30.20, 29.64, 29.49, 29.44, 29.42, 29.19, 28.61, 28.36, 28.26, 26.09, 25.90, 24.83 ppm. ATR-IR 2155 C-C, 1748 C=O, 1652 C=O cm⁻¹. *m/z* [ES]⁺ M+Na 1341.7. HRMS (NSI) Calcd for C₆₉H₉₉N₁₂O₁₀S₂, M+H, 1319.7050; Found 1319.7049. $[\alpha]_D^{25}$ +22 (c 1.0, CHCl₃).

Synthesis of (*S,S,R*)-(((1,1'-(13-(3-(oct-7-yn-1-yloxy)-3-oxopropyl)-6,12-dihydro-5,11-methanodibenzo[*b,f*][1,5]diazocine-2,8-diyl))bis(1*H*-1,2,3-triazole-4,1-diyl))bis(methylene))bis(oxy))bis(undecane-11,1-diyl) bis(5-((3*aS*,4*S*,6*aR*)-2-oxohexahydro-1*H*-thieno[3,4-*d*]imidazol-4-yl)pentanoate) (249)



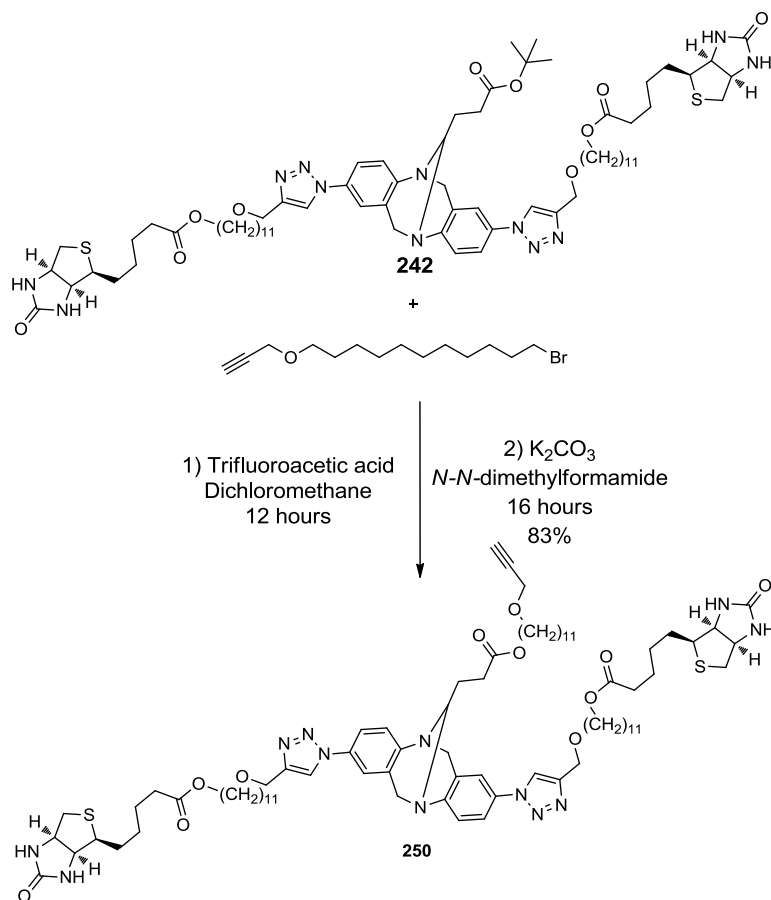
A 2.5 mL microwave vial was charged with (**242**) (*S,S,R*)-(((1,1'-(13-(3-(tert-butoxy)-3-oxopropyl)-6,12-dihydro-5,11-methanodibenzo[*b,f*][1,5]diazocine-2,8-diyl))bis(1*H*-1,2,3-triazole-4,1-diyl))bis(methylene))bis(oxy))bis(undecane-11,1-diyl) bis(5-((3*aS*,4*S*,6*aR*)-2-oxohexahydro-

1H-thieno[3,4-d]imidazol-4-yl)pentanoate) (145 mg, 0.108 mmol) in dichloromethane (2 mL). To this trifluoroacetic acid (418 μ l, 5.42 mmol) was added, the vial was sealed with a Teflon cap and left to stir for 12 hours. The solvent was removed under reduced pressure and the residue was dissolved in a minimum amount of dichloromethane (500 μ L) followed by addition of ether (3 mL). The precipitate was filtered off and used without further purification (**244**) (119 mg, 0.093 mmol, 86 % yield)

A 25ml round bottomed flask was charged with **244** (25 mg, 0.020 mmol) and potassium carbonate (4.04 mg, 0.029 mmol) in dimethylformamide (2mL) and left to stir for 30 minutes. To this 8-bromooct-1-yne (5.53 mg, 0.029 mmol) was added and the solution continued to be stirred for 16 hours. The resulting mixture was diluted with water (5 mL) and ethyl acetate (5 mL) then transferred to a 50 mL separating funnel. This was extracted with ethyl acetate (2 x 5mL) and the combined organic extracts were washed with water (5 x 10mL), brine (10 mL) and dried with magnesium sulfate. The suspension was filtered and the solvent removed under reduced pressure. The impure product was purified by flash chromatography on silica eluting with 5-10% methanol in dichloromethane to afford an off white solid. Subsequent physicochemical analysis confirmed this to be the title compound. **249** (23 mg, 0.017 mmol, 85 % yield)

^1H NMR (400 MHz, CDCl_3) δ 7.79 (s, 2H), 7.41 (dd, J 8.6, 2.3 Hz, 2H), 7.28 (dd, J 9.4, 2.2 Hz, 2H), 7.18 (s, 2H), 5.62 (s, 2H), 5.29 (s, 2H), 4.71 (d, J 16.9 Hz, 1H), 4.63 – 4.49 (m, 5H), 4.42 (dd, J 7.2, 5.1 Hz, 2H), 4.24 (m, 3H), 4.12 (t, J 6.9 Hz, 2H), 3.97 (t, J 6.7 Hz, 6H), 3.46 (t, J 6.6 Hz, 4H), 3.07 (t, J 5.6 Hz, 3H), 2.83 (dd, J 12.8, 4.9 Hz, 2H), 2.66 (d, J 12.8 Hz, 2H), 2.51 (t, J 7.3 Hz, 2H), 2.24 (t, J 7.4 Hz, 4H), 2.10 (m, 2H), 2.05 – 1.89 (m, 2H), 1.88 (t, J 7.0 Hz, 1H), 1.71 – 1.46 (m, 18H), 1.36 (m, 8H), 1.19 (s, 37H). ATR-IR 2145 C-C, 1743 C=O, 1650 C=O cm^{-1} . m/z $[\text{ES}]^+$ $\text{M}+\text{H}$, 1388.8 HRMS (NSI) Calcd for $\text{C}_{74}\text{H}_{112}\text{N}_{13}\text{O}_{10}\text{S}_2$, $\text{M}+\text{NH}_4$, 1406.8097; Found 1406.8095 $[\alpha]_{\text{D}}^{25} +15.4$ (c 1.0, CHCl_3 /10% MeOH).

(*S,S,R*)-(((1,1'-(13-(3-oxo-3-((11-(prop-2-yn-1-yloxy)undecyl)oxy)propyl)-6,12-dihydro-5,11-methanodibenzo[*b,f*][1,5]diazocine-2,8-diyl)*bis*(1*H*-1,2,3-triazole-4,1-diyl)*bis*(methylene))*bis*(oxy))*bis*(undecane-11,1-diyl)*bis*(5-((3*aS*,4*S*,6*aR*)-2-oxohexahydro-1*H*-thieno[3,4-*d*]-imidazol-4-yl)pentanoate) 250



A 5 mL microwave vial was charged with **242** (145 mg, 0.108 mmol) in dichloromethane (2 mL). To this trifluoroacetic acid (418 μ L, 5.42 mmol) was added, the vial was sealed and left to stir for 12 hours. The solvent was removed under reduced pressure and the residue was dissolved in a minimum amount of dichloromethane (500 μ L) followed by addition of diethyl ether (3 mL). The precipitate was filtered off and used without further purification **244** (119 mg, 0.093 mmol, 86 % yield)

A 25 ml round bottomed flask was charged with **244** (25 mg, 0.020 mmol) and potassium carbonate (4.04 mg, 0.029 mmol) in *N,N*-dimethylformamide (2 mL) and left to stir for 30 minutes. To this 1-bromo-11-(prop-2-yn-1-yloxy)undecane (8.46 mg, 0.029 mmol) was added and the solution continued to be stirred for 16 hours. The resulting mixture was diluted with water (5 mL) and ethyl acetate (5 mL) then transferred to a 50 mL separating funnel. This was extracted with ethyl acetate (2 x 5mL) and the combined organic extracts were washed with water (5 x 10mL), brine and dried with magnesium sulfate. The suspension was filtered and the solvent removed under reduced

pressure. The impure product was purified by flash chromatography on silica gel eluting with 5-10% methanol in dichloromethane to afford an off white solid. Subsequent physicochemical analysis confirmed this to be the title compound. **250** (24 mg, 0.016 mmol, 83 % yield)

$^1\text{H-NMR}$ (400 MHz, CDCl_3) δ 7.80 (s, 2H, ArH), 7.42 (dd, J 8.6, 2.3 Hz, 2H, ArH), 7.28 (dd, J 9.4, 2.3 Hz, 2H, ArH), 7.18 (s, 2H, ArH), 5.71 (s, 2H, 2NH), 5.35 (s, 2H, 2NH), 4.72 (d, J 16.9 Hz, 1H, CH), 4.65 – 4.54 (m, 5H, 2CH₂, CH), 4.49 – 4.35 (m, 2H, 2CH), 4.24 (m, 3H, 3CH), 4.17 – 4.10 (m, 1H, CH), 4.06 (d, J 2.4 Hz, 2H, 2CH), 3.98 (m, 5H, CH, 2CH₂), 3.52 – 3.34 (m, 6H, 2CH, 2CH₂), 3.08 (dd, J 12.7, 6.5 Hz, 2H, 2CH), 2.83 (dd, J 12.8, 4.9 Hz, 2H, 2CH), 2.66 (d, J 12.7 Hz, 2H, 2CH), 2.51 (t, J 7.4 Hz, 2H, 2CH), 2.35 (t, J 2.4 Hz, 1H, CH), 2.25 (t, J 7.5 Hz, 4H, 2CH₂), 2.09 – 1.75 (m, 2H, CH₂), 1.45 – 1.29 (m, 4H, 2CH₂), 1.71 – 1.44 (m, 20H, 10CH₂), 1.20 (m, 44H, 22CH₂). $^{13}\text{C-NMR}$ (101 MHz, CDCl_3) δ 173.76, 173.08, 163.54, 150.29, 146.19, 145.83, 133.19, 133.03, 129.42, 128.46, 127.47, 126.45, 120.59, 120.33, 119.88, 119.29, 119.11, 80.08, 74.07, 72.54, 71.04, 70.29, 64.80, 64.55, 64.28, 61.94, 60.59, 60.12, 58.00, 55.42, 52.23, 40.55, 33.96, 30.40, 29.64, 29.50, 29.45, 29.42, 29.40, 29.22, 29.19, 28.62, 28.36, 28.26, 26.09, 26.08, 25.90, 24.83 ppm. ATR-IR 3304 C-H, 1744 C=O, 1661 C=O cm^{-1} . m/z [ES]⁺ M+Na 1511.9. HRMS (NSI) Calcd for C₈₀H₁₂₁N₁₂O₁₁S₂, M+H, 1489.8720; Found 1489.8716. $[\alpha]_{\text{D}}^{25}$ +21.9 (c 1.0, CHCl₃/10% MeOH)

References

1. Tröger, J., Ueber einige mittelst nascirenden Formaldehydes entstehende Basen. *Journal für Praktische Chemie* 1887, 36, 225-245.
2. Spielman, M. A., The Structure of Tröger's Base. *J. Am. Chem. Soc.* 1935, 57, 583-585.
3. Wagner, E. C., Condensations of Aromatic Amines with Formaldehyde in Media Containing Acid. III. The Formation of Tröger's Base. *J. Am. Chem. Soc.* 1935, 57, 1296-1298.
4. Abella, C. A. M.; Benassi, M.; Santos, L. S.; Eberlin, M. N.; Coelho, F., The Mechanism of Troger's Base Formation Probed by Electrospray Ionization Mass Spectrometry. *J. Org. Chem.* 2007, 72, 4048-4054.
5. M. Valik, R. M. S., V. Kral, Trogers Base Derivatives - New life for old compounds. *Supramolecular Chemistry* 2005, 17, 347-367.
6. Anna Hansson, J. J. Ola F. W. K. W., Synthesis of Dihalo-Substituted Analogues of Trögers Base from ortho and meta-Substituted Anilines. *Eur. J. Org. Chem.*, 2003, 3179-3188.
7. Delphine Didier, S. S., Synthesis of symmetrical amino and amino methyl derivatives of Trogers base via Pd-catalysed C-C and C-N bond formation. *Tetrahedron* 2007, 63, 3864.
8. Redshaw, C.; Wood, P. T.; Elsegood, M. R. J., Synthesis and Structure of Pentamethylcyclopentadienyl Tungsten(V) Complexes Containing Functionalized 6,12-Epiiminodibenzo[b,f][1.5]diazocine Ligands. *Organometallics* 2007, 26, 6501-6504.
9. Sean P. Bew, L. L., Vincent Scholier, Sunil V. Sharma, a-Amino acid Tröger base derivatives, possible conformationally restricted scaffolds? *Chem. Commun.* 2007, 389-391.
10. Wilen, S. H.; Qi, J. Z.; Williard, P. G., Resolution, asymmetric transformation, and configuration of Tröger's base. Application of Tröger's base as a chiral solvating agent. *J. Org. Chem.* 1991, 56, 485-487.
11. Maitra, U.; Bag, B. G., First asymmetric synthesis of the Troger's base unit on a chiral template. *J. Org. Chem.* 1992, 57, 6979-6981.
12. Try, A. C.; Painter, L.; Harding, M. M., Rigid chiral carbocyclic clefts as building blocks for the construction of new supramolecular hosts. *Tetrahedron Lett.* 1998, 39, 9809-9812.
13. Hitoshi, T., Optical Activity and Absolute Configuration of 2,3 :6,7-Dibenzobicyclo [3.3.1]nona-2,6-diene Derivatives. *Bull. Chem. Soc. Jpn.* 1975, 48, 2473-2483.

14. Jacob Jenson, K. Warnmark., Synthesis of Halogen Substituted Analogues of Trogers Base. *Synthesis* 2001, 12, 1873-1877.
15. Jensen, J.; Tejler, J.; Warnmark, K., General Protocols for the Synthesis of C₂-Symmetric and Asymmetric 2,8-Disubstituted Analogues of Tröger's Base *via* Efficient Bromine-Lithium Exchanges of 2,8-Dibromo-6H,12H-5,11-methanodibenzo[b,f][1,5]diazocine. *J. Org. Chem.* 2002, 67, 6008-6014.
16. Lenev, D. A.; Chervin, I. I.; Lyssenko, K. A.; Kostyanovsky, R. G., Adducts of Troger Bases and activated acetylenes: synthesis and structure. *Tetrahedron Lett.* 2007, 48, 3363-3366.
17. Mahon, A. B.; Craig, D. C.; Try, A. C., Synthesis of 5,6,11,12-tetrahydrodibenzo[b,f][1,5]diazocines and a demonstration of their reactivity to afford methano strap-modified Tröger's base analogues. *ARKIVOC* 2008, XII 148-163.
18. Andrew B. Mahon, D. C. C. a. A. C. T., Synthesis of 5,6,11,12-tetrahydrodibenzo[b,f][1,5]diazocines and a demonstration of their reactivity to afford methano strap-modified Tröger's base analogues. *ARKIVOC* 2008, XII, 148-163.
19. Hamada, Y.; Mukai, S., Synthesis of ethano-Troger's base, configurationally stable substitute of Troger's base. *Tetrahedron: Asym.* 1996, 7, 2671-2674.
20. Try, A. C.; Mahon, A. B.; Craig, D. C., A New Class of Troger's Base Analogues Bearing Spiro[4.5] Lactone Straps. *Synthesis* 2009, 636-642.
21. Tomoshige Kobayashi, T. M., Masaya Tsubakiyama and Shihori Yoshida, Synthesis and functionalization of thiophene congeners of Tröger's base. *J. Chem. Soc., Perkin Trans. 1*, 2002, 1963-1967.
22. Valik, M.; Dolensky, B.; PetrIcková, H.; Vasek, P.; Král, V., Novel heterocyclic Tröger's base derivatives containing *N*-methylpyrrole units. *Tetrahedron Lett.* 2003, 44, 2083-2086.
23. Stoncius, S.; Orentas, E.; Butkus, E.; Ohrstrom, L.; Wendt, O. F.; Warnmark, K., An Approach to Helical Tubular Self-Aggregation Using C₂-Symmetric Self-Complementary Hydrogen-Bonding Cavity Molecules. *J. Am. Chem. Soc.* 2006, 128, 8272-8285.
24. Valik, M.; Cejka, J.; Havlik, M.; Kral, V.; Dolensky, B., calix-Tris-Troger's bases - a new cavitand family. *Chem. Commun.* 2007, 3835-3837.

25. Johnson, R. A.; Gorman, R. R.; Wnuk, R. J.; Crittenden, N. J.; Aiken, J. W., Tröger's base. An alternate synthesis and a structural analog with thromboxane A₂ synthetase inhibitory activity. *J. Med. Chem.* 1993, 36, 3202-3206.
26. Palivec, L.; Valík, M.; Král, V.; Urbanová, M., Interaction of chiral bis-distamycin derivatives with DNAs: electronic circular dichroism study. *Tetrahedron: Asym.* 2006, 17, 1049-1055.
27. S Neidle, L. H. P., P Herzyk, and H M Berman, A molecular model for proflavine-DNA intercalation. *Nucleic Acids Res.* 1988, 8999-9016.
28. Bailly, C.; Laine, W.; Demeunynck, M.; Lhomme, J., Enantiospecific Recognition of DNA Sequences by a Proflavine Tröger Base. *Biochem. Biophys. Res. Commun.* 2000, 273, 681-685.
29. Tatibouët, M. D., Chantal Andraud, André Collet and Jean Lhomme, Synthesis and study of an acridine substituted Tröger's base: preferential binding of the (–)-isomer to B-DNA. *Chem. Commun.* 1999, 161-162.
30. Sasagase, T.; Arai, T.; Kuwahara, M.; Ozaki, H.; Sawai, H., Interaction with and cleavage of DNA by novel phenanthroline polyamine derivative. *Nucl. Acids Symp. Ser. (OXF)* 2007, 51, 193-194.
31. Baldeyrou, B.; Tardy, C.; Bailly, C.; Colson, P.; Houssier, C.; Charmantray, F.; Demeunynck, M., Synthesis and DNA interaction of a mixed proflavine-phenanthroline Tröger base. *Eur. J. Med. Chem.* 2002, 37, 315-322.
32. Cocco, M. J.; Hanakahi, L. A.; Huber, M. D.; Maizels, N., Specific interactions of distamycin with G-quadruplex DNA. *Nucl. Acids Res.* 2003, 31, 2944-2951.
33. Claessens, N.; Pierard, F.; Bresson, C.; Moucheron, C.; Kirsch-De Mesmaeker, A., Optically active Ru(II) complexes with a chiral Tröger's base ligand and their interactions with DNA. *J. Inorg. Biochem.* 2007, 101, 987-996.
34. Lincoln, P.; Norden, B., DNA Binding Geometries of Ruthenium(II) Complexes with 1,10-Phenanthroline and 2,2'-Bipyridine Ligands Studied with Linear Dichroism Spectroscopy. Borderline Cases of Intercalation. *J. Phys. Chem. B* 1998, 102, 9583-9594.
35. Adrian, J. C.; Wilcox, C. S., Chemistry of synthetic receptors and functional group arrays. 10. Orderly functional group dyads. Recognition of biotin and adenine derivatives by a new synthetic host. *J. Am. Chem. Soc.* 1989, 111, 8055-8057.

36. Goswami, S.; Ghosh, K.; Dasgupta, S., Troger's Base Molecular Scaffolds in Dicarboxylic Acid Recognition. *J. Org. Chem.* 2000, 65, 1907-1914.
37. Webb, T. H.; Suh, H.; Wilcox, C. S., Chemistry of synthetic receptors and functional group arrays. 16. Enantioselective and diastereoselective molecular recognition of alicyclic substrates in aqueous media by a chiral, resolved synthetic receptor. *J. Am. Chem. Soc.* 1991, 113, 8554-8555.
38. Cowart, M. D.; Sucholeiki, I.; Bukownik, R. R.; Wilcox, C. S., Molecular recognition in aqueous media. Conformationally restricted water-soluble cyclophanes derived from 6H,12H-5,11-methanodibenzo[b,f][1,5]diazocine. *J. Am. Chem. Soc.* 1988, 110, 6204-6210.
39. Khoshbin, M. S.; Ovchinnikov, M. V.; Mirkin, C. A.; Golen, J. A.; Rheingold, A. L., Metallomacrocycles Incorporating a Hemilabile Troger's Base Derived Ligand. *Inorg. Chem.* 2006, 45, 2603-2609.
40. Lenev, D. A.; Lyssenko, K. A.; Golovanov, D. G.; Buss, V.; Kostyanovsky, R. G., Bis-ortho-Substitution by Methyl Groups Dramatically Increases the Racemization Barrier of Tröger Bases. *Chem. – Eur. J.* 2006, 12, 6412-6418.
41. Lenev, D. A.; Lyssenko, K. A.; Golovanov, D. G.; Malyshev, O. R.; Levkin, P. A.; Kostyanovsky, R. G., Absolute configuration of Troger bases: an X-ray diffraction and circular dichroism study. *Tetrahedron Lett.* 2006, 47, 319-321.
42. Rúnarsson, Ö. V.; Artacho, J.; Wärnmark, K., The 125th Anniversary of the Tröger's Base Molecule: Synthesis and Applications of Tröger's Base Analogues. *Eur. J. Org. Chem.* 2012, 7015-7041.
43. Bew, S. P.; Hiatt-Gipson, G. D.; Lovell, J. A.; Poullain, C., Mild Reaction Conditions for the Terminal Deuteration of Alkynes. *Org. Lett.* 2012 14 , 456-459.
44. Kushner, D. J.; Baker, A.; Dunstall, T. G., Pharmacological uses and perspectives of heavy water and deuterated compounds. *Can. J. Physiol. Pharmacol.* 1999, 77.
45. Harbeson, S. L.; Tung, R. D., Deuterium in drug discovery and development. *Annu. Rep. Med. Chem.* 2011, 46.
46. Foster, A. B., Deuterium isotope effects in studies of drug metabolism. *Trends Pharmacol. Sci.* 1984, 5, 524-527.
47. Belleau, B.; Burba, J.; Pindell, M.; Reiffenstein, J., Effect of Deuterium Substitution in Sympathomimetic Amines on Adrenergic Responses *Science* 1961, 133.

48. Tung, The Development of Deuterium-Containing Drugs; *J. Pharm. Innov. Tech.* 2008. <http://www.concertpharma.com/news/documents/IPT32ConcertPharma.pdf>
49. Buteau, K. C., Deuterated drugs: Unexpectedly unobvious. *J. High Tech. Law*, 2009, 22.
50. Trost, B. M.; Ball, Z. T.; Jorge, T., A Chemoselective Reduction of Alkynes to (E)-Alkenes. *J. Am. Chem. Soc.* 2002, 124, 7922-7923.
51. Vanier, G. S., Simple and Efficient Microwave-Assisted Hydrogenation Reactions at Moderate Temperature and Pressure. *Synlett* 2007, 1, 131-135.
52. Marion, N.; Ramoà, R. S.; Nolan, S. P., [(NHC)AuI]-Catalyzed Acid-Free Alkyne Hydration at Part-per-Million Catalyst Loadings. *J. Am. Chem. Soc.* 2008, 131, 448-449.
53. Agenet, N.; Bruisine, O.; SŁowinski, F.; Gandon, V.; Aubert, C.; Malacria, M., *Organic Reactions* 2007, 68, 302.
54. Hislop, J.-A.; Hunt, M. B.; Fielder, S.; Rowan, D. D., Synthesis of Deuterated β -Lactones for Use in Stable Isotope Dilution Assays. *J. Agric. Food Chem.* 2004, 52, 7075-7083.
55. Sabot, C.; Kumar, K. A.; Antheaume, C.; Mioskowski, C., Triazabicyclodecene: An Effective Isotope Exchange Catalyst in CDCl₃. *J. Org. Chem.* 2007, 72, 5001-5004.
56. Lewandos, G. S.; Maki, J. W.; Ginnebaugh, J. P., Kinetics of terminal alkyne sp carbon-hydrogen bond activation catalyzed by silver(I). *Organometallics* 1982, 1, 1700-1705.
57. Hashmi, A. S. K.; Rudolph, M.; Siehl, H.-U.; Tanaka, M.; Bats, J. W.; Frey, W., Gold Catalysis: Deuterated Substrates as the Key for an Experimental Insight into the Mechanism and Selectivity of the Phenol Synthesis. *Chem. – Eur. J.* 2008, 14, 3703-3708.
58. Tanaka, K.; Tanaka, K.; Takeo, H.; Matsumura, C., Intermediates for the degenerate and productive metathesis of propene elucidated by the metathesis reaction of (Z)-propene-1-d₁. *J. Am. Chem. Soc.* 1987, 109, 2422-2425.
59. Porcel, S.; Echavarren, A. M., Intramolecular Carbostannylation of Alkynes Catalyzed by Silver(I) Species. *Angew. Chem. Int. Ed.* 2007, 46, 2672-2676.
60. Egorova, O. A.; Seo, H.; Kim, Y.; Moon, D.; Rhee, Y. M.; Ahn, K. H., Characterization of Vinylgold Intermediates: Gold-Mediated Cyclization of Acetylenic Amides. *Angew. Chem. Int. Ed.* 2011, 50, 11446-11450.

61. Lowe, D. E.; Glomski, I. J., Cellular and physiological effects of anthrax exotoxin and its relevance to disease. *Front. Cell. Infect. Microbiol.* 2012, 2, 1-13
62. Diamandis, E. P.; Christopoulos, T. K., The Biotin-(strept)avidin system: Principles and applications in biotechnology. *Clin. Chem.* 1991, 37, 625-636
63. Stayton, P. S.; Nelson, K. E.; McDevitt, T. C.; Bulmus, V.; Shimoboji, T.; Ding, Z.; Hoffman, A. S., Smart and biofunctional streptavidin. *Biomol. Eng.* 1999, 16, 93-99.
64. Szychowski, J.; Mahdavi, A.; Hodas, J. J. L.; Bagert, J. D.; Ngo, J. T.; Landgraf, P.; Dieterich, D. C.; Schuman, E. M.; Tirrell, D. A., Cleavable Biotin Probes for Labeling of Biomolecules via Azide - Alkyne Cycloaddition. *J. Am. Chem. Soc.* 2010, 132, 18351-18360.
65. Crisp, G. T.; Gore, J., Preparation of biological labels with acetylenic linker arms. *Tetrahedron* 1997, 53, 1505-1522.
66. Rennhack, A.; Jumpertz, T.; Ness, J.; Baches, S.; Pietrzik, C. U.; Weggen, S.; Bulic, B., Synthesis of a potent photoreactive acidic β -secretase modulator for target identification in cells. *Bioorg. Med. Chem.* 2012, 20, 6523-6532.
67. Xu, W. Z.; Zhang, X.; Kadla, J. F., Design of Functionalized Cellulosic Honeycomb Films: Site-Specific Biomolecule Modification via Click Chemistry. *Biomacromolecules.* 2011, 13, 350-357.
68. Wong, J.; Chilkoti, A.; Moy, V. T., Direct force measurements of the streptavidin-biotin interaction. *Biomol. Eng.* 1999, 16, 45-55.
69. Hodneland, C. D.; Mrksich, M., Biomolecular Surfaces that Release Ligands under Electrochemical Control. *J. Am. Chem. Soc.* 2000, 122, 4235-4236.
70. Perez-Luna, V. H.; O'Brien, M. J.; Opperman, K. A.; Hampton, P. D.; Lopez, G. P.; Klumb, L. A.; Stayton, P. S., Molecular Recognition between Genetically Engineered Streptavidin and Surface-Bound Biotin. *J. Am. Chem. Soc.* 1999, 121, 6469-6478.
71. Dupont-Filliard, A.; Roget, A.; Livache, T.; Billon, M., Reversible oligonucleotide immobilisation based on biotinylated polypyrrole film. *Anal. Chim. Acta* 2001, 449, 45-50.
72. Fang, X.; Liu, X.; Schuster, S.; Tan, W., Designing a Novel Molecular Beacon for Surface-Immobilized DNA Hybridization Studies. *J. Am. Chem. Soc.* 1999, 121, 2921-2922.
73. Pan, S.; Rothberg, L., Chemical Control of Electrode Functionalization for Detection of DNA Hybridization by Electrochemical Impedance Spectroscopy. *Langmuir* 2005, 21, 1022-1027.

74. Love, J. C.; Estroff, L. A.; Kriebel, J. K.; Nuzzo, R. G.; Whitesides, G. M., Self-Assembled Monolayers of Thiolates on Metals as a Form of Nanotechnology. *Chem. Rev.* 2005, 105, 1103-1170.
75. Nuzzo, R. G.; Allara, D. L., Adsorption of bifunctional organic disulfides on gold surfaces. *J. Am. Chem. Soc.* 1983, 105, 4481-4483.
76. Li, J.; Thiara, P. S.; Mrksich, M., Rapid Evaluation and Screening of Interfacial Reactions on Self-Assembled Monolayers. *Langmuir* 2007, 23, 11826-11835.
77. Ulman, A., *An introduction to ultrathin organic films*. Academic press, London: 1991.
78. Weisbecker, C. S.; Merritt, M. V.; Whitesides, G. M., Molecular Self-Assembly of Aliphatic Thiols on Gold Colloids. *Langmuir* 1996, 12, 3763-3772.
79. Higashi, N.; Takahashi, M.; Niwa, M., Immobilization of DNA through Intercalation at Self-Assembled Monolayers on Gold. *Langmuir* 1998, 15, 111-115.
80. Wenz, G.; Liepold, P.; Bordeanu, N., Synthesis and SAM formation of water soluble functional carboxymethylcelluloses: thiosulfates and thioethers. *Cellulose* 2005, 12, 85-96.
81. Terrill, R. H.; Tanzer, T. A.; Bohn, P. W., Structural Evolution of Hexadecanethiol Monolayers on Gold during Assembly : Substrate and Concentration Dependence of Monolayer Structure and Crystallinity. *Langmuir* 1998, 14, 845-854.
82. Strong, L.; Whitesides, G. M., Structures of self-assembled monolayer films of organosulfur compounds adsorbed on gold single crystals: electron diffraction studies. *Langmuir* 1988, 4, 546-558.
83. Chidsey, C. E. D.; Loiacono, D. N., Chemical functionality in self-assembled monolayers: structural and electrochemical properties. *Langmuir* 1990, 6, 682-691.
84. Poirier, G. E.; Tarlov, M. J., The c(4X2) Superlattice of n-Alkanethiol Monolayers Self-Assembled on Au(111). *Langmuir* 1994, 10, 2853-2856.
85. Alves, C. A.; Porter, M. D., Atomic force microscopic characterization of a fluorinated alkanethiolate monolayer at gold and correlations to electrochemical and infrared reflection spectroscopic structural descriptions. *Langmuir* 1993, 9, 3507-3512.
86. Schreiber, F., Structure and growth of self-assembling monolayers. *Prog. Surf. Sci.* 2000, 65, 151-257.

87. Lopez, G. P.; Biebuyck, H. A.; Whitesides, G. M., Scanning electron microscopy can form images of patterns in self-assembled monolayers. *Langmuir* 1993, 9, 1513-1516.
88. Sharma, M.; Komiyama, M.; Engstrom, J. R., Observation from Scanning Tunneling Microscopy of a Striped Phase for Octanethiol Adsorbed on Au(111) from Solution. *Langmuir* 2008, 24, 9937-9940.
89. Keddie, J. L., Structural analysis of organic interfacial layers by ellipsometry. *Curr. Opin. Colloid Interface Sci.* 2001, 6, 102-110.
90. Biacore <http://www.biacore.com/lifesciences/company/index.html>
91. Tao, T. <http://www2.uic.edu/~stao3/SPR%20BIACORE.html>
92. Mrksich, M., Mass Spectrometry of Self-Assembled Monolayers: A New Tool for Molecular Surface Science. *ACS Nano* 2008, 2, 7-18.
93. Hillencamp, F.; Karas, M. *The MALDI Process and Method.* 2007, Wiley, Germany.
94. Su, J.; Mrksich, M., Using MALDI-TOF Mass Spectrometry to Characterize Interfacial Reactions on Self-Assembled Monolayers. *Langmuir* 2003, 19, 4867-4870.
95. Ha, T. K.; Oh, H. B.; Chung, J.; Lee, T. G.; Han, S. Y., Investigation of the MALDI Process Used to Characterize Self-Assembled Monolayers of Alkanethiolates on Gold. *Langmuir* 2009, 25, 3692-3697.
96. Ha, T. K.; Lee, T. G.; Song, N. W.; Moon, D. W.; Han, S. Y., Cation-Assisted Laser Desorption/Ionization for Matrix-Free Surface Mass Spectrometry of Alkanethiolate Self-Assembled Monolayers on Gold Substrates and Nanoparticles. *Anal. Chem.* 2008, 80, 8526-8531.
97. Su, J.; Mrksich, M., Using mass spectrometry to characterise self assembled monolayers presenting peptides, protiens and carbohydrates. *Angew. Chem. Int. Ed.* 2002, 41, 4715-4718.
98. Dal-Hee, M.; Wei-Jen, T.; Mrksich, M., Chemical screening by mass spectrometry to identify inhibitors of anthrax lethal factor. *Nat. Biotechnol.* 2004, 22, 717-723.
99. Yu, H.-Z., New chemistry on old CDs. *Chem. Commun.* 2004, 2633-2636.
100. Denise, L.; Eduardo, M. R.; Lúcio, A.; Mauro, B., Disposable Gold Electrodes with Reproducible Area Using Recordable CDs and Toner Masks. *Electroanalysis* 2006, 18, 89-94.
101. Li, Y.; Ou, L. M. L.; Yu, H.-Z., Digitized Molecular Diagnostics: Reading Disk-Based Bioassays with Standard Computer Drives. *Anal. Chem.* 2008, 80, 8216-8223.

102. Clair, J. J. L.; Burkart, M. D., Molecular screening on a compact disc. *Org. Biomol. Chem.* 2003, 1, 3244-3249.
103. Potyrailo, R. A.; Morris, W. G.; Leach, A. M.; Sivavec, T. M.; Wisnudel, M. B.; Boyette, S., Analog Signal Acquisition from Computer Optical Disk Drives for Quantitative Chemical Sensing. *Anal. Chem.* 2006, 78, 5893-5899.
104. Li, Y.-J.; Xu, L.; Yang, W.-L.; Liu, H.-B.; Lai, S.-W.; Che, C.-M.; Li, Y.-L., Amidetriazole: A Versatile Building Block for Construction of Oxyanion Anion Receptors. *Chem. – Eur. J.* 2012, 18, 4782-4790.
105. Bew, S. P.; Hiatt-Gipson, G. D., Synthesis of C-Propargylic Esters of N-Protected Amino Acids and Peptides. *J. Org. Chem.* 2011, 75, 3897-3899.
106. Bew, S. P.; Brimage, R. A.; L'Hermit, N.; Sharma, S. V., Upper Rim Appended Hybrid Calixarenes via Click Chemistry. *Org. Lett.* 2007, 9, 3713-3716.
107. Westheimer, F. H., The Magnitude of the Primary Kinetic Isotope Effect for Compounds of Hydrogen and Deuterium. *Chem. Rev.* 1961, 61, 265-273.
108. Burgers, P. C.; Holmes, J. L.; Mommers, A. A.; Szulejko, J. E., Generation and identification of four stable isomeric $[C_3H_3]^+$ ions by direct dissociative ionization or by charge reversal of anions. *J. Am. Chem. Soc.* 1984, 106, 521-525.
109. Hopf, H.; Priebe, H.; Walsh, R., Thermal isomerization. 9. The role of cyclopropene in the allene to propyne isomerization. A study of the thermal rearrangements of C_3H_3D isomers. *J. Am. Chem. Soc.* 1980, 102, 1210-1212.
110. Trambarulo, R., The Microwave Spectrum and Structure of Methyl Acetylene *J. Chem. Phys.* 1950, 18, 1613-1616.
111. Miyachi, A.; Takahashi, T.; Matsumura, S.; Mihara, H., Peptide Nanofibers Modified with a Protein by Using Designed Anchor Molecules Bearing Hydrophobic and Functional Moieties. *Chem. – Eur. J.* 16, 6644-6650.
112. Guerrero de la Rosa, V.; Ordez, M.; Llera, J. M., Asymmetric synthesis of both diastereomers of protected S-methyl-L-cysteine and S-n-propyl-L-cysteine sulphoxides. *Tet. Asymm.* 2001, 12, 1615-1620.
113. Goddard-Borger, E. D.; Stick, R. V., An Efficient, Inexpensive, and Shelf-Stable Diazotransfer Reagent: Imidazole-1-sulfonyl Azide Hydrochloride. *Org. Lett.* 2007, 9, 3797-3800.

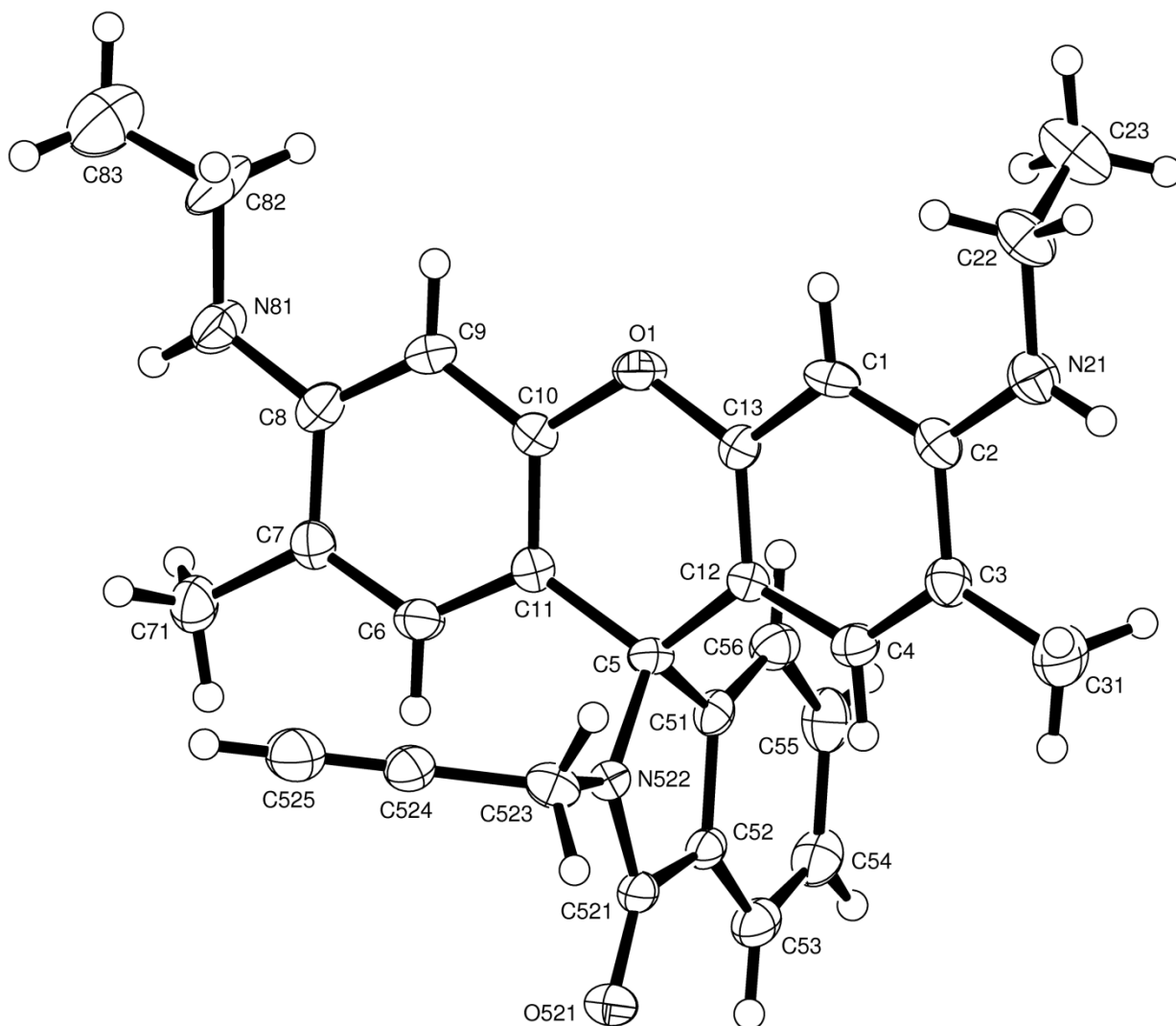
114. Yu, H.-Z., Self-Assembly on gold recordable CDs. *Anal. Chem.* 2001, 73, 4743-4747.
115. Wärnmark, K.; Jenson, J., Synthesis of Halogen Substituted Analogues of Trogers Base. *Synthesis* 2001, 12, 1873-1877.
116. Pardo, C.; Sesmilo, E.; Gutierrez-Puebla, E.; Monge, A.; Elguero, J.; Fruchier, A., New Chiral Molecular Tweezers with a Bis-Troger's Base Skeleton. *J. Org. Chem.* 2001, 66, 1607-1611.
117. Didier, D.; Sergeev, S., Synthesis of symmetrical amino and amino methyl derivatives of Trogers base via Pd-catalysed C-C and C-N bond formation. *Tetrahedron* 2007, 63, 3864 - 3869.
118. Scriven, E. F. V.; Turnbull, K., Azides: their preparation and synthetic uses. *Chem. Rev.* 1988, 88, 297-368.
119. Li, M.; Wong, K. K. W.; Mann, S., Organization of Inorganic Nanoparticles Using Biotin-Streptavidin Connectors. *Chem. Mater.* 1998, 11, 23-26.
120. Birkert, O.; Haake, H.-M.; Schatz, A.; Mack, J. r.; Brecht, A.; Jung, G. n.; Gauglitz, G. n., A Streptavidin Surface on Planar Glass Substrates for the Detection of Biomolecular Interaction. *Anal. Biochem.* 2000, 282, 200-208.
121. Zhang, L.; Zhang, Y.; Dong, J.; Liu, J.; Zhang, L.; Sun, H., Design and synthesis of novel photoaffinity probes for study of the target proteins of oleanolic acid. *Bioorg. Med. Chem. Lett.* 22, 1036-1039.
122. Sanda, F.; Araki, H.; Masuda, T., Serine-Based Helical Polyacetylenes. Effect of Hydroxyl Group on the Secondary Structure. *Macromolecules* 2005, 38, 10605-10608.
123. Loethen, S.; Ooya, T.; Choi, H. S.; Yui, N.; Thompson, D. H., Synthesis, Characterization, and pH-Triggered Dethreading of Cyclodextrin-Poly(ethylene glycol) Polyrotaxanes Bearing Cleavable Endcaps. *Biomacromolecules* 2006, 7, 2501-2506.
124. Sudhir, V. S.; Venkateswarlu, C.; Musthafa, O. T. M.; Sampath, S.; Chandrasekaran, S., Click Chemistry Inspired Synthesis of Novel Ferrocenyl-Substituted Amino Acids or Peptides. *Eur. J. Org. Chem.* 2009, 2120-2129.
125. Jones, J., *Amino Acid and Peptide Synthesis, 2nd edn.* Oxford University Press: 2002, Oxford, UK
126. Loeffler, L. J.; Sajadi, Z.; Hall, I. H., Antineoplastic agents. 1. N-Protected vinyl, 1,2-dihaloethyl, and cyanomethyl esters of phenylalanine. *J. Med. Chem.* 1977, 20, 1578-1584.

127. Kele, P.; Li, X.; Link, M.; Nagy, K.; Herner, A.; Lorincz, K.; Beni, S.; Wolfbeis, O. S., Clickable fluorophores for biological labeling-with or without copper. *Org. Biomol. Chem.* 2009, 7, 3486-3490.
128. Jockusch, S.; Li, Z.; Ju, J.; Turro, N. J., Two-photon excitation induced fluorescence of a trifluorophore-labeled DNA. *Photochem. Photobiol.* 2005, 81, 238-241.
129. Buer, B. C.; Chugh, J.; Al-Hashimi, H. M.; Marsh, E. N. G., Using Fluorine Nuclear Magnetic Resonance To Probe the Interaction of Membrane-Active Peptides with the Lipid Bilayer. *Biochemistry.* 2010, 49, 5760-5765.
130. Mereyala, H. B.; Gurrula, S. R., A highly diastereoselective, practical synthesis of allyl, propargyl 2,3,4,6-tetra-O-acetyl- α -D-glucopyranosides and allyl, propargyl heptaacetyl-D-lactosides. *Carbohydr. Res.* 1998, 307, 351-354.
131. Wardrop, D. J.; Zhang, W.; Fritz, J., Stereospecific Entry to [4.5]Spiroketal Glycosides Using Alkylidene-carbene CH Insertion. *Org. Lett.* 2002, 4, 489-492.
132. Severi, E.; Hood, D. W.; Thomas, G. H., Sialic acid utilization by bacterial pathogens. *Microbiology* 2007, 153, 2817-2822.
133. Baumberg, F.; Vasella, A.; Schauer, R., 4-Methylumbelliferyl 5-Acetamido-3,4,5-trideoxy- α -D-manno-2-nonulopyranosidonic Acid: Synthesis and Resistance to Bacterial Sialidases. *Helv. Chim. Acta* 1986, 69, 1927-1935.
134. Yohannes, F.; Vliegthart, G. *NMR spectroscopy of Sialic acids.* 1982, Springer, Vienna,
135. Tatibouët, M. D., Chantal Andraud, André Collet and Jean Lhomme, Synthesis and study of an acridine substituted Trögers base: preferential binding of the (-)-isomer to B-DNA. *Chem. Commun* 1999, 161-162.
136. Veale, E. B.; Gunnlaugsson, T., Synthesis, Photophysical, and DNA Binding Studies of Fluorescent Trögers Base Derived 4-Amino-1,8-naphthalimide Supramolecular Clefs. *J. Org. Chem.* 75, 5513-5525.
137. Furlan, R.; Garrido, L.; Brumatti, G.; Amarante-Mendes, G.; Martins, R.; Facciotti, M.; Padilla, G., A rapid and sensitive method for the screening of DNA intercalating antibiotics. *Biotechnol. Lett.* 2002, 24, 1807-1813.
138. Couty, F.; Durrat, F.; Prim, D., Expeditive synthesis of homochiral fused tri- and tetrazoles piperazines from amino alcohols. *Tet. Lett.* 2004, 45, 3725-3728.

139. Bew, S. P.; Legentil, L.; Scholier, V.; Sharma, S. V., α -Amino acid Träger base derivatives, possible conformationally restricted scaffolds? *Chem. Commun.* 2007, 4, 389-391.
140. Beavis, R. C.; Chait, B. T.; Barry L. Karger, W. S. H., [22] Matrix-assisted laser desorption ionization mass-spectrometry of proteins. In *Methods in Enzymology*, Academic Press: 1996; Vol. Volume 270, 519-551, Amsterdam.
141. Dean, B.; Oguchi, H.; Cai, S.; Otsuji, E.; Tashiro, K.; Hakomori, S.-i.; Toyokuni, T., Synthesis of multivalent lactosyl clusters as potential tumor metastasis inhibitors. *Carbohydr. Res.* 1993, 245, 175-192.
142. Ghosez, L. o.; Yang, G.; Cagnon, J. R.; Bideau, F. L.; Marchand-Brynaert, J., Synthesis of enantiomerically pure α -amino- β -hydroxy-cyclobutanone derivatives and their transformations into polyfunctional three- and five-membered ring compounds. *Tetrahedron* 2004, 60, 7591-7606.
143. Voorhees, V.; Adams, R., The use of the oxides of platinum for the catalytic reduction of organic compounds I. *J. Am. Chem. Soc.* 1922, 44, 1397-1405.
144. Khurana, J. M.; Arora, R., Rapid Chemoselective Deprotection of Benzyl Esters by Nickel Boride. *Synthesis* 2009, 7, 1127-1130.
145. Srinivasan, R.; Uttamchandani, M.; Yao, S. Q., Rapid Assembly and in Situ Screening of Bidentate Inhibitors of Protein Tyrosine Phosphatases. *Org. Lett.* 2006, 8, 713-716.
146. Schofield, C. L.; Field, R. A.; Russell, D. A., Glyconanoparticles for the Colorimetric Detection of Cholera Toxin. *Anal. Chem.* 2007, 79, 1356-1361.

Appendix

Crystal Structure and refinement for 107



Crystal and structure refinement data for a derivative of Rhodamine G

Identification code	glynhg8b
Elemental formula	$C_{29}H_{29}N_3O_2$
Formula weight	451.5
Crystal system	Triclinic
Space group	P-1 (no. 2)
Unit cell dimensions	$a = 8.8708(9) \text{ \AA}$ $\alpha = 88.826(8)^\circ$

$$b = 9.6838(11) \text{ \AA} \quad \beta = 79.174(8)^\circ$$

$$c = 15.8955(15) \text{ \AA} \quad \gamma = 63.088(10)^\circ$$

Volume	1192.7(2) \AA^3
No. of formula units, Z	2
Calculated density	1.257 Mg/m^3
F(000)	480
Absorption coefficient	0.080 mm^{-1}
Temperature	140(1) K
Wavelength	0.71073 \AA
Crystal colour, shape	pale brown plate
Crystal size	0.30 x 0.19 x 0.04 mm
Crystal mounting	On a glass fibre, in oil, fixed in cold N_2 stream

On the diffractometer:

Theta range for data collection 3.4 to 23.0 $^\circ$

Limiting indices $-9 \leq h \leq 9$, $-10 \leq k \leq 10$, $-17 \leq l \leq 17$

Completeness to theta = 23.0 99.5 %

Absorption correction Semi-empirical from equivalents

Max. and min. transmission 1.156 and 0.803

Reflections collected (not including absences) 13360

No. of unique reflections 3310 [R(int) for equivalents = 0.073]

No. of 'observed' reflections ($I > 2\sigma_I$) 1921

Structure determined by: direct methods, in SHELXS

Refinement: Full-matrix least-squares On F^2 , in SHELXL

Data / restraints / parameters 3310 / 0 / 309

Goodness-of-fit on F^2 0.884

Final R indices ('observed' data) $R_1 = 0.046$, $wR_2 = 0.099$

Final R indices (all data) $R_1 = 0.096$, $wR_2 = 0.108$

Reflections weighted:

$$w = [\sigma^2(F_o^2) + (0.0531P)^2]^{-1} \text{ where } P = (F_o^2 + 2F_c^2)/3$$

Largest diff. peak and hole 0.56 and -0.26 e.Å⁻³

Location of largest difference peak near H(82a)

Table 1. Atomic coordinates ($\times 10^5$) and equivalent isotropic displacement parameters ($\text{\AA}^2 \times 10^4$). U(eq) is defined as one third of the trace of the orthogonalized Uij tensor. E.s.ds are in parentheses.

	x	y	z	U(eq)
O(1)	3999(2)	6970(2)	3344.3(11)	260(5)
C(1)	5221(3)	4267(3)	3257.7(17)	254(7)
C(2)	6439(3)	2792(3)	2899.9(17)	242(7)
N(21)	6442(3)	1464(3)	3228.5(15)	328(7)
C(22)	5097(4)	1490(4)	3918.4(18)	343(8)
C(23)	5389(4)	1736(4)	4801(2)	495(10)
C(3)	7726(3)	2661(3)	2182.4(18)	247(7)
C(31)	9045(4)	1088(3)	1774(2)	410(9)
C(4)	7738(3)	3988(3)	1883.6(17)	242(7)
C(5)	6653(3)	6906(3)	1895.6(16)	209(7)
C(6)	4676(3)	9819(3)	1979.6(17)	245(7)
C(7)	3277(3)	11177(3)	2333.0(17)	231(7)
C(71)	2977(4)	12711(3)	1986.2(18)	321(8)
C(8)	2120(3)	11089(3)	3053.2(17)	246(7)

N(81)	756(3)	12456(3)	3467.1(15)	333(7)
C(82)	-488(4)	12457(4)	4205(2)	447(9)
C(83)	-1728(4)	14055(4)	4571(2)	630(12)
C(9)	2411(3)	9663(3)	3363.9(17)	239(7)
C(10)	3846(3)	8323(3)	2979.1(17)	199(7)
C(11)	5030(3)	8365(3)	2283.7(17)	200(7)
C(12)	6533(3)	5483(3)	2236.3(16)	194(7)
C(13)	5283(3)	5577(3)	2925.9(17)	199(7)
C(51)	8280(3)	6963(3)	2030.7(18)	210(7)
C(52)	9306(3)	6931(3)	1258.3(17)	205(7)
C(53)	10857(3)	6975(3)	1213(2)	285(8)
C(54)	11379(3)	7035(3)	1969(2)	313(8)
C(55)	10347(4)	7061(3)	2755(2)	322(8)
C(56)	8793(3)	7034(3)	2797.2(19)	264(7)
C(521)	8461(3)	6850(3)	558.9(19)	229(7)
O(521)	8960(2)	6817(2)	-218.2(12)	312(6)
N(522)	6965(3)	6817(2)	942.9(14)	202(6)
C(523)	5860(3)	6592(3)	448.2(18)	270(7)
C(524)	4400(4)	8041(4)	305.1(18)	284(8)
C(525)	3248(4)	9204(4)	193.5(19)	418(9)

Table 2. Molecular dimensions. Bond lengths are in Ångstroms, angles in degrees. E.s.ds are in parentheses.

O(1)-C(10)	1.381(3)	C(1)-C(2)	1.392(4)
O(1)-C(13)	1.386(3)	C(1)-C(13)	1.385(4)

C(2)-N(21)	1.377(3)	N(81)-C(82)	1.452(4)
C(2)-C(3)	1.416(4)	C(82)-C(83)	1.483(4)
N(21)-C(22)	1.452(3)	C(9)-C(10)	1.387(3)
C(22)-C(23)	1.516(4)	C(10)-C(11)	1.388(4)
C(3)-C(31)	1.501(4)	C(12)-C(13)	1.376(3)
C(3)-C(4)	1.365(4)	C(51)-C(52)	1.376(3)
C(4)-C(12)	1.400(3)	C(51)-C(56)	1.391(4)
C(5)-C(11)	1.520(3)	C(52)-C(521)	1.474(4)
C(5)-C(12)	1.512(4)	C(52)-C(53)	1.384(4)
C(5)-C(51)	1.523(4)	C(53)-C(54)	1.377(4)
C(5)-N(522)	1.484(3)	C(54)-C(55)	1.397(4)
C(6)-C(7)	1.370(3)	C(55)-C(56)	1.381(4)
C(6)-C(11)	1.393(4)	C(521)-O(521)	1.227(3)
C(7)-C(71)	1.499(4)	C(521)-N(522)	1.367(3)
C(7)-C(8)	1.416(4)	N(522)-C(523)	1.455(3)
C(8)-N(81)	1.392(3)	C(523)-C(524)	1.466(4)
C(8)-C(9)	1.384(4)	C(524)-C(525)	1.167(4)
C(10)-O(1)-C(13)	117.6(2)	C(3)-C(4)-C(12)	123.9(2)
C(13)-C(1)-C(2)	120.6(3)	C(12)-C(5)-C(11)	110.1(2)
N(21)-C(2)-C(1)	122.1(3)	C(11)-C(5)-C(51)	111.9(2)
C(1)-C(2)-C(3)	118.6(3)	N(522)-C(5)-C(11)	111.4(2)
N(21)-C(2)-C(3)	119.3(3)	C(12)-C(5)-C(51)	112.4(2)
C(2)-N(21)-C(22)	122.9(2)	N(522)-C(5)-C(12)	110.9(2)
N(21)-C(22)-C(23)	112.9(3)	N(522)-C(5)-C(51)	99.7(2)
C(2)-C(3)-C(31)	120.0(3)	C(7)-C(6)-C(11)	124.2(3)
C(4)-C(3)-C(2)	118.5(3)	C(6)-C(7)-C(71)	121.9(3)
C(4)-C(3)-C(31)	121.5(3)	C(6)-C(7)-C(8)	117.5(3)

C(8)-C(7)-C(71)	120.6(2)	C(52)-C(51)-C(5)	111.0(2)
N(81)-C(8)-C(7)	119.0(3)	C(56)-C(51)-C(5)	128.8(2)
C(9)-C(8)-C(7)	119.9(3)	C(52)-C(51)-C(56)	120.2(3)
C(9)-C(8)-N(81)	121.0(3)	C(51)-C(52)-C(521)	108.7(2)
C(8)-N(81)-C(82)	122.1(3)	C(51)-C(52)-C(53)	121.9(3)
N(81)-C(82)-C(83)	111.7(3)	C(53)-C(52)-C(521)	129.4(3)
C(8)-C(9)-C(10)	120.1(3)	C(54)-C(53)-C(52)	118.3(3)
O(1)-C(10)-C(9)	114.9(2)	C(53)-C(54)-C(55)	120.1(3)
O(1)-C(10)-C(11)	123.4(2)	C(56)-C(55)-C(54)	121.4(3)
C(9)-C(10)-C(11)	121.7(3)	C(55)-C(56)-C(51)	118.2(3)
C(6)-C(11)-C(5)	122.0(2)	O(521)-C(521)-C(52)	128.4(3)
C(10)-C(11)-C(5)	121.5(2)	N(522)-C(521)-C(52)	106.3(2)
C(10)-C(11)-C(6)	116.5(2)	O(521)-C(521)-N(522)	125.2(3)
C(4)-C(12)-C(5)	121.3(2)	C(521)-N(522)-C(5)	114.2(2)
C(13)-C(12)-C(4)	116.4(3)	C(523)-N(522)-C(5)	123.6(2)
C(13)-C(12)-C(5)	122.2(2)	C(521)-N(522)-C(523)	122.0(2)
C(1)-C(13)-O(1)	114.6(2)	N(522)-C(523)-C(524)	113.8(2)
C(12)-C(13)-C(1)	122.0(3)	C(525)-C(524)-C(523)	179.2(4)
C(12)-C(13)-O(1)	123.4(3)		

Table 3. Anisotropic displacement parameters ($\text{\AA}^2 \times 10^4$) for the

expression:

$$\exp \{-2\pi^2(h^2a^*U_{11} + \dots + 2hka^*b^*U_{12})\}$$

E.s.ds are in parentheses.

U₁₁ U₂₂ U₃₃ U₂₃ U₁₃ U₁₂

O(1)	289(11)	243(12)	227(11)	-10(9)	41(9)	-138(10)
C(1)	284(16)	339(19)	192(17)	50(14)	-5(13)	-205(15)
C(2)	273(17)	267(19)	251(18)	64(14)	-111(14)	-160(15)
N(21)	372(15)	230(15)	371(16)	63(13)	-21(12)	-149(13)
C(22)	467(19)	357(20)	343(20)	122(16)	-124(16)	-294(17)
C(23)	701(24)	575(24)	385(22)	190(18)	-187(18)	-420(20)
C(3)	260(16)	215(18)	273(18)	28(14)	-58(13)	-114(14)
C(31)	420(19)	253(19)	492(22)	23(16)	-29(16)	-122(16)
C(4)	211(15)	250(18)	252(18)	20(14)	-9(13)	-108(14)
C(5)	205(15)	240(17)	157(16)	5(13)	0(12)	-93(13)
C(6)	242(16)	301(19)	190(17)	24(14)	-22(13)	-131(15)
C(7)	265(16)	217(18)	209(17)	6(13)	-74(13)	-99(14)
C(71)	341(17)	246(18)	307(18)	0(15)	-76(14)	-69(15)
C(8)	200(16)	275(19)	231(18)	-58(14)	-55(13)	-75(15)
N(81)	267(13)	243(15)	429(16)	-38(13)	34(12)	-101(12)
C(82)	241(17)	332(21)	606(25)	-152(18)	134(16)	-65(16)
C(83)	505(22)	564(26)	676(28)	-113(22)	29(20)	-169(20)
C(9)	221(16)	278(19)	197(16)	-20(14)	10(12)	-114(14)
C(10)	227(15)	209(17)	186(16)	8(13)	-53(13)	-116(14)
C(11)	217(15)	190(17)	205(16)	7(13)	-56(13)	-100(13)
C(12)	195(15)	203(18)	174(16)	22(13)	-28(13)	-86(14)
C(13)	187(15)	188(17)	213(17)	-2(14)	-46(13)	-76(14)
C(51)	203(15)	159(16)	241(18)	-4(13)	-36(13)	-62(13)
C(52)	176(15)	154(16)	252(18)	16(13)	5(13)	-64(13)
C(53)	250(17)	210(18)	355(20)	5(14)	13(14)	-99(14)
C(54)	225(16)	272(19)	473(22)	42(16)	-57(16)	-145(15)
C(55)	315(18)	287(19)	391(21)	24(15)	-169(15)	-123(15)

C(56)	266(17)	246(17)	262(18)	-4(14)	-18(13)	-114(14)
C(521)	225(16)	151(17)	239(18)	16(13)	22(14)	-50(13)
O(521)	316(11)	313(13)	237(13)	42(10)	27(9)	-118(10)
N(522)	184(12)	197(13)	188(13)	12(10)	-13(10)	-65(11)
C(523)	327(17)	319(18)	197(17)	22(14)	-50(13)	-176(15)
C(524)	222(17)	342(20)	284(19)	54(15)	-30(13)	-136(16)
C(525)	316(19)	540(25)	360(21)	116(18)	-54(15)	-172(18)

Table 4. Hydrogen coordinates ($\times 10^4$) and isotropic displacement parameters ($\text{\AA}^2 \times 10^3$). All hydrogen atoms were included in idealised positions with $U(\text{iso})$'s set at $1.2 \cdot U(\text{eq})$ or, for the methyl groups, $1.5 \cdot U(\text{eq})$ of the parent carbon atom.

	x	y	z	U(iso)
H(1)	4358	4373	3724	30
H(21)	7277	580	3016	39
H(22A)	5043	516	3881	41
H(22B)	3995	2316	3845	41
H(23A)	4461	1755	5231	74
H(23B)	5430	2706	4845	74
H(23C)	6461	904	4885	74
H(31A)	9806	1205	1294	61
H(31B)	8473	556	1579	61
H(31C)	9699	499	2187	61
H(4)	8598	3894	1418	29

H(6)	5440	9870	1506	29
H(71A)	3918	12565	1525	48
H(71B)	2901	13403	2434	48
H(71C)	1920	13149	1777	48
H(81)	648	13330	3280	40
H(82A)	118	11872	4642	54
H(82B)	-1116	11946	4034	54
H(83A)	-2528	14011	5056	95
H(83B)	-2345	14631	4143	95
H(83C)	-1111	14557	4750	95
H(9)	1642	9603	3832	29
H(53)	11529	6965	686	34
H(54)	12420	7058	1956	38
H(55)	10715	7098	3261	39
H(56)	8107	7062	3323	32
H(52A)	5419	5926	747	32
H(52B)	6548	6061	-104	32
H(525)	2330	10130	104	50

Table 5. Torsion angles, in degrees. E.s.ds are in parentheses.

C(13)-C(1)-C(2)-N(21)	178.2(3)	N(21)-C(2)-C(3)-C(31)	1.7(4)
C(13)-C(1)-C(2)-C(3)	-0.9(4)	C(1)-C(2)-C(3)-C(31)	-179.2(2)
C(1)-C(2)-N(21)-C(22)	5.8(4)	C(2)-C(3)-C(4)-C(12)	-1.0(4)
C(3)-C(2)-N(21)-C(22)	-175.1(3)	C(31)-C(3)-C(4)-C(12)	179.5(3)
C(2)-N(21)-C(22)-C(23)	-83.9(3)	C(11)-C(6)-C(7)-C(8)	-0.1(4)
N(21)-C(2)-C(3)-C(4)	-177.8(2)	C(11)-C(6)-C(7)-C(71)	179.1(3)
C(1)-C(2)-C(3)-C(4)	1.3(4)	C(6)-C(7)-C(8)-C(9)	-1.1(4)

C(71)-C(7)-C(8)-C(9)	179.8(3)	C(51)-C(5)-C(12)-C(13)	113.2(3)
C(6)-C(7)-C(8)-N(81)	175.3(2)	N(522)-C(5)-C(12)-C(4)	46.4(3)
C(71)-C(7)-C(8)-N(81)	-3.9(4)	C(11)-C(5)-C(12)-C(4)	170.2(2)
C(9)-C(8)-N(81)-C(82)	-4.1(4)	C(51)-C(5)-C(12)-C(4)	-64.2(3)
C(7)-C(8)-N(81)-C(82)	179.5(3)	C(4)-C(12)-C(13)-C(1)	0.3(4)
C(8)-N(81)-C(82)-C(83)	175.5(3)	C(5)-C(12)-C(13)-C(1)	-177.3(2)
N(81)-C(8)-C(9)-C(10)	-175.4(2)	C(4)-C(12)-C(13)-O(1)	-179.9(2)
C(7)-C(8)-C(9)-C(10)	0.9(4)	C(5)-C(12)-C(13)-O(1)	2.6(4)
C(13)-O(1)-C(10)-C(9)	172.3(2)	C(2)-C(1)-C(13)-C(12)	0.1(4)
C(13)-O(1)-C(10)-C(11)	-8.2(4)	C(2)-C(1)-C(13)-O(1)	-179.8(2)
C(8)-C(9)-C(10)-O(1)	-179.9(2)	C(10)-O(1)-C(13)-C(12)	8.4(4)
C(8)-C(9)-C(10)-C(11)	0.5(4)	C(10)-O(1)-C(13)-C(1)	-171.7(2)
O(1)-C(10)-C(11)-C(6)	178.9(2)	N(522)-C(5)-C(51)-C(52)	0.8(3)
C(9)-C(10)-C(11)-C(6)	-1.6(4)	C(12)-C(5)-C(51)-C(52)	118.2(3)
O(1)-C(10)-C(11)-C(5)	-3.0(4)	C(11)-C(5)-C(51)-C(52)	-117.2(3)
C(9)-C(10)-C(11)-C(5)	176.5(2)	N(522)-C(5)-C(51)-C(56)	-179.1(3)
C(7)-C(6)-C(11)-C(10)	1.4(4)	C(12)-C(5)-C(51)-C(56)	-61.6(3)
C(7)-C(6)-C(11)-C(5)	-176.7(2)	C(11)-C(5)-C(51)-C(56)	63.0(3)
N(522)-C(5)-C(11)-C(10)	136.0(3)	C(56)-C(51)-C(52)-C(53)	-0.3(4)
C(12)-C(5)-C(11)-C(10)	12.5(3)	C(5)-C(51)-C(52)-C(53)	179.8(2)
C(51)-C(5)-C(11)-C(10)	-113.3(3)	C(56)-C(51)-C(52)-C(521)	179.8(2)
N(522)-C(5)-C(11)-C(6)	-46.0(3)	C(5)-C(51)-C(52)-C(521)	-0.1(3)
C(12)-C(5)-C(11)-C(6)	-169.5(2)	C(51)-C(52)-C(53)-C(54)	0.8(4)
C(51)-C(5)-C(11)-C(6)	64.7(3)	C(521)-C(52)-C(53)-C(54)	-179.4(3)
C(3)-C(4)-C(12)-C(13)	0.2(4)	C(52)-C(53)-C(54)-C(55)	-0.5(4)
C(3)-C(4)-C(12)-C(5)	177.8(3)	C(53)-C(54)-C(55)-C(56)	-0.2(4)
N(522)-C(5)-C(12)-C(13)	-136.1(2)	C(54)-C(55)-C(56)-C(51)	0.7(4)
C(11)-C(5)-C(12)-C(13)	-12.4(4)	C(52)-C(51)-C(56)-C(55)	-0.4(4)

C(5)-C(51)-C(56)-C(55) 179.5(3)
C(51)-C(52)-C(521)-O(521) 179.3(3)
C(53)-C(52)-C(521)-O(521) -0.6(5)
C(51)-C(52)-C(521)-N(522) -0.8(3)
C(53)-C(52)-C(521)-N(522) 179.4(3)
O(521)-C(521)-N(522)-C(523) 5.8(4)
C(52)-C(521)-N(522)-C(523) -174.2(2)
O(521)-C(521)-N(522)-C(5) -178.7(3)
C(52)-C(521)-N(522)-C(5) 1.3(3)
C(12)-C(5)-N(522)-C(521) -120.0(2)
C(11)-C(5)-N(522)-C(521) 117.0(2)
C(51)-C(5)-N(522)-C(521) -1.3(3)
C(12)-C(5)-N(522)-C(523) 55.4(3)
C(11)-C(5)-N(522)-C(523) -67.6(3)
C(51)-C(5)-N(522)-C(523) 174.1(2)
C(521)-N(522)-C(523)-C(524) -97.7(3)
C(5)-N(522)-C(523)-C(524) 87.2(3)
N(522)-C(523)-C(524)-C(525) 19(24)

Crystal structure analysis of a derivative of Rhodamine G

Crystal data: C₂₉H₂₉N₃O₂, M = 451.5. Triclinic, space group P-1 (no. 2), a = 8.8708(9), b = 9.6838(11), c = 15.8955(15) Å, α = 88.826(8), β = 79.174(8), γ = 63.088(10) °, V = 1192.7(2) Å³. Z = 2, D_c = 1.257 g cm⁻³, F(000) = 480, T = 140(1) K, μ(Mo-Kα) = 0.8 cm⁻¹, λ(Mo-Kα) = 0.71069 Å.

Crystals are pale brown plates. One, ca 0.30 x 0.19 x 0.04 mm, was mounted in oil on a glass fibre and fixed in the cold nitrogen stream on an Oxford Diffraction Xcalibur-3 CCD diffractometer equipped with Mo-Kα radiation and graphite monochromator. Intensity data were measured by thin-slice ω- and φ-scans. Total no. of reflections recorded, to θ_{max} = 23°, was 13360 of which 3310 were unique (R_{int} = 0.073); 1921 were 'observed' with I > 2σ_I.

Data were processed using the CrysAlisPro-CCD and -RED (1) programs. The structure was determined by the direct methods routines in the SHELXS program (2A) and refined by full-matrix least-squares methods, on F²'s, in SHELXL (2B). The non-hydrogen atoms were refined with anisotropic thermal parameters. Hydrogen atoms were included in idealised positions and their U_{iso} values were set to ride on the U_{eq} values of the parent carbon atoms. At the conclusion of the refinement, wR₂ = 0.108 and R₁ = 0.096 (2B) for all 3310 reflections weighted w = [σ²(F_o²) + (0.0531P)²]⁻¹ with P = (F_o² + 2F_c²)/3; for the 'observed' data only, R₁ = 0.046.

In the final difference map, the highest peak (ca 0.56 eÅ⁻³) was near H(82a).

Scattering factors for neutral atoms were taken from reference (3). Computer programs used in this analysis have been noted above, and were run through WinGX (4) on a Dell Precision 370 PC at the University of East Anglia.

References

Programs CrysAlisPro-CCD and -RED, Oxford Diffraction Ltd., Abingdon, UK (2008).

G. M. Sheldrick, SHELX-97 – Programs for crystal structure determination (SHELXS) and refinement (SHELXL), *Acta Cryst.* (2008) A64, 112-122.

'International Tables for X-ray Crystallography', Kluwer Academic Publishers, Dordrecht (1992). Vol. C, pp. 500, 219 and 193.

L. J. Farrugia, *J. Appl. Cryst.*, (1999) 32, 837-838 .

Legends for Figures

Figure 1. View of the molecule, indicating the atom numbering scheme. Hydrogen atoms have been omitted for clarity. Thermal ellipsoids are drawn at the 50% probability level.

Notes on the structure

The main C₁₃O three-ring system is basically planar, but there is a slight tilting about the central O(1)...C(5) vector; the angle between the normals to the two C₆ rings is 8.86(14)°.

Neither of the two amino hydrogen atoms is involved in hydrogen bonding – there are no acceptor atoms nearby. Nor is there any stacking of ring systems by π...π interactions. There is one

possible 'weak hydrogen bond', C(4)-H(4)...O(521'), where the symmetry operation, ' , is 2-x, 1-y, -x. Intermolecular contacts are principally by C-H... π and other van der Waals' interactions.

N.B.

The compound is a derivative of Rhodamine G, and its systematic name is :

3',6'-bis(ethylamino)-2',7'-dimethyl-2-(prop-2-ynyl)spiro[isoindoline-1,9'-xanthen]-3-one

Crystal structure analysis of ggipson3317 – (+/-)-111

Crystal data: C₃₁H₂₄N₈, CH₂Cl, M = 593.51. Orthorhombic, space group Pccn, a = 22.8378(19), b = 11.4030(12), c = 10.4557(7) Å, $\alpha = 90$, $\beta = 90$, $\gamma = 90$ °, V = 2722.9(4) Å³. Z = 4, D_c = 1448 g cm⁻³, F(000) = 1232, T = 140(1) K, $\lambda(\text{Mo-K}\alpha) = 0.71069$ Å.

Crystals are clear, colourless blocks. From a sample under oil, one, ca 0.70 x 0.15 x 0.15 mm, was mounted on a glass fibre and fixed in the cold nitrogen stream on an Oxford Diffraction Xcalibur-3/Sapphire3-CCD diffractometer, equipped with Mo-K α radiation and graphite monochromator. Intensity data were measured by thin-slice ω - and ϕ -scans. Total no. of reflections recorded, to $\theta_{\text{max}} = 30.5^\circ$, was 53410 of which 4155 were unique (Rint = 0.0738); 2518 were 'observed' with I > 2 σ _I.

Data were processed using the CrysAlisPro-CCD and -RED (1) programs. The structure was determined by the direct methods routines in the SHELXS program (2A) and refined by full-matrix least-squares methods, on F²'s, in SHELXL (2B). The non-hydrogen atoms were refined with anisotropic thermal parameters. Hydrogen atoms were included in idealised positions and their Uiso values were set to ride on the Ueq values of the parent carbon atoms. At the conclusion of the refinement, wR₂ = 0.1039 and R₁ = 0.0985 (2B) for all 4155 reflections weighted $w = [\sigma^2(F_o^2) + (0.0P)^2 + 1.P]^{-1}$ with $P = (F_o^2 + 2F_c^2)/3$; for the 'observed' data only, R₁ = 0.0465.

In the final difference map, the highest peaks (to ca 0.4 eÅ⁻³) were close to the chlorine atom.

Scattering factors for neutral atoms were taken from reference (3). Computer programs used in this analysis have been noted above, and were run through WinGX (4) on a Dell Precision 370 PC at the University of East Anglia.

References

Programs CrysAlisPro, Oxford Diffraction Ltd., Abingdon, UK (2010).

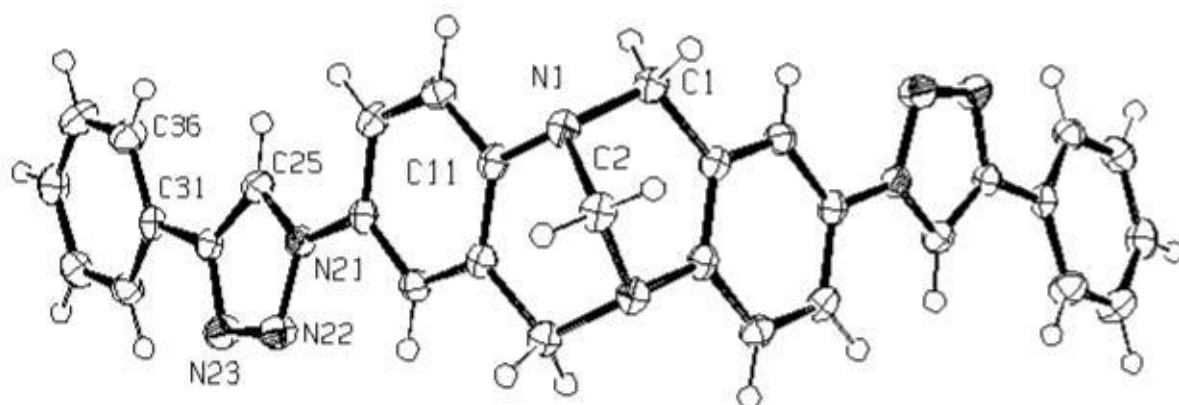
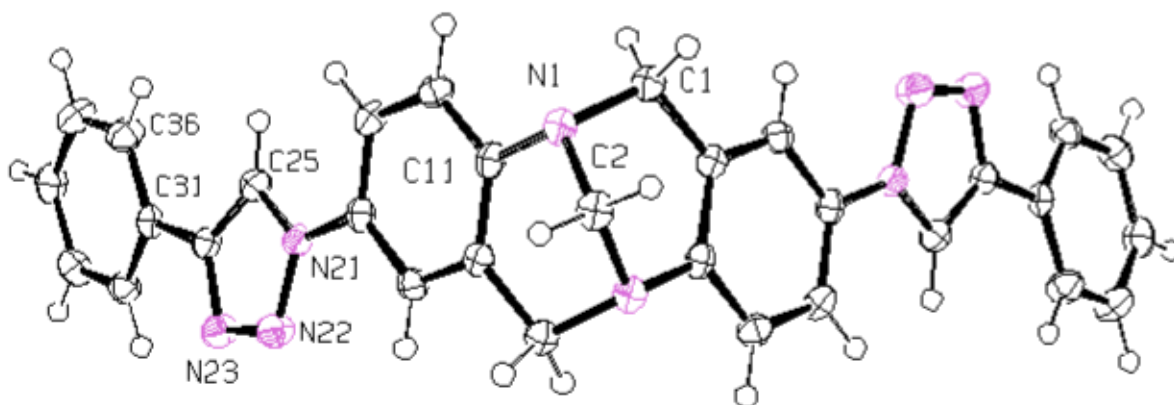
G. M. Sheldrick, SHELX-97 – Programs for crystal structure determination (SHELXS) and refinement (SHELXL), *Acta Cryst.* (2008) A64, 112-122.

'*International Tables for X-ray Crystallography*', Kluwer Academic Publishers, Dordrecht (1992). Vol. C, pp. 500, 219 and 193.

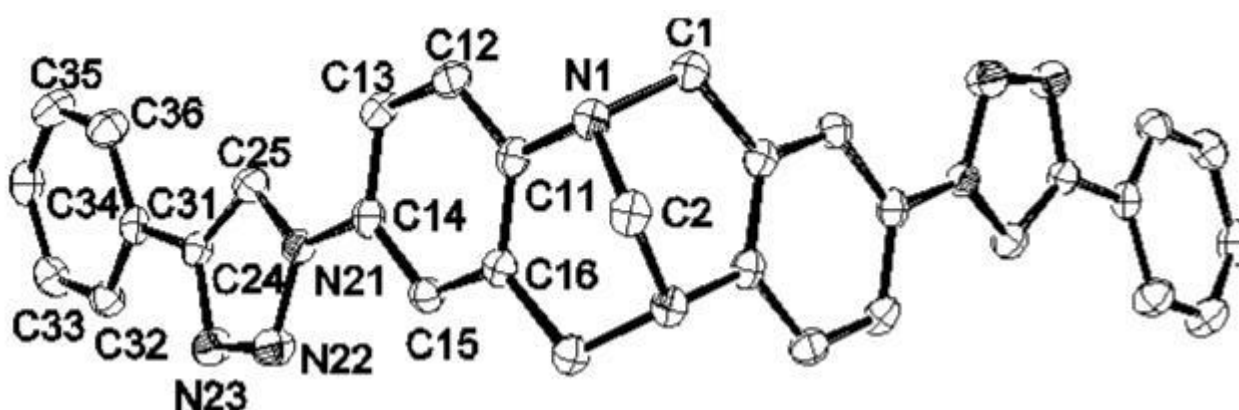
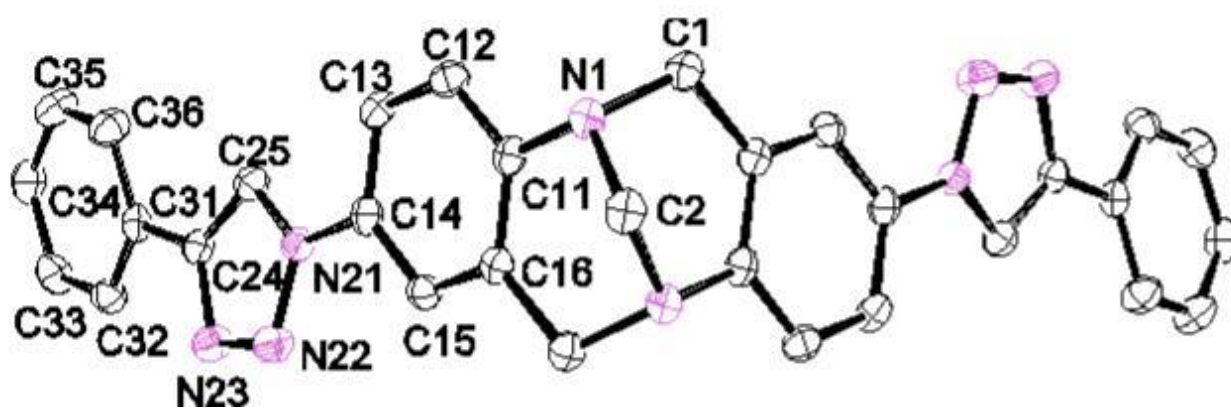
L. J. Farrugia, *J. Appl. Cryst.*, (1999) 32, 837-838 .

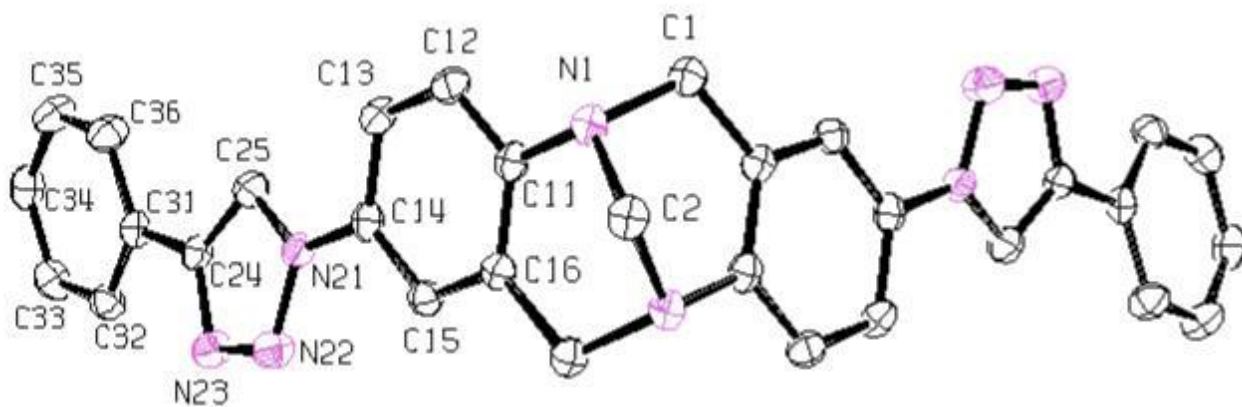
Figures for ggipson3317

Ellipsoids are drawn at 50% probability. The dichloromethane solvent molecule has been omitted for clarity. A center of symmetry is located at C2.

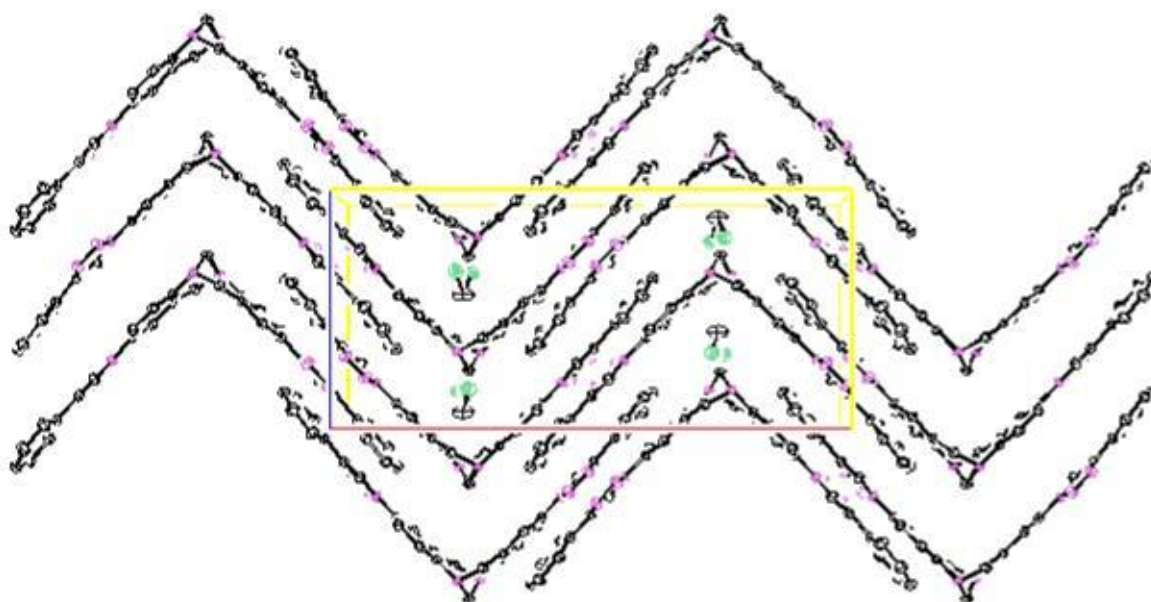


Ellipsoids are drawn at 50% probability. The dichloromethane solvent molecule and the hydrogen atoms have been omitted for clarity.





Packing diagram showing the unit cell contents: View normal to the 010 plane. Ellipsoids are drawn at 50% probability. Hydrogen atoms are omitted for clarity.



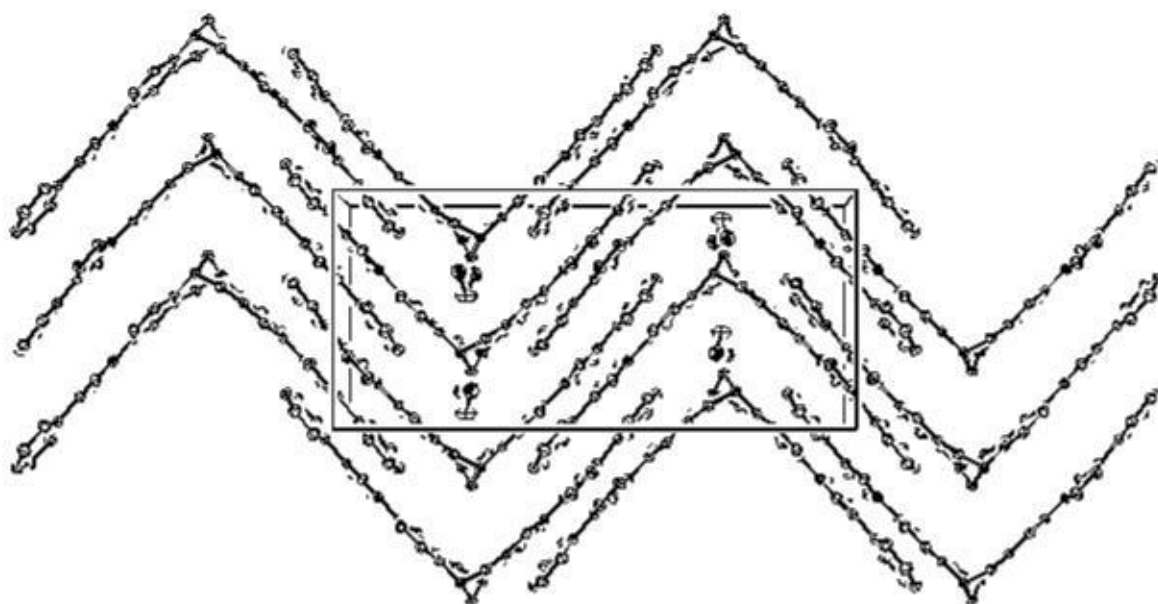


Table 1. Crystal data and structure refinement for ggipson3317.

Identification code	ggipson3317
Empirical formula	$C_{32} H_{26} Cl_2 N_8$
Moiety formula	$C_{31} H_{24} N_8 \times C H_2 Cl_2$
Formula weight	593.51
Temperature	140(1) K
Wavelength	0.71073 Å
Crystal system	Orthorhombic
Space group	Pccn
Unit cell dimensions	$a = 22.8378(19) \text{ \AA}$ $\angle = 90^\circ$.
	$b = 11.4030(12) \text{ \AA}$ $\angle = 90^\circ$.
	$c = 10.4557(7) \text{ \AA}$ $\angle = 90^\circ$.
Volume	$2722.9(4) \text{ \AA}^3$
Z	4
Density (calculated)	1.448 Mg/m^3
Absorption coefficient	0.279 mm^{-1}
F(000)	1232

Crystal size 0.70 x 0.15 x 0.15 mm³
 Theta range for data collection 3.57 to 30.51°
 Index ranges -32<=h<=32, -16<=k<=16, -14<=l<=14
 Reflections collected 53410
 Independent reflections 4155 [R(int) = 0.0738]
 Completeness to theta = 30.51° 99.9 %
 Refinement method Full-matrix least-squares on F²
 Data / restraints / parameters 4155 / 0 / 191
 Goodness-of-fit on F² 0.923
 Final R indices [I>2sigma(I)] R1 = 0.0465, wR2 = 0.0925
 R indices (all data) R1 = 0.0985, wR2 = 0.1039
 Largest diff. peak and hole 0.365 and -0.414 e.Å⁻³

Table 2. Atomic coordinates (x 10⁴) and equivalent isotropic displacement parameters (Å²x 10³) for ggipson3317. U(eq) is defined as one third of the trace of the orthogonalized U_{ij} tensor.

	x	y	z	U(eq)
C(15)	6384(1)		1604(1)	-544(1)20(1)
C(16)	6797(1)		1916(1)	375(1) 19(1)
C	7500	7500	4298(3)	63(1)
Cl	7380(1)		6240(1)	3362(1) 44(1)
N(1)	7296(1)		3480(1)	1607(1) 21(1)
N(21)	5629(1)		2125(1)	-2083(1) 20(1)
C(13)	6120(1)		3628(1)	-833(1)23(1)
N(22)	5479(1)		990(1)	-2263(1) 28(1)
C(31)	4574(1)		2353(1)	-4635(1) 21(1)
C(12)	6535(1)		3939(2)	66(1) 23(1)

C(25)	5330(1)	2821(2)	-2897(1)	23(1)
C(1)	7817(1)	4000(1)	1003(1)	22(1)
N(23)	5090(1)	969(1)	-3189(1)	26(1)
C(32)	4364(1)	1471(2)	-5425(1)	24(1)
C(35)	4019(1)	3752(2)	-5855(2)	32(1)
C(34)	3805(1)	2868(2)	-6628(2)	29(1)
C(11)	6873(1)	3098(1)	683(1)	20(1)
C(24)	4989(1)	2080(1)	-3599(1)	21(1)
C(33)	3978(1)	1728(2)	-6413(2)	27(1)
C(14)	6049(1)	2453(1)	-1133(1)	20(1)
C(36)	4398(1)	3501(2)	-4857(2)	29(1)
C(2)	7500	2500	2392(2)	23(1)

Table 3. Bond lengths [Å] and angles [°] for ggipson3317.

C(15)-C(14)	1.379(2)
C(15)-C(16)	1.394(2)
C(15)-H(15)	0.9300
C(16)-C(11)	1.397(2)
C(16)-C(1)#1	1.516(2)
C-Cl	1.7596(16)
C-Cl#2	1.7596(16)
N(1)-C(11)	1.4336(18)
N(1)-C(2)	1.4630(16)
N(1)-C(1)	1.472(2)
N(21)-C(25)	1.3480(19)
N(21)-N(22)	1.3518(18)
N(21)-C(14)	1.4309(18)
C(13)-C(12)	1.381(2)
C(13)-C(14)	1.385(2)

N(22)-N(23) 1.3144(18)

C(31)-C(32) 1.388(2)

C(31)-C(36) 1.389(2)

C(31)-C(24) 1.473(2)

C(12)-C(11) 1.391(2)

C(25)-C(24) 1.363(2)

C(1)-C(16)#1 1.516(2)

N(23)-C(24) 1.357(2)

C(32)-C(33) 1.388(2)

C(35)-C(34) 1.382(2)

C(35)-C(36) 1.385(2)

C(34)-C(33) 1.377(2)

C(2)-N(1)#1 1.4630(16)

C(14)-C(15)-C(16) 120.30(15)

C(15)-C(16)-C(11) 119.29(14)

C(15)-C(16)-C(1)#1 121.10(14)

C(11)-C(16)-C(1)#1 119.55(13)

Cl-C-Cl#2 112.44(15)

C(11)-N(1)-C(2) 111.11(11)

C(11)-N(1)-C(1) 112.20(11)

C(2)-N(1)-C(1) 106.91(10)

C(25)-N(21)-N(22) 110.35(12)

C(25)-N(21)-C(14) 128.55(14)

N(22)-N(21)-C(14) 121.10(12)

C(12)-C(13)-C(14) 118.91(15)

N(23)-N(22)-N(21) 106.92(12)

C(32)-C(31)-C(36) 118.88(14)

C(32)-C(31)-C(24) 120.50(15)

C(36)-C(31)-C(24)	120.61(14)
C(13)-C(12)-C(11)	121.30(15)
N(21)-C(25)-C(24)	105.32(15)
N(1)-C(1)-C(16)#1	112.23(12)
N(22)-N(23)-C(24)	109.27(13)
C(31)-C(32)-C(33)	120.64(15)
C(34)-C(35)-C(36)	120.76(16)
C(33)-C(34)-C(35)	119.40(15)
C(12)-C(11)-C(16)	119.32(14)
C(12)-C(11)-N(1)	118.51(14)
C(16)-C(11)-N(1)	122.16(13)
N(23)-C(24)-C(25)	108.15(13)
N(23)-C(24)-C(31)	122.60(14)
C(25)-C(24)-C(31)	129.25(15)
C(34)-C(33)-C(32)	120.19(15)
C(15)-C(14)-C(13)	120.86(14)
C(15)-C(14)-N(21)	119.89(14)
C(13)-C(14)-N(21)	119.24(14)
C(35)-C(36)-C(31)	120.13(15)
N(1)#1-C(2)-N(1)	111.75(16)

Symmetry transformations used to generate equivalent atoms:

#1 -x+3/2,-y+1/2,z #2 -x+3/2,-y+3/2,z

Table 4. Anisotropic displacement parameters ($\text{\AA}^2 \times 10^3$) for ggipson3317. The anisotropic displacement factor exponent takes the form: $-2 \sum [h^2 a^* 2 U^{11} + \dots + 2 h k a^* b^* U^{12}]$

	U ¹¹	U ²²	U ³³	U ²³	U ¹³	U ¹²
C(15)	20(1)	20(1)	20(1)	1(1)	3(1)	-1(1)

C(16)	19(1)	23(1)	15(1)	2(1)	2(1)	1(1)
C	86(3)	70(3)	33(2)	0	0	-1(2)
Cl	43(1)	44(1)	46(1)	9(1)	3(1)	2(1)
N(1)	21(1)	25(1)	16(1)	-2(1)	0(1)	1(1)
N(21)	19(1)	21(1)	21(1)	-1(1)	0(1)	1(1)
C(13)	22(1)	24(1)	23(1)	-1(1)	-2(1)	6(1)
N(22)	32(1)	24(1)	28(1)	-1(1)	-7(1)	1(1)
C(31)	16(1)	27(1)	20(1)	-1(1)	1(1)	0(1)
C(12)	25(1)	21(1)	23(1)	-4(1)	2(1)	3(1)
C(25)	22(1)	23(1)	25(1)	2(1)	-2(1)	2(1)
C(1)	22(1)	24(1)	19(1)	-2(1)	1(1)	1(1)
N(23)	28(1)	25(1)	26(1)	-2(1)	-6(1)	2(1)
C(32)	25(1)	23(1)	24(1)	2(1)	1(1)	-1(1)
C(35)	34(1)	29(1)	33(1)	-1(1)	-4(1)	11(1)
C(34)	23(1)	41(1)	22(1)	2(1)	-4(1)	2(1)
C(11)	18(1)	26(1)	15(1)	-2(1)	2(1)	2(1)
C(24)	19(1)	22(1)	21(1)	-1(1)	2(1)	2(1)
C(33)	29(1)	33(1)	21(1)	-2(1)	-3(1)	-7(1)
C(14)	17(1)	27(1)	16(1)	-1(1)	1(1)	1(1)
C(36)	32(1)	26(1)	28(1)	-8(1)	-5(1)	4(1)
C(2)	24(1)	29(1)	15(1)	0	0	1(1)

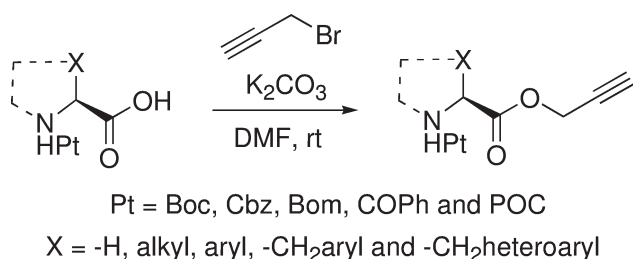
Synthesis of *C*-Propargylic Esters of *N*-Protected Amino Acids and Peptides

Sean P. Bew* and Glyn D. Hiatt-Gipson

School of Chemistry, University of East Anglia, Norwich, NR4 7TJ, United Kingdom

s.bew@uea.ac.uk

Received March 21, 2010



Recent years have seen a huge surge of interest in the application of alkyne-derived motifs for so-called “click” chemistry. Given the critical importance of amino acids in organic synthesis as well as their myriad of applications in “click” chemistry it is interesting to note that the synthesis of *C*-propargyl derived amino acid esters has not been particularly well served. We report a convenient, straightforward, and high-yielding synthesis of structurally diverse *C*-propargyl-derived *N*-protected amino acid esters.

A search of SciFinder reveals that to date over 1700 papers have been published on “click chemistry”. Critical to its continued success and development is the ready availability of structurally diverse alkyne (and azide) starting materials.

In an ongoing extension of a Tröger base project¹ we required an efficient, cheap, reliable, and straightforward synthesis of structurally diverse *N*-protected α -amino acid propargyl esters suited to “click” chemistry. Given the widespread availability of structurally diverse natural and unnatural amino acids and the extensive interest in “click” chemistry we were surprised that a search on SciFinder afforded a limited number of α -amino acid propargyl esters. Furthermore upon closer inspection many of the proposed syntheses employed elevated reaction temperatures, i.e., 70 °C,² multistep reaction processes, i.e., synthesis of propargyl ester **3** from methyl ester **1** via acid **2**,³ and the use of relatively expensive reagents, i.e., synthesis of esters **5** and **6** utilized

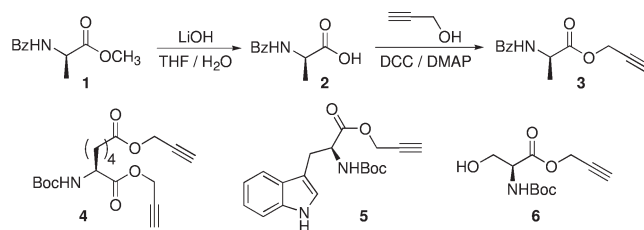
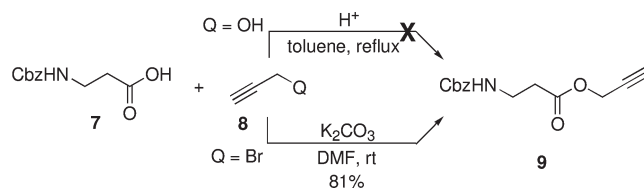


FIGURE 1. Previously synthesized *N*-protected *O*-propargylic α -amino acid esters.

SCHEME 1. Synthetic Routes to *N*-Cbz- β -aminoalanine Propargyl Ester **9**



N-(3-dimethylaminopropyl)-*N*-ethylcarbodiimide hydrochloride (\$22 per gram), were low yielding, i.e., 14% for **6**,⁴ required long reaction times, i.e., **5** took 48 h to go to completion,⁵ or employed DCC (dicyclohexylcarbodiimide), necessitating flash chromatography for the efficient and complete removal of the DCU (*N,N'*-dicyclohexylurea) byproduct, i.e., synthesis of **3** and **4** (Figure 1).⁶

Attempting the synthesis of ester **9** a solution of acid **7** was warmed with propargyl alcohol **8** (Q = OH) and 10 mol % tosic acid (Scheme 1). After 6 h an intractable brown tar had formed. Subsequent analysis (¹H NMR) indicated ~10% of ester **9** had formed but that this was embedded within a complex unidentifiable mixture.

An alternative procedure was required. The *O*-propargylation of α -amino carboxylic acids with use of propargyl bromide and base has been reported with (*S*)-tyrosine and (*S*)-aspartic acid.⁷ Reinvestigating the synthesis of ester **9** we stirred acid **7** in dimethylformamide with propargyl bromide and anhydrous potassium carbonate (1.2 equiv). After a simple workup, i.e., dilute with aqueous citric acid, extract with ethyl acetate, and filter through a Varian SPE cartridge (NH₂), an unoptimized 81% yield of ester **9** was afforded that was pure enough (¹H NMR indicated > 95%) to be used for a subsequent reaction.

With this result we set about investigating the scope of the reaction with alternative *N*-protected α -amino acids. Both aryl and alkyl side chain equipped α -amino acids such as *N*-Cbz-(*S*)-phenylalanine and *N*-Bz leucine (entries A and B, Table 1) afforded the corresponding propargyl esters **10** and

(1) Bew, S. P.; Legentil, L.; Scholier, V.; Sharma, S. V. *Chem. Commun.* **2007**, 389.

(2) Loeffler, L. J.; Sajadi, Z.; Hall, I. H. *J. Med. Chem.* **1977**, *20*, 1578.

(3) Werner, S.; Iyer, P. S.; Fodor, M. D.; Coleman, C. M.; Twining, L. A.; Mitasev, B.; Brummond, K. M. *J. Comb. Chem.* **2006**, *8*, 370.

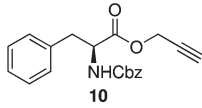
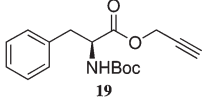
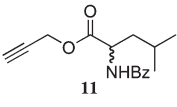
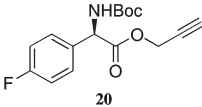
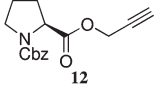
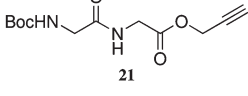
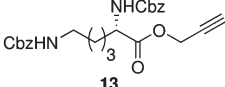
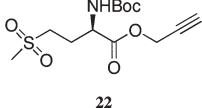
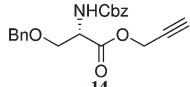
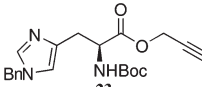
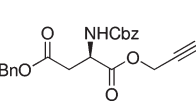
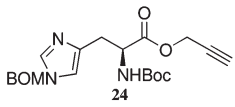
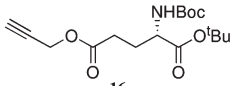
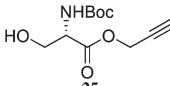
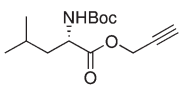
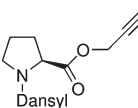
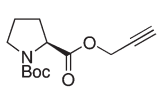
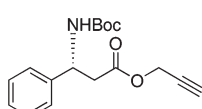
(4) Sanda, F.; Araki, H.; Masuda, T. *Macromolecules* **2005**, *38*, 10605.

(5) Loethen, S.; Ooya, T.; Soo, C. H.; Yui, N.; Thompson, D. H. *Biomacromolecules* **2006**, *7*, 2501.

(6) Haridas, V.; Lal, K.; Sharma, Y. K.; Upreti, S. *Org. Lett.* **2008**, *10*, 1645. Brummond, K. M.; Mitasev, B. *Org. Lett.* **2004**, *6*, 2245.

(7) Sudhir, V. S.; Venkateswarlu, C.; Musthafa, O. T. M.; Sampath, S.; Chandrasekaran, S. *Eur. J. Org. Chem.* **2009**, 2120. Mandal, P. K.; McMurray, J. S. *J. Org. Chem.* **2007**, *72*, 6599.

TABLE 1. Examples of Structurally Diverse N-Protected *O*-Propargylic Amino Acid Esters and Peptides Synthesized in This Study

Entry No	N-protected α -amino propargyl ester	Yield	Entry No	N-protected α -amino propargyl ester	Yield
A		86%	J		91%
B		83%	K		86%
C		95%	L		67%
D		85%	M		71%
E		81%	N		41%
F		82%	O		43%
G		89%	P		65%
H		92%	Q		85%
I		96%	R		75%

11 in 86% and 83% yields, respectively. Similarly the cyclic α -amino acid *N*-Cbz-(*S*)-proline derived propargyl ester (**12**, entry C) was returned in an excellent 95% yield and without recourse to flash chromatography. The synthesis of propargyl ester **13** derived from the doubly *N*-Cbz protected (*S*)-lysine was achieved in a pleasing 85% yield (entry D), again no column chromatography was required. Subjecting differentially *N,O*-diprotected *N*-Cbz-(*S*)-serine-*O*-benzyl to propargylation afforded the desired ester **14** (Table 1, entry E, 81% yield) with both *N*-Cbz and *O*-benzyl protecting groups remaining intact. Similarly the diprotected mono-*O*-benzyl ester *N*-Cbz aspartic acid precursor afforded the corresponding α -amino propargylic ester **15** in an 82% yield (entry F).

Incorporating an *N*-Boc protecting group within (*S*)-glutamic acid, (*S*)-leucine, (*S*)-proline, and (*S*)-phenylalanine

afforded (Scheme 1) the expected *N*-Boc protected α -amino acid propargylic esters **16–19** in 89%, 92%, 96%, and 91% yields, respectively (entries G–J), without recourse to column chromatography. Similarly incorporating an unnatural, aryl containing α -amino acid, i.e., *N*-Boc-4-fluoro-(*S*)-phenylglycine, afforded the corresponding propargylic ester **20** in a pleasing 86% yield (entry K).

All attempts at transforming *N*-acetylglycine, *N*-Fmoc-(*S*)-valine, *N*-Fmoc-(*S*)-phenylalanine, *N*-Fmoc- β -alanine, or *N*-Fmoc-(*S*)-alanine into the corresponding propargylic esters (not shown) employing the reaction conditions outlined in Scheme 1 failed to return any of the desired products. Seemingly the use of base labile *N*-protecting groups resulted in their cleavage during the reaction process.

A particularly useful application would focus on the ability to generate propargylic esters of dipeptides. With this in mind we subjected the simple monoprotected *N*-Boc-gly gly dipeptide to our standard propargylation reaction conditions (Scheme 1). After a simple workup we were delighted to isolate the desired propargyl ester of *N*-Boc-gly-gly (**21**) in an unoptimized 67% yield (entry L, Table 1).

The application of our O-propargylation reaction to α -amino acids that have heteroatoms embedded within their side chains was deemed worthy of investigation. Initiating this study we probed the O-propargylation of *N*-Boc-(*S*)-methionine sulfone. The desired ester (**22**) was afforded in an unoptimized but pleasing 71% yield (entry M). Similarly incorporating imidazole equipped α -amino acids such as 3-*N*-benzyl- α -*N*-Boc-(*S*)-histidine (entry N), 3-*N*-BOM- α -*N*-Boc-(*S*)-histidine (entry O) afforded the corresponding propargyl esters **23** and **24** in 41% and 43% yields, respectively.

The synthesis of (*S*)-serine derived propargylic ester **25** has been previously reported; however, the yield was a very poor 14%.⁴ We felt our procedure may offer this potentially valuable α -amino acid building block in a higher yield. Consequently we were delighted that subjecting *N*-Boc-(*S*)-serine to the reaction conditions outlined in Scheme 1 afforded ester **25** in a significantly improved 65% yield (entry P).

The dansyl group is routinely employed as a fluorogenic agent for the N-derivatization and analysis of α -amino acids and peptides.⁸ Furthermore Borthwick et al. has demonstrated that a series of *N*-dansyl-(*S*)-proline α -methylpyrrolidine-5,5-lactam derivatives display single-figure μ M inhibition of human cytomegalovirus (HCMV) protease.⁹ Thus the ability to generate a *N*-dansyl-(*S*)-proline propargyl ester **26** may have significant applications in the spectroscopic determination of amino acids or peptides as well as acting as a valuable tool for probing biological systems. With this in mind we subjected commercially available *N*-dansyl-(*S*)-proline to our standard propargylic reaction conditions. We were delighted that ester **26** (entry Q) was afforded in an 85% yield and, similar to previous examples, the product was pure enough to be used "as is".

Our study to date had focused on, in the majority of cases, investigating N-protected α -amino acids derived from natural sources. Although we did not envisage any issues it was thought prudent to establish that the procedure outlined in Scheme 1 also worked for unnatural N-protected β -amino

acids. With this in mind we took commercially available (*R*)-3-(Boc-amino)-3-phenylpropionic acid and subjected it to our standard conditions with propargyl bromide and potassium carbonate in dimethylformamide. The corresponding propargyl ester (**27**) was afforded as a white powder in a 75% yield (entry R).

In summary, the efficient synthesis of C-propargylated α -amino acids has been achieved by using very mild reaction conditions that tolerate the majority of commonly used amino acid protecting groups. Utilizing cheap reagents the desired products are afforded, in the majority of cases, pure enough to be employed as is, thus negating the cost and environmental impact of purification. It is envisaged that this protocol will be widely applicable, affording valuable C-propargylated amino acids building blocks that should find significant use in the synthetic chemistry community.

Experimental Section

General Procedure. A flame-dried 25-mL round-bottomed flask was charged with *N*-Cbz-(*S*)-proline (1 g, 4 mmol) and anhydrous potassium carbonate (830 mg, 6 mmol) in DMF (5 mL). The resulting suspension was stirred for 30 min under an atmosphere of nitrogen. Propargyl bromide (80% in toluene, 710 mg, 6 mmol) was added and the reaction was stirred for 16 h at ambient temperature. The resulting mixture was diluted with water (5 mL), acidified with citric acid (1 mL), and extracted with ethyl acetate (2 \times 2 mL). The combined organic extracts were washed with brine (2 mL), dried with magnesium sulfate, and filtered through NH₂ loaded silica. Solvent removal afforded **12** (1.1 g, 3.8 mmol) as a yellow oil in a 95% yield, with the following physicochemical properties.

¹H NMR (400 MHz, CDCl₃) δ 7.23 (m, 5H, ArH), 5.03 (m, 2H, CH₂(cbz)), 4.62 (m, 1H, CHH_(yne)), 4.45 (s, 1H, CHH_(yne)), 4.28 (m, 1H, α CH), 3.41 (m, 2H, δ CH₂), 2.41 (1H, CH_(yne)), 2.12 (d, *J* = 7.42 Hz, 1H, β CHH), 1.85 (m, 3H, β CHH, γ CH₂); ¹³C NMR (75 MHz, CDCl₃) δ 172.1, 171.9, 154.9, 154.2, 136.7, 136.6, 128.5, 128.4, 128.0, 127.9, 127.9, 127.8, 77.2, 75.3, 66.9, 66.9, 58.9, 58.6, 52.4, 52.3, 46.8, 46.3, 30.6, 29.6, 24.1, 23.3; FT-IR (KBr neat) 3285, 2956, 2883, 1753, 1704, 1452, 1417, 1353, 1167; *m/z* [ES] M + Na (found) 310.0, (calcd) 310.11; HRMS (NSI) calcd for C₁₆H₂₁N₂O₄ 305.1496, found 305.1496; [α]_D²⁵ -80.3 (*c* 1.0, CHCl₃).

Acknowledgment. The authors would like to acknowledge the financial assistance of the University of East Anglia, EPSRC and Chemistry Innovation. We would also like to thank Librarian for providing us with some of the α -amino acids used in this study.

Supporting Information Available: General experimental methods, additional experimental procedures, and compound characterization data. This material is available free of charge via the Internet at <http://pubs.acs.org>.

(8) Lam, S. J. *Chromatogr. Sci.* **1984**, *22*, 416. Chen, Z. *J. Chromatogr. Libr.* **2005**, *70*, 309. Takeuchi, T. *J. Chromatogr. Libr.* **2005**, *70*, 229.

(9) Borthwick, A. D.; Crame, A. J.; Ertl, P. F.; Exall, A. M.; Haley, T. M.; Hart, G. J.; Mason, A. M.; Pennell, A. M. K.; Singh, O. M. P.; Weingarten, G. G.; Woolven, J. M. *J. Med. Chem.* **2002**, *45*, 1. Borthwick, A. D.; Exall, A. M.; Haley, T. M.; Jackson, D. L.; Mason, A. M.; Weingarten, G. G. *Bioorg. Med. Chem. Lett.* **2002**, *12*, 1719.

Mild Reaction Conditions for the Terminal
Deuteration of Alkynes

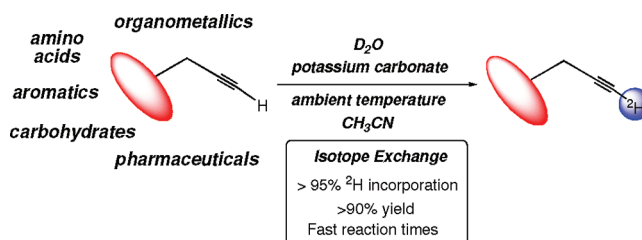
Sean P. Bew,* Glyn D. Hiatt-Gipson, Jenny. A. Lovell, and Christophe Poullain

School of Chemistry, University of East Anglia, Norwich Research Park, Norwich,
U.K., NR4 7TJ

s.bew@uea.ac.uk

Received October 28, 2011

ABSTRACT



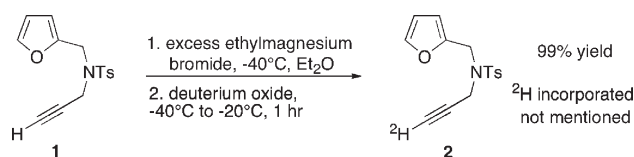
Routinely employed syntheses of terminally deuterated alkynes often utilize strong bases (i.e., LDA, *n*-BuLi, or Grignard reagents) or low (i.e., $-78\text{ }^{\circ}\text{C}$) or elevated (i.e., $56\text{ }^{\circ}\text{C}$) reaction temperatures; furthermore many of these procedures afford average yields and in some cases less than optimum deuterium incorporation. Herein we report the application of alternative extremely mild reaction conditions that readily afford quantitative yields of terminally deuterated alkynes in a matter of minutes with exceptional isotope incorporation at ambient temperature.

The development of protocols that afford high value, deuterated molecules in high yields and, importantly, with excellent levels of deuterium incorporation is very important to academia and biotechnology, medicinal, analytical, pharmaceutical, and agrochemical industries.

^2H -alkynes are valuable, synthetically useful entities¹ capable of being used for the synthesis of additional deuterated molecules; e.g., ^2H -alkyne hydrogenation generates *cis*- or *trans*- ^2H -alkenes² or ^2H -alkanes.³ Alternatively aqueous gold salts⁴ afford ^2H -ketones, and ^2H -alkyne cyclotrimerization affords ^2H -aromatics.⁵

Protocols for deuterated alkyne synthesis employ either elevated⁶ or subambient reaction conditions;⁷ extended, often hour-long reaction times;⁸ or strong bases, i.e. *n*-BuLi,⁹ Grignard reagents¹⁰ (Scheme 1), or LDA;¹¹ or an expensive transition metal salt,¹² a consequence of which is the requirement that anhydrous reaction conditions and solvents be maintained at all times.

Scheme 1. Synthesis of Deuterated Alkyne 2 from 1



(1) Diederich, F. *Acetylene Chemistry: Chemistry, Biology and Material Science*; Stang, P., Tykwinski, R. R., Eds.; Wiley-VCH: 2004. Denes, F.; Perez-Luna, A.; Chemia, F. *Chem. Rev.* **2010**, *110*, 2366. Willis, M. C. *Chem. Rev.* **2010**, *110*, 725. Amblard, F.; Cho, J. H.; Schinazi, R. F. *Chem. Rev.* **2009**, *109*, 4207. Alonso, F.; Beletskaya, I. P.; Yus, M. *Chem. Rev.* **2004**, *104*, 3079. Beletskaya, I.; Moberg, C. *Chem. Rev.* **1999**, *99*, 3435. Bunz, U. H. F.; Kloppenburg, L. *Angew. Chem., Int. Ed.* **1999**, *38*, 478.

(2) Lindlar, H.; Dubuis, R. *Org. Synth., Coll. Vol. 5* **1973**, 880. Trost, B. M.; Ball, Z. T.; Joege, T. *J. Am. Chem. Soc.* **2002**, *124*, 7922.

(3) Vanier, G. S. *Synlett* **2007**, 131. Mandal, P. K.; McMurray, J. S. *J. Org. Chem.* **2007**, *72*, 6556.

(4) Marion, N.; Ramon, R. S.; Nolan, S. P. *J. Am. Chem. Soc.* **2009**, *131*, 448.

(5) Agenet, N.; Bruisine, O.; Slowinski, F.; Gandon, V.; Aubert, C.; Malacria, M. *Organic Reactions* **2007**, *68*, 1–302.

(6) Zhang, G.; Cui, L.; Wang, Y.; Zhang, L. *J. Am. Chem. Soc.* **2010**, *132*, 1474.

(7) Hislop, J.-A.; Hunt, M. B.; Fielder, S.; Rowan, D. D. *J. Agric. Food Chem.* **2004**, *52*, 7075.

(8) Sabot, C.; Kumar, K. A.; Antheaume, C.; Mioskowski, C. *J. Org. Chem.* **2007**, *72*, 5001.

(9) Tsuchimoto, T.; Matsubayashi, H.; Kaneko, M.; Nagase, Y.; Miyamura, T.; Shirakawa, E. *J. Am. Chem. Soc.* **2008**, *130*, 15823.

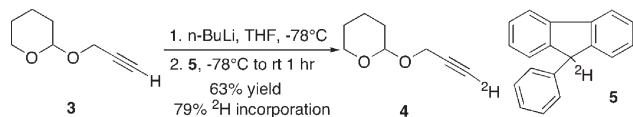
(10) Hashmi, A. S. K.; Rudolph, M.; Siehl, H.-U.; Tanaka, M.; Bats, J. W.; Frey, W. *Chem.—Eur. J.* **2008**, *14*, 3703.

(11) Chen, Y.; Lee, C. *J. Am. Chem. Soc.* **2006**, *128*, 15598.

(12) Lewandos, G. S.; Maki, J. W.; Ginnebaug, J. P. *Organometallics* **1982**, *1*, 1700.

Furthermore many afford subquantitative yields of product with reduced levels of deuterium incorporation or employ multistep procedures requiring presynthesized bespoke ‘not off the shelf’ reagents, i.e. **5** (Scheme 2),¹³ or hazardous to handle alkali metals.¹⁴

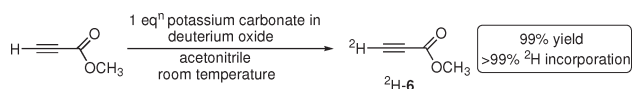
Scheme 2. Synthesis of Deuterated Alkyne **4** from **3** Using **5**



A mild, quick, and efficient protocol capable of generating terminal ²H-**6** was required (Scheme 3). Our initial thoughts focused on reacting methyl propiolate with sodium deuterioxide/D₂O mixtures; however significant ester hydrolysis was observed. Using *less* basic reaction conditions, the weaker base potassium carbonate was probed; furthermore using a water ether biphasic reaction medium we envisaged may negate the ester hydrolysis problem, affording high yields of ²H-**6**. After methyl propiolate was dissolved in ether, it was stirred with a 1 M aqueous (D₂O) potassium carbonate solution. ²H-**6** was generated in an average yield with relatively poor (25%) ²H-incorporation. Gratifyingly it seemed these less basic reaction conditions mediated significantly less ester hydrolysis but at the expense of lower deuterium incorporation. A solvent study using dichloromethane, toluene, 1,2-dichloroethane, *tert*-butylmethyl ether, ethyl acetate, hexane, toluene, and 1,1,1-trichloroethane and employing the same reaction conditions again generated ²H-**6**, but the yields were unacceptable and purification of ²H-**6** from methyl propiolate was tedious and time-consuming.

Aqueous potassium carbonate had negated the ester hydrolysis problem; however the efficiency of the reaction, i.e. conversion of methyl propiolate to ²H-**6**, was poor. We considered that part of the problem lies in the biphasic nature of the reaction system. Mindful that switching to water miscible acetonitrile and aqueous potassium carbonate would result in extensive ester hydrolysis, we were delighted to observe the formation of ²H-**6** in *both* quantitative yield and ²H-incorporation (Scheme 3).

Scheme 3. Mild Synthesis of Deuterated Propiolate Ester ²H-**6**



Probing the rate of the reaction, we dissolved methyl propiolate in CD₃CN and ran the ¹H NMR. To the same

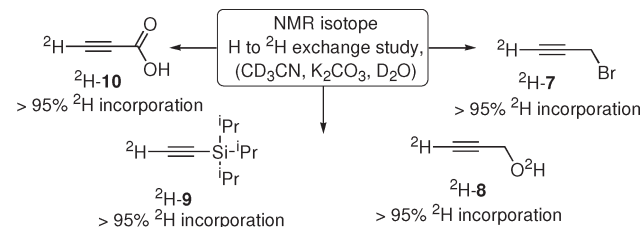
(13) Cintrat, J. C.; Pillion, F.; Rousseau, B. *Tetrahedron Lett.* **2001**, *42*, 5001.

(14) Sirokan, G.; Molnar, A.; Bartok, M. *J. Labelled Compds. Radiopharm.* **1989**, *27*, 439.

sample was added potassium carbonate (1 eqⁿ) in D₂O. Interestingly the deuteration of methyl propiolate was extremely fast, complete within minutes affording ²H-**6** in > 99% (Supporting Information (SI)).

Buoyed by this result we undertook a study using propargyl alcohol, propargyl bromide, montri(*isopropyl*)-silylacetylene, and propiolic acid (Scheme 4). Using ¹H NMR as an efficient, sensitive ‘real time investigative probe’ we established terminal alkyne deuteration was, again, fast and complete within minutes.

Scheme 4. Deuteration of Alkynes Monitored *via* ¹H NMR



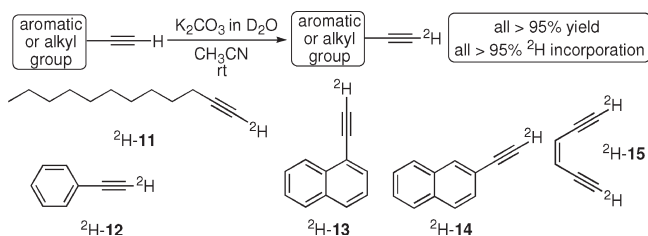
This limited substrate scope indicated our isotope exchange reaction tolerated a range of functionality that included the relatively base labile propargyl bromide, as well as propargyl alcohol, TIPS-acetylene (TMS-acetylene did not survive the reaction¹⁵), and electron-poor substrates such as propiolic acid. This simple protocol afforded ²H-**7**–²H-**10** via a straightforward process and with excellent levels of ²H-incorporation (see SI).

Confident our protocol was robust, we subjected dodec-1-yne to terminal deuteration. ²H-**11** was generated in both quantitative yield and ²H-incorporation (judged by the disappearance of the terminal alkyne triplet at 1.93 ppm). Similarly ethynylbenzene as well as 1- and 2-ethynyl-naphthalenes afforded ²H-**12**, ²H-**13**, and ²H-**14** in quantitative yields. Gratifyingly performing a one-pot double deuteration on (*Z*)-hexa-3-en-1,5-diyne generated ²H-**15** in a quantitative yield and with > 95% ²H-incorporation. Using ¹H NMR as our investigative tool no (*Z*)-²H-**15** or (*E*)-²H-**15** isomerization was observed.¹⁶

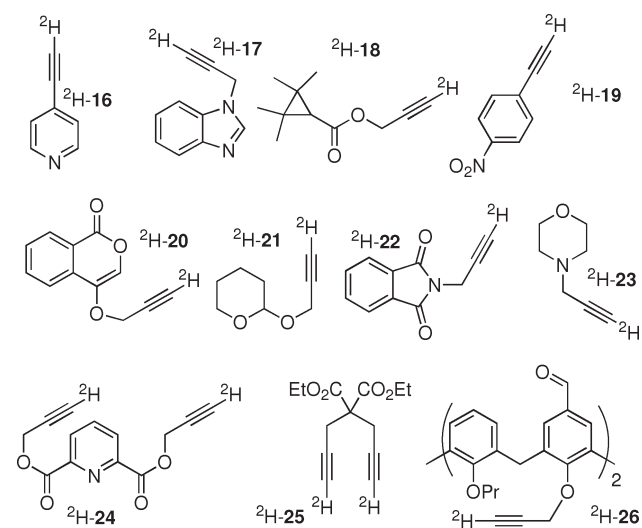
Using ethynylbenzene (**12**) we investigated, independently, water miscible dioxane and THF as possible alternatives to acetonitrile. Both afforded ²H-**12** with > 99% deuterium incorporation and essentially quantitative yields (K₂CO₃, rt, 1 h). To probe alternative inorganic or organic bases, the synthesis of ²H-**12** was attempted using cesium carbonate, sodium carbonate, sodium hydrogen carbonate, triethylamine, and polystyrene bound *tris*amine (all 1 eqⁿ). All the inorganic bases afforded ²H-**12** in excellent yield and deuterium incorporation, i.e. > 99%. Triethylamine and immobilized *tris*amine afforded ²H-**12** in good yields; however the ²H-incorporation was slightly lower, i.e. 95%.

(15) Diederich, F.; Stang, P. J. *Metal Catalyzed Cross-Coupling Reactions*; Wiley-VCH: Chichester, 1998.

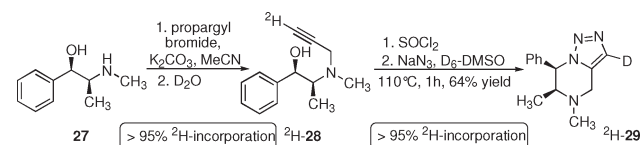
(16) McMahon, R. J.; Halter, R. J.; Fimmen, R. L.; Wilson, R. J.; Peebles, S. A.; Kuczkowski, R. L.; Stanton, J. F. *J. Am. Chem. Soc.* **2000**, *122*, 939–949.

Scheme 5. Synthesis of ^2H -Aliphatic and ^2H -Aromatic Species

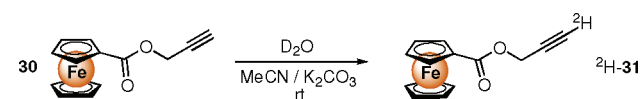
Probing the generality of the deuteration process, a series of structurally diverse heterocyclic and heteroatom alkynes were investigated. 4-Ethynylpyridine (**16**), 1-(prop-2-ynyl)-1*H*-benzo[*d*]imidazole (**17**), ethynyl 2,2,3,3-tetramethylcyclopropanecarboxylate (**18**), 1-ethynyl-4-nitrobenzene (**19**), 4-(prop-2-ynyloxy)-1*H*-isochromen-1-one (**20**), 2-(prop-2-ynyloxy)tetrahydro-2*H*-pyran (**21**), 2-(prop-2-ynyl)isoindoline-1,3-dione (**22**), and 4-(prop-2-ynyl)morpholine (**23**) reacted (standard reaction conditions employed in Scheme 5), within minutes, affording ^2H -**16**– ^2H -**23** in quantitative yields and excellent levels of deuterium (Figure 1). Incorporating multiple deuterium atoms into terminal *bis*- or *tetra*(alkynes) in quantitative yield and ^2H -incorporation had significant appeal. Subjecting diprop-2-ynyl pyridine-2,6-dicarboxylate and diethyl 2,2-di(prop-2-ynyl)malonate to our standard $\text{D}_2\text{O}/\text{K}_2\text{CO}_3$ (2.5 eqⁿ) reaction conditions afforded ^2H -**24** and ^2H -**25** in quantitative yields and, importantly, 100% deuterium incorporation. To exploit this further, the incorporation of four deuteriums was attempted using a calix[4]arene appended with four lower-rim *O*-propargyl ethers. To our delight ^2H -**26** was afforded in a quantitative yield and with outstanding levels of deuterium incorporation.

**Figure 1.** Examples of deuterated molecules ^2H -**16**– ^2H -**26**.

A terminally deuterated alkyne attached to an optically active molecule engenders it with synthetic ‘appeal’ especially if it can be used to synthesize optically active (deuterated) building blocks or drug-like molecules. Using an exceptionally mild, one-pot, two-step procedure, (1*R*,2*S*)-ephedrine (**27**) was *N*-propargylated using conditions reported¹⁷ by Couty et al. (Scheme 6); we were delighted that, without workup, the introduction of deuterium oxide afforded ^2H -**28** with quantitative ^2H -incorporation. Treatment of ^2H -**28** with thionyl chloride and subsequently sodium azide (D_6 -DMSO, 110 °C) afforded > 95% incorporated ^2H -**29** in a 64% yield. No reduction in ^2H -incorporation was observed for this transformation (*cf.* > 95% for ^2H -**28**). Worthy of note is that this exceeds the 80% ^2H -incorporation reported by Couty et al. for their low temperature (–78 °C) deprotonation (*n*-BuLi) electrophilic quench process using non- ^2H **28**.

Scheme 6. Synthesis of Deuterated Triazole Piperazine ^2H -29

To further demonstrate the broad scope of this exceptionally mild deuteration protocol, its exploitation for the chemoselective deuteration of an organometallic complex was sought. Synthesis of ferrocene propargyl acetate **30** (48% yield) was straightforward.¹⁸ Gratifyingly, dissolving **30** in acetonitrile, adding deuterium oxide and potassium carbonate, allowed the efficient synthesis of ^2H -**31** with > 95% deuterium incorporation and in an excellent 98% yield (Scheme 7); no evidence of cyclopentadienyl ^1H – ^2H exchange was detected.

Scheme 7. Synthesis of Isotopically Labelled Ferrocene ^2H -31

The synthesis of isotopically labeled α -amino acids and carbohydrates is critically important to (in)organic and biological mechanism elucidation, probing for kinetic isotope effects, and protein structure analysis. To validate the extremely mild nature of our protocol, the deuteration of variously *N*,*C*-protected- α -amino acids and *O*-protected carbohydrates was investigated. *N*-Boc-*C*-*tert*-butyl-*O*-

(17) Couty, F.; Durrat, F.; Prim, D. *Tetrahedron Lett.* **2004**, *45*, 3725.
(18) Bew, S. P.; Hiatt-Gipson, G. D. *J. Org. Chem.* **2010**, *75*, 3897.

propargyl-(*S*)-tyrosine, (*S*)-prop-2-ynyl-2-(tert-butoxycarbonylamino)pent-4-ynoate, *N*-Boc-C-propargyl-(*S*)-phenylalanine, and *N*-Boc-C-propargyl-(*S*)-4-fluorophenylglycine (unnatural α -amino acid) were transformed (standard conditions) into ^2H -**32**– ^2H -**35** (Figure 2) with > 99% ^2H -incorporation and excellent yields. The terminal deuteration (*S*)-*N*-Boc-C-propargyl methionine, (*S*)-*N*-dansylproline propargyl ester, and *N*-Bn-**38** afforded ^2H -**36**– ^2H -**38** in excellent yields and, again, levels of deuterium. Incorporating *O*-propargylated glucose, biotin, and lactose afforded the corresponding deuterated derivatives, ^2H -**39**– ^2H -**41** respectively, in excellent yields and levels of deuterium incorporation.

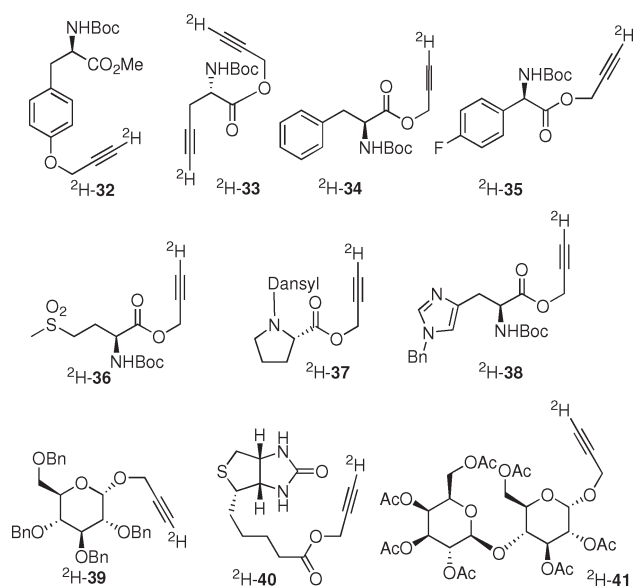
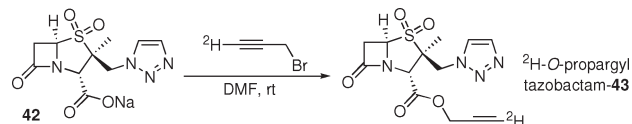


Figure 2. ^2H -alkyne derived α -amino acids and carbohydrates.

Isotopically labeled entities are crucial to the pharmaceutical, agrochemical, and biotechnology industries (ADME and PKME studies); therefore efficient routes to labeled drug compounds are very important. β -Lactam antibiotics are very sensitive to β -lactam ring opening under aqueous basic or acidic conditions. When *O*-propargyl tazobactam **42** was subjected to our standard slightly basic $\text{D}_2\text{O}/\text{K}_2\text{CO}_3$ ^2H -propargylating reaction conditions, none of the desired ^2H -**43** was isolated; instead as expected extensive decomposition was observed. While

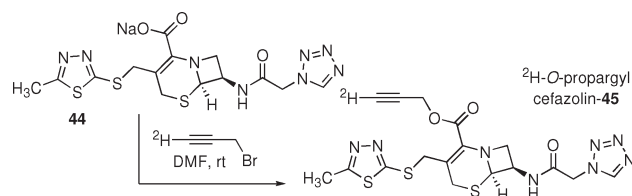
investigating (immobilized) base, solvent, and temperature conditions, we were unable to prevent ring-opening.

Scheme 8. Synthesis of ^2H -*O*-Propargyltazobactam ^2H -**43**



Negating this, 3-deutero propargyl bromide ^2H -**7** (see Scheme 4) reacted directly with the sodium salt of the β -lactam tazobactam **42** affording ^2H -**43** in excellent yield and > 95% ^2H -incorporation (Scheme 8). Similarly reacting the sodium salt of **44** with **7** at ambient temperature in DMF afforded the desired ^2H -*O*-propargylcefazolin **45** in excellent yield and deuterium incorporation (Scheme 9).

Scheme 9. Synthesis of ^2H -*O*-Propargylcefazolin **45**



In summary, this is an exceptionally mild, synthetically versatile, extremely practical protocol that efficiently transforms terminal alkynes into their deuterated analogs; is straightforward; does not use low temperature, anhydrous solvent, or strong base; is cheap and environmentally friendly; and should prove useful to the organic, inorganic, medicinal and agrochemist alike.

Acknowledgment. The authors would like to acknowledge UEA, Chemistry Innovation and Librarian for financial support and the Mass Spectroscopy Service at the University of Wales for MS analysis.

Supporting Information Available. Data for compounds ^2H -**11**– ^2H -**41**, ^2H -**43**, and ^2H -**45**. This material is available free of charge via the Internet at <http://pubs.acs.org>.